# Nuclear Physics GANIL 1992 - 1993

M. Bex, J. Galin

LABORATOIRE COMMUN IN2 P3 (CNRS) - DSM (CEA)

# NUCLEAR PHYSICS GANIL 1992-1993

a COMPILATION

# NUCLEAR PHYSICS AT GANIL

## A COMPILATION 1992 - 1993

Editors : Monique BEX, Joël GALIN
Typing and layout of the manuscript : S. GESWEND

April 1994

# FOREWORD

Investigations in nuclear physics achieved at GANIL during the 1992-1993 years are presented in this compilation. For this period, the accelerator was running more than 10 000 hours and delivered several dozens of different ion beams . The new control system design is now into operation on the machine and provides new capabilities for the beam tuning applications.

During the recent period, the exploration of the isospin degree of freedom which is an important field of research at GANIL has been actively pursued in two main avenues illustrated by the following examples : the $^{112}Sn$ projectile fragmentation has allowed to produce and identify with the LISE spectrometer the new $^{102}Sn$ and $^{101}Sn$ isotopes and then prepare the road towards the doubly magic nucleus for the very near future. On the other hand radioactive beams are more and more routinely used for nuclear structure studies. Thus, the Coulomb excitation of the bound excited state of the $^{11}Be$ neutron halo nucleus has been measured for the first time.

There is a long list of research topics concerning the behaviour of hot nuclei. An experiment showed nicely the transition from fission to multifragmentation regimes with excitation energies. The analysis of emitted fragment properties gives clear indications on the character of the disassembly process. Last spring 1993, the new INDRA detector was set into operation and a first series of experiments was performed which should improve considerably our understanding of the multifragmentation phenomenon. Besides these new measurements, theoretical studies in nuclear dynamics and the development of instabilities have been pursued.

The TAPS detector was again at GANIL for few months during this period and several experiments were successfully achieved, some of them in connection with the SPEG spectrometer.

An original experiment was set to search for a signature of a colour Van der Waals force in nuclei. This study of the Mott Scattering for the $^{208}Pb + ^{208}Pb$ system, was a real technical challenge, requiring very high precision on both the incident energy and the angular definition. Results indicate clearly the influence of atomic effects other than the usual screening.

We are indebted to the authors for the quality of their contributions.

**Samuel HARAR**
**Director**

**Daniel GUERREAU**
**Deputy Director**

# CONTENTS

# I. COMPILATION

# A - NUCLEAR STRUCTURE

## A1 - NUCLEAR SPECTROSCOPY

## A2 - EXOTIC NUCLEI AND DECAY MODES

# B - NUCLEAR REACTIONS

## B1 - PERIPHERAL COLLISIONS. PROJECTILE-LIKE FRAGMENTS

## B2 - DISSIPATIVE COLLISIONS

## B3 - FLOW AND RELATED PHENOMENA

## B4 - MULTIFRAGMENT EMISSION

## B5 - MESONS AND PHOTONS

# C - MISCELLANEOUS

# A - NUCLEAR STRUCTURE

# A1 - NUCLEAR SPECTROSCOPY

# EXCLUSIVE AND RESTRICTED INCLUSIVE REACTIONS INVOLVING THE $^{11}$Be ONE-NEUTRON HALO

R. Anne[1], R. Bimbot[2], S. Dogny[2], H. Emling[3], D. Guillemaud-Mueller[2], P.G. Hansen[4], P. Hornshøj[4], F. Humbert[5], B. Jonson[6], M. Keim[7], M. Lewitowicz[1], P. Møller[4], A.C. Mueller[2], R. Neugart[7], T. Nilsson[6], G. Nyman[6], F. Pougheon[2], K. Riisager[4], M.-G. Saint-Laurent[1], G. Schrieder[5], O. Sorlin[2], O. Tengblad[8], and K. Wilhelmsen Rolander[6]

1) GANIL, F-14 021 Caen Cedex.
2) Institut de Physique Nucléaire, IN2P3-CNRS, F-91 406 Orsay Cedex.
3) GSI, Postfach 11 05 52, D-64220 Darmstadt.
4) Institut for Fysik og Astronomi, Aarhus Universitet, DK-8000 Aarhus C.
5) Institut für Kernphysik, Technische Hochschule, D-64289 Darmstadt.
6) Fysiska Institutionen, Chalmers Tekniska Högskola, S-412 96 Göteborg.
7) Institut für Physik, Universität Mainz, D-55099 Mainz.
8) PPE Division, CERN, CH-1211 Genève 23.

The nuclei with a neutron halo pose a peculiar experimental problem. Having in most cases only one bound state in addition to an almost structureless continuum, they are not amenable to the usual spectroscopic methods of nuclear structure physics. The attention has instead focused on nuclear reactions. Among those, the study of momentum distributions from the fragmentation of halo nuclei has turned out to be especially fruitful.

Our 1990 experiment on $^{11}$Li led to the first observation of an extremely narrow transverse momentum distribution of the outgoing neutrons from the break-up of this nucleus. This experiment has recently been confirmed at the NSCL (M.S.U.) by an elegant measurement of the longitudinal momentum distribution of the $^{9}$Li fragment. Although it is qualitatively correct to say that the narrow distributions via Heisenberg's uncertainty principle are a measure of the extended halo, we now know that there are unavoidable modifications caused by the reaction mechanisms, and these become a major problem when it comes to studying the finer points such as the expected existence of neutron-neutron correlations.

In order to clarify the interplay between structure and reaction mechanism, the present work has investigated fragmentation reactions of $^{11}$Be, so far the only known case of a one-neutron halo. We measured the dissociation cross-sections, energy spectra and angular distributions of the forward fast neutrons from reactions with three targets: beryllium (Z=4), titanium (Z=22), and gold (Z=79). These were chosen in order to illuminate the relative contributions of nuclear and Coulomb interactions, dominant for beryllium and for gold, respectively. An essential part of our experimental strategy was that the fast charged fragments from the reactions were recorded in a counter telescope and in coincidence with the neutrons so that the information could be sorted according to different reaction channels. Since the $^{10}$Be

core has little chance of remaining intact after a collision with the target nucleus, the channel with this nucleus as a fast outgoing fragment must predominantly represent collisions that take place for impact parameters larger than the sum of the core and target radii. We refer to the single-neutron-exclusive reactions leading to $^{10}$Be as dissociation reactions. These are very sensitive to the halo structure.

The results for these were compared with two sets of theoretical estimates. The first [1] was a calculation of Coulomb excitation to the continuum in a perturbation treatment. The second [2] is based on the sudden approximation and describes the combined effect of Coulomb and nuclear dissociation. In both cases it turns out to be possible to give analytical expressions describing the cross-sections and the momentum distributions of the neutrons. There is no attempt to "fit" the data; our estimates of cross-sections are on an absolute scale and contain no free parameters. The calculations give a very good description of the data, both for the angular distributions and for the longitudinal energy spectra. The conclusion is that the dissociation reactions are well accounted for with three theoretial ingredients: Coulomb excitation and the Serber and Glauber (diffraction dissociation) mechanisms. As an example of these results we show in Fig. 1 the systematics of the dissociation cross-sections.

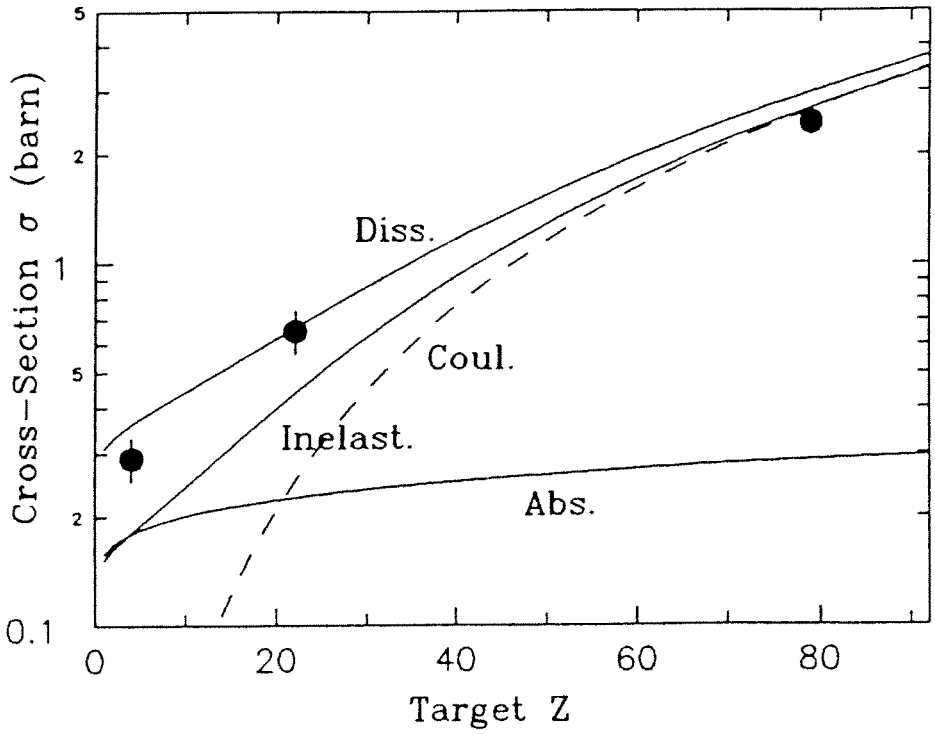


*Fig. 1:The experimental dissociation cross-sections for the reaction ($^{11}$Be,$^{10}$Be+X). The full-drawn lines are the calculated contributions from absorption, inelastic reactions (i.e. final states of $^{11}$Be consisting of $^{10}$Be and a free neutron) and (top) the sum of the two. The dashed line has been calculated with the nuclear terms set equal to zero. It shows what Coulomb dissociation alone would give in the same calculation. The inelastic nuclear contribution in the absence of Coulomb terms can be obtained by setting $Z_2$=0. The result would be indistinguishable from the absorption contribution and is not shown.*

Instead of discussing separately the single-neutron inclusive angular distributions, we have found it more instructive to present these data with the dissociation reactions removed. The result of this is what we have chosen to call "restricted inclusive distributions", which represent the channel "neutron plus anything except $^{10}$Be". This anti-coincidence requirement selects events for which the impact parameters are smaller than the sum of the core and target radii. The corresponding angular distributions are shown for the beryllium target as the top line of experimental points in Fig. 2. Similar data were obtained with the titanium target, and the results for the gold target were very similar in absolute magnitude, but had much inferior statistics.We believe that the restricted inclusive distributions are more interesting than might seem to be the case at first sight

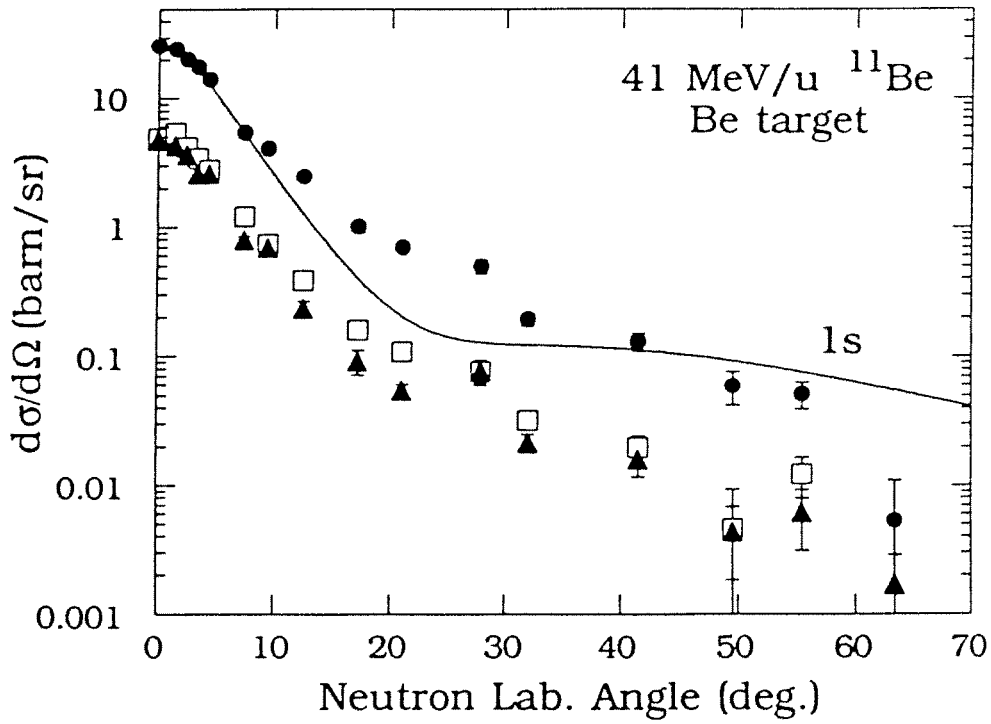


*Fig. 2: Angular distributions of fast neutrons (25<$E_n$<75 MeV) produced by a 41 MeV/u beam of Be on a target of beryllium. The filled circles are the restricted inclusive events, i.e. events not accompanied by an outgoing $^{10}$Be. Also shown are two sub-sets of exclusive events corresponding to coincidences with outgoing helium (Z=2, filled triangles) and lithium (Z=3, open squares) ions, independent of their mass. The curve, arbitrarily normalized to fit the points at zero degrees, is the angular distribution obtained by transforming to laboratory coordinates the momentum distribution of a finite-size square well with depth adjusted to reproduce the experimental neutron separation energy of 0.5 MeV. The integrated restricted inclusive cross-section is 1.5±0.3barn.*

In this connection we note first of all, that a halo neutron has a probability distribution that extends far beyond the core and that as a consequence it must have an appreciable probability of going clear of the debris from the core-target conflagration. This is an obvious case for the sudden approximation: The neutron viewed in the coordinate system following the beam should, as in Serber's model of the deuteron break-up, emerge with a momentum distribution characteristic of the halo wave function. Under the right experimental conditions this

could then permit a mapping of the Fourier transform of the halo wave function. In order to extract this contribution from that arising from that of neutrons from core-target collisions, the experiment should then be repeated with the core (e.g. $^{10}$Be) as a projectile and at the same beam velocity as that used for the halo nucleus. The difference would then reflect the contribution of the halo neutron. We have recently proposed such an experiment to GANIL.

Some support to the interpretation just given comes from numerical estimates [2] of the cross-sections and from the essentially identical shapes emerging for exclusive events involving outgoing helium and lithium ions, fragmentation products of the projectile core. The strongest argument, however, is that the angular distributions of Fig. 2 have a shape that seems to indicate a superposition of a narrow and a broad component, where the former presumably is the one that we associate with the halo neutron. The calculated momentum distribution of a 1*s* state of a finite well is seen to be in very good agreement with the measured shape at small angles.

In summary, the experiments have shown that dissociation reactions of $^{11}$Be (*i.e.* those that leave the $^{10}$Be core intact) are dominated by the neutron halo and that all cross-sections can be understood in a quantitative way that conveys information about the halo structure.

The results of the experiments have been published in the following journal papers:

[1] R. Anne, S.E. Arnell, R. Bimbot, S. Dogny, H. Emling, H. Esbensen, D. Guillemaud-Mueller, P.G. Hansen, P. Hornshøj, F. Humbert, B. Jonson, M. Keim, M. Lewitowicz, P. Møller, A.C. Mueller, R. Neugart, T. Nilsson, G. Nyman, F. Pougheon, K. Riisager, M.-G. Saint-Laurent, G. Schrieder, O. Sorlin, O. Tengblad, K. Wilhelmsen Rolander and D. Wolski, Phys. Lett. **B304** (1993) 55-59.

[2] R. Anne, R. Bimbot, S. Dogny, H. Emling, D. Guillemaud-Mueller, P.G. Hansen, P. Hornshøj, F. Humbert, B. Jonson, M. Keim, M. Lewitowicz, P. Møller, A.C. Mueller, R. Neugart, T. Nilsson, G. Nyman, F. Pougheon, K. Riisager, M.-G. Saint-Laurent, G. Schrieder, O. Sorlin, O. Tengblad and K. Wilhelmsen Rolander, submitted to Nuclear Physics A

The results were reported in the following conferences:

P.G.Hansen :
- International Conference on Nuclear Physics, Wiesbaden, Germany, August 1992, Nucl. Phys. **A553** (1993) 89c.
- Study Week-end on the Neutron Halo, Copenhagen, Denmark, March1993
- ECT* International Workshop on High Spins and Novel Deformations, Trento, Italy, December 1993.

B. Jonson
- International Conference on Perspectives in Nuclear Structure, Copenhagen, Denmark, June 1993, to be published in Nucl. Phys. A.
- Nordic Meeting on Nuclear Physics, Vigso, Denmark, August 1992
- Midsummer Workshop on Nuclear Physics, Jyväskylä, Finland, June 1993

-European Physical Society Meeting, Florence, Italy, September 1993

A.C.Mueller
-Advances in Nuclear Dynamics, Jackson Hole, WY, USA, January 1992
-Spring Meeting of the American Chemical Society, San Francisco, CA, USA, April 1992
-VI Journee Saturne, Le Mont St Odile, France, Mai 1992
-Sixth International Conference on Nuclei far from Stability, Bernkastel Kues, Germany, July 1992
-Nuclear Structure & Interdisciplinary Topics, St Malo, France, October 1992
-XXI Int. Winter Meeting on Nuclear Physics, Bormio, Italy, January 1993
-European Physical Society Meeting, Florence, Italy, September 1993
-Ecole Joliot Curie, Maubuisson, France, September 1993
-Summer School on Nuclear Structure, Varenna, Italy, October 1993

F.Pougheon
-2nd Int. Conf. on Atomic and Nuclear Clusters,Santorini, Greece, July 1993

K. Riisager
-Third Radioactive Nuclear Beams, East Lansing, MI, USA, May 1993
-Gordon Conf. on Nuclear Chemistry, New London, NH, USA, July 1993
-Summer School on Exotic Nuclei and Radioactive Beams, Leuven, Belgium, September 1993
-Summer School on Nuclear Structure, Varenna, Italy, October 1993.

# COULOMB EXCITATION OF BOUND EXCITED STATES OF THE NEUTRON HALO

R. Anne[1], D. Bazin[1], R. Bimbot[3], M.G.J. Borge[8], J.M. Corre[1], S. Dogny[3], H. Emling[4], D. Guillemaud-Mueller[3], P.G. Hansen[5], P. Hornshoj[5], P. Jensen[5], B. Jonson[2], M. Lewitowicz[1], A.C. Mueller[3], R. Neugart[6], T. Nilsson[2], G. Nyman[2], F. Pougheon[3], K. Riisager[5], M.G. Saint-Laurent[1], G. Schrieder[4], O. Sorlin[3], O. Tengblad[8], K. Wilhelmsen-Rolander[2]

1) GANIL, BP 5027, F-14021 Caen
2) Fysika institutionen, Chalmers Tekniska Högskola, S-412 96 Göteborg
3) Institut de Physique Nucléaire, BP 1, F-91406 Orsay
4) Gesellschaft für Schwerionenforschung (G.S.I.), D-6100 Darmstadt
5) Institut for Fysik og Astronomi, Aarhus Universitet, DK-8000 Aarhus C
6) Institut für Physik, Universität Mainz, D-6500 Mainz
7) Institut für Kernphysik, Technische Hochschule, D-6100 Darmstadt
8) CERN, Div. PPE, CH-1211 Genève 23

Abstract:

A new method, based on Coulomb excitation of a radioactive beam, permits for the first time the spectroscopy of $1^-$ excitations of nuclei with a neutron halo. The $\gamma$ transitions of the de-excitation are clearly identified by the Doppler shift. We could thus observe the transition $1/2^- \rightarrow 1/2^+$ of $^{11}$Be and determine its Coulomb excitation cross section. It is interesting that this number is about a factor two smaller than that calculated from the measured lifetime of the state. Explanations are in progress. Limits are presented for the excitation of hypothetical bound excited states in $^{12,14}$Be and $^{8}$He halo nuclei.

Introduction:

The characteristics of light exotic nuclei at the neutron drip-line have now been studied by several experiments at GANIL [1]. Systems with one ($^{11}$Be) or two ($^{8}$He, $^{11}$Li, $^{14}$Be ) slightly bound neutrons ("halo neutrons") have been investigated by measurements of reactions cross-sections and of neutron angular distribution from the break-up of the neutron halo. The goal of the present work was to pursue these studies by searching for bound excited levels in halo nuclei using Coulomb excitation. We took advantage of the very high polarizability of the loosely bound halo, which is expected to give a very large cross-section for E(1) excitation. As a test case, we

have chosen the nucleus $^{11}$Be, which so far is the only halo system with a known bound excited state (at 320 keV). Furthermore the lifetime and hence the B(E1) for this state is known from the Doppler-shift experiment of Millener et al.[2]. We have populated this $1/2^-$ state and observed the transition back to the $1/2^+$ ground state and thus achieved for the first time a Coulomb excitation experiment with a high energy (45 MeV/A) radioactive beam. We shall briefly describe the experimental set-up, aspects of the analysis , show experimental results for $^{11}$Be and propose some limits for the existence of bound excited states in the $^{12,14}$ Be and $^{8}$He nuclei.

Experimental set-up:

The experiment was performed at GANIL, on the LISE3 [3] spectrometer, using fragmentation of a primary $^{18}$O beam (63 MeV/A) for the production of neutron-rich light nuclei. Three independent selection criteria of LISE3, viz. magnetic rigidity, energy loss in an achromatic wedge and velocity, are combined in order to produce and transmit the secondary beams with a very high isotopic purity. Fig. 1 shows the experimental set-up. The radioactive beam impinges onto a lead target chosen for its high atomic number, which strongly enhances Coulomb excitation. We used plastic scintillators (NE102) for particle identification in order to accept high count rates. Three large-volume hyperpure germanium counters are used for the detection of in-flight $\gamma$ de-excitation. The Doppler shift of these rays will be sensitive to the angle of detection. The distances from the target indicated on fig.1 result from a compromise between Doppler broadening and solid angle efficiencies.

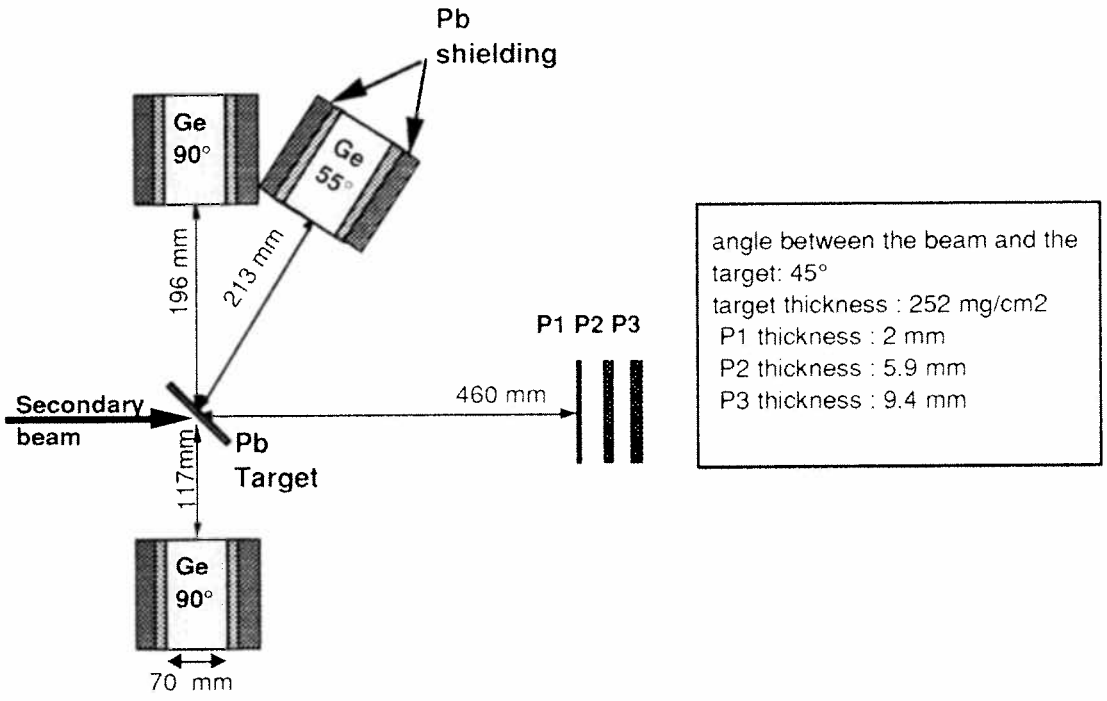


*Fig. 1 Experimental set-up*

Analysis and results

Contours on two-dimensional spectra, the particle identification (energy loss vs. time of flight) are used in order to eliminate the residual impurities of the secondary beam and the products of nuclear reactions in the target. A time window (100 ns) selects the gamma rays emitted in coincidence with a particle of the secondary beam resulting in strong suppression of background. The key to identification of lines arising from projectile excitation is their Doppler shift. The mean energies of the peaks observed at 55° and 90° should follow the Doppler formula:

$$E\gamma = \frac{E\gamma_0\sqrt{1-\beta^2}}{1-\beta\cos\theta}$$ where $\beta$ is the secondary beam velocity.

Fig. 2 shows the regions of interest of the $\gamma$ spectra for the $^{11}$Be. We clearly see peaks with different positions and widths.These peaks are probed with 2 criteria to see whether they originate from excitation or not:

-The observed widths were consistent with the Doppler broadening induced by the energy spread of the secondary radioactive beam and the solid angle acceptance of the detectors.

- The positions of the centers of gravity observed for each angle in the experiment agree very well with the expected positions of the 320 keV line calculated under the following assumption: the mean energy of $^{11}$Be at the middle of the target is derived from the magnetic rigidity of the second dipole of LISE and the energy loss in the Coulomb excitation target by means of the program STOPX [4].

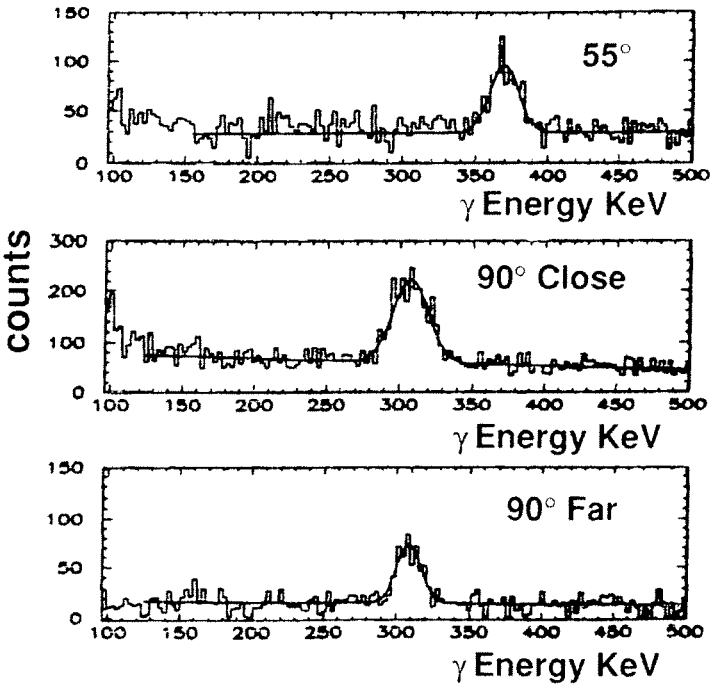


*Fig.2: Parts of the γspectra in the relevant energy -range for the 320 keV transition in 11Be.*

From the number of incident $^{11}$Be in Ne102 plastic scintillators, and from the number of 320 keV $\gamma$ detected in each germanium detector and geometrical and intrinsic efficiencies, it is possible to determine cross-sections and then to deduce the transition probability of bound excited level.The experimental cross section for the 320 keV level of $^{11}$Be is:

$\sigma$(320 keV, $^{11}$Be) = 191± 26 mb.

The lifetime of the 320 keV state has been measured by a Doppler-shift technique by Millener et al. [2]. From this, it is possible to calculate the B(E1) and the (pure) Coulomb excitation cross-sections by means of the theory for high-energy Coulomb excitation developed by Winther and Alder [5].

The cross-section can be expressed as :

$$\sigma = \left(\frac{Z_2\alpha}{\beta}\right)^2 \frac{B(E1)}{e^2}\frac{16\pi}{9}\left\{g_1(\xi)+(1-\beta^2)g_0(\xi)\right\}$$

where other parameters are defined in their paper and $\xi$ is the adiabaticity parameter defined as:

$$\xi = \frac{1}{197.3}E^*(MeV)\frac{R(fm)}{\beta\gamma}$$

and R is the sum of the projectile and target nuclear radii. From this, we deduce a theoretical cross section $\sigma_{th}$ = 480±50 mb, for the $^{11}$Be level ($E^*$= 320 keV, B(E1) = 0.116 $e^2fm^2$ ± 0.012 [2]); the error bars of the theoretical cross-section are due to the experimental uncertainties of the lifetime measured by Millener et al.[2].

Our experimental results for the cross-sections are thus a factor 2 lower than the result expected for pure Coulomb excitation : Apart from the possibility of an experimental error, we see two possible avenues for a theoretical explanation of this difference :

- In spite of the fact that incident $^{11}$Be nuclei were detected inside the grazing angle, Coulomb and nuclear strengths can, because of the halo, interfere in a destructive way, decreasing the cross section for the excitation of the 320 keV level.
- A two step process : Coulomb dissociation of the $^{11}$Be ->$^{10}$Be + n can, due to the strong Coulomb field of the heavy target, follow the excitation of the 320 keV level ( bound against the separation energy of one neutron by only 180 keV), leading to a $^{10}$Be nucleus, at the detriment of the observation of the 320 keV $\gamma$ transition.

The same method was used for $^{12,14}$Be and $^{8}$He nuclei to excite their eventual unknown E1 level and to determine their energies and transition probabilities.

No new $\gamma$ transitions are seen in the corresponding $\gamma$ spectrum. To search with the best accuracy, a mathematical procedure consisting of a $\chi^2$ comparison of background fit with and without a gaussian peak was performed. Inside the factor 2 between experimental and theoretical cross sections determination, the non-excitence of E1 levels having transition probabilities B(E1) greater than the value of 0.01 Wu. was extracted for the $^{12}$Be and $^{8}$He nuclei, and no level was observed in a B(E1) limit of 0.5 Wu. for the $^{14}$Be nucleus.

Conclusion

Using a weak (compare to stable beams) radioactive beam of high energy, it was possible, for the first time, to observe, the Coulomb excitation of the halo nucleus $^{11}$Be. The photons from the $1/2^- \rightarrow 1/2^+$ E(1) transition to the ground state were observed by means of a highly efficient germanium detectors. This positive result will allow us to put meaningful limits for other halo nuclei studied by this technique. One should note, in this context, that at the low energy, Coulomb excitation of secondary beam has been reported recently by Brown et al.[6] for $^{8}$Li and by Oshima et al [7] for $^{76}$Kr. However, their secondary beams were produced by inelastic scattering and fusion reactions, respectively, which limit this technique to nuclei close to the valley of stability. Our method is based on fragmentation of high energy particles, which allows to reach nuclei at the drip-line and to use a magnetic spectrometer for an efficient separation and purification of the secondary beams. More generally, we believe also that Coulomb excitation experiments may constitute a powerful tool for nuclear structure studies of unstable nuclei post-accelerated after an ISOL system. Such future facilities are presently considered at several laboratories [8], including the GANIL project .

Acknowledgements: We would like to thank F. Geoffroy, R. Hue and L. Petizon for their technical assistance during the experiment.

References

[1] see for example
M.G. Saint-Laurent et al., Z Phys. A332 (1989) 457
A.C.C. Villari, Phys. Lett. B268 (1991) 345
R. Anne et al., Phys. Lett. B250 (1990) 19.
K. Riisager et al., Nucl. Phys. A540 (1992) 365
R. Anne et al., Phys. Lett. B (1993) in press
[2] Millener et al, Phys. Rev C 28 (1983) 497
[3] A.C.Mueller and R.Anne, Nucl. Inst. Meth. B56 (1991) 559
[4] T. Awes, Oak Ridge National Laboratory (1983)
[5] Winther et Alder, Nuc.Phys. A319 (1979) 518-532
[6] Brown et al,. Phys. Rev. Let. 66 (1991) 2452-2455
[7] Oshima et al, NIM A312 (1992) 425-430
[8] see, e. g., Proc. Int. Workshop on the Physics and techniques of Secondary Nuclear Beams, Dourdan, March 1992, J.F. Bruandet, B. Fernandez, M. Bex, eds., Editions Frontières (Gif sur Yvette)

# Investigations of Giant Resonances Through Photon Absorption and Emission*

R. L. Varner, P. E. Mueller, J. R. Beene, F. E. Bertrand, M. L. Halbert,
D. J. Horen, and D. H. Olive
Oak Ridge National Laboratory, Oak Ridge, Tennessee 37831, USA†

B. Sherrill and M. Thoennessen
National Superconducting Cyclotron Laboratory and
Department of Physics and Astronomy,
Michigan State University, East Lansing, Michigan 48824, USA‡

P. Lautridou, F. Lefèvre, M. Marqués, T. Matulewicz,
W. Mittig, R. Ostendorf, P. Roussel-Chomaz, and Y. Schutz
GANIL, BP 5027, 14021 Caen CEDEX, France

J. van Pol and H. W. Wilschut
Kernfysisch Versneller Instituut, 9747 AA Groningen, The Netherlands

J. Díaz, G. Martinez, and A. Marín
IFIC 46100 Burjassot, Valencia, Spain

December 7, 1993

## 1 Introduction

The inelastic scattering of heavy-ion beams at the energies available at GANIL is an excellent tool for the excitation of giant resonances in nuclei. These beams, coupled with the high resolution magnetic spectrometer SPEG and the TAPS photon detector array [Nov91], allow us to explore the excitation and decay of the giant resonance region, with a detail which is otherwise difficult to achieve. This brief report outlines some preliminary results of an experiment made at GANIL in 1992. See also [Bar88, Bee90a, Bee90b, Hor91] and the 1989-1991 edition of Nuclear Physics at GANIL.

## 2 Two-Phonon Giant Resonances

It has long been expected that multiple excitations of strongly collective states like the giant resonances (GR) should exist. These multiphonon states should, in principle, be a rich source of information on the limits of collective descriptions of excitations in finite systems. This will require systematic spectroscopic investigations. Recent experiments have reported observation of the two-phonon GDR⊗GDR state (DGDR) excited by Coulomb excitation by heavy ions at about 1 GeV/nucleon [Sch93, Rit93]. The first evidence for the existence of a DGDR came from pion double charge exchange [Mor88].

We have investigated the two-phonon giant dipole resonance (GDR) strength in $^{208}$Pb using beams of $^{36}$Ar at 95 MeV/nucleon and $^{86}$Kr at 60 MeV/nucleon in an earlier experiment at GANIL. In 1992, we used a beam of $^{64}$Zn at 80 MeV/nucleon and the TAPS array to extend the search. These experiments used Coulomb excitation in inelastic scattering to excite the nucleus into the region where the DGDR strength lies, at about $2\times E_{GDR}$. We then looked for a coincident decay photon at energies near $E_{GDR}$ using the TAPS array. Our

*Experiment performed with TAPS

†Oak Ridge National Laboratory is managed by Martin Marietta Energy Systems, Inc. under contract DE-AC05-84OR21400 with the United States Department of Energy.

‡Supported by the National Science Foundation.

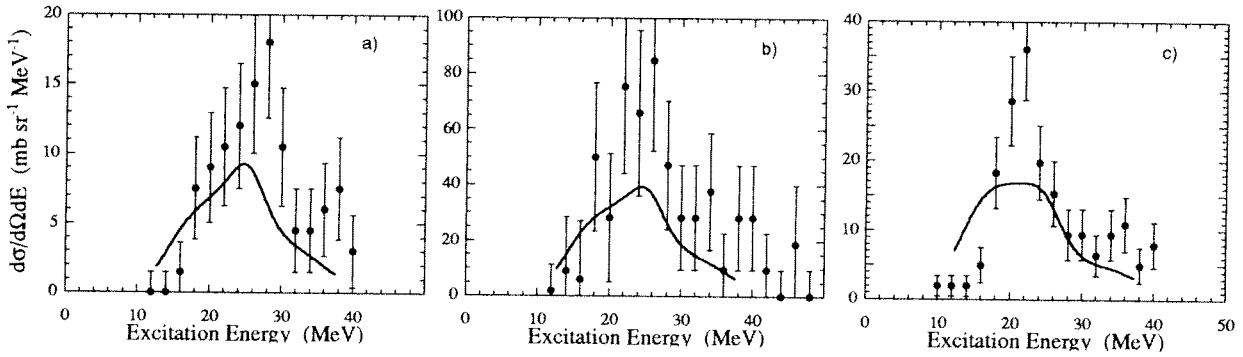


Figure 1: Excitation spectrum for the two-GDR-phonon state: a) $^{36}$Ar (95 MeV/nucleon) on $^{208}$Pb, b) $^{64}$Zn (80 MeV/nucleon) on $^{209}$Bi, and c) $^{86}$Kr (60 MeV/nucleon) on $^{208}$Pb. Note the different cross section scales. The solid curves are essentially parameter-free calculations folding the photonuclear cross section for the GDR with itself and the virtual photon spectrum to obtain the two-phonon excitation.

identification of the 2-phonon state is based on two features of the experiment. First, we depend on the identification (Z and A) of the ejectile and direct determination of the excitation energy with approximately 1 MeV resolution from SPEG and the coincident photon detection from the DGDR to GDR deexcitation. The branching ratio for GDR photon decay to the ground state is approximately 0.02. The DGDR to GDR photon decay branch is expected to be similar. While this branch is small, the yield from this decay is expected to be two orders of magnitude larger than the yield of similar energy photons from other processes in this excitation energy region.

The second feature of the identification comes from the use of different Z beams at different velocities to perform the measurements. The cross section for a single-phonon excitation in the target is directly proportional to the virtual photon flux, which is itself proportional to $Z^2$, whereas the two-phonon excitation is proportional to $Z^4$. By measuring with beams of different Z, we can distinguish the double-phonon excitation strength from single-phonon excitation strength in the same region. Another feature of the use of the different beams is that the spectrum of virtual photons depends on projectile velocity, so that the different measurements will produce differently shaped excitation yields for the two-phonon states.

The results of the measurements are shown in Figure 1 which shows the two-phonon GDR excitation resulting from the scattering of $^{36}$Ar and $^{86}$Kr from $^{208}$Pb and $^{64}$Zn from $^{209}$Bi. Note the different excitation spectrum shapes, especially comparing the $^{36}$Ar and $^{86}$Kr scattering, and how they each qualitatively resemble the calculations. The data from all three reactions are consistent with a DGDR strength distribution centered at about $2 * E_{GDR} = 27MeV$. The combined result is $< E >= 27.5 \pm 0.8MeV$.

There are two interesting features in the comparison of the calculations with the data. The first is that the calculations underestimate the magnitude of the excitation. The second is that the width of the two-phonon state is smaller than predictions. This is especially evident in the $^{86}$Kr data in Figure 1c. This is remarkable because the width in the calculation results entirely from the width of the one-phonon GDR strength distribution. One

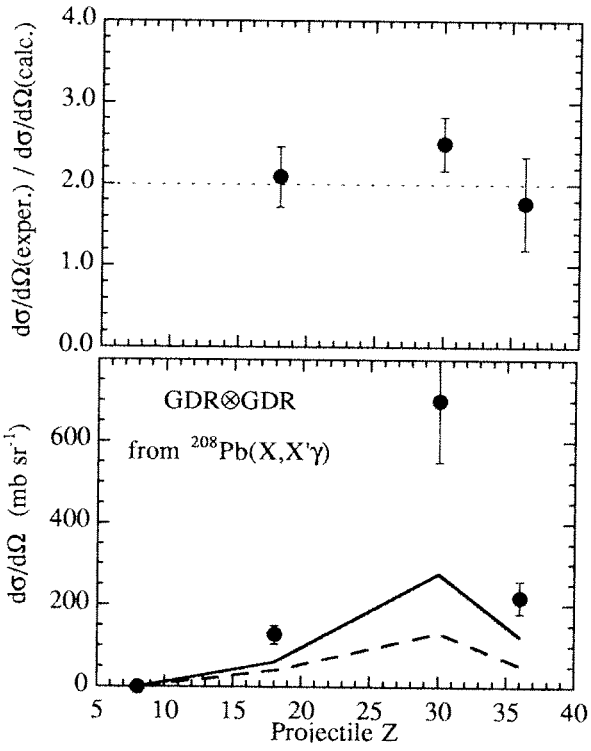


Figure 2: Cross sections for two-GDR-phonon excitation. The lower panel shows energy integrated data from Figure 1 for the data (points) and the calculations (the solid line). The dashed line is a calculation assuming a $\delta$-function GDR excitation function. The upper panel shows the ratio of the experimental cross sections to the calculations.

might expect some additional broadening from damping of the DGDR state, but we would not expect a width smaller than can be accounted for by convolution of the one-phonon excitation alone.

To further explore the excess cross section, we display in Figure 2 the measured and calculated cross sections for the two-phonon GDR as a function of projectile Z. Also, we display the ratio of the experimental to theoretical cross sections. Note that the ratios are approximately 2.0 for all projectiles. This behavior lends strong support to our identification of these structures as the DGDR. The excess yield suggests to us a larger than expected photon decay branch of the DGDR. Other experiments, cited in the introduction, have also observed comparable enhancement of the cross section.

## 3 Contamination from Pickup and Decay Reactions

The presence of the forward angle, charged-particle hodoscope developed by the KVI group permitted us to investigate contaminant contribution to our inelastic scattering yields because of pickup and decay reactions such as

$$^{64}Zn + ^{208}Pb \Rightarrow ^{65}Cu + ^{207}Tl \Rightarrow ^{64}Zn + p + ^{207}Tl$$

in which we detect a $^{64}$Zn projectile-like fragment which did not result from inelastic scattering. We had never before been able to quantify this contamination of our data.

We compared the spectrum of $^{64}$Zn scattering events measured in SPEG with the spectrum of the subset of $^{64}$Zn scattering events in which a charged particle was detected in the hodoscope. The ratio of these shows that in the region of interest to us, 0 MeV to 40 MeV, there is a less than 2% contamination in the excitation spectrum from projectile pickup and decay.

## 4 Time dependence of the GDR decay

In intermediate-energy heavy-ion scattering, the time scale of the interaction responsible for GDR excitation is comparable to the time of damping of the giant resonances. For example, the time of interaction for the $^{64}$Zn projectiles at 80 MeV/nucleon is about 51 fm/c, and, for a GDR of width $\Gamma^{\downarrow}$ of 4 MeV, the damping time, $\tau_D = \hbar/\Gamma^{\downarrow}$, is about 49 fm/c. This suggests that the excitation amplitudes sampled by semi-direct processes, which occur over a time scale limited by $\tau_D$, could be influenced by the interaction, i.e. by the proximity of the projectile. We have searched for such an effect in the angular distribution of emitted photons. The GDR in $^{208}$Pb is particularly interesting because, according to our earlier analyses [Bee90b], the lower excitation energy part of the GDR emits about equal numbers of photons from the semi-direct (fast) and compound (slow) decays, whereas photon emission from the higher excitation energies are dominated by semi-direct decays. Thus, we should see an evolution in the angular distributions as a function of energy [Bee90b].

We designed our 1992 experiment at GANIL to measure the angular distribution of photons emitted from the decay of the GDR to the ground state. Calculations indicate that at 90° out of the scattering plane, the yield is independent of the decay time, so we placed a small 19-detector $BaF_2$ array at that angle, to provide a normalization.

An additional check upon this measurement was to use a $^{209}$Bi target. In Bi, the excitation of the GDR is nearly identical to that of $^{208}$Pb, but the contribution of compound decays is much smaller, so that semi-direct decay photons should dominate across the entire resonance [Bee90b].

Our results are shown in Figure 3. It is clear that there is a difference in the angular distribution between low and high excitation for $^{208}$Pb. The quantity plotted is the ratio of the photon yield along the momentum transfer direction to that perpendicular to the scattering plane. For comparison, we show curves of the expected ratio considering only very slow decays and the case of $\Gamma^{\downarrow} \approx 4MeV$. The experimental angular distribution does indeed seem to evolve between the extremes with increasing excitation energy. Preliminary results on $^{209}$Bi show no statistically significant energy dependent variation, in agreement with our expectation. Both the data analysis and the calculations upon which Figure 3 is based are very preliminary.

## 5 Summary

We have been using the fast, heavy-ion beams of GANIL to great advantage for several years in the investigation of giant resonance decay. Our latest experience with TAPS at GANIL has yielded strong confirming evidence for direct observation of the two-GDR-phonon excitation in $^{208}$Pb, as well as striking evidence for a direct observation of the variation in time scale of photon emission from the ground state GDR in $^{208}$Pb. We hope that ongoing theoretical treatment of the properties of the two-GDR-phonon state will unravel the discrepancy between the simple calculations presented here and the data.

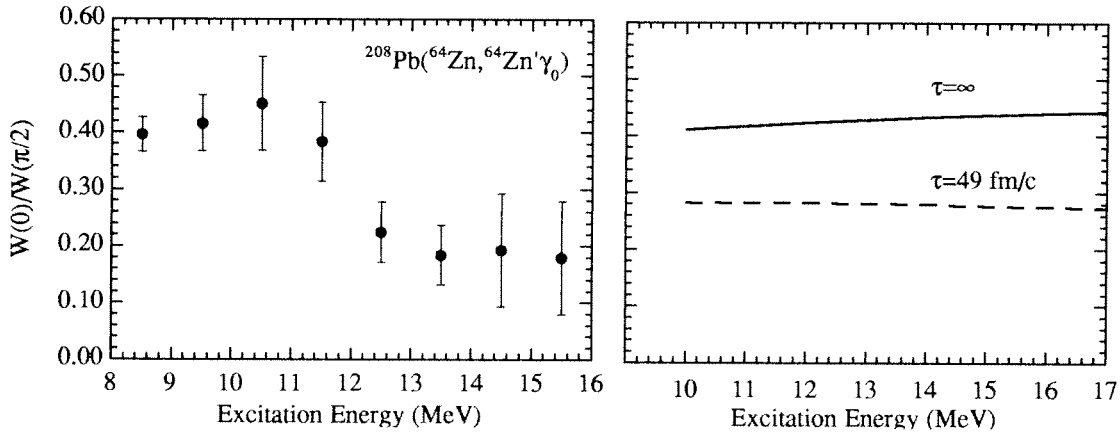


Figure 3: Ratio of photons emitted along the momentum transfer direction to those emitted perpendicular to the scattering plane. Points are preliminary data for $^{208}$Pb inelastic scattering. The curves show the expected ratio for $\Gamma^{\downarrow} \approx 4MeV$ (solid) and for $\Gamma^{\downarrow} = 0MeV$ (dashed).

## References


[Bar88] J. Barrette, N.Alamanos, F. Auge, B. Fernandez, A. Gillibert, D. J. Horen, J. R. Beene, F. E. Bertrand, R. L. Auble, B. L. Burks, J. Gomez del Campo, M. L. Halbert, R. O. Sayer, W. Mittig, Y. Schutz, B. Haas, and J. P. Vivien, Phys. Lett. B 209 (1988) 182.

[Bee90a] J. R. Beene, F. E. Bertrand, D. J. Horen, R. L. Auble, B. L. Burks, J. Gomez del Campo, M. L. Halbert, R. O. Sayer, W. Mittig, Y. Schutz, J. Barrette, N. Alamanos, F. Auger, B. Fernandez, A. Gillibert, B. Haas, and J. P. Vivien, Phys. Rev. C 41 (1990) 920.

[Bee90b] J. R. Beene, F. E. Bertrand, D. J. Horen, J. Lisantti, M. L. Halbert, D. C. Hensley, W. Mittig, Y. Schutz, J. Barrette, N. Alamanos, F. Auger, B. Fernandez, A. Gillibert, B. Haas, J. P. Vivien, and A. M. Nathan, Phys. Rev. C 41 (1990) R1332.

[Hor91] D. J. Horen, F. E. Bertrand, J. R. Beene, G. R. Satchler, W. Mittig, A.C.C. Villari, Y. Schutz, Zhen Wenlong, E. Plagnol, and A. Gillibert, Phys. Rev. C 44 (1991) 2385.

[Mor88] S. Mordechai, N. Auerbach, M. Burlein, H. T. Fortune, S. J. Greene, C. Fred Moore, C. L. Morris, J. M. O'Donnell, M. W. Rawool, J. D. Silk, D. L. Watson, S. H. Yoo, and J. D. Zumbro, Phys. Rev. Lett. 61 (1988) 531.

[Nov91] R. Novotny, IEEE Transactions on Nuclear Science, 38 (1991) 379.

[Rit93] J. Ritman, F.-D. Berg, W. Kühn, V. Metag, R. Novotny, M. Notheisen, P. Paul, M. Pfeiffer, O. Schwalb, H. Löhner, L. Venema, A. Gobbi, N. Herrman, K. D. Hildenbrand, J. Mösner, R. S. Simon, K. Teh, J. P. Wessels, and T. Wienold, Phys. Rev. Lett. 70 (1993) 533.

[Sch93] R. Schmidt, Th. Blaich, Th. W. Elze, H. Emling, H. Freiesleben, K. Grimm, W. Henning, R. Holzmann, J. G. Keller, H. Klingler, R. Kulessa, J. V. Kratz, D. Lambrecht, J. S. Lange, Y. Leifels, E. Lubkiewicz, E. F. Moore, E. Wajda, W. Prokopowicz, Ch. Schütter, H. Spies, K. Stellzer, J. Stroth, W. Walus, H. J. Wollersheim, M. Zinser, and E. Zude, Phys. Rev. Lett. 70 (1993) 1767.

# NEUTRON DECAY OF THE GIANT RESONANCE REGION AND THE HIGH-ENERGY CONTINUUM IN $^{208}$Pb, $^{124}$Sn, and $^{90}$Zr.

A.M. van den Berg[a], J. Blomgren[b], D. Chmielewska[a], J.A. Bordewijk[a], S. Brandenburg[a], A. van der Woude[a], Y. Blumenfeld[c], N. Frascaria[c], J.C. Roynette[c], J.A. Scarpaci[c], T. Suomijärvi[c], L. Nilsson[d], N. Olsson[e], N. Alamanos[f], F. Auger[f], A. Gillibert[f], P. Roussel-Chomaz[f], and R. Turcotte[g].

(a) *Kernfysisch Versneller Instituut, 9747 AA Groningen, The Netherlands*
(b) *Department of Radiation Sciences, S-751 21 Uppsala, Sweden*
(c) *Institut de Physique Nucléaire, $IN_2P_3$-CNRS, 91406 Orsay, France*
(d) *The Svedberg Laboratory, S-751 21 Uppsala, Sweden*
(e) *Department of Neutron Research, S-751 21 Uppsala, Sweden*
(f) *SEPhN, DAPNIA, CEA Saclay, 91191 Gif sur Yvette, France*
(g) *Foster Radiation Laboratory, McGill University, Montreal, Canada, H3A 2B2*

Two main mechanisms are responsible for the decay of Giant Resonances (GR): direct decay which de-excites directly the particle-hole state by emission of a particle into the continuum and statistical decay where the GR couples to more complicated n-particle n-hole states before decaying statistically like a compound nucleus. Direct decay is of particular interest since it can yield information on the wave function of the GR. Experimentally, the direct component can be obtained by subtracting the statistical component, calculated using the Hauser-Feschbach formalism, from the total measured decay. Up to now, the most reliable systematics concerning GR decay have been obtained for the Isoscalar Giant Monopole Resonance (ISGMR)[1] for which the non-statistical decay branch ranges from 5% to 30% in the nuclei investigated so far. Results concerning the Isovector Giant Dipole Resonance (IVGDR), the Isoscalar Giant Quadrupole Resonance (ISGQR), as well as the region above the GRs, are much more fragmentary.

The aim of the present experiment[2,3] was to take advantage of the large differential cross sections and favourable peak-to-continuum ratios for GR excitation provided by intermediate energy heavy-ion beams[4], to study the neutron-decay modes of the region between the neutron threshold and 60 MeV excitation energy in $^{208}$Pb, $^{124}$Sn, and $^{90}$Zr nuclei. Targets of $^{208}$Pb, $^{124}$Sn, and $^{90}$Zr, with a thickness of 5 mg/cm$^2$, were bombarded with the 84 MeV/u $^{17}$O beam from GANIL. The $^{17}$O ejectiles were detected with the SPEG spectrometer, centered at $\Theta_{lab} = 3°$, associated with its standard detection system. The decay neutrons were measured with four large detectors (30 cm diameter and 5 cm thick) positioned at backward angles with respect to the recoiling target, and seven smaller detectors in order to determine the angular distributions. The neutrons were discriminated from $\gamma$-rays through a pulse-shape analysis and their energies were deduced from a time-of-flight measurement with respect to the cyclotron RF.

During the experiment, downscaled $^{17}$O singles spectra were recorded along with the coincidence data. The singles spectra are very similar to those measured for the same reactions in ref.[4], albeit with a poorer energy resolution due to the thick targets. Singles spectra on all targets exhibit a large GR bump, followed by a rather smooth continuum at higher excitation energies. The analysis of ref.[4] concluded that, in the case of $^{208}$Pb, the GR bump is dominated by the IVGDR, while for the two lighter targets, the IVGDR, ISGMR, and ISGQR exhibit comparable contributions.

In order to study the statistical and non-statistical decay, missing-energy spectra ($E_m = E^* - E_n - E_r$, where $E^*$ is the excitation energy, $E_n$ the neutron energy, and $E_r$ is the energy of

the recoil) were constructed for all target nuclei for $E^*$ bins ranging from the neutron threshold up to 60 MeV. Note that, in the region below the threshold for two-neutron emission, $E_m$ is directly related to the final-state energy in the residual nucleus. Some examples of $E_m$ spectra for $^{208}$Pb and $^{90}$Zr are shown in fig.1. These spectra show a large bump, corresponding to low-energy neutrons, which is ascribed to statistical decay. Decay to hole states of the residual nuclei, $^{207}$Pb and $^{89}$Zr, is also apparent up to rather high excitation energies.

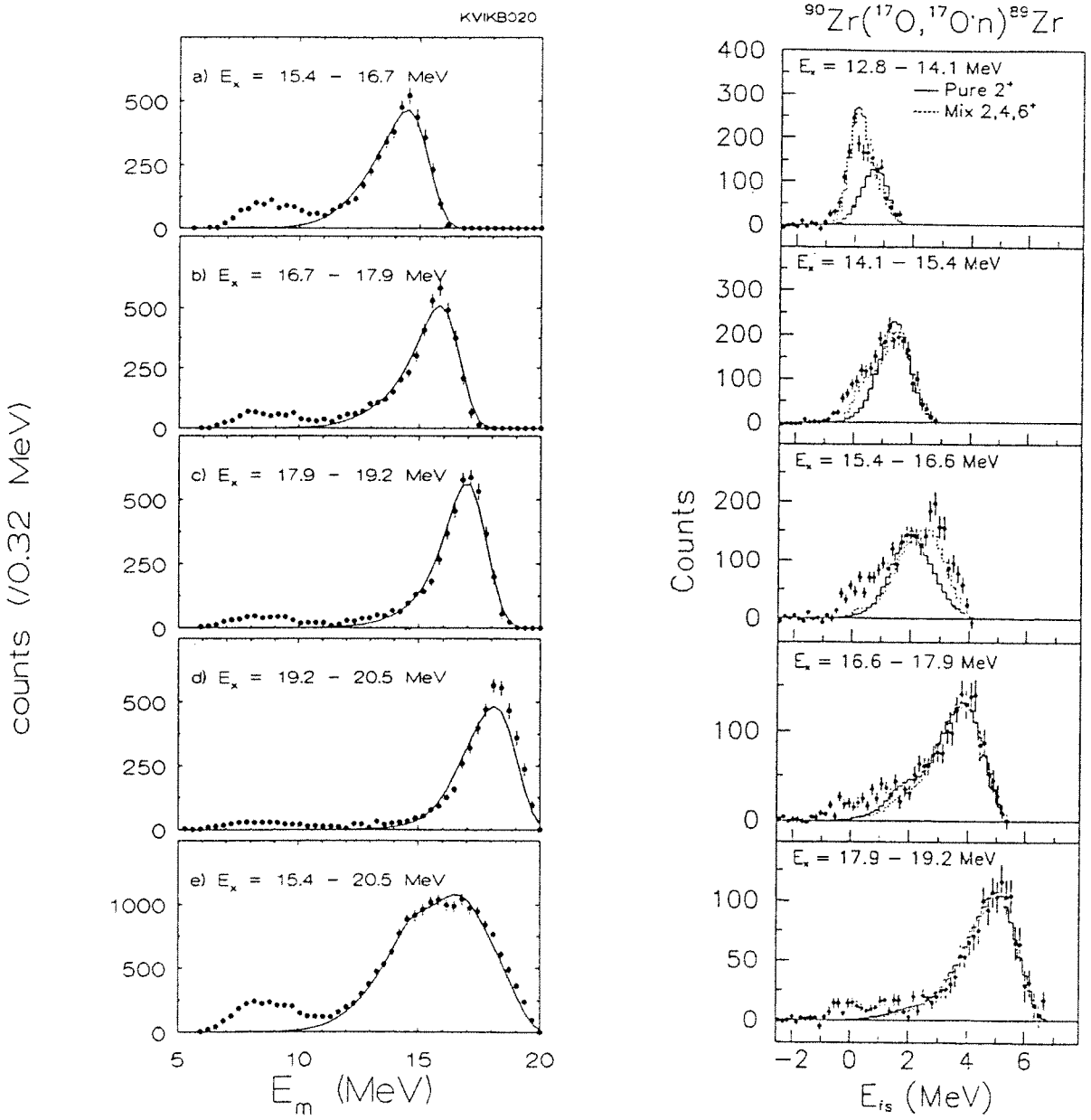


Fig. 1: Missing-energy spectra for typical excitation energy bins in $^{208}$Pb (left panel) and $^{90}$Zr (right panel). The scale for $^{90}$Zr is in final state energy. Solid lines are CASCADE calculations. Dashed lines for $^{90}$Zr are CASCADE calculations assuming a mixture of spins.

To distinguish between statistical and non-statistical decay, calculations were performed

with the code CASCADE. At low excitation energies, individual levels were included for the nuclei of interest. At higher excitation energies, the level densities were obtained from the back-shifted Fermi gas model, and above 30 MeV, the liquid-drop model was used with a level-density parameter $a = A/8$. The results of the calculations (solid lines on fig.1), using a spin $J^\pi = 1^-$ for the decaying states in $^{208}$Pb and $J^\pi = 2^+$ in $^{90}$Zr, were folded with the neutron detection efficiency, and normalized so as to never overshoot the data.

The main trends are similar for all three target nuclei. In the region just above the neutron threshold the distinction between statistical and non-statistical decay cannot easily be made because both modes will populate the same levels and, moreover, the choice of the spin of the decaying states influences the relative population of final states significantly. Above approximately 13 MeV in $^{208}$Pb and 16 MeV in $^{90}$Zr the choice of the spin has only a minor influence. Apart from some small effects to be discussed later, the bump corresponding to low-energy neutrons is well reproduced by the CASCADE calculations. This agreement gives confidence in the statistical model calculations using standard parameters.

The most conspicuous feature of fig.1 is the presence of a direct decay branch towards the hole states of the (A-1) nuclei, decreasing with increasing excitation energy, but distinctly persisting up to 30 MeV in Pb and 40 MeV in Zr. Various processes are known to contribute to the population of hole states. In addition to the direct decay of excited states there is the process of knock-out which is expected to peak in the direction of the recoiling nucleus. For the $^{208}$Pb target, fig.2 shows the angular distribution for the population of hole states as a function of excitation energy. No evidence for an excess population in the recoil direction is observed, leading to the conclusion that the contribution from the knock-out process is small in the present experiment. This is quite different from what is found in inelastic $\alpha$-scattering. It shows a pronounced angular pattern which is strongly asymmetric around the anti-recoil direction. This is contrary to what is expected for the decay of excited states which should be symmetric around an angle close to the recoil angle. Note that the same phenomena are observed for the $^{124}$Sn target, although less pronounced than for $^{208}$Pb, whereas they seem absent for $^{90}$Zr.

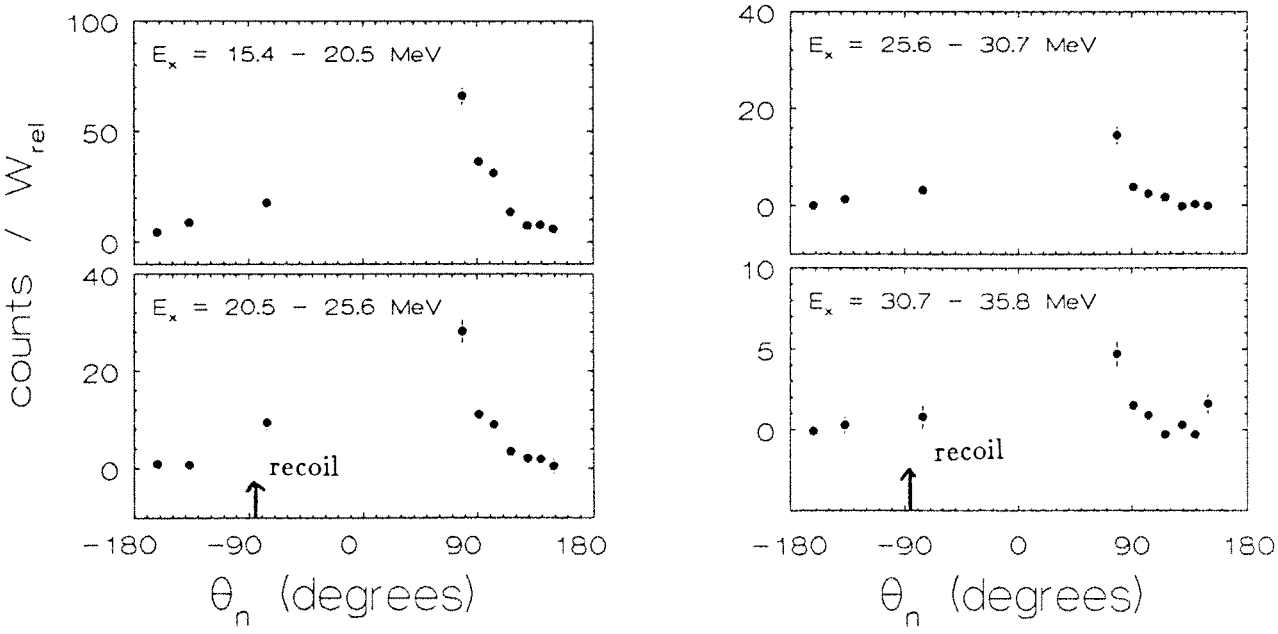


Fig. 2: Angular distributions for hole-state population for different excitation-energy bins in $^{208}$Pb.

A possible explanation of the above observations would be the coexistence of two different processes feeding the hole states: the direct decay of excited structures having an angular distribution approximately symmetric around the anti-recoil direction, and another, hitherto unknown process. It should be pointed out that this novel process would be related more strongly with the conditions in the entrance channel rather than with a decay process. In fact, it seems to be present only under conditions where the cross section is dominated by Coulomb scattering: small scattering angles and high-$Z$ targets.

In addition to non-statistical decay to hole states, there is a small but distinct non-statistical decay branch to other states as well. In $^{207}$Pb, there is an excess population of states located at $11 < E_m < 14$ MeV from the excitation energy region between 20 and 25 MeV in $^{208}$Pb, which cannot be reproduced by the statistical calculations. This excess can be interpreted as pre-equilibrium decay towards the 1p-2h states in $^{207}$Pb, described as the coupling of the collective $J^\pi = 3^-$ state of $^{208}$Pb to the hole states of $^{207}$Pb. In the same way the spectrum for the 15 - 16.5 MeV region in $^{90}$Zr exhibits a non-statistical peak at final-state energies around 3 MeV. This would be pre-equilibrium decay towards phonon-hole coupled states, in which the ground state of $^{89}$Zr is coupled to the $3^-$ state in $^{90}$Zr[5].

The decay spectra from the excitation-energy region between 20 and 30 MeV in $^{208}$Pb also shows non-statistical decay towards $E_m \approx 20$ MeV, which corresponds approximately to the region of the ISGQR in $^{207}$Pb. Two tentative explanations can be advanced for this observation: the excitation of the two-phonon ISGQR state, expected at twice the excitation energy of the ISGQR, which would decay towards the one-phonon state in the $(A-1)$ nucleus[6], or the presence of the Isovector Giant Quadrupole Resonance (IVGQR), which would strongly couple to the ISGQR of the $(A-1)$ nucleus due to isospin mixing. In $^{90}$Zr, when gating on low-energy neutrons, a resonance-like structure is observed in the inelastic spectrum around 27 MeV. This again corresponds to the region where the double ISGQR and the IVGQR are expected. Note that no such structure is observed in $^{124}$Sn.

In conclusion, the present data have shown that a detailed study of the small but measurable direct decay component of the neutron decay of structures located in the excitation-energy region of 15 - 30 MeV which are excited in small-angle scattering of fast heavy ions, is quite possible and gives a number of interesting and partly unexplained results. A more extensive data set with higher statistics and a larger angular coverage is necessary to answer the questions raised by the present data set. Such experiments will benefit from the availability of large multi-detector systems for neutrons, such as EDEN[7], which recently became operational.

## 1. References


[1] A. van der Woude in "Electric and Magnetic Giant resonances", ed. J. Speth, World Scientific, Singapore 1991, p.100.

[2] A.M. van den Berg et al., submitted to Nucl. Phys. A.

[3] J. Blomgren et al., submitted to Nucl. Phys. A.

[4] R. Liguori-Neto et al., Nucl. Phys. **A560** (1993) 733.

[5] W.T.A. Borghols et al., Nucl. Phys. **A504** (1989) 231.

[6] J.A. Scarpaci et al., Phys. Rev. Lett. **71** (1993) 3766.

[7] H. Laurent et al., Nucl. Inst. Meth. Phys. Res. **A326** (1993) 517.

# PRE-EQUILIBRIUM GIANT DIPOLE EMISSIONS

*Ph. Chomaz* [1], *M.Di Toro*[2], *A.Smerzi*[2] *and Zhong Jiquan*[2,3] *

[1]) *GANIL, BP 5027, 14021 Caen, France*

[2])*Laboratorio Nazionale del Sud, INFN*
*44, Via S.Sofia, 95125 Catania, Italy*
*and*
*Dipartimento di Fisica dell' Universitá di Catania,*

[3])*Institute of Modern Physics, Lanzhou, China*

ABSTRACT

We discuss the possibility of a direct observation of pre-equilibrium giant dipole photons in relatively fast fusion reactions induced by charge asymmetric entrance channels. Independent information on the damping of Giant Dipole Resonances ($GDR$) in excited nuclei can be extracted. These experiments appear particularly appropriate for the new available radioactive beams.

At lower energies giant dipole $\gamma$-decays from long-living intermediate nuclear systems can be used to get a direct insight into the dynamics of fusion and deep inelastic collisions.

Pre-equilibrium emission is a well known mechanism in nuclear collisions. Pre-equilibrium light particles and incoherent photons have been well detected. We stress here the possibility of observing pre-equilibrium emissions of collective dipole photons in *fast* fusion processes. Charge asymmetry in the entrance channel is playing an essential role and consequently these experiments seem to be very appropriate for the new available radioactive beams.

$GDR$'s in very hot nuclei have been extensively studied at GANIL [1,2]. Since in order to get such highly excited compound nuclei we need fusion reactions at relatively high energy (between 15 and $30 MeV/u$ beam energy), we have looked at the possibility of a pre-equilibrium collective dipole $\gamma$- emission due to the fact that the charge can be not fully equilibrated when a fused nucleus is formed [3].

A thorough analysis has been performed in ref.s [4,5] where a $GDR$ phonon gas coupled to a compound nucleus without any phonon has been considered. The $\gamma$-emission probability, integrated over the Giant Dipole region, will be much dependent on the $GDR$ strength present in the fused system before a complete equilibration:

$$P_\gamma = P_\gamma^{eq} \frac{\mu}{\mu + \gamma_{ev}} [1 + n_0 \frac{\gamma_{ev}}{\lambda}] = P_\gamma^{eq} + (n_0 - \lambda/\mu) \frac{\gamma_\gamma}{\mu + \gamma_{ev}} \qquad (1)$$

where $\mu$ and $\lambda$ are the phonon decay and excitation rates ( the $GDR$ spreading width being $\Gamma^{\downarrow} = \hbar\mu$), $\gamma_{ev}$ is the particle evaporation rate and $n_0$ is the mean number of $GDR$ phonons present at the time of compound nucleus formation;

---

* *Partial reference to the MEDEA exp.s E142 series*

$$P_\gamma^{eq} = \frac{\gamma_\gamma}{\gamma_{ev}} \frac{\lambda}{\mu} \tag{2}$$

is the statistical equilibrium prediction, $\gamma_\gamma$ being the partial width for photon emission.

In general eq.(1) says that if $n_0 > \lambda/\mu$ (equilibrium value of the number of $GDR$ phonons) we should expect to actually see an enhancement of Giant Dipole photon emissions. This seems indeed to be a quite likely case since, from level density considerations,

$$\frac{\lambda}{\mu} = \frac{\rho(E_x - E_{GDR})}{\rho(E_x)} << 1. \tag{3}$$

and particularly for $N/Z$ asymmetric entrance channels.

In order to check this point we have performed a fully microscopic dynamical calculation [6,7] for a central collision, leading to a fused system in the Sn region, at 26 MeV/n beam energy in different entrance channels $^{36}Ar$ $(N/Z = 1.0) + {}^{96}Zr$ $(N/Z = 1.4)$, charge asymmetric, and $^{40}Ar$ $(N/Z = 1.22) + {}^{90}Zr$ $(N/Z = 1.25)$, charge symmetric.

In fig.1 we report the time evolution of the isovector dipole moment in momentum space for the composite system

$$D(t) = \frac{N\ Z}{A} \left[ \frac{< P_z >_{proton}}{N} - \frac{< P_z >_{neutron}}{Z} \right] \tag{4}$$

in the N/Z asymmetric fig(1a) and N/Z symmetric (fig.1b) case. The difference seems quite evident. In the same figure we have the corresponding isoscalar quadrupole moment, which gives a measure of the overall equilibration of the fused nucleus. We see that at $t \simeq 140 fm/c$ the fused system is equilibrated for both entrance channels. At the same time in the N/Z asymmetric entrance channel we still see quite clear dipole oscillations.

This effect is particularly evident from the Fourier transforms, shown in Fig.2, defined as

$$S(\omega) = |F(\omega)|^2$$

with

$$F(\omega) = \int_0^{t_{max}} dt\ e^{i\omega t} D(t) \tag{5}$$

We have chosen $t_{max} = 300 fm/c$ in order to avoid the contribution from the compound nucleus. For the asymmetric case (fig.2a) we clearly see a nice peak around 16 MeV, which roughly corresponds to the $GDR$ energy for the compound system. It is interesting to notice a peak in the same position, but with a much reduced strength (the scale is different) also for the symmetric entrance channel (fig.2b): this could be interpreted as due to $N/Z$ fluctuations present in incomplete fusion events.

We can conclude that studying different reactions with or without asymmetry in the N/Z ratio one should be able to observe the presence of a pre-equilibrium collective dipole $\gamma$-emission [8]. More experimental work is certainly needed in this

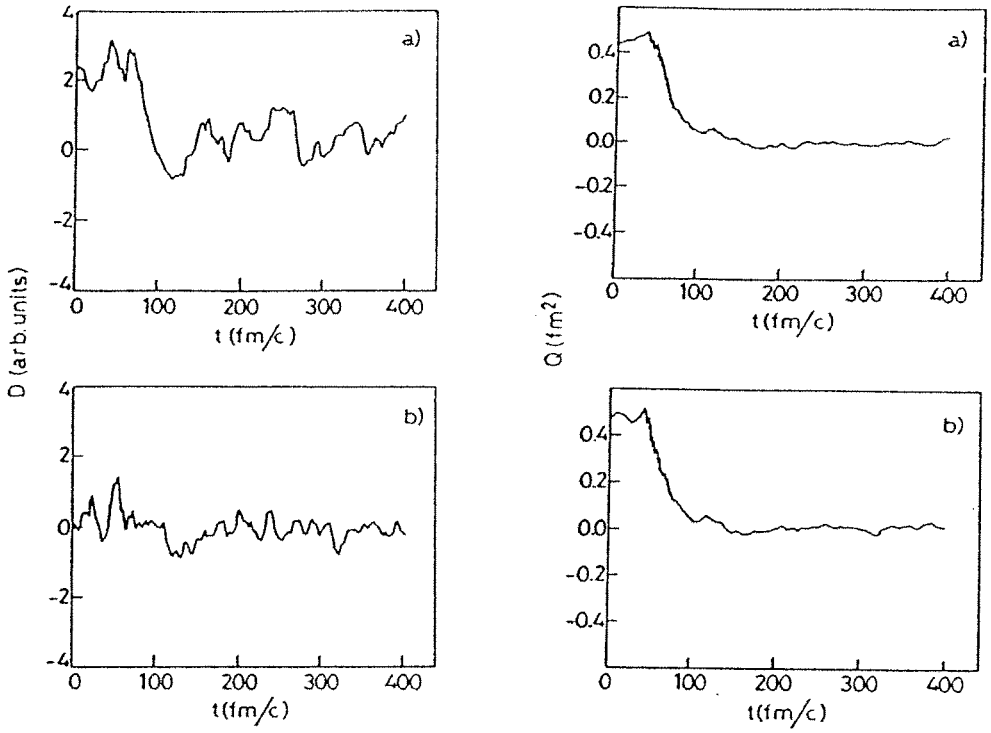


**Fig. 1.** Time evolution of isovector dipole (left) and isoscalar quadrupole (right) moments for central collisions of charge asymmetric (a) and symmetric (b) $Ar + Zr$ entrance channels.

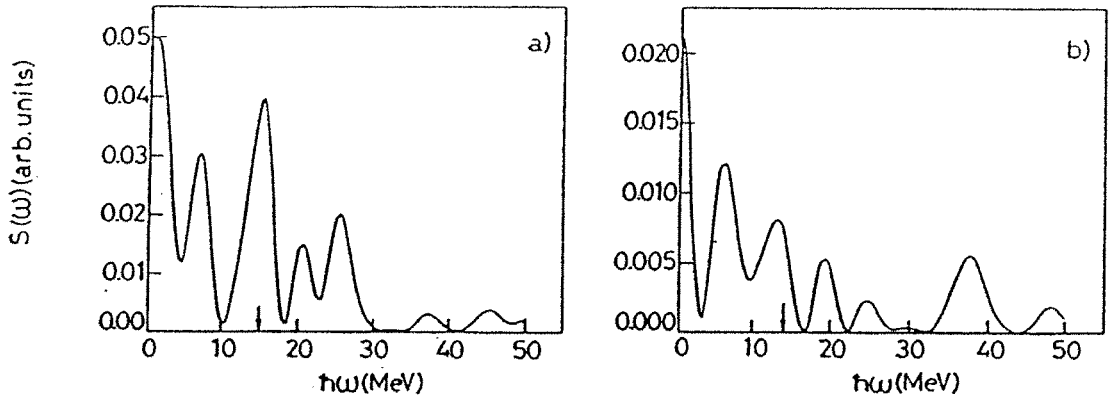


**Fig. 2.** Fourier transforms of the dipole oscillations of fig.1 for a) the asymmetric case and b) symmetric.

medium energy region, possibly also with radioactive beams in order to enhance the range of $N/Z$ asymmetries.

Moreover in ref.s [4,5] it has been also shown that in this way one could get independent information on the excitation energy dependence of the $GDR$ spreading width. Indeed if the damping due to the coupling to other c.n. states becomes large entrance channel effects will disappear since the mean number of $GDR$ phonons is quickly reaching the equilibrium value.

Inspired by the quite exciting results obtained at intermediate energies we have also looked at the influence of the entrance channel $N/Z$ asymmetry at lower energies: we actually see a clear disappearance of the effect with decreasing beam energy [5]. Now the time involved to form a fused system is longer and there is enough time for the charge to equilibrate. However the fusion dynamics seems to allow the possibility of a direct observation of pre-fusion $GDR$'s in highly deformed intermediate nuclear system. But this is another chapter of the never ending Nuclear Giant Resonance Story.

Indeed in the low energy region only some mass-asymmetry effects have been observed so far, which are related to different time scales for the fusion process [9]. Of course this effect would be enhanced from the presence of some angular momentum, i.e. for more peripheral collisions. We have started a systematic study in order to check if it would be possible to detect pre-equilibrium giant photon decays from these intermediate states in fusion and deep inelastic collisions at low energies.This could represent a direct picture of the fusion and $DIC$ dynamics, particularly interesting for the study of fusion paths leading to hyperdeformed bands.

It would be also interesting to check if for this type of $GDR$ emission the entrance channel charge asymmetry is not so important as in the fast fusion processes previously discussed.

We warmly thank A.Bonasera, D.M.Brink and the MEDEA collaboration for very helpful discussions.

## References

1) T.Suomijarvi et al. "Study of hot Giant Dipole Resonance with the MEDEA detector" Preprint Orsay IPNO DRE 92-35, Proc. INFN-RIKEN meeting "Perspectives in Heavy Ion Physics", Ed.s M.DiToro and E.Migneco, SIF Bologna 1993, pp.189-197
2) T.Suomijarvi private communication and J.H.Le Faou et al. "Towards limiting temperatures in nuclei: the behavior of collective motion" IPN-Orsay preprint Oct.93
3) Ph. Chomaz, invited talk, Colloque Franco-Japonais St.Malo Oct. 1992, Preprint GANIL 92-27
4) Ph. Chomaz, M. Di Toro and A. Smerzi, Nucl.Phys. A563 (1993) 509
5) Ph.Chomaz, Zhong Jiquan, A.Smerzi and M. Di Toro "New pieces into the Hot Giant Dipole Resonance puzzle" Int.Winter Meeting on Nuclear Physics, Bormio 1993, Ed.I.Iori, p.427-450
6) A.Bonasera et al. Phys.Lett. B221 (1989) 233; B244 (1990) 169 and B259 (1991) 399
7) A.Smerzi, Ph.D.Thesis, Catania 1993
8) R.Alba et al., OUVERTURE Proposal with the first test $Ni$ beams of the $LNS$ Superconducting Cyclotron, Catania 1993.
9) M.Thoennessen et al., Phys.Rev.Lett. 70 (1993) 4055

# SIGNATURE OF MULTIPHONON STATES BY PROTON EMISSION IN HEAVY ION INELASTIC SCATTERING

J.A.Scarpaci[a)], Y.Blumenfeld[a)], Ph.Chomaz[b)], N.Frascaria[a)], J.P.Garron[a)], M.Lamehi-Rachti[a)][1], I.Lhenry[a)], J.C.Roynette[a)], T.Suomijärvi[a)], D.Beaumel[a)], P.Massollo[c)][2], N.Alamanos[d)], A.Gillibert[d)], and A.Van der Woude[e)]

*a) Institut de Physique Nucléaire, $IN_2P_3$-CNRS, 91406 Orsay, France*

*b) GANIL, BP 5027, 14021 Caen Cedex, France*

*c) University of La Plata, La Plata, Argentine*

*d) SEPhN, DAPNIA, CEA Saclay, 91191 Gif sur Yvette, France*

*e) Kernfysisch Versneller Institut, 9747 AA Groningen, Netherland*

## 1. Introduction

It is now well established that inelastic scattering of intermediate energy heavy ions is a powerful tool for the study of giant resonances and their decay. In such reactions, giant resonances are excited with very large differential cross sections and larger peak-to-background ratios than with light projectiles. Moreover, between 20 and 60 MeV excitation energy, structures superimposed on a large background were also observed[1,2]. In order to investigate these structures, numerous inclusive experiments were performed at GANIL, covering a wide range of incident energies and projectile-target combinations, as well as different ejectile detection systems such as silicon detectors coupled to a time of flight measurement[3] or the energy loss spectrometer SPEG[4]. These experiments demonstrated that such structures are excited in all the studied targets, in a small angular range around the grazing angle[3]. They are regularly spaced and have narrow widths (a few MeV) and from the large amount of data obtained in these inclusive experiments, it was concluded that these structures are due to target excitations[4]. The most consistent interpretation[5] is given by multiphonon states built with isoscalar giant resonances (GR).

In order to get a better understanding of these structures and to disentangle the different mechanisms contributing to the inelastic spectrum, coincidence experiments for which both the ejectile and light particles are detected are necessary. The measurement of particles emitted by the target allows to study the decay of highly excited states and gain insight into their microscopic structure.

In this contribution, we report on the first signature of a multiphonon state built with the isoscalar giant quadrupole resonance (GQR) excited by the nuclear interaction in $^{40}$Ca.

## 2. Experiment

The experiment was performed at the GANIL facility using the SPEG spectrometer associated with its standard detection system to measure the ejectiles[6]. The energy resolution was about 800 keV. Light charged particles were detected in 30 cesium iodide

[1] On leave from University of Teheran, Iran

[2] Deceased

elements of the multidetector array PACHA[7], positioned in the reaction plane and covering the whole angular domain with the exception of a small wedge of $\pm 7^o$ around the beam direction. The proton energy resolution was about 2% and the detection threshold ranged between 1 and 3.5MeV. In order to sum the spectra from various detectors, a software threshold of 4MeV protons in the center of mass of the recoiling $^{40}$Ca nucleus was set for the analysis.

## 3. Results and discussion

In the inclusive inelastic spectrum, the giant resonance is observed split into 2 components centered at 14 and 17.5MeV excitation energy. By comparison with D.W.B.A. calculations, both components can be mainly attributed, in the studied angular range (from $1.2^o$ to $5^o$ in the laboratory), to the excitation of the isoscalar GQR[7]. At higher excitation energies small bumps are also observed superimposed over a large plateau due to 3-body processes such as pick-up break-up[8].

At backward angles, only protons emitted by the target are present. Thus, coincidence measurements with these protons allow to select only target excitations[8]. The $^{40}$Ca inelastic spectrum in coincidence with backward protons is shown in fig.1a. It must be corrected for the multiplicity of emitted protons[7]. The multiplicity correction function

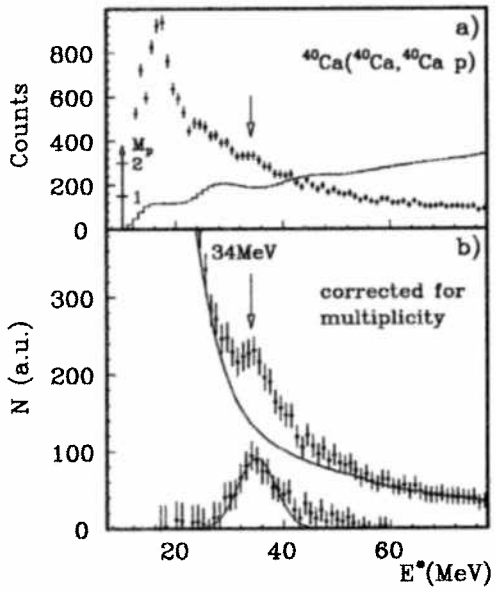


Fig. 1: a) Inelastic spectrum in coincidence with one proton emitted backwards, displayed along with the multiplicity correction. b) Inelastic spectrum corrected for the proton multiplicity. The solid line corresponds to a polynomial fit of the background. The result of the background subtraction is shown below, fit by a gaussian.

calculated with the code LILITA[9] is shown in fig.1a and the corrected spectrum is displayed in fig.1b. In such a correction, the main assumption is that particle emission is purely statistical and the direct contribution is neglected. In this coincidence spectrum a very prominent structure at twice the GQR excitation energy shows up, which is barely visible in the inclusive spectrum. To roughly estimate the characteristics of this structure, several polynomial fits of the background were subtracted. An example is shown as

a solid line in fig.1b, and the result, fit by a gaussian, is displayed on the bottom of the figure. The width of the structure is estimated to be 9±2 MeV and its cross section is 8±2 times smaller than the giant resonance cross section. These characteristics are compatible with the multiphonon model[10] which predicts for the two-phonon state, a width equal to $\sqrt{2}$ times the width of the one-phonon state and a ratio of 15. However, theoretical calculations for this energy region predict the presence of both the two-phonon state and other high lying giant resonances. Therefore, additionnal information is needed to demonstrate the existence of the two-phonon state.

To sign unambiguously the origin of this structure, a detailed study of its decay and a comparison with the direct decay pattern of the GQR is called for. Particle decay of GRs can occur through various processes. The coupling of the particle-hole (1p-1h) states to more complicated configurations: 2p-2h, 3p-3h, ... until a completely equilibrated system is reached, leads to the population of states which decay as compound nuclear states. This process, measured by the spreading width $\Gamma^{\downarrow}$, can be analysed by statistical calculations. The coupling of the 1p-1h states to the continuum gives rise to direct decay into hole states of the A-1 residual nucleus with an escape width $\Gamma^{\uparrow}$. The study of such direct decay only provides information on the microscopic structure of the GR and can give a signature of a multiphonon state.

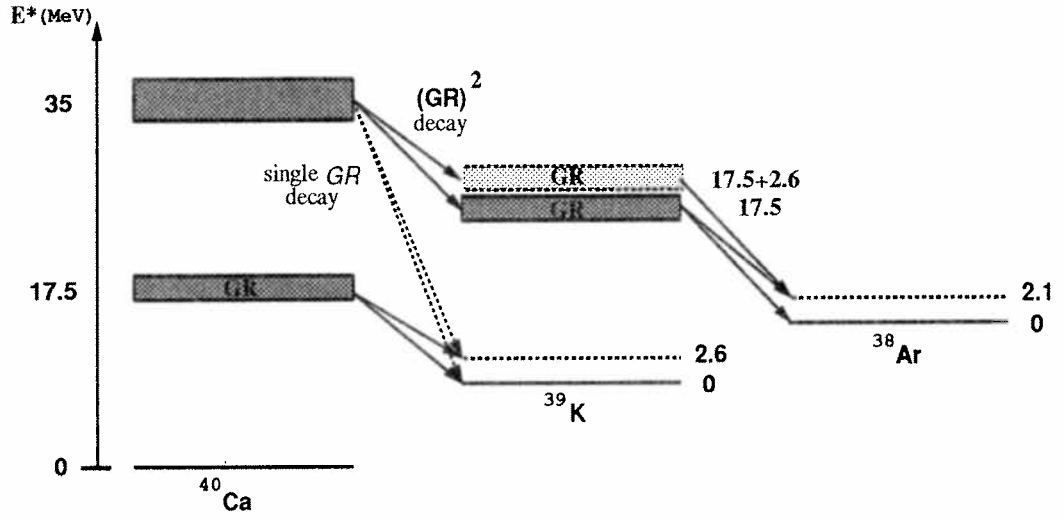


Fig. 2: Direct decay pattern of a GR and a high lying state at twice the excitation energy of the GR.

Assuming a weak coupling between phonons, each of them would undergo a direct decay exhibiting the same features as the direct decay of the GR. Figure 2 sketches the direct decay of a GR and a high lying state in $^{40}$Ca. The GR decays towards hole states in $^{39}$K. Similarly, a one-phonon high lying state will decay into the same hole states through the emission of one high energy proton (dashed arrows), while a two-phonon direct decay will proceed through the emission of two protons. The first proton will populate the GR or (GR $\otimes$ first hole state) in $^{39}$K, and the second will deexcite this GR, leading to two-hole states in $^{38}$Ar.

Experimentally, the direct decay part of the GQR is extracted by constructing missing energy spectrum $E_{miss} = E^{\star}_{^{40}Ca} - E_p^{CM}$, where $E^{\star}_{^{40}Ca}$ is the initial excitation energy in $^{40}$Ca and $E_p^{CM}$ the proton energy in the center of mass of the recoiling $^{40}$Ca target,

and comparing with the equivalent spectrum calculated with the statistical decay code CASCADE[11]. Figure 3 compares the statistical calculation (histograms) to the data, for two excitation energy regions in $^{40}$Ca: the GQR region ( fig 3a) and the two-phonon state region (fig 3b). The calculation has been normalized so as to never overshoot the data, in order to obtain the maximum contribution consistent with statistical decay. An excess of cross section for decay to the GS and the first excited hole state of $^{39}$K is observed, which can be ascribed to direct decay.

For excitation energies in $^{40}$Ca around 34MeV, corresponding to the structure, the missing energy spectrum (Fig.3b) shows two very striking features. First of all, population of the GS and the 2.6MeV state in $^{39}$K should correspond to the direct decay of a GR present in this energy region, and a symmetric angular correlation around the recoil direction is expected. However, the fast protons populating the hole states of $^{39}$K, are only present in the forward hemisphere. Such an assymetry suggests that a more exotic phenomenon occurs in this reaction.

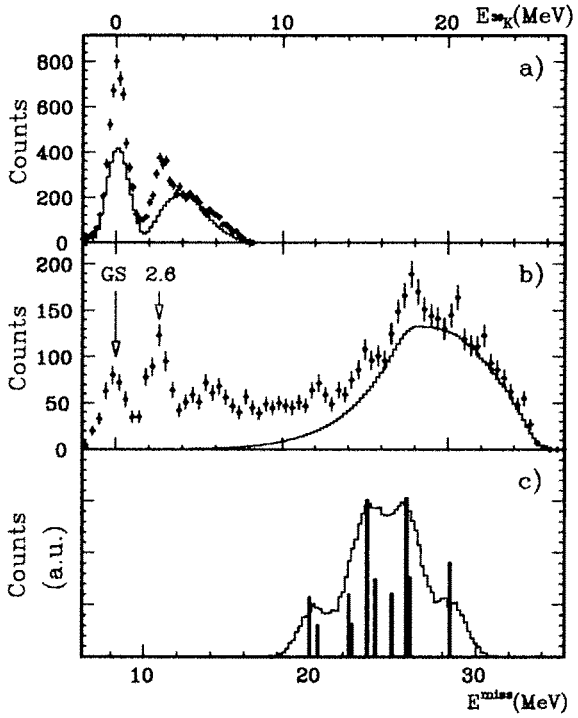


Fig. 3: Missing energy spectra, for the GQR region (a) and the 34MeV bump (b). Statistical calculation are shown (histograms). (c): Calculation for the direct decay of a two phonon state built with the GQR.

More surprisingly, four peaks located around 25MeV missing energy show up, superimposed on a broad contribution (histogram) which can be attributed to statistical emission. At these high excitation energies in $^{40}$Ca, two protons can be emitted, while only one is detected. If the first proton is detected, peaks in the missing energy spectrum mean that a small number of states must be preferentially populated in $^{39}$K around 17MeV excitation energy. In the same way, if we detect the second emitted proton which populates the $^{38}$Ar, peaks will show up only if the initial excited nucleus, $^{40}$Ca, has decayed through particular states in $^{39}$K, to well defined low lying states in $^{38}$Ar. This is precisely the picture expected for the direct decay of a two-phonon state.

Figure 3c presents a simulation[12] of a two phonon direct decay. The different decay combinations should give rise to ten peaks which are shown by bars. However, due to the experimental resolution (800 KeV) and the phonon width, the final result (histogram) exhibits only 4 peaks which are in remarkable agreement with those observed in the experimental missing energy spectrum (Fig.3b). This is a clear signature of the existence of the double phonon built with the GQR in $^{40}$Ca.

At excitation energy in $^{40}$Ca of about 50MeV, one still observes bumps in the missing energy spectrum. They are located about the energy of a double phonon which could be the signature of a direct decay of a 3-phonon state in $^{40}$Ca. However to low statistics does not allow us to perform any complete analysis. Transitions to the GS and first excited states of $^{39}$K are still observed, and again correspond to fast moving protons in the forward direction.

## 4. Conclusion

Inelastic scattering of $^{40}$Ca on $^{40}$Ca at 50MeV/n was studied in coincidence with protons measured over a large angular domain.

At about $\pm 60^{o}$, a component of fast moving protons is observed which feeds the GS and the first excited states of $^{39}$K. However their angular distribution does not seem consistent nor with the direct decay of high energy giant resonances, nor with pick-up break-up reactions. Their production mechanism remains for the moment an open question.

Backward emitted protons allow to investigate target excitation with no pollution from other mechanisms. The GQR in $^{40}$Ca was found to have a sizeable direct decay branch. Furthermore, through the observation of its specific direct decay pattern, the presence of the double GQR has been demonstrated in the excitation energy region between 30 and 40 MeV. This confirms the prediction of the calculations coupling the quasi-boson approximation for nuclear excitations to classical trajectories[5]. Heavy ion inelastic scattering combined with coincident decay measurements is thus a unique tool to investigate multiphonon states built with isoscalar giant resonances in nuclei.

## 5. References


[1] N.Frascaria et al., Phys. Rev. Lett. **39**, 918 (1977)
[2] Ph. Chomaz et al., Z. Phys. **A318**, 1 (1984)
[3] N.Frascaria et al., Nucl. Phys. **A474**, 253 (1987)
[4] N.Frascaria, Nucl. Phys. **A482**, 245c (1988)
[5] Y.Blumenfeld and Ph.Chomaz, Phys. Rev. **C38**, 2157 (1988)
[6] L.Bianchi et al., Nucl. Inst. and Meth. **A276**, 568 (1989)
[7] J.A.Scarpaci, PhD Thesis, Université d'Orsay, report IPNO-T-90-04, 1990 (France)
[8] J.A.Scarpaci et al., Phys. Lett. **B258**, 279 (1991)
[9] J.Gomez del Campo and R.G.Stokstad, Internal report ORNL TM7295
[10] Ph.Chomaz and N.V.Giai, Phys. Lett. **B282**, 13 (1992)
[11] F.Pühlhofer, Nucl. Phys. **A280**, 267 (1977)
[12] J.A.Scarpaci et al., Phys. Rev. Lett. **71**, (1993) 1766

# ($^{12}$C,$^{12}$B) AND ($^{12}$C,$^{12}$N) REACTIONS AT E/A = 70 MeV AS SPIN PROBES: CALIBRATION AND APPLICATION TO $1^+$ STATES IN $^{56}$Mn

N. Anantaraman,[1] J.S. Winfield,[1] Sam M. Austin,[1] J.A. Carr,[2] C. Djalali,[1] A. Gillibert,[3] W. Mittig,[3] J.A. Nolen, Jr.,[1] and Zhan Wen Long[3]

[1] *National Superconducting Cyclotron Laboratory, Michigan State University, East Lansing, Michigan 48824-1321, USA*
[2] *Supercomputer Computations Research Institute, Florida State University, Tallahassee, Florida 32306-4052, USA*
[3] *GANIL, B.P. 5027, 14021 Caen Cedex, France*

## 1. INTRODUCTION

In principle, heavy-ion charge-exchange reactions like ($^{12}$C,$^{12}$N) and ($^{12}$C,$^{12}$B) offer significant advantages for studies of spin excitations in nuclei in that the quantum numbers of the states involved can be chosen to limit the transitions strictly to $\Delta S = \Delta T = 1$, thus giving cleaner spectra than (p,n) and (n,p). In addition, both the initial and final states involve charged particles, so that better resolution is often possible. There are, however, complexities that are not present for high-energy (p,n) and (n,p) reactions. First among these issues is that the reactions must be dominated by the one-step process if the selection rules noted above are to hold and if there is to be a close correlation between the observed cross section and isovector spin strength. In the case of the ($^{12}$C,$^{12}$N) reaction, it was shown[1] that the one-step mechanism should be dominant above about 50 MeV/nucleon for $0^+ \rightarrow 1^+$ transitions. Experimental data[1,2] and detailed calculations[3] both support this conclusion. A second issue is that of the strong absorption in heavy-ion reactions; only the surface region of the projectile and target transition densities is sampled in the reaction. We address the question of the suitability of heavy-ion charge-exchange reactions for the measurement of Gamow-Teller (GT) strengths by attempting to establish an empirical calibration curve for $\hat{\sigma}$, the cross section per unit GT strength B(GT), as a function of target mass, by studying a variety of ($^{12}$C,$^{12}$B) transitions whose B(GT) values are known. This calibration curve and a measurement of the cross section for the $^{56}$Fe($^{12}$C,$^{12}$N) reaction are used to obtain the GT strength of known $1^+$ states in $^{56}$Mn. These results have been published.[4]

## 2. EXPERIMENT

Cross sections were measured for the ($^{12}$C,$^{12}$B) and ($^{12}$C,$^{12}$N) reactions on a variety of nuclei at a laboratory bombarding energy of 70 MeV/nucleon. The ($^{12}$C,$^{12}$B) results on $^{12}$C, $^{26}$Mg, $^{54}$Fe, $^{58}$Ni, and $^{90}$Zr were used to establish a calibration curve. The outgoing particles were analyzed by the magnetic spectrometer SPEG. Emphasis was placed on obtaining measurements at small angles, including 0°.

In the forward angle spectra for the $^{56}Fe(^{12}C,^{12}N)^{56}Mn$ reaction, besides a contaminant peak due to the $H(^{12}C,^{12}N)n$ reaction, two sharp and cleanly-resolved peaks were observed. From the focal plane calibration, we estimated the excitation energies in Mn for these peaks to be 0.025±0.15 MeV and 1.20±0.26 MeV. By comparison with the $(t,^{3}He)$ spectrum of Ajzenberg-Selove et al.,[5] and assuming that the spins of the states we observe are $1^+$, we identified these states with the 0.11 MeV and 1.17 MeV levels in $^{56}Mn$. The Hydrogen peak in the $^{56}Fe$ spectra was subtracted by scaling from the spectra obtained with a $(CH_2)_n$ target. This was a significant correction only for laboratory angles of 0.53° and 1.01°.

**3. RESULTS**

A comparison of the measured cross sections with the results of distorted-wave approximation (DWA) calculations shows that $0^+ \rightarrow 1^+$ transitions are predominantly one-step at the bombarding energy of E/A = 70 MeV. The calculated cross sections are generally in good agreement with the measured cross sections, requiring normalizations that are typically less than 40%, which is in the range of the overall calculational and experimental uncertainties. In many cases the angular distributions are well described quantitatively.

The following procedure was used to obtain the unit cross section, the ratio of the experimental cross section extrapolated to q = 0 to the GT strength B(GT). First, DWA calculations were done to provide L = 0 and L = 2 angular distributions. The relative strengths of these distributions were adjusted to yield an optimal fit to the cross section, corresponding to a minimum in $x^2$. This yielded the L = 0 cross section at 0°, i.e. at zero transverse momentum transfer. In order to obtain the cross section corresponding to zero total momentum transfer (q = 0), this cross section was multiplied by the ratio, F(Q), of the L = 0 cross section calculated at Q = 0 to that at the actual Q of the reaction (typically around -20 to -30 MeV). Dividing this cross section by the corresponding B(GT) gives $\hat{\sigma}$, the cross section per unit GT strength. The results are plotted in Fig. 1. The dashed and the dot-dashed curves shown in Fig. 1 were obtained assuming a linear and a quadratic form, respectively, for the A-dependence of $\hat{\sigma}$. These assumptions were made in the absence of any theoretical input as to the A-dependence. The parameters of the fits, determined by least-squares fittings in which the data points were weighted by their relative uncertainties, are:

$\hat{\sigma} = (4.078\pm0.390) - (0.0382\pm0.006)A$ (linear fit);

$\hat{\sigma} = (6.275\pm0.794) - (0.134\pm0.030)A + [(0.814\pm0.256)/1000]A^2$ (quadratic fit).

The calibration curves thus determined are essentially phenomenological in nature and not dependent on detailed reaction calculations; for example, they are relatively insensitive to the choice of optical potentials used to extrapolate to q=0, since that procedure involves only the ratio of two calculated cross sections. They were used to obtain $\beta^+$ GT strengths from the cross sections measured for the $^{56}Fe(^{12}C,^{12}N)^{56}Mn$ reaction.

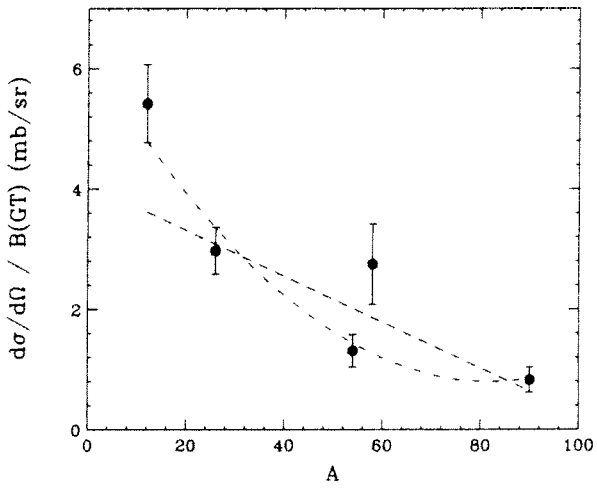


Fig. 1. Calibration curves determined from the ($^{12}$C, $^{12}$B) reaction on several nuclei at E/A = 70 MeV, as described in the text. The dashed and dot-dashed curves represent a linear and a quadratic fit, respectively.

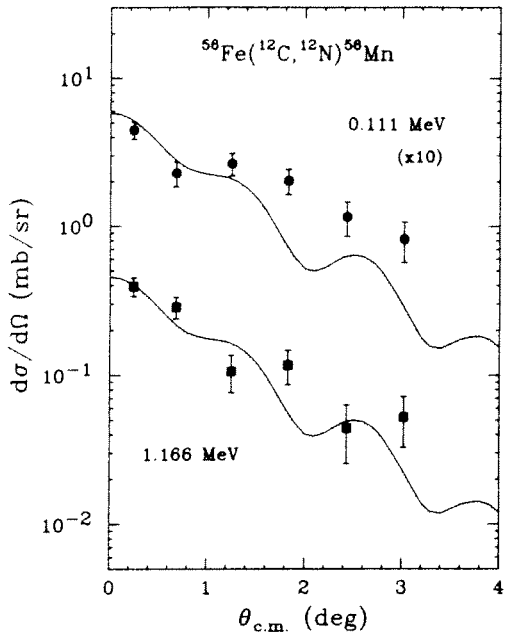


Fig. 2. Angular distributions for the $^{56}$Fe($^{12}$C, $^{12}$N)$^{56}$Mn reaction at E/A = 70 MeV, leading to two states. The curves represent results of DWA calculations normalized to the data.

The angular distributions for the two isolated $1^+$ states in $^{56}$Mn are shown in Fig. 2, along with the results of DWA calculations normalized to the data. The DWA calculations used shell-model wave functions we calculated. Next, a multipole decomposition of the two angular distributions was done in the manner described above. The normalizations N'(L=0) and N'(L=2) thus obtained show that the transition to the 0.11-MeV state has more L = 2 strength than predicted with the shell-model wave functions used, whereas that for the 1.17-MeV state is correctly predicted as regards the relative L = 0 and L = 2 contributions. From the L = 0 cross section data, $\sigma(L=0,\theta=0,Q=0)$ values for the two transitions were obtained in the same way as described above. To convert them to B(GT), the unit cross section $\hat{\sigma}$ at A=56 was read off from the two calibration curves shown in Fig. 1. The values of $\hat{\sigma}$(A=56) determined by the linear and the quadratic calibrations are 1.94 and 1.35 mb/sr, respectively. The average of these was used to convert $\sigma(L=0,\theta=0,Q=0)$ to B(GT). The uncertainty in B(GT) was determined by adding in quadrature the statistical error in the measured cross sections (±17%), the error in the procedure for extrapolating to $\theta$=0 and Q=0 (±10%), and the uncertainty in $\hat{\sigma}$ corresponding to half the difference between the linear and the quadratic fits (±18%). The B(GT) values thus obtained were then corrected for the fact that the reaction used to measure the A=56 cross sections was ($^{12}$C, $^{12}$N) whereas the calibration curves of Fig. 1 are based on data from the ($^{12}$C, $^{12}$B) reaction.

The B(GT) values obtained by the above procedure for the $1^+$ states at $E_x$ = 0.11 and 1.17 MeV in $^{56}$Mn are shown in Table I, where they are compared with the results of three shell-model calculations. One of these is the calculation of Bloom and Fuller[6] and the

other two are our calculations in two model spaces: a zero-order model space (a 2p2h configuration for the initial state and a 3p3h configuration for the final state) and a larger space in which 1p1h excitations in both initial and final states are included. The extracted strengths appear to agree better with our calculated results than with those of Ref. 6. The average quenching factor for the sum of the two transitions obtained by comparing the extracted strengths to Bloom and Fuller's calculation, our calculation in the smaller model space, and our calculation in the larger model is 0.49, 0.70, and 0.75, respectively. Calculations of the supernova process have previously been made using the results of Ref. 6. It remains to be seen how these calculations will be affected by the different B(GT) values obtained in the present experiment.

Table I. Results for B(GT) values for $1^+$ states in $^{56}$Mn from analysis of the $^{56}$Fe($^{12}$C,$^{12}$N)$^{56}$Mn data and from shell-model calculations.

| State | Expt | | Theory A[a] | | Theory B[b] | Theory C[c] |
|---|---|---|---|---|---|---|
| | $E_x$(MeV) | B(GT) | $E_x$(MeV) | B(GT) | B(GT) | B(GT) |
| 1 | 0.11 | 0.65±0.17 | 0.24 | 0.26 | 0.88 | 0.83 |
| 2 | 1.17 | 0.83±0.22 | 1.3 | 2.73 | 1.23 | 1.14 |

[a] Reference 6. The numbers given for $E_x$ and B(GT) do not appear in this form in Ref. 6; they were provided by S.D. Bloom.
[b] Present calculation in the smaller model space described in the text; energy spacing between the two $1^+$ states is 1.26 MeV, compared to 1.06 MeV experimentally.
[c] Present calculation in the larger model space described in the text; energy spacing between the two $1^+$ states is 1.45 MeV, compared to 1.06 MeV experimentally.

The calculated B(GT) values have a significant dependence on both the two-body interaction and the model spaces involved. Further measurements such as those presented here will be required to constrain the shell-model calculations so as to facilitate reliable calculations for transitions which are important in astrophysical phenomena but which cannot be measured in the laboratory.

**4. REFERENCES**


1. J.S. Winfield et al., Phys. Rev. C33 (1986) 1333; C35 (1987) 1166 [E].
2. H.G. Bohlen et al., Nucl. Phys. A488 (1988) 89c.
3. H. Lenske, H.H. Wolter, and H.G. Bohlen, Phys. Rev. Lett. 62 (1989) 1457.
4. N. Anantaraman et al., Phys. Rev. C44 (1991) 398.
5. F. Ajzenberg-Selove et al., Phys. Rev. C30 (1984) 1850; C31 (1985) 777.
6. S.D. Bloom and G.M. Fuller, Nucl. Phys. A440 (1985) 511.

# ASTROPHYSICAL RATE OF THE $^{11}C$ + p REACTION FROM COULOMB BREAK-UP OF A $^{12}N$ RADIOACTIVE BEAM

P. Aguer[1], C. Angulo[1], F. Attalah,[2] G. Bogaert[1], A. Coc[1], D. Disdier[3], Ph. Eudes[4], S. Fortier[5], F. Guilbault[4], C. Grunberg[6], J. Kiener[1], L. Kraus[3], A. Lefebvre[1], I. Linck[3], Th. Reposeur[4], P. Roussel-Chomaz[6], J.A. Scarpaci[5], C. Stephan[5], L. Tassan-Got[5], J.P. Thibaud[1]

1) C.S.N.S.M. IN2P3-CNRS, Bât. 104-108, 91405 Orsay (France)
2) CENBG, IN2P3-CNRS et Univ. Bordeaux I, 33170 Gradignan (France)
3) C.R.N. IN2P3-CNRS, Univ. Louis Pasteur, B.P. 20, 67037 Strasbourg Cedex (France)
4) Laboratoire de Physique Nucléaire, IN2P3 et Univ. Nantes 44072 Nantes Cedex (France)
5) I.P.N. IN2P3-CNRS et Univ. Paris Sud, 91406 Orsay (France)
6) GANIL, IN2P3-CNRS et IRF-CEA, BP 5027, 14021 Caen Cedex (France)

*ABSTRACT*

*The Coulomb break-up technique has been used to determine the radiative widths of excited states in $^{12}N$ . The radioactive beam of $^{12}N$ was produced through transfer and fragmentation of a primary 95.5 MeV/u $^{14}N$ beam at GANIL. A value of 6 meV was extracted for the width of the 1.19 MeV level in $^{12}N$ .*

## 1. Introduction

In stellar evolution models, the description of an explosive type of scenario needs reaction rates involving radioactive materials. Actually, when the stellar temperature rises higher than 0.2 $T_9$ ( $T_9 = 10^9$K ) the proton or alpha capture on nuclei can compete with their $\beta$ decay. This is the case for explosive hydrogen burning, hot CNO burning, hot p-p chain or the rp process. To determine when and where that competition can take place, one has to know proton or alpha capture reaction rates, but experimental problems arise due to the need of handling either radioactive beams or radioactive targets.

Direct experiments seem to be the most appealing way of determining reaction rates. However direct measurements of radiative capture cross sections require the observation of a very low gamma ray yield mixed with the noise coming from the radioactive beam stopped in the target or the slits. An alternative technique has been

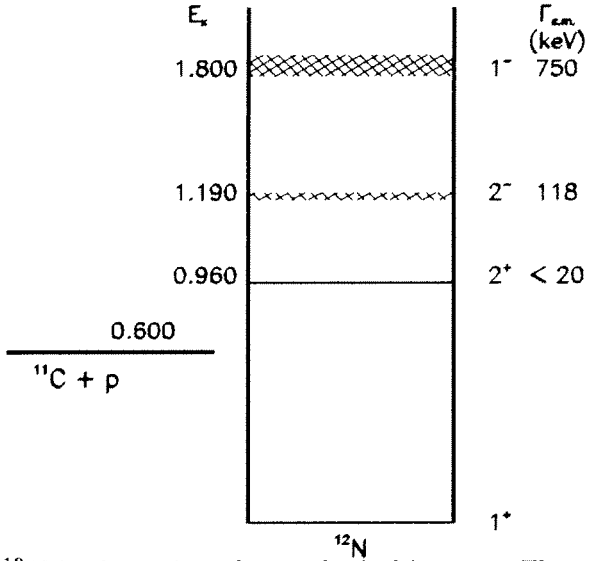


Fig. 1: Level scheme of $^{12}N$ in the region of astrophysical interest. The total widths of the levels are extracted from ref. 2

proposed for the determination of astrophysical reaction rates[1]. Instead of measuring the cross section for the reaction $A + b \rightarrow C + \gamma$, one looks at the inverse one $C+\gamma \rightarrow A+b$. Compared with the direct process, the cross section of the inverse one is enhanced due to the high density of virtual photons. We report here an experimental result on the Coulomb break-up of a $^{12}N$ beam in order to get informations on the $^{11}$C + p $\rightarrow$ $^{12}N$ + $\gamma$ reaction rate

## 2. The $^{11}$C + p $\rightarrow$ $^{12}$N reaction rate

Figure 1 shows the $^{12}N$ levels in the region of interest. Two resonances are expected to dominate the reaction rate. The $J^{\pi}$ =$2^+$ state ($E_x$= 0.960 MeV, $E_{cm}$ = 0.360 MeV), where $E_{cm}$ is the center of mass energy above the proton threshold and the $2^-$ state ($E_x$= 1.19 MeV, $E_{cm}$ = 0.59 MeV) which presents a *s*-wave component, and is allowed to decay to the ground state by an E1 transition. The radiative widths of these levels are unknown. For the 1.19 MeV level, Wiescher *et al* [3] suggest $\Gamma_\gamma$= 2 meV on the basis of a $\gamma$-transition strength estimate. Using a code based upon the generator coordinate method, P. Descouvemont and I. Baraffe [4] find $\Gamma_\gamma$= 140 meV. With such a large value, the 1.19 MeV level in $^{12}N$ is expected to play a major role in the burning of $^{11}$C.

The large difference between both estimates shows the need of an experimental determination of the radiative widths of the first excited levels in $^{12}N$ , and this

requires to produce either a $^{11}$C beam ($T_{1/2}$ = 20 mn) for a direct measurement, or a $^{12}N$ beam ($T_{1/2}$ = 11 ms) for a Coulomb break-up type experiment.

## 3. $^{12}$N radioactive beam production

The Coulomb break-up technique with radioactive material requires the production of a high energy (about 30-100 MeV/u) radioactive beam. The 70.9 MeV/u $^{12}N$ beam was produced through transfer reaction and fragmentation of a stable $^{14}N$ primary beam of 95.5 MeV/u on a primary target of 800 mg/cm$^2$ graphite foil. The radioactive species were analysed with the GANIL alpha spectrometer (deviation angle 270 °).

Since the alpha spectrometer drives to the target area all the species with the correct magnetic rigidity, the selected beam is composed of several species. With a large amount of the residual primary $^{14}N$ nuclei, the other elements in the secondary beam are $^{11}$C (32%), $^{13}$N (15%), $^{12}$C (14%), $^{7}$Be (10%), $^{10}$C (4%), the $^{12}N$ contributes for only 7 %. However, all the selected elements having the same magnetic rigidity but different energies are easily discriminated by energy-loss and time-of-flight methods. Hence the secondary beam can be purified using a foil degrader. The remaining composition after an aluminum purification foil was 18% $^{12}$N, 73% $^{11}$C and 9% $^{10}$B, at the cost of a reduction of the $^{12}N$ intensity by a factor of 3. The beam resolution depends on the spectrometer acceptance and was set to $\Delta E/E$ = 0.3%. For safety reasons, the Ganil beam power load is limited to 400 Watts (2 $\mu$A maximum $^{14}N$ beam intensity) and the $^{12}N$ beam intensity remains at the best lower than $10^4$ particles/s when using a foil purification method.

## 4. Experimental procedure and results

The $^{12}N$ beam was sent onto a $^{208}$Pb target, and the $^{11}$C and protons issued from the reaction were observed using the SPEG spectrometer detection system for the heavy fragment, and 12 CsI detectors of 1 cm diameter set at 40 cm from the target for the protons. In the focal plane of the spectrometer, two drift chambers allow the determination of the magnetic rigidity and the angle of a particle triggering the plastic scintillator at the end of the spectrometer. The relative energy of the break-up fragments was computed event by event from their energy and their relative angle. Figure 2 displays the spectrum of the Relative energy between the proton and the $^{11}$C, where the contribution of the levels at 0.960 MeV ($E_{cm}$ = 0.36 MeV), 1.19 MeV ($E_{cm}$ = 0.59 MeV) and 1.8 MeV ($E_{cm}$ = 1.2 MeV) are clearly present.

This spectrum has been decomposed into the components coming from these levels. The fitting shapes are obtained from a Monte Carlo simulation of the experiment.

The differences between the three gaussian shapes in the analysis come from the natural widths of the three levels (see figure 1). From the intensity of the line at 1.19 MeV ($E_{cm}$ = 0.59 MeV), we infer a radiative width of (6 $\pm$ 4) meV and from the peak at 1.8 MeV, a value of (70 $\pm$ 20) meV. The large uncertainty comes mainly from

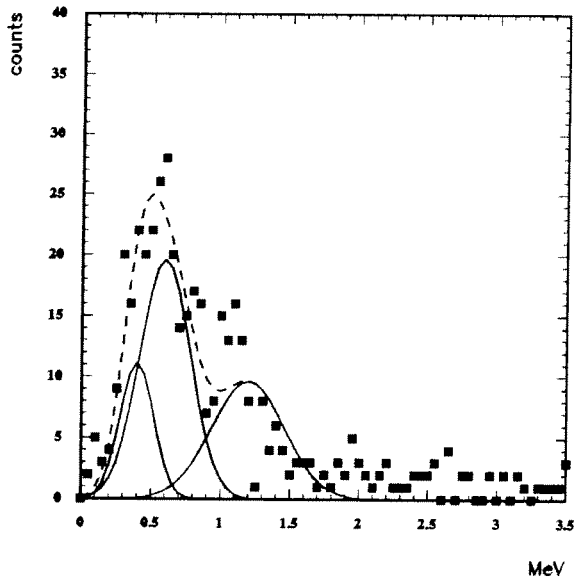


Fig. 2: relative energy spectrum of $^{11}$C and the proton in the Coulomb break-up of a $^{12}N$ beam. The dotted line is the sum of the three fitted peaks

the fitting of the relative energy spectrum, and the determination of the $^{12}N$ beam intensity.

The value for the 1.19 MeV state is in agreement with the Wiescher *et al* [3] estimate (2 meV), but not with the Descouvemont and Baraffe computation (140 meV) [4]. The Coulomb break-up method does not allow to extract any value for the first level at 0.960 MeV in $^{12}$N. That level decays through an M1 + E2 gamma transition and the M1 decay mode is the dominant one when looking at the analog nucleus $^{12}$B. The E2 Coulomb excitation being about 1300 times larger than the M1 one, a small E2 admixture gives a contribution larger than the M1 one. The astrophysical consequences of that result are actually evaluated.

## 5. References

[1] G. Baur, C.A. Bertulani, H. Rebel Nucl.Phys. A458 (1986) 188
[2] F. Ajzenberg-Selove Nucl. Phys. A506 (1990) 1
[3] M. Wiescher, J. Görres, S. Graff, L. Buchmann, F.K. Thielemann Ap.J. 343 (1989) 352
[4] P. Descouvemont, I. Baraffe, Nucl. Phys. A514 (1990) 66

# Search for the observation of Resonant Coherent Nuclear Excitation of Channeled Isomeres

S. Andriamonje[1], B. Blank[1], M. Chevallier[2], C. Cohen[3], N. Cue[4], D. Dauvergne[2], R. Del Moral[1], J.P. Dufour[1], J. Dural[5], L. Faux[1], A. Fleury[1], R. Kirsch[2], A. L'Hoir[3], J.C. Poizat[2], M.S. Pravikoff[1], J. Remillieux[2], D. Schmaus[3], M. Toulemonde[5]

[1] *Centre d'Etudes Nucléaires de Bordeaux-Gradignan and IN2P3*
*BP 120, Le Haut Vigneau, F-33175 Gradignan Cedex, France*
[2] *Institut de Physique Nucléaire de Lyon*
*IN2P3-CNRS/Université Claude Bernard, 69622 Villeurbanne Cedex, France*
[3] *Groupe de Physique des Solides*
*Universités Paris VII et VI, 75251 Paris Cedex 05, France*
[4] *Departement of Physics, University of Science and Technology, Kowloon, Hong Kong*
[5] *Centre Interdisciplinaire de Recherche sur les Ions Lourds*
*14040 Caen Cedex, France*

## Abstract

The possibility of observing Resonant Coherent Excitation (RCE) of an isomere nucleus by the periodic field of an aligned crystal is described. The results of a test centered on the production of $^{45}Ti^{m}$ and on the measurement of background resulting from the interaction of the $^{45}Ti^{m}$ with amorphous targets are given.

## 1. Introduction

When energetic heavy ions are channeled along a crystal axis, the ions travel far from the target nucleus and interact only with loosely bound target electrons. This aspect of channeling allows one to study the interaction of heavy ions with quasi-free target electrons, which we have done at GANIL, where we have studied non-resonant process, the Radiative Electron Capture (REC) which is the inverse of the Photoelectric effet [1], and a resonant process, the Resonant Transfer and Excitation (RTE) which is the inverse of the Auger effect [2].

Other interesting possibilities offered by energetic heavy-ions channeling is the search for Resonant Coherent Nuclear Excitation of the projectile by the periodic field of an aligned crystal. It happens that radioactive projectiles seem to be the best candidates for the observation of the process [3].

## 2. Coherent Nuclear Excitation of Channeled Isomeres

Channeled ions moving with velocity v along atomic rows experience a coherent periodic perturbation at the frequency $\nu$ ($\nu = K(\gamma v/d)$, K = 1, 2, 3,..., $\gamma = 1/\sqrt{1-\beta^2}$ where $\beta = v/c$, and d is the distance between the atoms in the rows). If one of these frequencies coincides with $\nu_r = \Delta E_{ij}/h$, where $\Delta E_{ij}$ is the difference between atomic or nuclear levels of the ion, a Resonant Coherent Excitation might occur.

This effect predicted by Okorokov in 1965 [4] has been observed in Oak Ridge, at Tandem energies, through the **atomic excitation** (from n = 1 to n = 2 states) of H-like and He-like ions [5].

The possibility of exciting **nuclear transitions** by RCE has been suggested also by Okorokov [4], and later was reconsidered by Fusina and Kimball [5] and by Pivovarov et al [6] but has never been observed because it requires very high incident energies in order to match the resonance condition. For example, RCE of the 110 keV level in $^{19}F$ requires an incident momentum per nucleon of about 20 GeV/c to reach the first harmonic for the most open channel of a diamond crystal [6]. It is very difficult to consider high harmonic numbers, and then lower incident energies, since RCE probabilities decrease rapidly when the harmonic number increases. For the moment, such relativistic heavy-ion beams are not easily available.

The possibility of producing secondary nuclear beams makes it possible to observe coherent nuclear excitation of some metastable nuclei in crystals for the following reasons.

Consider a nucleus in an excited level of long half-life ($\tau \geq 1\mu s$) and having a neighbouring level separated by a small transition energy ( 0.3 to 10 keV).

The **excitation** (if the neighbouring level is situated **above** the metastable state) or the **de-excitation** (if the neighbouring level is situated **below** the metastable state) into these short-lived nuclear states could then be reached at "low" incident energies (20 to 100 MeV/u). The observation of nuclear RCE (or de-excitation) could be performed by measuring the gamma-ray cascade to the ground state as a function of the incident secondary beam energy.

We considered only the excitation process for the $^{45}Ti^{m}$ ion. In channeling along the $< 111 >$ axis of a tungsten crystal at an incident energy of about 70 MeV/u, the $(3/2)^-$ metastable state ($\tau_{1/2} = 3.1\ \mu s$) could be excited to the $(5/2)^-$ state ($M_1$ transition of 3.4 keV) [8]. The decay ($\tau_{1/2} = 12$ ns) of this state to the ground state is followed by the emission of a 40 keV photon (Cf. Fig. 1).

The observation of this decay could be performed by stopping the Ti beam in an absorber.

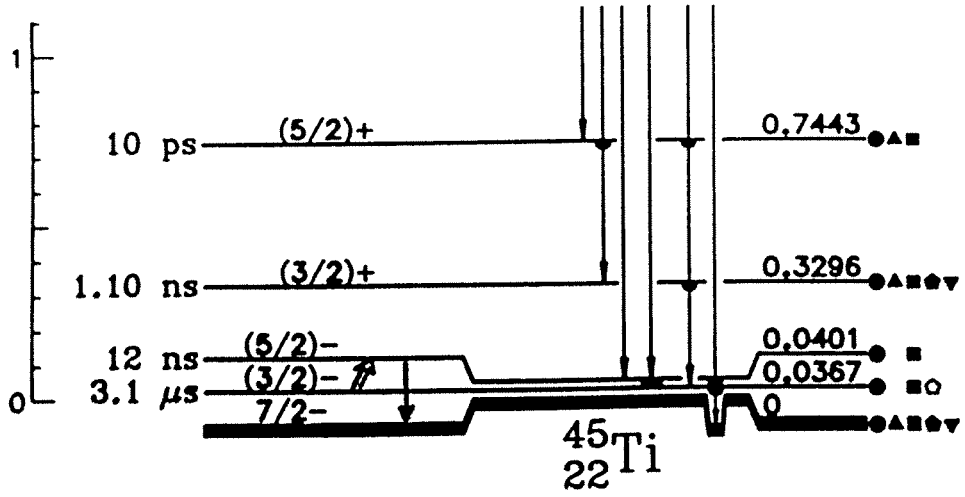


Fig. 1 *Principe of the Coherent Excitation of the $^{45}$ Ti isomeric state*

The experimental method is based on two techniques:

First, we produce the radioactive ions having a nuclear isomeric state ($^{45}$Ti) by the PFIS (Projectile Fragments Isotopic Separation) method [9] and we isolate the secondary beam using two magnetic spectrometers.

Second, these radioactive ions are channeled in suitable crystals and along appropriate axes. The resonant effect will be searched for by varying the beam energy, using the method described in the study of the Resonant Transfer and Excitation [2].

## 3. Measurement of the non-coherent excitation

The first experiment devoted to the production of a $^{45}$Ti secondary beam and to the measurement of the **non-coherent excitation** of the 40 keV level, in an amorphous target has been performed at GANIL in collaboration with the machine team (M. Bajard and D. Bibet).

The $^{45}$Ti has been produced by the fragmentation of a primary beam of $^{52}$Cr at 75 MeV/u on an Al target. The high-resolution alpha spectrometer associated with an achromatic degrader placed at the intermediate focal plane, has been used to separate $^{45}$Ti (Cf. Fig.2) and the identification has been performed by a $\Delta$E-TOF measurement (Cf. Fig. 3). The secondary beam is purified by the Wien filter and their passage in the center of the target chamber is signed by the detection of electrons produced in a thin aluminium foil. Several degrader foils ( Al to Pb) have been used to adjust the range of the $^{45}$Ti before stopping it in front of a X-ray detector (1000 mm$^2$ active area and 216 eV resolution at 5.9 keV). One of the goals of the experiment is the measurement of the production rate of the 40 keV $\gamma$ (background for RCE effect) as a function of the nature of the degrader and of the stopper.

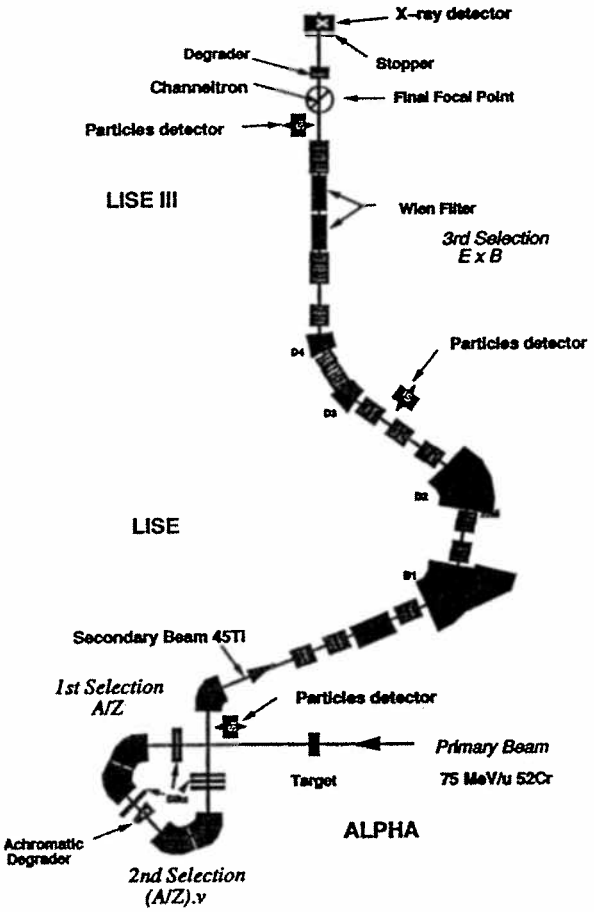


Fig. 2 *Experimental set up*

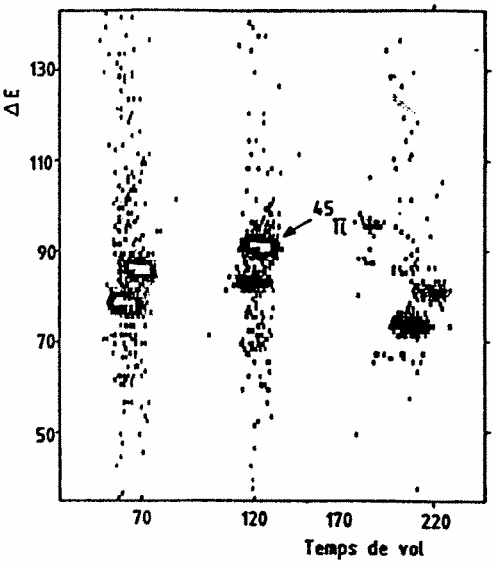


Fig. 3 *$\Delta$E-ToF spectrum for the identification of $^{45}$Ti*

Examples of the $\gamma$-ray spectra are given in Fig. 4. The absolute rate of the production of $^{45}$Ti$^{m}$ is deduced from the intensity of the 37 keV $\gamma$ ray (Fig. 4 a) and the intensity of the 40 keV $\gamma$ ray is obtained from the $\gamma$-ray spectra in coincidence with heavy ions within a time interval below 60 ns(Fig. 4 b).

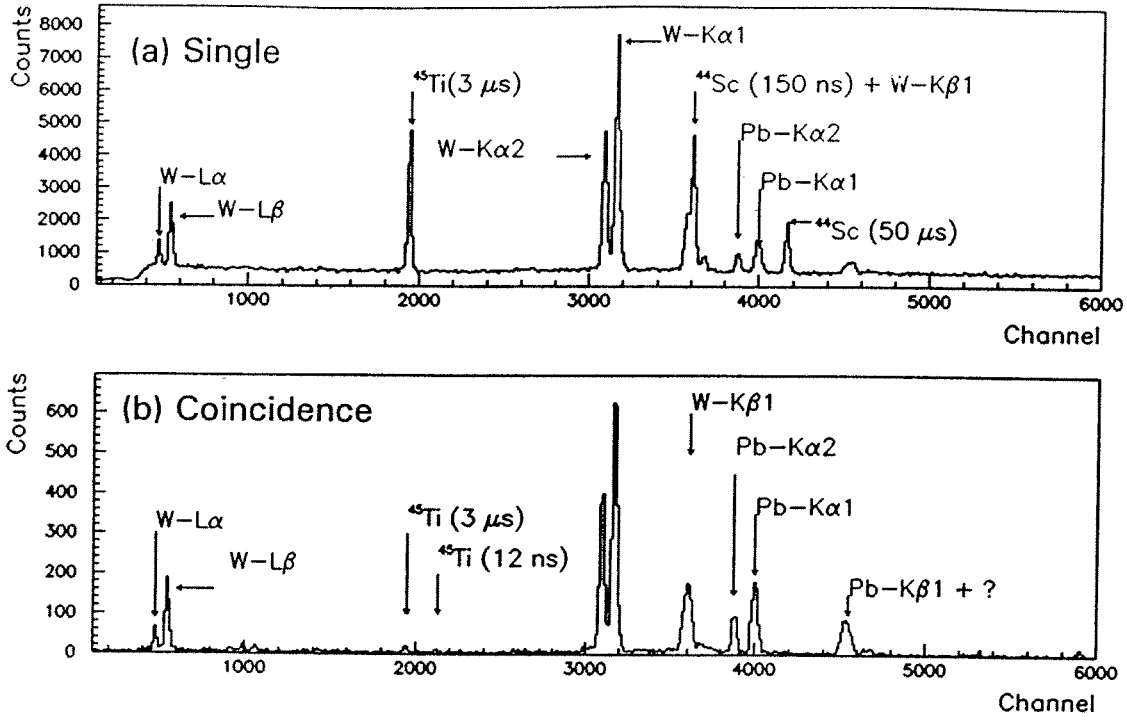


**Fig. 4** *a) Single $\gamma$-ray spectrum*
*b) Prompt ($\Delta t \leq 60$ ns) $\gamma$-ray spectrum in coincidence with heavy ions.*

This experiment permitted also to measure with good precision the transition energy between the two states ($(3/2)^-$ to $(5/2)^-$). The peaks corresponding to these two transitions are shown in figure 5.

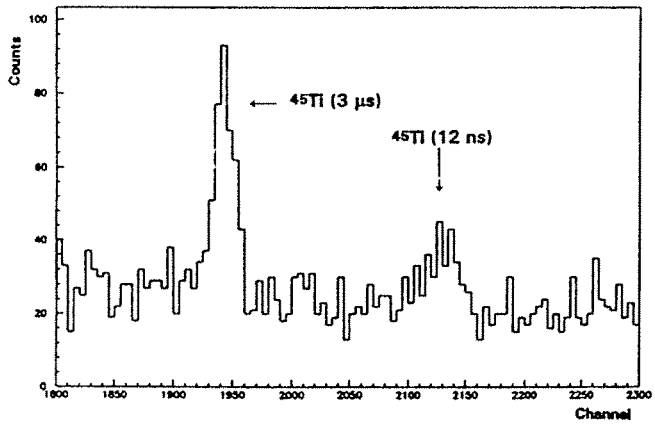


**Fig. 5** *Prompt ($\Delta t \leq 60$ ns) $\gamma$-ray spectrum around 40 keV (in coincidence with heavy ions)*

From the K-X-rays emitted by the degrader and the stopper we can extract also the contribution of the light-particles contaminants. In Fig. 6 we can see clearly the energy shift (190 eV) of the K-X-ray of the Tungsten stopper for the X-ray spectrum in coincidence with the heavy ion, which is characteristic for the presence of L-shell holes in the Tungsten atom target during the K hole de-excitation by X-ray emission, i.e. the signature of the interaction of highly or fully stripped heavy ions with atom targets [10].

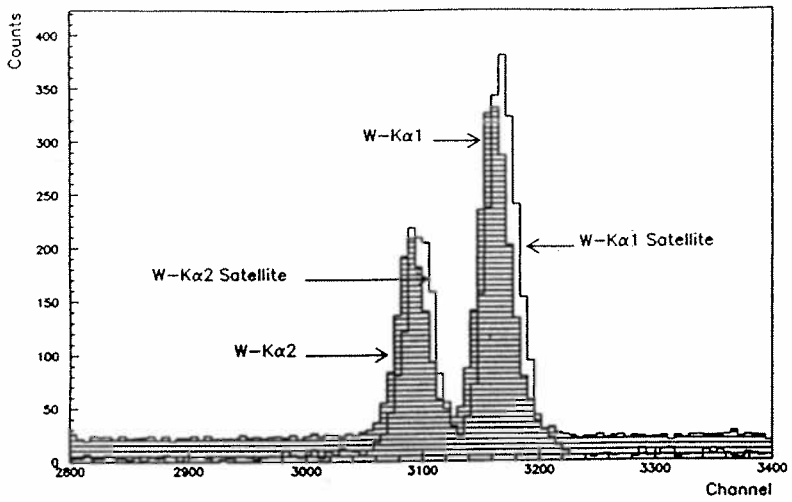


**Fig. 6** *$K_\alpha$ X-rays of Tungsten stopper (single divided by ten (stripped) and in coincidence with the heavy ions)*

## 4. Conclusion

The results obtained show that actually the observation of the RCE effect for the $^{45}Ti^m$ is not possible at GANIL with the considered experimental set up for three reasons :

i) The absolute rate for the production of metastable $^{45}$Ti is only 200/s. This represents only 20% of the total production of stable $^{45}$Ti.

ii) The cross section for the excitation of the 40 keV level is too large (40 to 100 mb depending on degrader and stopper) compared with the 20 mb RCE cross section.

iii) Our precisely measured value of the transition between the excited state and the metastable state of $^{45}$Ti is equal to 3.48 keV instead of 3.4 keV in the table [8] and the maximum energy delivered by GANIL for $^{52}$Cr (75 MeV/u) is now to low to reach the RCE resonance.

We study at the moment the possibility to find another candidate and another experimental set up in particular to use a new method for X-ray detection which is based in "channeling" photons [11].

## References :

[1] S. Andriamonje et al, Phys. Rev. Lett. **59** (1987) 2271.
[2] S. Andriamonje et al Phys. Lett. **A 164** (1992) 184.
[3] J. Remillieux, in: Physics and Techniques of Secondary Nuclear Beams, eds., J.F. Bruandet, B. Fernandez and M. Bex, (Editions Frontières, 1992) p.239.
[4] V.V. Okorokov, Pis'ma Zh. Eksp. Teor. Fiz. **2** (1965) 175 [JETP Lett. **2** (1965) 111].
[5] S. Datz et al, Phys. Rev. Lett. **40** (1978) 843.
[6] R. Fusina, J.C. Kimball, Nucl. Inst. Meth. **B27** (1987) 368 and **B33** (1988) 77.
[7] Yu. Pivovarov et al, Nucl. Phys. **A509** (1990) 800.
[8] C.M. Lederer et al, Table of Isotopes
[9] J.P. Dufour et al, Nucl. Inst. Meth. **A248** (1986) 267.
[10] S. Andriamonje et al, Z. Phys. A : Atoms and Nuclei **317** (1984) 251.
[11] M.A. Kumakhov, Nucl. Inst. Meth. **B48** (1990) 283.

# A2 - EXOTIC NUCLEI AND DECAY MODES

# PRODUCTION OF RADIOACTIVE BEAMS WITH MASS LESS THAN 65

Y. Yong Feng[1], R. Anne[1], P. Aguer[2], D. Bazin[1], T. Benfoughal[3], R. Bimbot[3], C. Cabot[3], F. Clapier[3], Th. Ethvignot[4], J. Fares[5], R. Freeman[6], A. Hachem[5], A. Lefevre[2], A. Lepine[1], M. Lewitowicz[1], M. Mirea[7], P. Roussel-Chomaz[1], M.G. Saint-Laurent[1], J.E. Sauvestre[4], J.L. Sida[8], C. Stephan[3]

*1) GANIL BP 5027 14021 Caen Cedex FRANCE*
*2) CSNSM 91405 Orsay FRANCE*
*3) IPN 91406 Orsay FRANCE*
*4) PNN/DAM Bruyères-le-Chatel FRANCE*
*5) Fac. Des Sciences, 28 Av. Valrose, 06034 Nice FRANCE*
*6) CRN Strasbourg, BP 20, 67037 Strasbourg Cedex FRANCE*
*7) Univ. Bucharest ROUMANIE*
*8)DAPNIA CEN Saclay 91191 Gif-sur-Yvette cedex FRANCE*

## 1-Motivations

The radioactive beams produced by projectile fragmentation at intermediate energy have already been used in various experiments: study of the fundamental properties of exotic nuclei (mass, period, radius...) and of their structure ($\gamma$ spectroscopy, halo...), nuclear astrophysics (Coulomb break-up). For each of these studies the production of the radioactive beam was optimized during the experiment, but very few systematic measurements[1] were ever performed in order to determine the optimum production for a given beam.

The aim of the present study is twofold:

1) obtain experimental data on differential cross sections near 0° for a large ensemble of reactions. These data should be completed in the future with data covering a larger angular range, in order to obtain integrated cross section and to be used as tests of mechanism models.

2) Provide us with a large experimental data base concerning the production of radioactive beams by fragmentation. These data should be directly applicable to the experiments on LISE, and with acceptance corrections also to other spectrometers such as SISSI and SPEG. They should be useful in order to improve the simulations existing on this subject, allowing us to extend the predictions for the production rates to other systems and other incident energies.

## 2-Experimental set-up

The first experiment of this program was performed with a 95 A.MeV $^{12}C$ beam. Beryllium, copper and gold targets of three different thicknesses were used. For each element, the thicknesses were chosen to induce a primary beam energy loss of about 1%, 15% and 40% . The secondary fragments produced by projectile fragmentation were separated by the doubly achromatic spectrometer LISE and were detected in a telescope of two silicon detectors (300 $\mu$m

and 1000 μm) placed at the achromatic focal point. The energy slits located at the dispersive focal point of LISE were set at +/-3mm, which corresponds to a total momentum acceptance of 0.35%. The angle of LISE was zero degree and the angular acceptance was left at its maximum value (±17 mrad in both planes). For each of the nine targets used in this experiment, measurements were performed for magnetic fields ranging from 0.7 up to 1.6 T by step of 0.05 T. In order to obtain counting rates acceptable by the silicon detectors, the primary beam intensity had to be reduced between 0,1 enA and a few tens of enA depending on the magnetic field settings. The intensity transformer usually used for normalisation was not sensitive enough to give a reliable measurement for such low intensities. Furthermore it appeared that the secondary emission detector located in front of the target induced perturbations on the counting rates for secondary fragments on the telescope. Therefore it was not possible to leave this normalisation detector in the beam path during the measurements. The procedure which was finally adopted for normalisation purpose was the following: the secondary emission detector was first calibrated with respect to a Faraday cup for high beam currents. It was assumed that this calibration could be extrapolated to low intensities. Then for each target and each magnetic field settings, the global (total) production yield of secondary beams, defined as the ratio of secondary to primary beam intensities, was measured by the following method: the primary beam intensity was monitored using the secondary emission detector. Then this monitor was taken off the beam, and the total number of particles reaching the telescope was recorded during a short time period (generally 10 seconds). Finally, the secondary emission detector was inserted again in order to check that no variation of the beam intensity had occured. The total production yield, measured by this method was then used to normalise the "individual" production yields of identified fragments which were extracted from the energy loss/time of flight bidimensional plots recorded for the same target and magnetic settings. The uncertainty due to this normalisation procedure should not exceed 5 to 10%.

3-Data analysis and first results

The secondary fragments were identified unambiguously by their energy loss and time of flight. The ratios of secondary beam productions to the primary beam intensity as a function of $B/B_0$ is presented in Fig. 1 for the thinnest Be target ($B_0$ is the magnetic field corresponding to the transmission of the primary beam after passing through the considered target). The data are shown by the dots whereas the solid and dashed lines present the results obtained with the LISE[2] and INTENSITY[3] programs. These two programs calculate an estimation of secondary beam intensities. They are very similar in their basic principles: both assume projectile fragmentation in a production target, they calculate the energy loss, multiple scattering and equilibrium charge state distribution in the target and any other system components, and they simulate the magnetic separation through a doubly achromatic magnetic spectrometer.

The shift between the maxima of the calculated distributions is related to different assumptions which are made in the two calculations. With LISE we assumed that the velocity of the fragment is equal to the beam velocity, whereas the calculations with INTENSITY were performed with a velocity shift, which was equivalent to assume that 8 MeV are required to remove an ablated nucleon. The data lie in between these two assumptions, but seem to be closer to the high velocity hypothesis. Both calcultations assume a pure fragmentation process and are therefore unable to reproduce the low energy tail observed experimentally, which is due to more dissipative processes. Concerning the absolute values of the maxima, the calculations are in good agreement with the observed production for isotopes not far from the stability : $^{6}$Li, $^{7}$Li, $^{7}$Be, $^{10}$B, $^{9}$C, $^{10}$C. However the calculations underestimate the production of $^{11}$C, $^{11}$B, because they do not take into account the transfer reactions which participate also in the production of these isotopes. Note that the production of $^{12}$B and $^{13}$C, which can only be formed via transfer reactions, is also observed. Finally, the production for $^{9}$Be and $^{8}$B is overestimated, and this can probably be related to the low binding energy of these nuclei.

The evolution of the production rates with the target thickness is in good agreement with the calcultations, as shown on Fig.2. First, the production increases linearly with the target thickness, but this progression is stopped and even inverted because of the broadening of the momentum and energy distribution of the secondary beam which decreases drastically the fraction which can be transmitted within the spectrometer acceptance. A maximum secondary beam intensity is thus obtained for an optimum target thickness (1300 mg/cm$^2$ for the Be target in the example of Fig. 2).

## 4-Conclusion

Although only the production of isotopes relatively close to the stability was studied in this first experiment, the most important shortcomings of the two codes could be clearly pointed out. However, the results of these codes are quite satisfactory for nuclei not too far from stability. For more exotic nuclei, the predictions are usually overestimated by roughly one order of magnitude. Three other experiments were performed with $^{13}$C at 75 A.MeV, $^{36}$Ar at 44 and 95 A.MeV in mid 1993. Their analysis should be completed soon. With these new data, and the already existing ones for $^{12}$C, $^{18}$O, $^{40}$Ar primary beams, a fair set of data will be available for light beams. The next step will be to study the production with heavier beams such as Ni and Cu.

## References


1) R. Bimbot, Proceedings of the RIKEN-IN2P3 Symposium on Heavy-Ion Collisions, Oct 1987

2) J.A. Winger et al, Nucl. Inst. and Meth. B70 (1992) 380

3) D. Bazin and O. Sorlin, private communication

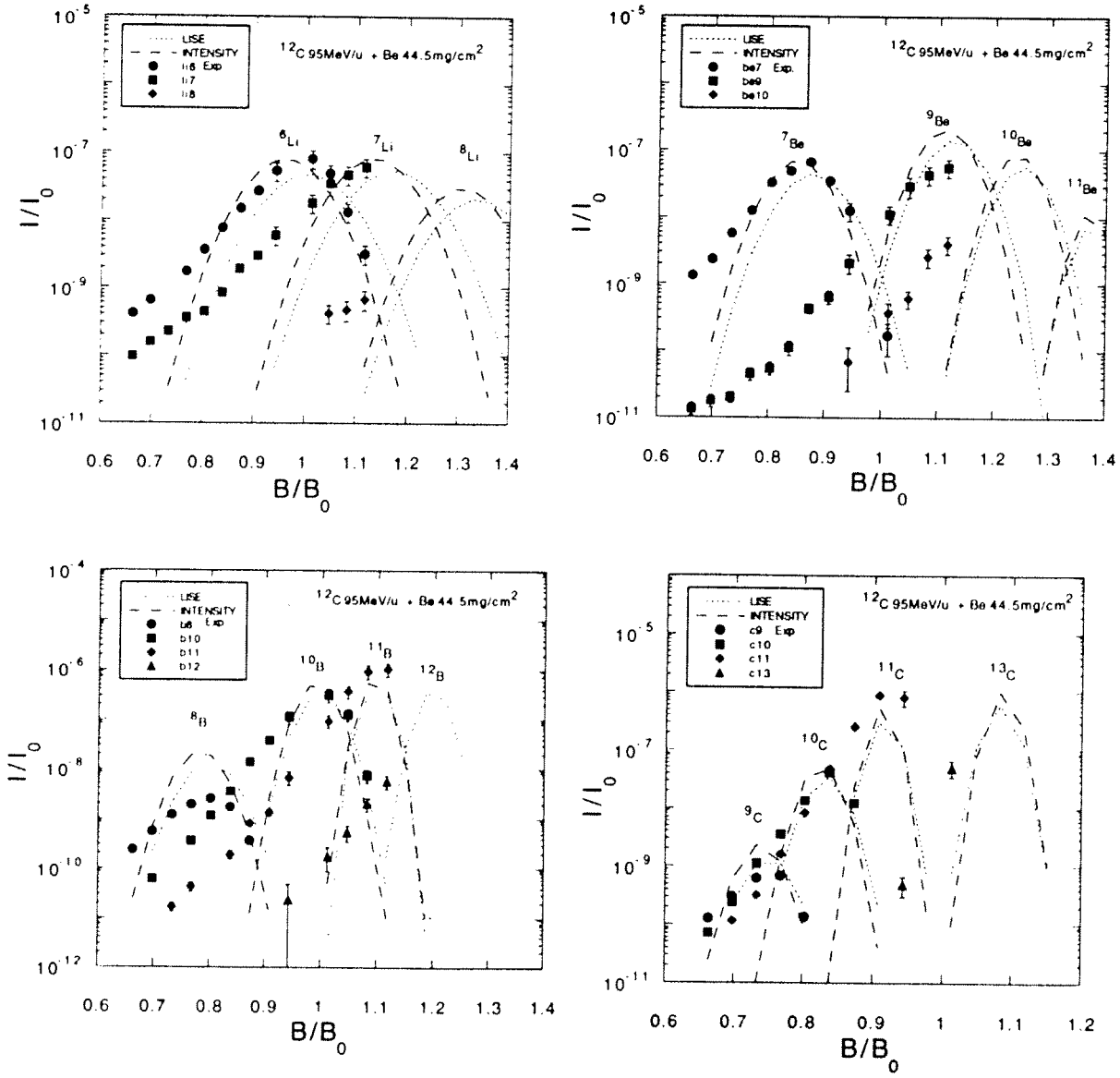


Fig.1: Ratios of secondary beam productions to the primary beam intensity as a function of $B/B_0$.

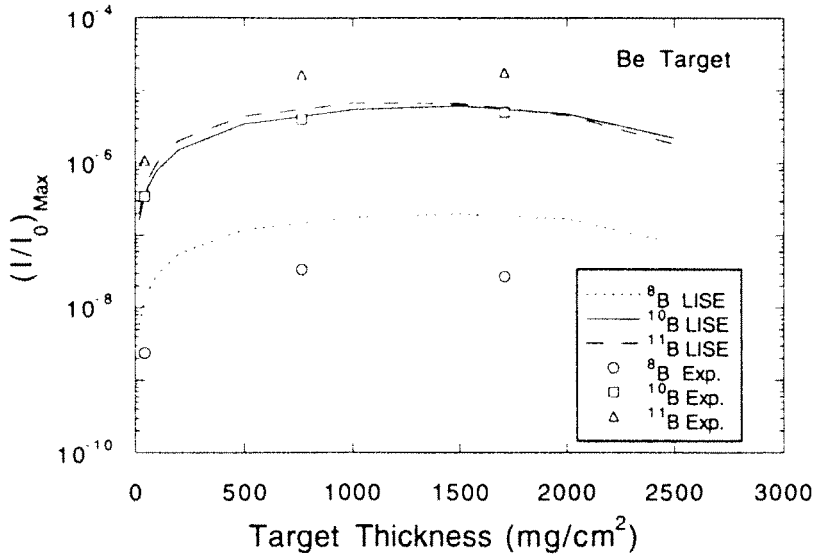


Fig.2: Production of B isotopes as a function of the Beryllium target thickness.

# TOWARDS $^{100}$Sn

M.Lewitowicz, R. Anne, G. Auger, D. Bazin, M.G. Saint-Laurent **GANIL Caen**

R. Grzywacz, M. Pfützner, K. Rykaczewski, J. Zylicz **University of Warsaw**

S. Lukyanov, A. Fomichov, Yu. Penionzhkevich, O. Tarasov **FLNR, JINR Dubna**

V. Borrel, D. Guillemaud-Mueller, A. C. Mueller, H. Keller, O. Sorlin, F. Pougheon **IPN Orsay**

M. Huyse, T. Pluym, J. Szerypo*) , J. Wauters **KU Leuven**

C. Borcea **IAP Bucharest**

Z. Janas*), K. Schmidt **GSI Darmstadt**

**Abstract**: Fragmentation reactions analyzed by means of the projectile fragment separator LISE3 at GANIL were exploited to enable the nuclei in the closest neighborhood of $^{100}$Sn to be identified and their decay properties studied. Preliminary results of the first experiment performed with the $^{112}$Sn beam are presented. The first identification of $^{102}$Sn and confirmation of an existence of $^{101}$Sn open new possibilities in the study of nuclei close to $^{100}$Sn.

## I. Motivation

Studies of doubly-closed-shell and neighboring nuclei are obviously important for testing and further development of nuclear models . Such studies on nuclei far from stability [1] have additionally an astrophysical context. Reliable predictions of nuclear structure and disintegration rates, especially for the Gamow-Teller (GT) beta decay, are crucial for understanding the nucleosynthesis scenarios under stellar conditions. In case of neutron-deficient nuclei these scenarios include the rapid proton-capture process.

The decay of nuclei in the $^{100}$Sn region has been investigated in several experiments on beta decay using the on-line mass-separators at GSI Darmstadt, ISOLDE CERN and LISOL Leuven. However, $^{100}$Sn has not been discovered. Progress towards this nucleus using on-line mass-separator based studies is made very difficult by a drastic decrease of the production cross-section in both spallation and heavy ion fusion-evaporation reactions. The yield is further reduced by the small overall release efficiency

*) On leave of absence from Warsaw University

caused by the short half-lives of investigated nuclei. Obviously, new production methods and separation techniques have to be tested in order to cross the border line of known nuclei (see next section).

Therefore we proposed [2] studies of the nuclei in the $^{100}Sn$ region using the fragmentation reactions and LISE3 projectile fragment separator at the GANIL facility. It was expected that, relative to earlier experiments, production yields of the most neutron deficient nuclides will be increased, and the limit for detectable half-lives will be essentially improved. These two improvements offer an opportunity to reach $^{100}Sn$. The expected increase of the production yields is mainly due to the use of $^{112}Sn$ as a projectile. This rare primary beam is developed at GANIL in a close and already very fruitful collaboration with the Laboratory of Nuclear Reactions, JINR at Dubna.

## III. Experiment

In the experiment performed at GANIL (26 Oct. - 4 Nov., 1993) we used $^{112}Sn^{43+}$ beam at 58 MeV/nucleon impinging on a 78mg/cm$^2$ thick $^{nat}Ni$ target. The mean intensity of the primary beam was about 130enA and it was limited by the data acquisition system. The choice of the nickel target enhances a transfer-type reaction.This in particular increases in an important way production of the nuclei with Z>50. A 9.5mg/cm$^2$ thick carbon foil placed just behind the target decreased a width of the charge state distribution in this way that about 90% of all tin isotopes were produced in the 48+ and 49+ charge states.

The experimental device used to select the exotic nuclei was the LISE3 spectrometer [3]. Briefly described, LISE3 is a doubly achromatic system providing selection of reaction products following the ratio $Av/Q \sim B\rho$ where A, Q and $v$ are, respectively, the mass, the ionic charge and the velocity of the ions and $B\rho$ is the magnetic rigidity of the spectrometer. The Wien filter placed at the end of the spectrometer allows for an additional velocity selection of the reaction products. In order to have a good velocity determination and to decrease the counting rate we reduced the momentum acceptance of LISE to ±0.1%.

A schematic view of the experimental set-up used in the present study is shown in fig. 1. All selected nuclei were stopped at the last image point of the spectrometer in a four-member silicon detector telescope (E1,E2,E3,E4) providing energy-loss (ΔE) and total-kinetic-energy (TKE) measurements. Furthermore, we measured the $B\rho 1$ and $B\rho 2$ values of the dipoles with a nuclear magnetic resonance probes, and the time-of-flight (TOF) between the target and the telescope, the start signal being given by the first silicon detector E1, and the stop by the radiofrequency of the last GANIL cyclotron. Two removable silicon detectors DED4 and ED4 and two removable position-sensitive avalanche counters XY1 and XY2 were used for a fine tuning of reaction products along the LISE spectrometer. Four big (80-90%) germanium detectors and a NE102 plastic

scintillator surrounding the final telescope served for measurements of beta and gamma radiation coming from the nuclei implanted in the silicon detectors.

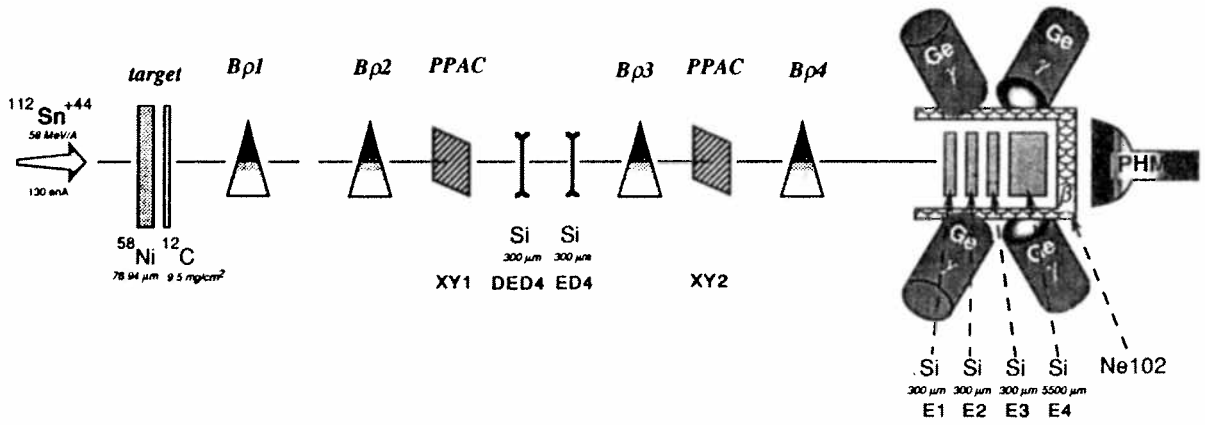


*Fig. 1. Schematic view of the experimental set-up.*

## IV. Data analysis and results

The analysis of the experimental data aims at a correct identification of all nuclei selected by the spectrometer. The atomic number is determined by a combination of the energy loss ΔE and time-of-flight (TOF) measurements according to the Bethe formula.

The determination of Z is done using the primary beam (Z=50) and by taking into account cross-checks such as the non-existence of $^{8}$Be on the A/Q=2 line and other equal-A/Q alignments. The Z spectrum obtained in the experiment for a tin region is presented in an upper part of fig. 2.

The charge state Q of each isotope can be calculated from the relativistic formula:

$$Q=3.33\times10^{-3}\frac{TKE\,\beta\gamma}{B\rho(\gamma-1)}$$

where the TKE has dimensions of MeV.

The TKE is calculated as a sum of energy losses in each silicon detector. A very careful energy calibration of E1,E2,E3 and E4 detectors was done using the primary $^{112}$Sn beam of five different energies. This calibration, which is valid in the energy region corresponding to the expected TKE for nuclei around A=100, takes into account non-linear effects in the electronic chains and the silicon detectors themselves.

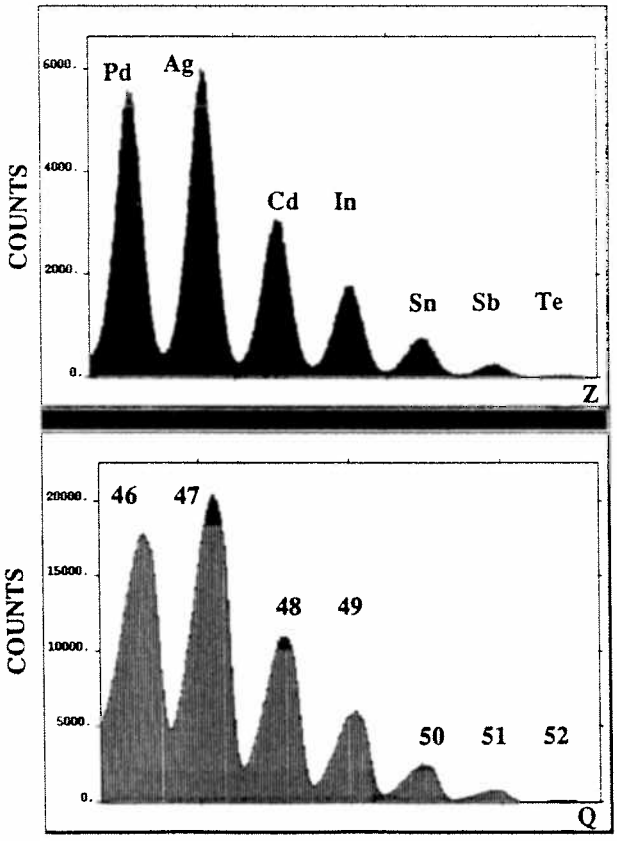


***Fig. 2.*** *Atomic-number and charge-state distributions obtained from the experimental data at Bρ=1.98835Tm.*

Once the charge state has been identified, the mass A of each nucleus expressed in a.m.u. can be extracted from the equation:

$$A=\frac{B\rho\, Q}{3.105\ \beta\gamma}$$

Since the charge resolution was sufficiently good (see a lower part of fig. 2), it was possible to improve the mass resolution by forcing integer values for Q. These integers were assigned for tin isotopes by putting the ΔQ=0.5 wide windows on the Q=50+,49+ and 48+ charge states. The resulting mass distributions for selected Q values are shown in fig. 3. In the distributions corresponding to Q=49+ and Q=48+, the events from $^{102}$Sn are clearly visible. It is a first observation of this tin isotope. In the second of these distributions, four events due to $^{101}$Sn are present.

The above results were obtained at Bρ=1.98835Tm which was chosen after test measurements performed at several Bρ values. The above spectra represent statistics obtained after about 30 hours of measurement with a mean intensity of primary beam of about 80enA.

The complete data evaluation which includes the analysis of beta-gated gamma spectra, is in progress.

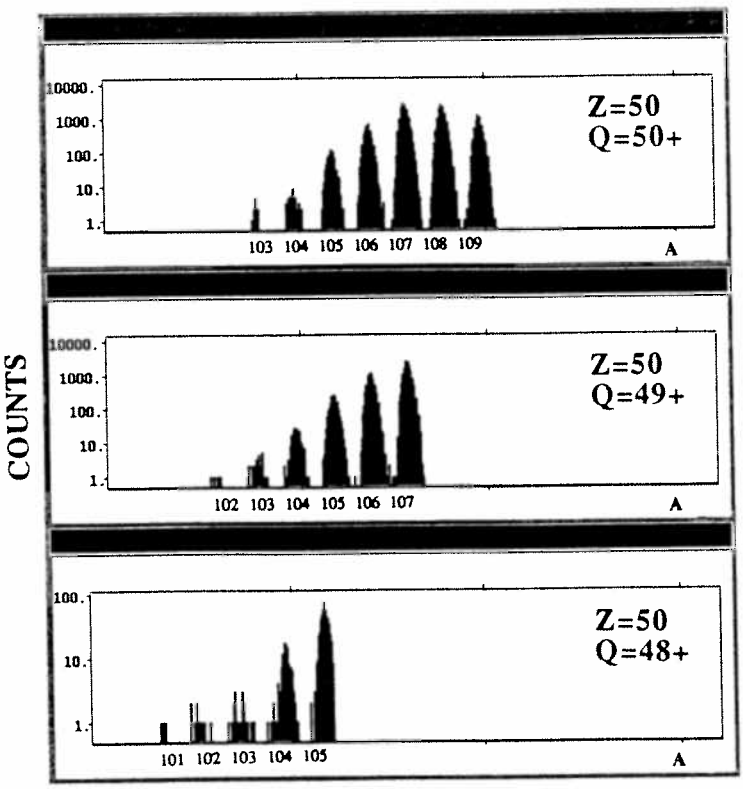


*Fig. 3. Mass distributions for tin isotopes for selected charge states Q at Bρ=1.98835Tm.*

## IV.Conclusions

The first GANIL experiment with the $^{112}$Sn beam, aiming at an identification and studies of nuclei near $^{100}$Sn, brought promising results and an important experience. With this experience, after an upgrading of the experimental set-up (adding SISSI solenoids right after the CSS2 and a new dipole magnet at the end of LISE3), there will be a good chance to identify $^{100}$Sn unambiguously and to start the decay spectroscopy in this region of highly neutron-deficient nuclei.

The experience gained during such studies and the detection equipment which will be developed will also be used at the Warsaw Heavy-Ion Cyclotron Laboratory coming into operation in 1994 and also in the future Radioactive Nuclear Beam ISOL-type facility (SPIRAL).

## References

1. Proceedings of the Sixth NFFS and the Ninth AMCO Conference, Bernkastel-Kues, Germany, 19-24 July, 1992 , Edited by R. Neugart and A. Wöhr, IOP, Bristol 1992
2. K. Rykaczewski et al. Towards the study of Gamow-Teller beta decay of $^{100}$Sn, Proposal for the GANIL experiment E226, June 1993
3. R. Anne and A. C. Mueller , Nucl. Instr. Meth. B70 (1992) 276, and ref. therein

# Production of a $^{42}Sc^{m}$ isomeric beam (E199)

Uzureau J.L., Bonnereau B., Delbourgo-Salvador P., Ethvignot T.,
Sauvestre J.E., Szmigiel M., Trochon J.
*Centre d'Etudes de Bruyères-le-Châtel,*
*B.P.12, 91680 Bruyères-le-Châtel*
Anne R., Bazin D., Corre J.M., Lewitowicz M., St Laurent M.G.
*GANIL,BP 5027,14021 Caen Cedex*
Bimbot R., Keller H., Mueller A.C., Sorlin O.
*Institut de Physique Nucleaire,B.P. 1, 91406 Orsay Cedex*

## 1 Introduction

The availability of the last generation of heavy ion accelerators and their sophisticated equipment has opened new ways for producing and studying radioactive nuclear beams (RNBs). In particular, secondary beams of nuclei in metastable states could be produced. Such isomeric beams are of great interest in order to study the nuclear structure by measuring the total reaction cross-section, direct reaction cross-sections on light nuclei or sub-barrier fusion cross-section. Comparison to results with ground state nuclei induced reactions will confirm or constrain theoretical models.

In this experiment, we test a method, based on transfer reactions, for producing pure isomeric heavy ion beams. Indeed, the selectivity of transfer reactions should lead, in principle, to extremely pure isomeric beams. Becchetti et al.(1990) reported the production of a short lived RNB of $^{18}F^{m}$ using the $(^{17}O,^{18}F)$ proton pick up reaction. We have chosen to produce an isomeric beam of $^{42}Sc^{m}$ which has a high spin $J^{\pi} = 7^{+}$, a long lifetime of $\tau = 62s$ and an excitation energy of 0.617 MeV. In its ground state the $^{42}Sc$ has a lifetime of 681ms and $J^{\pi} = 0^{+}$. The basic idea is to transfer a neutron-proton pair on a primary $^{40}Ca$ beam using a target of either $^{4}He$ or $^{12}C$:

$$^{40}Ca + ^{4}He \rightarrow ^{42}Sc + d$$

$$^{40}Ca + ^{12}C \rightarrow ^{42}Sc + ^{10}B$$

These two reactions favor the transfer of high orbital angular momentum (L=6 to produce the isomeric state of $^{42}Sc$ ) due to the momentum mismatch

between the entrance and the exit channels and the selection rules authorize the transfer S=1,T=0 to the isomeric state and other T=0 high spin states.The S=0,T=1 transfer to the ground state are forbidden.

The $^{40}Ca(^4He,d)^{42}Sc$ reaction has been already studied in direct kinematics at 10 MeV/u (Nann et al. 1977) and at 12.5 MeV/u (Rivet et al 1966). They clearly show the dominance of the isomeric state ($J^\pi = 7^+$ ,Ex=0.617 MeV ) in the deuteron spectrum. This reaction could thus be used to produce $^{42}Sc^m$ with a good purity.

The $(^{12}C,^{10}B)$ reaction is as selective as the $(^4He,d)$ reaction and will preferentially produce the isomeric state (Kraus et al.1987 for the reaction $^{16}O(^{12}C,^{10}B)^{18}F$).

## 2 Experimental set-up

The experiment was performed at the GANIL facility. A $^{40}Ca$ beam of an energy of 30 MeV/u and an intensity of 5 nAp bombarded three targets: one self supported $^{12}C$ target of 5 $mg/cm^2$ thickness, one gaseous target filled with $^4He$ (isotopic purity of 99.99 %) or $^3He$ (same isotopic purity but 5ppm of CO2 were measured) at atmospheric pressure (the cylindrical cell dimensions were 10mmx100mm and it was closed at both ends by a 4 micron Havar foil). The LISE3 spectrometer (R.Anne et al. 1987) was used to separate the outgoing fragments at 0 deg. It essentially consists of two dipoles (A/Z selection) with a 138 $\mu m$ wedge shape degrader in between ($A^3/Z^2$ selection). The Wien filter (velocity selection) was not utilized for this experiment. The angular acceptance of the apparatus (below one degree) is sufficient to allow collection of all the fragments produced on helium targets. However, a significant fraction of $^{42}Sc^m$ produced with the $^{12}C$ target was not detected, because the angular distribution extends well above one deg. at this energy. A removable silicon detector (300 microns) was placed at the first achromatic focal point, in order to record the time-of-flight (TOF) vs. energy loss identification maps.

At the end of the beam line, a silicon detector telescope was mounted. The thicknesses of the two detectors (209 and 406 microns) were chosen to optimize the $^{42}Sc^m$ detection. Energy losses, TOF, and a periodic clock signal (T=1.001s) were recorded on 8mm data cartridges. Independently, a high resolution germanium detector was placed behind the telescope, in order to measure the $\beta$-delayed $\gamma$-ray activity of the implanted $^{42}Sc$ ions. Indeed, the $^{42}Sc$ $\beta$-decays on an excited level of $^{42}Ca$ that promptly emits three $\gamma$ rays of well known energies: 437,1227 and 1524 keV . The targets were irradiated for 3 mn ( $\approx 3\tau$ ). Then the $\gamma$-ray activity was recorded for 5 minutes. Calibration of the silicon detectors was performed with direct irradiation of a $^{36}Ar$ beam.$^{56}Co$ and $^{60}Co$ $\gamma$-ray sources were used to calibrate the Ge detector in situ. The efficiency for the total absorption peak at 1227 keV was found to be $2.6 \pm .1\%$

# 3 Results

The average energy of the outgoing $^{42}Sc$ coming from the transfer reaction ($^{12}C$,$^{10}B$) was calculated to be 27.4 MeV/u. Thus the first dipole rigidity was set to $B\rho_1$ = 1.5019 T.m and the second dipole after the Aluminium degrader to $B\rho_2$ =1.312 T.m. The secondary beam was transported to the end of the beam line (D6). On Figure 1,a typical Total Energy vs Energy Loss scatter plot is shown. The $^{42}Sc$ beam is contamined by 10 % of $^{40}Ca$ and 0.1 % of $^{44}Ti$.

We present on Figure 2 a $\gamma$-ray spectrum. The three characteristic peaks of the isomeric state of $^{42}Sc^m$ are indicated by arrows. The total number of isomers was calculated knowing the Germanium detector efficiency. The lifetime of the isomer was also confirmed by the time analysis of the characteristic decay peaks.

Finally, a beam intensity of 114 pps was obtained with an isomeric purity of $85 \pm 5\%$.

Concerning the gaseous targets, a problem with the positionning of the Al degrader occured, leading to an uncertainty on its effective thickness. Thus, the selection of the nuclei was not optimum. The statistics collected with the $^3He$ target was very poor and the results are not significant.

However, a beam of 14 pps with a purity of $90 \pm 8\%$ was produced with the $^4He$ target.

# 4 Conclusion

For the first time, a pure isomeric beam was produced at GANIL with a $^{40}Ca$ beam impinging a $^{12}C$ target and measurements of the total reaction cross section of the $^{42}Sc^m$ is planed in a near future. However, the results with the Helium targets need to be confirmed. We also plan to produce a similar beam via heavy projectile fragmentation in order to improve the secondary beam intensity.

# References


[1] Becchetti *et al*, 1990, Phys.Rev., **C42**, 801

[2] Nann *et al*, 1977, Nucl.Phys., **A292**, 195

[3] Rivet *et al*, 1966, Phys.Rev., **141**, 1021

[4] Kraus *et al*, 1987, Phys. Rev., **C37**, 2529

[5] Anne *et al*, 1987, NIM, **A257**, 215

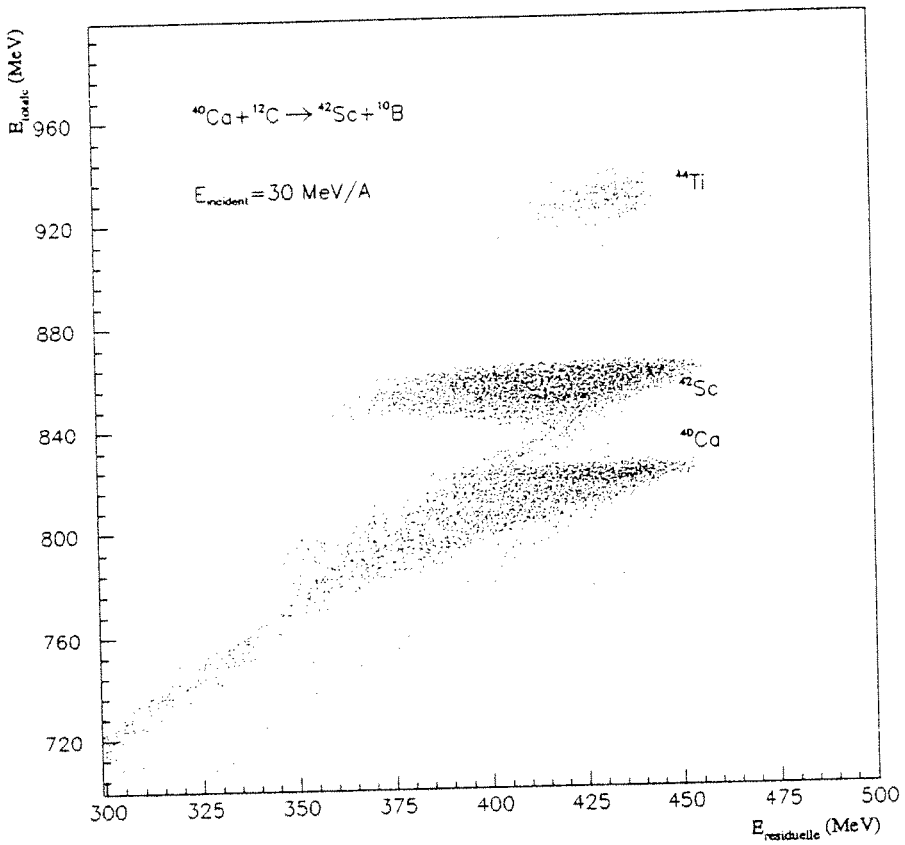


Figure 1 : Total energy (in the two junctions) vs. residual energy (in the E junction).

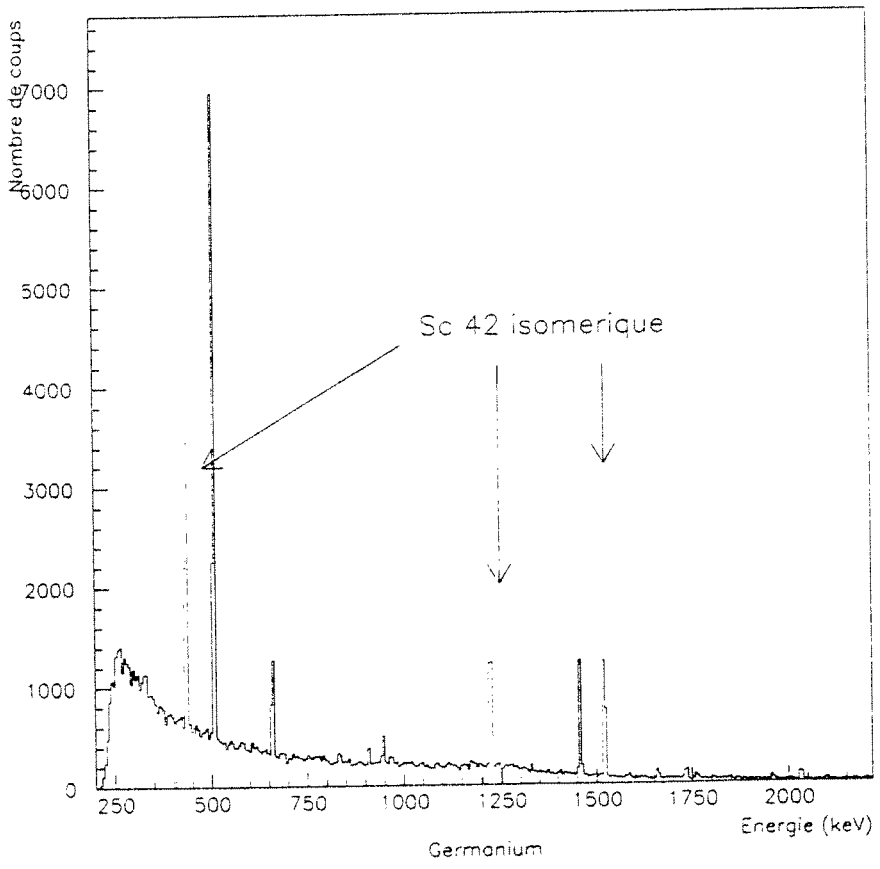


Figure 2 : $\gamma$ spectrum at the end of LISE.

# THE BETA-DECAY OF $^{20}$MG AND ITS IMPLICATIONS FOR THE ASTROPHYSICAL rp-PROCESS

A. Piechaczek[1], M. F. Mohar[1], R. Anne[2], V. Borrel[3], B. A. Brown[1,4], J. M. Corre[2], D. Guillemaud-Mueller[3], R. Hue[2], H. Keller[1], S. Kubono[6], V. Kunze[7], M. Lewitowicz[2], P. Magnus[8], A. C. Mueller[3], T. Nakamura[9], M. Pfützner[10], E. Roeckl[1], K. Rykaczewski[10], M. G. Saint-Laurent[2], W.-D. Schmidt-Ott[7], O. Sorlin[3]
[1]GSI, Darmstadt, [2]GANIL, Caen, [3]IPN, Orsay, [4]MSU, East Lansing, [5]RIKEN, Wako, [6]INS, Univ. of Tokyo, [7]II. Phys. Inst., Univ. Göttingen, [8]Dept. of Physics, Univ. of Washington, Seattle, [9]Dept. of Physics, Univ. of Tokyo, [10]Inst. of Exp. Physics, Univ. of Warsaw

## 1 Introduction

In 1981 Wallace and Woosley [1] proposed an astrophysical breakout-process from the 'hot' CNO cycle, which would ignite the burning of neon and hydrogen and would lead, following a path close to the borderline of proton instability, to the formation of heavy elements up to the nickel-iron region or even beyond. This rp-process is expected to take place in dense stellar sites, $\rho \geq 5 \times 10^3 g/cm^3$, under the condition of high temperatures, $T \geq 0.5 \times 10^9$. The breakout proceeds by the reaction sequence $^{15}O(\alpha,\gamma)^{19}Ne(p,\gamma)^{20}Na$. While the $(\alpha,\gamma)$ reaction is fairly well understood, there are considerable uncertainties concerning the $(p,\gamma)$ reaction which depends on the detailed structure of the $^{20}$Na-levels in the Gamow window above the proton threshold and in particular on the properties of the first unbound $^{20}$Na level at 2646 keV.
The first attempt to experimentally clarify the nuclear structure of $^{20}$Na around the proton threshold was undertaken by Kubono et al. [2] utilizing (p,n) and ($^3$He,t) reactions. The ($^3$He,t) reaction has meanwhile been reinvestigated by several other groups [3]. Coszach et al. [4] studied the $^1H(^{19}Ne,\gamma)^{20}Na$ reaction but did not observe the 2646 keV state either. In this paper we report on a detailed study of the $^{20}$Mg $\beta$-decay, which includes $\beta$-p and $\beta$-$\gamma$ coincidence measurements and thus considerably improves previous measurements of this decay [5].

## 2 Experimental techniques

We performed the experiment at the LISE3-facility [6] at GANIL. A secondary beam of $^{20}$Mg ions was produced in reactions between a 95 MeV/u $^{24}$Mg beam and a 300 $\mu$m $^{nat.}$Ni target. The isotopic identification was performed by the $\Delta$E-TOF method. The achromatic degrader, situated at the intermediate focal plane of the spectrometer, and the the velocity filter in front of the final focus, enabled us to achieve an overall purity of the $^{20}$Mg-beam of 93%. The main contaminant was the isotonic $^{18}$Ne with a fraction of 3%. The remaining activity of 4% is dispersed over several other isotopes. The $^{20}$Mg intensity at the final LISE3 focus amounted to 150 atoms/s for a $^{24}$Mg beam of $\approx 10^{11}$ atoms/s. The $^{20}$Mg beam was implanted into a 300 $\mu$m thick silicon strip detector ('implantation detector') inclined by an angle of 45° relative to the beam axis. The full width of the $^{20}$Mg range distribution in the implantation detector was $\approx$ 200 $\mu$m. The implantation detector was positioned between two large-area silicon detectors ('$\beta$-detectors') of 500 $\mu$m thickness which detected $\beta$-rays emitted from the implantation detector. A low energy loss of the $\beta$-particle in those detectors implies also a low energy loss in the implantation detector. Thus, by setting a window on small signals in the $\beta$-detectors, the $\beta$-summing of the particle spectra was reduced considerably. The silicon detector array was surrounded by three large-volume germanium detectors for $\gamma$-ray detection. Due to the high background rate of these detectors, they were only read out if triggered by an event in the implantation detector, i.e. either by the implantation of a heavy ion or by the subsequent positron, proton or alpha decay event.

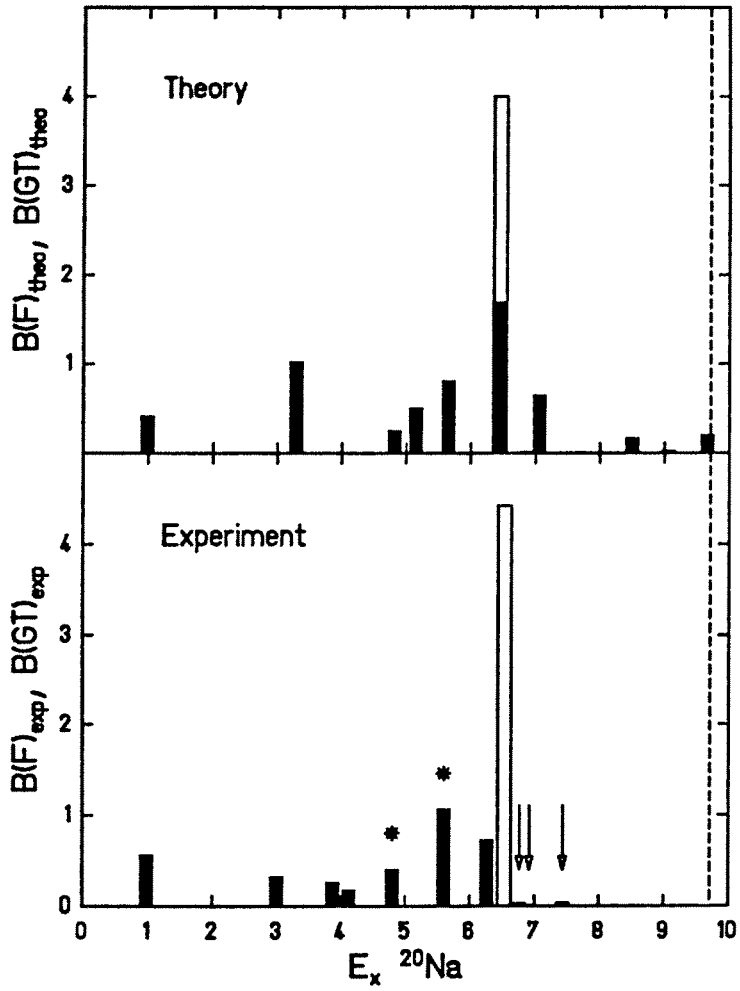


Figure 2: *Comparison of experimental and theoretical B(F) and B(GT) values for the $^{20}Mg$ decay. The full bars denote the B(GT) values, the empty bars the B(F) values. For the transitions indicated by an arrowhead only lower bounds of the B(GT) values have been determined. The levels marked by an asterix may represent broad levels or groups of several unresolved states. The dashed line represents the maximum possible Q value for positron decay.*

The branching ratio of the $\beta$-decay to proton-unbound $^{20}$Na states was found to be (30.3±1.2)% from the measured number of implanted $^{20}$Mg atoms and the spectrum of $\beta$-delayed particles obtained in the implantation detector, after having subtracted the low energy $\beta$-background as well as the $^{20}$Na contribution. The value of (30.3±1.2)% yields a branching ratio of (69.7±1.2)% for the $^{20}$Na level at 984.2 keV, since there are no other $1^+$ levels known below the proton threshold. The $\beta$-branching ratio for this level, independently determined from $\beta$-$\gamma$ coincidence data to be (70.5±1.4)%, is fully consistent with this assumption.

We identified a total of six or maybe even 9 $1^+$levels above the proton threshold. The $^{20}$Na level, at 6521 keV represents the T=2, $T_Z$=-1 isobaric analogue state of the $^{20}$Mg ground state. The $\beta$-branching ratios for the proton-unbound levels in $^{20}$Na were deduced from the proton and proton-$\gamma$ coincidene data. An upper limit of 0.1% was estimated for the feeding of the level at 2646 keV. This result was deduced from the nonobservation of 447 keV protons in the $\beta$-gated proton spectra, in which the background due to $\beta$-decay into bound states of $^{20}$Na and $^{20}$Ne is strongly reduced. In the $\gamma$-spectrum we did not find any lines that would correspond to the electromagnetic deexcitation of the 2646 keV level.

With the measured half-life of 98(15) ms, the $Q_\beta$ value of 10731(28) keV [8] and the experimental branching ratios, the log ft values given in Figs. 1 and 2 have been calculated. It is interesting to compare the log ft values to those in the decay of mirror nucleus $^{20}$O [9]. The $^{20}$Mg → $^{20}$Na [$^{20}$O → $^{20}$F] log ft values are 3.795(17) [3.740(6)] for decays to the first $1^+$ state at 984 [1057] keV, and 4.18(4) [3.65(6)] for the decays to the $1^+$ state at 3001 [3488] keV. The asymmetry observed for the second $1^+$ state is among the largest ever observed [10] and will be a theoretical challenge to interpret.

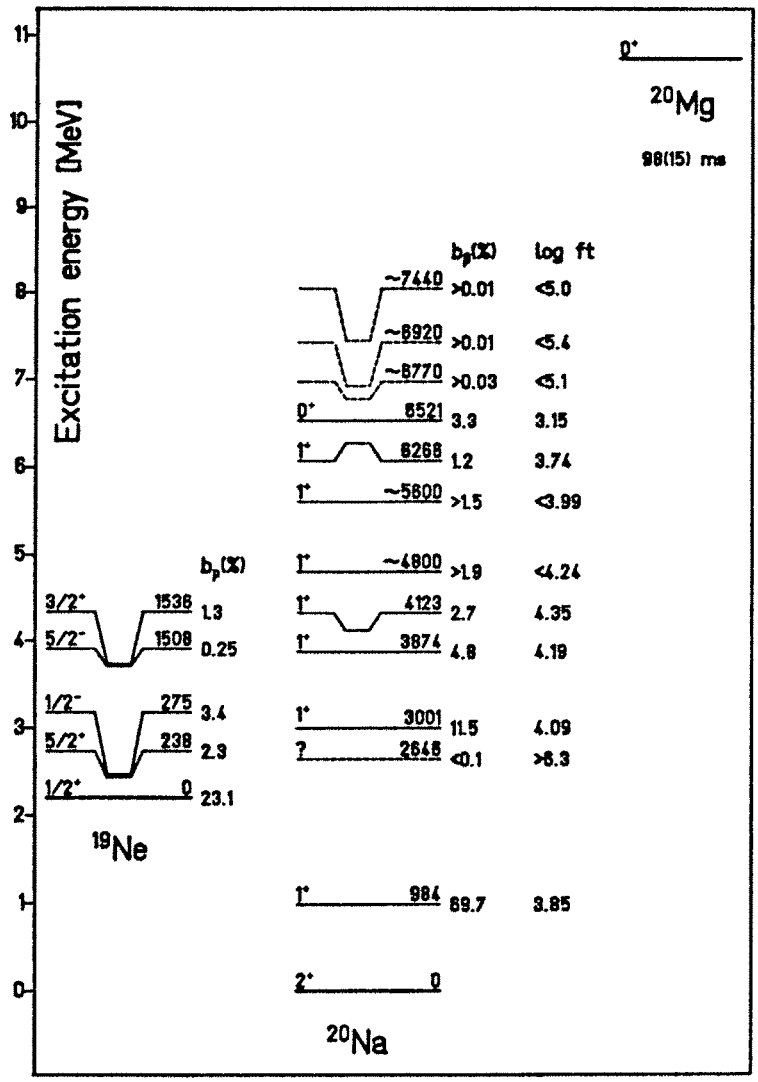


Figure 1: *Proposed decay scheme of $^{20}Mg$. The levels at 4800 and 5600 keV may represent broad levels or groups of several unresolved states.*

## 3 Results and Discussion

Figure 1 shows the decay scheme of $^{20}$Mg derived from this work, including in particular experimental results for the $^{20}$Mg half-life, the excitation energies of $^{20}$Na levels, the log ft values and the $J^{\pi}$ assignments. By operating the LISE3-spectrometer in a pulsed-beam mode (200 ms beam on, 800 ms beam off), the $^{20}$Mg half-life was redetermined yielding, together with results from previous measurements [5], a mean value of 98(15)ms. The excitation energy of 984.2(3) keV for the first excited (bound) $1^+$ level of $^{20}$Na was determined from the $\gamma$-ray measurement, whereas the excitation energies of higher lying states were deduced from the measured proton data and the known proton separation energy of 2199 keV[8]. In principle, the energies of the observed proton lines can be determined by using the well known $\alpha$-energies [7] from the subsequent $\beta$-delayed $\alpha$-decay of $^{20}$Na. However, for the energy calibration two effects have to be taken into account, namely (i) the difference between nuclear energy losses of the recoil atoms $^{19}$Ne and $^{16}$O, and (ii) the difference in ionization power of protons compared to $\alpha$ particles, which is of the order of $\approx 1\%$. In order to avoid the uncertainties caused by the effect (i) we adopted the energy of the first excited $1^+$ level above the proton threshold from the work of Coszach [4] as 3001(2) keV. An independent determination of these energies, using the known [7] $\alpha$-energies of the $^{20}$Na decay for energy calibration, yielded a value of 2987 keV. The slope of the calibration was determined by evaluating the proton transitions feeding the excited state of $^{19}$Ne at 1536 keV.

The limit of the log ft value for the 2646 keV state is consistent with a proposed assignment of $3^+$ for this level based on Coulomb shift systematics [11]. With this $3^+$ assignment the $^{19}$Ne(p,$\gamma$)$^{20}$Na reaction rate is increased by about an order of magnitude over earlier results [2][3] due to a large spectroscopic factor for d-wave proton decay to the $^{19}$Ne ground state and also due to a large $\gamma$-width. With this increased rate, the flow into the rp-process becomes limited by the slower $^{15}$O($\alpha$,$\gamma$)$^{19}$Ne reaction.
The $\beta$-decay of $^{20}$Mg and the subsequent proton decay properties of states in $^{20}$Na to positive parity states in $^{19}$Ne have been calculated within the sd-shell model space following the methods of refs. [12] and [13]. The calculated Gamow-Teller (GT) strength values B(GT) take into account the global quenching factor (about 0.6) as obtained from the empirical effective GT operator of ref. [12]. For all states the calculated proton decay widths are dominated by s-wave decay to the $1/2^+$ ground state, being with the summed proton intensity to the lowest $5/2^+$ and $3/2^+$ states relative to the $1/2^+$ ground state 0.13 and 0.01, respectively. The agreement with experiment (see Fig. 1) is good for the $5/2^+$ but an order of magnitude underpredicted for the $3/2^+$. The total calculated widths range from 0.3 keV for the isospin forbidden proton decay of the IAS to about 2 MeV for the isospin allowed decay of the 6th theoretical $1^+$ state which lies near the IAS and has the largest B(GT) value (see Fig. 2). There is some evidence in the data for the occurrence of broad states (or groups of levels) near the IAS (see Fig. 2). Due to the limitation of the calculations to the sd-shell model space, one may expect intruder $1^+$ levels from excitations into other shells, and the GT-strength may be fragmented over these intruder states. The comparison of experiment and theory in Fig. 2 shows evidence for this fragmentation. Taking into account the fragmentation, the total GT-strength below about 4 MeV is in reasonable agreement with theory. We note that 79% of the total calculated GT-strength is predicted to lie within the Q-value window (see Fig. 2), a fraction which is high compared to most other cases.

One of us (BAB) would like to acknowledge support from the Humboldt foundation and NSF grant 90-17077.

## References

[1] R. K. Wallace and S. E. Woosley, Astrophys. J. Suppl. 45(1981)389

[2] S. Kubono et al., Z. Phys. A331(1988)359 and Astrophys. J. 344(1989)460

[3] N. M. Clarke al., J. Phys. G16(1990)1547; L. O. Lamm et al., Nucl. Phys. A510(1990)503; M. S. Smith et al., Nucl. Phys. A536(1992)333

[4] R. Coszach et al., Proc. 2nd Int. Symposium on Nuclear Astrophysics 'Nuclei in the Cosmos', eds. F. Käppeler and K. Wisshak, IOP Publishing Ltd, 1993, p. 295

[5] D. M. Moltz et al., Phys. Rev. Lett 42(1979)43; J. Äystö et al., Phys. Rev. C23(1981)879; S. Kubono et al., Phys. Rev. C46(1992)361; J. Goerres et al., Phys. Rev. C46(1992)R833

[6] A. C. Mueller and R. Anne, Nucl. Instr. Meth. B56/57(1991)559

[7] E. T. H. Clifford et al., Nucl. Phys. A493(1989)293

[8] A. H. Wapstra, G. Audi and R. Hoekstra, Atomic Data and Nucl. Data Tables 39(1988)281

[9] D. E. Alburger et al., Phys. Rev. C35(1987)1479

[10] W. T. Chou, E. K. Warburton and B. A. Brown, Phys. Rev. C47(1993)1163

[11] B. A. Brown et al., Phys. Rev. C48(1993)1456

[12] B. A. Brown and B. H. Wildenthal, At. Data Nucl. Data Tables 33(1985)347

[13] B. A. Brown, Phys. Rev. Lett. 65(1990)2753

# ELECTRON ENERGY THRESHOLD EFFECT IN THE DEPENDENCE OF THE RADIOACTIVE DECAY CONSTANT ON THE IONIC CHARGE STATE

*F. Attallah* [1], *P. Aguer* [2], *M. Aiche* [1], *G. Boggaert* [2], *J.F. Chemin* [1], *J.P. Goudour* [1], *J.P. Grandin* [3], *C. Grunberg* [4], *J. Kiener* [2], *A. Lefevre* [2], *W.E. Meyerhof* [5], *J.N. Scheurer* [1], *J.P. Thibaud* [2]

1. CENBG - Le Haut-Vigneau BP 120 33175 GRADIGNAN Cedex
2. CSNSM - BP 1 - Bât 104 91406 ORSAY
3. CIRIL - BP 5133 14040 CAEN Cedex
4. GANIL - BP 5027 14021 CAEN
5. STANFORD UNIVERSITY - Department of Physics STANFORD California 94305 USA

## I - MOTIVATIONS

It was considered for a long time that the electronic environment of a nucleus can only induce small changes on the nuclear decay processes[1]. Such perturbations of the electron configurations on the nuclear decay modes have been evidenced in few cases for nuclear levels decaying by internal conversion or by electron capture. Nevertheless, up to a recent periode, the observed relative changes remain of the order of few percents in relation with the modifications of the chemical composition and the physical environments of the target reflecting the weak influence of the outer shell electrons on the electronic structure of the inner shells[2].

Since the apparition of heavy ions accelerators, like GANIL, highly ionized ions can be accelerated, leading to the possibility of a wide choice in the nature, the energy and the charge state of the ion beams.

Recently, two experiments have demonstrated in highly ionized atoms that the electronic configurations can have a drastic effect on the nuclear decay processes. First, the bound state β decay has been observed in bare $^{163}$Dy nuclei with the FSR storage ring at GSI[3]. Second, the half-life of the 14,4 keV level in $^{57}$Fe has been found to vary strongly when the electronic configuration evolves from a lithium-like to helium-like and hydrogen-like configuration[4].

The aim of the present experiment is to demonstrate that a very large variation (one order of magnitude) of the lifetimes of some nuclear levels is expected, when the energies of the transitions are slightly larger than the binding energy of the K shell electrons in the neutral atoms. For technical reasons we have used a beam of $^{125}$Te. Nevertheless the same effect could be found in some other nuclei such as $^{191}$Ir.

## EXPERIMENTAL APPROACH

For the first time at GANIL, a beam of $^{125}$Te, has been accelerated at an energy of 27 MeV/amu. The charge state of the beam was $q = 38^+$. The first $(3/2)^+$ excited level in $^{125}$Te is located at an energy of 35.46 keV above the ground state. This level decays by an almost pure $M_1$ transition. In a neutral $^{125}$Te atom, the main decay channel of this level is the internal conversion of the $M_1$ transition on a K shell electron. The K shell internal conversion coefficient in the neutral atom, is $C_K$ = 12.01 corresponding to an energy of the K shell electron $E_K^o$ = 31,8 keV. The lifetime of the transition in this neutral atom is $T^o$ = to 1.5 ns[5].

After acceleration, the $^{125}Te$ beam was sent on a 1 mg/cm$^2$ target of $^{232}Th$ mounted at a distance d = 11 cm from the entrance of the magnetic spectrometer SPEG[6]. At the exit of the target, the $^{125}Te$ beam has a charge state distribution centered on the $47^+$ charge state. The full width at half maximum of the charge states distribution is $\Delta q = 2$, in agreement with theoretical predictions[7]. Futhermore after passing through the $^{232}Th$ target a fraction of the $^{125}Te$ nuclei are excited by Coulomb excitation. Sergolle et al[8] and Barrette et al[9] have measured the $B(E_2)$ values for a number of excited levels in $^{125}Te$ which partially decay to the 35.46 keV level within 0.1 ns.

Due to the changes in the mean electric field viewed by the inner shell electrons for different configurations in the outer electronic shells, the binding energy of one K shell electron increases as the charge state increases. For one particular charge called hereafter the critical charge state $q_c$, the binding energy of the K shell, $E_K^{qc}$, becomes larger than the available energy in the nuclear transition. In such case, the internal conversion on a K shell electron becomes energetically forbidden, in spite of the presence of the two K shell electrons. Consequently, the mean half-life of the transtion is modified by a factor which is approximately equal to $T^o/T^{qc} = (1 - \Gamma_K^o / \Gamma_T^o)$, where $\Gamma_T^o$ and $\Gamma_T^o$ are respectively the K conversion and total decay widths in the neutral atom.

At the exit of the Th target we have selected the $^{125}Te$ ions which have been scattered at an angle of (42 ± 4) mrad with respect to the incident beam direction. The angular direction was defined by a 1 mm wide rectangular aperture in front of the target and a movable 0.1 mm wide slit mounted at d = 11 cm away from the target. This slit is set just in the entrance plane of the dispersive spectrometer SPEG. The grazing angle in the system $^{135}Te$ + $^{232}Th$ at 27 MeV/amu is equal to 105 mrad in the laboratory system. For the selected scattering angle, the feeding probability of the first nuclear level at 35.46 keV by Coulomb excitation has been calculated equal to $1.3\ 10^{-3}$.

After the slit, different species of $^{125}Te$ ions are coexisting.

a) $^{125}Te$ ions in the nuclear ground state and in different atomic charge states ranging between q = 50 and q = 43. They follow trajectories which are defined by the magnetic field, the angle of incidence in the spectrometer, the energy resolution of the beam and the charge state[6]. The X and Y positions of the $^{125}Te$ at the exit of the magnetic spectrometer are detected event by event in two identical systems separated by a distance of 1.783 m. Each system consists of a parallel plate giving a fast trigger signal and a drift chamber to analyze the position. At the end the ions are stopped in an ionization chamber which gives the value of the energy of each ion with an energy resolution of 2 %

b) $^{125}Te$ ions which have been excited in the first nuclear state by Coulomb interaction with a charge state $q < q_c$. Before entering the magnetic field, most of the excited nuclear states have time to decay to the nuclear ground state by internal conversion because the lifetime of the first excited nuclear state in the neutral atom is of the order of the time of flight between the target and the magnetic field entrance. During the process, a conversion electron has been emitted in the continuum. These $^{125}Te$ ions enter into the spectrometer with a charge state (q + 1). They cannot be distinguished from the Te ions seen in (a) which have been formed directly in a charge state (q + 1).

c) $^{125}Te$ ions which are nuclear excited with a charge state $q \geq q_c$. Their decay length is larger than the distance d because the half-life $T^{qc}$ is increased by a large factor. The greatest part of such ions enters into the magnetic field with a charge state q and begins to follow the corresponding trajectory of the $^{125}Te$ (q). At some position inside of the spectrometer SPEG the nuclear state decays. One part

of the decay arises by photon emission and the other part arises by internal conversion on the remaining L shell electrons, inducing a change in the charge state. The $^{125}Te$ (q) becomes then a $^{125}Te$ (q + 1) which follows a different trajectory in the magnetic field. Once detected in the drift chambers, its position is located between $^{125}Te(q)$ and $^{125}Te(q + 1)$ peaks.

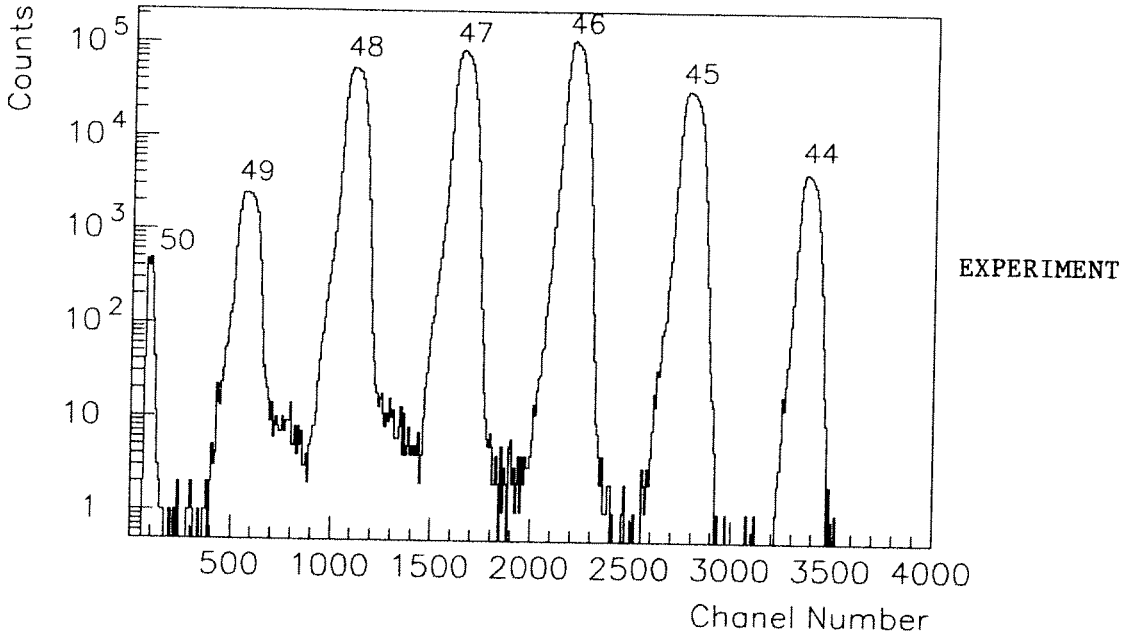


**Fig. 1** : Expérimental distribution of the $^{125}Te^{q}$ ions location in the drift chamber showing the charge of the trajectories of the $q \geq 46$ ions inside of SPEG anording to the different nuclear lifetimes of the first excited state

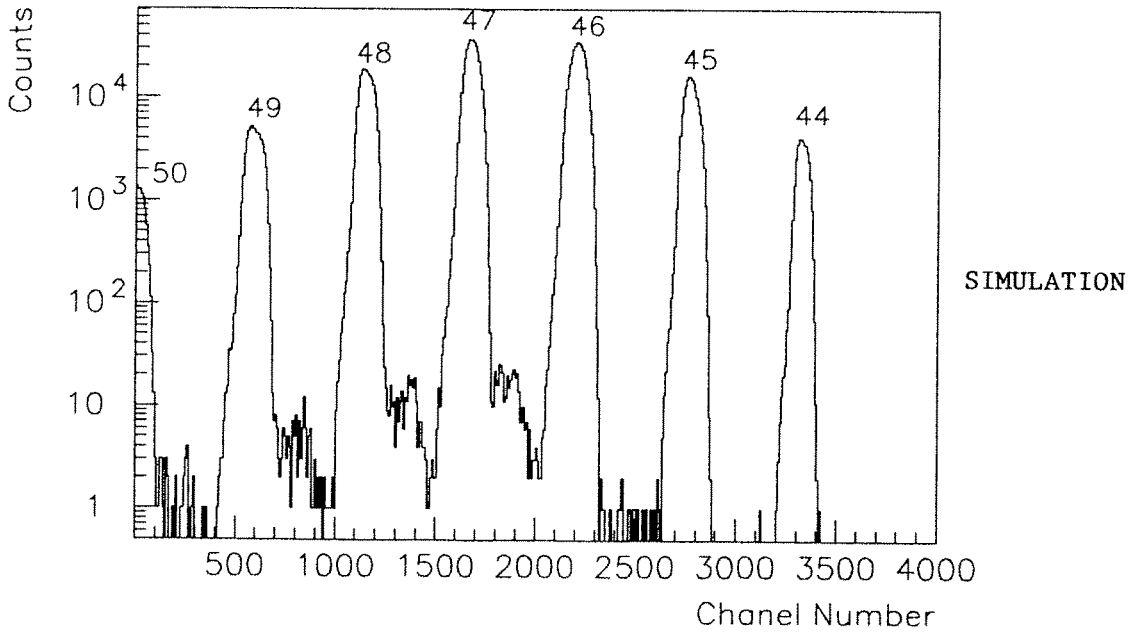


**Fig. 2** : Result of a computer simulation of the decay of the $^{125}Te$ ions inside the magnetic spectrometer SPEG for different charge states (see the text)

The actual position in the detection system plane depends on the location where the decay has taken place. If the decay happens soon after the penetration in the magnetic field, the ion is detected in the drift chamber at a position which is closed to the peak of $^{125}Te$ associated with the charge state (q + 1). On the contrary a long lifetime corresponds to a location in the drift chamber which will be close to the low energy side of the $^{125}Te$ peak associated with the charge state q.

Fig. (1) presents the distribution of the $^{125}Te$ ions in the second drift chamber. A gate has been set on the elastic part of the energy distribution of ions scattered at 42 mrd . The effect of the critical charge is clearly seen in Fig. (1) between the charges q = 46 and q = 47. The change in the mean lifetime of the nuclear level is evidenced by the filling of the valley between the corresponding peaks. Since the modification of the charge during the flight produces events located on the high energy side of the peaks, such events cannot be confused with energy loss background events.

The total intensity and the distribution of the counts are used to deduce the lifetimes associated to the different charge states. A simulation program, based on the code Turtle[10], has been achieved to give a quantitative interpretation of the data. Fig (2) shows the result of a simulation corresponding to our experimental situation. In this case, we have assumed a half-life $T^o$ = 1.5 ns for the first excited level of $^{125}Te$ with charge state $q \leq 45$ and a constant value of $T^{qc}$ = 12 ns for $^{125}Te$ in charge states q = 46, q = 47, q = 48, q = 49. The feeding probability of the first state has been taken equal to $P_c = 1.3\ 10^{-3}$ for all decaying charge states.

It is seen that the simulation reproduces very well the major features of the experimental data, evidencing the large enhancement of the nuclear period for a critical charge state q = 46.

## REFERENCES


1) Emery - Ann. Rev. Nucl. Sc. 22, 165 (1972)

2) H. Ulrickson et al - Phys. Rev. C9, 326 (1974)

3) M. Jung et al - Phys. Rev. Lett. 69, 2164 (1992)
K. Takahaski et al - Phys. Rev. C36, 152 (1987)

4) W.R. Phillips et al - Phys. Rev. Lett. 62, 1025 (1989)

5) Table of isotopes, seventh edition, ed. by M. Lederer and V. Shirley, p. 611

6) L. Bianchi et al - NIM A276, 509 (1989)

7) W.E. Meyerhof - Private communication

8) H. Sergolle et al - Nucl. Phys. A145, 351 (1970)

9) J. Barrette et al - Phys. Rev. C11, 282 (1974)

10) K.L. Brown, C.H. Iselin - CERN Report 74-2

# B - NUCLEAR REACTIONS

# B1 - PERIPHERAL COLLISIONS PROJECTILE-LIKE FRAGMENTS

# Peripheral Collisions at Very Forward Angles.

Ch.O. Bacri, P. Roussel, R. Anne[1], M. Bernas, Y. Blumenfeld, V. Borrel, F. Clapier,

H. Gauvin, J. Hérault, J.C. Jacmart, F. Pougheon, J.L. Sida[2], C. Stéphan,

T. Suomijarvi, L. Tassan-Got.

Institut de Physique Nucléaire,IN2P3, Université Paris Sud, 91406 Orsay Cedex, France

1 Ganil, B.P. 5027, F14021 Caen Cedex

2 Dapnia, CEA, Saclay, F91191 Gif-sur-Yvette Cedex

The mixture of several contributions in the reaction mechanism makes difficult a complete understanding of heavy-ion peripheral collisions at the Ganil energies. Friction, coulomb deflection, nucleon exchanges, fragmentation and diffraction are possible participant to this mixture. The latter has been demonstrated to play a dominant role in the analysis of $^{11}$Li breakup reactions [1]. A detailed study of characteristic angular parameters involved in peripheral collisions shows the necessity of a good knowledge of the angular range from around the grazing angle down to $0^{o}$, the beam direction [2].

The corresponding experimental study has begun, essentially on the $^{40}$Ar + Ni system, at 44MeV/A , so far performed only at $0^{o}$. The required angular accuracy (+/-3mr) has been obtained by the use of the telescopic mode on the LISE spectrometer [3]. The analysis of the results and their comparison with already performed measurements at the grazing angle ($3^{o}$) [4] have brought new constraints on reaction mechanisms. In particular, the observed variation with the angle of the most probable velocities of all the detected nuclei (Fig. 1) requires the role of the dissipation to be studied again. Diffraction might explain this angular behaviour.

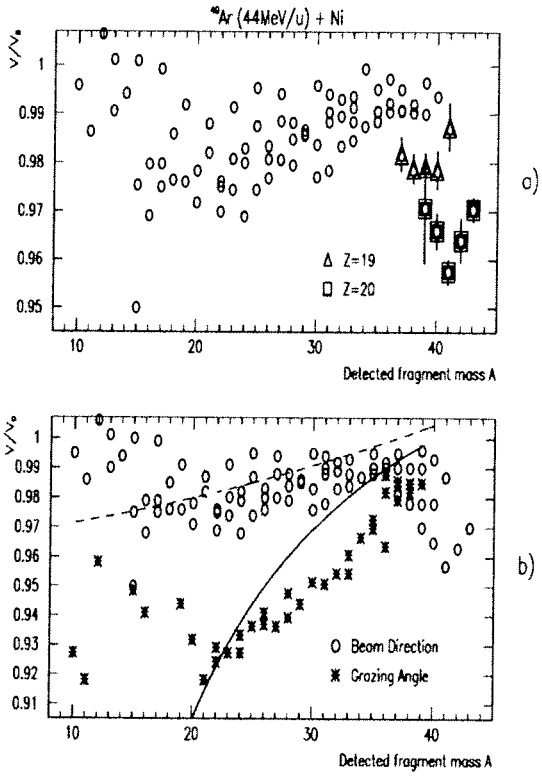


**Fig. 1:** Most probable value of the projectile-like-fragment velocity distributions versus the fragment mass A. **(a)** Measured in the beam direction. The points for fragments with one (Z=19) or two (Z=20) protons more than the projectile have been tagged respectively with a triangle and a square. For more clarity, experimental errors bars are not indicated, except for Z>18. **(b)** Compared to the grazing angle results [4], and to model evaluations (see ref. 2,5).

Although all the angular distributions have been found to be peaked at $0^{o}$, the ratio $\sigma(0^{o})/\sigma$(grazing angle) is strongly N and Z dependant (Fig. 2). Moreover, these measurements modify the previously established yield evaluations. All theses results are detailed in [2,5].

In order to complete these results, we have begun to measure neutrons and charged particles in coincidence with quasi-projectiles emited from around the grazing angle down to $0^{o}$. A modular neutron detector has been constructed and tested under beam, in the reaction chamber of the LISE spectrometer. It is hoped that the experiment will be performed during the year 1994.

## References :


[1] P. Roussel, Ch.O. Bacri, F. Clapier, Nucl. Phys. **A559**(1993)646.

[2] Ch.O. Bacri, P. Roussel, V. Borrel, F. Clapier, R. Anne, M. Bernas, Y. Blumenfeld, H. Gauvin, J. Herault, J.C. Jacmart, F. Pougheon, J.L. Sida, C. Stéphan, T. Suomijarvii, L. Tassan-Got, Nucl. Phys. **A555**(1993)477.

[3] Ch. O. Bacri, P. Roussel, Nucl. Inst. Meth. **A300**(1991)89.

[4] V. Borrel, B. Gatty, D. Guerreau, J. Galin, D.Jacquet , Z. Phys.**A324**(1986)205.

[5] Ch.O. Bacri, P. Roussel, V. Borrel, F. Clapier, R. Anne, M. Bernas, Y. Blumenfeld, H. Gauvin, J. Herault, J.C. Jacmart, F. Pougheon, J.L. Sida, C. Stéphan, T. Suomijarvii, L. Tassan-Got, XXXI **International Winter Meeting on Nuclear Physics**, Bormio, Italy(1993).


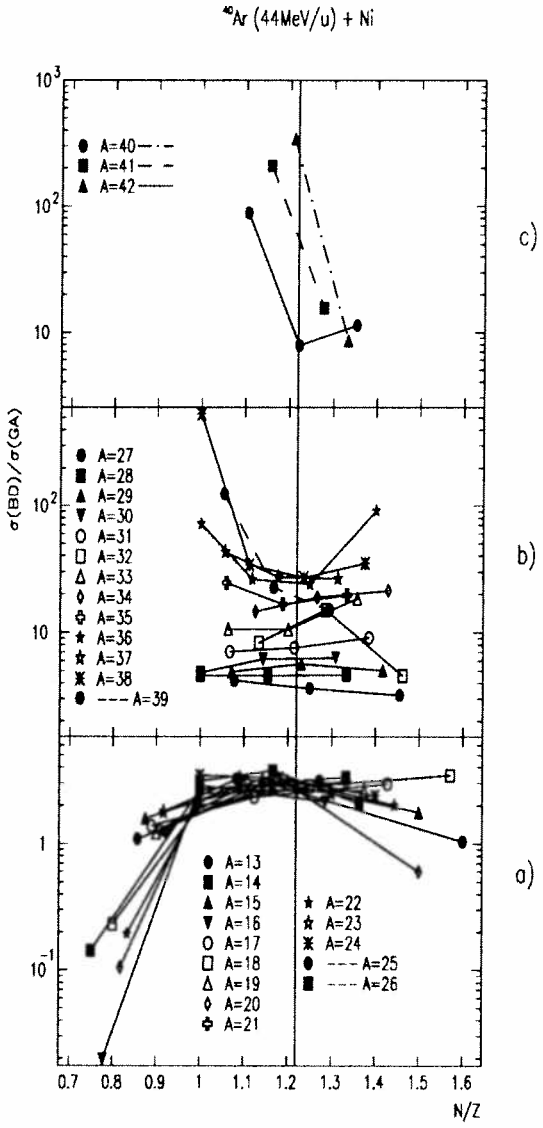


**Fig. 2:** Ratio of the differential cross section in the beam direction (BD) to that at the grazing angle (GA) versus the N/Z value of the detected fragment. The different fragment masses have been split into : (a) 12<A<27, (b) 26<A<40 and (c) A>39, in order to make clear the observed different behaviour between the three sets. The vertical line indicates the N/Z value of the projectile.

# Breakup of the projectile in heavy ion collisions at intermediate energies

A. Badalà[1)], R. Barbera[1,2)], A. Palmeri[1)], G. S. Pappalardo[1)]
F. Riggi[1,2)], A. C. Russo[1)], G. Russo[2,3)], R. Turrisi[1,2)]
[1)]Istituto Nazionale di Fisica Nucleare, Sezione di Catania
[2)]Dipartimento di Fisica dell'Università di Catania
[3)]Istituto Nazionale di Fisica Nucleare, Laboratorio Nazionale del Sud

**Abstract**

The 4-He disassembly channel of the $^{16}O$ on $^{27}Al$, $^{58}Ni$ and $^{197}Au$ targets has been studied at 94 MeV/nucleon, both inclusively and in coincidence with charged pions.

# 1 INTRODUCTION

It is well known that heavy ion collisions at energies well above the Fermi energy represent a useful tool to prepare nuclear matter in states far from normal conditions. In the so-called intermediate energy range, the competition which exists between mean field effects and two-body collisions allows to investigate interesting and still open questions such as the existence of a limit of the excitation energy that a nucleus can sustain before its breaking and the space-time evolution of the reaction with regard to its mechanism. In the last few years some attention has been turned to the study of projectile breakup in peripheral collisions induced by light nuclei, mainly $^{16}O$, on different targets spanning the whole stable mass range at various bombarding energies from 32.5 to around 100 MeV/nucleon [1]. In this contribution we report on an experiment in which the 4He breakup channel of the $^{16}O$ projectile has been studied, inclusively [1] and in coincidence with charged pions [2], in reactions induced at 94 MeV/nucleon bombarding energy on various targets. Section II is devoted to a description of the experimental setup and selection criteria on treated data. Section III.A and III.B contain a general review of the results for inclusive (4He) and exclusive ($\pi^{\pm}\cap$4He) events, respectively.

# 2 EXPERIMENT AND DATA SELECTION

The overall detection apparatus is sketched in Fig. 2. Light charged particles have been detected by two large-area multidetectors, which were able to identify the charge $Z$ of the fragments, from hydrogen to oxygen, by a standard $\Delta$E-TOF (time of flight) technique [1]. They were the *Mur* (a plastic wall) [3] and one half of the *Tonneau* (a plastic barrel) [4], both installed in the *Nautilus* vacuum chamber at the GANIL facility. Charged pions of kinetic energy ranging from 23.4 up to 74.1 MeV have been detected, at laboratory angles 70°, 90° and 120°, using a *range* telescope of plastic scintillators [5, 6]. Most of other particles impinging on the telescope was on-line rejected by a suitable adjusting of the electronics and the residual contaminants were eliminated in the off-line data reduction performing a multiple $\Delta$E-E and $\Delta$E-$\Delta$E analysis of the relative energy loss in each scintillator element of the telescope. In the study of both inclusive and exclusive data we restricted the analysis to those events with only four particles with $Z = 2$, all detected in the angular range between 3° and about 20° (the first five rings of the *Mur*, see Fig. 2) with a velocity larger than 8 cm/ns. These severe conditions reasonably select those events resulting from the breakup of the primary projectile-like nucleus (PLN), as it is shown in Ref. [1].

# 3 RESULTS

## 3.1 Inclusive events

Figure 3.1 shows the PLN excitation energy distribution ($E^*_{PLN}$) for the Au target compared to those obtained for the same target at lower bombarding energies [7]. The spectra are normalized to the

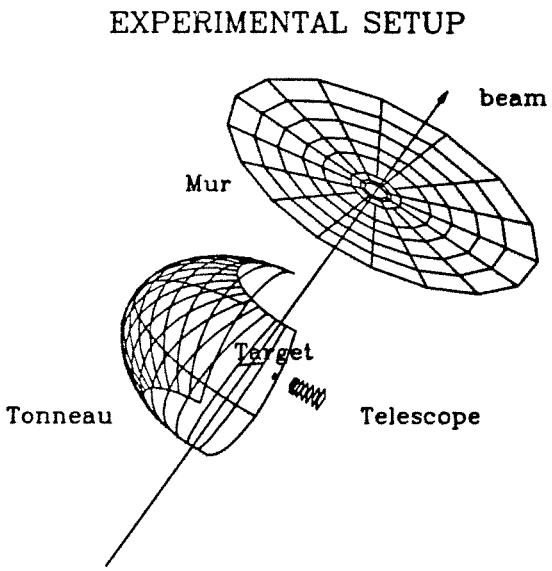


Figure 1: Global view of the experimental setup

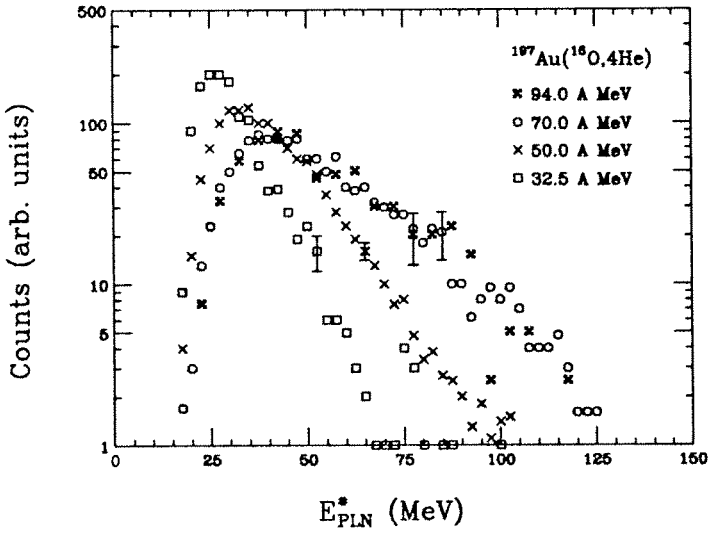


Figure 2: Experimental excitation energy distributions of the primary projectile-like nucleus for the breakup process $^{16}O \rightarrow 4He$ in the reaction $^{16}O + ^{197}Au$ at different bombarding energies. The data at 32.5, 50 and 70 MeV/nucleon come from Ref. 7. The data at 94 MeV/nucleon come from Ref. [1].

same number of counts. The shape of the spectrum taken at 94 MeV/nucleon is very similar to that of the spectrum taken a 70 MeV/nucleon both in slope and location of the maximum. $E^*_{PLN}$ mean values show a slight increase with the incident energy going from 30 MeV at 32.5 MeV/nucleon [7] to 53 MeV at 70 MeV/nucleon [7]. The value of $54 \pm 2$ MeV at 94 MeV/nucleon is equal, within the statistical uncertainties, to that observed at 70 MeV/nucleon, revealing a saturation of the excitation energy which can be stored in such a projectile, for the observed disassembly channel. This effect has been found to be independent of the target mass and its presence is confirmed also in efficiency-corrected data, as it is shown with more details in Ref. [1]. The experimental data have been also submitted to an event-by-event analysis performed to extract some global variable distributions that could describe the entire fragmenting system and investigate the process time scale [1]. Figures 3.1 and 3.1 show the distributions of the events in the coplanarity-sphericity plane (functions of the eigenvalues of the kinetic flow tensor) and on the relative angle axis [1], respectively. In both figures experimental data are

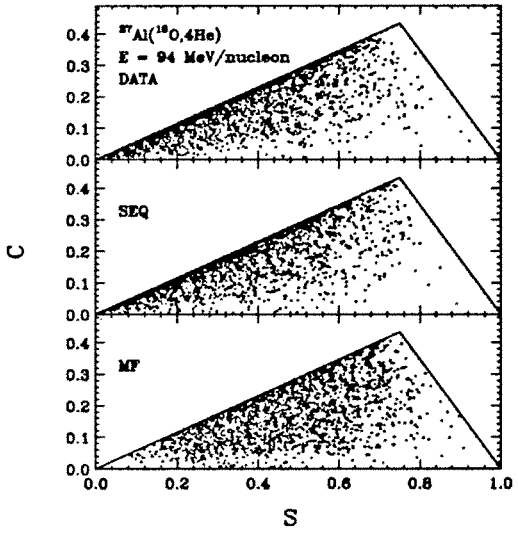


Figure 3: Comparison between the experimental and the simulated SEQ and MF sphericity-coplanarity distributions for the reaction $^{16}O+^{27}Al \rightarrow$ 4He at 94 MeV/nucleon [1].

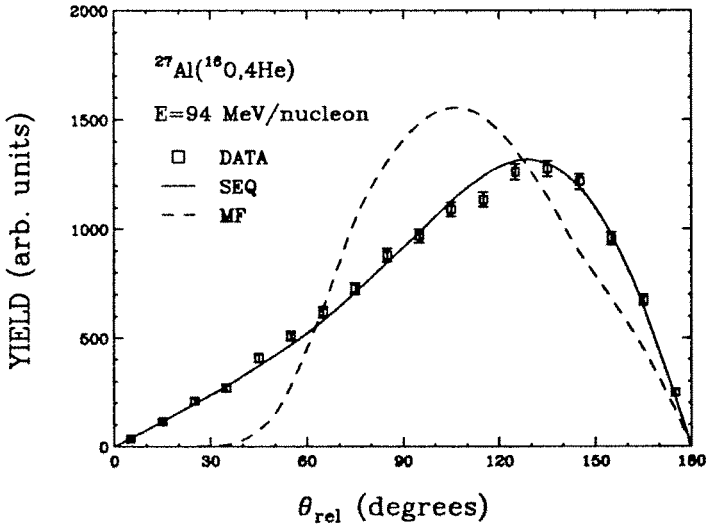


Figure 4: Relative angle distribution for the reaction $^{27}$Al($^{16}$O,4He) at 94 MeV/nucleon. The full and dashed curves indicate the results of SEQ and MF simulations [1], respectively.

compared with the results of Montecarlo simulations based on sequential (SEQ) and multifragmentation (MF) mechanisms [1]. Wichever global variable is taken into account, the experimental distribution is closer to a sequential-emission picture than to a multifragmentation one.

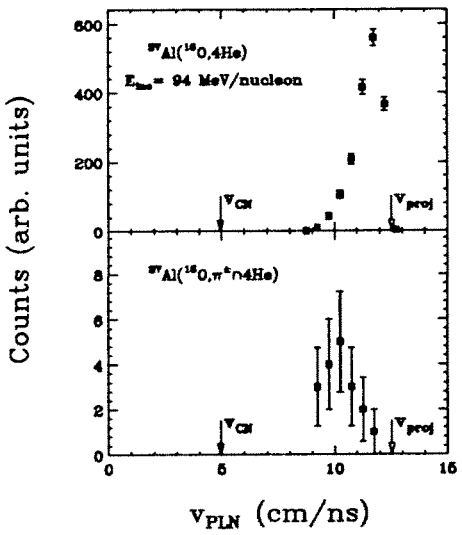


Figure 5: Projectile-like nucleus velocity distributions for 4-He inclusive breakup events (upper part) and for coincidence ones (lower part) [1]. In each plot right and left arrows indicate the projectile velocity and the compound nucleus velocity, respectively.

### 3.2 Exclusive events

Figure 3.2 shows the distribution of the projectile-like velocity ($v_{PLN}$), defined as that of the center of mass of the four He ions detected in each event, for inclusive (4He; upper part) [1] and coincidence events ($\pi^{\pm}\cap$4He; lower part) [2]. The inclusive velocity distribution has the usual shape observed in projectile fragmentation at the intermediate energies. The net effect of charged pion detection in coincidence with four He ions is the shift of the velocity spectrum to lower values. The peaks of the PLN velocity spectra are shifted by about 1.5 cm/ns which is, at these velocites, more than five times the velocity indetermination due to the experimental uncertainties. This corresponds to a projectile energy loss of 200-250 MeV, large enough to produce a charged pion in the measured kinetic energy range. So, by detecting all projectile breakup fragments inclusively and in coincidence with pions and measuring their velocities, we are able to select for the first time a well defined class of events in which the total pion energy is provided by the coherent slowing down of the projectile [2].

## References

[1] A. Badalà, R. Barbera, A. Palmeri, G. S. Pappalardo, F. Riggi, Phys. Rev. C **48**, 633 (1993) and references therein.

[2] A. Badalà *et al.*, Phys. Lett. B **316**, 240 (1993).

[3] G. Bizard, A. Drouet, F. Lefebvres, J. P. Patry, B. Tamain, F. Guilbault, C. Lebrun, Nucl. Instrum. Methods A **244**, 483 (1986).

[4] A. Peghaire *et al.*, Nucl. Instrum. Methods A **295**, 365 (1990).

[5] V. Bernard *et al.*, Nucl. Phys. A **423**, 511 (1984).

[6] A. Badalà *et al.*, Phys. Rev. C **43**, 190 (1990).

[7] J. Pouliot *et al.*, Phys. Lett. B **263**, 18 (1991).

# Statistical signatures of the quasi-projectile breakup at 70A MeV

D. Doré[1], L. Beaulieu[1], R. Laforest[1], J.L. Laville[2], O. Lopez[2], J. Pouliot[1], R. Régimbart[2], R. Roy[1], J.C. Steckmeyer[2], C. St-Pierre[1].

[1]Laboratoire de physique nucléaire, Département de physique, Université Laval, Sainte-Foy, QC, Canada, G1k 7P4

[2]ISMRA-Laboratoire de Physique Corpusculaire, Blvd Maréchal Juin, 14050 Caen Cedex, France

## 1. Introduction

The deexcitation of hot nuclei in the intermediate energy domain has been investigated in many works in order to obtain information on nuclear matter properties [1]. At these energies where low and high energy mechanisms compete, it is interesting to follow the evolution of a particular observable as a function of the bombarding energy. In the present work, we focus on the source thermalization and look for statistical signatures at 70A MeV, near the end of the intermediate energy domain. Source identification is an important basis for this search ; the projectile-target system and the configuration of the experimental setup are selected accordingly. In this report peripheral collisions in the $^{24}Mg$ + $^{197}Au$ reaction at 70A MeV are studied although the experiment has been done also at 50A MeV. The quasi-projectile breakup cross sections are measured and the excitation energy distributions reconstructed. Entrance channel effects in transfer reactions are also investigated by comparing oxygen quasi-projectile formed by $^{16}O$ and $^{24}Mg$ beams on a gold target.

The experiment has been performed at GANIL in the reaction chamber Nautilus with an arrangement of 88 detectors : a phoswich array covering polar angles from 1.4 to 15°, a phoswich ring from 16 to 24° and two rings of thin time-of-flight scintillators from 25 to 38° [2]. Charges up to Z=12 were identified. The energy calibration has been achieved with secondary beams : a $^{24}Mg$ beam at 70A MeV was stopped in a thick target to produce particles of Z=1 up to Z=8, with several isotopes for each charge. Isotopes were then selected by a Br value corresponding to 2.06 T·m. Energy thresholds were of 14.5A MeV for protons and alphas and went up to 38.5A MeV for Z=12. A more detailed description of the experimental setup will be presented elsewhere [3]. With such a setup covering almost totally the angular region from 1.4 to 38° for all azimuthal angles, fragments emitted from a rapid source were efficiently detected and therefore sources could be clearly identified. Also the good granularity of the system permitted the detection of high multiplicity events.

## 2. Quasi-projectile breakup

The quasi-projectile breakup events were selected by imposing a condition on the total charge detected. The breakup of quasi-projectiles can lead to many exit channels. All deexcitation possibilities for a given charge combination contributed to the same exit channel. For example, $^{23}Na$-$^{1}H$, $^{22}Na$-$^{2}H$, $^{22}Na$-$^{1}H$-n, etc. were included in the same exit channel Na-H, for the study of the projectile fragmentation with the condition $\Sigma Z=12$. We have also grouped channels where one $^{8}Be$ (two $^{4}He$ in the same detector are considered like a $^{8}Be$) or two $^{4}He$ were present [4].The least negative separation energy (Q-value) of all isotopic combinations of a given channel was attributed to that channel. With the charge, the energy, the position and the Q-value, it was possible to reconstruct the quasi-projectile velocity and build excitation energy spectra of the quasi-projectile [4] in an event-by-event analysis. The excitation energy spectrum of the Mg is presented in fig. 1a. It can be seen that even for peripheral collisions, high excitation energies are reached [5,6].

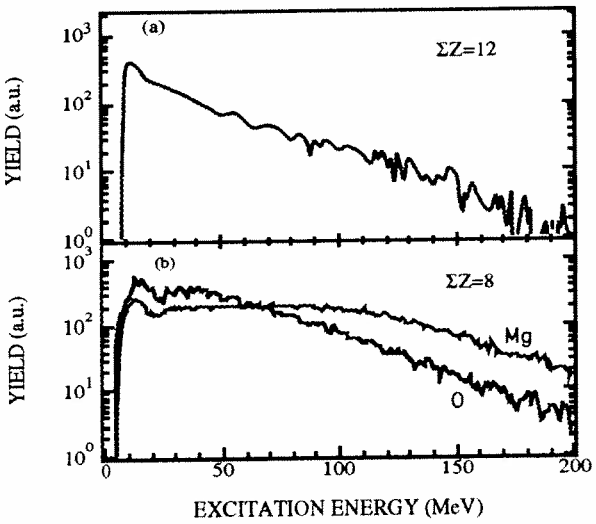


Fig.1. (Above) Excitation energy spectra. Projectile ($\Sigma Z=12$) excitation energy distribution in (a) shows that even for peripheral collisions, high excitation energies are reached. In (b) excitation energy distribution for an excited oxygen produced by a $^{24}Mg$ beam and a $^{16}O$ beam on gold target. The contribution of the exit channel N+H is not included.

Fig.2. (Right) Cross sections versus the least negative Q-value for each channel. Statistical calculated yields (circles) and experimental fragmentation cross sections (full squares) are shown in a. The breakup absolute cross sections of an excited oxygen produced by a $^{24}Mg$ beam (full symbols) are compared with the yields produced with a $^{16}O$ beam (open symbols) using a full (b) and a partial ($60<E^*<80$) excitation energy distribution (c). Curves with full symbols in (a) and (b) are absolute cross sections. Other curves are arbitrarily normalized.

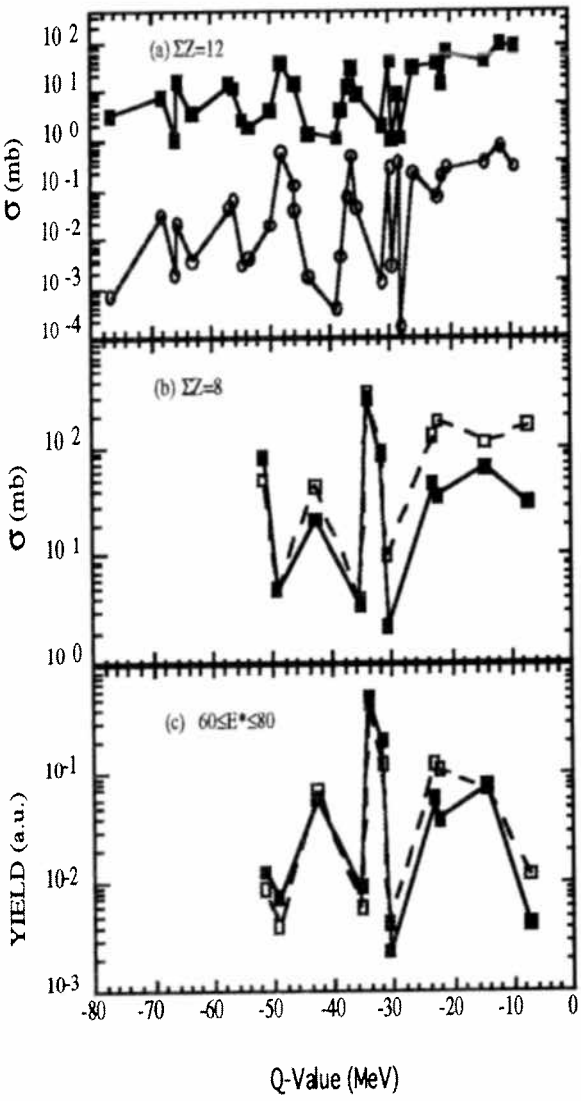


A total detected charge of 12, equal to the beam charge, was requested to select a quasi-elastic reaction. This condition yielded 64 different exit channels. The requirement on the total charge was sufficient to isolate a given quasi-projectile with a good precision. The energy of the particles emitted by the target is below detector thresholds, but particles coming from an intermediate velocity source or emitted prior to equilibrium might pollute peripheral data. A severe condition on the particle velocity, a minimum of 64% of the beam velocity known to eliminate a great part of these events [7,8], brings no significant changes to the results presented here. The breakup channel cross sections have been measured and corrected for detection efficiencies. Exclusive angular distributions have been used to calculate these detection efficiencies for charges 1 to 11. By assuming that the angular distribution of a particle is independent of the exit channel [4], the channel detection efficiency is obtained from the product of efficiencies for each charge composing that channel. Corrected cross sections for the 31 most abundant exit channels are presented as a function of Q-values in fig. 2a (squares). The general trend of the cross section is to decrease with increasing separation energy (more negative Q-value), as obtained with $^{16}O$ projectiles [5,6,9], but the fluctuations are larger with the $^{24}Mg$ projectile. These fluctuations can be attributed to the number of isotopic combinations included in each exit channel [5-6]. The number of combinations is partially dependent of the nucleus stability composing a channel [10].

The experimental cross sections were compared with the predictions of the statistical code Brandex [11]. This code, based on the experimental quasi-projectile excitation energy distribution, deexcites the source through a sequential binary process. It provides the relative breakup channel cross sections presented in fig. 2a (circles). The similarities between the experimental and calculated results seem to indicate the statistical nature of the quasi-projectile deexcitation. So, even at 70A MeV where the collision time is short and excitation mechanisms fast, it appears that the quasi-projectile reaches equilibrium before breakup. A similar observation has already been made with a different approach [12].

## 3. Transfer reactions

It has already been shown that transfer reactions are still present at 60A MeV [13]. Charge transfers from quasi-projectile to target can be studied by selecting a total charge smaller than 12. It was particularly interesting to observe an excited oxygen because many results are available for this source. A total charge of eight has therefore been selected. Corrected exit channel yields as a function of Q-value are presented in fig. 2b (full symbols) for this quasi-projectile. The probability that a particle misses the detection system is low and contamination from higher charge quasi-projectiles does not contribute in a significant way to the results. For example, contamination from incompletely detected $\Sigma Z=12$ events in $\Sigma Z=8$ events is only 10%. It is also clear in fig. 2b that most of $\Sigma Z=8$ events come from real transfer reactions since the total cross section is larger than in fig. 2a for quasi-elastic reactions.

Transfer reaction cross sections obtained for the $\Sigma Z=8$ quasi-projectile with the $^{24}Mg$ beam are compared, in fig. 2b (full symbols), to the equivalent quasi-elastic cross sections in $^{16}O+^{197}Au$ at 70A MeV (open symbols) [5]. The cross sections present a similar pattern. Comparable observations have been made for other quasi-projectiles [2], but with different beam energies. Similarities between breakup channel yields for an excited oxygen produced by two different beams have also been noticed for quasi-elastic and pickup reactions [14]. In fig. 2b, in spite of different quasi-projectile production processes, no strong differences in the relative yields are seen for the same beam energy.

Excitation energy distributions produced from the two different processes are different (fig. 1b). Some characteristics in one spectrum might compensate some particularities in the other spectrum to produce similar relative cross sections. It was therefore important to verify the agreement between the curves of fig. 2b. To achieve that, we have selected a range in the excitation energy spectra. The excitation energy region from 60 to 80 MeV, where the curves were rather regular (see fig. 1) and possible exit channels abundant, has been selected. The effect of this selection can be seen in the cross sections presented in fig. 2c. The relative cross sections are the same for both sources, showing very similar variations with Q-value, although their formation was different. This result has also been obtained by selecting energy regions from 40 to 60 and 80 to 100 MeV. It appears that the decay of the quasi-projectile is not influenced by the way it has been formed. This is another indication that quasi-projectiles were thermalized and their decay was statistical.

## 4. Decay probabilities

Another approach to verify whether thermal equilibrium is reached in the quasi-projectile has been suggested by Moretto et al. [15]. They look at the relation between the logarithm of the ratio of n-fold ($P_n$) to the 2-fold probability ($P_2$) as a function of $E^{-1/2}$ where E is the excitation energy. Considering that the decay probability is proportional to the level density, they concluded that the dependence between the logarithm of the ratio of decay probabilities ($\ln(P_n/P_2)$) and $E^{-1/2}$ will be linear if the decay is statistical. In particular, this relationship has been applied to the decay of an excited oxygen into four-alpha particles [16] and showed its statistical nature. We followed this approach to study two excited nuclei produced in quasi-elastic and transfer reactions : magnesium and oxygen both formed in the reaction $^{24}Mg + ^{197}Au$. Results are shown in figs. 3a and 3b. The

linear dependence is observed and confirms that the disintegration is governed by the available phase space.

## Conclusion

In summary, projectile breakup and transfer reaction events have been selected in the $^{24}Mg$ + $^{197}Au$ reaction and their excitation energy distributions deduced. Exit channel cross sections have been measured. The relation between breakup channel yields and Q-values seems to indicate a source thermalization to a high degree both for projectile breakups and transfer reactions. For the latter case, no entrance channel effects have been observed. These observations have been reinforced by the linearity observed between the logarithm of $(P_n/P_2)$ and $E^{-1/2}$. We can then conclude that even at 70A MeV, close to the high energy limit of the intermediate energy domain, the sources studied are thermalized and their deexcitation is mainly governed by the available phase.

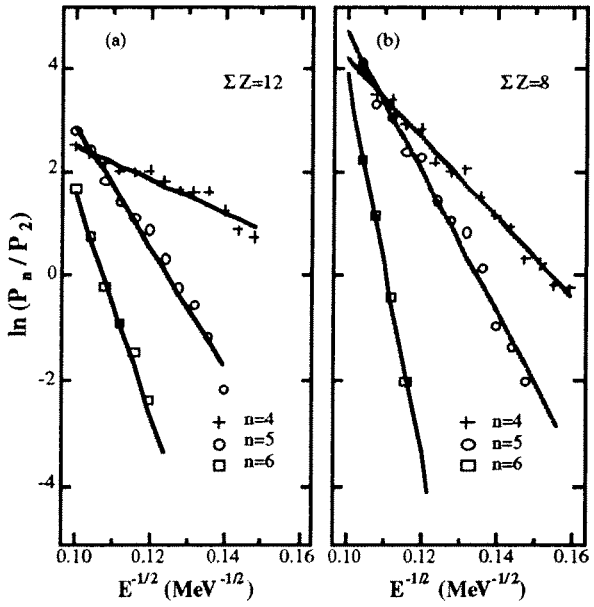


Fig.3. Logarithm of $P_n/P_2$ versus $E^{-1/2}$. Quasi-elastic events (a) and transfer reaction events (b) give both a linear relation which indicate the statistical nature of deexcitation.

## References


[1] B. Tamain, Proceedings of the International School of Physics Enrico Fermi, Course CXII 1989, edited by C. Detraz and P. Kienle (Italian Physical Society, North-Holland,1991) 1.
[2] L. Beaulieu et al., Compilation GANIL (1989-91) 106, unpublished.
[3] D. Doré, Ph. D. Thesis, to be presented at Laval University
[4] J. Pouliot et al., Phys. Rev. C43 (1991) 735.
[5] J. Pouliot et al., Phys. Lett. B 263 (1991) 1.
[6] R. Laforest et al., accepted for publication in Nucl.Phys. A
[7] A. Badala et al., Phys. Rev. C48 (1993) 633.
[8] R.J. Charity et al., Phys. Rev. C46 (1992) 1951.
[9] D. Doré et al., Nucl. Phys. A 545 (1992) 363c.
[10] B. Harvey et al., Phys. Rev. C45 (1992) 1748.
[11] T. Knop et al., LBL-Report 26439 (1988), unpublished.
[12] M.I. Adamovitch et al., Phys. Rev. C40 (1989) 66.
[13] J.C. Steckmeyer et al., Nucl. Phys. A500 (1989) 372.
[14] R.G. Stokstad et al., XX International Summer School on Nuclear Physics (1988).
[15] L.G. Moretto et al.,Prog. Part. Nucl. Phys. Vol. 30 (1993) 135.
[16] J. Pouliot et al., Phys. Rev. C48 (Nov. 1993) 2514.

# Angular momentum transfer in the $^{208}Pb+^{197}Au$ reaction at 29 A.MeV

S. BRESSON, M. MORJEAN, E. CREMA, J. GALIN, D. GUERREAU, C. PAULOT, J. POUTHAS
*GANIL, BP 5027, 14021 Caen Cedex, France*

B. GATTY, D. JACQUET
*I.P.N., BP 1, 91406 Orsay Cedex, France*

E. PIASECKI, A. KORDYASZ
*Inst. of Exp. Phys., Warsaw Univ, Hoza 69, 00-681 Warsaw, Poland*

J. JASTRZEBSKI, L. PIENKOWSKI, W. SKULSKI
*Heavy Ion Lab., Warsaw Univ., ul. Banacha 4, 02-097 Warsaw, Poland*

B. LOTT
*C.R.N., BP 20 CRO, 67037 Strasbourg Cedex, France*

R. BOUGAULT, J. COLIN, A. GENOUX-LUBAIN, D. HORN, C. LEBRUN, J.F. LECOLLEY, M. LOUVEL
*L.P.C., Bd Marechal Juin, 14032 Caen Cedex, France*

B. QUEDNAU, W.U. SCHROEDER, J. TOKE
*Univ. of Rochester, Rochester, NY,14627, USA*

U. JAHNKE
*Hahn Meitner Institut, D1000 Berlin 39, Germany*

The reaction mechanisms involved in nuclear reactions induced by heavy-ion projectiles at intermediate velocities (a few tens of MeV per nucleon) are yet not well understood. No clear signature of the expected transition between the low energy domain in which one body dissipation mainly occurs and the high energy domain in which two body interactions are dominant has been found: large amounts of excitation energy are thermalized in the two partners of peripheral reactions induced in this energy range[1,2] and even for incident energies up to 200 A.MeV[3,4]; rather large excitation energies are measured even in very peripheral collisions for which the net nucleon transfers between the projectile and the target nuclei remain small. The amount of angular momentum transferred in intrinsic spin of the projectile- and target-like nuclei as well as the spin alignment are then a crucial piece of information for understanding the reaction mechanism: in a one body dissipation picture, large spins, strongly aligned along a direction perpendicular to the reaction plane, are expected whereas, in a two body dissipation picture, smaller spins are expected as well as weaker alignments. The persistence of large spin effects in the $^{208}Pb+^{197}Au$ reaction at 29 A.MeV has been previously reported after a careful study of the characteristics of the projectile-like fragment (PLF) fission fragments[5]. In this report, quantitative estimates of the transferred spins will be given as a function of excitation energy of the fissioning PLF.

Fission fragments of the PLF were detected between 6° and 20° by two silicon strip detectors, providing us with the emission angle, the atomic number and the energy of one of the two fission fragments. The associated neutron multiplicity $M_n$ was measured by Orion, a $4\pi$ neutron detector. More detail on the experimental set-up can be found in refs.[5,6]. Binary fission events have been unambiguously identified for $M_n<35$. For higher neutron multiplicities, it has not been possible to distinguish binary fission events, if any, from more complex events. The main characteristics (atomic number, velocity, excitation energy and deflection angle) of the fissioning PLF's have been deduced on the average for 3 $M_n$ bins corresponding to average PLF excitation energies E* = 82, 165 and 255 MeV. Using these average characteristics, a Monte-Carlo simulation has been performed taking into account the effect of the spin on the angular distributions of the fission fragments[7]:

$$W(\theta) \alpha \exp(p \cos^2\theta)$$

with: $$p = \frac{J^2}{2 K_0^2} \quad \text{and} \quad K_0^2 = \frac{T I_{eff}}{\hbar^2}$$

where J is the angular momentum of the fissioning PLF (J is supposed to be totally aligned along a direction perpendicular to the reaction plane), T is the PLF temperature at the saddle point and $I_{eff}$ its effective moment of inertia. In the following, we shall first find the p values that give the best fit to the data, then we shall deduce the initial spins of the PLF's with some assumptions on the deexcitation step.

Fig.1 shows the results of these simulations, filtered by the detection capability (energy thresholds, angular resolution and opening of the detectors), for a fission fragment with Z=40 and with 14<Mn<25 (E* = 165 MeV) and for 5 different p values. The experimental data are also presented for the comparison in the middle lower part of Fig.1. The quantity S represents the sum between 9° and 20° of the Galilei-invariant cross sections.

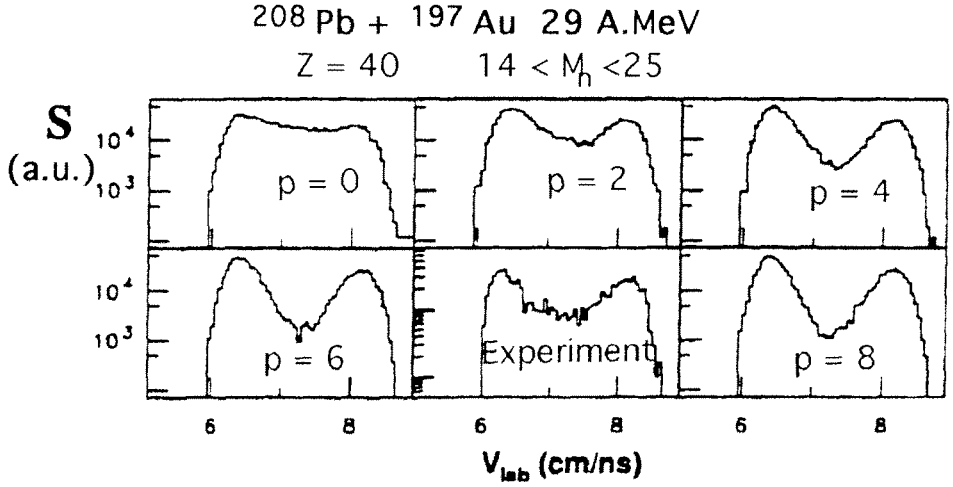


*Fig.1*: Comparison between the experimental data and the results of simulations for 5 different p values. S represents the sum between 9° and 20° of the galilei invariant cross sections.

The p values deduced from these simulations correspond to the minimum p values in agreement with the data. They are given as $p_{min}$ in table 1. In order to get more realistic p values, fluctuations around the PLF average velocities and deflection angles (that have been determined in 3 $M_n$ bins) have been taken into account in the simulations. Fluctuations around the average PLF velocities had only a very small

effect on the deduced p values, whereas fluctuations around the deflection angle lead to much larger effects. A constant 4.7° full-width-half-maximum value ($\sigma$=2°) for the deflection angle distributions has been adopted following the data by Lecolley et al.[8], for the 3 bins in $M_n$ considered. The p values $p_{fluct}$ obtained by taking into account these distributions are given in Table 1.

| E* (MeV) | $P_{min}$ | $P_{fluct}$ |
|---|---|---|
| 82 | 2.0 | 4.0 |
| 165 | 2.5 | 5.0 |
| 255 | 3.4 | 5.5 |

*Table 1*: E* is the PLF excitation energy.

The PLF temperature as well as the effective momentum $I_{eff}$ are defined within this model at the saddle point for fission. In order to get a minimum value $J_{min}$ of the aligned component of the angular momentum, the temperature has been assumed to be that predicted at the scission point from the systematics by Hilscher et al.[9]. The $J_{min}$ values presented as full dots in Fig. 2 have been calculated assuming $K_0^2 = 100\ \hbar^2$ (corresponding roughly to liquid drop model predictions and in agreement with the systematics of Dyer et al.[10]). These $J_{min}$ values remain smaller than 35 $\hbar$ even for the largest PLF excitation energy. The angular momentum actually transferred to the PLF during the interaction is much larger than these $J_{min}$ values since evaporation prior to fission removes a large amount of angular momentum. As an example, for the largest PLF excitation energy, 30 neutrons are detected on the average. After correction for detection efficiency and assuming an equal sharing of the emitted neutrons between the projectile- and the target-like fragment (this assumption is realistic on the average for this almost symetrical system), 22 neutrons are found to be emitted by the PLF. Hence, according to Hilscher et al.[9], 17 neutrons are evaporated by the PLF prior to scission. As a rough estimate of the evaporation effect, all these pre-scission neutrons have been supposed evaporated before the PLF reaches the saddle point and the emission of each of them has been supposed to decrease the total angular momentum by $1.5 \pm 0.5\ \hbar$. The resulting spins after correction are given in Fig.2 as triangles, the error bars corresponding to the uncertainty on the angular momentum removed by each neutron. With these assumptions, the PLF angular momenta reach $59 \pm 9\ \hbar$ for the most dissipative collisions leading to binary fission.

Spin values deduced from fission fragment detection confirm that, for the $^{208}Pb+^{197}Au$ reaction at 29 A.MeV, a one body dissipation process still plays an important role. Accurate determination of spin for the most central collisions leading to binary fission requires a good knowledge of both the time scale for the fission process (time needed to move from the saddle point to the scission point) and of the time scale for the evaporation process (time needed to decrease the initial spin by particle evaporation). In any case, the amount of transferred angular momentum increases when the impact parameter decreases ($M_n$ increases) as expected from Landau-Vlasov simulations[6,11] that predict intrinsic angular momenta as large as 100 $\hbar$ for the PLF. However, for these latter high spin values, high excitation energies are involved and the PLF might not undergo pure binary fission anymore. In that case, a large part of the spin could be removed rapidly either by alpha particle emission or by intermediate mass fragment emission.

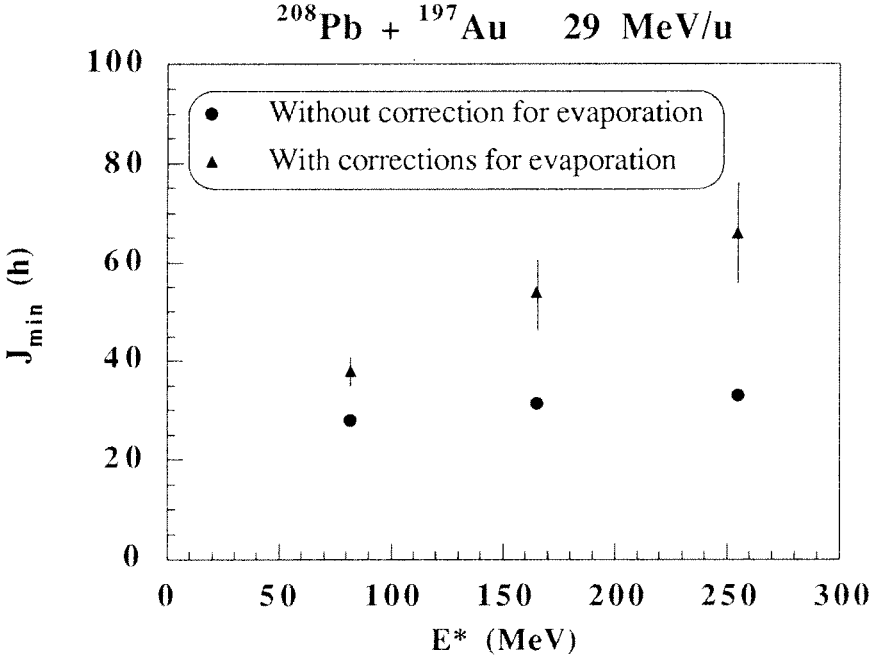


*Fig.2*: Intrinsic spin of the PLF as a function of its excitation energy

## *References*


1- M. Morjean et al., Nucl. Phys. A529 (1991) 179
2- J.C. Steckmeyer et al., Nucl. Phys. A500 (1989) 372
3- C. Stephan et al., Phys. Lett. B262 (1991) 6
4- B. Quednau et al., to be published
5- S. Bresson et al., Phys. Lett. B294 (1992) 33
6- S. Bresson, thesis Université de Caen 1993
7- See for example R. Vandenbosch and J.R. Huizenga, Nuclear Fission (Academic Press, 1973) 179 and ref therein
8- J.F. Lecolley et al., submitted to Phys. Lett. B
9- D. Hilscher et al., Phys. Rev. Lett. (1989) 1099
10- P. Dyer et al., Nucl. Phys. A322 (1979) 205
11- F. Sebille et al., to be published

# B2 - DISSIPATIVE COLLISIONS

# HOT NUCLEI WITH TEMPERATURE ABOVE 10 MEV PRODUCED IN Ar + Al COLLISIONS FROM 55 TO 95 MeV/u

S.C. Jeong[1-8)], D. Cussol[1)], J.C. Angélique[1)], G. Auger[2)], G. Bizard[1)], R. Brou[1)], A. Buta[1-a)], C. Cabot[2-c)], Y. Cassagnou[3)], E. Crema[1-b)], Y. El Masri[4)], Ph. Eudes[5)], Z.Y. He[7)], A. Kerambrun[1)], C. Lebrun[5)], R. Legrain[3)], J.P. Patry[1)], A. Péghaire[2)], J. Péter[1)], R. Popescu[1-a)], R. Regimbart[1)], E. Rosato[6)], F. Saint-Laurent[2)], J.C. Steckmeyer[1)], B. Tamain[1)], E. Vient[1)],

*1) LPC Caen, 14050 CAEN - FRANCE, 2) GANIL, 3) DAPNIA, CEN Saclay, 4) Institut de Physique Nucléaire, LOUVAIN-LA-NEUVE, BELGIUM, 5) Laboratoire de Physique Nucléaire, NANTES , 6) Dipartimento di Scienze Fisiche and INFN, NAPOLI, 7) Institute of Modern Physics, LANZHOU , CHINA, 8) Department of Physics, Soongsil University, SEOUL, KOREA, a) Permanent address : I.F.A., Heavy Ion Department, BUCHAREST, ROMANIA, b) Permanent address : Inst. di Fisica, Univ. de SAO PAULO, BRAZIL, c) On leave of absence from IPN ORSAY, France*

## 1 - MOTIVATIONS

One of the open questions related to the formation of hot nuclei in nucleus-nucleus collisions is the determination of the amount of energy which has been thermalized. This is obtained by determining the mass A, the excitation energy $E^*$ and the temperature T of the system. At high excitation energies the relation between T and $E^*$ has not yet been established and one must measure separately $E^*$ (or $E^*/A$) and T. This can be done only via exclusive measurements. We have already performed similar measurements for $^{40}Ar + ^{27}Al$ reactions at energies ranging from 25 to 65 MeV/u[1)]. We present here the results of temperatures measurements for the $^{36}Ar + ^{27}Al$ system at incident energies of 55, 67, 79, 86 and 95 MeV/u.

## 2 - EXPERIMENTAL SET-UP AND IMPACT PARAMETER SORTING

The experiments were performed in the reaction chamber Nautilus with the complementary multidetector systems MUR and TONNEAU : see fig. 1. The improvement relative to ref. 1 was the addition of 7 large solid angle silicon telescopes installed 60 cm from the target and covering polar angles from 3° to 30°.

A minimum bias trigger was used in which all events with a multiplicity larger than 1 were recorded. The first step in the analysis was to select the events in which sufficient information was collected. This was achieved by requiring that the total parallel momentum be above 60 % of the projectile linear momentum (the average value is ~85 %). The global variable used for the impact parameter sorting was the total tranverse momentum $P_\perp$, which selects the most dissipative collisions without contamination from other events.

## 3 - RESULTS

As in ref 1, invariant cross section maps $d_2\sigma / \beta_\perp d\beta_{//} d\beta_\perp$ exhibits three sources of particles. Since all the products of the "fast" source have velocities well above the detection threshold, we can study these nuclei. An improvement relative to ref. 1 was to select those events in which the heaviest fragment is detected in a telescope, thus ensuring a good kinematical reconstruction of the excited primary nucleus. The source velocity vector was reconstructed for each event from the momentum vectors of its products with $Z \geq 2$. A cut on $\beta$ // around $\beta$cm eliminated most pre-equilibrium particles and retained most of the products from the primary nucleus.

One can now plot the distribution of particles versus their velocity components in the *frame of the primary nucleus* (f.p.n.) : fig. 2 at 55 MeV/u (they are quite similar at the other energies). At negative $\beta_{//}$ values, the pre-equilibrium "mid-rapidity" component adds up for light products. The angular distribution of Z = 2 particles (mostly $\alpha$-particles) in the f.p.n. is displayed in fig. 3. Below 90°, the distribution is flat for central collisions and gradually evolves towards a 1/sin $\theta$ distribution as the angular momentum of the primary nucleus increases with increasing impact parameter ; the kinetic energy distributions are independent of angle. These features are in agreement with de-excitation from thermally equilibrated nuclei.

The apparent temperature $T_{app}$ as a function of the impact parameter and incident energy is displayed in fig. 4. Temperatures around 9 MeV are reached at 55 MeV/u and increases to more than 11 MeV at 95 MeV/u. The initial temperatures are even larger, but how can a nucleus - or at least an equilibrated system - live long enough and reach thermal equilibrium as indicated by isotropic decay ? Above T = 5 MeV, the average decay time calculated in the framework of the statistical theory is below $10^{-22}$s [1] which implies that the time needed to thermalize the excitation energy would be below $10^{-22}$s.

## 4 - CONCLUSIONS

Hot nuclei with masses A ~35 in thermal equilibrium are found to be formed at all incident energies and impact parameters. The temperature of these nuclei increases slowly but steadily with the incident energy ; no saturation is observed in the present energy range. In central collisions, it reaches more than 10 MeV, implying that thermal equilibrium is reached very quickly and that light nuclei can sustain higher temperatures than heavy ones.

**REFERENCES :** D. Cussol et al, Nucl. Phys. A561 (1993) 298

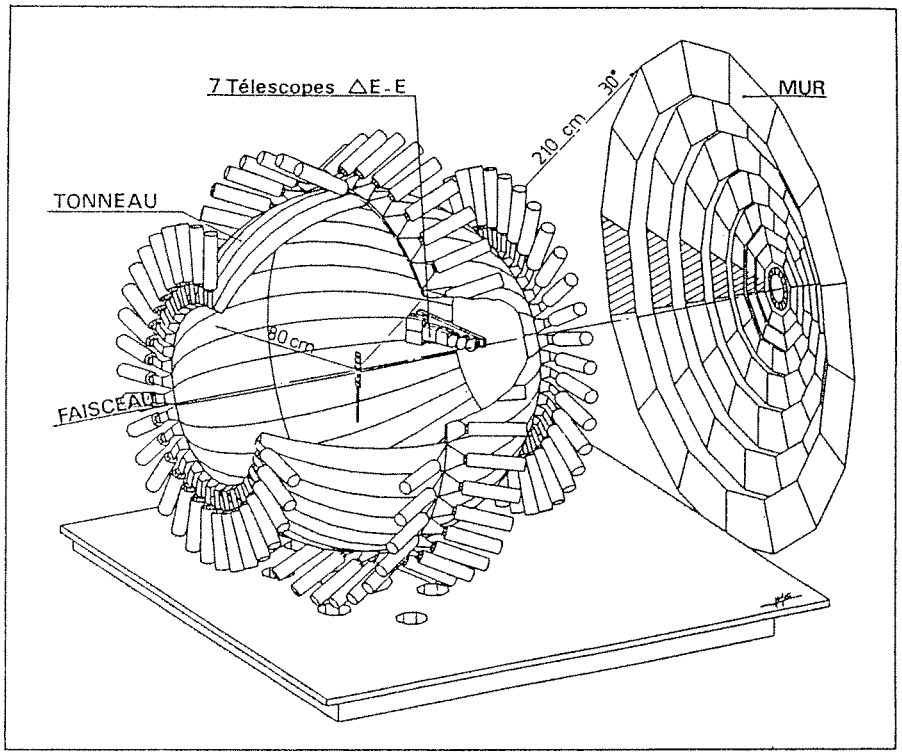


Fig. 1 : Experimental set-up

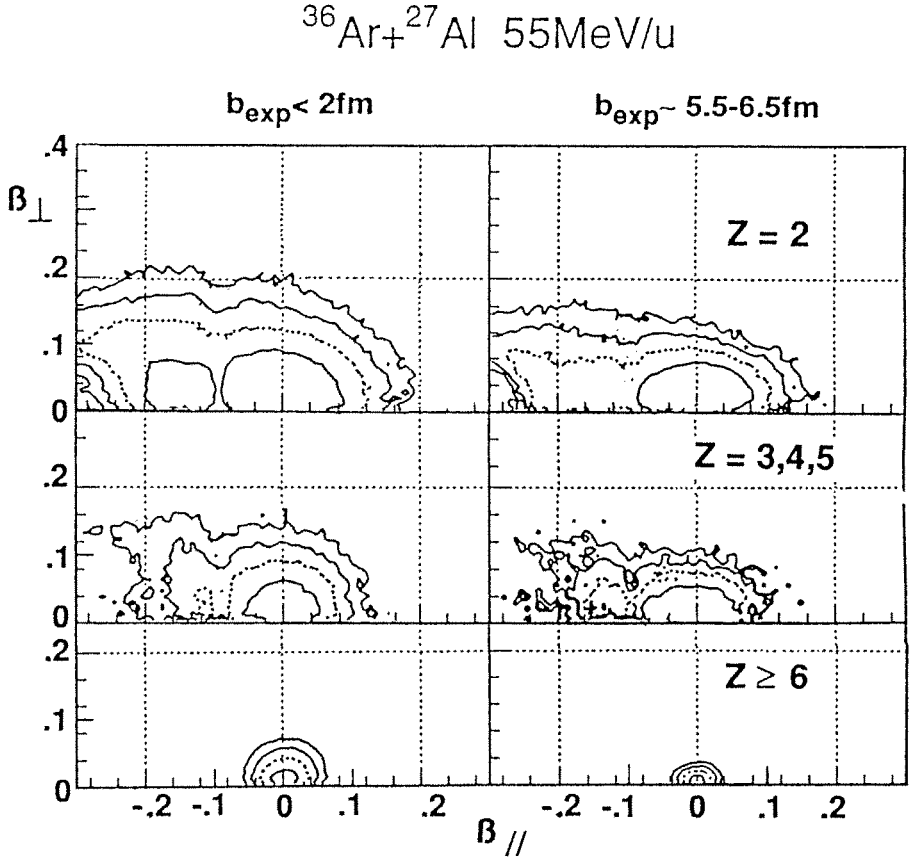


Fig. 2 : Contour plots of $d^2N / \beta\perp \, d\beta \, // \, d\beta_\perp$ in the reference frame of the reconstructed primary nucleus for central collision and semi-peripheral collision events. The plot for Z = 1 is very similar to Z = 2.

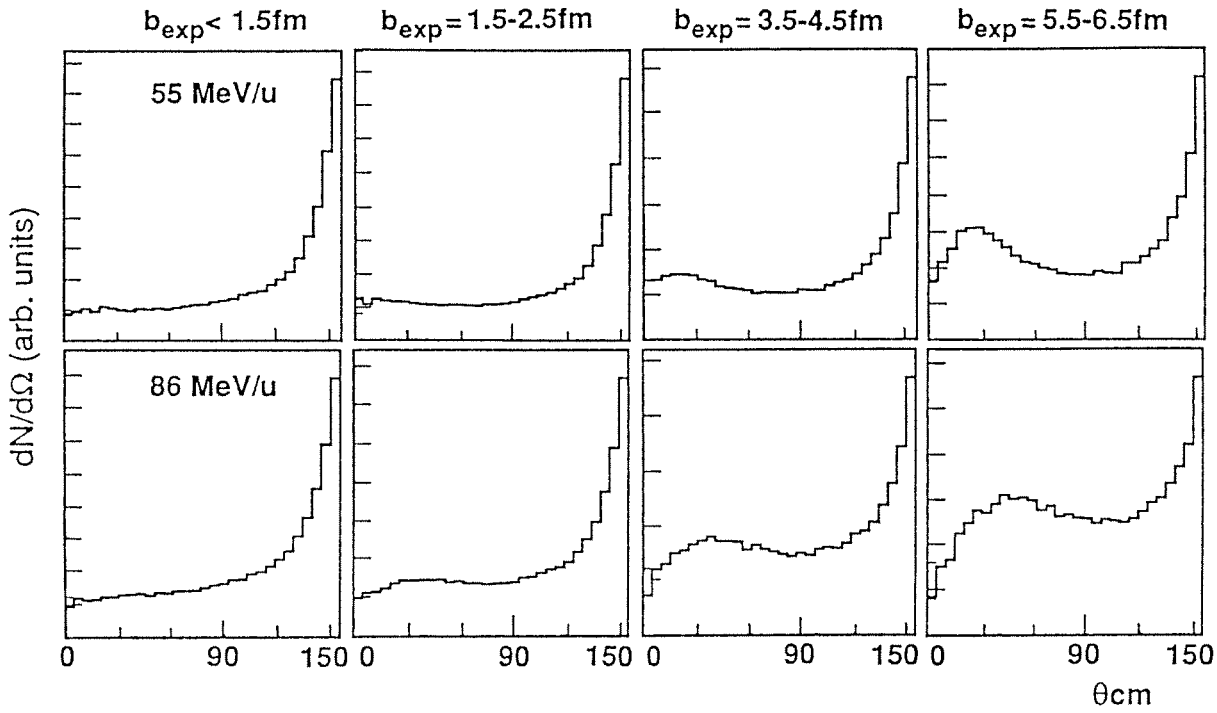


Fig. 3 : Angular distributions of Z = 2 particles (mostly α particles) in the frame of the primary nucleus at 55 and 86 MeV/u. The decrease near 0° is due to the 3.2° hole at forward laboratory angles,enlarged in the f.p.n . The increase at backward angles is due to the contributions from mid-rapidity particles and target-like emission.

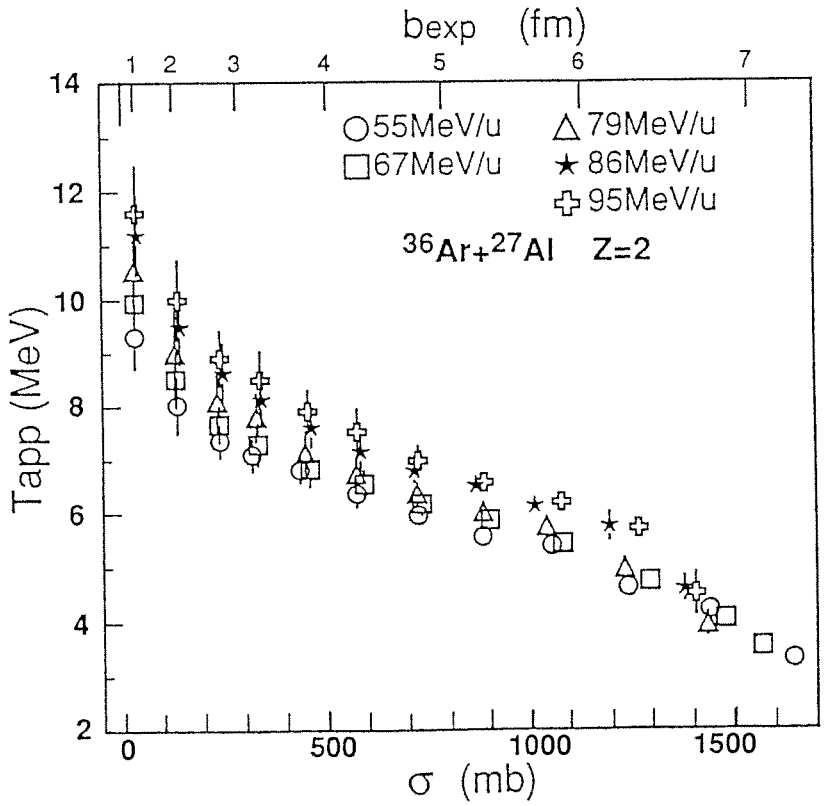


Fig. 4 : Apparent temperature of the equilibrated nuclei as a function of the impact parameter (top scale) at incident energies 55, 67, 79, 86 and 95 MeV/u. For clarity not all error bars are drawn. The grazing impact parameter value is ~8 fm. The bottom scale represents the cross section integrated from b $_{exp}$ = 0 to b $_{exp}$ ($\sigma = \pi\ b_{exp}^2$).

# THE GIANT DIPOLE RESONANCE IN VERY HOT NUCLEI

J.H. Le Faou[a], T. Suomijärvi[a], Y. Blumenfeld[a], P. Piattelli[b], C. Agodi[b], N. Alamanos[c], R. Alba[b], F. Auger[c], G. Bellia[b,d], Ph. Chomaz[e], R.Coniglione[b], A. Del Zoppo[b], P. Finocchiaro[b], N. Frascaria[a], J.J. Gaardhøje[f], J.P. Garron[a], A. Gillibert[c], M. Lamehi-Rachti[a 1], R. Liguori-Neto[c 2], C. Maiolino[b], E. Migneco[b,d], G. Russo[b,d], J.C. Roynette[a], D. Santonocito[b], P. Sapienza[b] and J.A. Scarpaci[a]

(a) *Institut de Physique Nucléaire, $IN_2P_3$-CNRS, 91406 Orsay, France*
(b) *INFN - Laboratorio Nazionale del Sud, Via S. Sofia 44, 95123 Catania, Italy*
(c) *SEPhN, DAPNIA, CEA Saclay, 91191 Gif sur Yvette, France*
(d) *Dipartimento di Fisica dell'Università di Catania, Italy*
(e) *GANIL, BP 5027, 14021 Caen, France*
(f) *The Niels Bohr Institute, University of Copenhagen, DK-2100 Ø, Denmark*

Information concerning hot nuclei produced in heavy ion collisions has been gathered through very detailed measurements of their numerous decay products: light particles, intermediate mass fragments, fission fragments, and evaporation residues. Complementary information can be obtained from the study of the Giant Dipole Resonance (GDR) excited in these hot systems. This allows to probe the collective behavior of nuclei at extreme excitation energies, and, in particular, assess the limiting temperatures for collective motion in nuclear matter. The GDR has already been extensively studied for nuclei in the vicinity of A≈115 at moderate excitation energies[1]. At higher excitation energies ($E^*$ >300 MeV) experimental results are more fragmentary[2,3]. In order to pursue the study of the GDR at very high excitation energies ($E^* \approx$ 500 MeV), we have measured $\gamma$-rays emitted by hot nuclei formed in the $^{36}Ar + {}^{90}Zr$ reaction at 27 MeV/u bombarding energy.

Gamma-rays and LCPs were detected with the MEDEA multidetector[4], which consists of a ball built with 180 barium fluoride ($BaF_2$) crystals that covers the angular range between $30^o$ and $170^o$. Fusion-like residues were detected in two rectangular parallel plate avalanche counters (PPAC) covering between $6^o$ and $22^o$ on either side of the beam. The time of flight and energy loss information from these counters allowed to clearly distinguish fusion-like residues, of interest in the following, from projectile-like and target-like fragments. The trigger was given by one PPAC firing in coincidence with at least one $BaF_2$ detector. This requirement eliminates cosmic ray contamination of the $\gamma$ spectra.

Before studying the $\gamma$-spectra it is necessary to correctly characterize the emitting hot nuclei. This was done by combining the residue and the light charged particle measurements. The data have been sorted into three bins according to the ratio $v_R/v_{CM}$ between the velocity of the detected recoil and the velocity of the center of mass. The mean velocities of each bin are 0.52, 0.69 and 0.92 $v_{CM}$. According to the massive transfer model these correspond to excitation energies of 360, 480 and 630 MeV and to initial masses of 105, 113 and 122 respectively. To confirm these estimations, proton spectra were extracted for each velocity bin, for several angles covering between $69^o < \theta_{lab} < 160^o$, and analysed in terms of a moving source fit assuming an isotropic maxwellian surface emission. Only two sources, a compound nucleus-like source (CN) and an intermediate velocity source simulating pre-equilibrium emission, were necessary to fit the data over the angular range studied. The velocities of the CN source extracted from the fit for each bin are in good agreement with the measured residue velocities. The temperature

[1] On leave from University of Teheran, Iran.
[2] On leave from University of São Paolo, Brasil.

and proton multiplicity of the CN source increase with increasing residue velocity. However, this increase is stronger between the first two bins than from the second to the third. From the temperature of the CN source, excitation energies of 350, 500 and 550 MeV can be inferred for the three velocity bins. The combination of the residue and particle measurements clearly establish that increasing residue velocities correspond to increasing excitation energies and that hot nuclei with excitation energies well in excess of 300 MeV are populated in the reaction studied.

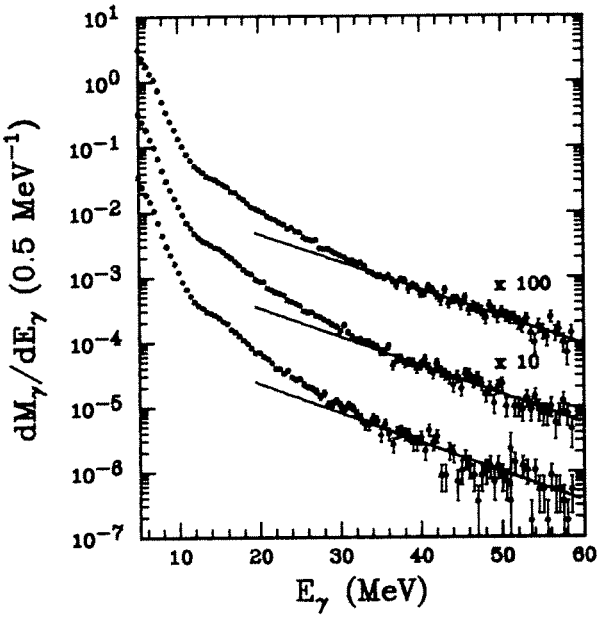


Fig. 1: Normalized gamma spectra measured for three excitation energy bins at 350 MeV, 500 MeV ($\times$10) and 550 MeV ($\times$100). The solid lines are a fit to the high energy component of the spectra ($E_\gamma > 35$ MeV).

Fig.1 shows gamma spectra measured at 90°, where the Doppler shift is negligible, in coincidence with fusion events for the three excitation energy bins, normalized over $4\pi$. One can notice the high statistics in the spectra up to $E_\gamma = 60$ MeV. The high energy photons are interpreted as due to the nucleon-nucleon bremsstrahlung during the initial stages of the collision process. This high energy $\gamma$ yield can be represented by an exponential function, fitted to the spectrum for $E_\gamma > 35$ MeV. The slope parameter for all three bins is $9.5 \pm 1.0$ MeV which is in good agreement with the known systematics[5]. Moreover, the high energy $\gamma$-yield increases with increasing residue velocity, in agreement with a simple geometrical picture in which the highest momentum transfers correspond to the most central collisions for which the number of primary nucleon-nucleon collisions is largest. At about 15 MeV, a pronounced bump can be seen. At this energy, $\gamma$-rays due to the direct decay of the GDR excited in a nucleus of mass around 115 are expected. Finally, at low energies, statistical $\gamma$-rays emitted by the compound nucleus at the end of its decay chain give rise to a steep exponential decay.

To investigate the evolution of the direct gamma decay from the GDR as a function of excitation energy, the bremsstrahlung component was subtracted from the spectra and the gamma multiplicity was integrated between 12 and 20 MeV corresponding approximately to the GDR region in the spectra. The integrated multiplicities are $(3.5\pm0.2)10^{-3}$,$(3.8\pm0.2)10^{-3}$, $(4.1\pm0.4)10^{-3}$ for 350, 500 and 550 MeV respectively. They increase only very slightly over the

excitation energy region populated in the reaction, and can even be considered constant within the error bars.

Statistical calculations using the code CASCADE were performed at different excitation energies assuming $E_{GDR} = 76.5 \times A^{-1/3} MeV$, $\Gamma_{GDR} = 12 MeV$, and $S_{GDR} = 100\%$EWSR, for the energy, width and strength of the GDR. The temperature dependent level density parameter from ref.[6] was used. The calculations were folded with the detector response. As an example, the calculation at 500 MeV is compared to the data in fig 2. Such standard CASCADE calculations clearly overshoot the data in the GDR region. Moreover, the calculated multiplicity increases strongly with excitation energy, in contrast to the experimental results. It should be noted that the choice of an other level density parameter can slightly change the calculated yields but does not affect the above conclusions[7].

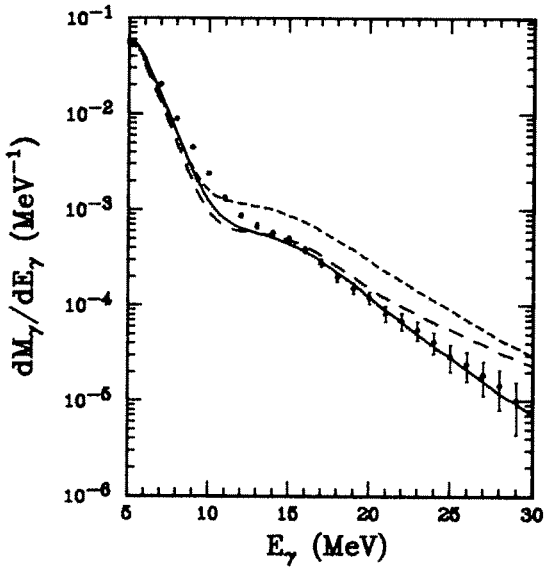


Fig. 2: Comparison of the experimental data for the 500 MeV bin after bremsstrahlung subtraction (points) with a standard CASCADE calculation (dotted line), a calculation following the model of Smerzi et al. (dashed line), and a calculation including a cutoff of the GDR $\gamma$-emission above $E^* = 250$ MeV (full line).

It was proposed [8,9] that the observed saturation could be related to a strong increase of the width of the GDR with excitation energy. Indeed, increasing the width of the GDR will spread the $\gamma$-rays over a larger energy range and thus lead to a quenching of the yield between 12 and 20 MeV. As an example, the result of a calculation using the model of Smerzi et al.[8] is compared to the data in fig. 2 (dashed line). These authors predict a strong increase of the GDR spreading width with excitation energy due to the damping through two-body collisions. This width can be parametrized for all excitation energies by $\Gamma_{GDR} = \Gamma_0 + 0.0026(E^*)^{1.6}$. This model furnishes an acceptable prediction for the integrated $\gamma$-multiplicity between 12 and 20 MeV. However, it strongly overpredicts the $\gamma$-spectra above 20 MeV. Calculations using other prescriptions[9] for a continuous increase of the GDR width with excitation energy give rise to similar conclusions[7]. Therefore it can be concluded that current models which predict a continuous increase of the GDR width without a suppression of $\gamma$-emission at high temperatures cannot reproduce the data.

The simplest way to simulate the complete $\gamma$-spectrum above 12 MeV is to introduce a sharp suppression of the $\gamma$ emission above a given excitation energy. Such a calculation using a constant width of 12 MeV for the GDR, and a cut-off excitation energy of 250 MeV allows to reproduce the $\gamma$ spectra above 12 MeV measured for the three excitation energy bins. An example is shown for 500 MeV excitation energy in fig. 2 (solid line).

In ref.[2] it was suggested that the observed saturation could be due to a loss of collectivity at high temperature. In a recent paper[9] it was discussed that a transition from collective to chaotic motion should occur around 300 MeV excitation energy. Another possibility could be that the GDR is gradually shifted to lower energy or replaced by some low-lying strength as one approaches the highest excitation energies that the nucleus can sustain. This tendency can be found in Random Phase Approximation calculations at high temperatures[10,11]. Moreover, the experimental data present some strength at low excitation which is not accounted for in any of the CASCADE simulations and which might be an indication of the presence of a new low lying component. However, before any definite conclusion about the origin of this low lying component in the $\gamma$-spectrum can be drawn more experimental work and new theoretical predictions are called for.

In summary, $\gamma$-rays were measured in coincidence with well characterized hot nuclei at excitation energies above 300 MeV. The $\gamma$-yield above 12 MeV from the GDR decay is constant as a function of excitation energy. We have shown that an increase with temperature of the width of the GDR could account for the integrated $\gamma$-yield between 12 and 20 MeV but is unable to reproduce the spectra above 20 MeV. To reproduce the data a quenching of the $\gamma$-emission at excitation energies above approximately 250 MeV must be supposed.

Very recently we have measured, with the same experimental set-up, $\gamma$-rays from the $^{36}$Ar + $^{94}$Zr reaction at 32 MeV/u and $^{36}$Ar + $^{98}$Mo reaction at 37 MeV/u in order to study the photon emission from hot nuclei in the regime where multifragmentation and vaporization is expected to set in.

## 1. References


[1] J. J. Gaardhøje, Ann. Rev. Nucl. Part. Sci. **42**, 483 (1992)
[2] J. J. Gaardhøje et al., Phys. Rev. Lett. **59**, 1409 (1987)
[3] K. Yoshida et al., Phys. Lett. **245 B**, 7 (1990)
[4] E. Migneco et al., Nucl. Instr. and Meth. **A314**, 31 (1992)
[5] H. Nifenecker and J.A. Pinston, Annu. Rev. Nucl. Part. Sci. **40**, 113 (1990)
[6] W. E. Ormand et al., Phys. Rev. **C40**, 1510 (1989)
[7] T. Suomijärvi et al., Proc. of the Gull Lake Nucl. Phys. Conf. on Giant Resonances, August 17-21, 1993, Gull Lake, Michigan, to be published in Nucl. Phys. A
[8] A. Smerzi et al., Phys. Rev. **C44**, 1713 (1991); A. Bonasera et al., Proc. of the Gull Lake Nucl. Phys. Conf. on Giant Resonances, August 17-21, 1993, Gull Lake, Michigan, to be published in Nucl. Phys. A
[9] Ph. Chomaz, Proc. of the Gull Lake Nucl. Phys. Conf. on Giant Resonances, August 17-21, 1993, Gull Lake, Michigan, to be published in Nucl. Phys. A.
[10] H. Sagawa and G. F. Bertsch, Phys. Lett. **146B**, 138 (1984)
[11] P. F. Bortignon et al., Nucl. Phys **A460**, 149 (1986)

# HOT NUCLEI FORMATION AND DECAY : THE Ar+Ag SYSTEM AT 50 AND 70 MeV/u

*E. Vient [1], A. Badala [4], R. Barbera [4], G. Bizard [1], R. Bougault [1], R. Brou [1], D. Cussol [1], J. Colin [1], D. Durand [1], A. Drouet [1], J.L. Laville [1], C. Le Brun [1], J.F. Lecolley [1], M. Louvel [1], J.P. Patry [1], J. Péter [1], R. Régimbart [1], J.C. Steckmeyer [1], B. Tamain [1], A. Peghaire [2], P. Eudes [3], F. Guilbault [3], C. Lebrun [3], E. Rosato [5], A. Oubahadou [6]*

[1] LPC, ISMRA, IN2P3-CNRS, 14050 CAEN CEDEX (France)
[2] GANIL, B.P. 5027, 14021 CAEN CEDEX (France)
[3] LPN, Université de Nantes, 44072 NANTES CEDEX (France)
[4] Istituto Nazionale di Fisica Nucleare, 95129 CATANIA (Italy)
[5] Dipartimento di Scienze Fisiche, Univ. di Napoli, 80125 NAPOLI (Italy)
[6] Laboratoire de Physique Nucléaire, Faculté des Sciences de Rabat (Maroc)

## INTRODUCTION

Two important questions are raised concerning hot nuclei : their limit of existence and their decay properties. The fact that the so called " fusion bump " vanishes for argon induced reactions at bombarding energies exceeding 40 MeV/u [1)] can be understood either as an entrance channel or an exit channel effect. In the first case, fusion would be inhibited by preequilibrium mechanisms or by the limit of existence of hot nuclei. In the second case, the opening of new decay channels (multifragmentation) would prevent the occurence of standard binary fission products or evaporation residues.

In the present work, we have investigated to which extent " standard " decay processes (i.e. those which are dominant at limited excitation energy) are still observed for very large excitation energies. The system we have studied is Ar+Ag at 50 and 70 MeV/u . For such medium mass systems, the expected standard decay is sequential evaporation leading to an evaporation residue. In the present work, it is shown that such a statistical decay still exists even for very large involved excitation : the opening of new decay channels (namely multifragmentation) does not inhibit other processes, and the competition of " standard " decay processes remains efficient.

## EXPERIMENTAL SET UP

The present experiment was performed with two multidetectors installed in the Nautilus chamber : the " Mur " [2] and the " Tonneau " [3]. These devices detected all the charged particles emitted in coincidence with a heavy residue forward detected in a time of flight silicon telescope. The residue was identified in mass and energy and the coincident particles were identified in charge and velocity. An event by event analysis was performed in order to reconstruct the initial hot nucleus [4]. For this purpose, it was necessary to discriminate preequilibrium from evaporated particles ; this has been performed in assuming that the angular distribution of evaporated particles is forward-backward symmetric in the hot nucleus frame and that all backward emitted particles are evaporated.

## RESULTS [4] [5]

In figure 1 are shown the excitation energy distributions for hot nuclei which were recognized at 50 and 70 MeV/u . The abscissa indicates the measured excitation

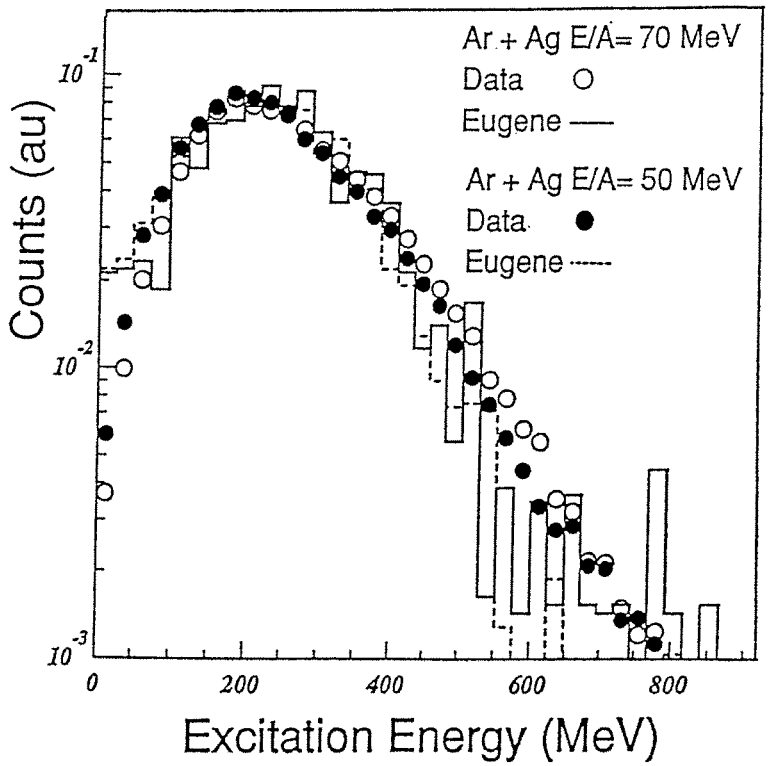


*Figure 1 :*
*Comparison between the excitation energy distributions obtained at 50 and 70 MeV/u .*
*Points : experimental results ; lines : Eugene simulations taking into account the experimental filter.*

energy. It has been experimentally obtained by adding the contributions (kinetic and binding energies) of all evaporated particles. Points are experimental. It turns out that excitation energy distributions look quite similar at 50 and 70 MeV/u . Histogramms have been obtained in a theoretical simulation (Eugene code [6]) in which the decay step is based on a sequential emission mechanism. The calculations are in good agreement with data, thus showing that very hot nuclei decay can be reproduced in assuming a "standard" sequential evaporation process.

Excitation energies which are reached are quite large : if one corrects measured values for thresholds and inefficiency effects, it turns out that 600 MeV are reached for 10 % of events, i.e. a cross section of about 100 mb/rad for the forward detected residue. The corresponding temperatures have been deduced from the slopes of proton kinetic energy spectra. Initial temperatures values of 7 MeV have been obtained.

An important question is to know to which extent still larger excitation energies can be reached. A possibility would be that these extreme excitations would lead to new decay mechanisms (namely multifragmentation). In order to check this hypothesis, we have used another trigger condition, namely the total multiplicity of charged particles in the $4\pi$ set up. In other words, we have relaxed the requirement on the forward heavy residue detection. With this new trigger condition, any violent collision was registered. In figure 2 , the abscissa is the charged particle multiplicity which is an indication of the

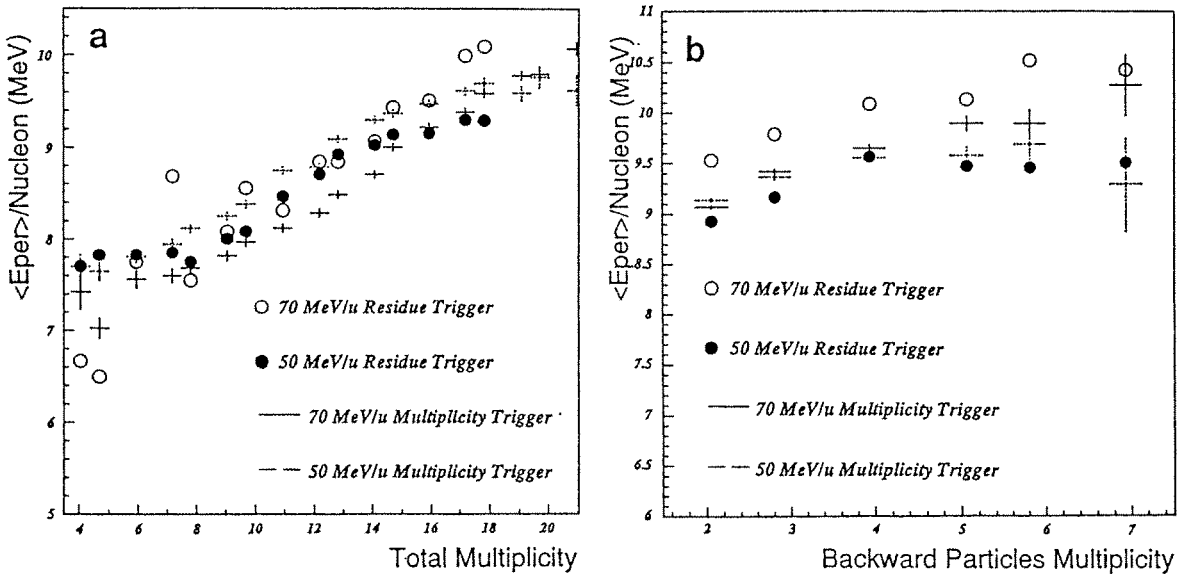


***Figure 2***

*Evolution of $E_{per}/A$ as a function of the total charged particle multiplicity (left side), or the multiplicity of backward emitted particles (right side). In each case, $E_{per}/A$ has been calculated in selecting particles backward emitted in the hot nucleus frame. It has hence been possible to avoid the preequilibrium contribution. In every case, $E_{per}/A$ has about the same behaviour whatever the trigger is : residue trigger or multiplicity trigger.*

violence of the collision. The ordinate is the perpendicular energy per nucleon of the outgoing particles in an event by event analysis. The results (points) are compared with the corresponding perpendicular energy obtained if a forward evaporation residue is required. They are quite similar. This means that whatever the triggering conditions are (with or without the evaporation residue requirement), similar excitation energies are obtained.

Even at very large excitation energies, competition between standard decay processes leading to an evaporation residue and more exotic phenomena (multifragmentation) remains open.

## REFERENCES


1 - M. CONJEAUD et al ; Phys. Lett. B159 (1985) 244

2 - G. BIZARD et al ; NIM A244 (1986) 483

3 - A. PEGHAIRE et al ; NIM A295 (1990) 365

4 - E. VIENT et al ; accepted to Nucl. Phys. A

5 - E. VIENT et al ; proceedings of the 30$^{th}$ International Winter Meeting on Nucl. Phys. Bormio, 1992

6 - D. DURAND ; Nucl. Phys. A541 (1992) 266

# EXPLOSION OF $^{64}$Zn + $^{nat}$Ti ?

A. KERAMBRUN, J.C. STECKMEYER, J.C. ANGELIQUE, G. BIZARD, R. BROU, D. DURAND, Z.Y. HE[1], J. PÉTER, R. REGIMBART, B. TAMAIN, E. VIENT,
*Laboratoire de Physique Corpusculaire, ISMRA, IN2P3 - CNRS, 14050 CAEN CÉDEX, France,*
G. AUGER, C. CABOT[2], E. CREMA[3], A. PEGHAIRE, F. SAINT-LAURENT,
*GANIL , BP 5027 , 14021 Caen cédex, France*
M. GONIN[4], K. HAGEL, R. WADA,
*Cyclotron Institute , Texas A & M University , College Station, Texas 77843,*
P. EUDES, C. LE BRUN,
*Laboratoire de Physique Nucléaire, Institut de Physique, 44072 Nantes cédex 03, France*
Y. EL MASRI,
*Université Catholique de Louvain, Institut de Physique Nucléaire, 1348 Louvain-la-Neuve, Belgium*
E. ROSATO,
*Dipartemento di Science Fisiche, Universita di Napoli, 80125 Napoli, Italy,*

**Abstract**

The reaction of a $^{64}$Zn beam with a $^{nat}$Ti target has been studied at several bombarding energies between 35 and 79 MeV/nucleon using two multidetectors with large solid angle coverage (84 % of 4π ). Only quasicomplete events were retained in the subsequent analysis. The hot nuclei produced in the $^{64}$Zn + $^{nat}$Ti reactions were found to deexcite by isotropic emission of light particles and intermediate mass fragments (IMF). Very high excitation energies were reached in the most central collisions, up to 11 - 12 MeV/nucleon. The observed multiplicities and slope parameters were compared to the predictions of several statistical models. The data are in qualitative agreement with a model in which an explosive phase is included. Differences between the experimental and predicted relative velocity distributions between IMF's suggest the existence of a compression mode.

*1) Permanent address : Institute of Modern Physics, POB 31, 730000 Lanzhou, P. R. China,*
*2) Permanent address : Institut de Physique Nucléaire, BP 1, 91401 Orsay cédex, France,*
*3) Permanent address : Instituto de Fisica, Universidade de Sao Paulo, CP 20516, 01498 Sao Paulo, Brazil,*
*4) Permanent address : Brookhaven National Laboratory, Up ton, New-York 11973*

## I INTRODUCTION

By using heavy ions at intermediate bombarding energies ($20<E_{bomb}<100$ MeV/nucleon), composite systems with very high excitation energies are formed in the most violent collisions. As these excitation energies are of the order or larger than the binding energy of the so-called hot nuclei, new phenomena are expected to be observed, such as the emission of several fragments (multifragmentation), or the complete vaporization of the nucleus into single nucleons.

## II EXPERIMENTAL PROCEDURE

Beams of $^{64}Zn$ with energies between 35 and 79 MeV/nucleon were used to bombard a $^{nat}Ti$ target ($400\mu g/cm^2$). The experimental consisted of two multidetectors which provided the identification of light particles and nuclei up to Z=8 using the Q-TOF method [1 - 2]. They covered 84 % of the $4\pi$ solid angle with polar angles coverage from 3 to 150 degrees. A set of seven telescopes with a limited coverage was also used to allow for the identification of fragments with charges greater than 8.

## III ANALYSIS AND RESULTS

Only events for which sufficient information had been collected were kept in the subsequent analysis. This was done by requiring that the total detected parallel momentum was greater than 60 % of the projectile incident momentum. For these events, an average of 85 % of the incident linear momentum and 70 % of the total charge were collected.

Selection of the hotest nuclei requires, first of all, the knowledge of the impact parameter. Here, the impact parameter was determined from the experimental cross section, assuming that the most violent collisions (i.e. the most central ones) correspond to the highest values of the total transverse momentum [3].

Once the events were sorted as a function of the impact parameter, the characteristics of the sources were investigated. Emission sources were recognized by studying the invariant cross section in the $V_{//}$ - $V_{\perp}$ velocity plane. For all impact parameters and all particles, a high velocity source lying between the projectile velocity and the center of mass velocity was found. Also seen, an important component approximately at half the beam velocity especially for the Z=1 and 2 particles.

Of particular interest is the high velocity source. In order to determine the characteristics of these hot nuclei, the reconstruction of the primay masses is needed. The angular distribution of particles and fragments were constructed in the moving source frame. The angular distributions of Z=1 and 2 particles and IMF exhibit a flat behaviour at angles smaller than 90 degrees, indicating that the excitation energy has equilibrated

inside the hot nucleus. For center of mass angles larger than 90 degrees, an important component shows up, relative to a pre-equilibrium and/or a target-like emission.

As it has been ascertained that light particles and IMF were emitted by an equilibrated nucleus, the mass of the initial hot nucleus could be determined from the characteristics of the ejectiles and of the cold residue. This was done by doubling in the center of mass the contribution of particles and IMF which had been isotropically emitted in the forward hemisphere. The number of emitted neutrons has been estimated and taken into account. The excitation energy was calculated from the center of mass kinetic energies of all forward emitted particles and fragments and from the mass balance as well [4]. The experimental excitation energies per nucleon *(E*/A)* are displayed in fig. 1 for four bombarding energies as a function of the experimentally determined impact parameter. For a fixed bombarding energy, the excitation energy increases with the decreasing impact parameter. From 35 to 49 MeV/nucleon the excitation energy rises rapidly and then, only slightly from 49 to 79 MeV/nucleon. As shown in fig. 1, very high excitation energies, up to 11 - 12 MeV/nucleon, were reached in the most violent collisions , while lower values of the excitation energy ($\cong$ 2 MeV/nucleon) are, as expected, associated with collisions occurring at large impact parameters. In the most violent collisions, average multiplicities of charged products of the order of 14 were found, providing some indication for multifragmentation of the hot nuclei studied here.

## IV COMPARISON WITH MODELS

The data have been compared with the results of statistical model calculations. Two of these models [ 5 - 6 ] employ a standard evaporation formalism while in the third one, the FREESCO code [ 7 ], an explosion stage arises when the excitation energy of the hot nucleus is larger than its binding energy. This latter model has been employed to search for any deviations from a standard evaporation behaviour usually observed at moderate excitation energies.

The mean multiplicities of Z = 1 and 2 particles and IMF, emitted by the hot nuclei, are displayed in fig. 2 as a function of the impact parameter. The yield of Z = 1 particles is underpredicted by a factor of 2 whatever the model.

The Z = 2 multiplicity is rather well predicted by the EUGENE code. The trends of the data are also reproduced by FREESCO, for low and high impact parameters. The disagreement at medium impact parameters is related to the sudden change of regime since for these impact parameters the excitation energy is close to the threshold for disassembly. The comparison between the results of FREESCO and the data favours a smooth transition from an evaporation mode to an explosive mode as intituively expected. The same conclusion is reached by looking at the evolution of the IMF multiplicity versus the impact parameter (see fig. 2).

That FREESCO reproduces qualitatively the number of clusters ($Z \geq 3$) emitted by the hot nuclei both in peripheral and central reactions argues in favour of a new desintegration mode of hot nuclei with high excitation energies.

## V CONCLUSIONS

The formation and decay of hot nuclei has been studied in the $^{64}Zn + ^{nat}Ti$ reaction using large solid angle multidectors. The analysis was carried out on quasi-complete events as a function of the experimentally determined impact parameter. The observed hot nuclei were produced with high excitation energies, up to 12 MeV/nucleon in the most violent collisions and decay by emission of light particles and IMF's. The experimental multiplicities and relative velocity distributions (not presented here) were compared to different statistical models predictions. Only the FREESCO code in which an explosive phase is included reproduces qualitatively the experimental data. It should be noted that a study performed on a similar system, $^{40}Ca + ^{40}Ca$ at 35 MeV/nucleon [ 8 ], led to the conclusion that an expansion phase must be incorporated in order to explain the experimental results. In agreement, our results seem to indicate that some expansion following a compression step is also necessary at 79 MeV/nucleon. Further comparisons with dynamical calculations need to be performed in order to identify unambiguously the key processes involved in multifragmentation

## REFERENCES


[ 1 ] G. BIZARD et al., Nucl. Inst. and Meth. A244 (1986) 489

[ 2 ] A. PEGHAIRE et al., Nucl. Inst. and Meth. A295 (1990) 365

[ 3 ] D. CUSSOL et al., XXXI Int. Winter Meeting on Nuclear Physics, Bormio, Italy, 1993

[ 4 ] D. CUSSOL et al., Nucl. Phys. A 561 (1993) 298

[ 5 ] R.J. CHARITY et al., Nucl. Phys. A483 (1988) 371

[ 6 ] D. DURAND, Nucl. Phys. A 541 (1992) 266

[ 7 ] G. FAI and J. RANDRUP, Nucl. Phys. A 381 (1982) 557

[ 8 ] K. HAGEL et al., Phys. Rev. Lett. 68 (1992) 2141

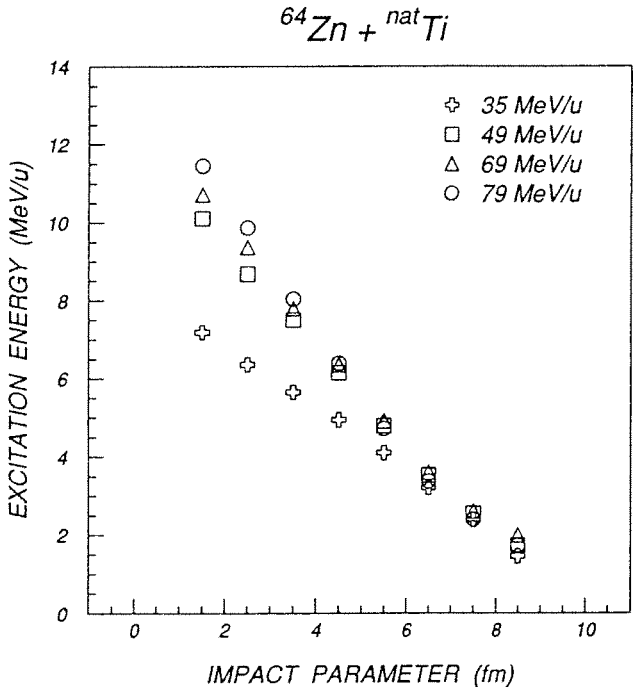


*Fig. 1 : Mean values of the distributions of the excitation energy of the hot nuclei formed in the $^{64}Zn + ^{nat}Ti$ reaction at different bombarding energies, as a function of the experimentally determined impact parameter.*

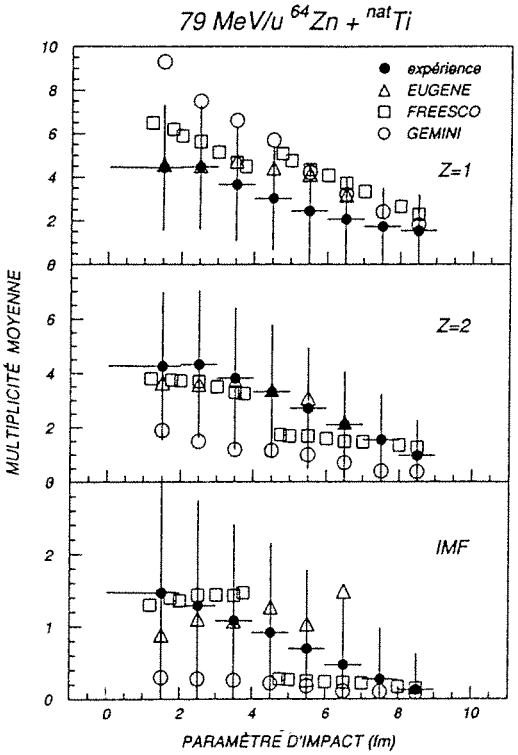


*Fig. 2 : Mean values of the distributions of Z = 1 ands 2 particles and IMF's emitted by the hot nuclei in the reaction $^{64}Zn + ^{nat}Ti$ at 79 MeV/nucleon (closed circles) as a function of the experimentally determined impact parameter. Also shown, results of calculations : GEMINI (ref. 5), EUGENE (ref. 6) and FREESCO (ref. 7).*

# HEAVY FRAGMENTS PROPERTIES IN THE $^{40}Ar + ^{232}Th$ SYSTEM AT 27, 44 AND 77 MeV/u

E.Berthoumieux[1], E.De Filippo[2] *, R.Barth[3], B.Berthier[1], Y.Cassagnou[1], Sl.Cavallaro[4], J.L.Charvet[1], A.Cunsolo[2] R.Dayras[1], N.Foti[2], S.Harar[5], G.Lanzanó[2], R.Legrain[1], V.Lips[6], C.Mazur[1], E.Norbeck[7], H.Oeschler[6], A.Pagano[2], E.C. Pollacco[1], S.Urso[2] and C.Volant[1]

[1] DAPNIA/SPhN CEN Saclay, 91191 Gif-Sur-Yvette Cedex, France
[2] Istituto Nazionale di Fisica Nucleare and Dipartimento di Fisica, Corso Italia 57, 95129 Catania, Italy
[3] GSI Darmstadt, D-6100 Darmstadt, Germany
[4] Dipartimento di Fisica and INFN-Laboratorio Nazionale del Sud, Viale Andrea Doria, Catania, Italy
[5] GANIL BP 5027, 14021 Caen, France
[6] Institut für Kernphysik, Technische Hochshule Darmstadt, Germany
[7] Department of Physics, University of Iowa, Iowa City, Iowa 5242, USA

## 1 Motivations.

In the reaction $^{40}Ar+^{232}Th$ above 30 MeV/u angular correlations between fission fragments show a decrease in cross section for central collisions (CC) with increasing incident energy ($E_{Ar}$) . At 44 MeV/u there is no visible CC peak [1]. Several scenarios have been invoked to explain this effect with two extreme examples being related to multifragmentation and heavy residues production. In the first case the cross section for hot nuclei is assumed to go into multifragmentation processes. Although this is a stimulating possibility for, it would infer that temperature for change in regime are being reached, no expected increase in yield for intermediate mass fragments (IMF) has been observed for the system and incident energies in question [2, 3]. In the second case it is considered that the highly excited nuclei (via complete or incomplete fusion) suffer a large loss of nucleons in the early stage of decay process [4] yielding nuclei with a high fission barrier. This gives rise to a decreasing of the fission cross section, the difference going into evaporation residues. The heavy residue description is plausible, however the actual mechanism is likely to be more complex in that it: a) might involve the memory of the entrance channel [5, 6] (mechanism which go under the titles like *deep inelastic* and so on); b) might include large mass asymmetries and hence intermediate mass fragments (IMF) production. The objective of the present experiment (E157) was to establish the existence and characterize events where a large fraction of the incident energy is dissipated, leading to a heavy mass in the exit channel.

## 2 Experimental procedure.

A primary 77 MeV/u $^{40}Ar$ beam was used to bombard a 700 $\mu g/cm^2$ $^{232}Th$ target. The energies of 44 and 27 MeV/u were obtained by slowing down the primary beam. The timing reference was taken from the RF of the cyclotron and an overall time resolution of 700 ps was obtained.

The experimental set-up is shown in figure 1. The Z axis in the figure lies along the beam direction. The detection of heavy fragments (HF) and fission fragments (FF) has been achieved by 32 high field silicon (Si) diodes ($3 \times 3$ $cm^2$), 140 $\mu m$ thick, located at 40 cm from the target and spanning an angular range between -8.5 to -45°. Energy [7] and time [8] defect corrections were employed to build the mass and velocity.

A parallel plate avalanche counter (PPAC) ($30 \times 30$ $cm^2$) located at 30 cm from the target at a mean angle of 145° was used to eliminate fission fragments arising from peripheral collisions in coincidence with their partners detected in the silicon array.

IMF ($3 \leq Z \leq 16$) were detected in 8 ionisation chambers (TEGARA) [9]. Each ionisation chamber consisted of a splitted anode coupled to four $5 \times 5$ $cm^2$ silicon diodes 500 $\mu m$ thick. A $CF_4$ gas volume, 5.4 cm depth, operating at 30 torrs was used. These detectors were located at angles of 35, 48, 60, 65, 100, -110 and -120°.

The honey comb arrangement containing 36 $BaF_2$,

*Present address: DAPNIA/SPhN CEN Saclay 91191 Gif-Sur-Yvette Cedex, France

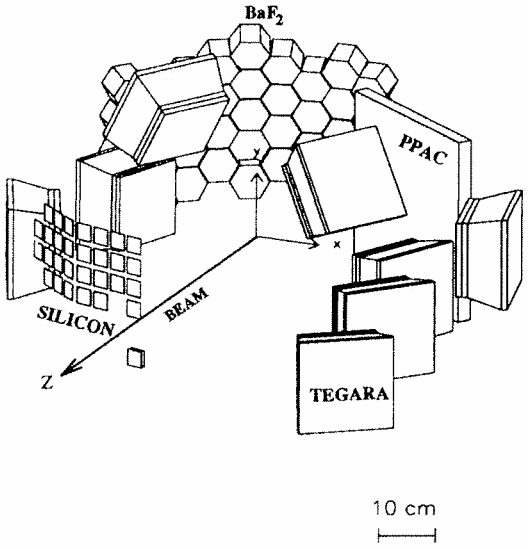


Figure 1: Experimental set-up of the E157 experiment.

5 cm thick, each of 25 $cm^2$ area [10], covering angles between -130 and -175$^o$, was employed to detect light charged particles (LCP) (p,d,t,$^3$He,$\alpha$).

# 3 Identification of heavy fragments.

Analysis of the single data for the Si counters at 44 MeV/u shows a strong fission contribution in the velocity versus mass bidimensional spectra (fig 2 up) but no apparent HF peak. However, introducing at least one LCP or one IMF and rejecting fission-fission events detected in coincidence with the PPAC (fig 2 down), selects events in Si where two peaks at 90 and 160 amu become apparent. The peak at 90 amu is attributed to FF and we denote the higher peak as the heavy fragments (HF). It is to note that imposing an IMF yields the strongest enhancement for the HF peak. Similar results are obtained at 77 MeV/u, but the HF mass peak is shifted to lower values. At 27 MeV/u there are some indications for the presence of events containing a HF, however the background from fission is very high.

# 4 Cross section evaluations.

To evaluate cross sections from the single measurements a deconvolution procedure is adopted to separate fission from HF. The coincidence PPAC-Si shows

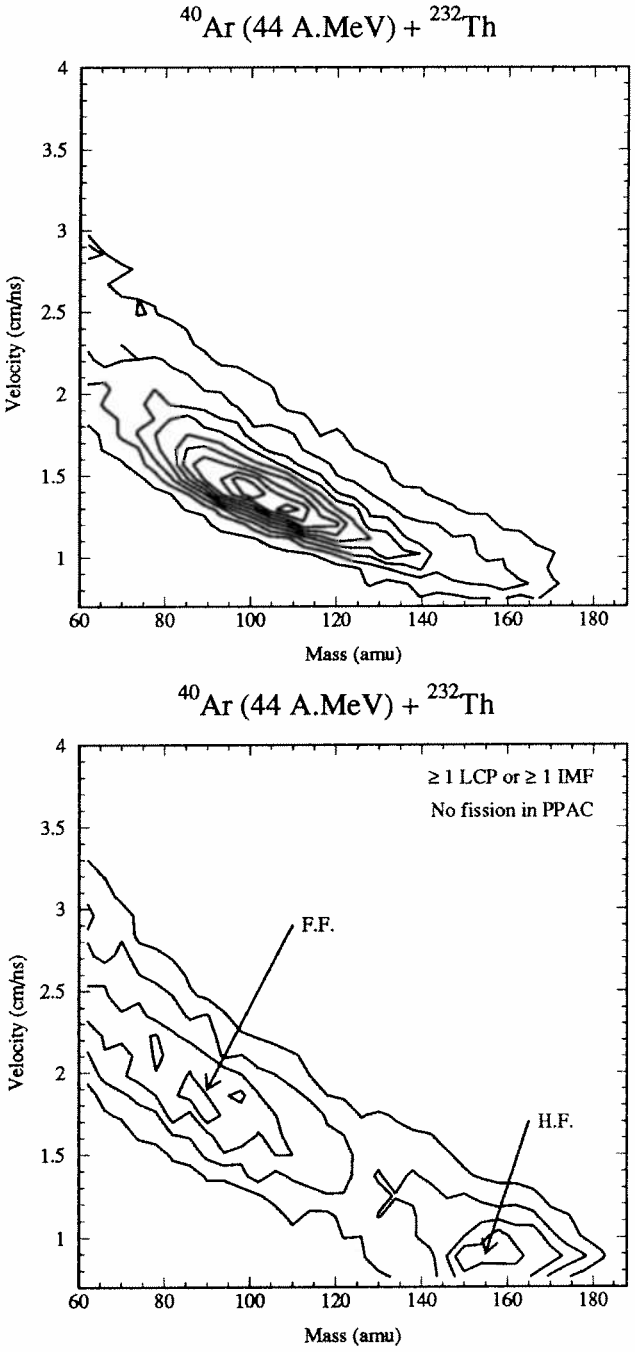


Figure 2: Velocity versus mass bidimensional spectra of products detected in a silicon at -8.5$^o$ at 44 MeV/u bombarding energy. Up: Single measurements. Down: Coincidence data with at least one LCP or one IMF and with veto on fission fragments detected in PPAC.

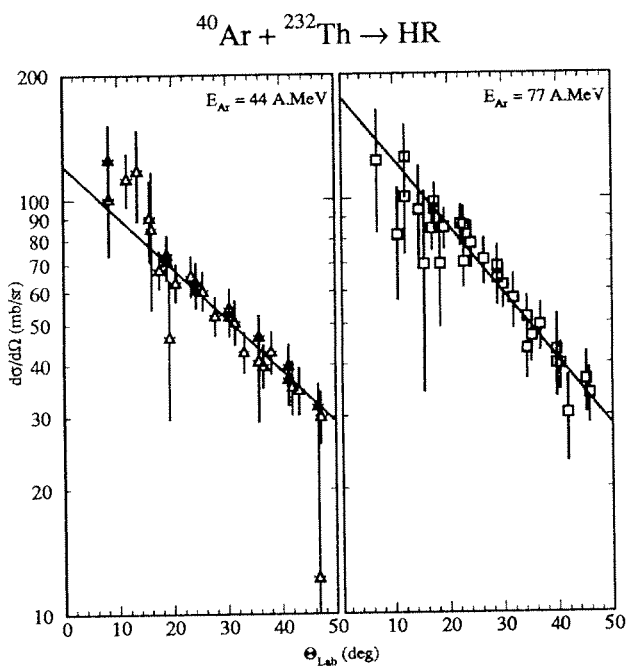


Figure 3: Heavy fragments angular distribution at 44 and 77 MeV/u for a velocity $\geq$ 0.5 cm/ns.

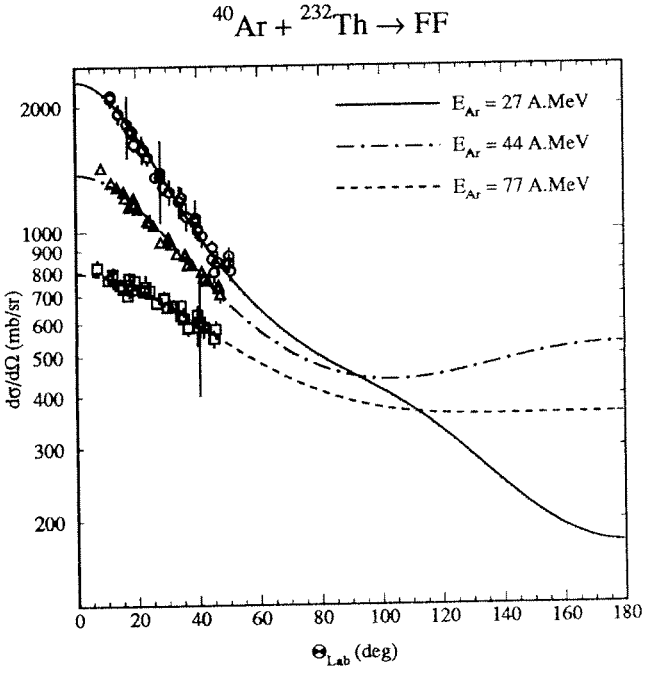


Figure 4: Fission fragments angular distribution at 27, 44 and 77 MeV/u.

that the velocity spectra for fission are quite gaussian (2 gaussians needed at 27 MeV/u). A gaussian shape was assumed for the HF, whose characteristics are extracted from the coincidence LCP-Si. The main difficulty with this procedure is related to the velocity thresholds (0.5 cm/ns) for the heavier masses. Angular distributions are given in figures 3 and 4 and show that the HF have a steeper fall off with angle compared to the FF. To extract HF cross sections the angular distributions are fitted using an exponential law. The FF angular distribution is fitted using formulation of [12, eq. (20)], the recoil velocity being calculated using the dependence in angle of FF mean velocity. Integrated cross sections over the total solid angle are given in table 1, and show, in the limit of the experimental threshold, that there is no noticeable increase for the HF cross section between 44 and 77 MeV/u. FF cross sections are also given and show a drop of approximatly 30% between 44 and 77 MeV/u. Those results are in reasonable agreement with [1] and [11].

## 5 Characteristics of heavy fragments.

The mass distributions at the two higher energies are extracted using the HF-LCP correlations. A summary of the data mean values are given in the table. The mass decreases with incident energy. For the selected events, the velocities (0.89 and 0.84 cm/ns at 44 and 77 MeV/u respectively) are consistent with values extracted for the CC using FF correlations [1]. To depict further the HF, the coincident LCP energy spectra and their multiplicities were studied. The LCP energy spectra were transformed in the rest frame of the HF and fitted using a Maxwell-Boltzmann function. The alpha spectra are well fitted over the whole of the dynamic range. For the protons the fits were limited to 30 MeV, for beyond, the data show an enhancement which cannot be reproduced using the chosen distribution. Extracted temperature parameters are given in the table. Also given in the table are the mean LCP multiplicities. These were obtained by performing a simulation where the experimental geometry is reproduced (GEANT 3.15) and the HF and LCP distributions are those found experimentally. The angular distributions of the LCP are assumed to be isotropic in the frame of the HF.

The results given in this section agree with a picture where the HF emerge from a nuclear complex raised to high excitation energy. The neutrons [11, 13] and LCP multiplicities support this view. As for the the extracted apparent temperatures, they are at best average values in a long chain of evaporation, nonetheless, they are consistent with high temperatures being reached. Assuming that the HF are indeed evaporation residues, the low mean mass indicates that large amounts of energy are liberated in long evaporation chains. Further, the tabled values support a process where at 77 MeV/u higher excitation energies are reached. It is important to note that the extracted angular and velocity distributions for HF are not inconsistent with the evaporation hypothesis.

| $E_{Ar}$ | (MeV/u) | 27 | 44 | 77 |
|---|---|---|---|---|
| $\sigma_{HF}$ ($V_{HF} \geq 0.5$ cm/ns) | (mb) | | $200 \pm 100$ | $200 \pm 100$ |
| < Mass > | (amu) | $\approx 175$ | $160 \pm 10$ | $145 \pm 10$ |
| $M_{LCP}$ | | | $6.5 \pm 1$ | $8 \pm 1$ |
| $T_p$ | (MeV) | | $4.9 \pm 0.2$ | $6.0 \pm 0.2$ |
| $T_\alpha$ | (MeV) | | $5.1 \pm 0.2$ | $5.0 \pm 0.2$ |
| $E^*_{calc}$ | (MeV) | | 900 | 1170 |
| $M_{calc}$ | (amu) | | 195 | 170 |
| $\pi \int_{10°}^{50°} \frac{d\sigma_{FF}}{d\Omega} \sin\theta d\theta$ | (mb) | $1300 \pm 150$ | $970 \pm 100$ | $680 \pm 90$ |
| $\sigma_{FF}$ | (mb) | (3580) | (3550) | (2770) |

Table 1: For the 3 studied energies $E_{Ar}$, are given: HF cross-section $\sigma_{HF}$, HF mean mass, mean LCP multiplicity $M_{LCP}$ for the HF, apparent temperatures for proton $T_p$ and for alpha $T_\alpha$ extracted from the LCP spectra in coincidence with HF, the calculated excitation energy $E^*_{calc}$ associated with HF, the calculated mass $M_{calc}$, and fission cross-sections in the measured angular range and integrated $\sigma_{FF}$

To comment on the experimental results and estimate the excitation energy, $E^*_{calc}$, a simple model, using linear momentum balance is employed [14]. It is considered that the HF are indeed evaporation residues and that they recoil along the beam axis with measured mean velocities. The results of the calculation are included in the table. Qualitatively, the calculations are consistent with the data in that large amounts of $E^*_{calc}$ is involved and that higher values are reached at 77MeV/u. Also, the calculated temperatures (level density parameter assumed to a be constant 8 MeV) are close to the experimental values. The calculated mass $M_{calc}$, however, are too high when compared to the data (using reasonable values for the energy removed per evaporated nucleon 15 MeV [1]). This discrepancy persists even outside the context of the above model. Summing the emitted neutrons, LCP and HF nucleons relative to FF mean total mass [1] shows a too low HF mass. Preliminary analysis of the coincident IMF coincidence data shows that this inconsistency is less severe, however, it does also suggest that a more elaborate production mechanism is probably involved.

# 6 Conclusion

In conclusion, the data show that in $^{40}Ar+^{232}Th$ at 44 and 77 MeV/u heavy fragments are observed which are products from a complex of high excitation energy. The measurements show that at 27 MeV/u these events have negligible contribution to the total cross section. Between 44 and 77 MeV/u the probability for heavy fragments remains relatively constant, in the limit of the experimental thresholds.

# References


[1] M. Conjeaud et al., Phys. Lett. **159B**, 244 (1985).

[2] Y. Cassagnou et al., Proc. Symp. on Nuclear Dynamics and Nuclear Disassembly, Dallas 1989, p. 386.

[3] C. Volant et al., Contribution to the third international conference on nucleus nucleus collisions, Saint-Malo, France, June 6-11, 1988, p. 100.

[4] D. Jacquet et al., Phys. Rev. **C32**, 1594 (1985).

[5] V. Lips et al., submitted to Phys. Rev. C rapid communications (1993).

[6] B. Borderie et al., Phys. Lett. **205B**, 26 (1988).

[7] S.B. Kaufman et al., Nucl. Inst. and Meth., **115** (1974), 47-55.

[8] H.O. Neidel and H. Henschel, Nucl. Inst. and Meth., **178** (1980), 137-148.

[9] R. Dayras et al., Note DPHN 90-1, CEN Saclay 1990, p. 68.

[10] G. Lanzanó et al., Nucl. Inst. and Meth. **A312**, 515 (1992).

[11] E. Schwinn et al., HMI preprint, Berlin 1993.

[12] N.N. Ajitanand et al., Phys. Rev. **C34**, 877 (1986).

[13] D. Utley et al., Progress in Research, Texas A&M (April 1, 1992 - March 31, 1993), p. I-11.

[14] E. C. Pollacco et al., Phys. Lett. **146B**, 29 (1984).

# INTERMEDIATE ENERGY Ar - Th COLLISIONS

**K Aleklett[a], J O Liljenzin[b], W Loveland[c], A. Srivastava[c] and R. Yanez[a]**

a) Uppsala University, Studsvik Neutron Research Lab., S-611 82 Nyköping, Sweden
b) Chalmers University of Technology, S-412 96 Göteborg, Sweden
c) Oregon State University, Corvallis, OR 97331-5903, USA

The Ar + Th reaction has played an important role in our understanding of intermediate energy nuclear collisions. Measurements[1,2] of the fission fragment folding angle distributions for this reaction showed the disappearance of fusion-like events at a projectile energy of 39-44 MeV/nucleon. Originally this disappearance was linked to the idea of the maximum excitation energy that could be contained in a nucleus, but similar studies[3] of the Ni + Th reaction showed the persistence of fusion-like events up to E* ~900 MeV, a value greater than that achieved in the Ar + Th reaction. Measurement[4,5] of the neutron multiplicities for the Ar + Th reaction showed a constant average multiplicity with Ar energy varying from 27 to 77 MeV/nucleon and the occurrence of similar multiplicity distributions. So it was clear that large multiplicity (large p transfer, fusion-like) events were occurring at projectile energies above 40 MeV/nucleon even though they seemed to be absent from the folding angle distributions.

Two possible reaction exit channels in which one might find the "missing" fusion-like events were the heavy residues and true multifragmentation events that do not leave a heavy target residue [The frequently used term "intermediate mass fragments" can include lower Z (Z = 1-5) fragments whose production also includes that of a heavy target-like fragment]. Independent evidence was found[6-9] that the time scale of fission events for the Ar + Th system was ~ $10^{-20}$ sec which is long compared to the time for neutron emission of ~ $10^{-22}$ sec. Thus fission was expected to be severely inhibited for E* > 50-75 MeV.

We thought it would be useful to measure, using radiochemical techniques, the gross cross sections for heavy residue and intermediate mass fragment production, and their momenta for the Ar + Th reaction at energies (77 and 95 MeV/A) where the fusion-like events were absent from the folding angle distributions, but present in the neutron multiplicities. The use of radiochemical techniques to study the heavy residue properties was to insure that no residues would be missed due to detection thresholds, etc.

Thick targets of Th metal (~ 56 mg/cm$^2$) were surrounded by 18 mg/cm$^2$ Mylar catcher foils and irradiated in the external Ar beams from GANIL. Two Ar energies, 77 and 95 MeV/nucleon, were used. A short (~ 10 m) and a long irradiation (~ 1 hr) was performed at each energy with typical Ar fluences of 3 x $10^{13}$ and 2 x $10^{14}$, respectively. The irradiated target and catcher foils were analyzed by off-line $\gamma$-ray spectroscopy. Using techniques described previously,[10] target fragment mass distributions were deduced from the $\gamma$-ray spectrometric data. (Figure III-C-1 and III-C-2.)

The two isobaric yield distributions are similar. Integration of the region from A = 60 to A = 155 and A = 160-215 gives fission (multiplicity = 2) and heavy residue (multiplicity = 1) production cross sections of 3400 and 900 mb for 77 MeV/nucleon $^{40}$Ar + $^{232}$Th and 3100 and 700 mb for 95 MeV/nucleon $^{36}$Ar + $^{232}$Th.

The integral catcher analysis method of Tobin and Karol[11] was used to deduce the average longitudinal momentum transfer associated with various fragments (Figure III-C-3). The intermediate mass fragments are the events which correspond to fusion-like events while the momentum transfers leading to the heavy residues are low. (For fusion-like events in the $^{36}$Ar (95 MeV/A) + $^{232}$Th system, one would expect $\overline{v_{\parallel}/v_{CN}} \sim 0.4$.)

This association of the "missing" high linear momentum transfer events with the lighter fragments is consistent with theoretical predictions[12] and studies of heavy residues in other systems[13] which showed a disappearance of fusion-like residues at Ar projectile energies less than 44 MeV/A. Other studies[14] of heavy residue production at higher projectile energies have shown very low residue energies corresponding to their formation in low momentum transfer events. The aforementioned neutron multiplicity measurements indicated a cross section for fusion-like events of $\sim 2$ b for the Ar + Th system which is in rough agreement with the estimated lower Z fragment cross sections of $\sigma_{rxn} - \sigma_t - \sigma_{HR} \sim 1200$ and 1600 mb for the 77 and 95 MeV/nucleon Ar-induced reactions, respectively.

References


1. E.C. Pollacco, et al., Phys. Lett. B146, 29 (1984).
2. M. Conjeaud, et al., Phys. Lett. B159, 244 (1985).
3. M. Mostefai, et al., J. Phys., Suppl. 8, Vol. 47, C4-361 (1986).
4. D.X. Jiang, et al., Nucl. Phys. A503, 560 (1989).
5. J. Galin, et al., Nuclear Dynamics and Nuclear Disassembly, J.B. Natowitz, Ed. (World, Singapore, 1989), pp. 320-336.
6. H. Delagrange, C. Gregoire, F. Scheuter and Y. Abe, Z. Phys. A323, 437 (1986).
7. D. Guerreau, GANIL, P91-15.
8. E.M. Eckert, et al., Phys. Rev. Lett. 64 2483 (1990).
9. E. Mordhurst, et al., Phys. Rev. C43, 716 (1991).
10. D.J. Morrissey, et al., Phys. Rev. C21, 1783 (1980).
11. M.J. Tobin and P. Karol, Nucl. Instr. Meth. A270, 511 (1988).
12. H.W. Barz, et al., Phys. Rev. C46, R42 (1992).
13. J. Blachot, et al., Proc. XXIII Winter Meeting on Nucl. Phys., Bormio, 1985, p. 598.
14. K. Aleklett, et al., Nucl. Phys. A499, 591 (1989).


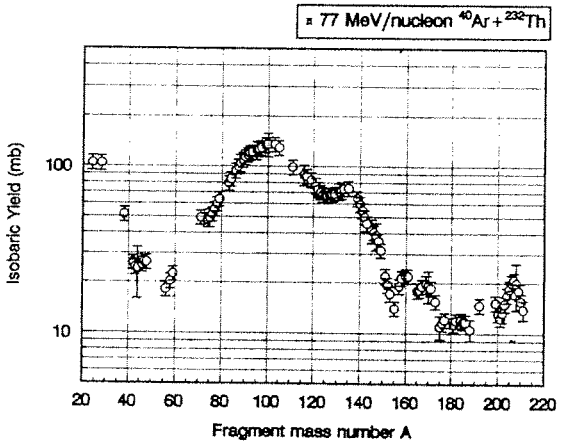


Figure 1. Target fragment mass distribution for the 77 MeV/nucleon $^{40}$Ar + $^{232}$Th reaction.

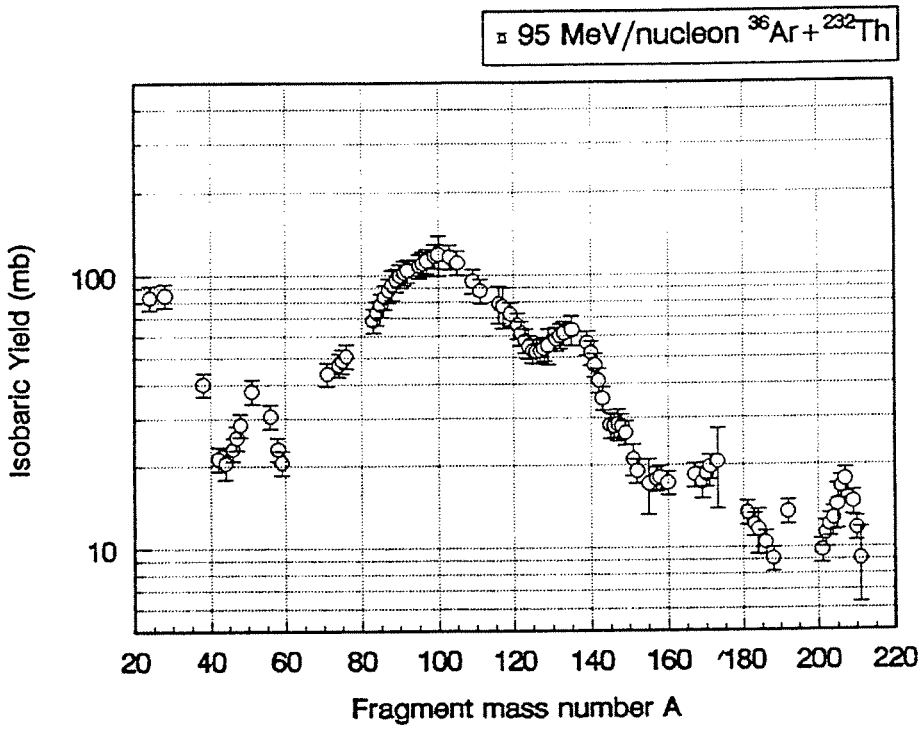


Figure 2. Target fragment mass distribution for the 95 MeV/nucleon $^{36}Ar$ + $^{232}Th$ reaction.

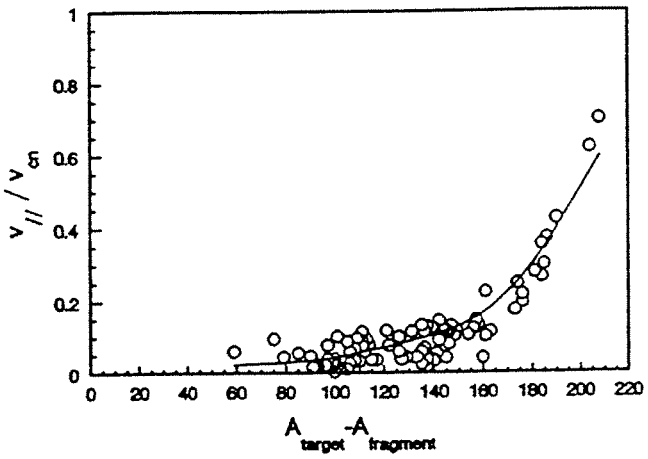


Figure 3. Target fragment longitudinal velocity (as a fraction of $v_{CN}$) vs. the mass removed from the target nucleus for the reaction of 95 MeV/nucleon $^{36}Ar$ with $^{232}Th$.

# *EXCITATION ENERGY AND THE TIME SCALES INVOLVED IN THE FORMATION AND DECAY OF VERY HOT NULCEI.*

T. Hamdani[1)], M. Louvel [1)], A. Genoux-Lubain [1)], G. Bizard [1)], R. Bougault [1)], R.Brou[1)], A. Buta [1)], H. Doubre [2)], D. Durand [1)], Y. El Masri [3)], H. Fugiwara [4)], K. Hagel [1-5)], F.Hanappe[6)], S.C. Jeong [4)], G.M. Jin [2-7)], S. Kato [4)], J.L. Laville [1)], C. Le Brun[1)], J.F. Lecolley [1)], S.M.Lee[4)], T. Matsuse [8)], T. Motobayashi [1-9)], A. Péghaire [2)], J. Péter [1)], R. Regimbart [1)], F. Saint-Laurent [2)], J.C. Steckmeyer [1)], and B. Tamain [1)]

1) LPC ISMRA, 14050 Caen Cedex, France
2) GANIL, 14021 Caen Cedex, France
3) FNRS-I.P.N.(UCL), 1348 Louvain la Neuve, Belgium
4) Institute of Physics, University of Tsukuba, Ibaraki-ken 350, Japan
5) Cyclotron institute, Texas A&M University, College Station, TX77843, USA
6) FNRS-ULB, Bruxelles, Belgium
7) Institute of Modern Physics, Lanzhou, China
8) Shinshu University, Japan
9) Rikkyo University, Toshima-ku, Tokyo 171, Japan

## 1. Introduction:

The formation of very hot nuclei by incomplete fusion provides for the investigation of complex phenomena such as the sequential decay of highly excited nuclei or multifragmentation. In the present work the main goal has been to study the emergence of the production of several fragments and follow their propreties when the excitation energy increases. In particular we have investigated the relationship between the excitation energy and the temperature of nuclei produced in central collisions of Ar on Au at 30 and 60 MeV/u. In addition, we have studied the evolution of the decay mechanism by fragment emission with increasing bombarding energy from 30 to 60 MeV/u.

## 2. Experiments:

In these experiments the detection system, which was described in ref 1 and 2, consisted of three multidetectors in the reaction chamber NAUTILUS: DELF for fragments with Z larger than 8 and velocity V > 0.5 cm/ns, emitted in the angular range 130°-150°, the Mur and Tonneau for light particles in the polar angular range 3°-150°. In addition, four large area silicon telescopes were located at forward angles to detect projectile like fragments and four CsI detectors at backward angles (located at 160° with respect to the beam axis) to detect, with low energy-threshold, light charged particles. Two triggering conditions were adopted: trigger 1 required at least the detection of one fragment in one of any of the forward telescopes in coincidence with two fragments in DELF, trigger 2 required coincidences between at least three fragments in DELF. In this paper, we present only the results obtained with trigger 2 where the events corresponding to more central collisions were treated.

## 3. Results and discussion:

*a) Excitation energy and temperatures:*

The results in this section concern events where at least 3 large fragments were detected at angles larger than 30° (DELF). It has been established that these fragments are emitted from an equilibrate source (ref 1). To characterise the composite system we have reconstructed the recoil velocity of the source, in the laboratory frame, from the velocity vector of the detected fragments,

$$\vec{V_R} = (\sum_{i=1}^{N_d} Z_i \vec{V_i}) / \sum_{i=1}^{N_d} Z_i$$

Where $N_d$ is the number of detected fragments and $Z_i$ their atomic number

This variable has allowed us to estimate the linear momentun transfered (LMT) in the reaction. It was 75% of the incident momentum at 30 MeV/u and 50% at 60 MeV/u in agreement with systematics. By using the simple assumption of massif transfer, we have calculated the excitation energy. In reference 2, it has been established that this method gives a correct estimate of the true excitation energy of the composite system. At 30 MeV/u the excitation energy per nucleon ($\varepsilon^*$) was around 3.3 MeV and reached 5.5 MeV when the bombarding energy was increased to 60 MeV/u. It is also important to relate these values of the excitation energy to the nuclear temperatures in order to determine the Fermi gas level density parameter. The procedure used to derive the initial temperature as deduced from the average temperature extracted from the kinetic energy spectra of alpha particles detected in the CsI telescopes is described in reference 2. An initial temperature (Tin) of 7.5 MeV is obtained for 60 MeV/u bombarding energy and 5.5 MeV for 30 MeV/u. With respect to the corresponding excitation energies the Fermi gas level density parameter estimated are A/10. In Table 1, we have also reported the corrected alpha particles multiplicites along with the two above mentioned variables. It is seen that all these quantities increase when the bombarding energy increases. Such a result demonstrates that it is possible to produce hotter nuclei by increasing the bombarding energy.

| *E/A* | *$\varepsilon^*$ MeV/u* | *Tin (MeV)* | *Multi alpha* | *Emission Time (fm/c)* |
|---|---|---|---|---|
| *30 MeV/u* | *3.3* | *5.5* | *3* | *500* |
| *60 MeV/u* | *5.5* | *7.5* | *5.5* | *50* |

*Table 1: Excitation energy, initial temperature, multiplicities of alpha particles and emission time obtained for central collisions.*

*b) From sequential decay processes to prompt fragment emission:*

To look for such an effect, we have employed a kinematical method based on the measurement of the vector velocities of the fragments. We have also developed a Monte Carlo simulation (ref 3) to search for any difference in the Coulomb trajectories of the emitted frgaments. In fig.1 correlation functions built with the relative angle distributions simulated between the three pairs of the fragments are compared with the three-fold data at 30 and 60 MeV/u.

At 30 MeV/u (3.3 MeV/u excitation energy), the emission time is long, $\tau = 500$ fm/c or more, as for longer emission times, the trajectory of one fragment is not modified by the other fragments which are still within the range of the Coulomb interaction. The decay mechanism is sequential with multifragment emission involving very long times between each splitting.

At 60 MeV/u (5.5 MeV/u excitation energy), the decay mechanism is different. The differences shown in the correlations between the characteristics of the fragments indicate a large influence of the excitation energy on the decay time. The time interval beween two successive splittings is so small ($\tau$ = 50 fm/c) that the concept of prompt sequential emission becomes equivalent to spontaneous multifragmentation.

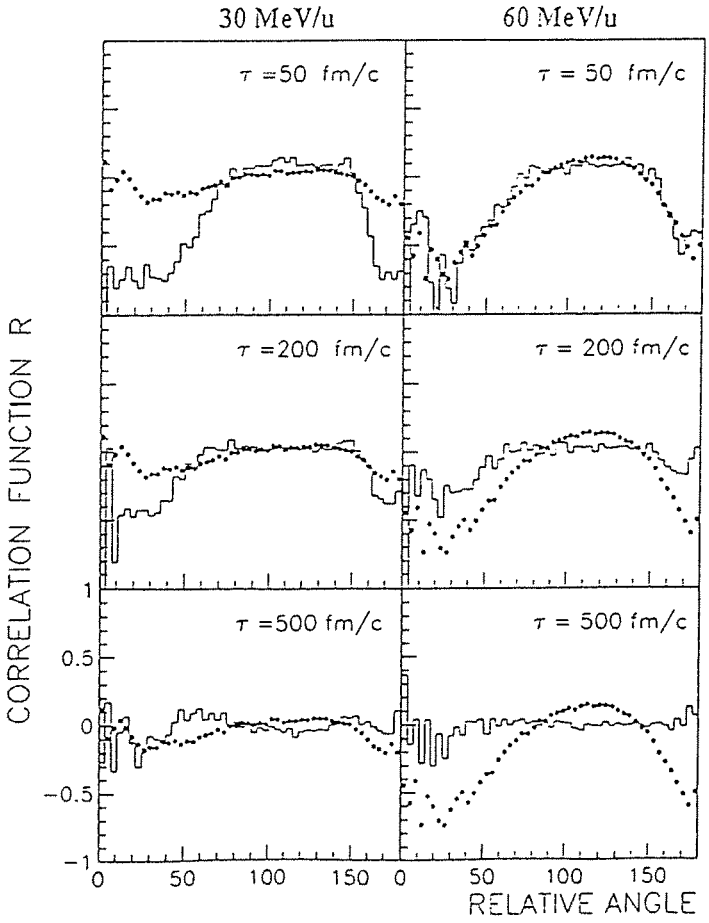


*Figure 1 : Correlation functions of the relative angle summed over all pairs of fragments in the 30 MeV/u (left side) and 60 MeV/u (right side) Ar+Au three fold events. The full dots are the data. The histograms are the calculated correlation functions for emision times of 50, 200 and 500 fm/c .*

**REFERENCES:**


1) M. Louvel et al, Nucl. Phys A559 (1993)137

2) T. Hamdani, Thesis, University of Caen (1993) LPCC T 93-05

3) M. Louvel et al, to appear in Phys. Lett B.

# Dissipative collisions around 20 A·MeV

A.A. Stefanini[1], J.P. Wessels[2,e], G. Casini[1], P.R. Maurenzig[1], A. Olmi[1]
R.J. Charity[2,a], R. Freifelder[2,b], A. Gobbi[2], N. Herrmann[2],
K.D. Hildenbrand[2], M. Petrovici[2,c], F. Rami[2,d], H. Stelzer[2], M. Gnirs[3],
D. Pelte[3], J. Galin[4], D. Guerreau[4], U. Jahnke[4,f], A. Peghaire[4] J.C. Adloff[5],
B. Bilwes[5], R. Bilwes[5,g] and G. Rudolf[5]

[1] INFN and Università di Firenze, Largo E. Fermi 2, I-50125, Italy
[2] Gesellschaft für Schwerionenforschung, Postfach 110552, W-6100 Darmstadt, Germany
[3] Physikalisches Institut der Universität Heidelberg, W-6900 Heidelberg, Germany
[4] GANIL, BP 5027, F-14021 Caen Cedex, France
[5] CRN and Université Louis Pasteur, BP 20, F-67037 Strasbourg Cedex 2, France

[a] Present address: Dept. of Chemistry, Washington Univ., St. Louis, USA
[b] Present address: Dept. of Radiology, Univ. of Pennsylvania, Philadelphia, USA
[c] On leave from: INPE, Bucharest, Roumania
[d] On leave from: CRN and Univ. Louis Pasteur, 67037 Strasbourg, France
[e] Present address: Dept. of Physics, SUNY, Stony Brook, USA
[f] On leave from: Hahn-Meitner-Institut, D-1000 Berlin 39, Germany
[g] Deceased

ABSTRACT

Results from a kinematic analysis of 3-body events in the collision $^{100}$Mo + $^{100}$Mo have been compared at the two bombarding energies of 18.7 and 23.7 A·MeV.
Small but detectable differences are interpreted as due to pre-equilibrium effects which removes mass and energy from the interacting system.

The symmetric collisions $^{100}$Mo + $^{100}$Mo and $^{120}$Sn + $^{120}$Sn were extensively studied at GSI and GANIL (experiment **E73**) in exclusive experiments at bombarding energies between 12 and 23.7 A·MeV, with the aim of characterizing as precisely and as completely as possible at least the most relevant components of the total reaction cross-section. Such a study allows to investigate the evolution of dissipative processes with increasing bombarding energy, from the low-energy domain into the intermediate energy region, where new phenomena (like multifragmentation) are predicted to appear.

The experimental set-up consisted of twelve [1] large-area position-sensitive parallel-plate avalanche counters (PPAC), mounted in an axially symmetric configuration around the beam axis. The detectors covered, altogether, about 75% of the solid angle in the forward hemisphere, which is the most important in this work, as most heavy products are expected to be emitted there. Behind each PPAC, two hybrid telescopes [2, 3] were used for the detection of light charged particles and intermediate-mass fragments.

From the measurement of time of flight and position by means of the PPACs, one can obtain, for each heavy fragment ($A \geq 20$), the secondary velocity vector, which is expected to coincide, on the average, with the primary one (i.e. before evaporation). Kinematic reconstruction yields primary masses and energies in an unambiguous way for events with up to four fragments in the final state [4]. With realistic and iteratively tuned Monte

Carlo simulations, the experimental data have been corrected to take into account the efficiency of the detecting system and the possible distortions introduced by the kinematic reconstruction.

The results show that a large part of the reaction cross section is exhausted by the 2- and 3-body channels, while less than 20% of the cross section is left in the 4-body or in other unobserved channels.

The gross features (diffusion- and Wilczynski-plot) of the 2-body cross section [1, 5] are, even at 23.7 A·MeV, entirely consistent with the behaviour typical for dissipative collisions at lower bombarding energies. This fact has now become quite generally accepted, being confirmed by several other works, recently even up to 30 A·MeV [6] in the reactions $^{208}$Pb + $^{197}$Au and $^{136}$Xe + $^{209}$Bi.

A fast emission of Light Charged Particles from the composite system [7, 8] as well as possible pre-equilibrium effects [1] may sizably limit the amount of excitation energy which one can deposit into the nuclei.

One of the main goals in the analysis of 3–body events was to determine the nature of their production mechanism (prompt or sequential). If they originate from the sequential decay of one of the fragments of a deep–inelastic interaction, then one of the three final nuclei should be located in the phase–space region typical of the 2–body events (which is efficiently measured in these experiments) and this property could be used to help distinguishing such events from prompt break–up processes. In this way, we showed [9, 10] that most of the 3–body events are produced in a sequential process, suggesting the picture of an initial binary deep–inelastic interaction followed by the fission–like decay of one of the fragments.

After having identified which is the pair of fragments produced in such a decay ("fission-fragments"), one can study various properties of this second reaction-step, including the total mass $M_{fiss}$ of the fissioning nucleus, the asymmetry $\eta$ of the mass division, the angles defining the direction of the fission axis and the relative velocity $v_{rel}$ between the fission fragments. They will be presented in detail elsewhere [10], together with indications that, at the end of the deep–inelastic phase, the emerging nuclei are not fully equilibrated [10, 11]. Here we like to put in evidence one particular aspect, which seems to indicate the need for some "pre-equilibrium" emission in order to give a consistent picture in terms of the decay of hot nuclei.

Fig.1 shows the reconstructed distributions of mass asymmetry $\eta$ in the second reaction step. The mass-asymmetry parameter is defined as $\eta = (m_1 - m_2)/(m_1 + m_2)$, where $m_1$ and $m_2$ are the masses of the two fragments resulting from the fission of a former deep-inelastic fragment of mass $m_{12}$; we choose $m_1 \geq m_2$ so that $0 \leq \eta < 1$. The data refer to fissioning primary masses in the range from 90 to 130 amu and from 110 to 150 amu for the $^{100}$Mo + $^{100}$Mo and $^{120}$Sn + $^{120}$Sn systems, respectively. The indicated values of the TKEL bins refer to the systems $^{120}$Sn + $^{120}$Sn (open squares) and $^{100}$Mo + $^{100}$Mo at 18.7 A·MeV (open circles).

The figure shows that the rise of the $\eta$ distributions at large mass asymmetries is somewhat more abrupt for the $^{120}$Sn + $^{120}$Sn system than for the $^{100}$Mo + $^{100}$Mo one and that, for both systems, the distributions tend to become flatter with increasing TKEL. The $\eta$ distributions of the system $^{100}$Mo + $^{100}$Mo at 23.7 A·MeV (filled circles) do not match the corresponding distributions at the lower bombarding energy when the comparison is

performed in the same TKEL bins. A similar situation had already been observed in ref. [1] for the probability of occurrence of a 3-body event $P_3$. At 23.7 A·MeV, a given value of $P_3$ was reached for a reconstructed TKEL larger than at 18.7 A·MeV. Assuming that $P_3$ reflected mainly the decay properties of the excited primary fragments, the difference in TKEL was tentatively attributed to a stronger emission of pre-equilibrium light particles at 23.7 A·MeV. Their removal of energy in an early phase of the collision has the consequence that equal values of reconstructed TKEL do not represent the same excitation in the two reactions. Therefore, for the 23.7 A·MeV data of fig.1, the adopted TKEL bins have been chosen in such a way as to give the same $P_3$ values as at 18.7 A·MeV (see e.g. fig.12 of ref. [1]); the shifts of TKEL necessary to do so are indicated in the caption of fig.1.

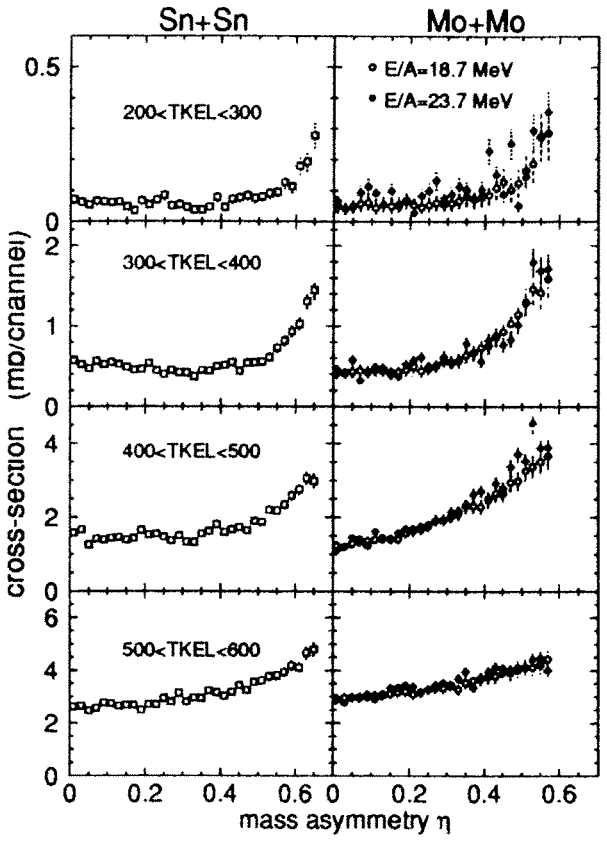


Figure 1: Distributions of mass asymmetry $\eta$ in the second reaction step, from 3-body events in the collisions $^{120}$Sn + $^{120}$Sn at 18.4 A·MeV (left, open squares) and $^{100}$Mo + $^{100}$Mo at 18.7 A·MeV (right, open circles). Distributions from the collision $^{100}$Mo + $^{100}$Mo at 23.7 A·MeV (right, filled circles) refer to bins at larger values of TKEL, namely, from top to bottom, 250–350, 370–470, 500–600 and 600–700 MeV.

It is evident that now the curves of the $^{100}$Mo + $^{100}$Mo system at the two bombarding energies coincide within the experimental errors. This suggests that in the $^{100}$Mo + $^{100}$Mo reaction at these two energies, the shape of the $\eta$ distributions and the sequential-fission probability are correlated. Also the widths of the out-of-plane angular distributions for these two cases seem to be consistent with about the same shifts.

It has been suggested [1, 10] that this seeming discrepancy between the results at the two bombarding energies may be ascribed to some kind of pre-equilibrium emission, which reduces the mass and the energy available for the interaction. In a symmetric colliding system, this emission does not distort the kinematics, on the average, but causes just an overestimation of masses and energies.

Further support for this interpretation is obtained by correlating primary quantities obtained from the kinematic reconstruction and secondary quantities measured in the telescopes. Fig.2 presents the "total charge loss" $\Delta Z$ vs. TKEL. $\Delta Z$ is taken as twice the difference between Z=42 (atomic number of Molibdenum) and the secondary charge Z measured in the telescopes, for fragments with reconstructed primary mass A=100±5.

It is therefore an estimate of the charge which is not found in the heavy fragments, but has presumably left the system, for whatever mechanism, in the form of light charged particles or intermediate-mass fragments.

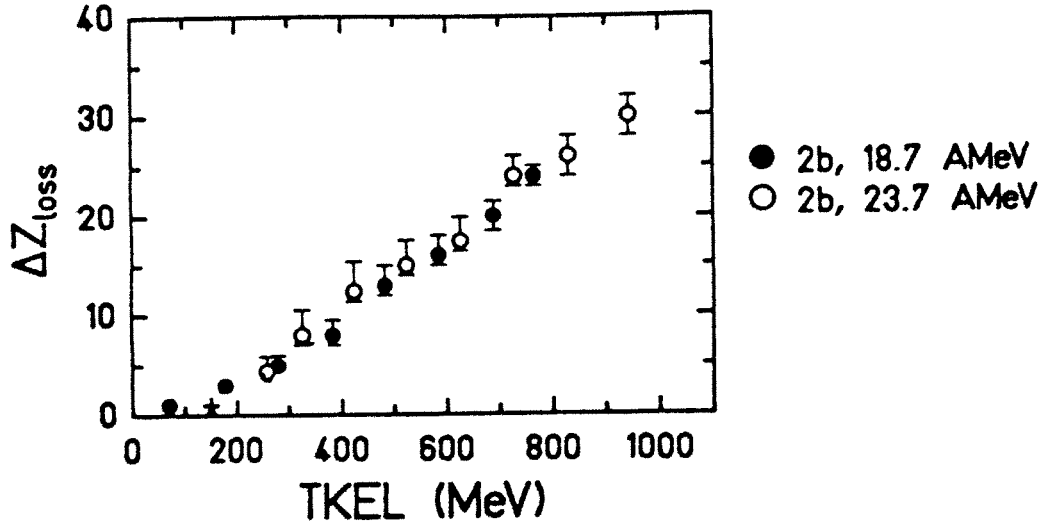


Fig.2 Total charge loss ($\Delta Z$) as a function of the total kinetic energy loss (TKEL) for the $^{100}$Mo + $^{100}$Mo system at 18.7 (filled circles) and 23.7 A·MeV (open circles).

The open and filled circles of fig.2 show the result for the $^{100}$Mo + $^{100}$Mo system at 23.7 and 18.7 A·MeV, respectively. One can first notice that (apart from the first $\approx$100 MeV, where there may be a preferential emission of neutrons) $\Delta Z$ correlates linearly with TKEL (with about 25 MeV for each charge unit at 18.7 A·MeV) even at the highest energy losses, where the probability of 3-body events $P_3$ presented a saturation or even a decrease [1]. A second observation concerns the above mentioned shifts of the TKEL-scale at 23.4 A.MeV attributed to the energy removed by pre-equilibrium particles. The good agreement of fig. 2 for the two sets of data indicates that (within the precision of the methode) there is no significant difference between the energy released by pre-equilibrium or evaporated charged particles.

## References


[1] R. Charity et al. Z. Phys, **A341** (1991) 53
[2] J.P. Wessels Master thesis, University of Heidelberg (1986)
[3] M. Gnirs Master thesis, University of Heidelberg (1986)
[4] G. Casini et al. Nucl. Inst. & Meth. **A277** (1989) 445
[5] A. Olmi in Proc. 8th High Energy Heavy Ion Study (Berkeley, U.S.A. 1987) 288
[6] B. Lott et al. Phys. Rev. Lett. **68** (1992) 3141
B.M. Quednau et al. Phys. Lett. **B309** (1993) 10
[7] J.P. Wessels PhD thesis, University of Heidelberg (1990)
[8] M. Gnirs PhD thesis, University of Heidelberg (1991)
[9] P.R. Maurenzig in Perspectives in Heavy Ion Physics (Catania, Italy 1992) 275
[10] A.A. Stefanini et al. to be published.
[11] G. Casini et al. Phys. Rev. Lett. **71** (1993) 2567

# Angular and velocity analysis of the three-fold events in the Xe + Cu reaction at 45 MeV/u.

M.Bruno[b], P.Buttazzo[e], M.D'Agostino[b], A.Ferrero[d], M.L.Fiandri[b], E.Fuschini[b], F.Gramegna[c], F.Gulminelli[d], I.Iori[d], L.Manduci[b], G.V.Margagliotti[e], P.F.Mastinu[b], P.M.Milazzo[b], A.Moroni[d],R.Scardaoni[d],G.Vannini[e], E. Plagnol[f], G. Auger[g].

[b] Department of Physics and INFN Bologna, [c] INFN, Laboratori Nazionali di Legnaro, [d] Department of Physics and INFN Milano, [e] Department of Physics and INFN Trieste, [f] IPN Orsay , [g] GANIL

The experiment was performed in the Nautilus scattering chamber at the GANIL facility by bombarding a Cu target with Xe beam at 45 MeV/u. Fragments were detected in the MULTICS apparatus(1). This apparatus is an array of 48 identical modules with front surface tangent to a sphere (with radius 50 cm) centered in the target position; the array covers the angular range $3^o$-$23^o$ with a geometrical efficiency of 72%. Each module consists in a three element telescope: an axial ionization chamber (IC length 8.5 cm), a two dimensional position sensitive solid state detector (Si), 500 μm thick and a CsI scintillator, 25 mm thick with photodiode read-out. The energy threshold, operating the IC at 200 mbar of $CF_4$, is ≈ 2.5 MeV/u, corresponding to a velocity≈ 2.2 cm/nsec.
The overall energy resolution is better than 2%, the angular resolution ranges from $0.2^o$ to $0.3^o$(2) and the atomic numbers can be identified up to Z=56.
The trigger was given by the 45/48 Si detectors working during the measurement; the Z identification was possible only for the telescopes with low threshold, due to some technical problems, that is≈ 50% of total detectors; the angular coverage considered in the analysis was $\theta > 5.5^o$ . Thus, since the grazing angle for this reaction is less than $2^o$ , most of the events coming from peripheral reactions were not detected, as the projectile-like fragments were outside the acceptance of the apparatus.

*Inclusive data*

The experimental cross sections as a function of the IMF (Z>2) multiplicity and the inclusive Z cross sections are shown in Fig. 1. A non negligible contribution of high multiplicity events has been found, not reproduced by a statistical binary decay model (Gemini code(3)) with inputs obtained from the incomplete fusion systematics.
Since the gross features of the data mainly depend on the weight of the impact parameter, we took then into account the entrance channel dynamics, coupling the Gemini code to a dynamical model based on the BNV equation(4). Theoretical predictions were then filtered, event by event, through the detector acceptance, in order to allow a meaningful comparison with the data. A fairly good agreement between inclusive data and calculations results which indicates that the entrance channel characteristics like masses, charges, excitation energies and angular momenta of the sources were correctly calculated using the BNV dynamics: the results filtered by the acceptance of the apparatus show that, due to the minimum detection angle, the contribution of b>6 fm to the cross section is negligible.

*Exclusive data*

The analysis was then focused on three and four-fold coincidence data. These data are predicted to come mostly from impact parameters≈ 5 fm, where two sources

with sufficiently high excitation and angular momentum are formed and at least one of them undergoes a binary decay.
The fact that three and four-fold events can be associated to central and medium impact parameters was confirmed by studying both the observable $Y_{3\,3}=\langle V_{rel}\rangle - V_{rel(min)}$[5], as shown in Fig.2, were the experimental data do not show the typical ridges corresponding to peripheral reactions, and by analyzing the Z correlation and the angular and velocity distributions of three fold events[6,7].
Different sets of events in the charge correlation triangle (Fig.3) have been observed: regions I and II of high and low charge asymmetry come from reactions at different impact parameters. The angular and velocity analysis shows that the events with three nearly equal fragments (region I) seem to correspond to very central collisions ($b<2$). The relative velocities and angles of these IMF are typical of a simultaneous multifragmentation of an expanding hot source. The three fold events coming from region II, on the contrary, seem to come from more peripheral collisions ($b>3$); the argument relies in the similiarity of these fragments with the projectile and the target as far as the angular and velocity distributions are concerned.
We have compared our data with two different de-excitation models following a BNV dynamical calculation, namely a sequential decay[3] and a prompt multifragmentation[8] model. The events corresponding to the region I cannot be due to a binary statistical sequential de-excitation of a hot equilibrated source: the distributions of the relative velocities and angles demand a prompt multifragment emission; some promising agreement with the statistical model by D.H. Gross is found, even if some discrepancies are still present. The main discrepancy relies to the theoretical multiplicities that are higher than the observed ones.
These results may indicate that the assumption of an homogeneous isoentropic expansion of the intermediate source may be correct if it could be possible to change some ingredient of the calculation: disregarding infact the lightest fragments the overall agreement between predictions and experimental data looks reasonable. Fig.4 show the predictions of the multifragmentation model filtered by the apparatus without any constraint (a,b) and with the constraint $Z>6$ (c,d).

*References*


1) M. Bruno et al. NIM **A325**(1993)458
2) M. Bruno et al. NIM **A311**(1992)189
3)R. J. Charity et al. Nucl. Phys. **A483**(1988)371
4) A. Bonasera et al. XXIX Int. Wint. Meeting Bormio(1991) p.193
5) M. Louvel et al. XXX Int. Wint. Meeting Bormio(1992) p.11
6) M. Bruno et al. Phys. Lett. **B292**(1992)251
7) M. Bruno et al. submitted to Nucl. Physics
8) D.H.E. Gross et al. Phys. Rev. Lett.**56**(1986)1544
and A.R. De Angelis and D.H.E. Gross, Comp.Phys.Comm.**76**(1993)113

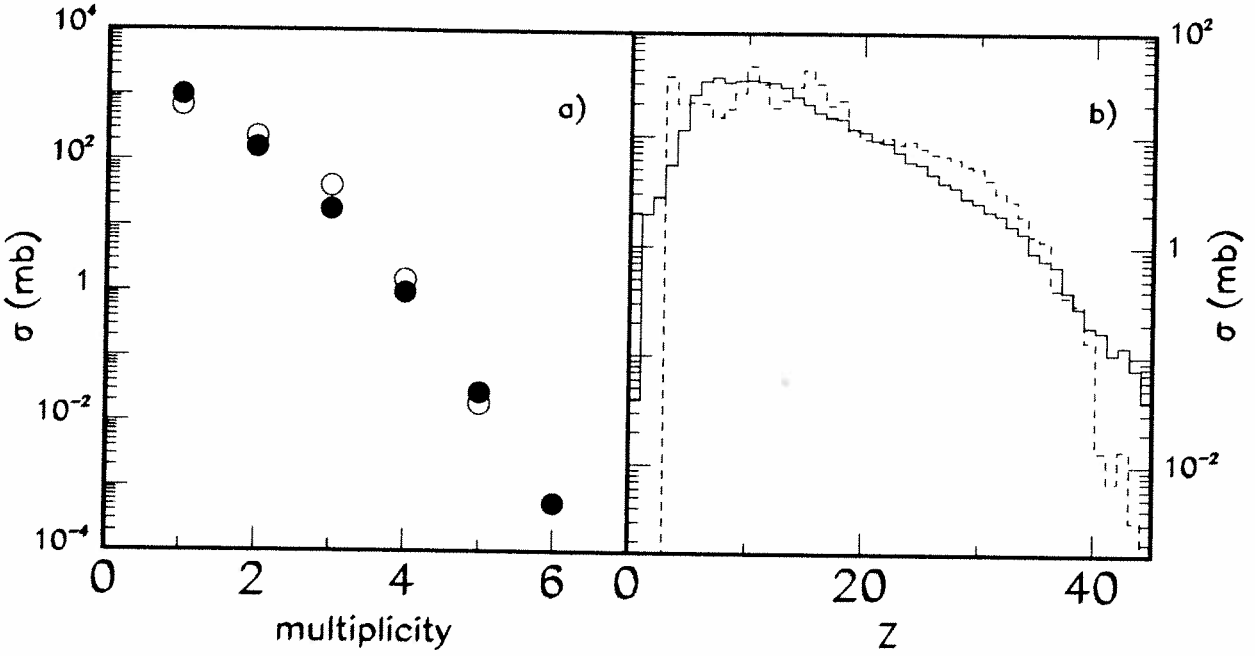


Fig. 1 - Cross section as a function of the multiplicity for the overall apparatus. Full circles show the experimental results, the open ones predictions from the coupled dynamical and statistical approach, filtered by the apparatus.

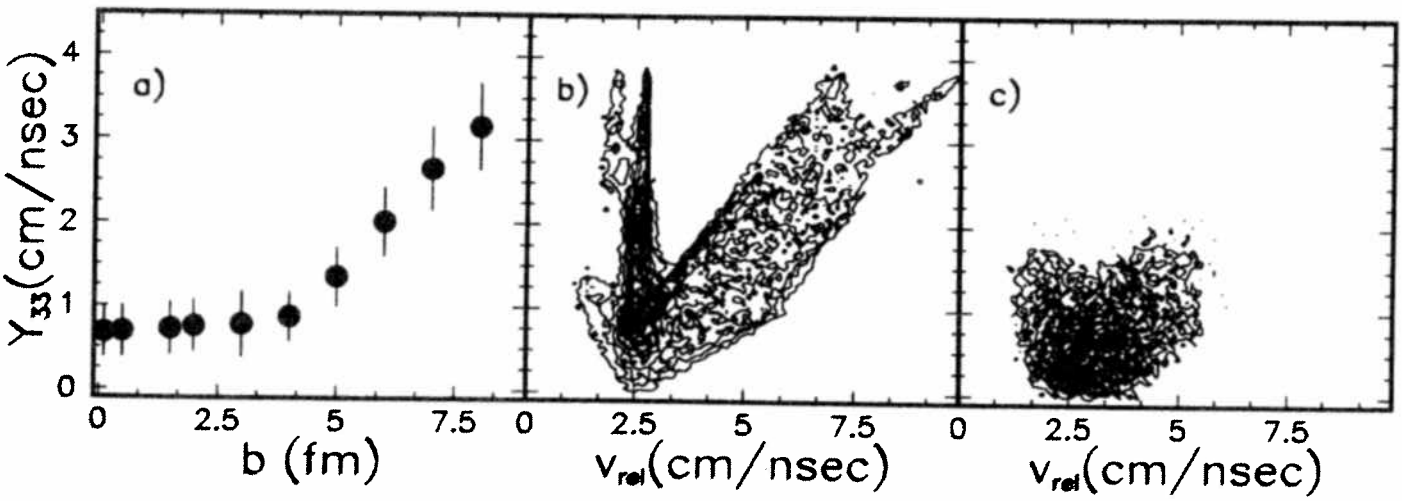


Fig. 2 -

a) Plot of Y33 (cm/ns) vs b(fm) predicted by BNV+Gemini calulations.
b) Contour plot of the predicted Y33 vs $v_{rel}$ for the 3-fold event.
c) same as b) but experimental

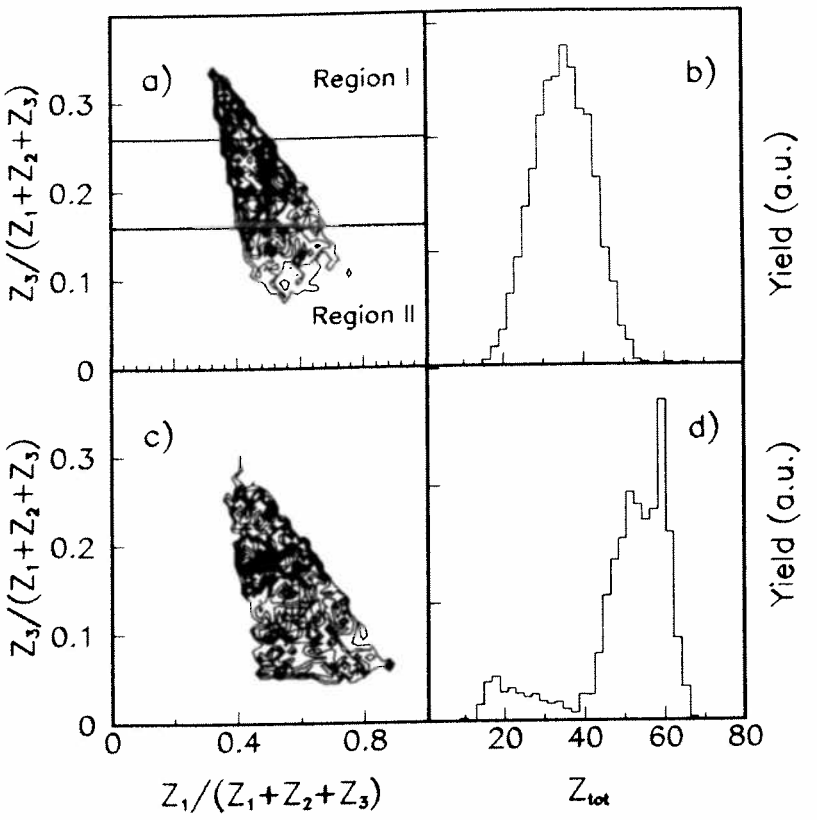


Fig. 3 - a) Plot of $Z_{min}/(Z_1+ Z_2+ Z_3)$ versus $Z_{max}/(Z_1+ Z_2+ Z_3)$ for 3-fold events. The lines delimitate the regions I and II as explained in the text.
b) Sum of the charges of all IMF detected in three-fold events.

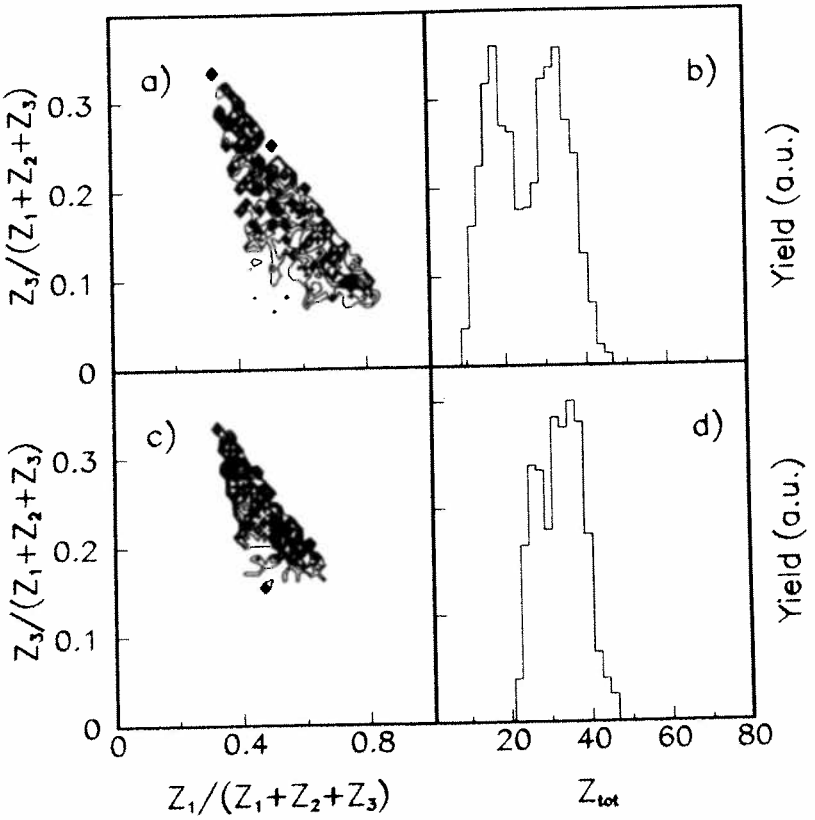


Fig. 4 - Prediction of the multifragmentation model, filtered by the acceptance the apparatus:
a) $Z_{min}/(Z_1+ Z_2+ Z_3)$ versus $Z_{max}/(Z_1+ Z_2+ Z_3)$ for 3-fold events
b) Sum of the charges of the IMF for 3-fold events
c) $Z_{min}/(Z_1+ Z_2+ Z_3)$ versus $Z_{max}/(Z_1+ Z_2+ Z_3)$ for 3-fold event ($Z \geq 6$).
d) Sum of the charges of the IMF for 3-fold events ($Z \geq 6$).

# Damped Reaction Dynamics in $^{197}$Au+$^{208}$Pb Collisions at E/A = 29 MeV

B.M. Quednau, S.P. Baldwin, B. Lott[†], W.U. Schröder, B.M. Szabo, J. Tõke
*University of Rochester*[‡]; D. Hilscher, U. Jahnke, H. Rossner *HMI Berlin*;
S. Bresson, J. Galin, D. Guerreau, M. Morjean *GANIL*; D. Jacquet *IPN Orsay*

## 1. Motivation

The purpose of the experiment was to establish characteristic features of the intermediate-energy reaction mechanism by identifying the mechanisms of neutron emission and evaluating the energy deposited in the nuclear system. The system $^{197}$Au + $^{208}$Pb at $E/A$ = 29 MeV was chosen for study, because for a heavy system the well-known low-energy reaction mechanism [1,2] is expected to evolve gradually with bombarding energy and impact parameter. The experimental technique employed in this work consists in the measurement of emission patterns of neutrons associated with charged reaction products ranging from intermediate-mass fragments (IMF) to projectile-like fragments detected at selected angles. With this technique, it is possible to study the evolution of energy dissipation for the full range of impact parameters, since all reaction products from such a heavy, neutron-rich system cool preferentially by the emission of neutrons[3,4]. A partial account of the data has been given in [5].

## 2. Experimental Setup

A beam of $^{208}$Pb projectiles was used to bombard a 2.1 mg/cm$^2$-thick gold target placed in the center of a thin-wall scattering chamber. Three silicon-detector telescopes, located at angles of $+8.5°$, $-6.5°$, and $-21.5°$, detected heavy fragments. Three large-area multi-strip silicon detectors covering angles between $+28°$ and $+81°$ were used to measure the recoil angles of target-like fragments (TLF), in kinematical coincidence with their projectile-like collision partners (PLF) detected at -6.5°. Neutrons were detected using a time-of-flight (TOF) spectrometer consisting of 21 scintillation counters placed in a plane common with the charged-particle detectors. The cyclotron RF and timing signals from the anodes of the photomultipliers were used to provide start and stop signals, respectively, for the TOF measurement. Discrimination between neutrons and $\gamma$-rays was accomplished employing pulse-shape analysis. A more detailed description of the experimental setup can be found elsewhere[5].

## 3. Fragment Distributions

In Fig. 1, the yield of charged products detected at $-6.5°$ is plotted in form of a contour diagram versus kinetic energy ($E$) and atomic number ($Z$). The most prominent feature in this distribution is the peak at $Z \approx 82$ and $E \approx 6$ GeV formed by quasi-elastic events. From this peak, a continuous ridge of cross section extends down into the region of IMF. Superimposed on this ridge are two components of fragments with $Z \approx 40$, and $E \approx 2$ GeV and 3.5 GeV, respectively. These latter fragment groups correspond to the two kinematical solutions for fragments from fission of the fast-moving PLF.

---

[†] on leave from Centre de Recherches Nucléaires, F-67037 Strasbourg, France

[‡] supported by the U.S. Department of Energy under Grant No. DE-FG02-88ER40414.

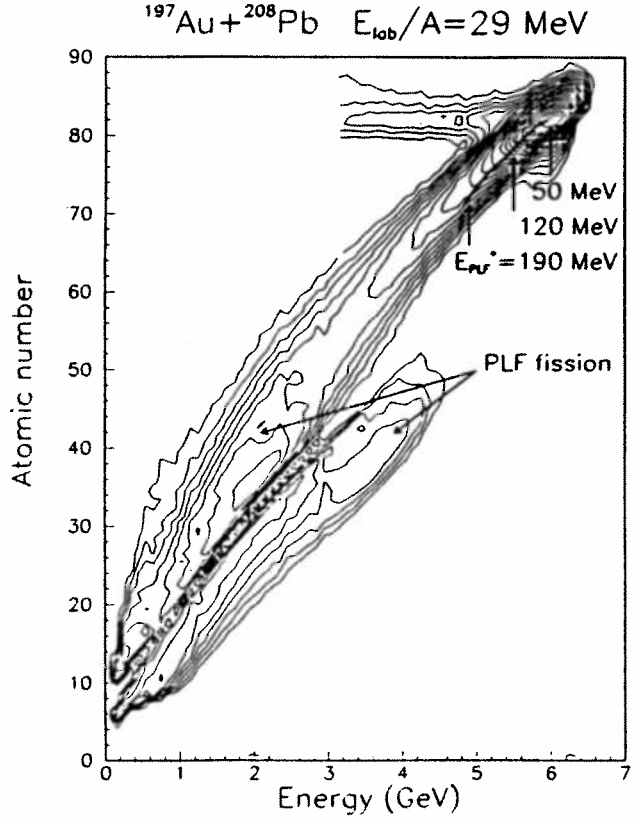


Figure 1: Logarithmic contour diagram of the charged fragment yield at -6.5°, versus atomic number and laboratory energy. The solid line represents results of theoretical calculations for the ridge line of the distribution assuming a damped-collision model. The horizontal ridge and the diagonal discontinuity seen in this figure are instrumental artifacts due to slit scattering and an inactive layer in one of the telescope elements, respectively.

The strong correlation between atomic number and kinetic energy of the PLF, represented by the narrow ridge in Fig. 1 cannot be explained in terms of an overall drift of the primary PLF charge distribution. Because of the mass symmetry of the system, there is no effective driving force for proton transfer. However, as shown by simulation calculations[5], such correlations can be attributed to the effect of a competition between fission and evaporation on a primary fragment distribution whose width increases with increasing dissipation.

Results of model calculations for relatively peripheral collisions, assuming a binary damped reaction scenario, are represented by the solid line in Fig. 1 The primary fragment distributions were calculated with the nucleon-exchange model[6] (NEM) in the non-adiabatic, frozen-density approximation[7]. The decay of the primary fragments was then simulated with the evaporation code[8] EVAP. As seen in Fig. 1 the calculations reproduce the experimentally observed average correlation between atomic number and kinetic energy rather well. The arrows in Fig. 1 indicate excitation energies for the PLF.

The validity of the binary reaction scenario and of other model predictions was confirmed in a kinematical coincidence measurement of PLF-TLF pairs. In particular, for given secondary fragments, the coincidence data provided values of the total kinetic energy loss that are in agreement with those obtained from the simulation calculations and are also compatible with the emission patterns of associated neutrons discussed below.

## 4. Neutron Distributions

The evolution of the dissipative reaction mechanism with impact parameter was inferred from velocity distributions of neutrons measured in coincidence with different types of charged reaction products, representing different degrees of dissipation. These distributions are nonisotropic even for most dissipative collision events and indicate the presence

of at least two major neutron components.

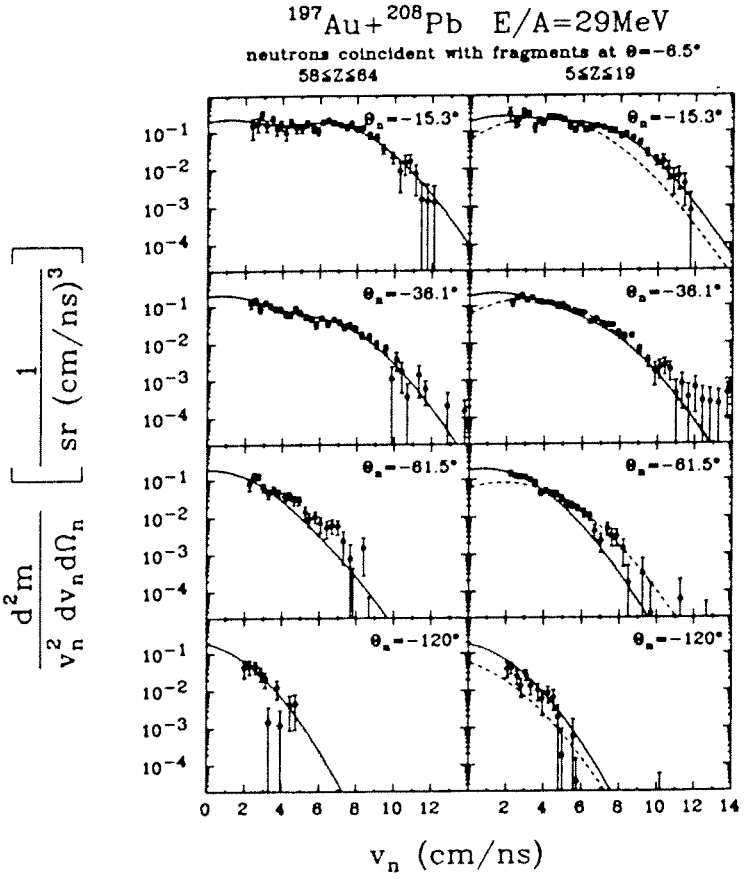


Figure 2: Galilei-invariant velocity spectra for neutrons at selected detection angles $\Theta_n$ coincident with PLF of $58 \leq Z \leq 64$ (left side) and IMF of $5 \leq Z \leq 19$ (right side) detected at $\Theta = -6.5°$. The dotted curves show results of a fit to the data assuming a source representing the composite system. The solid curves result from a fit assuming an average PLF and TLF source.

Very high degrees of energy dissipation were found in the present experiment for events associated with the following two classes of fragments measured at $\Theta = -6.5°$, massive fragments with $58 \leq Z \leq 64$ and IMF with $5 \leq Z \leq 19$. As could be inferred from the experimental velocity-angle correlations[5], the emission pattern of neutrons in coincidence with massive fragments has a bimodal shape, with a fast-neutron component aligned with the detection direction of the PLF, indicating significant emission from this fragment. Representative one-dimensional neutron velocity spectra are displayed in the left-hand column of Fig. 2 for four (out of 21) neutron detection angles $\Theta_n$. The solid curves represent a fit of the neutron spectra with a theoretical evaporation spectrum, assuming isotropic emission from effective PLF and TLF described by common source parameters. This assumption provides a satisfactory description of the neutron spectra at most angles. At intermediate angles, $30° < |\Theta_n| < 70°$, an additional, relatively weak component is seen, attributed to a nonequilibrium (neq) emission process. From this fit, source parameter values of $m_{PLF} = m_{TLF} = 25 \pm 4$ and $\tau_{PLF} = \tau_{TLF} = (3.7 \pm 0.4)$MeV, as well as a kinetic-energy loss of $E_{loss}$= $(1500 \pm 200)$MeV and a PLF scattering angle of $\Theta_{PLF} = -3°$, were deduced. This energy loss is significantly smaller than the available kinetic energy of $E_{cm} - V_c = 2.5$ GeV. As ascertained by statistical-model calculations, the above set of parameters is internally consistent. It corresponds to initial temperatures of PLF and TLF of $T_{PLF} = T_{TLF} \approx 5$MeV. From the fit and an extrapolation of the excess

yield, assuming azimuthal isotropy, the average total neutron multiplicity is estimated to $m_{tot} = 58 \pm 2$. A value of $m_{neq} = 8 \pm 2$ is estimated for the multiplicity of the nonequilibrium component.

The second class of highly dissipative events is accompanied by IMF emission, an observation in agreement with other works.[9,10,11] A selection of one-dimensional velocity spectra of neutrons is shown on the right-hand side of Fig. 2 along with theoretical fit curves for two different emission scenarios. The dashed curves in Fig. 2 are calculated assuming a scenario in which a single equilibrated composite system (CS) is formed, moving with the velocity of the center of mass and evaporating IMF as well as neutrons. A neutron multiplicity of $m_{CS} = 45$ and an effective source temperature of $\tau_{CS} = 5$ MeV are obtained from this fit. The neutron spectra at intermediate angles are mostly accounted for by such a single-source scenario. However, significant and systematic discrepancies between the data and predictions by this model are present at both forward and backward angles, as illustrated by the spectra at $\Theta_n = -15.3°$ and $\Theta_n = -120°$ shown in Fig. 2 Moreover, the relatively low effective temperature and low total neutron multiplicity are inconsistent with complete dissipation of the total kinetic energy of $E_{cm} = 2.9$ GeV, as would be required by this single-source scenario. These inconsistencies suggest that, in the present $^{197}$Au+$^{208}$Pb reaction, evaporation from a composite system is not seen with significant cross section.

The second reaction scenario considered explicitly assumes two effective sources of neutrons representing fully accelerated PLF and TLF. This somewhat more complex scenario is still an oversimplification of the actual process in which neutrons could be evaporated, e.g., also from excited IMF. However, such additional sources are not expected to affect the neutron yields significantly. Results of a fit based on the above two-source model are shown by solid curves in Fig. 2. In the fitting procedure, first a value of $E_{loss}$ =(1900 $\pm$ 200) MeV was inferred from data at forward and backward angles, PLF and TLF "master" angles, respectively, in order to reduce the sensitivity of this energy loss value to the nonequilibrium component discussed previously. Next, only the common source parameters were varied in an overall fit to the data at all angles. The resulting values for the source parameters are $m_{PLF} = m_{TLF} = 27 \pm 2$ and $\tau_{PLF} = \tau_{TLF} = (4.0 \pm 0.4)$MeV ($T_{PLF} = T_{TLF} \approx 5.5$MeV). This set of parameters, including the value deduced for the energy loss, is internally consistent, quite in contrast to that for the one-source scenario discussed previously. The average total multiplicity obtained for this second class of highly dissipative events is $m_{tot} = 60 \pm 2$.

It is interesting to note that the respective values for neutron multiplicity and effective source temperature for the two classes of highly dissipative events, identified by PLF ($58 \leq Z \leq 64$) or IMF ($5 \leq Z \leq 19$) detected at $\Theta = -6.5°$, are very similar to each other. Most significantly, these types of highly dissipative events are associated with similar energy losses, accounting for only 60% – 80% of the available total kinetic energy. It is worth noting that the limit on $E_{loss}$deduced in this work represents an ensemble average that is characteristic of highly dissipative $^{197}$Au+$^{208}$Pb collisions. Therefore, it can not be excluded that events with significantly higher energy losses are present with a small cross section.

## 5. Conclusion

In conclusion, the experimental results reported in this work on the reaction $^{197}$Au + $^{208}$Pb reflect the dominantly binary, dissipative character of the reaction mechanism, for all degrees of dissipation. For all event triggers, the neutron emission patterns are essentially bimodal and characteristic of sequential neutron emission from primary PLF and TLF with only a small contribution of prompt, nonequilibrium processes. Values of source velocities, neutron multiplicities, and spectral temperatures are found to be consistent with dissipation of total kinetic energy of not more than $E_{loss} \approx 1900$MeV. No evidence was found in the experimental data that either the entire available kinetic energy of $E_{cm} = 2.9$GeV or the energy above the interaction barrier $E_{cm} - V_c = 2.35$GeV is dissipated. The observations made in this work reveal features of the reaction mechanism that, if confirmed, present a clear challenge to theoretical reaction scenarios assuming the formation of essentially mono-nuclear systems in central heavy-ion collisions at intermediate bombarding energies.


1. W.U. Schröder and J.R. Huizenga, in: Treatise on Heavy-Ion Science, Vol. 2, ed. D.A. Bromley (Plenum, New York and London, 1984) p. 113, and references therein.
2. R.G Stokstad, in: Treatise on Heavy-Ion Science, Vol. 3, ed. D.A. Bromley (Plenum, New York and London, 1984) p.81 , and references therein.
3. E. Piasecki et al., Phys. Rev. Let. 66 (1991) 16.
4. B. Lott et al., Phys. Rev. Let. 21 (1992) 3141.
5. B. Quednau et al., Phys. Lett. B309 (1993) 10.
6. J. Randrup, Nucl. Phys. A383 (1982) 468.
   J. Døssing et al., Nucl. Phys. A433 (1985) 215; A433 (1985) 280.
7. J. Błocki et al., Ann. Phys. 105 (1977) 427.
8. N.G. Nicolis, et al., private communication.
9. L.G. Moretto et al., Prog. Part. Nucl. Phys. 21 (1988) 401.
10. Y.D. Kim et al., Phys. Rev. C45 (1992) 338.
    D.R. Bowman et al., Phys. Rev. Lett. 67 (1992) 1527.
11. K. Kwiatkowski, Nucl. Phys. A471 (1987) 271c.

# Production of very hot (E/A = 6 MeV/u) heavy nuclei through binary fully damped $^{208}Pb$ + $^{197}Au$ collisions at 29 MeV/u [1]

D. Jacquet[1], R. Bougault[2], S. Bresson[3], J. Colin[2], E. Crema[3], J. Galin[3], B. Gatty[1], A. Genoux-Lubain[2], D. Guerreau[3], D. Horn[2], U. Jahnke[4], J. Jastrzebski[5], A. Kordyasz[6], C. Le Brun[2], J.F. Lecolley[2], B. Lott[7], M. Louvel[2], M. Morjean[3], C. Paulot[3], E. Piasecki[6], L. Pienkowski[5], J. Pouthas[3], B. Quednau[8], W.U. Schroder[8], W. Skulski[5], J. Toke[8]

*1) I.P.N., BP 1, 91406 Orsay Cedex, France*
*2) L.P.C., Bd Marechal Juin, 14032 Caen Cedex, France*
*3) GANIL, BP 5027, 14021 Caen Cedex, France*
*4) Hahn Meitner Institut, D1000 Berlin 39, FRG*
*5) Heavy Ion Lab, Warsaw Univ., ul. Banacha 4, 02-097 Warszawa, Poland*
*6) Inst. of Exp. Phys., Warsaw Univ, Hoza 69, 00-681Warszawa, Poland*
*7) C.R.N., BP 20 CRO, 67037 Strasbourg Cedex, France*
*8) Univ. of Rochester, Rochester, New-York 14627, USA*

## Motivation

Within the last decade , (incomplete) fusion reactions have been extensively used to produce hot nuclei. However, for incident kinetic energies higher than about 30MeV/u, a large part of the available energy can be taken away by promptly emitted particles and nuclei or can be dissipated in non thermal excitation energy (compressional energy, rotational energy...). Recently [1,2] the persistence of deep-inelastic collisions has been claimed in the Fermi energy region. The large energy damping associated to the most relaxed collisions brings an interesting alternative way to produce hot nuclei close to their limit of stability.
As the energy deposit is expected to be more effective for symmetric systems, and as the pre-equilibrium emission involved in central collisions will be minimized with very heavy symmetric systems, the $^{208}Pb$+$^{197}Au$ system at 29 MeV/u has been studied.

The determination of the thermal excitation energy has been done from the measurement of evaporated neutron multiplicities [3,4]. By following the evolution of the population of charged products detected in a large angular range with the neutron multiplicity, it has been possible to study the evolution of the reaction mechanism over a large range of impact parameters with gradually varying initial conditions.

## Experiment

Neutrons were counted by ORION[5], a $4\pi$ detector, whose efficiency has been computed with various reaction scenario. Assuming a quasi elastic reaction, a partly damped reaction, a fully damped reaction, or a more or less incomplete fusion reaction leads always, due to compensation effects, to an overall efficiency close to 64%.

A small scattering chamber was located inside ORION and contained the target and various charged particle detectors: The first set of detectors was a telescope covering an angular range between 6° and 20°. It consisted of two Silicon detectors (200

[1] Experiments performed at Ganil

$\mu$m and 500 $\mu$m) followed by a 300 $\mu$m silicon detector backed by 8cm CsI detectors. The first member was separated in 6 horizontal independent strips and the second member, in 6 vertical independent strips. The combination of these two detectors allows for the identification of fragments ranging from Z=4 up to Z=48 and provided us with the position of the detected fragments with a precision better than 1°. For fragments with atomic number higher than Z=48, only a rough Z identification has been performed.

Beside this Si hodoscope, five conventional silicon telescopes consisting of three members ( whose typical thicknesses were 30$\mu$m, 300$\mu$m, 5000$\mu$m ) were located at 6.2°, 8°, 20°, 30° and 50°. They allowed for the identification of fragments of Z > 6 with a typical threshold of 3.5 MeV/u for Z=20 fragments. The results concerning the fission events [6] are given in another paper; the present contribution is dedicated to these very dissipative collisions in which the system disassembles into a large number of neutrons, light charged particles and intermediate mass fragments[7] (IMF).
To get further insight into the origin of these IMF's, a possible common source for these fragments has been looked for. Fig. 1 presents for Z=25 fragments the quantity $\frac{\partial^2\sigma}{\partial v_{\|}\partial v_{\perp}}$ plotted in the $(v_{\|}, v_{\perp})$ plane for different neutron multiplicity bins.
From these plots one can see a rather fast component, associated with the projectile-like nucleus, and the tail of a much slower component, severely cut by detection thresholds, probably associated to its target-like partner. A tentative assignment of these two sources has been done following the assumptions listed below:
The system is considered as a perfectly symmetric system at each step of the collision process, and the properties of the target-like nucleus have been completely inferred from those of the projectile-like nucleus assuming binary kinematics.
The detected IMF's are then supposed emitted either by the projectile-like fragment ( PLF) or by the target like fragment ( TLF). The velocity and deflection angle of the PLF is derived from the position of the center of the circular contours which can be drawn through the data. The radii of these circles correspond to the coulomb velocity between the IMF and the remnant of the PLF whose charge is thus simply deduced. This procedure , similar to what has been applied to fission data [6], has been extended to lighter fragments and high neutron multiplicity bins, where the detection thresholds prevented us to isolate the entire circular isocontour.

From Fig. 1 it appears that for the two highest neutron multiplicity bins the relative velocity between the PLF and the TLF nuclei corresponds roughly to the Coulomb repulsion between gold and lead nuclei, indicating clearly that the full damping of the incident energy has been reached, in agreement with conclusions of ref [8] for the same system and with ref [1] for the Mo + Mo system at slightly lower bombarding energy.

In such collisions the dissipated energy amounts to 2.5 GeV, i.e. excitation energies greater than 6 MeV/n can be stored in a quasi-lead nucleus ( the energy removed by pre-equilibrium emission has been shown to be small [9]). Such an excitation energy appears to exceed the amount of heat that a nucleus can sustain, remaining a self-bound object, as computed by of Bonche et al [10] ( 3MeV/n for such heavy nuclei).

*Figure 1:* $\frac{\partial^2\sigma}{\partial v_{\parallel}\partial v_{\perp}}$ *plotted in the* $(v_{\parallel}, v_{\perp})$ *plane for Z=25 fragments, for four neutron multiplicity bins. The figure has been symmetrized with respect to the beam axis. The experimental thresholds for the telescopes located at 6, 8, 20, 30 and 50° are much lower than those of the Si stripped detector covering the angular range 6-20°.*

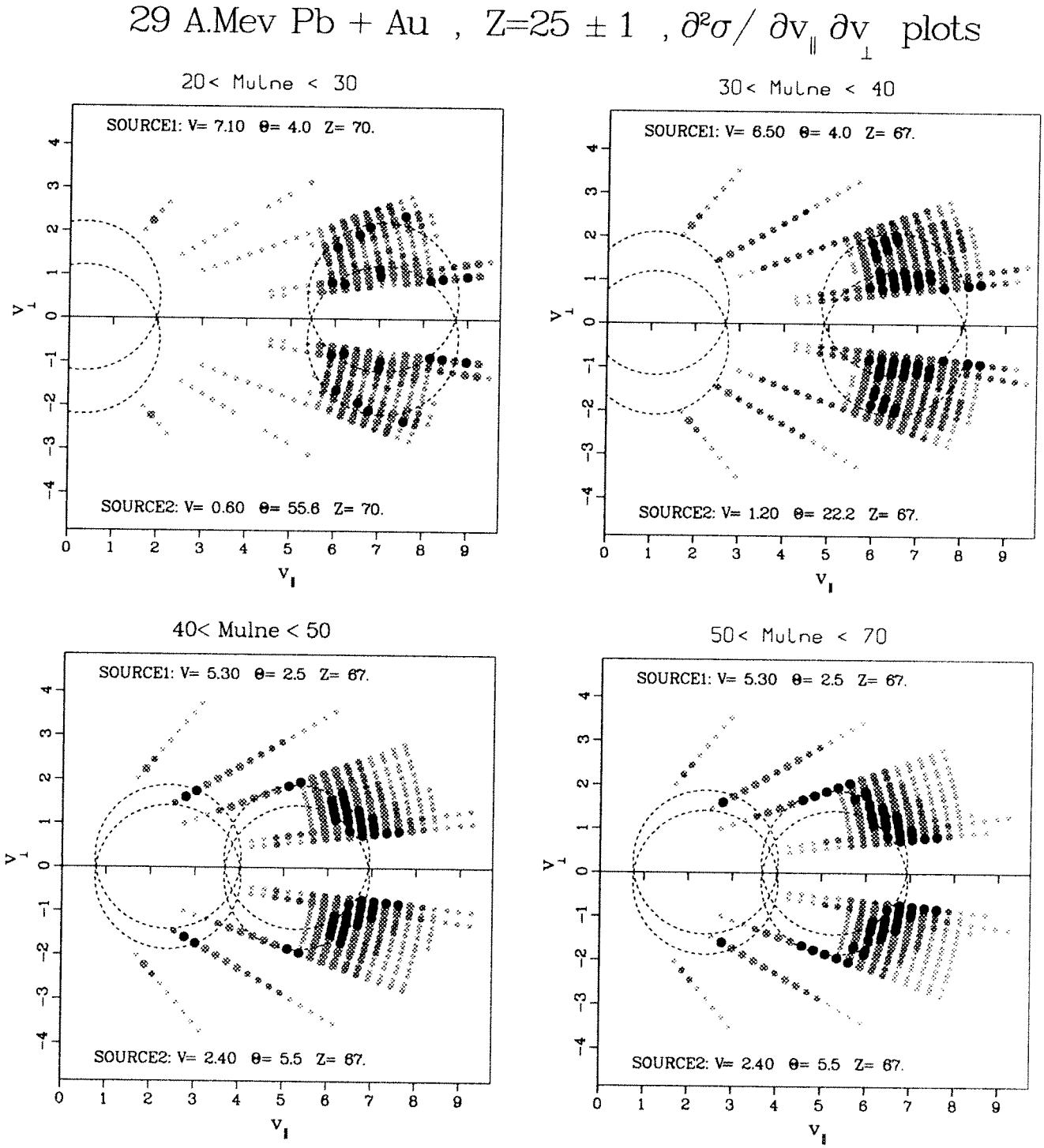

The average multiplicity of fragments of charge ranging from Z=6 to Z=50 has been integrated from measured differential cross sections between $6^o$ and $50^o$ as a function of the neutron multiplicity.

From these measured multiplicities if one assumes :
- All the fragments originate on the average from the same source that has been identified for emitted Z = 25 fragments for the different neutron multiplicity bins
-An isotropic emission in the rest frame of these sources
then it is possible to estimate the ImF multiplicities integrated over $4\pi$ as listed in table 1.

| *Mn* *uncorrected for* $\epsilon$ | *Mimf* *as measured from* 6 *to* 50 $^o$ | *Mimf* *integrated over* $4\pi$ |
|---|---|---|
| 0 – 10 | 0.00 | 0.0 |
| 10 – 20 | 0.2 | 0.3 |
| 20 – 30 | 0.9 | 1.5 |
| 30 – 40 | 2.1 | 3.2 |
| 40 – 50 | 3.5 | 4.7 |
| 50 – 70 | 3.8 | 5.0 |

**Table 1**
Intermediate mass fragments ( $50 \geq Z \geq 6$ )multiplicities
for different neutron multiplicity bins

For the most dissipative collisions, these integrated multiplicities are in excellent agreement with those of ref [8] obtained for the same system. Further investigations have to be carried out in order to determine whether the disassembly of the system results from a classical sequential evaporation from a highly excited system or from a simultaneous multifragmentation mechanism which might sign that, for this system, the limits of excitation energy that a nucleus can sustain have been reached in the most dissipative collisions.

## References


1. Charity et al, *Z. Phys.* **A 341** (1991) 53
2. B. Borderie et al, *Phys. Lett.* **B205** (1988) 26
3. D.X. Jiang et al, *Nucl. Phys.* **A503** (1989) 560
4. E. Crema et al, *Phys. Lett.* **B258** (1991) 266
5. J. Galin et al, in *Proc. of the 2nd IN2P3-RIKEN Symposium, Obernai*, ed B. Heusch and M. Ishihara (World Scientific, 1990)
6. S. Bresson et al, *Phys. Lett.* **B294** (1992) 33
7. E. Piasecki et al, *Phys. Rev. Lett.* **66, 10** (1991)1291
8. J.F. Lecolley et al , *Rapport LPCC 93-15* and M. Aboufirassi et al, *Rapport LPCC 93-14*
9. B. Quednau et al, *Phys. Lett.* **B309** (1993) 10
10. S. Levit et al, *Nucl. Phys.* **A437** (1985) 426 and J. Besprosvany et al, *Phys. Lett.* **B217** (1989)1

# *HEAVY NUCLEI SUSTAIN HIGH EXCITATION ENERGIES IN 29 MeV/u Pb+Au REACTIONS*

M. Aboufirassi [a)], A. Badala [a-e)], B. Bilwes [b)], R. Bougault [a)], R. Brou [a)], J. Colin [a)], F. Cosmo [b)], D. Durand [a)], G. Galin [c)], A. Genoux-Lubain [a)], D. Guerreau [c)], D. Horn [a-f)], D. Jacquet [d)], J.L. Laville [a)], C. Le Brun [a)], J.F. Lecolley [a)], F. Lefebvres [a)], O. Lopez [a)], M. Louvel [a)], M. Mahi [a)], M. Morjean [c)], A. Peghaire [c)], G. Rudolf [b)], F. Scheibling [b)], J.C. Steckmeyer [a)], L. Stuttge [b)], B. Tamain [a)], S. Tomasevi [b)]

a) *Laboratoire de Physique Corpusculaire (IN2P3-CNRS/ISMRA)*, Boulevard du Maréchal Juin, F-14050 CAEN cédex, FRANCE.
b) *Centre de Recherches Nucléaires (IN2P3-CNRS/Université Louis Pasteur)*, B.P. 20, F-67037 STRASBOURG cédex, FRANCE.
c) *GANIL (DSM-CEA/IN2P3-CNRS)*, B.P. 5027, F-14021 CAEN cédex, FRANCE.
d) *Institut de Physique Nucléaire (IN2P3-CNRS/Université Paris Sud)*, B.P. 1, F-91406 ORSAY cédex, FRANCE.
e) on leave from *INFN-Catania*, Catania, ITALY.
f) on leave from *CRL (AECL)*, Chalk River, Ontario, CANADA.

## 1) Introduction

The purpose of this study is to answer the following questions:

1) Results (1) have shown that the deep inelastic mechanism is still present at 20 MeV/u for lighter systems and lower available center-of-mass energy as compared to the present case. Accordingly, is there for such high relative velocities between the two partners a complete damping of the kinetic energy or is the collision too fast to prevent the dissipation from being fully achieved (2)(3)

2) What is the evolution of the decay modes of massive and highly excited nuclei produced in reactions when the dissipated energy increases ? (4). In particular, is a nucleus able to sustain high temperatures without undergoing multifragmentation ?

## 2) Experimental description and data sampling

The experiment was performed at the GANIL facility in the Nautilus scattering chamber by bombarding a 500 $\mu g/cm^2$ Au target with a 1 particle nA Pb beam at 29 MeV/u. Fragments (Z>8) were detected using the low velocity threshold detectors Delf (5) and XYZT (6), while light charged-particles were detected with the Mur (7) and the Tonneau (8). The covered angular range is from 3°-150° with a 55 % geometrical acceptance. The measured parameters are the atomic number Z, the fragment velocity V and the angle, with a resolution better than one degree for fragment detection. The Mur and the Tonneau were not used in the triggering condition which was decided among the 30 PPACs of Delf and XYZT.

Since we will be interested here in n-fragment production, it is of primary importance to select events which are as completely detected as possible (i.e. as well characterized as possible) in order to avoid mixing between different n-fold coincidences. To this end, we have retained only events leading to detection of more than 80 % of both the available total parallel momentum and total charge.

These measured values take into account fragments and light charged-particles. The latter, which did not contribute to the triggering condition, were corrected by a factor of 2 to take into account the 50% geometrical acceptance of the Mur and Tonneau.

Large values (up to 7) of fragment multiplicity have been reached with sizeable cross sections. The azimuthal symmetry of the experimental set-up allows us to perform a first order cross section correction for n-fragment production (no correction has been made for any lack of in plane angular coverage and velocity thresholds), and this leads to values of 4180 mb, 669 mb, 260 mb, 82 mb for fragment multiplicity equal to 2, 3, 4, and greater than 4 respectively.

### 3) Analysis in term of excitation energy

In figure (a), the number of detected light charged-particles (LCP) for various values of the fragment multiplicity are displayed. The pattern of the total distribution (fragment multiplicity>1, histogram) is consistant with what has been measured as a function of neutron multiplicities for the same system at the same incident energy [9]. There is a large contribution at small multiplicity values associated essentially with peripheral collisions (elastic and quasi-elastic collisions) and a shoulder around 8-10 (which is a bump in the neutron data) associated with the largest fragment multiplicities and extending up to 15 measured LCP (recall that the average LCP detection acceptance is around 50%). As the fragment multiplicity increases, the LCP multiplicity distribution evolves steadily towards a more symmetric distribution peaked around 8. A striking result is found when comparing the 2-fold fragment case to higher folds : the probability of finding large LCP multiplicities does not depend strongly on the associated number of fragments. If we assume that the multiplicity of light particles is a good measure of the violence of a collision, then this is the first indication that violent collisions (at least the most violent selected with our experimental set-up) can lead to two-body production.

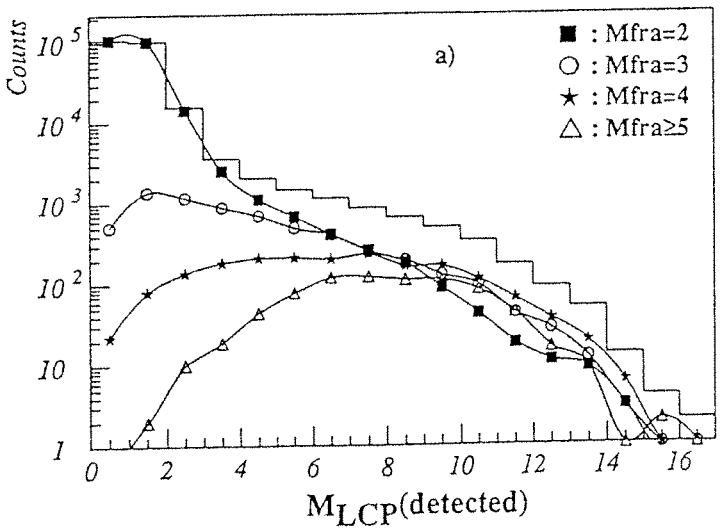

To confirm this in a more quantitative way, the correlation between the n-fold fragment production and the total kinetic energy (TKE) or the total kinetic energy loss (TKEL) was examined.

$$TKE = 0.5\ \mu\ V_{rel}^2 \qquad TKEL = Ecm - TKE \qquad (1)$$

Where $E_{cm}$ is the available center of mass energy (2.9 GeV), $\mu$ the reduced mass of the dinuclear system just before separation, and $V_{rel}$ the relative velocity between the two fragment partners after separation. For a two-body final state the relative velocity calculation could easily be performed whereas for higher n-fold coincidences the calculation was achieved with reconstructed velocities in the reaction frame where a clear separation is observed between fragments originating from the projectile-like and the target-like nuclei respectively. The evaporation process does not affect, on the average, the fragment velocities. It is crucial, however, for the determination of the reduced mass of the transient dinuclear system. As far as the evaporation mechanism takes place only after the separation of the two partners, the average reduced mass is simply given by $\mu=(A_{Pb}\ A_{Au})/(A_{Pb} + A_{Au})$, where $A_{Pb}$ and $A_{Au}$ are respectively the mass of the projectile and the target nuclei. This evaporation scheme was confirmed by the velocity distributions of the light charged particles detected in coincidence with the fragments. The TKEL can be transformed in excitation energy per nucleon for each partner by

$$E^*\ (MeV/u) = TKEL\ /\ (A_{Pb}+A_{Au}) \qquad (2)$$

Although pre-equilibrium emission is weak for the studied system [10], it can affect the TKEL values. But for symmetric systems, with the only hypothesis of equal number of nucleons of pre-equilibrium issued from the target and the projectile nuclei, one can easily shows that equation (2) leads to the exact excitation energy per nucleon when TKEL is calculated through equation (1).

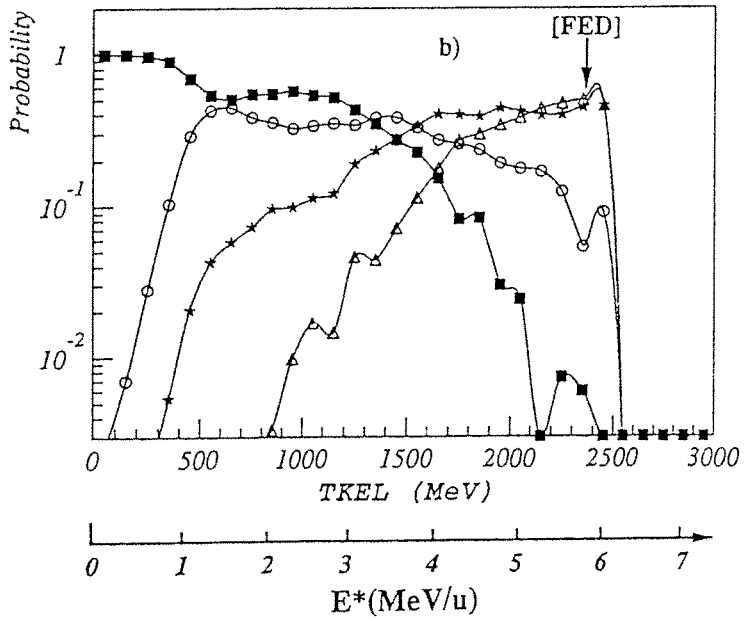


Excitation energy spectra are displayed in fig (b). Fig (a) and (b) can be paralleled, showing the strong correlation between LCP multiplicity and TKEL.

An other interesting remark about the TKEL spectra is that full energy damping (FED=$E_{cm}$-$E_{Coulomb}$) is reached whatever the fragment multiplicity. For moderate values of the excitation

energy, there are essentially two main bodies in the exit channel. Then, with increasing excitation energy, multifragment emission sets in, beginning with binary fission of one of the two partners to binary fission of both partners. Finally, above 4 MeV/u, the multifragment production becomes dominant. This is the energy domain in which multifragmentation (defined as the simultaneous emission of several frament) is believed to replace the standard low excitation energy processes (LCP evaporation, binary fission, sequential fragment emission). However, even at such high energies, there remains a sizeable number of 2-fold events. The cross sections for 2-fold events with E* larger than 3 MeV/u is around 25 mbarns (corrected value), is still around 5 mbarns (corrected value) for excitation energies larger than 4 MeV/u. The value E*=5.9 MeV/u corresponding to full energy damping (7 MeV temperature for $E^*=A/8\ T^2$) is achieved for 2-fold events. The cross section for heavy nuclei sustaining high excitation energies is even larger than the quoted value if one considers the 3-fold events for which one of the partners has been identified as either a projectile-like or a target-like nucleus. These excitation energy values are very large and rather unexpected.

In conclusion, we have studied Pb+Au collisions at 29 MeV/u. The detection of fragments and light charged particles in coincidence allowed us to perform a completely recorded events selection (>80% of detected atomic number and parallel momentum relative to the entrance channel) for the analysis. Large fragment multiplicities have been observed correlated with large light charged-particle multiplicities and large values of the dissipated energy. However, we have found that the two-body final state is still present in violent collisions corresponding to fully damped deep inelastic reactions which, for the present system, correspond to excitation energy values as high as 5.9 MeV/u . This rather unexpected result indicates that the limits of stability of highly excited massive nuclei could be much higher than predicted by static calculations (11). These results should provide interesting constraints on the models describing the decay properties of hot nuclei.

## references


1) R.J. Charity et al Z. Phys. A341 (1991) 53
2) B.M. Quednau et al Phys. Lett. B309 (1993) 10
3) B. Lott et al Phys. Rev. Lett. 68 (1992) 3141
4) E. Suraud, B. Tamain, C. Gregoire Progress of Nuclear and Particle Science 23 (1989) 357
5) R. Bougault et al. NIM A259 (1987) 473
6) G. Rudolf et al. NIM A307 (1991) 325
7) G. Bizard et al. NIM A244 (1986) 483
8) A. Peghaire et al. NIM A295 (1990) 365
9) E. Piasecki et al Phys. Rev. Lett. 66 (1991) 1291
10) S. Bresson Thesis University of Caen (1993)
11) P. Bonche et al Nucl. Phys. A427 (1984) 278

# THE DECAY OF PRIMARY PRODUCTS IN BINARY HIGHLY DAMPED $^{208}Pb + ^{197}Au$ COLLISIONS AT 29 MeV/u

J.F. Lecolley [a], L. Stuttgé [b], M. Aboufirassi [a], A. Badala [a-e], B. Bilwes [b], R. Bougault [a], R. Brou [a], F. Cosmo [b], J. Colin [a], D. Durand [a], J. Galin [c], A. Genoux-Lubain [a], D. Guerreau [c], D. Horn [a-f], D. Jacquet [d], J.L. Laville [a], F. Lefebvres [a], C. Le Brun [a], J. Lemière [a], O. Lopez [a], M. Louvel [a], M. Mahi [a], M. Morjean[c], C. Paulot [c], A. Péghaire [c], N. Prot [a], G. Rudolf [b], F. Scheibling [b], J.C. Steckmeyer [a], B. Tamain [a], S. Tomasevic [b].

*a) Laboratoire de Physique Corpusculaire, ISMRA, IN2P3-CNRS*
*14050 CAEN CEDEX, France*
*b) Centre de Recherches Nucléaires, IN2P3-CNRS, Université Louis Pasteur, B.P. 20*
*67037 STRASBOURG CEDEX, France*
*c) GANIL, B.P. 5027 - 14021 CAEN CEDEX, France*
*d) Institut de Physique Nucléaire, B.P. 1 - 91406 ORSAY CEDEX, France*
*e) On leave from INFN - Catania, Catania, Italy*
*f) On leave from CRL (AECL), Chalk River, Ontario, Canada*

**Abstract :**

Events with fragment multiplicities up to eight have been detected with a large detector array in Pb+Au reactions at 29 MeV/u. All collisions show a binary character irrespective of a possible further disassembly of the two highly excited primary partners. For the most violent collisions, dissipative orbiting is observed as well as full energy damping corresponding to excitation energies as high as 5.9 MeV/u.

## 1) MOTIVATION

At low bombarding energies, i.e. close to the Coulomb barrier, the cross section for reactions between very heavy nuclei is dominated by deep inelastic collisions. Indeed, the strong Coulomb repulsion completely inhibits the formation of the compound nucleus. At intermediate energies (several tens of MeV per nucleon), a number of studies have shown that this mechanism still exists or have demonstrated at least partial damping. The transition from this low energy behaviour to a more violent regime dominated by transfer or abrasion mechanisms is not fully elucidated. We present results concerning the nearly symmetric system $^{208}Pb+^{197}Au$ at 29 MeV/u. This system is well suited for studying the above-mentioned problem. In addition, such reactions have the advantage of dissipating the initial energy over a wide and continuous range as a function of impact parameter and offer the opportunity to follow the decay properties of massive excited nuclei over a large domain of excitation energy up to 5.9 MeV/u in case of fully damped collisions.

## 2) EXPERIMENTS

A 29 MeV/u $^{208}Pb$ beam of about 1 part-nA was used to bombard a self supporting 500 $\mu g/cm^2$ Au target. Reaction products were detected with an apparatus consisting of 30 multiwire proportionnal counters able to detect with full efficiency fragments with $Z \geq 8$ and $v > 2$ cm/ns (2.07 MeV/u) in the angular range 3-30 degrees (XYZT) and with $Z \geq 8$ and $v \geq 0.5$ cm/ns (0.13 MeV/n) in the angular range 30-150 degrees (DELF). These systems were installed in the large vaccuum chamber NAUTILUS at GANIL. Behind these detectors, plastic scintillators (the "MUR" and "TONNEAU" were used to detect light charged particles ($Z < 6$ and $v > 2.2$ cm /ns : 2.5 MeV/n) in the same angular range. The set-up covered 55% of the total solid angle. The triggering condition was a multiplicity requirement amongst the 30 cells (XYZT and DELF). The parameters measured for each ion were the atomic number Z and the velocity vector $\vec{V}$. For each event the fragment multiplicity $M_f$ ($Z \geq 8$) and the light charged multiplicity $M_l$ ($Z < 8$) were obtained.

A coherent description of the reaction process requires a complete kinematical analysis on an event-by-event basis. Thus, the present investigation has been restricted to events in which at least 80% of both total charge (including light charged particles, hereafter called LCP) and total linear momentum were recorded.

## 3) RESULTS

Two results have been obtained :

- First, we demonstrate by applying an event-by-event analysis, that it is possible to reconstruct kinematically the two primary partners of the collision irrespective of the final fragment multiplicity and thus emphasize the binary character of the reaction for the whole range of impact parameters.

- Second, we confirm the possibility for a complete damping of the relative energy for the most violent collisions whatever the number of fragments in the exit channel. This finding is supported by classical trajectory calculations which can reproduce the mean values of several kinematical observables of the target-like and projectile-like nuclei.

The mean values of these reconstructed observables are shown in figure 1 as a function of the total kinetic energy loss TKEL. The evolution of $V_{QP}$, $\theta_{QP}$, $V_{QT}$, $\theta_{QT}$ (these are the laboratory velocity and angle for the projectile-like and the target-like nuclei respectively) are similar whatever the fragment multiplicity. This evolution is consistent with a predominantly binary character for the reaction. It shows a gradual damping of the relative motion as the TKEL increases until the Coulomb velocity (corresponding to full damping) between the projectile-like and target-like nuclei is reached for large values of TKEL (~ 2,4 GeV).

The results of the classical trajectory calculations are shown in figures 1-b and 1-c (solid lines) in which the calculated kinematical quantities (velocities and deflection

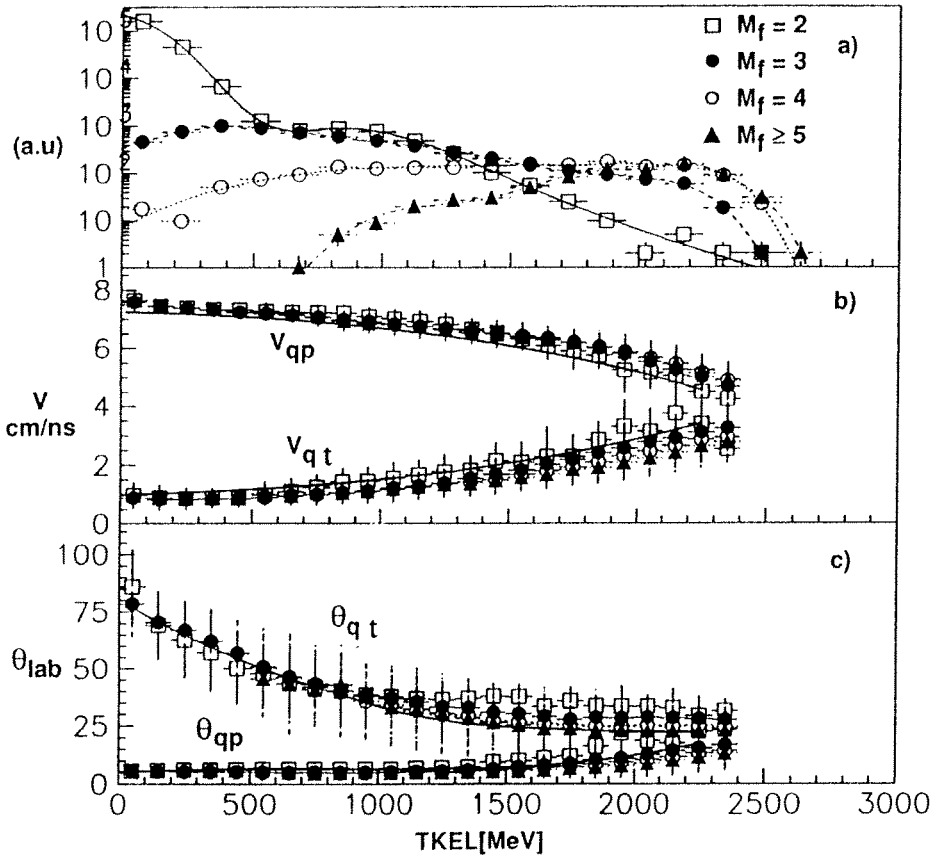


**Fig. 1**

angles) of the projectile-like and target-like nuclei are shown. We conclude from the good agreement of the calculations with the data that the first step of the interaction is basically similar to what is observed for other systems at lower bombarding energies.

The other convenient way to present the experimental results is to plot the differential cross section $d^2\sigma/d\theta\, dE$ versus the deflection angle $\theta_{CM}$ and the TKE of the fragments (Wilczynski plot). Figure 2 shows the relationship between TKE and $\theta_{CM}$ for $M_f = 3$ (2a) and $M_f \geq 4$ (2b). For moderately damped events (high values of TKE), a well-developed peak is seen near the grazing angle. This phenomenon of angular focusing close to the grazing angles shows the equal influence of the Coulomb field compared to the nuclear one as is expected from systematics for the value of the reduced Sommerfeld parameter ($\eta' \sim 210$) for this reaction. The angular distributions become broader and broader with decreasing TKE and reflects the fluctuations in the flow of nucleons between the two partners. This effect is more pronounced for $M_f \geq 4$ events (fig. 2b) than for $M_f = 3$ ones (fig. 2a). This is due to the fact that the angular threshold at 3 degrees has little influence on events for which the projectile-like nucleus has fragmented. In the low TKE domain, the angular distribution becomes progressively isotropic, indicating the existence of a long-lived di-nuclear system. The solid line (fig. 2b) is the mean angle-energy correlation predicted by the calculations using the trajectory calculations. The relationship between the most probable deviation $\theta_{CM}$ and TKE is well reproduced by the model. We have also indicated the time (the initial time is taken as when the two nuclei touch in the entrance channel) for which the two partners ceased to interact. This time goes from 100 fm/c for moderately dissipative collisions up to more than 270 fm/c for the most violent collisions.

Fig. 2

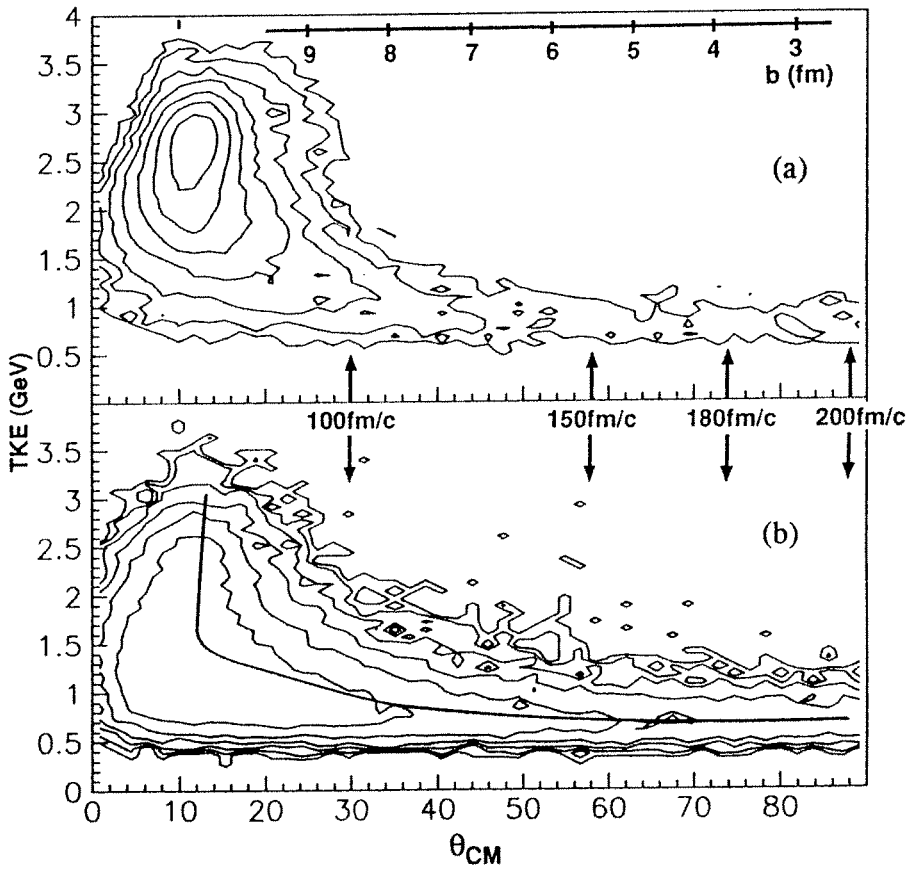


## 4) CONCLUSIONS

To summarize, we have studied the $^{208}Pb+^{197}Au$ system at 29 MeV/u by using selected events in which more than 80% of both the total charge and total linear momentum were detected and by analysing coincidences between two to eight fragments with $Z > 8$. From the kinematical reconstruction on an event-by-event basis of the two primary partners of the collision with the help of shape analysis, we have demonstrated the binary character of the reaction irrespective of the final fragment multiplicity for all impact parameters. This result could be reproduced using a simple standard deep-inelastic scattering model. The data seem to indicate that no significant new processes set in in this energy range for the first step of the reaction as compared with previous results at lower incident energies. We have also shown that complete damping occured (even for this relatively high incident energy) leading to excitation energies as high as 5.9 MeV/u. In this excitation energy region there is a strong competition between all possible decay modes. Lastly, dissipative orbiting has been displayed through Wilczynski plots, thus indicating the existence of a rather long-lived di-nuclear system.

# SELECTION OF VIOLENT COLLISIONS BY NEUTRON CALORIMETRY FOR INTERFEROMETRY MEASUREMENTS

L. Sezac[1], C. Lebrun[1], H. Dabrowski[4], A. Chbihi[3], B. Erazmus[1],P. Eudes[1], J. Galin[3], D. Guerreau[3], F. Guilbault[1], C. Ghisalberti[1], P. Lautridou[2,3], R. Lednicky[5], M. Morjean[3], A. Peghaire[3], J. Pluta[6], J. Quebert[2], A. Rahmani[1], T. Reposeur[1], R. Siemssen[7], D. Ardouin[1].

*1- Laboratoire de Physique Nucléaire(CNRS/IN2P3 et Université de Nantes) 2, rue de la Houssinière, 44072 NANTES, cedex 03 (France)*

*2- Centre d'Etudes Nucléaires de Bordeaux-Gradignan, le Haut Vigneau, 33170 GRADIGNAN (France)*

*3- Laboratoire GANIL,BP 5027, 14021 CAEN (France)*

*4- Institute of Nuclear Physics, im. H.Niewodniczanskiego, Zaklad I - Radzikowskiego 152, 31342 CRACOW (Poland)*

*5- Institute of Physics, Academia of Sciences of the Czech Republic, CZ-18040 Prague, Czech Republic*

*6- Institut of Physics, Warsaw Technical University, ul. Koszykoma 75, 00-662 WARSAW (Poland)*

*7- K. V. I. Zernikelaan 25-9747 AA GRONINGEN (The Netherlands).*

## 1) Introduction

Two-particle correlation measurements have been often used to study heavy-ion collisions at intermediate energy in order to get information on the space-time characteristics of the emitting source as well as on the temperature deduced from the population of excited states. The results [1-3] confirmed the relevance of the method but also the dependence of such results on various parameters (impact parameter, emission angles...). In this spirit, one can point out two important effects. The first one is the preequilibrium emission during which two particles can be emitted in a very short time scale (less than $10^{-22}$s). The second one concerns the evaporation from an equilibrated nucleus for which the deduced characteristic times concern either the projectile-like or the target-like nucleus, depending on the location of the detectors. For instance the p-p and p-t correlation data [4-7] measured at backward angles with the Ar + Ag system at 39 MeV per nucleon reflect an equilibrium emission from the target-like nucleus.

Improvement in this approach can be obtained by selecting the involved impact parameter interval. In a previous experiment [8] the charged particle multiplicity in a limited part of the space has been tentatively used as a selection parameter but the selectivity appeared to be rather poor. In a recent measurement on the $^{36}Ar + ^{45}Sc$ reaction at 80 MeV per nucleon [9] p-p correlations were analysed using the total tranverse energy of charged particles detected in a $4\pi$ multidetector as a filter of the violence of the collisions.

The aim of the experiment presented here was to choose experimental conditions in order to observe mainly light particle correlations coming from heavy equilibrated quasi-projectile nuclei and to sort the events in several intervals of violence. In his report we want to demonstrate that one can use a high efficiency $4\pi$ neutron detector as a calorimeter and gain with such an instrument high selectivity on the violence of a collision. (for more details see reference 10).

## 2) Experimental set-up.

The experiment was performed in the scattering chamber of ORION at GANIL. In order to favour the emission of neutrons a $^{208}Pb$ beam at 29 MeV per nucleon has been used to bombard a $^{93}Nb$ target. This beam energy was chosen to reach high excitation energy with a small amount of preequilibrium emission. Reverse kinematic allows to observe in the forward direction the particles emitted by the heaviest partner, limit the observation of the preequilibrium particles associated with the light partner and minimize the threshold limitations due to higher momenta of the detected particles.

So far, the $4\pi$ ORION detector was essentially devoted to neutron multiplicity ( Mn ) measurement. Interesting results [11-14] have been reported which show the relevance of Mn for the determination of the initial excitation energy involved in each reaction.The neutrons are detected in five tanks surrounding the scattering chamber which are filled with liquid scintillator loaded with Gd. The scintillation light generated by the recoiling protons and carbon nuclei of the medium after multiple scattering of the neutrons is collected by means of 30 phototubes surrounding the tanks, giving rise to the QPP signal related to the total kinetic energy of the neutrons (prompt signal). Later on, i. e. approximatively 700 ns after the neutron emission, and for several tens of microseconds, the phototubes are fired by $\gamma$ rays resulting from the radiative capture of the thermalised neutrons by gadolinium nuclei, giving the opportunity to measure the neutron multiplicity Mn for any event (delayed signals). The detector acts as a calorimeter and a multiplicity meter. Due to the large capture time the Mn measurement imposes a slow counting rate. This limiting factor makes it difficult to use the neutron multiplicity information in interferometry measurements for which good statistics in a reasonable amount of beam are needed. On the contrary, the signal issued from the slowing down of the neutrons being orders of magnitude shorter, appears well suited for faster measurements. In the present contribution we want to demonstrate the relevance of such an approach, first by studying the correlation between Mn and QPP and then by considering other observables which are known to be very sensitive to the violence of the collision [16].

The scattering chamber is a cylinder (59 cm in diameter and 120 cm long) with the beam direction as a symmetry axis. Particles were detected by 48 CsI detectors (1.27 cm in diameter). Among them 4 detectors (10 cm long) were put in a plane at 5.5 , 10 , 15 and 20 degrees in the forward direction. At backward angles, 4 other detectors (4.5 cm long) were set at 100, 120, 140 and 160 degrees. The correlator itself was formed with the 40 scintillators (4.5 cm long) left in a compact geometry covering radial angles between 25 and 80 degrees and spanning 50 degrees in azimuth. The minimum relative angle between two detectors was 4.7 degrees. The energy calibration was obtained by detecting secondary beam of light particles with known magnetic rigidity with the detectors positionned near the beam axis. Those particles were identified from the conventional pulse shape analysis. An algorithm has been developped [15] which can automatically deduce the value of an identification parameter from the slow and fast components of the integrated charge.

## 3) The calorimeter selectivity.

In order to study the correlation between the neutron multiplicity Mn and the prompt pulse charge QPP a short beam time has been devoted to a measurement with a chopped beam. During this time, any prompt pulse from ORION was triggering the data acquisition, so that the total reaction cross section was investigated (inclusive data). Figure 1 shows the correlation plot between the Mn and QPP data. A strong correlation is observed, giving confidence that ORION used as a calorimeter leads to a similar selectivity as when it is used as a multiplicity meter.

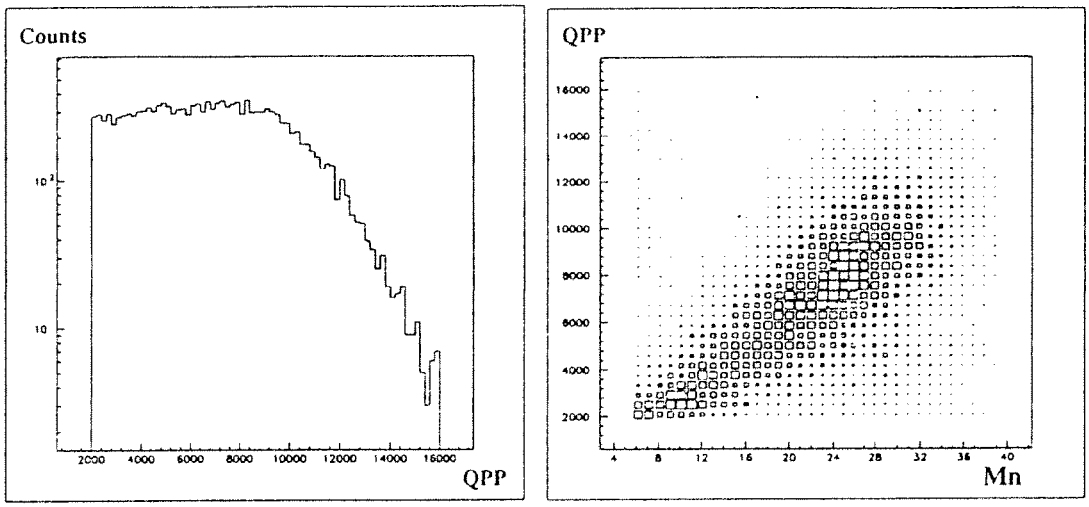


Figure 1: *Correlation plots between QPP and Mn and the projection on the QPP axis for inclusive data.*

The evolution of the characteristics of the projectile-like source is shown on the energy spectra recorded at very small angle (Fig. 2). The double bumped structure corresponding to the two kinematical solutions for alpha-particle evaporation is well observed for the less dissipative collisions (small QPP). A steady shift from 240 MeV to 190 MeV in the location of the high energy bump is clearly observed as expected with higher energy damping and demonstrates the good sensitivity of the QPP selection. The low energy peak (second kinematical solution) truncated at low energy by the detection thresholds, overlaps more and more with target-like particle emission when the energy damping increases.

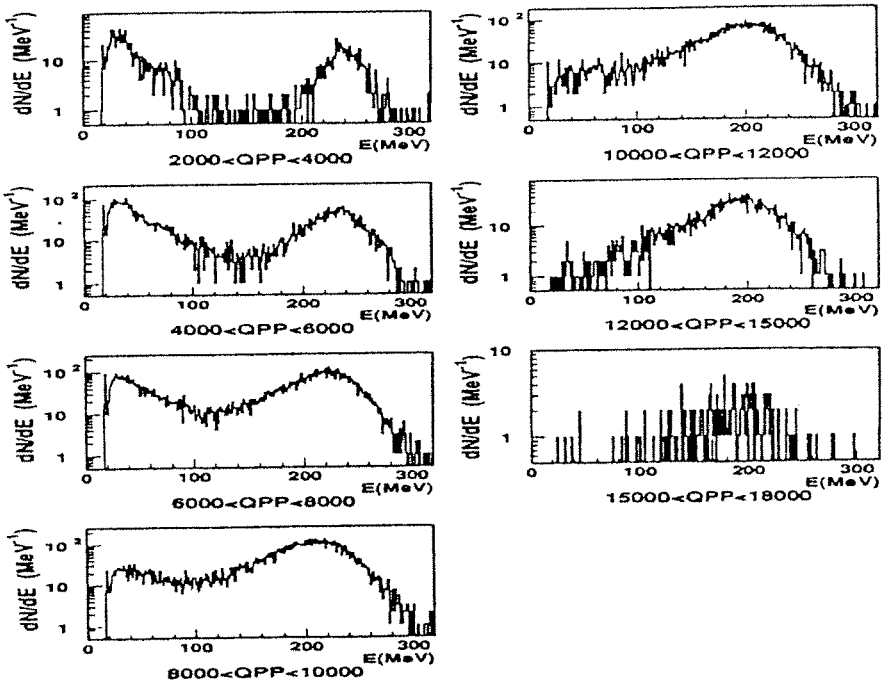


Figure 2: *Alpha particle energy spectra at 5.5° for seven adjacent QPP bins.*

By applying the massive transfer model one can tentatively correlate the QPP information with the impact parameter. In this model it is assumed that the heavy partner (the Pb nucleus) captures nucleons from the light one and that the number of captured nucleons is simply function of the overlap between nuclei i. e. depends on impact parameter. Velocity and temperature values deduced from this model are reported in the table 1.

| QPP min / QPP max | | 2000 / 4000 | 4000 / 6000 | 6000 / 8000 | 8000 / 10000 | 10000 / 12000 | 12000 / 15000 |
|---|---|---|---|---|---|---|---|
| $\frac{V_R}{c}$ | minimisation | 0.24 | 0.24 | 0.22 | 0.22 | 0.20 | 0.19 |
| | model | 0.23 | 0.23 | 0.22 | 0.21 | 0.20 | 0.18 |
| T (MeV) | minimisation | 3.4 | 3.7 | 4.9 | 5.8 | 7.2 | 8.6 |
| | model | 3.1 | 3.7 | 4.8 | 5.6 | 6.1 | 6.8 |

Table 1 . *Velocity and temperature values extracted from minimisation procedure ("minim") and from massive transfer model comparison ("mod") for six QPP bins.*

Finally the high energy part of the spectra of Fig. 2 have been fitted by a single Maxwell-Boltzman distribution assuming that these spectra represent pure sequential evaporation from the projectile-like nucleus without any contaminant from other sources. As it can be seen in table 1, both the recoil velocity and the slope parameter (temperature) match reasonably well those deduced from the massive transfer model. The temperatures deduced with these rough assumptions reach hudge values that have to be confirmed by the interferometry data, the analysis of which is in progress.

**References:**


*[1] J. Quebert Ann. Phys. Fr. 17 (1992) 99*
*[2] W. G. Lynch et al. Phys. Rev. Lett. 51 (1983) 1850*
*[3] J. Pochodzolla et al. Phys. Rev. C35 (1987) 1695*
*[4] D. Ardouin et al. Nucl. Phys. A495 (1989) 57c*
*[5] D. Goujdami et al. Zeits. für Phys. A339 (1991) 293*
*[6] H. Dabrowski et al. Phys. Lett. B247 (1990) 223*
*[7] P. Lautridou Thesis Univ. of Bordeaux 1 (1989)*
*[8] A. Ferragut Thesis Univ. of Caen (1990)*
*[9] M.A. Lisa et al. Phys.Rev. Lett. 70 (1993) 3709*
*[10] L. Sézac Thesis Univ. of Grenoble 1 (1993)*
*[11] M. Morjean et al. Nucl. Phys. A524 (1991) 179*
*[12] E. Piasecki et al. Phys. Rev. Lett. 66 (1991) 1291*
*[13] S. Bresson et al. Subm. for publ. in Phys. Lett. B*
*[14] J. Galin Second IN2P3-RIKEN Symp. on Heavy Ion Collisions, Obernai (April 90)*
*[15] C. Ghisalberti et al. Nouv. du GANIL 43 (1992) 11*

# BINARY FISSION STUDIES IN 24 MeV/u $^{238}$U INDUCED REACTIONS ON C, Si, Ni and Au

E.Piasecki[1], A.Chbihi[2], E.Crema[3], W.Czarnacki[4], J.Galin[2], B.Gatty[5], D.Guerreau[2], J.Iwanicki[6], D.Jacquet[5], U.Jahnke[7], J.Jastrzębski[6], M.Kisieliński[4], A.Kordyasz[1], M.Lewitowicz[2], M.Morjean[2], M.Muchorowska[8], L.Pieńkowski[6], J.Pouthas[2] and A.Tucholski[4]

1) Institute of Experimental Physics, Warsaw University, Hoża 69, 00-681 Warsaw, Poland
2) GANIL, BP 5027, 14021 Caen cedex, France
3) Instituto de Fisica, Universidade de Sao Paulo, Sao Paulo, Brasil
4) Sołtan Institute for Nuclear Studies, 05-400 Świerk, Poland
5) Institut de Physique Nucleaire, BP 1, 91406 Orsay, France
6) Heavy Ion Laboratory, Warsaw University, Banacha 4, 02-097 Warsaw, Poland
7) Hahn Meitner Institut, D1000 Berlin, Germany
8) SGGW-AR, Warsaw, Poland

Fission has been often used as a means to probe either the reaction mechanism or the properties of nuclei formed in intermediate energy heavy ion reactions. In our experiment the reaction chamber was placed inside of the neutron calorimeter ORION, which purpose has been to count with good efficiency the number of neutrons accompanying each registered reaction event. As it is known [1,2,3] the neutron multiplicity can be used as a measure of reaction violence. The $^{238}$U beam, after transmitting through the $^{12}$C, $^{28}$Si, $^{58}$Ni or $^{197}$Au target, passed through an annular telescope consisting of 150μm, 500μm and 4.5mm Si detectors. This instrument was used to detect, identify charge (with resolution better than 1 for Z<40) and measure the energy of reaction products. Moreover, since the first member of telescope was a multistrip circular detector, while the other two were multistrip radial ones, we could also identify position and in this way determine the angular information. In this communication we will present some preliminary results concerning the events in which two charged fragments (in addition to neutrons) were detected in coincidence.

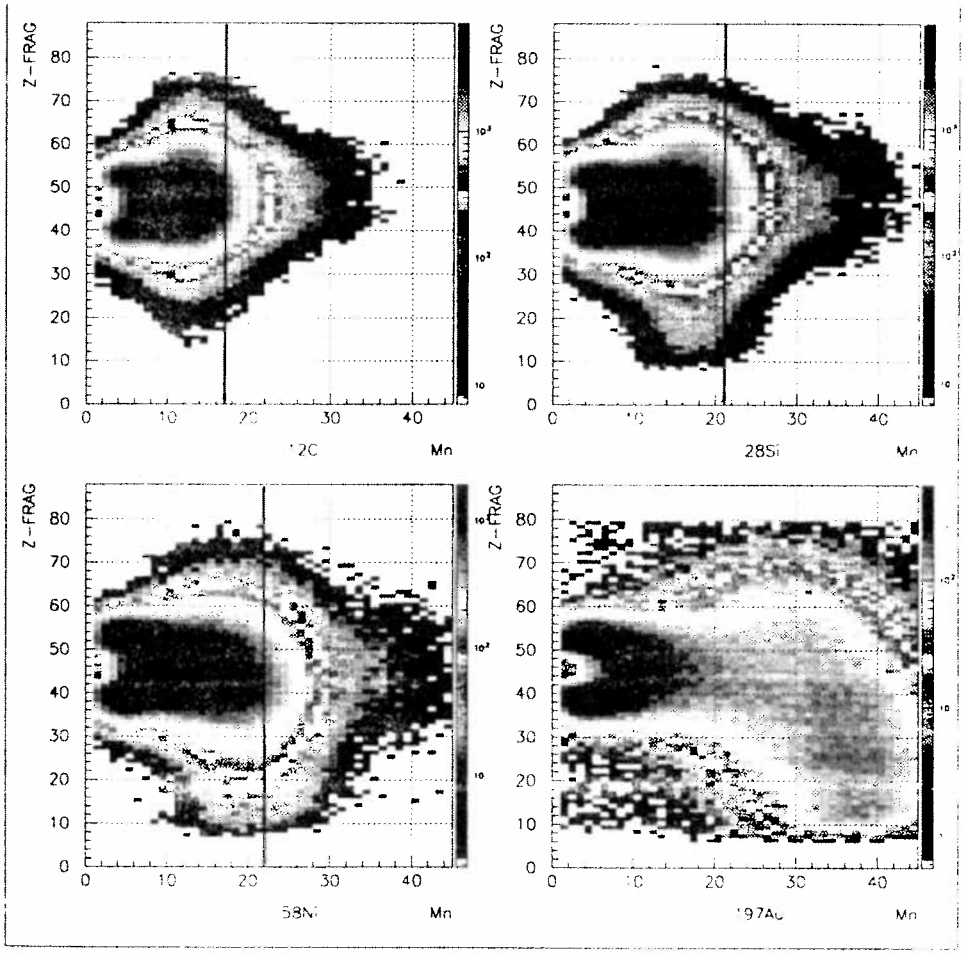


Fig. 1. Fission fragment charge and neutron multiplicity distributions (log scale). The vertical line marks the limit, above which the neutron multiplicity measurements are not reliable because of significant admixture of pile-ups. In all the figures the neutron multiplicities are uncorrected for registration efficiency.

The fission product charge distribution as a function of the associated neutron multiplicity are presented in fig. 1, for all the targets used. We see here, how the asymmetric fission of heavy projectile-like nuclei, characte-ristic for peripheral scattering (low neutron multiplicity) evolves gradually to symmetric fission with increasing violence of reaction. For even higher neutron multiplicity the charge distributions widen rapidly and finally we see evolution of typical fission fragments towards very light, IMF-like. They can be produced in extremely asymmetric binary fission, see fig. 2, but the results point also to change of the reaction mechanism from binary to nonbinary fission.

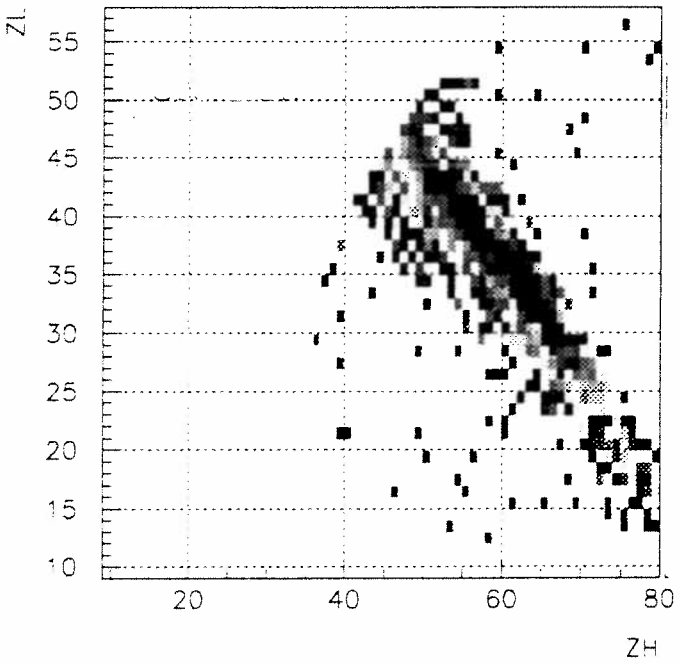


Fig. 2. Distribution of light and heavy fragment charges from fission of nuclei produced in reaction of 238U with 12C (log scale). Neutron multiplicity Mn = [13,18].

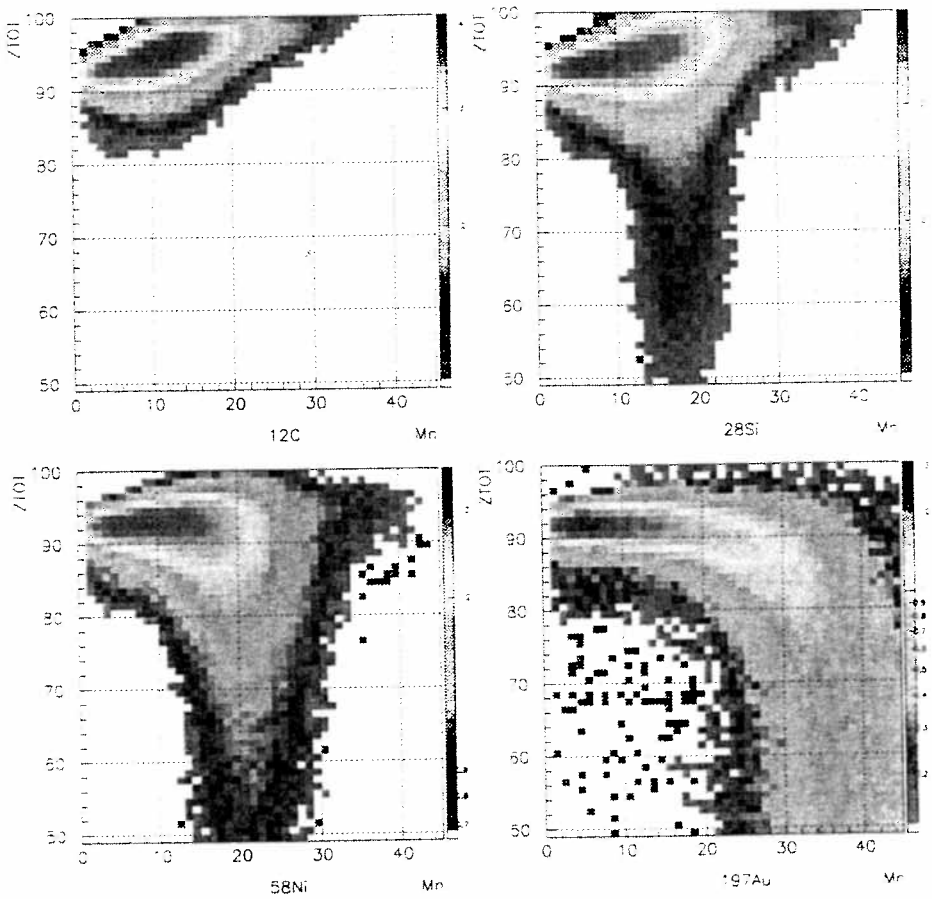


It is well seen in fig. 3, where the distributions of ZTOT (sum of charges of two coincident fragments) are plotted as a function of neutron multiplicity. This figure shows also that for the lightest targets the increasing centrality of collision conducts to complete or incomplete fusion, while for the heavier targets the Coulomb barrier renders such an evolution difficult or impossible.

Fig. 3. Charge distribution of nuclei undergoing fission, produced in reaction of 24 MeV/u $^{238}$U with $^{12}$C, $^{28}$Si, $^{58}$Ni and $^{197}$Au (log scale)

Increasing centrality of scattering is reflected not only in the fissioning nuclei composition, but also in the linear momentum transfer from projectile to target. The distributions of fissioning nuclei velocity (normalised to the beam velocity) were determined from fission fragment energies and the results are presented in fig. 4. Note the peaks at low velocity, corresponding to large linear momentum and charge/mass transfer, which are clearly seen for the lightest targets [3].

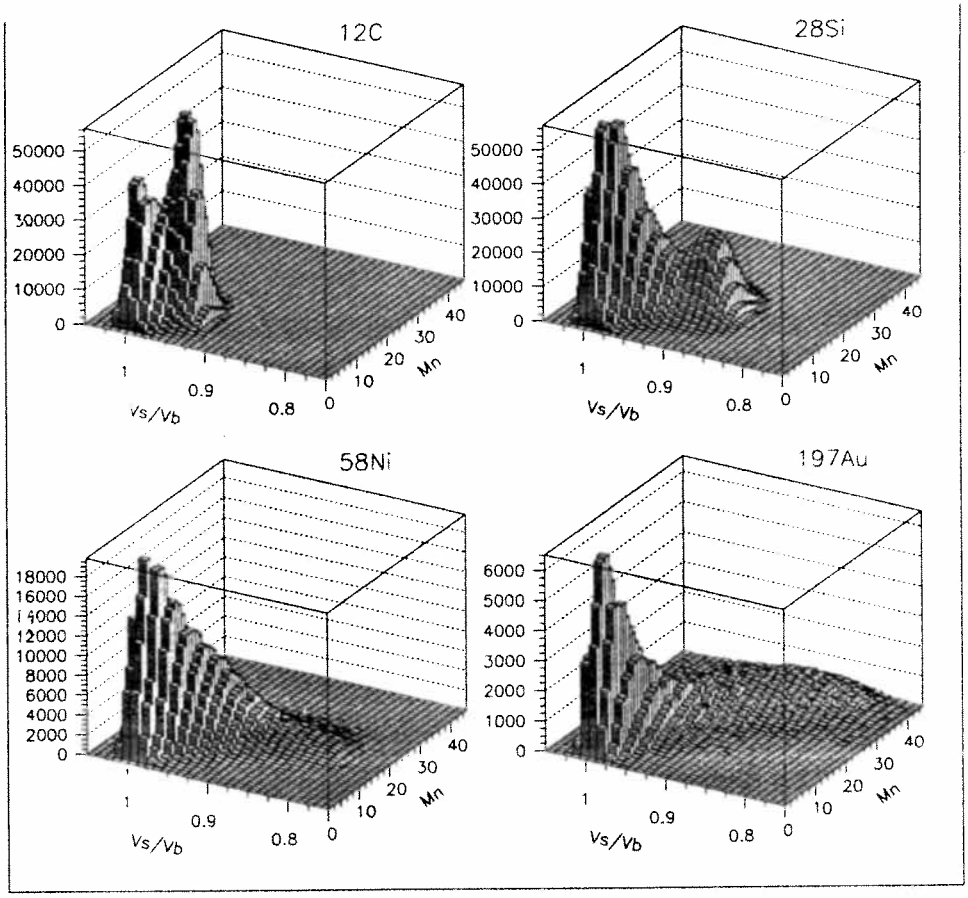


Fig. 4. Normalized to the beam velocity of fissioning nuclei in function of neutron multiplicity.

Another interesting result, shown in fig. 5, regards the total kinetic energy release (TKE) in fission. As it is well known [4,5], in low energy fission the TKE depends on fission mass asymmetry: for nuclei with Z = 88 - 98 it is greatest when heavy fragments have a mass of AH = 132 - 134 (or ZH = 50 - 51). Since this energy comes mainly from Coulomb interaction between fission fragments, the maximum energy should correspond to the most compact scission configuration, or - in other words - the least deformed fission fragments. However, as we know, the deformation depends on nuclear shell structure, which in turn should depend on the system excitation energy. Perhaps just this is illustrated in fig. 5, where the dependence of the mean TKE on fission asymmetry and neutron multiplicity is presented. For Mn = 0 we see the well known maximum at Z = 50 - 51, but it is remarkable, how rapidly this maximum fades away with increasing neutron multiplicity. Whether this is caused by thermal damping of shell structure, the temperature dependence of fission dynamics or by some other reason - it remains to be seen.

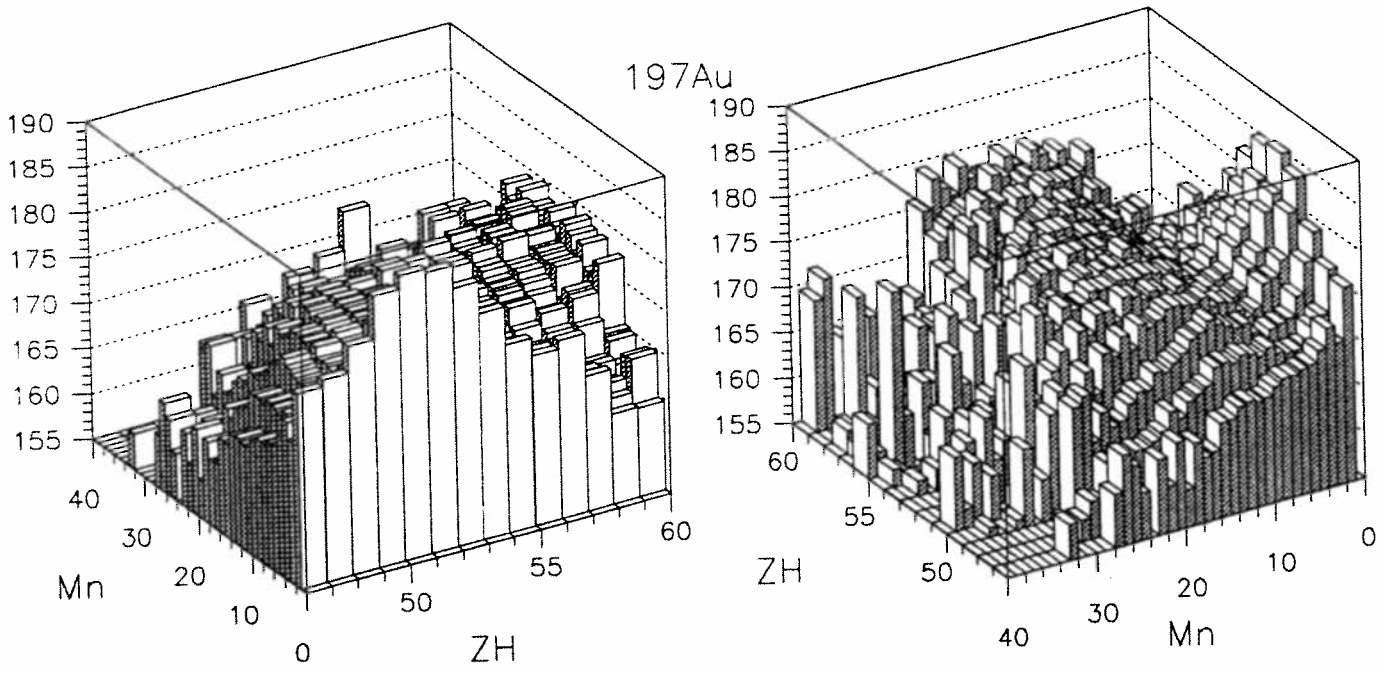


Fig. 5. Dependence of the mean kinetic energy of fission fragments (in cms) on heavy fragment charge and neutron multiplicity in $^{238}U + ^{197}Au$ reaction. For better visibility the distribution is shown from two sides. Note the maximum at ZH = 50 - 51 vanishing with increasing neutron multiplicity.

References

1. M. Morjean et al., Phys.Lett. B203 (1988) 215
2. E. Piasecki et al., Phys.Rev.Lett. 66 (1991) 1291
3. K. Knoche et al., Z.Phys. A342 (1992) 319
4. R. Vandenbosh and J.R.Huizenga, *Nuclear Fission* (Academic Press, New York, 1973)
5. T. Ohtsuki et al., Phys.Rev.Lett. 66 (1991) 17

# Two-proton correlation function measured at very small relative momenta

L.Martin, B.Erazmus, J.Pluta,
D.Ardouin,P.Eudes, F.Guilbault, P.Lautridou, C.Lebrun
R.Lednicky[1], A.Rahmani, T.Reposeur, D.Roy, L.Sézac
*Laboratoire de Physique Nucléaire , 2 rue de la Houssinière, 44072 Nantes Cedex 03, France*
M.Lewitowicz, W.Mittig, P.Roussel – Chomaz
*GANIL, BP 5027, 14021 Caen Cedex, France*
N.Carjan
*Centre d'Etudes Nucléaires de Bordeaux-Gradignan,33175 Gradignan Cedex , France*
P.Aguer,
*CSNSM, 91405 Orsay, France*
W.Burzynski,W.Peryt,
*Warsaw University of Technology, Warsaw, Poland*
H.Dabrowski, P.Stefanski
*Institut of Nuclear Physics, Krakow, Poland*

[1] *Permanent adress: Institut of Physics, Academia of Sciences of the Czech Republic CZ-18040 Prague, Czech Republic*

## 1. Introduction

Numerous studies using the intensity interferometry technique have been performed in order to estimate the size and the lifetime of a hot emitting nucleus. However the experimental resolution often reduces the quality of the mesured correlation function namely in the region of small relative momenta. The accuracy of the extracted physical information is thus quite limited and the theoretical predictions cannot be strongly constrained [1]. A recent theoretical study has revealed an interesting feature of two-proton correlation function characteristic of sequential emission [2]: the region of very small relative momenta ($q < 10$MeV/c) appears to be particularly well suitable to extract precisely the lifetime of an evaporating source whereas the intermediate region ($10$MeV/c $< q <$ $30$MeV/c) allows one to estimate the relative weight of each effect giving rise to correlations between two particles. Using the GANIL accelerator facility we have performed a measurement of two-proton coincidences at relative momenta between 1 and 100 MeV/c. It should be

emphasized that the region of very small relative momenta of a few MeV/c cannot practically be reached using a classical compact detector array.For this purpose an original experimental setup has been employed.

## 2. Experimental procedure

We studied the reaction $^{129}Xe + ^{48}Ti$ at 45 MeV/nucleon in reverse kinematics. The thickness of the Ti target was 1 mg/cm$^2$ only, in order to reduce the energy and angular straggling of the detected particles. The intensity of the Xe($45^+$) beam was set at 50 nAe in order to limit the random coincidence rate. Looking for the excited projectile-like decay the detection system was centered at 25° in the laboratory frame. It was composed of the SPEG magnetic spectrometer and twelve Csi(Tl) scintillators placed in the reaction chamber. The use of a spectrometer is justified by its high resolution allowing an accurate measurement of the angles and the momenta of the particles. Moreover it serves as a trigger of small relative momenta selecting a very narrow region of the angular and energy distribution of the emitted protons. The detection system of the spectrometer, usually used to record heavy ions, was adapted to detect light particles in coincidence. We have used a plastic scintillator providing energy and time measurements and four drift chambers.Each chamber delivered three position and one energy loss signals. It should be noted that the detection of protons requiered to tune the drift chamber characteristics to extreme operating values [3].The magnetic field was set to detect protons with a kinetic energy of 30 MeV.

## 3. Results and discussion

The identification of protons measured in the spectrometer was done using the residual energy signal delivered by the plastic scintillator and the energy loss signals provided by each drift chamber . The (E, $\Delta$E) matrix has allowed a good separation between the two-proton coincidences and the single protons (Fig. 1). The final selection of both types of events was performed by applying geometrical criteria to the three position signals delivered by each drift chamber. Then, based on the position measurements, the trajectories of the protons and their initial momenta were calculated.

The experimental two-proton correlation function constructed from the proton coincidences recorded in the spectrometer covers the range from 1 to 10 MeV/c . The uncorrelated background spectrum required to construct the correlation function was generated from pairs of single protons. The two-proton coincidences were corrected for a rate of 20% of random ones deduced from a careful analysis of the single proton production rate

evolution during the experiment. The correlation function was normalized by requiring equal areas of correlated and uncorrelated spectra. A good resolution, of the order of 1 MeV/c, in the whole range of the relative momenta covered by the spectrometer results from a good position resolution (estimated at 3 mm) of the drift chambers.

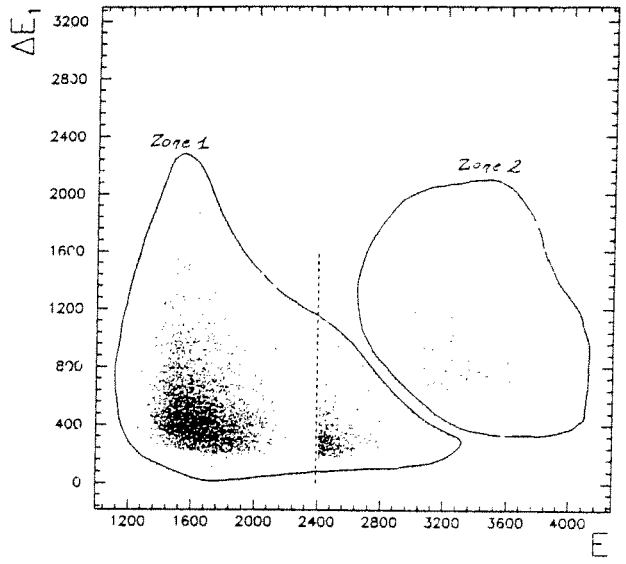


*Figure 1 : - Energy loss in the first chamber versus total energy delivered in the plastic scintillator for proton events. Zone 1 contains single events. Zone 2 corresponds to proton pairs. The dashed line represents an on-line cut in energy reducing the dominant contribution of single protons.*

In order to extract the space-time dimensions of the emitting source we have compared the experimental correlation function to the predictions of a classical approach [4]. In the frame of this model, three-body tridimensional trajectory calculations were performed describing two light charged particles sequentally emitted from a recoiling nucleus. The main characteristics of the source have been fixed assuming a projectile-like emitter and according to the experimental results obtained for similar reactions [5,6] :a mean charge and a mass equal to those of the projectile, a mean velocity equals to 90% of the beam velocity and a temperature equals to 4.5 MeV. One can note that by choosing a mean mass of the emitter we have fixed the size of the source. Nevertheless, in the case of a sequential emission the predominant lifetime effect conceals the sensitivity of the correlation function to space dimensions.

A realistic comparison between experimental data and theoretical predictions requires the convolution of the theoretical correlation function with the response function of the SPEG spectrometer including its magnetic and resolution characteristics. Thus, the value

of the mean lifetime of the hot nucleus was extracted taking advantage of the strong sensitivity of the coincidence spectra and the correlation function to the lifetime for very small relative momenta. The best agreement with experimental data was obtained with the mean lifetime $\tau_0 = (3.90 \pm 0.15)\ 10^{-21}$s (Fig. 2). From this large value one can conclude that the long-range Coulomb interaction is the most important source of the two-proton correlations measured in this experiment.

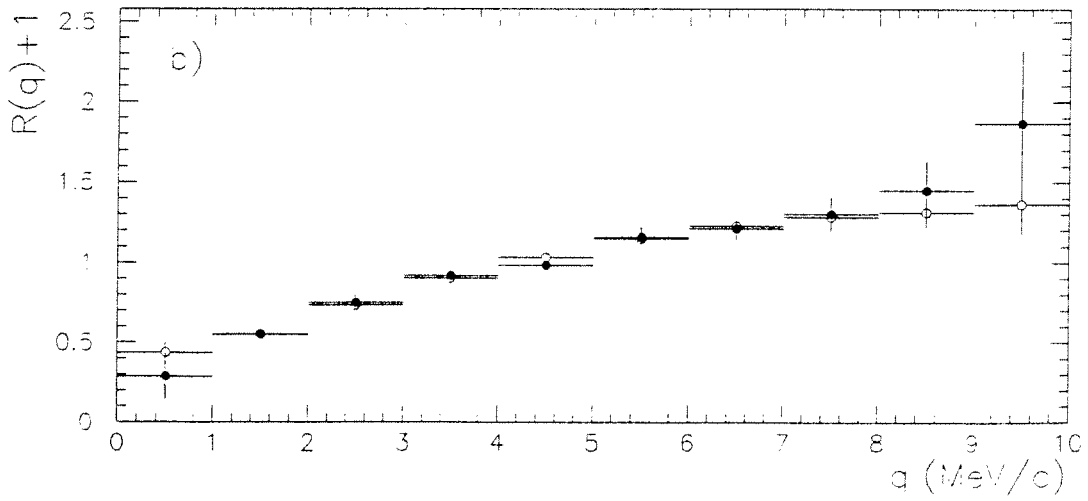


*Figure 2 : - Experimental correlation function (solid circles) measured in SPEG compared to the correlation function (open circles) predicted by the classical model for mean lifetime* $\tau_0 = 3.9\ 10^{-21}$s *and convoluted with the response function of the spectrometer.*

Studies of directional effects in particle correlations may give an important new insight to the space-time development of the particle emission process. Recently, such directional effects have been observed in p-p correlations in a non-equilibrium emission [7]. In the case of a sequential equilibrium emission, a quantum model taking into account the quantum satistics and the final state interaction effects predicts a surprising result [8,2]: a strong suppression of the correlation in the case of both extreme longitudinal ($\vec{q}\|\vec{v}$) and transverse ($\vec{q}\perp\vec{v}$) orientations of the relative momentum and the pair velocity (Fig. 3). In order to study this effect, we have constructed the experimental two-proton correlation function for three gates of the relative orientation of the vector of momentum difference and the pair velocity (Fig. 4). The shape of the correlation function obtained for the intermediate orientation clearly differes from that observed for the extreme relative orientations. This qualitative result may be a first signature of directional effects in particle correlations in the sequential decay of an excited source in statistical equilibrium. A detailed analysis requires to include the SPEG resolution in the predictions of the quantum model.

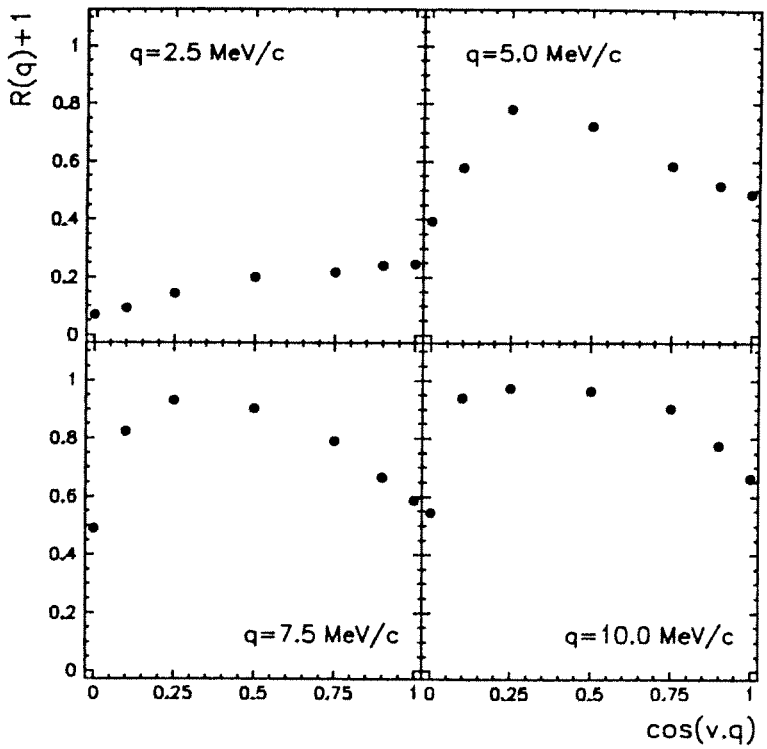


*Figure 3 : Dependence of the theoretical p-p correlation function on the relative orientation between the velocity and the relative momentum of the pair predicted by quantum model for lifetime* $\tau_0 = 3.6\ 10^{-21}$s.

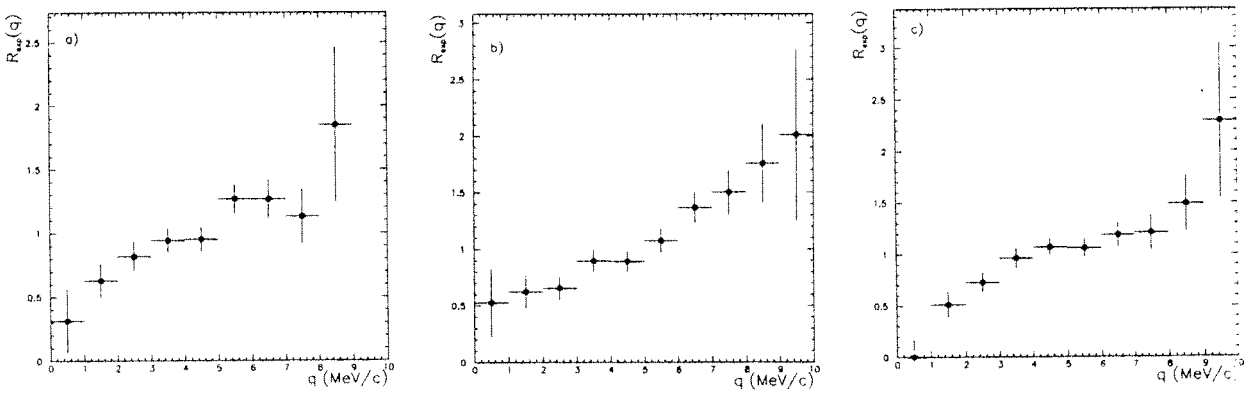


*Figure 4 : Experimental two-proton correlation function constructed for three different gates on the relative orientation of the vector of the momentum difference and the pair velocity :* $\cos(\vec{q}.\vec{v}) \in [0, 1/3]$ *(a),* $\cos(\vec{q}.\vec{v}) \in [1/3, 2/3]$ *(b),* $\cos(\vec{q}.\vec{v}) \in [2/3, 1]$ *(c).*

## 4. Conclusions

We have presented the first results of an experiment performed in order to measure the two-proton correlation function at very small relative momentum. Coincidences of two protons emitted with almost equal momenta by an excited nucleus have been detected in the SPEG spectrometer. The experimental p-p correlation function was constructed and analyzed :

- By realistic comparison with the predictions of a classical approach, a precise value $\tau_0 = (3.90 \pm 0.15)\ 10^{-21}$s was deduced for the source lifetime.
- For three different relative orientations of the velocity and the relative momentum of the proton pairs the experimental correlation function exhibits different shapes in qualitative agreement with the predictions of the quantum model.

Twelve CsI(Tl) scintillators were used during the experiment. Events measured in these detectors will allow to construct the p-p correlation function at higher relative momenta and to study unlike particle correlation functions.

Finally, we conclude that the SPEG spectrometer appears to be a powerful tool for a detailed analysis of the correlation function of identical particles at very low relative momenta. Therefore the sophisticated interferometry method combined with the high quality of the SPEG spectrometer offers a precious way to charaterize hot nuclei produced in heavy-ion reactions.

## 5. References


[1] B.Erazmus, L.Martin, R.Lednicky and N.Carjan, Phys. Rev. C 49 (1994).
[2] L.Martin, Thèse de Doctorat Université de Nantes (1993).
[3] L.Martin et al, Nouvelles du GANIL N°43 (1992).
[4] B.Erazmus, N.Carjan and D.Ardouin, Phys. Rev. C 44 (1991) 2663.
[5] L.G. Moretto et al, Int. Rep LBL-30930 (1991).
[6] W.G. Gong et al, Phys. Rev. C 43 (1991) 1804.
[7] M.A. Lisa et al, Phys. Rev. Lett. 71 (1993) 2863.
[8] R.Lednicky and V.L. Lyuboshitz, Yad. Fiz 35 (1982) 1316,
Sov. J. Nucl. Phys. 35 (1982) 770.

# B3 - FLOW AND RELATED PHENOMENA

# From in-plane to out-of-plane enhancement of the directed flow in $^{64}Zn$ on $^{58}Ni$ collisions between 35 and 79 MeV/u.

R. Popescu[1-a)], J.C. Angélique[1)], G. Auger[2)], G. Bizard[1)], R. Brou[1)], A. Buta[1-a)], C. Cabot[2-c)], Y. Cassagnou[3)], E. Crema[1-b)], D. Cussol[1)], Y. El Masri[4)], Ph. Eudes[5)], Z.Y. He[7)], S.C. Jeong[1-8)], A. Kerambrun[1)], C. Lebrun[5)], R. Legrain[3)], J.P. Patry[1)], A. Péghaire[2)], J. Péter[1)], R. Regimbart[1)], E. Rosato[6)], F. Saint-Laurent[2)], J.C. Steckmeyer[1)], B. Tamain[1)], E. Vient[1)],

*1) LPC Caen, 14050 CAEN - FRANCE, 2) GANIL, 3) DAPNIA, CEN Saclay, 4) Institut de Physique Nucléaire, LOUVAIN-LA-NEUVE, BELGIUM, 5) Laboratoire de Physique Nucléaire, NANTES , 6) Dipartimento di Scienze Fisiche and INFN, NAPOLI, 7) Institute of Modern Physics, LANZHOU , CHINA, 8) Department of Physics, Soongsil University, SEOUL, KOREA, a) Permanent address : I.F.A., Heavy Ion Department, BUCHAREST, ROMANIA, b) Permanent address : Inst. di Fisica, Univ. de SAO PAULO, BRAZIL, c) On leave of absence from IPN ORSAY, France*

## -I- MOTIVATIONS

The in-plane flow parameter describes only one aspect of the directed collective flow. Another aspect lies in the azimuthal distribution of particles relative to the reaction plane. The azimuthal distribution of mid-rapidity particles was found to be not uniform. Opposite effects have been observed at high and low incident energies. A maximum was observed in the direction perpendicular to the reaction plane on both sides from 150 to 1 050 MeV/u : squeeze-out effect [1, 2]. Below 100 MeV/u, maxima in the reaction plane have been observed on both the target and projectile sides "rotation-like effect" [3, 4, 5]. It was studied as a function of energy, impact parameter and emitted particle mass in the collisions of $^{40}Ar$ on $^{27}Al$ at energies from 36 to 65 MeV/u (4) and $^{36}Ar$ on $^{27}Al$ from 55 to 95 MeV/u (5) : the anisotropy of mid-rapidity particles increases both with the particle mass and the impact parameter, and decreases with increasing energy, reaching very low values at 95 MeV/u.

We report on the first observation of the transition from in-plane enhancement ("rotation-like") to out-of-plane enhancement (squeeze-out) on the system $^{64}Zn + ^{58}Ni$ when the energy increases from 36 to 79 MeV/u.

## -II- EXPERIMENTAL SET-UP AND ANALYSIS

The experiments were performed at the Ganil facility in the reaction chamber Nautilus. The set-up, the selection of well characterized events and the impact parameter sorting are described in the contribution "Hot nuclei with temperature..." by S.C. Jeong et. al.

A meaningful determination of the reaction plane of an event required a high completeness of detection of this event, an axially symmetric detection array and a sufficient granularity. These three conditions were satisfied by MUR and TONNEAU. The selection of well characterized events ensured us that the first condition is fullfiled. We have used two methods : the well-known transverse momentum analysis method (ref. Dan - Ody) and the azimuthal correlation method (ref. Wilson) which gave close results.

## -III- RESULTS

The 0° azimuth is in the reaction plane on the side of the high rapidity products. The azimuthal distribution was fitted by a polynomial

$$dN/d\phi = 1 \text{ (or } a_0) + a_1 \cos\phi + a_2 \cos 2\phi \qquad (1)$$

where $a_1$ is due to the in-plane flow and has a zero value at mid-rapidity. The anisotropy factor $a_2$ (or $a_2/a_0$) is negative for out-of-plane enhancement, zero for an uniform

distribution and positive for in-plane enhancement. The rotation axis is the beam direction [4, 5], whereas in ref. 2, it was the in-plane flow direction. The effects of this choice is discussed in ref. [6].

Two examples of the azimuthal distributions for Z = 2 mid-rapidity particles are shown in fig.1. Mid-rapidity means Y/Ybeam = 0.4 to 0.6. The minima near 0° and 180°are due to the shadow of the telescopes on the MUR [6]. At 35 MeV/u, in-plane enhancement occurs and increases from central to semi-peripheral collisions, as already observed for Ar + Al reactions (ref. Shen, Angélique). The anisotropy $a_2 \cos 2\phi$, shifted up by 1/3, is shown by the dotted line. The 69 MeV/u data exhibit an opposite trend, namely out-of-plane enhancement.

Figure 2 shows the average transverse momentum $< pt >$ versus $\phi$. The same in-plane enhancement is observed, revealing that not only the density of particles is enhanced in-plane but also that these particles are emitted with a higher average transverse velocity. Therefore, the energy flowing in-plane is significantly larger than out-of-plane.

The evolution from in-plane enhancement to squeeze-out as a function of incident energy is shown in fig. 3. When the flow vanishes, $\theta_F = 0$, the flow axis lies along the beam direction and the anisotropy measured is relative to the flow axis. The corresponding balance energies $E_{bal(b)}$ are indicated by the thick bars [6]. Above and below, $| \theta_F |$ increases and contributes to increase N (0°) and N (180°). Had the flow axis been used, the slopes in fig. 3 would be gentler below $E_{bal}$ and steeper above $E_{bal}$, but the general behaviour would not be modified.

The anisotropy ratio increases from central to semi-peripheral collisions (5 - 7 fm), and decreases in more peripheral collisions (7 - 9 fm), similarly to the flow parameter.

Let us call $E_{uni(b)}$ the energy at which the azimuthal distribution is uniform ($a_2$ = 0, N(90°) / N(0°) = 1). $E_{uni(b)}$ shifts to higher values when the impact parameter increases, in the same way as $E_{bal(b)}$. BUU calculations on the system Ar + Al have shown that mean field effects produce an in-plane enhancement (rotation-like effect) [7]. Since the relative importance of mean field decreases when the energy increases, in-plane enhancement decreases until finally compression in the reaction zone, which QMD calculations found to be responsible for squeeze-out [8], dominate and out-of-plane enhancement is obtained.

The values of $E_{uni(b)}$ are lower than the values of $E_{bal(b)}$, which confirms they are related to different aspects of the directed flow. Their relative position varies with the mass of the system. Indeed, for the system $^{35}Ar + ^{27}Al$, uniform distributions were observed at energies higher than or equal to $E_{bal(b)}$ [5].

## -IV- CONCLUSIONS

The use of a high efficiency $4\pi$ detector array and the good characterization of each analyzed event made it possible to study the azimuthal distribution of mid-rapidity particles relative to the beam axis, for the system $^{64}Zn + ^{58}Ni$. At the lowest energies the azimuthal distribution exhibits an in-plane enhancement in the average transverse momentum value as well as in the number of particles . The distribution becomes uniform at an energy which is ~ 50 MeV/u in central collisions and increases with the impact parameter. At higher energies (69, 79 MeV/u), the sqeeze-out effect is observed. These additionnal data related to the competing roles of mean field and two body collisions provide another check for dynamical calculations of the first instants of the nucleus-nucleus encounter.

REFERENCES

1 : - J. Gosset et al., Talk at Int. Advanced Courses on "The Nuclear Equation of State", Peniscola (Spain) 1989, NATO ASI series Physics 216.
- M. Demoulins et al., Phys. Lett. B 241 (1990) 476
2 : - H. H. Gutbrod et al., Phys. Lett. B 216 (1989) 267
3 : - W. K. Wilson et al., Phys. Rev. C41 (1990) R1881
4 : - W. Q. Shen et al., Nucl. Phys. A 551 (1993) 333
5 : - J. C. Angélique et al., XXXI Int. Winter Meeting on Nuclear Physics, Bormio (Italy) January 1993
- J. C. Angélique et al., 9th Winter Workshop on Nuclear Dynamics, Key West (U.S.A.) February 1993
6 : - R. Popescu, Ph. D. thesis and paper to be submitted
7 : - Y. G. Ma et al., Z. für Phys. A344 (1993) 469
- Y. G. Ma et al., Phys. Rev. C48 (1993) 1492
8 : - C. Hartnack et al., Nuc. Phys. A538 (1992) 53C


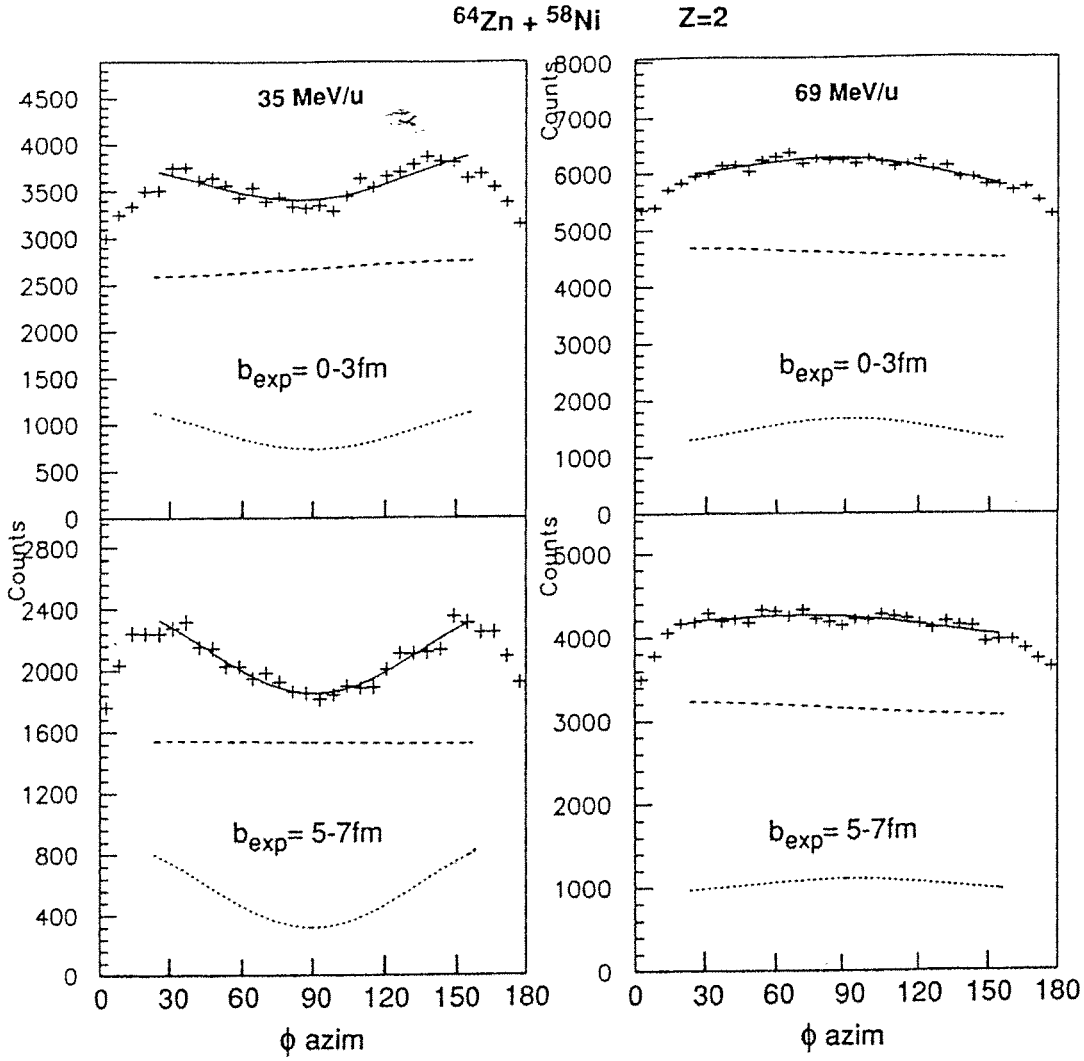


**Fig. 1 :** Azimuthal distributions of mid-rapidity Z=2 particles (mostly α-particles) emitted in central (top) and semi-peripheral (bottom) collisions at 35 and 69 MeV/u. The minima at 0° and 180° are due to the detector set-up. The solid lines are fits with expression (1). The dashed and dotted lines show the cos ϕ and cos 2ϕ terms.

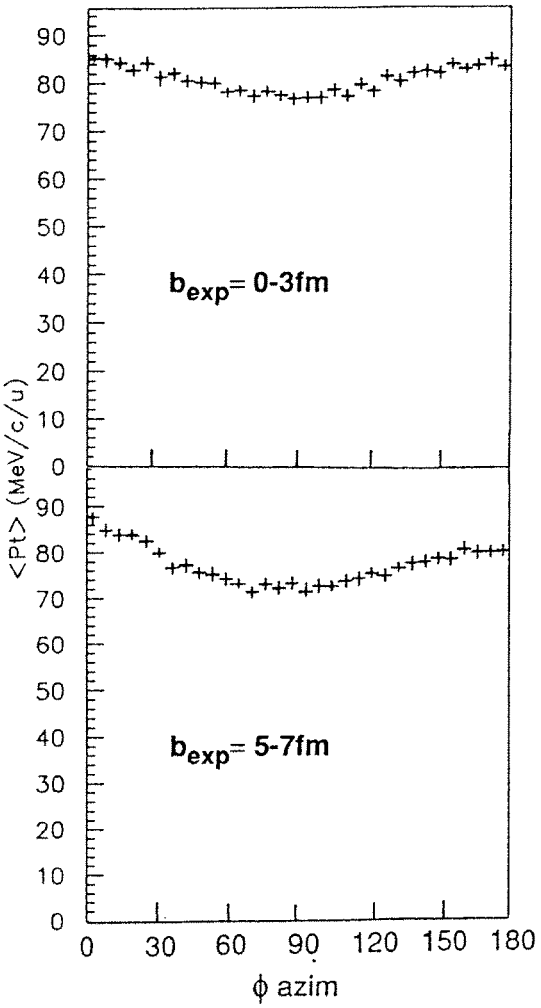


**Fig. 2 :** Azimuthal variation of the average transverse momentum per nucleon of mid-rapidity Z=2 particles (mostly α-particles) emitted at 35 MeV/u in central (top) and semi-peripheral (bottom) collisions.

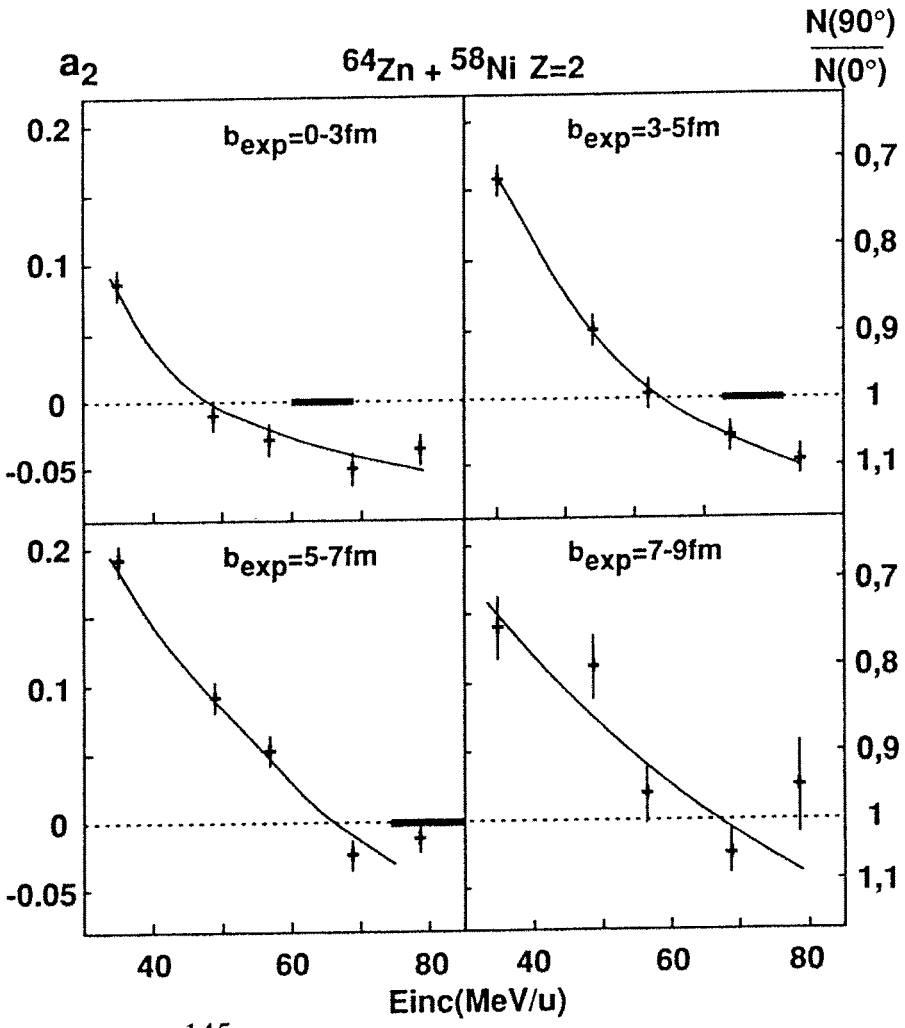


**Fig. 3** : Excitation functions for the anisotropy factor $a_2$ (left scale) and the number ratio N (90°)/N(0°) (right scale) in four bins of the estimated impact parameter $b_{exp}$. The thick horizontal bars show the location of the balance energies. The thin solid lines are just to guide the eyes.

# INVERSION OF COLLECTIVE MATTER FLOW AND EQUATION OF STATE

J.C.Angélique[a], G. Bizard[a], R. Brou[a], D. Cussol[a], M. Louvel[a], J.P. Patry[a], J.Péter[a], R. Regimbart[a], W.Q. Shen[a)n], J.C. Steckmeyer[a], B. Tamain[a], E. Crema[b,i], H. Doubre[b], K. Hagel[b,f], G.M. Jin[b)h], A. Péghaire[b], F. Saint-Laurent[b], Y. Cassagnou[c], R. Legrain[c], C. Lebrun[d], E. Rosato[e], R. MacGrath[g], S.C. Jeong[i], S.M. Lee[i], Y. Nagashima[i], T. Nakagawa[i], M. Ogihara[i], J. Kasagi[j], T. Motobayashi[a)b)k)]

*a) LPC Caen, ISMRA, 14050 Caen, France, b) GANIL Caen, c) DPhN/BE CEN, Saclay 91191, d) LPN Nantes, e) Dipart. di Scienze Fisiche, Univ. di Napoli, Italy, f) Present address : Cyclotron Institute Texas A&M Univ. , USA, g) SUNY, Stony Brook, USA, h) Inst. of Modern Physics, Lanzhou, China, i) Inst. of Physics, Tokyo, Japan, Inst. of Technology, Tokyo, k) Rikkyo University, Tokyo, Japan, l) Permanent address : Inst. de Fisica, Univ. de Sao Paulo, Brazil, m) Present address : P2 Division, Los Alamos National Laboratory, USA, n) Permanent address : Institute of Nuclear Research, Shanghaï, China.*

## 1 - MOTIVATION

The study of mid-rapidity particles provides information on nuclear matter in the interaction region (also called participant nucleons). The directed flow of matter in the reaction plane (sidewards flow) is a signature of this interaction.

At high energies, the flow parameter is positive and attributed to a repulsive momentum transfer in the compressed interaction region. Conversely, at a few tens of MeV/u , the interaction is dominated by the attractive mean field. There, fragments have been shown to be deflected to negative angles. The continuous evolution from negative to positive flow values as a function of incident energy has been studied with the Boltzmann equation [1] and the microscopic Landau-Vlasov model [2]: the flow values are sensitive both to the nucleon-nucleon cross section $\sigma_{NN}$ in nuclear medium and to the equation of state through the incompressibility modulus $K_\infty$ of infinite nuclear matter. In order to disentangle the respective influences of two parameters ($\sigma_{NN}$ and $K_\infty$) by comparing the results of such calculations to experimentally determined flow values, the flow should be measured as a function of two variables, namely the incident energy and the impact parameter.

We have performed measurements on the system $^{36}Ar$ on $^{27}Al$ from 55 to 95 MeV/u. This experiment complements a previous one made at GANIL for the $^{40}Ar$ on $^{27}Al$ system from 25 to 85 MeV/u [3]. The experimental set-up consisted in the complete MUR [4] and TONNEAU [5] and 7 silicon telescopes covering the azimuthal angles between 3° and 30°.The exclusion of poorly characterized events (in very peripheral reactions) and the sorting of events versus the impact parameter value are achieved by using the methods described in reference [6].

## 2 - EXPERIMENTAL RESULTS

The method created by Danielewicz and Odyniec [7] has been used to find the location of the reaction plane.

Figures 1 shows the measured average transverse momentum in the reaction plane $< p^{x'}/A >$ versus the particle rapidity (y) obtained at 55 MeV/u for Z=2 , in bins corresponding to different estimated impact parameter values. The rapidities of the projectile, $y_p$ , the nucleon-nucleon center-of-mass $y_{NN}=y_p/2$ , and the center-of-mass, $y_{cm}$ , are shown by arrows.

The flow parameter of the participants is the slope at $y_p/2$ multiplied by $(y_p-y_p/2)$. The variation of the absolute value of flow parameter versus $b_{exp}$ is plotted in figure 2 for Z=1 and Z=2 at the five incident energies. These values decrease rapidly at small $b_{exp}$ values,

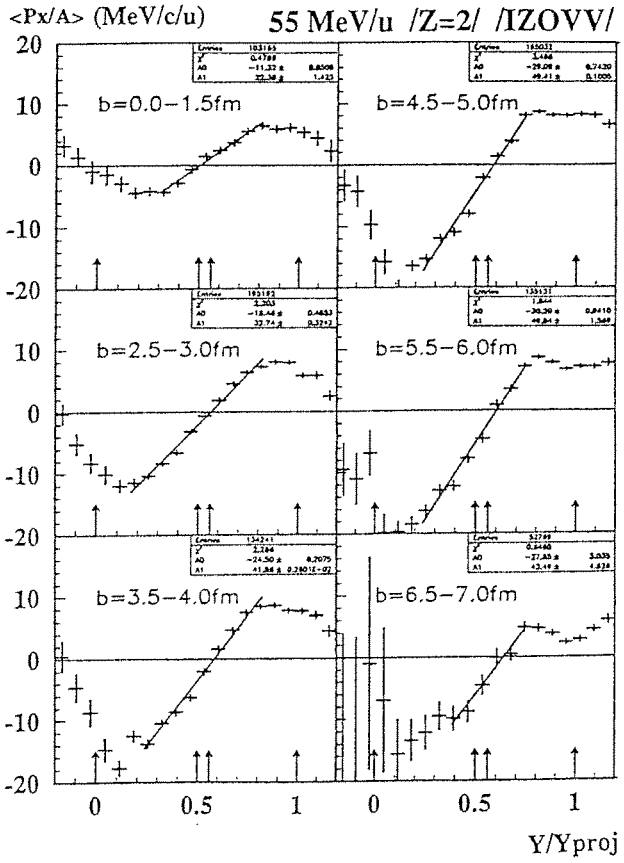


**Figure 1:** *Average value of the projected tranverse momemtum for Z=2 at 55 MeV/u for different impact parameter. values*

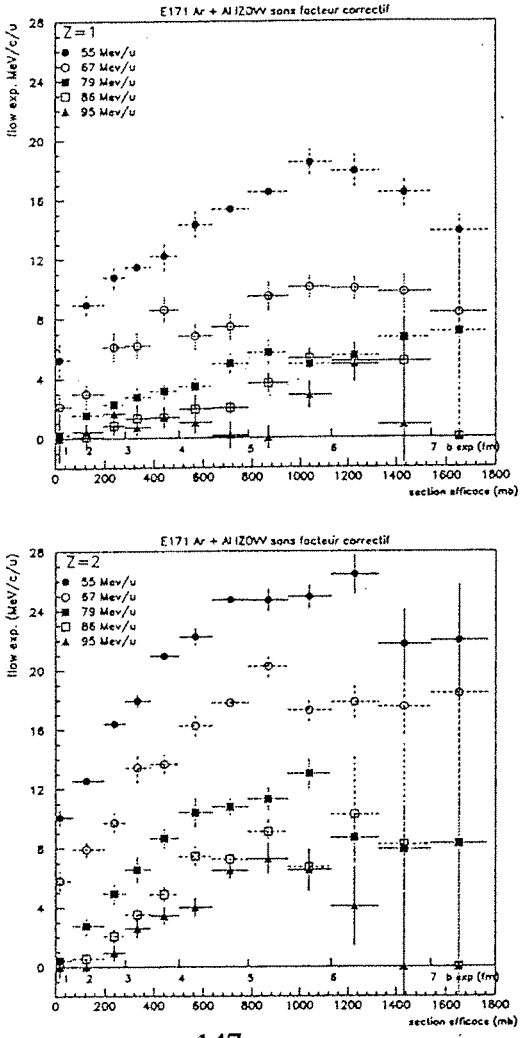


**Figure 2:** *Evolution of the flow parameter with the impact parameter for Z=1 (upper) and Z=2 (lower) from 55 to 95 MeV/u .*

since they must be zero at b=0, and at large impact parameter values ( $b_{grazing}$ = 8 fm). They decrease (i.e. the negative flow parameter increases) when the energy increases, at a different place for different impact parameters. Larger flow values are observed for Z=2 than for Z=1 . This effect has already been observed. It has been attributed to the role of thermal motion which tends to reduce the alignment into the reaction plane due to collective motion. An objection to this explanation is that thermal motion should not modify the average value of $< p^x/A >$ (which is used to get the flow parameter). It has been shown that Coulomb repulsion is, at least partially, responsible for this increase of flow with Z [2].

## 3 - REAL AND MEASURED FLOW VALUES

An experimental value of the flow parameter is normally less than the true value because the experimentally determined direction of the reaction plane is not exactly the real one. It is important to understand that this deviation from the real reaction plane is mainly due to the thermal energy which leads to the emission of particles having a randomly oriented momentum, superimposed to the flow momentum. If the thermal momentum is small relative to the flow momentum, the final direction of the particles remain close to that of the reaction plane and Danielewicz's method will lead to a good location of the reaction plane. In the opposite case, the influence of the flow momentum on the direction of the particle is washed out by the large thermal momentum.

The ratio between the real and measured flow parameters is needed when analyzing data so that the measured flow parameter can be corrected to give the true value before the effects of the method and detector limitations have changed it. There are several different methods for estimating this correction factor first formulated by Danielewicz and co-workers.

However, instead of correcting the experimental data, it is much better to analyse the theoretical calculations in a way similar to the experimental data : one forgets that the reaction plane is known and one finds its direction with the Danielewicz's method, firstly for a perfect detector, secondly after applying a software filter which reproduces the detector limitations. One must perform separately these two steps and watch their effect.

## CONCLUSIONS

Fig. 3 shows the flow measured at different energies for an impact parameter value b around 3 fm , for Z=1 (open circles). $E_{bal}$ (3fm) appears to be close to 95 MeV/u . Similar plots for Z=1 and Z=2 indicate that $E_{bal}$ (1fm) is in the range 80-90 MeV/u and $E_{bal}$ (5 fm) is above $E_{bal}$ (3 fm) . This increase of $E_{bal}$ with b is in qualitative agreement with theoretical predictions.

The value corrected for the difference between the true and measured reaction plane are shown as closed circles .Calculations, based on the Landau-Vlasov equation using a Gogny force and including Coulomb effects, compared to the experimental results indicate that the effective nucleon-nucleon cross section in medium is arround 80% of the value usually used in the calculation.

Fig. 4 shows the evolution of Ebal with the total mass of the system deduced from theoretical calculations (open circles, reference 2), for different systems studied with MUR and TONNEAU (filled circles), and for other experiments (filled triangles, MSU experiments).These data show that $E_{bal}$ evolves like $A^{-1/3}$ for a given impact parameter value. The agreement with the calculations indicates that in these LVUU calculations the relative importance of the mean field and the two body collisions is properly taken into account.

### References


1) G.F.Bertsch, W.G.Lynch and M.B.Tsang, Physics Letters **B189** (1987) 384.
2) V.DeLaMota, F.Sebille et al., Physical Review **C46** (1992) 677.
3) J.P.Sullivan et al., Physics Letters **B249** (1990) 8.
4) G.Bizard et al., Nuclar Instruments & Methods **A244** Vol. 3 (1986) 483.
5) A.Péghaire et al., Nuclar Instruments & Methods **A295** Vol. 3 (1990) 365.
6) J.Péter et al., Nuclear Physics **A519** (1990) 611.
7) P.Danielewicz and G.Odyniec, Physics Letters **B157** (1985) 146

## PUBLICATIONS


1) J.P. Sullivan and J. Péter ; Nucl. Phys. **A540** (1992) 275.
2) J.Péter et al.; Nucl. Phys. **A 538** (1992) 75c
3) J.C.Angélique et al.; Communication at XXXI Meeting on Nuclear Physics, Bormio (January 1993)
4) G.Bizard et al.; Symposium on Nuclear Physics, Tours 1992.


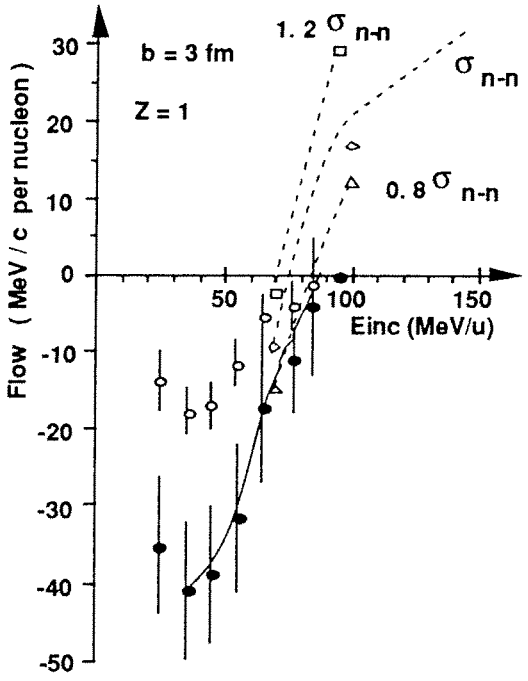


**Figure 3:** *Evolution of the flow parameter at b=3 fm with the incident energy for Z=1. The open and full circles represent respectively the uncorrected and the corrected experimental data. The theoretical calculations correspond to 0.8 $\sigma_{nn}$ (triangles), $\sigma_{nn}$ (diamonds) and 1.2 $\sigma_{nn}$ (squares).*

**Figure 4:** *Evolution of $E_{bal}$ with the size of the system. The open circles represent theoretical predictions and the full symbols represent experimental data from GANIL and MSU experiments.*

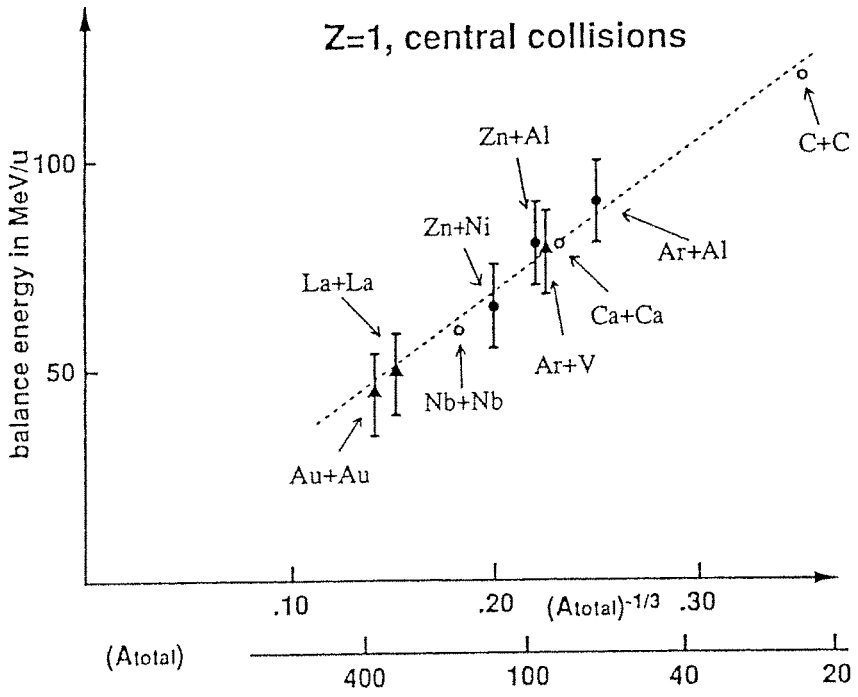

# Velocity and azimuthal distributions produced in 45 MeV/nucleon $^{84}$Kr reactions

L.G. Sobotka, Z. Majka*, D.W. Stracener, D.G. Sarantites, and R.J. Charity
*Department of Chemistry, Washington University, St. Louis Missouri 63130*

G. Auger, E. Plagnol, and Y. Schutz
*GANIL, BP 5027, F14021 Caen CEDEX, France*

R. Dayras and J.P. Wieleczko†
*Service de Physique Nucléaire-Basse Energy, 91191 Gif-sur-Yvette CEDEX, France*

J. Barreto
*Instituto de Física da UFRJ-CP21945-RJ, Brazil*

E. Norbeck
*Department of Physics, University of Iowa, Iowa City, Iowa 52242*

## I. INTRODUCTION

A few recent studies have claimed that bulk volume expansion is needed in order to explain the production of intermediate mass fragments in intermediate energy heavy-ion collisions. [1,2] If this is so, these collisions are providing a means of studying the decay of subsaturation density nuclear systems. However, in order to have confidence in these results, the reaction dynamics must be better understood than they presently are, and in particular how the dynamics is reflected in the few selected parameters which are used in comparisons with theory.

This contribution reports on complete velocity and azimuthal correlations for both asymmetric and symmetric systems as a function of a few global event variables. The velocity distributions are elongated, and suggestive of two main sources, for all values of global event parameters. A 180° azimuthal correlation between the heaviest fragment in each event and all other fragment types exists for all values of the event parameters, however this correlation is dominated by fragments with very low transverse velocity, $V_\perp$. Taken together, these data indicate that most of the reaction cross section has dynamical features bearing a resemblance to only moderately kinetic energy damped binary reactions with the breakup of the projectile-like component dominating the azimuthal correlations. However, as the forward component has very small $V_\perp$, procedures which weight by the $V_\perp$ (or momentum) do generate flat azimuthal correlations.

*Permanent Address: Institute of Physics, Jagellonian University of Kraków, Poland.

†Permanent Address: GANIL, BP 5027, F14021 Caen Cedex, France.

## II. EXPERIMENTAL

A beam of 45 MeV/u $^{84}$Kr was used to bombard targets of $^{45}$Sc, $^{93}$Nb, and $^{159}$Tb. The Dwarf Ball/Wall detector system was used to detect and identify the charged particles [3]. This system subtends approximately 88% of $4\pi$ and is composed of 104, fast plastic - CsI(Tl) phoswich detectors. The energy calibration of the light charged particles (lcp = p,d,t,$^3$He, and $\alpha$-particles) was obtained from the punch-through points. The calibration of the energies of the heavy ions was done by the procedure described in ref. [3]. The identification thresholds for protons and alpha particles are 4 and 2 MeV/nucleon, respectively, for a large angular region, from $\approx$ 167° to near 55°. The energy thresholds increase at more forward angles. For protons, which is the worst case, the threshold increases to as much as 2 times the value at the backward angles. The azimuthal angular resolution, which is determined by the detector granularity, is approximately 30° for most of the subtended solid angle. The exceptions are for the most forward and backward angles, where the resolution is a factor of two worse. For the purpose of this study the angles of each detected particle were randomly selected from those subtended by the hit detector.

## III. RESULTS AND DISCUSSION

The global event parameters used in this study are the light charged particle multiplicity ($M_{lcp}$), the total detected charge ($\sum Z_{det}$), and the maximum individual charge detected ($Z_{max}$). Some of these distributions have been presented previously. [4]

Cross section plots, in a Galilean invariant form $d^2\sigma/(V^2 d\Omega dV)$, are shown in Fig. 1. This figure displays maps for protons, $\alpha$ particles, deuterons and carbon fragments emitted from the reaction 45 MeV/u $^{84}$Kr + $^{93}$Nb. These maps clearly indicate the presence of two strong

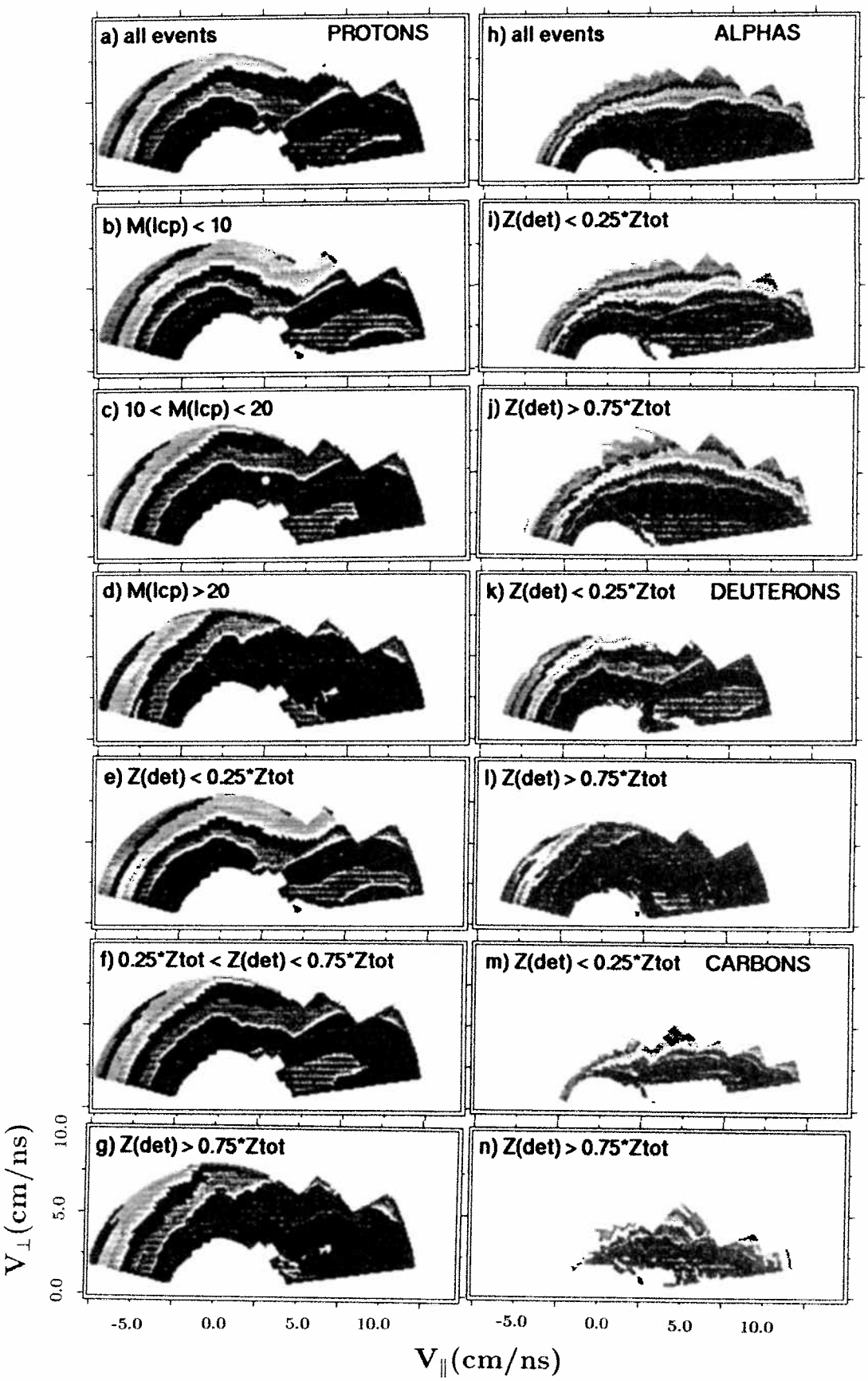


FIG. 1. Invariant cross section plots, [$V_\parallel$(cm/ns) vs $V_\perp$(cm/ns)], for the reaction 45 MeV/u $^{84}$Kr + $^{93}$Nb. The individual maps in the left column are for protons selected for a) all events, b) $M_{lcp} < 10$, c) $10 \leq M_{lcp} < 20$, d) $20 \leq M_{lcp}$, e) $\sum Z_{det} \leq 19$, f) $19 < \sum Z_{det} \leq 57$, g) $\sum Z_{det} > 57$. In the right column there are selected maps for $\alpha$ particles, deuterons, and carbon nuclei, (frames h-n).

sources of particles: one with a value of $V_{\parallel}$ of only a few cm/ns and another with velocity slightly less than that of the beam, $V_b$ = 9.3 cm/ns. Of course, one expects this for the most peripheral collisions and it is true that the characteristic Coulomb "hole" for the projectile-like source is only clearly seen for the gates on either $M_{lcp}$ < 10 (section b) or $Z_{det}$ less than 25% (section e).

What is perhaps surprising is that these two features, while somewhat blurred, remain visible even for the most violent events, The persistence of a bimodal emission pattern for light ions from the most violent collisions has also been observed for the very heavy system, 28.2 MeV/u $^{136}Xe + ^{209}Bi$ [5].

The bimodal structure of the other deuterons is also clearly seen. On the other hand, the maps for the heavier particles, provide only a hint of a bimodal nature for the least violent collisions, with an evolution into a single eccentric distribution for the most violent collisions. Further examination of these maps clearly shows that the eccentricity of the ellipses of constant invariant cross section decreases as the collisions become more violent. The weaker bimodal structure and the "compacting" of the ellipses of constant cross section could be taken as evidence of an increased contribution of a true intermediate rapidity source for heavier particles. However, it is also possible that these emissions are primarily from one fragment or the other, but emerge at a latter time (than the lighter fragments), when the relative velocity is less.

Figure 2 shows an example of an azimuthal correlation in the two $V_{\perp}$ coordinates. In this example the correlation is between fragments with Z > 2 and the heaviest fragment in the event, which is going to the right in this plot. These fragments are generally emitted to forward angles with low $V_{\perp}$. As the detector used to detect the "heaviest" fragment can not be used to detect another fragment, a large dip in yield in seen at $\phi = 0$. The dip is quite pronounced for about $\pm 35°$ at small transverse velocities. This is due to the fact that many of the "heaviest" fragments are detected in the innermost ring, which consists of 5 detectors.

Figure 3a shows a few selected azimuthal correlations which result from the radial integration of plots such as the one shown in Fig. 2. Needless to say, the outstanding features of these plots are the prominent correlation at 180° and the strong negative autocorrelation at 0° and 360°. (These plots are normalized such that the average value is 100.)

The 180° correlation diminishes with either increasing values of $M_{lcp}$ or decreasing values of $Z_{max}$ (shown). One would like to differentiate between two mechanisms for producing this correlation. If the particle emission is focussed into a plane as the result of spin polarization, one would find the azimuthal correlation to have peaks at both 0° and 180°. On the other hand, if the plane is defined by a two body breakup, momentum balance will produce only a 180° enhancement. Overall momentum balance must produce a 180° correlation originating from the different (forward-backward) center of mass hemispheres. While, breakup of a forward ($\theta \approx 0°$) going projectile-like subsystem, will send particles to both sides of the beam, and therefore the 180° correlation will be confined to the forward hemisphere.

The 180° correlation is present when one selects only those fragments forward of $90°_{C.M.}$. Therefore the peaks are not the result of overall momentum balance.

The differentiation between whether these correlations are driven by spin or the result of a dynamical breakup is difficult due to the strong negative autocorrelation in one of the regions of interest. However, inspection of Fig. 3a shows satellite peaks at small $\Delta\phi$ for the gates on the smaller values of $Z_{max}$. These satellite peaks suggest that angular momentum does influence the shape of the azimuthal correlations for these gates.

Rather than integrating radially, one can study the correlations in plots such as Fig. 2., by examining the eccentricities of the ellipses of constant intensity, as a function of $V_{\perp}$ and particle type. We find that the correlations (as indicated by the eccentricity) are stronger for the gate on low values of $M_{lcp}$ than for the gate on high values, stronger for Z > 2 fragments than for $\alpha$ particles, which in turn exhibit a stronger correlation than for protons, and it is much stronger at low values of $V_{\perp}$ than for high values. The last observation is the most interesting. One would not expect such a trend if angular momentum produced the correlation. On the other hand, if a projectile fragment going near $\theta = 0°$ breaks up, both the heaviest piece (which generates the reference angle) and the lighter fragment would have low transverse velocity, as well as exhibit a 180° correlation.

The azimuthal correlations relative to the heaviest fragment illustrate a specific facet of the reaction. In order to get a more global picture of azimuthal correlations, another procedure was used to generate the reference angle. Here we follow the procedure of Wilson et al. [6], where the reference angle is taken as collinear with the line in the x-y plane (with z as the beam axis) from which the sum of the squares of the perpendicular distances of all of the momenta is a minimum. This procedure, still has an 180° ambiguity. This is resolved by choosing the reference angle consistent with the direction of the transverse momentum vector, Q.

This procedure yields the following general results, see fig. 3b for a few examples.

1) The 180° correlations from the "azimuthal + Q" method are smaller than those from the method which uses the heaviest fragment to generate the reference angle.

2) The correlation observed at 180° is still significantly stronger than at 0° or 360° for all but the most violent collisions.

3) The correlations for the gates which should correspond to central collisions, the largest values of $M_{lcp}$ and $\sum Z_{det}$, are essentially flat, (not shown).

4) The azimuthal correlations for selected charges from more peripheral collisions show the expected trend that the heavier the fragment the more pronounced the cor-

relation.

The first observation is due to the fact that the method which uses the heaviest fragment to generate the reference angle emphasizes the strong correlations between fragments each which have low $V_\perp$ while the "azimuthal + Q" method, which weights by $V_\perp$, deemphasizes these components. The second observation, is found not to be due to the autocorrelations of this method and therefore indicates (again) that these correlations are, in general produced by dynamical breakup rather than by the influence of angular momentum. The third observation provides strong evidence that these gates, ones which select the most violent collisions, select events in which the bulk of the particles are emitted isotropically in the transverse directions. The last observation is not surprising, and has been reported before [7,8]. However, the discussion above indicates that this correlation is not due to the influence of spin on the decay of excited fragments, but rather due to a dynamical process.

## IV. CONCLUSION

We conclude that the azimuthal correlations, and thus reaction plane determinations, are dominated by a process or processes which send particles to opposite sides of the beam in the forward direction. While this might be projectile-like fragmentation, particles knocked out of the target could also contribute. The importance of this type of dynamics has been made previously [7,9–11], however the generality of the phenomenon (in terms of global event gating conditions and system mass asymmetry) has not been demonstrated previously. Methods used to determine the reaction plane which are weighted by $V_\perp$, such as the "azimuthal + Q" procedure, deemphasize this component, however it is present in all event gates.

Returning to the $V_\parallel$ versus $V_\perp$ plots, we have found that one can not clearly identify a participant region for the reactions, 45 MeV/nucleon $^{84}$Kr with targets of $^{45}$Sc, $^{93}$Nb, and $^{159}$Tb. For all light charged particle multiplicity bins as well as all bins on the total collected charge the event shapes are quite elongated.

In summary, we find all gating conditions generate observables which are dominated by dynamics and reflect the entrance channel. This highlights the importance of comparing this kind of data to simulations which do not decouple the latter stages (where the system might be at low mean density) from the initial dynamics.


[1] D.R. Bowman, et al., Phys. Rev. Lett. **67**, 1527 (1991).
[2] K. Hagel, et al., Phys. Rev. Lett. **68**, 2141 (1992).
[3] D.W. Stracener, et al., Nucl. Instru. Meth. **A294**, 485 (1990).
[4] Z. Majka, et al., in the proceedings of the symposium on Nuclear Dynamics and Nuclear Disassembly, World Scientific, ed. J.B. Natowitz, pp 424, Dallas 1989.
[5] B. Lott, et al., Phys. Rev. Lett., **68**,3141 (1992).
[6] W.K. Wilson, et al., Phys. Rev. **C45**, 738 (1992).
[7] H.J. Rabe, et al., Phys. Lett. **B196**, 439 (1987).
[8] M.B. Tsang, et al., Phys. Rev. **C44**, 2065 (1991).
[9] B. Borderie, et al. Phys. Lett. **B205**, 26 (1988).
[10] R. Wada, et al., Nucl. Phys. **A539**, 316 (1992).
[11] T. Ethvignot, et al., Phys. Rev. **C46**, 637 (1992).


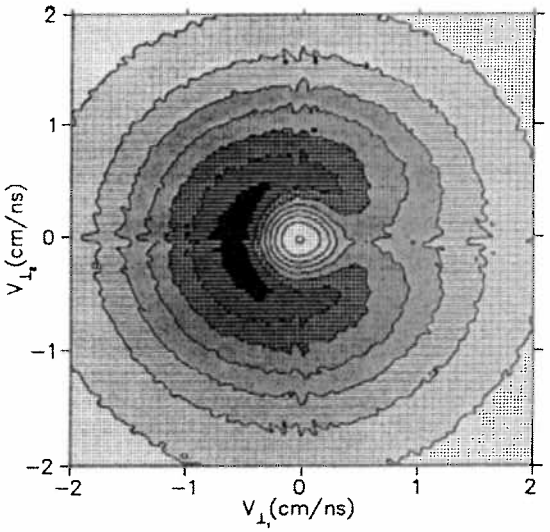


FIG. 2. Azimuthal distribution of fragments with $Z > 2$ relative to the direction of the heaviest detected fragment (going to the right) for the reaction 45 MeV/u $^{84}$Kr + $^{93}$Nb. These data have the requirement that $M_{lcp} < 10$.

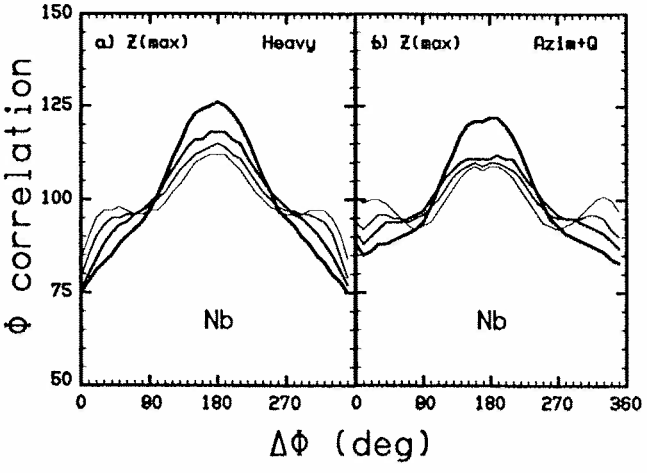


FIG. 3. Azimuthal correlations for the reaction 45 MeV/u $^{84}$Kr + $^{93}$Nb. a) is the correlation relative to the direction of the heaviest detected fragment while b) is the correlation relative to the direction deduced by the "azimuthal + Q" procedure. The thicker the line is, the larger the values of $Z_{max}$ .

# PRE-EQUILIBRIUM PROTON EMISSION IN $^{40}$Ar AND $^{132}$Xe INDUCED REACTIONS AT 44 MeV/u

R. Alba[1], R. Coniglione[1], A. Del Zoppo[1], C. Agodi[1], G. Bellia[1,2], P. Finocchiaro[1], K. Loukachine[1,+], C. Maiolino[1], E. Migneco[1,2], P. Piattelli[1], D. Santonocito[1], P. Sapienza[1], A. Peghaire[3], I. Iori[4,5], L. Manduci[4], A. Moroni[4]

(1) *INFN - Laboratorio Nazionale del Sud, Via S.Sofia 44, 95129 Catania (ITALY)*
(2) *Dipartimento di Fisica dell'Università di Catania (ITALY)*
(3) *GANIL - Caen (FRANCE)*
(4) *INFN - Sezione di Milano (ITALY)*
(5) *Dipartimento di Fisica dell'Università di Milano (ITALY)*

## 1. Motivations

In several experimental works, aimed at the study of the proton emission in heavy ion collisions, very energetic protons have been observed even at rather large polar angles[1]. A standard data analysis based on three moving sources[2] has evidenced the presence of a half-beam velocity source (IS) interpreted in terms of pre-equilibrium emission from the participant zone of the colliding system[3-5].

We have performed an experimental study of the fast protons production with the aim of investigating its impact parameter dependence.

## 2. Experiment and data analysis

The experiment was performed at the GANIL facility using the MEDEA $4\pi$ detection system[6], studying the following reactions: 44 MeV/u $^{40}$Ar on $^{27}$Al, $^{51}$V, $^{197}$Au and 44 MeV/u $^{132}$Xe on $^{51}$V, $^{158}$Gd, $^{197}$Au. In this experiment the MEDEA array consisted of 150 $BaF_2$ and 80 phoswich detectors, located in the angular range $42^o \div 170^o$ and $10^o \div 30^o$, respectively, giving a total geometrical efficiency of 80% altogether. Events triggered by a multiplicity $M \geq 1$ of particles above a threshold level corresponding to about 5 MeV protons were recorded. Protons were identified as in ref.[6] and the energy calibration was performed as described in ref.[7].

Inclusive proton energy spectra at different angles between $14^o$ and $160^o$ in the laboratory frame were analyzed using moving source parametrization. Three sources with velocities close to those of the projectile, a slow spectator and the IS and with inverse slopes T in the range 4÷6 MeV, 4÷6 MeV and 13÷14 MeV, respectively, give a satisfactory description of the data. We notice that the velocity of IS equals that of the nucleon-nucleon (N-N) center of mass even for the most asymmetric colliding

[+] On leave from Nuclear Physics Institute, St. Petersburg, Russia

systems and the inverse slope parameters, well described by the estimation of ref.[3] in the framework of the first chance p-N collision model, are in agreement with the systematics as reported, for instance, in ref.[1].

The results of the three sources analysis suggest a way to perform a clean separation of the IS from the spectators by imposing suitable constraints in the phase space. In fact for $\theta \geq 42^o$ and $E_p \geq 40$ MeV in the laboratory frame, at least 96% of the fast proton yield is given by the IS only for all the investigated systems. Using the parameters extracted from the moving source fit, the filtered fraction $\Omega_F$ of IS protons detected with these constraints has been determined. We have found $\Omega_F \approx 0.15 \pm 0.02$, independently of the impact parameter and of the system.

To study the impact parameter dependence of the pre-equilibrium proton multiplicity $\langle m \rangle$, two-dimensional $Y(M, m_F)$ data sortings, $m_F$ being the multiplicity of protons with $E_p \geq 40$ MeV detected at $\theta \geq 42^o$ and $M$ the charged particle multiplicity, were performed. The multiplicity $M$ was used as indicator of the impact parameter $b$.

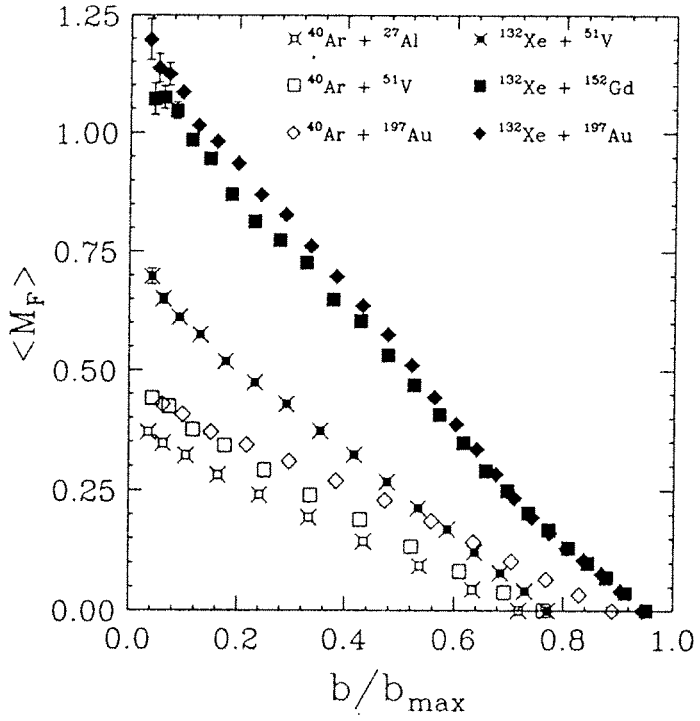


**Fig.1** -First moment of the multiplicity distributions of fast protons with $E_p \geq 40$ MeV and $\theta \geq 42^o$ as a function of $\frac{b}{b_{max}}$ for all the systems investigated.

## 3. Results and discussion

We have performed a standard $M$ to impact parameter conversion based on the geometric prescription of ref.[8]

$$\frac{b(M)}{b_{max}} = \left[ \frac{\sum_M^{M_{max}} \sigma(M)}{\int_0^{b_{max}} 2\pi b db} \right]^{\frac{1}{2}}$$

with $b_{max} = R_P + R_T$, $R_{P,T} = r_0 A_{P,T}^{1/3}$ being the projectile (target) radius with $r_0 = 1.2$ fm, and $\sigma(M)$ the measured cross section of events with multiplicity $M$. The first moment of the $m_F$-distribution is reported in fig.1 as a function of $\frac{b}{b_{max}}$ for all the systems studied. The data show clearly that the mean multiplicity of the IS protons increases strongly with the centrality of the collision as expected in the hypothesis that their origin is the projectile-target overlap region. However,to compare this experimental result to a model and to extract a scaling law with the size of colliding system a more reliable $M \rightarrow b$ conversion is necessary. The fluctuactions of the emitted charged particle multiplicity, in fact, generate an impact parameter mixing when the simple conversion described above is performed. A method to correct for such an effect is under study.

## References


1. B.H. Jacak et al., *Phys. Rev.* **C 35** (1987) 1751 and refs. therein.
2. J. Pochodzalla et al., *Phys. Rev.* **C 35** (1987) 1695.
3. H. Fuchs and B. Homeyer, *International Workshop on Particle Correlation and Interferometry in Nuclear Collisions*, Nantes (1988) 305.
4. M. Blann and B. Remington, *Phys. Rev.* **C 37** (1988) 2231.
5. W. Bauer, *Nucl. Phys.* **A471** (1987) 604; J. Aichelin et al., *Phys. Rev.* **C 31** (1985) 1730; W. Cassing, *Z. Phys.* **A 329** (1988) 471; S.J. Luke et al., *Phys. Rev.* **C 48** (1993) 857.
6. E. Migneco et al., *Nucl. Instr. and Meth.*, **A314** (1992) 31.
7. A. Del Zoppo et al., *Nucl. Instr. and Meth.*, **A 327** (1993) 363.
8. C. Cavata et al., *Phys. Rev.* **C 42** (1990) 1760.

# B4 - MULTIFRAGMENT EMISSION

# DYNAMICS AND INSTABILITIES IN NUCLEAR FRAGMENTATION

*M.Colonna*[1,2], *M.Di Toro*[1], *A.Guarnera*[1,2], *V.Latora*[1] *and A.Smerzi*[1]

[1])*Laboratorio Nazionale del Sud, INFN*
*44, Via S.Sofia, 95125 Catania, Italy*
*and*
*Dipartimento di Fisica dell' Universitá di Catania,*

[2])*GANIL, B.P. 5027, F-14021 Caen Cedex, France*

ABSTRACT

A general procedure to identify instability regions which lead to multifragmentation events is presented. The method covers all possible sources of dynamical instabilities. Informations on the instability point, like the time when the nuclear system enters the critical region, the most unstable modes and the time constant of the exponential growing of the relative variances, are deduced without any numerical bias. Some hints towards a fully dynamical picture of fragmentation processes are finally suggested.

Heavy ion collisions at intermediate energy have been widely described through some kinetic approaches ($VUU, BUU, BNV$) which are able to correctly reproduce the mean trajectory of the system in phase space. However, when one is interested in unstable processes such as, for instance, multifragmentation events, these methods are not valid anymore since they do not contain fluctuations, which are very important in a not equilibrated system. Nevertheless we will show that the use of such kinetic equations, solved within the test particle approach, can still be very useful to extract quite precise informations on physical properties of the instability regions. The test particle method introduces some numerical fluctuations in the initial conditions and in the Pauli blocking. In critical regime the fluctuations are growing exponentially and this numerical noise can substantially modify the relative dynamics[1]. In this paper we will show that any noise, in a good mean trajectory dynamics, is suitable to extract informations on the instability point (most unstable modes and instability time); on the contrary, in order to get the right fragment formation, we should be able to reproduce the correct physical fluctuations at the instability point.

We have checked these ideas solving $BNV$-type transport equations in a simplified model. We consider a two-dimensional collision between two slabs of nuclear matter in a box of lengths 63 $fm$ and 21 $fm$; in order to reduce the computational time, the mean field has been averaged on the $y$ direction. The $x$ radius of the two nuclei is equal to 4 $fm$ (the radius of a $^{40}Ca$ nucleus) while the total number of nucleons is fixed requiring that the density of the two slabs is equal to the normal density, which is 0.55 $fm^{-2}$ in two dimensions. We have simulated a central

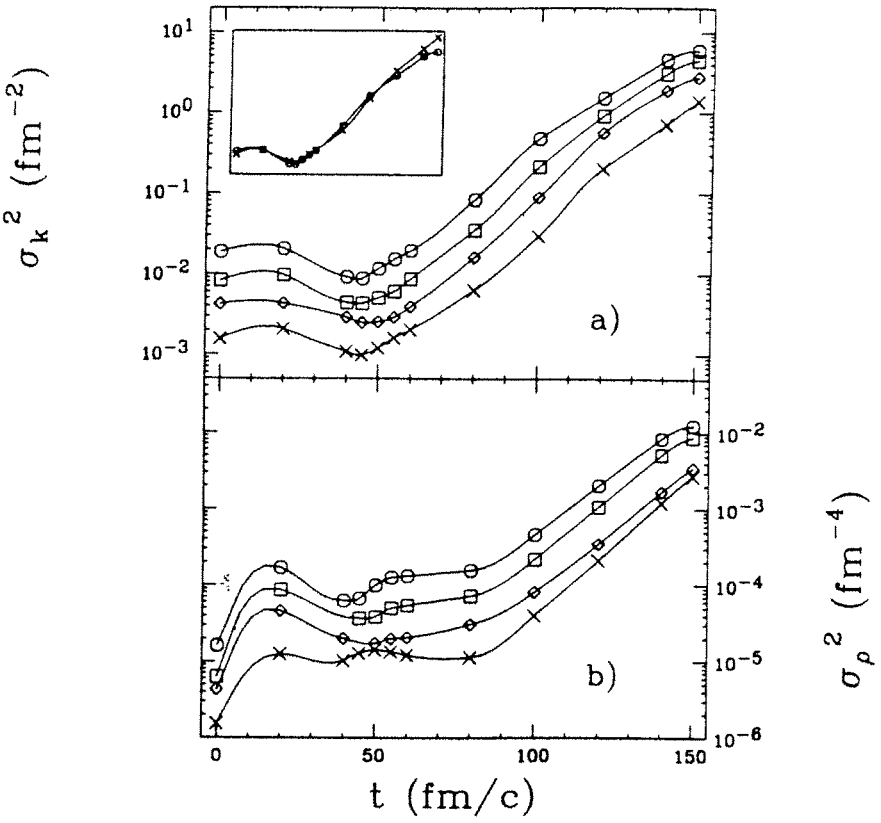


**Fig. 1.** Time evolution of variances for the two slab collision described in the text. a): $\sigma^2(t)$ of the most unstable modes; b) $\sigma^2(t)$ of the monopole mode. Circles: $N_{TP} = 20$; squares: $N_{TP} = 40$; diamonds: $N_{TP} = 80$; crosses: $N_{TP} = 200$.

collision at a beam energy $E_{lab}/A = 40\ MeV/u$. As the time increases we see the formation of a nearly uniform region at half normal density and at a temperature around $T = 8\ MeV$. This system lies in the spinodal instability region[2]. In such a simplified situation it is possible to demonstrate that, for infinite nuclear matter, the eigenmodes of the density are plane waves, characterized by a wave number $k$. Even if, in our case, the system is finite, it is interesting to perform a Fourier analysis of the density fluctuation and therefore to define the following quantity:

$$\sigma_k^2 = \int_0^{L_x} dx \int_0^{L_x} dx' e^{-ik(x-x')} < \delta\rho(x)\delta\rho(x') > . \qquad (1)$$

The quantity $\sigma_k^2$ represents the spectral correlator.

In fig. 1a) is shown the time behaviour of $\sigma_k^2$ for the most unstable mode ($k = 5 \div 6$), calculated using 20, 40, 80 and 200 test particles per nucleon, 50 trajectories are considered. We see that all the variances reach the minimum point at the same time $t_{inst} = 45 fm/c$; this point does not depend on the noise and it corresponds to

the time when the system enters the instability region. The scaling law is preserved also in the next evolution of $\sigma_k^2$; it means that the time $\tau$, characteristic of the exponential growing, does not depend on the number of test particles. The scaling disappears when the system enters a saturation regime, corresponding to a new equilibrium reached by cluster formation. This can be seen in the box inside fig.1a where we report two curves of this figure ($N_{TP} = 20, 200$) suitably rescaled. As expected the saturation appears earlier for the trajectories with less test-particles.

The fragmentation time, *i.e.* the time when we observe fragment formation, is therefore fully dominated, in this representation, by the value of the fluctuation $\sigma_k^2$ at $t = t_{inst}$. In this sense it would be extremely important to know the right physical amount of fluctuations that are present at that point.

We have also studied the time dependence of the density variance of the trajectories in the a circle of radius 4 fm in the overlapping zone:

$$\sigma_\rho^2 = \frac{1}{N_{events}} \sum_{i=1}^{N_{events}} (\rho_i(t) - \bar{\rho}(t))^2 \tag{2}$$

which is related to the fluctuations of the distribution function, after some phase space averaging. In the stability region the variance follows the density as it should be in a Poisson-type distribution of test particles. Indeed if the variance on the number of test particles in the circle follows a Poisson law $\sigma_n^2 = \bar{n}$ we get for the variance on density the relation:

$$\sigma_\rho^2(t) = \frac{\bar{\rho}(t)}{S\ N_{TP}} \tag{3}$$

where $S$ is the surface of the circle. The presence of this classical behaviour of fluctuations is not surprising since we are looking at properties of phase space averaged observables and then we expect quantum fluctuations to be washed out.

When the system enters the instability region we observe a sharp transition to an exponential behaviour:

$$\sigma_\rho^2(t) = \sigma_0^2 e^{2t/\tau} \tag{4}$$

which clearly indicates the presence of an unstable mode with associated imaginary energy $E = i\hbar/\tau$ [3,4]. $\sigma_0^2$ represents the amount of fluctuations present at the time of instability and clearly scales with the number of test particles per nucleon $N_{TP}$. But it is very important to remark that the time of instability, *i.e.* the time of the transition to the exponential, and the time $\tau$, characteristic of the exponential growing of fluctuations, do not depend on the number of test particles we are using, *i.e.* on the noise introduced in the calculation. They are related just to the mean evolution and to the mean properties (density and temperature) of the system which, as we explained before, is always well described until the instability spinodal region is reached. Starting from this point, the amount of fluctuations present in the system becomes of crucial importance since the dynamics is now dominated

by the exponential amplification of the initial noise and consequently calculations using a different number of test particles will lead to different results.

In fig.1b) is displayed the density variance. The scaling behaviour here is less evident because in $\sigma_\rho^2$ we have the superposition of different modes corresponding to different values of $k$. This superposition seems to create an uncertainty on the time when the system enters the instability region, since, using 200 test particles, the exponential growing starts later. Actually this time does not change and it is still $t = 45\ fm/c$ for all curves. When the amplitude of fluctuations is not large enough (as it happens using 200 test particles per nucleon), the system expands before exploding and therefore the growing time $\tau$ reduces, according to the reduced new density, until the explosion becomes the dominant one. In this case it happens at $t = 80\ fm/c$.

In conclusion we have shown that, when one is interested in the dynamics of critical situations, it is possible to extract very important informations just solving the $BNV$ equation within the test particle approach. In fact, if the number of test particles is large enough to avoid spurious effects, the dynamical evolution is correctly described until the system becomes unstable. Therefore the time when the spinodal region is reached and all the observables related to the mean properties (density, temperature, etc...) at that point may be calculated without any ambiguity. In particular we can extract the growing time $\tau$, characteristic of the exponential increasing of fluctuations, which will lead to fragmentation. On the other hand we have also proved that time and pattern of this fragment formation depends, in a crucial way, on the noise present in the system, *i.e.* on the number of test particles. Therefore the right physical value of fluctuations is needed in order to correctly describe the dynamics. Concerning this subject, work is presently in progress. It is finally evident that the method presented here is not limited to the study of spinodal (volume) instabilities. The recipe is to look at the time dependence of the variances $\sigma_i^2$ of various collective degrees of freedom, that can be done within the test particle approach. In this way all possible sources of instabilities (surface, Coulomb and so on) will be revealed and suitably studied.

We warmly thank Ph.Chomaz for very helpful discussions.

## References

1. L.G.Moretto, Kin Tso, N.Colonna, and G.J.Wozniak, *Phys. Rev. Lett.* **69** (1992) 1884.
2. G.F.Burgio, Ph.Chomaz, J.Randrup, *Phys. Rev. Lett.* **69** (1992) 885
3. M.Colonna, Ph.Chomaz, and J.Randrup, preprint LBL-33402 (Dec'92)
4. M.Colonna, G.F.Burgio, Ph.Chomaz, M.Di Toro and J.Randrup, *Phys. Rev. C* (in press)

# THE DECAY MODES OF HEAVY EXCITED NUCLEI: FROM BINARY FISSION TO MULTIFRAGMENTATION

G. Bizard [1], R. Bougault [1], R. Brou [1], J. Colin [1], D. Durand [1], A. Genoux-Lubain [1]
J.L. Laville [1], C. Le Brun [1], J.F. Lecolley [1], M. Louvel [1], J. Péter [1], J.C. Steckmeyer [1]
B. Tamain [1], A. Badala [1-2], T. Motobayashi [1-3], G. Rudolf [4], L. Stuttgé [4]

*1) LPC -ISMRA, Bld Marechal Juin , 14050 Caen Cedex, France*
*2) INFN Catania, Corso Italia, Catania, Italy*
*3) Rikkyo University, Rikkyo, Japan*
*4) CRN Strasbourg, BP 20 CRO, F-67037, Strasbourg Cedex,France*

Abstract :

The decay modes of heavy excited nuclei formed in dissipative collisions for the systems Ar+Au at 60 MeV/u and Kr+Au at 43 MeV/u are studied. A transition from binary fission towards multi-fragment emission is observed around 3 MeV/u excitation energy, independently of the considered system. The charge distributions of the three target-emitted fragments suggest a smooth change from "fission" events (as a "natural" continuity of binary fission) to "residue production" then to "symmetric ternary fragmentation" events when the excitation energy increases from 3 MeV/u to 5 MeV/u.

## 1) MOTIVATION

The evolution with excitation energy of the decay modes of excited nuclei is of key interest for the understanding of the fundamental properties of nuclear matter as well as of the dynamics of nucleus-nucleus collisions. In this work, we have studied the competition between binary fission and the three-(or possibly more)- body decay process of a massive excited target-like nucleus produced in a nucleus-nucleus collision around the Fermi energy.

## 2) EXPERIMENTS

The experiments were performed at the Ganil facility in the Nautilus scattering chamber. Two different systems were studied: Ar+Au at 60 MeV/u and Kr+Au at 43 MeV/u. Light charged particles were detected in Mur and Tonneau while fragments were detected in Delf, XYZT and additional solid-state detectors. In this work we concentrated on peripheral events characterized by the presence of one fast fragment associated with two or three slow target-emitted fragments. The characteristics of the fast

fragment were the following: Z and velocities larger than 10 and .75 $V_{beam}$, respectively, in the Ar+Au experiment and larger than 25 and .85 $V_{beam}$ in Kr+Au. Due to the thresholds of the fragment detectors, the characteristics of the massive slow target-emitted fragments were: Z larger than 8 and velocities larger than .5 cm/ns (.13 MeV/u) for Delf and 3 cm/ns (4.7 MeV/u) for XYZT in the forward direction.

## 3) RESULTS

To describe conveniently the onset of multi-fragment emission, we defined R as the probability for the target-like nucleus to emit at least three fragments divided by the corresponding probability to emit two fragments. We made use of the so-called Kinematical Coincidence Method to account for detection biases induced by dead zones and thresholds. In order to obtain the evolution of R as a function of the excitation energy, an estimate of R on an event by event basis was performed. Two methods were used to estimate the excitation energy of the target-like nucleus. The first one used the information carried by the fast light-charged particles to estimate the degree of the so-called "elasticity" of the collision while the second one took advantage of the information associated with the heavy detected fragments. In this case, the excitation energy per nucleon was related to the kinematical properties of the fragments using the massive transfer hypothesis.

The two methods of estimating the excitation energy have been compared and a good agreement between the two has been found. The evolution of R as a function of the excitation energy is displayed for the two systems in fig 1. It is observed that R is independent of the considered system and appears to depend only on the excitation energy of the decaying composite system. Lastly, the three fragment production is negligeable at low excitation energies as expected and increases exponentially around 3 MeV/u to become substantial around 5 MeV/u.

We have also analyzed the charge distribution of the three target-emitted fragments using Dalitz plot in fig 2. A clear evolution is observed. Starting from moderate excitation energies, most of the events are concentrated in the "fission" region. Increasing the excitation energy first tends to populate the "residues" area and then for the highest reachable excitation energies, the "symmetric ternary fragmentation" region. We have indicated for each excitation energy bin the average Zfrag defined as the sum of the charge of the fragments. One may note that Zfrag decreases with increasing excitation energy as expected since light particle evaporation becomes more and more abundant.

## 4) CONCLUSIONS

To conclude, we have found a transition from binary fission towards multi-fragment emission in the decay of massive excited nuclei around 3 MeV/u. In this excitation energy range the charge distributions displayed in Dalitz plots exhibit two

massive fragments in coincidence with a lighter one, suggesting a "natural" continuity with the standard low-energy-like binary decay fission process. On the other hand as the energy is increased, there is a gradual transition from "fission" to "residue production", then to "symmetric ternary fragmentation" around 5 MeV/u indicating a change in the decay mechanism and the onset of multifragmentation.

G. Bizard et al Physics Letters B302 (1993) 162

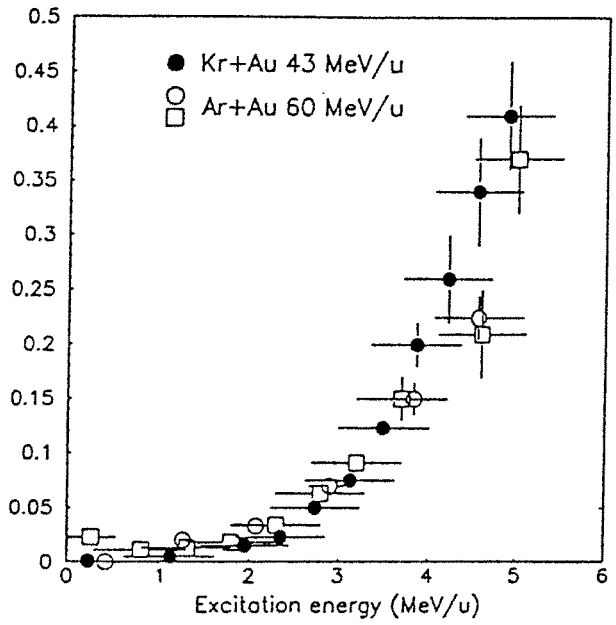


*Fig. 1:*
*Evolution of the two-fold vs three-fold fragment production as a function of the excitation energy per nucleon E*. Symbols correspond to different methods for estimating E* and to two studied systems.*

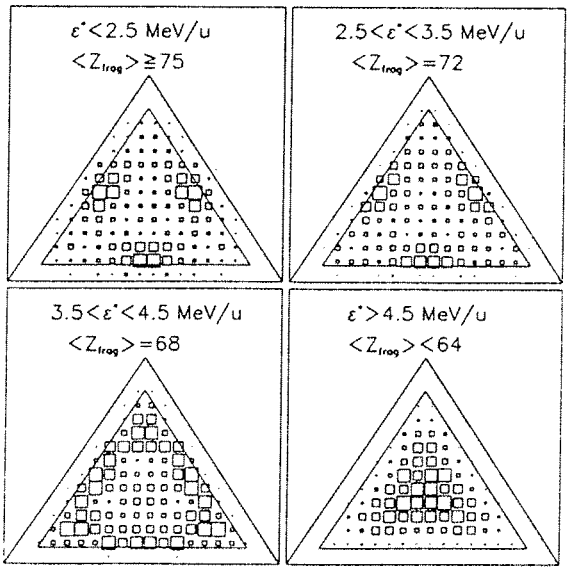


Fig. 2. Dalitz plots for the three fragments (called TEF in the text) for the Kr+Au system. The events have been sorted according to the excitation energy per nucleon. For each bin, the average $Z_{frag}$ (see text) is indicated. The area being possibly covered by the data because of experimental limitations (lowest detectable charge is 8) is indicated by the interior triangle.

# PHYSICS WITH INDRA: THE FIRST RESULTS

**C.O. Bacri, B. Borderie, P. Box, L. Lakehal-Ayat, A. Ouatizerga, E. Plagnol, M.F. Rivet, M. Squalli, L. Tassan-Got**
*IPN Orsay, France*

**B. Berthier, Y. Cassagnou, J.L. Charvet, R. Dayras, E. de Filippo, R. Legrain, L. Nalpas, E.Pollacco, C. Volant**
*DAPNIA Saclay, France*

**G. Auger, A. Benkirane, J. Benlliure, A. Chbihi, P. Ecomard, A. Lefevre, N. Marie, J. Pouthas, F. Saint-Laurent, J.P. Wieleczko**
*GANIL, France*

**R. Bougault, R. Brou, J. Colin, D. Cussol, D. Durand, A. Genoux-Lubain, J.L. Laville, C. Le Brun, J.F. Lecolley, M. Louvel, V. Métivier, J. Peter, R. Regimbart, E. Rosato, J.C. Steckmeyer, B. Tamain, E. Vient**
*LPC Caen, France*

**A. Demeyer, D. Guinet, P. Lautesse, L. Lebreton**
*IPN Lyon, France*

**P. Eudes, D. Gourio, A. Rahmani, T. Reposeur**
*LPN Nantes, France*

## 1 Motivations

Several theoretical models predict that multifragmentation becomes the dominant deexcitation mode of highly compressed or heated nuclear systems. Indeed, when high energy heavy ions collide, the composite system is predicted to suffer first a severe compression, followed by an expansion phase; during the latter it may enter the mechanical instability region (spinodal) and remain long enough in it to break into several fragments. For light systems, this phenomenon is expected to occur typically above 40 MeV/nucleon [1, 2]. Conversely for very heavy systems, the strong Coulomb repulsion enhances the expansion, and multifragmentation could occur after a more gentle compression step, and consequently at lower energies (above 25 MeV/nucleon). In this case, the entity which undergoes multifragmentation might present very exotic shapes such as bubbles, donuts, disks ... [3, 4]

A careful study of this phenomenon requires the best possible detection of all the produced species. This was the main reason for building the $4\pi$ multidetector INDRA: it is designed to detect and identify *charged* products over very large Z and energy ranges [5, 6]. A first set of experiments was run in March-April 1993 for studying multifragmentation, varying the total mass and the initial asymmetry of the system, and the incident energy. More precisely four projectile-target couples were chosen:

$^{36}Ar + {}^{58}Ni$, between 32 and 95 MeV/nucleon.

$^{36}Ar + KCl$, between 32 and 74 MeV/nucleon.

$^{129}Xe + {}^{nat}Sn$, between 25 and 50 MeV/nucleon.

$^{155}Gd + {}^{nat}U$, at 36 MeV/nucleon.

## 2 Results

The easiest results which could be sorted in a short time were multiplicity distributions, by rejecting $\gamma$ rays, and separating roughly light charged particles (H, He isotopes) from heavier fragments, *without more precise identification*; only qualitative comments can be given at the present time, these curves however point out unambiguously the excellent global efficiency of INDRA (geometry and thresholds).

### *2.1 Total charged product multiplicities*

The charged product multiplicity distributions are displayed in Fig 1: they have the well-known shape for this kind of distribution [7], namely a strong low-multiplicity component, associated with very peripheral collisions, and a broad peak for higher multiplicities. Both the position and the width of the peak increase with incident energy, the peak eventually turns into a plateau at the highest explored incident energies. Moreover the position of the tail of the multiplicity distributions keeps shifting upward with incident energy, indicating that more and more violent collisions occur; indeed for the $Ar + Ni$ system at 95 MeV/nucleon the highest measured value of the charged product multiplicity is close to that which corresponds to the vaporisation of the system ( Z = 46).

### *2.2 Fragment multiplicity versus total multiplicity*

Spectra showing the fragment ($Z \geq 3$) multiplicity versus the total charged product multiplicity are presented in Fig 2 for some of the studied systems. As no fragment identification was performed, *these curves should be regarded as preliminary.* One observes an increase of the fragment number with the total multiplicity; more fragments are therefore emitted in the most violent collisions. The evolution of this general trend with the incident energy is however depending on the size of the system:

For $Ar + Ni$ the average fragment number associated with the largest multiplicities does not change between 40 and 95 MeV/nucleon, while the maximum value of the total multiplicity keeps increasing. This finding, already observed on a neighbour system $Zn + Ti$ [8], is probably connected with a decrease of the fragment size at higher energy; it should be noticed that the Z conservation line (corresponding to all fragments having Z=3 and all light charged particles being protons) is reached at 95 MeV/nucleon, and that it is far from being so at 40 MeV/nucleon.

Conversely for the $Xe + Sn$ system a strong increase of the average fragment number with the incident energy is visible. Very high fragment multiplicities are observed (12-14), which should be confirmed when all fragments will be properly identified.

Finally the picture obtained for the $Gd + U$ system at 36 MeV/nucleon is comparable to that of $Xe + Sn$ at 50 MeV/nucleon. Reactions on the Carbon backing of the target show up clearly at multiplicities smaller than 12, and will be easily removed as soon as more severe constraints (total Z, linear momentum, energy) will be applied.

## 3 Comparison with data from other detectors

Comparison of the results on raw data (i.e. non efficiency-corrected) with those obtained with previous $4\pi$ detectors gives a quality label to the detectors ( particularly on their granularity and detection thresholds). A systematics of multiplicity distributions for

reactions induced by 50 MeV/nucleon Xe projectiles on targets ranging from C to Au has been realized by a group from MSU, using the Miniball [9] . Our measurement on the Sn target well enters this series of measurements. Similarly the distributions for 50 and 80 MeV/nucleon Ar beams impinging on Ni and Au targets can be compared [10] . It appears from Fig 3 that INDRA can detect more complete events than the Miniball: at 50 MeV/nucleon, the INDRA multiplicity distributions for $Ar + Ni$ $(Xe + Sn)$ coincide with the Miniball $Ar + Au$ $(Xe + Au)$ ones, despite total charge numbers smaller by 50 (30) units. Moreover, for the Xe beam, the average number of fragments detected with INDRA is larger.

We will therefore obtain with INDRA high quality physical results, on events where a very large fraction of the total charge has been detected. This will provide very stringent constraints for theoretical models.

## References


1. E. Suraud, D. Cussol, C. Grégoire, D. Boilley, M. Pi, P. Schuck, B. Remaud, F. Sébille, Nucl. Phys. **A495** (1989) 73c
2. S. Levit and P.Bonche, Nucl. Phys. **A347** (1985) 426.
3. B.Borderie et al. , Phys. Lett. **B302** (1993) 15.
4. L.G. Moretto et al. Phys. Rev. Lett. **69** (1992) 1884 and preprint LBL-34724.
5. B. Borderie et al., XXXI Int. Winter Meeting on Nuclear Physics, Bormio (1993).
6. G. Auger et al., Nouvelles du GANIL 44 (1993).
7. E Schwinn et al, GANIL- A compilation 1989-1991, p 142
8. A. Kerambrun Thèse LPCC 1993
9. D.R. Bowman et al, Phys. Rev. **C46** (1992) 1834
10. D. Fox et al., Phys. Rev. **C47** (1993) R421.

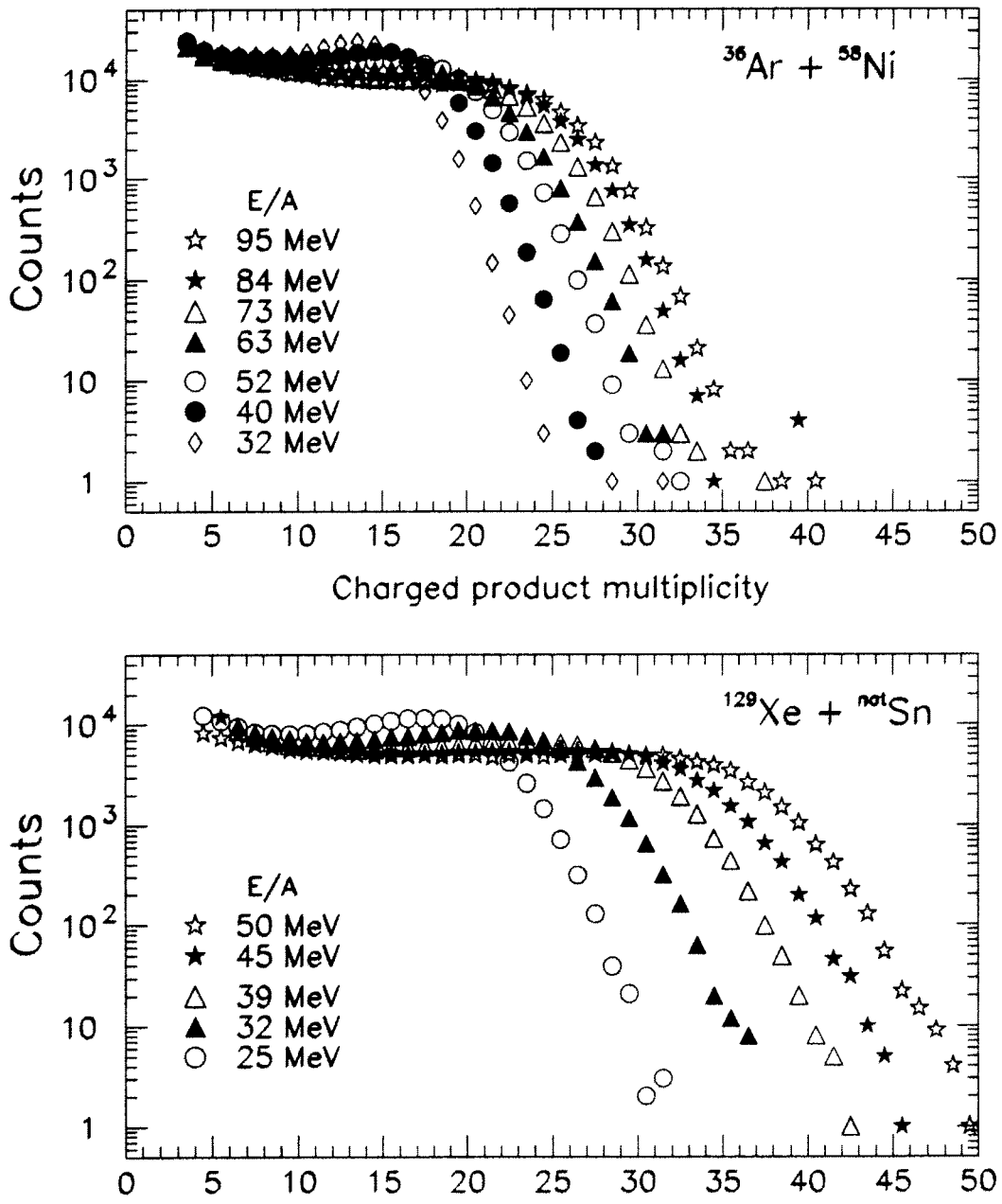


**Fig 1:** *Charged product multiplicity distributions. Events were recorded when at least N INDRA modules fired ($N = 3$ for 32-73 MeV/nucleon Ar beams, and $N = 4$ otherwise).*

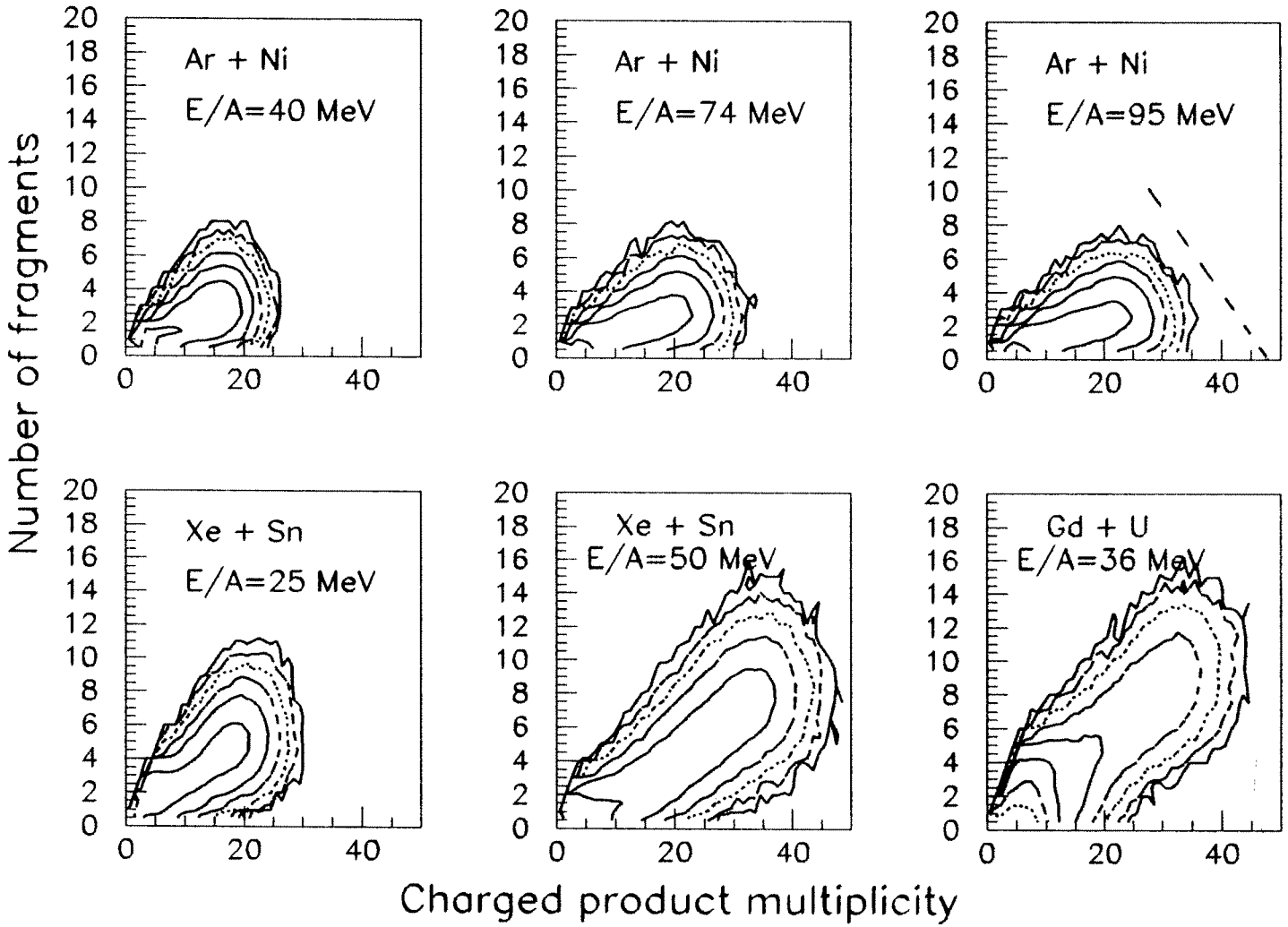


**Fig 2**: *Fragment multiplicity versus charged product multiplicity for several systems at different energies. The dotted line for 95 MeV/nucleon Ar + Ni represents the Z conservation line*

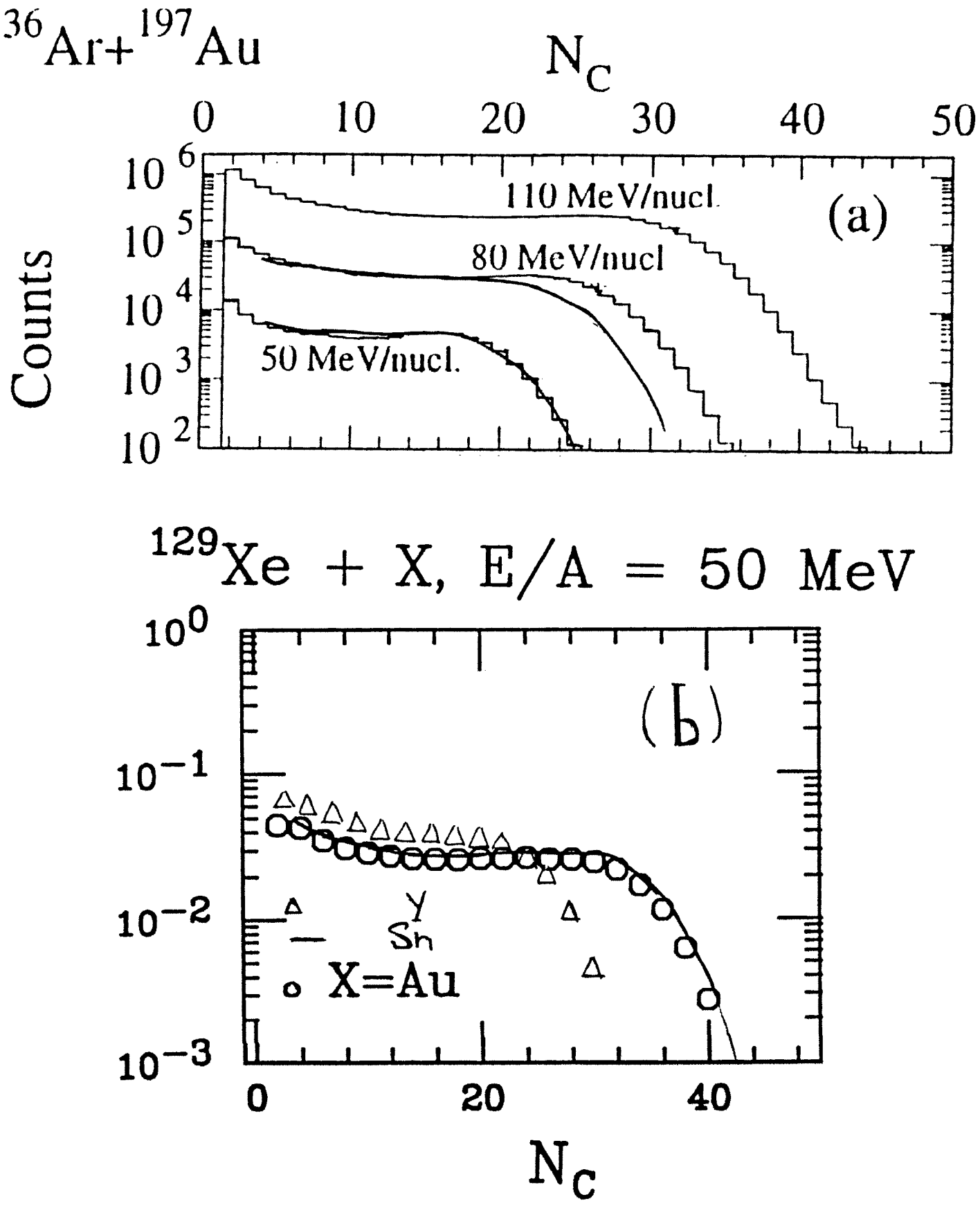


**Fig 3:** *Charged product multiplicity distributions obtained with INDRA and with the MSU miniball. a) Ar + Au* [10] (histograms-MSU) and Ar + Ni (solid lines-INDRA). b) Xe + Y, Au (points-MSU) and Xe + Sn (solid line-INDRA)

# *Multifragmentation in central Kr+Au collisions at 60 MeV/u*

O. Lopez [a], M.Aboufirassi [a], A Badala [a-e], B. Bilwes [b], R. Bougault [a], R. Brou [a], F. Cosmo [b], J. Colin [a], D. Durand [a], A. Genoux-Lubain [a], D. Horn [a-d], J. L. Laville [a], J. F. Lecolley [a], F. Lefebvres [a], C. Le Brun [a], M. Louvel [a], M. Mahi [a], C. Paulot [a], A. Peghaire [c], G. Rudolf [b], F. Schiebling [b], J. C. Steckmeyer [a], L. Stuttgé [b], B. Tamain [a], S. Tomasevic [b].

*a) Laboratoire de Physique Corpusculaire, ISMRA, IN2P3-CNRS 14050 CAEN CEDEX, France.*

*b) Centre de Recherches Nucléaires, IN2P3-CNRS, Université Louis Pasteur, B.P. 20 67037 STRASBOURG CEDEX, France.*

*c) GANIL, B.P. 5027, 14021 CAEN CEDEX, France.*

*d) Chalk River Laboratories, AECL, Chalk River, Ontario, Canada.*

*e) INFN Catania, Corso Italia, Catania, Italy.*

## 1) Motivations

One important issue of central collisions in the intermediate energy range concerns the decay modes of very excited nuclei produced in the reactions[1]. When the energy dissipated in the collisions is sufficiently high, many fragments can be emitted during the collision, thus leading to a complete disassembly of the excited matter. This process often referred to as multifragmentation[2], is presently being intensively investigated with help of $4\pi$ detectors. In this paper, we want to address the following topic :

*- Is the disassembly process prompt and simultaneous or is it sequential ?*

The answer to this question requires, in addition to the charge distributions, the knowledge of the kinematical characteristics of the fragments produced in the most violent collisions. Moreover, the events used in this analysis must be as well characterized as possible in order to correctly select central collisions and estimate the degree of equilibration reached during the reactions. This last point is of primary importance since we wish to compare the data with two statistical models.

## 2) Experiment and data sampling

The experiment was performed in the Nautilus scattering chamber at the GANIL facility by bombarding a Au target with a low intensity Kr beam at 60 MeV/u. Fragments were detected in the DELF[3] and XYZt[4] detectors. They constitute an ensemble of 30 position sensitive plate avalanche counters (PPAC), each followed by an ionisation chamber. The

angular range covered was 3-150° with a geometrical acceptance of 55%. Full detection efficiency for atomic numbers equal to or larger than 8 was obtained. The setup had low velocity thresholds : .5 cm/ns ( .13 MeV/u ) for DELF and 2 cm/ns ( 2.1 MeV/u ) for XYZt in the forward direction. The measured parameters were the atomic number Z, the velocity V and the angles. Light charged particles were detected in coïncidence by two plastic detectors MUR[5] and TONNEAU[6] covering the same angular range as DELF and XYZt. In the present work, we will consider only events with a detected fragment multiplicity equal to or larger than 3, which corresponds to a rough elimination of peripheral events[7].

In order to select central events for which global equilibrium have been achevied, we have introduced the following condition in the sorting of data : events in which at least one fragment have been emitted at an angle smaller than a given "cutting" angle were rejected. The evolution as a function of the "cutting" angle of the fragment angular distribution ( calculated in the center-of-mass of the detected fragments, called hereafter "event frame" ) and the associated parallel and perpendicular ( with respect to the beam axis ) velocity distributions are displayed in fig. 1.

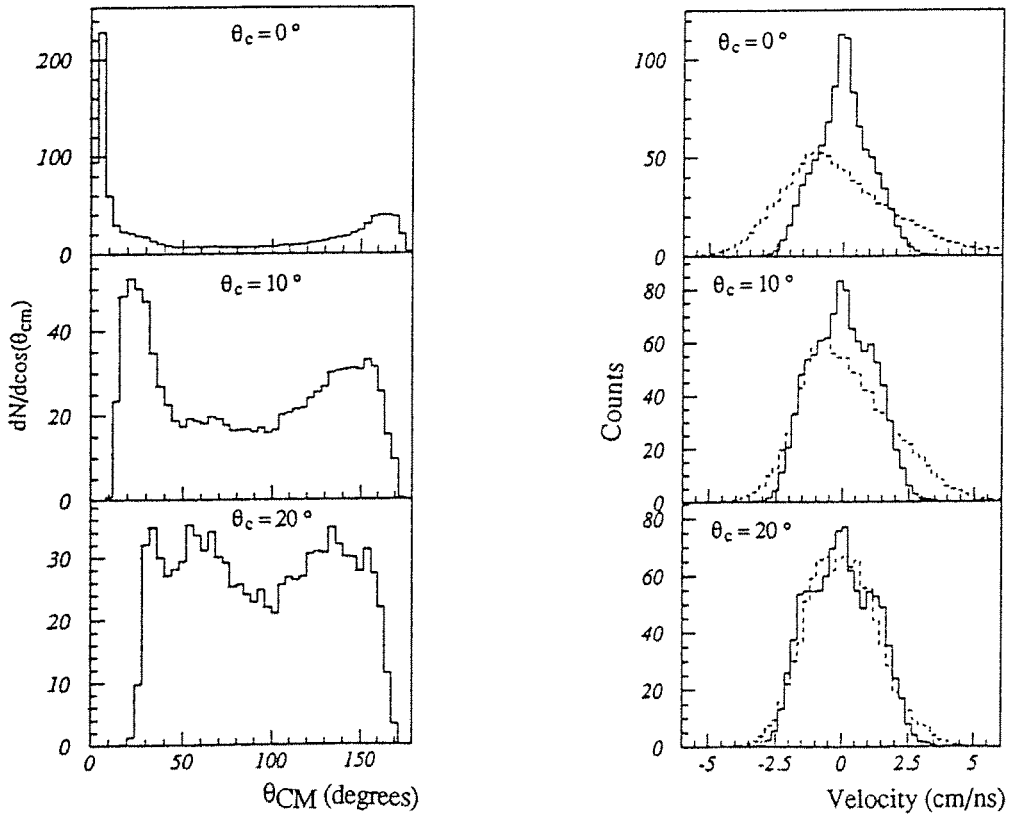


*Fig. 1. Left : angular distributions in the "event" frame (see text) for different values of the "cutting" angle θc. Right : same as left but for parallel ( solid histogram ) and perpendicular ( dashed histogram ) velocity distributions in the "event" frame.*

For small values of the "cutting" angle, the distributions do not correspond to equilibrium : the angular distribution is forward-peaked. However, for a value of 20° the selected events exhibit global equilibrium : the angular distribution is forward-backward symmetric and the two velocity distributions are nearly identical. Therefore, for these events, fragments are emitted isotropically by an equilibrated source[8].

## 3) Comparison between models and data.

Since the main question addressed in this study is related to the time scale of the disassembly process, two computer simulations were performed based on very different assumptions. In the first one, standard statistical prescriptions[9-11] have been used and fragments are emitted sequentially with no correlation between successive splittings. In the second one, we have used the Lopez-Randrup formalism[12] describing the multifragmentation mechanism as a extension of the transition state method and assumed that fragments are emitted simultaneously. In both models, it was supposed that the fragments were produced by a unique thermalized source, the characteristics of which (mass, velocity and excitation energy ) were chosen in order to reproduce the charge distributions and evaporated light charged particles multiplicities[8]. The best agreement was obtained for a value of the excitation energy around 4.5 MeV/u and a mass around 230.

In order to answer to the question addressed here, kinematical correlations between fragments have been studied since they provide different patterns according to different decay times[13,14]. In the case of sequential emission, no correlation between fragments issued from different splitting must be present while in the "simultaneous" one, repulsive Coulomb interactions between all fragments should set in. To explore such behaviours, the distributions of relative velocities and relative angles (in the event frame) between the fragments taken two by two have been built and compared to those resulting from the two simulations, filtered through the experimental setup acceptance. The relative velocity distributions are presented in fig. 2(a) for three different n-fold events. The distributions corresponding to the sequential model ( dotted histogram ) are peaked at low values while those of the "simultaneous" model (solid histogram ) are in reasonnable ageement with the data (black points).

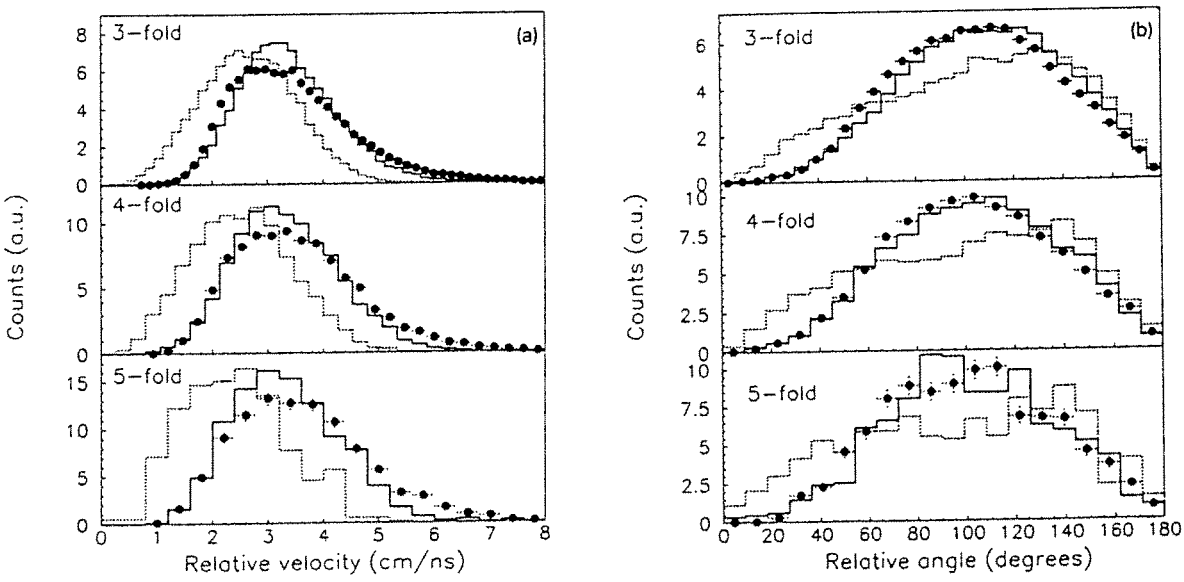


*Fig. 2. (a) Relative velocity distributions between fragments taken two by two for three different fragment multiplicities ( indicated in the left corner of each panel ). Black points correspond to data, the dotted line to the results of the "sequential" model calculations and the solid line to those of the "simultaneous" model.*
*(b) Same as (a) but for relative angle distributions.*

In fig. 2(b) , a nice agreement with the data is still obtained with the "simultaneous" model for the relative angle distributions showing the existence of correlations between fragments ( repulsive Coulomb interactions ).

To summarize, we have detected and analysed multi-fragments events produced in central Kr+Au collisions at 60 MeV/u. After a careful selection of central events by requiring identical parallel and transverse center-of-mass velocity distributions (i. e. global equilibrium ), events have been compared with two computer simulations. Nice agreement with the simultaneous model has been found leading to the conclusion that the disassembly process is compatible with prompt and simultaneous fragment emission.

## REFERENCES :


*1) E. Suraud, B. Tamain, C. Gregoire, Prog. of Nuclear and Particle Science 23(1989) 357*

*2) B. Tamain, Conference EPS-8 " Trends in Physics" (1991).*

*3) R. Bougault et al, NIM A259 (1987) 473.*

*4) G. Rudolf et al, NIM A307 (1991) 325.*

*5) G. Bizard et al, NIM A244 (1988) 483.*

*6) A. Peghaire et al, NIM A295 (1990) 365.*

*7) O. Lopez et al, Contribution to "The second European Biennal Workshop in Nuclear Physics", Megeve (1993).*

*8) O. Lopez et al, University Thesis, Caen (1993).*

*9) L. G. Moretto, Nucl. Physics A247 (1975) 641.*

*10) R. J. Charity et al, Nucl. Physics A483 (1988) 371 and A511(1990) 59.*

*11) D. Durand, Nucl. Physics A541 (1992) 266.*

*12) J. Lopez, J. Randrup, Nucl. Phys. A512 (1990) 345.*

*13) R. Trockel et al, Phys. Rev. Letters Vol.29 (1987) 2844.*

*14) M. Louvel et al, Nucl. Physics A559 (1993) 137.*

# B5 - MESONS AND PHOTONS

# Nuclear Bremsstrahlung as a probe to study dissipation mechanisms

J.H.G. van Pol[1], H. Löhner[1], R.H. Siemssen[1], H.W. Wilschut[1], R. Holzmann[2], A. Schubert[2], S. Hlaváč[2,6], R.S. Simon[2], V. Wagner[2,7], P. Lautridou[3], F. Lefèvre[3], M. Marqués[3,5], T. Matulewicz[3], W. Mittig[3], R.W. Ostendorf[3], P. Roussel-Chomaz[3], Y. Schutz[3], M. Franke[4], W. Kühn[4], M. Notheisen[4], R. Novotny[4], F. Ballester[5], J. Díaz[5], A. Marín[5], G. Martinez[5], A. Kugler[7]

[1] *Kernfysisch Versneller Instituut, NL-9747 AA Groningen, The Netherlands*
[2] *Gesellschaft für Schwerionenforschung, D-64220 Darmstadt, Germany*
[3] *Grand accélérateur National d'Ions Lourds, F-14021 Caen, France*
[4] *II. Physikalisches Institut, Universität Gießen, D-35392 Gießen, germany*
[5] *Instituto de Física Corpuscular, SP-46100 Burjassot Valencia, Spain*
[6] *Slovak Academy of Sciences, Bratislava, Slovak Republic*
[7] *Nuclear Physics Institute, Řež u Prahy, Czech Republic*

## 1 Introduction

For bombarding energies well below the Fermi energy it has been shown that nucleus-nucleus collisions are dominated by mean field effects (one-body dissipation). Going beyond the Fermi energy the dominating factor is increasingly that of incoherent nucleon-nucleon collisions (two-body dissipation). The motivation of the present experiment is to try to determine the relative importance of one- and two-body dissipation near the Fermi energy. For this the hard photon probe is used: Hard photons (Bremsstrahlung) are known to originate from incoherent proton-neutron collisions so the observation of these highly energetic photons is an indication of two-body dissipation. The reaction studied was $^{36}$Ar + $^{159}$Tb at 44 $MeV/u$. The experiment mainly focussed on peripheral collisions for which the outcoming particle will have approximately beam velocity and mass, i.e. a projectile-like fragment (*PLF*). In the participant-spectator model for peripheral reactions, the number of proton-neutron collisions is directly related to the number of protons and neutrons removed from the projectile and can be determined from the $N$ and $Z$ of the *PLF* provided that this fragment remains particle stable. If not, the primary mass should be determined by measuring the decay products in addition. The participant-spectator model thus assumes only two-body dissipation and, therefore, provides a convenient test of the Bremsstrahlung method.

## 2 Experimental setup

For the experiment three detector systems where used (figure 1): TAPS for the photon detection, SPEG (the ganil spectrograph) to detect the *PLF's* and the KVI forward wall (FW) to detect the light charged particles (*LCP's*) evaporated by the *PLF*. The forward wall consists of 60 phoswich modules [1] covering angles between 3.7° and 24.5°. Two types of phoswiches were used, small ones ($32.5 \cdot 32.5 \cdot 50$ $mm^3$) around the center and large ones ($65 \cdot 65 \cdot 50$ $mm^3$) on the outside. For the data discussed here the spectrograph was set to a rigidity of 91% of the beam. In this contribution only preliminary results concerning the FW and coincidences with SPEG are discussed.

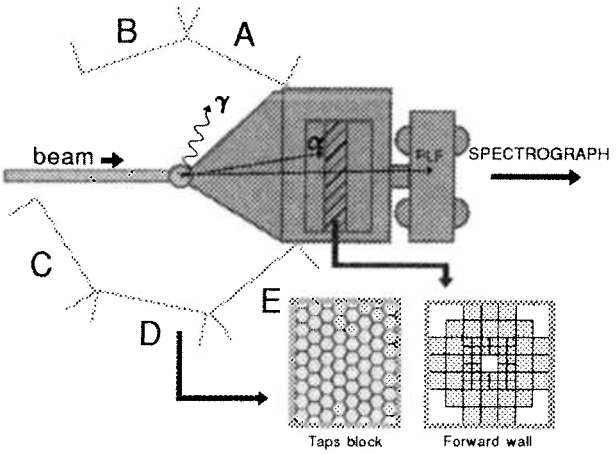


Figure 1: Setup for Ganil experiments

## 3 First results

Assuming for the moment 100% acceptance for particles evaporated by the *PLF's* and complete rejection for particles evaporated by the *TLF's*, a reconstruction of the primary *PLF* can be done. Since the forward wall can not detect neutrons it is assumed (as a first estimate) that for every emitted proton also a neutron is emitted. The primary *PLF* can then be calculated with

$$\begin{aligned} Z_{PLF_{primary}} &= N_p + 2 \cdot N_{He} + 3 \cdot N_{Li} + ..... + Z_{PLF_{detected}}, \\ A_{PLF_{primary}} &= 2 \cdot N_p + 4 \cdot N_{He} + 7 \cdot N_{Li} + ..... + A_{PLF_{detected}}, \end{aligned}$$

where $N_p$, $N_{He}$ and $N_{Li}$ are the number of *LCP's* observed in the forward wall in coincidence with a *PLF* detected in the spectrograph ($PLF_{detected}$). In figure 2 the inclusive yield of the

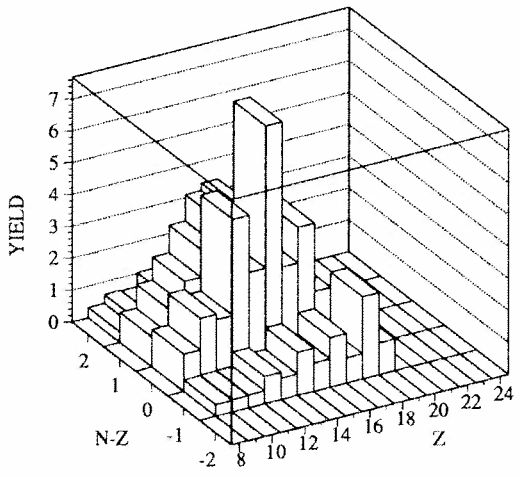


Figure 2: Detected PLF distribution

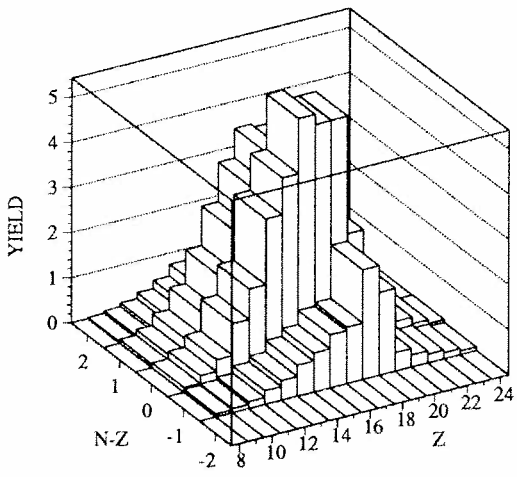


Figure 3: Primary PLF distribution

detected *PLF's* is plotted as a function of $Z$ and $N$-$Z$. This figure shows a clear enhancement of *PLF's* with even $Z$ relative to *PLF's* with odd $Z$. Comparing this to the yield for primary *PLF's* (figure 3), where $Z$ and $N$-$Z$ have been calculated as shown above, this effect has disappeared. Thus the odd-even staggering in figure 2 expresses a nuclear structure effect: the excited *PLF's* tend to decay towards even-$Z$ nuclei. The inclusive *PLF* distribution peaks at $Z$=14 and is spread out widely in $Z$ while the distribution of reconstructed *PLF's* peaks at $Z$=16 and shows

a more steep behaviour. Note that the maximum of the distribution is expected near $Z=18$ for peripheral reactions. Whereas the observed yield for $Z>18$ is absent, it is clearly present in the primary $PLF$ yield although it drops very rapidly. After having determined the primary $PLF$ distribution one can calculate the $\gamma$-multiplicity ($M_\gamma$).

$$M_\gamma \propto \frac{\sum_Z N_\gamma(Z,A)}{\sum_Z N_{singles}(Z,A)}.$$

The results are shown in figure 4 and figure 5 for the detected and primary $PLF$, respectively. From these figures one can see that $M_\gamma$ scales linearly with the mass difference between projectile

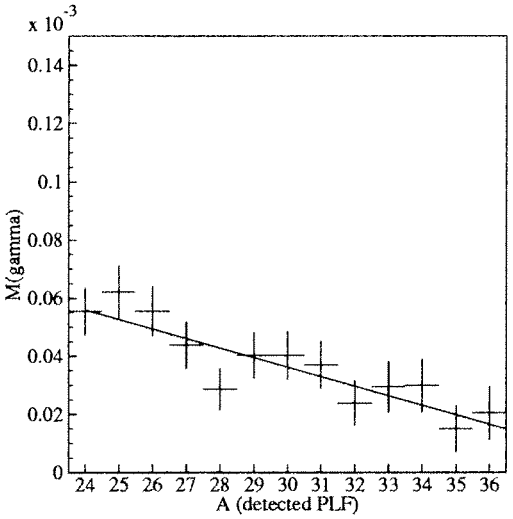


Figure 4:

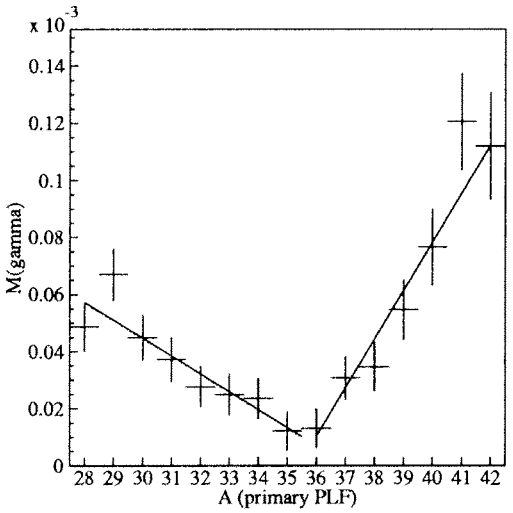


Figure 5:

and $PLF$. The $\gamma$-production probability per removed nucleon is then defined as:

$$P_\gamma = \frac{dM_\gamma}{dA}$$

If we consider only the cases where nucleons have been removed from the projectile one finds for the detected $PLF$'s $P_\gamma^{rem} = (3.3 \pm 0.6) \cdot 10^{-6}$ (figure 4) and for the reconstructed $PLF$'s $P_\gamma^{rem} = (6.1 \pm 1.2) \cdot 10^{-6}$ (figure 5). The fact that different values for $P_\gamma$ are obtained shows the importance of reconstructing the primary $PLF$ and is one of the important improvements with respect to previous work by Rieß et al.[2]. To compare the latter number to the systematics [2,3], obtained from inclusive measurements, it's necessary to determine the probability per pn-collision. Assuming that the number of pp + nn collisions equals the number of pn collisions $P_\gamma^{pn,rem} = 2 \cdot P_\gamma^{rem} = (1.2 \pm 0.24) \cdot 10^{-5}$. This value is smaller than the value given by the systematics ($P_\gamma^{pn,sys} = (2.3 \pm 0.4) \cdot 10^{-5}$), where also the inverse slope parameter ($E_0 = 10 \pm 1 MeV$) is taken into account (cf.[2]). This could indicate that the mass difference is not completely due to nucleon-nucleon collisions. For $PLF$'s heavier than the projectile a higher value for the $\gamma$-production probability is obtained ($P_\gamma^{pn,add} = (3.6 \pm 0.4) \cdot 10^{-5}$). This may suggest that incoherent nucleon-nucleon collisions are relatively more important when mass transfer to the projectile occurs. Further analysis is in progress.


1 H.K.W. Leegte et al., Nucl.Instr.Method **A313**(1992)26

2 S. Rieß et al., Phys.Rev.Lett. **69**(1992)1504

3 see e.g. W. Cassing et al., Phys.Rep.**188**(1990)363

# Hard photon spectrum from the 60 AMeV Kr+Ni reaction[1]

T. Matulewicz[1], M. Marqués[1], R.W. Ostendorf[1], P. Lautridou[1], F. Lefèvre[1], W. Mittig[1], P. Roussel-Chomaz[1], Y. Schutz[1], J. Québert[2], F. Ballester[3], J. Díaz[3], A. Marín[3], G. Martínez[3], R. Holzmann[4], S. Hlávač[4,5], A. Schubert[4], R.S. Simon[4], V. Wagner[4,6], H. Löhner[7], J.H.G. van Pol[7], R.H. Siemssen[7], H.W. Wilschut[7], M. Franke[8], Z. Sujkowski[9]

[1] Grand Accélérateur National d'Ions Lourds, BP 5027, 14021 Caen, France
[2] Centre d'Etudes Nucléaires de Bordeaux-Gradigan, 33175 Gradignan, France
[3] Instituto de Física Corpuscular, 46100 Burjassot, Valencia, Spain
[4] Gesellschaft für Schwerionenforschung, D-6100 Darmstadt, Germany
[5] Slovak Academy of Sciences, Bratislava, Slovakia
[6] Czech Academy of Sciences, Řež u Prahy,Czech Republic
[7] Kernfysisch Versneller Instituut, 747 AA Groningen, The Netherlands
[8] II Physikalisches Institut Universität Gießen, D-6300 Gießen, Germany
[9] Soltan Institute for Nuclear Studies, 05-400 Swierk, Poland

The production of very energetic particles provides a unique tool to study the initial phase of the collision between heavy nuclei well above the Coulomb barrier [1]. In this phase of a collision, where the initial collective motion has not been dissipated, one expects maximum energy density and compression to be reached, allowing one to study the equation of state of nuclear matter. Very energetic photons are the perfect probes of the initial phase as: (i) they leave the production zone virtually unaffected, as they interact only electromagnetically, and (ii) their production is strongly suppressed in the later phase of the reaction. However, in practice, several factors limit their applicability, namely: (i) the low production rate and (ii) the background at higher beam energies coming from the copiously produced neutral pions, which disintegrate predominantly into two photons.

A typical photon spectrum exhibits three basic features. In the low-energy part ($E_\gamma < 15$ MeV), the exponential spectrum originates from photons emitted during the cooling down of the reaction remnants (statistical decay). The accumulation seen around 20 MeV is the signature of the EM deexcitation of Giant Resonances (GR) excited in the reaction fragments. In a commonly used convention, photons above 30 MeV, i.e. above the GR region, are called high-energy photons and are produced predominantly in first chance proton-neutron collisions. The spectrum of high energy photons is also exponential in the photon energy range studied so far. This range is rather limited, as the high energy end of the spectrum reaches up to 2-3 times the beam energy per nucleon.

The knowledge of the high energy end of the photon spectrum is an interesting challenge to the theoretical models. The production of such energetic photons requires either not yet specified collective phenomena or may be the signature of a very long and unexpected tail of the nucleon momentum distribution within the collision zone. It is also of prime importance since it allows to access the region where one expects to observe the EM decay of baryonic resonances. This could thus provide a unique way to study the behaviour of the $\Delta$ resonance within hot and compressed nuclear matter.

[1]Experiment performed with TAPS

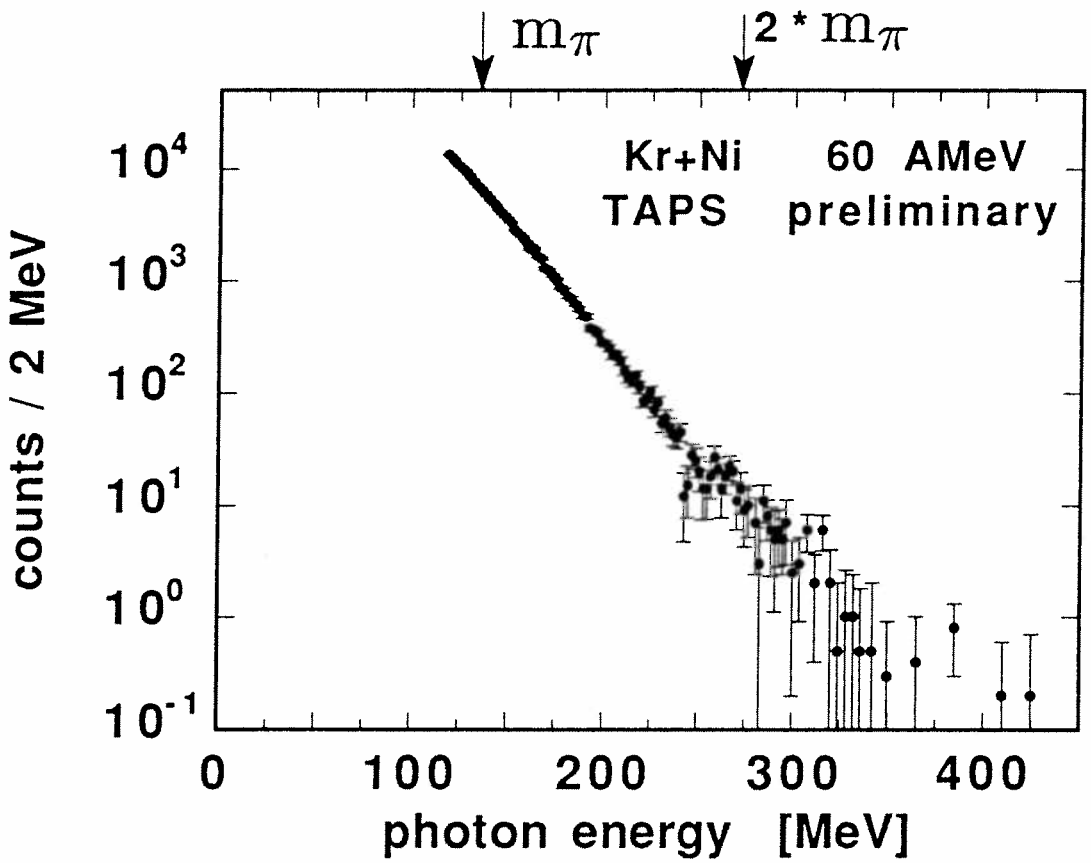


Figure 1: *Integrated energy spectrum of photons in the NN center-of-mass system. The arrows indicate the energy scale in terms of the pion rest mass.*

In an experiment performed by the TAPS collaboration, we have studied the reaction $^{86}$Kr + $^{nat}$Ni at 60 AMeV. While the main goal of this experiment was to measure the correlation between two hard photons [2], it permitted a measurement to be made of the photon spectrum [3] over a much wider energy range than all previous experiments. As may be seen in Fig.1, the integrated photon spectrum extends up to 350 MeV, i.e., almost 6 times the beam energy per nucleon! The shape of this spectrum remains exponential up to energies exceeding twice the pion rest mass. The purely exponential shape and source velocity equal to the half beam velocity indicate that the mechanism for the production of so much energetic photons remains first chance proton-neutron collision. However, the nucleon pairs participating in collisions producing these very energetic photons must have a CM energy much higher than the energy available from the beam related velocity and the standard Fermi motion inside the nucleus at rest ($E_F \sim 40$ MeV). Therefore, the very high energy photons observed for the first time in this experiment suggest that the momentum distribution, as known in the nucleus at rest, may be strongly modified by the dynamics of the collision.

## References

[1] W. Cassing, V. Metag, U. Mosel and K. Niita, Physics Reports 188 (1990) 363

[2] M. Marqués *et al.*, this issue

[3] T. Matulewicz, talk presented at the XXIII Mazurian Summer School on Nuclear Physics, Piaski, Poland, 18-28 August 1993; GANIL P 93-21

# Exclusive Hard Photon Production in the 60 AMeV Kr+Ni reaction[1]

G. Martínez[1], F. Ballester[1], J. Díaz[1], A. Marín[1], M. Marqués[2], R.W. Ostendorf[2], P. Lautridou[2], F. Lefèvre[2], T. Matulewicz[2], W. Mittig[2], P. Roussel-Chomaz[2], Y. Schutz[2], J.-P. Wieleczko[2], J. Québert[3], R. Holzmann[4], S. Hlávač[4,5], A. Schubert[4], R.S. Simon[4], V. Wagner[4,6], H. Löhner[7], J.H.G. van Pol[7], R.H. Siemssen[7], H.W. Wilschut[7], M. Franke[8], Z. Sujkowski[9] [1] Instituto de Física Corpuscular, 46100 Burjassot, Valencia, Spain

[2] Grand Accélérateur National d'Ions Lourds, BP 5027, 14021 Caen, France
[3] Centre d'Etudes Nucléaires de Bordeaux-Gradigan, 33175 Gradignan, France
[4] Gesellschaft für Schwerionenforschung, D-6100 Darmstadt, Germany
[5] Slovak Academy of Sciences, Bratislava, Slovakia
[6] Czech Academy of Sciences, Řež u Prahy,Czech Republic
[7] Kernfysisch Versneller Instituut, 747 AA Groningen, The Netherlands
[8] II Physikalisches Institut Universität Gießen, D-6300 Gießen, Germany
[9] Soltan Institute for Nuclear Studies, 05-400 Swierk, Poland

Hard photon production has been studied as a function of impact parameter for the system $^{86}Kr+^{nat}Ni$ at 60 AMeV. From the established systematics [1], it has been established that the total flux of hard photons originates mainly from the incoherent superposition of bremsstrahlung radiation emitted during individual neutron-proton collisions within the participant zone. A few experiments have investigated the dependence of the hard photon production mechanism with impact parameter selected, with the latter selected by making use of either the charged particle multiplicity or the mass of the projectile like fragments (PLF). A strong variation of the photon multiplicity was observed such that the multiplicity is largest for the most central collisions thus strengthening the case for the n-p bremsstrahlung model. The exclusive measurements also yielded the observation that the photon energy spectrum depends on the impact parameter, with softer spectra being measured for the more peripheral collisions. It was suggested that the dependence of the energy spectrum could reflect the momentum distribution of the nucleons within the collision zone.

In the present wpork, we have studied the properties of hard photon production as a function of impact parameter, covering a broad range of reactions from peripheral to central. The hard photons were detected using the TAPS photon spectrometer [3], which consisted of 320 hexagonal $BaF_2$ scintillation detectors each associated with a plastic detector (CPV) "tagging" charged particles. Peripheral and mid-central reactions were selected using the mass of the PLF (identified using the SPEG spectrometer[5]). More central reactions were selected by using the multiplicity of the charged particles detected using the KVI Hodoscope [4].

The inclusive photon production was analyzed assuming an exponential energy spectrum characterized by the inverse slope parameter, $E_0$, and the angular distribution to be isotropic with a dipolar contribution characterized by the parameter $\alpha$. The measured photon source velocity, $\beta_S = 0.172 \pm 0.007$ is compatible with the velocity of the N-N center-of-mass, $\beta_{NN} =$

[1]Experiment performed with TAPS

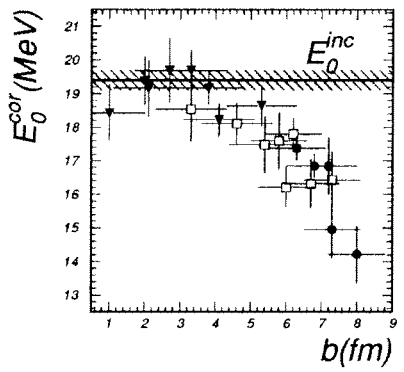


Figure 1: Variation of the slope parameter of the hard photon spectra with the impact parameter measured in the reaction $^{86}$Kr+$^{nat}$Ni at 60 MeV/u. The triangles indicate data selected with the charged particle multiplicity, the circles (SPEG at 85% $B\rho$) and squares (SPEG at 90% $B\rho$) indicate data selected with the mass of the PLF.

0.177 in addition, the measured cross section, $\sigma_\gamma = 3.6 \pm 0.2$ mb, is in fair agreement with the existing systematics [1].

Assuming that the probability to produce a photon per NN collision, $P_\gamma$, depends only on the bombarding energy one can calculate the number of participants and deduce, as suggested in reference [2], the corresponding impact parameter. We have made use of this observation to select a given impact parameter using the charged particle multiplicity, or the projectile like fragment mass or even a combination of both and for each selection to deduce the impact parameter from the associated photon multiplicity.

To study the evolution of the hard photon production we have constructed for each impact parameter the angular distribution and the energy spectrum. We have assumed that the gross properties of the photon production remain over all impact parameters the same. We have found that the source velocity and the anisotropy of the angular distribution do not change with the impact parameter and remain equal to the values obtained in the inclusive measurement. This result suggests that the mechanism which produces hard photons does not change with the centrality of the collision, over the whole range of impact parameters which have been probed (bremsstrahlung radiation emitted in individual first chance neutron-proton collision).

The slope parameter, $E_0$, corrected for the detector response is plotted versus the impact parameter in figure 1. One observes a strong decrease (25%) as one goes from central to peripheral collisions. In our data we observe that the hardness of the photon spectrum remains constant from the most central collisions to 4-5 fm, that is as long as projectile and target fully overlap. The energy spectrum becomes softer as one selects toward more peripheral collisions. In the neutron-proton bremsstrahlung model the energy of the photon depends only on the energy available in the NN center of mass, that is the combination of the beam momentum and the momentum of both nucleons. Therefore the photon energy spectrum reflects the momentum distribution of the nucleons within the participant zone. We can then interpret the observed changes in the shape of the energy spectrum in two ways. The first interpretation assumes that the momentum distribution in the collision zone is the same as in the nucleus at rest and, therefore, the changes in $E_0$ indicate a change of the momentum distribution inside the nucleus. The second interpretation takes into account the fact that the dynamics associated with the collision may perturb the momentum distribution within the projectile-target overlap zone. One therefore measures a dynamical momentum distribution which could be related to the compression reached at the very beginning of the collision, during the photon emission.

## References


[1] W. Cassing *et al.*, Phys. Rep. **188**, 365 (1990);
H. Nifenecker and J.A. Pinston, Prog. Part. Nucl. Phys. **23**, 271 (1989).

[2] S.Riess *et al.*, Phys. Rev. Lett. **69**, 1504 (1992).

[3] R. Novotny, IEEE Trans. Nucl. Sc. **38-2**, 379 (1991).

[4] H.K.W. Leegte *et al.*, Nucl. Instr. Meth. Phys. Res. Sect. A **313**, 26 (1992).

[5] L. Bianchi *et al.*, Nucl. Instr. and Meth. **A276**, 509 (1989).

# Hard photon interferometry in the reaction Xe + Au at 44 $A$·MeV[1]

R. W. Ostendorf[1], Y. Schutz[1], F. Lefèvre[1], H. Delagrange[1], T. Matulewicz[1], R. Merrouch[1], W. Mittig[1], P. Lautridou[2], J. Québert[2], F. D. Berg[3], W. Kühn[3], V. Metag[3], R. Novotny[3], M. Pfeiffer[3], A. L. Boonstra[4], H. Löhner[4], L. B. Venema[4], H. W. Wilschut[4], W. Henning[5], R. Holzmann[5], R. S. Mayer[5], R. S. Simon[5], F. Ballester[6], E. Casal[6], J. Díaz[6], J. L. Ferrero[6], M. Marqués[6], G. Martínez[6], D. Ardouin[7], H. Dabrowski[7], B. Erazmus[7], C. Lebrun[7], L. Sézac[7], H. Nifenecker[8], Z. Sujkowski[9], B. Fornal[10], L. Freindl[10]

[1] Grand Accélérateur National d'Ions Lourds, BP 5027, 14021 Caen, France
[2] Centre d'Etudes Nucléaires de Bordeaux-Gradigan, 33175 Gradignan, France
[3] II Physikalisches Institut Universität Gießen, D-6300 Gießen, Germany
[4] Kernfysisch Versneller Instituut, 747 AA Groningen, The Netherlands
[5] Gesellschaft für Schwerionenforschung, D-6100 Darmstadt, Germany
[6] Instituto de Física Corpuscular, 46100 Burjassot, Valencia, Spain
[7] Laboratoire de Physique Nucléaire, 44072 Nantes, France
[8] Institut des Sciences Nucléaires, 38026 Grenoble, France
[9] Soltan Institute for Nuclear Studies, 05-400 Swierk, Poland
[10] Institute of Nuclear Physics, 31-342 Krakow, Poland

It is rather well established that hard photon emission in heavy-ion reactions at intermediate energies originates mainly from the incoherent superposition of bremsstrahlung radiation emitted in individual first chance proton-neutron collisions [1]. Since photons only interact weakly with the surrounding nuclear matter, they provide an undistorted probe of the early stage of the nuclear reaction, where one expects to reach a maximum temperature and density.

To measure the space-time extent of the photon source we have employed the method of intensity interferometry, developed in astronomy to measure the diameter of stars and commonly used in nuclear physics to extract the space-time extent of an emitting source. The correlation signal arises from the quantum statistical nature of the particles involved, i.e., symmetrization (for bosons) or antisymmetrization (for fermions) of the two-particle wave function.

The main difficulty in measuring correlations between hard photons is the low production cross section of hard photon pairs ($\sim 1\mu$b), thus implying the need for a high efficiency setup with good energy and angular resolutions. The availability of the photon detector TAPS, a modular array of $BaF_2$ crystals, made, for the first time, a measurement of the correlation between hard photons feasable (247 modules were assembled in 13 blocks of 19 detectors [2, 3]).

To optimize the photon production, which scales with the number of participants, the system $^{129}$Xe + $^{197}$Au at 44 MeV/u was selected. These data were also used in an independent analysis studying reabsorption effects of neutral pions [4].

Photons were identified using pulse-shape and time-of-flight information [2, 3]. Due to a contamination of the data by cosmic-ray events with a yieid about 10 times superior to the production of hard photon pairs, it was necessary to introduce 3 extra conditions: (1) the two

[1] Experiment performed with TAPS

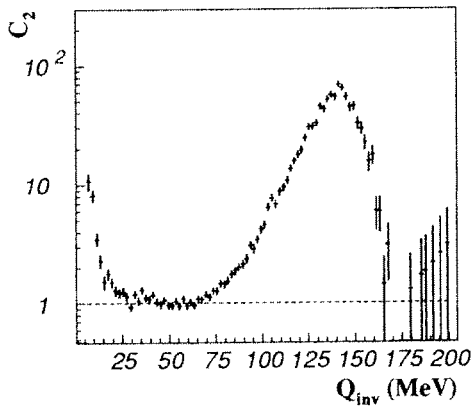


Figure 1: Hard photon correlation function.

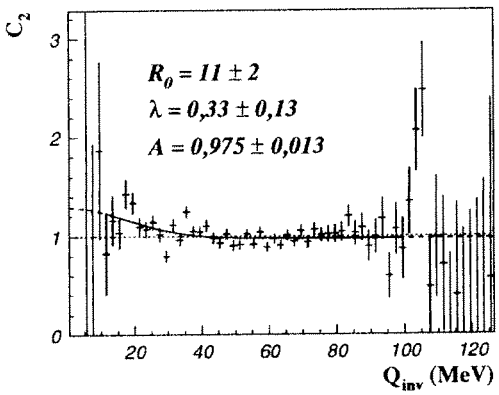


Figure 2: Corrected correlation function (see text).

photons must have been detected by two different blocks; (2) to tag a nuclear reaction, at least two particles (neutrons, protons) must have been detected in coincidence; and (3) events in which more than 3 detectors had recorded an energy larger than 25 MeV were eliminated. There were 14,046 events with a pair of hard photons ($E_\gamma > 25$ MeV in the nucleon-nucleon center-of-mass frame) satisfying these conditions.

The correlation function was constructed as the ratio of the coincident yield, $Y_2$, over an uncorrelated background generated by folding the the single photon yields, $Y_1 \otimes Y_1$. The correlation function is represented as a function of the invariant transfered momentum, $Q_{\rm inv} = (-(p_1 - p_2)^2)^{1/2}$, that for photons is equivalent to the invariant mass and therefore very suitable for the recognition of the contribution of decaying neutral pions.

This correlation function is shown in figure 1. Three components can be distinguished: (1) a sharp rise at $Q_{\rm inv} < 20$ MeV due to events where the electromagnetic shower of a single photon is registered in two different blocks; (2) a large peak centered around 135 MeV due to $\pi^0 \rightarrow \gamma\gamma$-events; and (3) a slow rise of the correlation function from 60 MeV to 20 MeV, the region in which one would expect to observe the intensity interference.

In order to investigate whether this latter structure can be attributed to an interference effect, it is necessary to correct the correlation function for all contaminants. This is shown in figure 2 where the contributions of left over cosmic-ray events (350 events), events in which a single photon is detected as a pair (210 events), and (3) decaying neutral pions (6,700 events), are subtracted. The data were fitted to the function, $A(1 + \lambda \exp(-Q_{\rm inv}^2 R_0^2/2\hbar^2c^2))$, and the resulting parameters are reported in the figure. Though the result of the fit gives us a hint about the observation of the interference effect searched for, the dispersion of the data points and their large statistical errors prohibit any strong conclusion.

From this experiment we can therefore conclude that it is of prime importance to understand, recognize and eliminate all possible contaminants with high efficiency. This experience was used in the follow-up experiment Kr + Ni at 60 $A$·MeV also reported here.

## References

[1] W. Cassing, V. Metag, U. Mosel and K. Niita, Phys. Rep. **188** (1990) 363.

[2] R. Merrouch, Thesis University of Caen, GANIL Report T-90-01, (1993).

[3] R. W. Ostendorf, Thesis University of Caen, GANIL Report T-93-05, (1993).

[4] R. S. Mayer et al., Phys. Rev. Lett. **70** (1993) 904.

[5] R. Ostendorf et al., Contribution to XV Nuclear Physics Symposium, Oaxtepec, Mexico, Revista Mexicana de Física **38** (1992) 184.

# The HBT effect for hard photons in the reaction Kr + Ni at 60 $A$·MeV[1]

M. Marqués[1], R.W. Ostendorf[1], P. Lautridou[1], F. Lefèvre[1], T. Matulewicz[1], W. Mittig[1], P. Roussel-Chomaz[1], Y. Schutz[1], J. Québert[2], F. Ballester[3], J. Díaz[3], A. Marín[3], G. Martínez[3], R. Holzmann[4], S. Hlávač[4,5], A. Schubert[4], R.S. Simon[4], V. Wagner[4,6], H. Löhner[7], J.H.G. van Pol[7], R.H. Siemssen[7], H.W. Wilschut[7], M. Franke[8], Z. Sujkowski[9]

[1] Grand Accélérateur National d'Ions Lourds, BP 5027, 14021 Caen, France
[2] Centre d'Etudes Nucléaires de Bordeaux-Gradigan, 33175 Gradignan, France
[3] Instituto de Física Corpuscular, 46100 Burjassot, Valencia, Spain
[4] Gesellschaft für Schwerionenforschung, D-6100 Darmstadt, Germany
[5] Slovak Academy of Sciences, Bratislava, Slovakia
[6] Czech Academy of Sciences, Řež u Prahy,Czech Republic
[7] Kernfysisch Versneller Instituut, 747 AA Groningen, The Netherlands
[8] II Physikalisches Institut Universität Gießen, D-6300 Gießen, Germany
[9] Soltan Institute for Nuclear Studies, 05-400 Swierk, Poland

In reference [1], the motivation to measure the interference between hard photons (known in Astronomy as the HBT effect) produced in heavy ion collisions has been developed. To overcome the difficulties previously encountered to identify the photon interference effect among other sources (mainly dileptons, comic-rays and neutral pions), two new experiments were performed with TAPS at GANIL [2]. We have studied two systems with different sizes in an attempt to observe not only the HBT effect, but also to verify the dependence on the source size. The systems were $^{86}$Kr + $^{nat}$Ni at 60 $A$·MeV and $^{181}$Ta + $^{197}$Au at 39.5 $A$·MeV, but beam time constraints forced us to concentrate on the first one.

The data were analysed as described in reference [3] and we have identified 20,649 two-hard-photon events. The contamination from cosmic-rays has been reduced to 4 events using a shower shape filter [4]. The $e^+e^-$ conversion pairs were identified using the information of the charged particle veto detector and by demanding a separation of $\Delta\theta \approx 18°$ between coincident showers. The remaining contribution from conversion pairs amounts to 6 events in the invariant mass region between 20 and 80 MeV.

The correlation function was constructed as the ratio of the two photon coincidence yield, $Y_2(p_1, p_2)$, over an uncorrelated background generated by folding the single photon yields, $Y_1(p_1)$ and $Y_1(p_2)$, where the $p_i$ are the four-momenta of the photons. At $Q_{\rm inv} = 135$ MeV the spectrum of the coincidence photons, $Y_2$, exhibits a peak due to photons stemming from $\pi^0$ decay. By requiring that at least 20% of the shower energy was deposited in the fiducial volume of a TAPS block, the invariant mass resolution of the $\pi^0$ peak was reduced to 10% FWHM, thus limiting the contribution of $\pi^0$ decay to the low invariant mass region. The uncorrelated yield, $Y_1 \otimes Y_1$, is normalized to the coincidence yield, $Y_2$, by fitting the experimental correlation spectrum to a distribution of the form,

$$f(Q_{\rm inv}) = K_0 + K_1 \cdot g_{\gamma\gamma}(Q_{\rm inv}) + K_2 \cdot g^{\rm A}_{\pi^0}(Q_{\rm inv} - m_{\pi^0})$$

[1]Experiment performed with TAPS

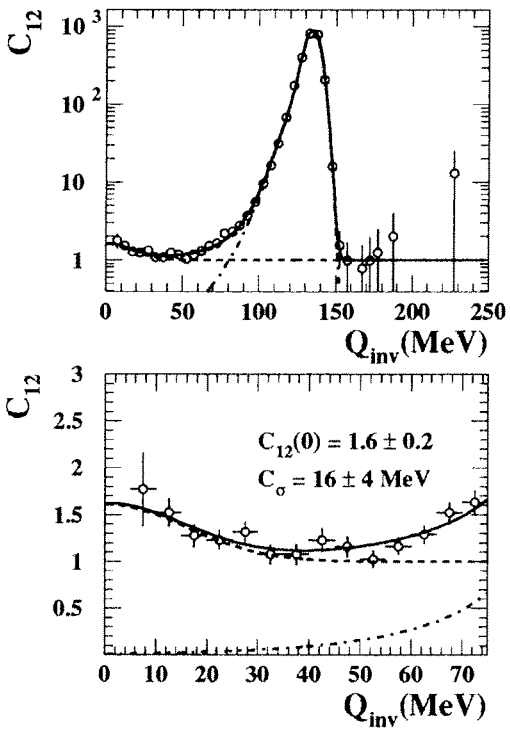


Figure 1: Hard photon correlation function for the Kr+Ni system

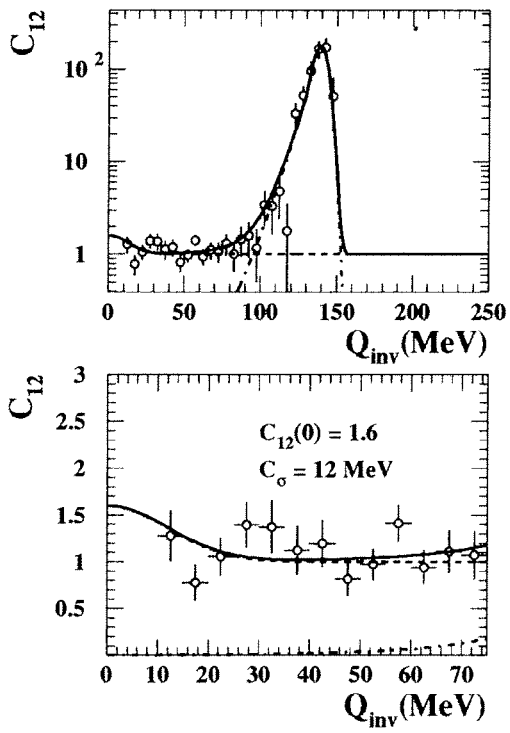


Figure 2: Hard photon correlation function for the Ta+Au system

where $K_0$ was chosen so that the correlation function is equal to 1 for non-interfering photons and $g_{\gamma\gamma}$ is a Gaussian function describing the interference effect at low $Q_{\rm inv}$. A Gaussian density distribution for the source was assumed. The $\pi^0 \rightarrow 2\gamma$ contribution is described by an asymmetric gaussian function, $g^{\rm A}_{\pi^0}$, for which the parameters were deduced from the corresponding simulated distribution. After the fit the correlation function can be written as,

$$C_{12}(Q_{\rm inv}) = 1 + \lambda_{\rm inv} \cdot \exp\left(-\frac{Q^2_{\rm inv}}{2C^2_\sigma}\right) + \alpha \cdot g^{\rm A}_{\pi^0}(Q_{\rm inv} - m_{\pi^0}) \qquad (1)$$

where the parameter $\lambda_{\rm inv}$ $(K_1/K_0)$ includes the effects that reduce the interference, such as partial coherence of the source and random coincidences. The result of the fit to the whole spectrum is shown in Fig.1 as the solid line. The first two terms of Eq. 1 (the HBT effect) are shown as the dashed line and the third one (the neutral pion contribution) as the dot-dashed line. The intercept is found to be $C_{12}(0) = 1.6 \pm 0.2$, consistent with the values predicted in references [5, 6]. The width of the correlation function (correlation length) is found to be $C_\sigma = (16 \pm 4)$ MeV, which corresponds to an invariant radius of the source $R_{\rm inv} \equiv \hbar c/C_\sigma = (12 \pm 3)$ fm. A geometrical estimate [7] of the average number of participant nucleons producing two-hard-photons gives $\langle N_{\rm part}\rangle_{\gamma\gamma} = 76.6$, which leads to an average impact parameter of $\langle b\rangle = 3.1$ fm and a Gaussian radius [8] of the overlap zone of two nuclei of $R_{\rm ov} = \sqrt{2/5}\left(1.2\langle N_{\rm part}\rangle^{1/3}_{\gamma\gamma}\right) = 3.2$ fm. This value is smaller than $R_{\rm inv}$, although it should be noted that $R_{\rm inv}$ includes both the space and time dimensions.

For the heavier system, the poor statistics and the relatively large error do not allow a fit to be made over the whole spectrum and thus to obtain a normalization. However, we can assume that the correlation function has the shape described by equation 1 and compare it to the data. The geometrical considerations lead for Ta+Au to $\langle N_{\rm part}\rangle_{\gamma\gamma} = 213.4$, $\langle b\rangle = 4.1$ fm

and $R_{ov} = 4.5$ fm. Assuming that $R_{inv}$ scales as in the Kr+Ni system, we should have $R_{inv} = 17$ and $C_\sigma = 12$ MeV. In Fig. 2 the data are compared to equation 1 assuming also an intercept $C_{12}(0) = 1.6$ and that the shape of the $\pi^0$ contribution does not change. The poor statistics and the absence of data points below $Q_{inv} = 10$ MeV does not allow a firm conclusion on the presence or not of the interference effect to be made, although the data do not exclude it.

## References


[1] R.W. Ostendorf *et al.*, this issue.

[2] P. Lautridou *et al.*, Nouvelles du GANIL **44** (1993) 29.

[3] M. Marqués *et al.*, Nouvelles du GANIL **45** (1993) 45.

[4] T. Matulewicz *et al.*, Nouvelles du GANIL **45** (1993) 33.

[5] D. Neuhauser, Phys. Lett. **B182** (1986) 289.

[6] L.V. Razumov and R.M. Weiner, in Proceedings of the II TAPS Workshop, Guardamar, Spain (1993), edited by J. Díaz and Y. Schutz, World Scientific, to be published.

[7] H. Nifenecker and J.P. Bondorf, Nucl. Phys. **A442** (1985) 478.

[8] W.A. Zajc *et al.*, Phys. Rev. **C29** (1984) 2173.

# SUBTHRESHOLD PIONS AND HARD PHOTONS AS COMPLEMENTARY PROBES OF REACTION DYNAMICS

R. Holzmann[1], A. Schubert[1], S. Hlaváč[1,8], R. Kulessa[1,7], W. Niebur[1], R.S. Simon[1], V. Wagner[1,9], P. Lautridou[2], F. Lefèvre[2], M. Marqués [2,4], T. Matulewicz[1], W. Mittig[2], R.W. Ostendorf[2], P. Roussel-Chomaz[2], Y. Schutz[2], H. Löhner[3], J.H.G. van Pol[3], R.H. Siemssen[2,3], H.W. Wilschut[3], F. Ballester[4], J. Díaz[4], A. Marín[4], G. Martínez[4], W. Kühn[5], V. Metag[5], R. Novotny[5], J. Québert[6]

[1] *Gesellschaft für Schwerionenforschung, D-64220 Darmstadt, Germany*
[2] *Grand Accélérateur National d'Ions Lourds, F-14021 Caen, France*
[3] *Kernfysisch Versneller Instituut, NL-9747 AA Groningen, The Netherlands*
[4] *Instituto de Física Corpuscular, SP-46100 Burjassot Valencia, Spain*
[5] *II. Physikalisches Institut, Universität Gießen, D-35392 Gießen, Germany*
[6] *Centre d'Etudes Nucléaires de Bordeaux-Gradignan, F-33175 Gradignan, France*
[7] *Jagellonian University, Cracow, Poland*
[8] *Slovak Academy of Sciences, Bratislava, Slovak Republic*
[9] *Nuclear Physics Institute, Řež u Prahy, Czech Republic*

## 1 Introduction

Besides the study of nucleon and fragment collective observables, the measurement of particle production offers an alternative sensitive approach to the investigation of nuclear collision dynamics. At intermediate bombarding energies, hard photons and pions are the main probes at hand, and while it is generally assumed that at these energies both are mostly produced in incoherent first-chance nucleon-nucleon collisions, it is not clear to what extent this simple scenario really holds. Indeed, whereas transport calculations support the picture of particle production primarily in the early stage of the nuclear collision, they also lead to expect some sensitivity to the later, dissipative phase. While the spacial and temporal properties of the particle source can in principle be studied with correlation techniques, we expect to obtain relevant information already from a careful investigation of more easily accessible global observables, like the source velocities and angular distributions. Furthermore, as photons leave the reaction system virtually unperturbed, while pions interact strongly with the surrounding nuclear medium, both constitute a pair of truly complementary probes. We have measured with the photon spectrometer TAPS at GANIL inclusive and exclusive hard-photon and $\pi^0$ production in the reactions $^{36}$Ar + $^{12}$C and $^{36}$Ar + $^{197}$Au at 95 MeV/u.

## 2 Experiment and Data Reduction

In our measurement, gold targets of 20 mg/cm$^2$ and carbon targets of 15 mg/cm$^2$ were irradiated with a 95 MeV/u $^{36}$Ar beam of typically 0.5 pnA. Photons were registered in 320 $BaF_2$ detectors from the two-arm photon spectrometer TAPS, arranged in 5 blocks of 64 scintillators each. The blocks were placed in the horizontal plane at a distance of 62 cm from the target, with their centers at angles of 65°, 109°, 212°, 258°, and 309° with respect to the beam axis. Furthermore, all $BaF_2$ crystals were equipped with individual plastic charged-particle veto (CPV) detectors. This setup yielded a detection efficiency of 12.3% for photons (with $E_\gamma \geq 30$ MeV) and of 1.6% for neutral pions (detected via their 2-photon decay). Light charged particles (LCP) were detected and identified in the KVI forward wall (FW) made of 60 plastic-scintillator phoswich detectors[1], covering an angular range of $\theta$ = 3.5°-23°, with charge separation up to Z=5. Finally, projectile-like

fragments (PLF) were registered in the GANIL magnetic spectrograph SPEG positioned at 0°, giving an angular acceptance of ±2.0°, both horizontally and vertically. With a magnetic field setting at 93.5 % of the beam rigidity, we obtained PLF charge and mass resolutions of respectively 0.6 and 0.2 units FWHM.

In the data analysis, a very clean separation of $\gamma$ rays from charged particles and neutrons was achieved by requiring : (i) the absence of a signal in the CPV modules in front of the hit $BaF_2$ modules, (ii) the proper time of flight and, (iii) the correct pulse shape of the $BaF_2$ signals. High-energy background produced by cosmic muons traversing a $BaF_2$ block were eliminated by a cut on the lateral extension of the hit pattern in the block.

## 3 Photon Source Velocities

The photon spectra contain, besides bremsstrahlung events, also a sizable contamination from $\pi^0$ decay photons. To subtract this component, a Monte-Carlo simulation has been performed with a $\pi^0$ event generator, carefully adapted to the simultaneously measured pion energy and angular distributions. The resulting clean bremsstrahlung spectrum displays an exponential shape up to the highest measured energies, i.e. 300 MeV, with an inverse slope parameter of $E_0^{NN} = 29.4 \pm 1.4$ MeV in the $N-N$ cm frame for both systems studied here.

In Ar+Au we have investigated the behavior of the photon source velocity with increasing photon energy. The mean velocity $\beta_S$ of the $\gamma$ source has been extracted using a moving-source fit with the expression proposed in Ref. 2. Figure 1(a) shows the angle-differential cross sections for different cuts on $E_\gamma$, together with the corresponding moving-source fits. It appears that $\beta_S$ has a nearly constant value of 0.15 up to $E_{cut} \simeq 120$ MeV, but then increases, to reach 0.19 for $E_\gamma \geq 165$ MeV. Evidently, very high-energy photons are emitted from a source with a velocity much closer to $\beta_{NN} = 0.22$. The angular distributions measured for Ar+C display however no significant variation with $E_{cut}$ and yield $\beta_S = 0.21$.

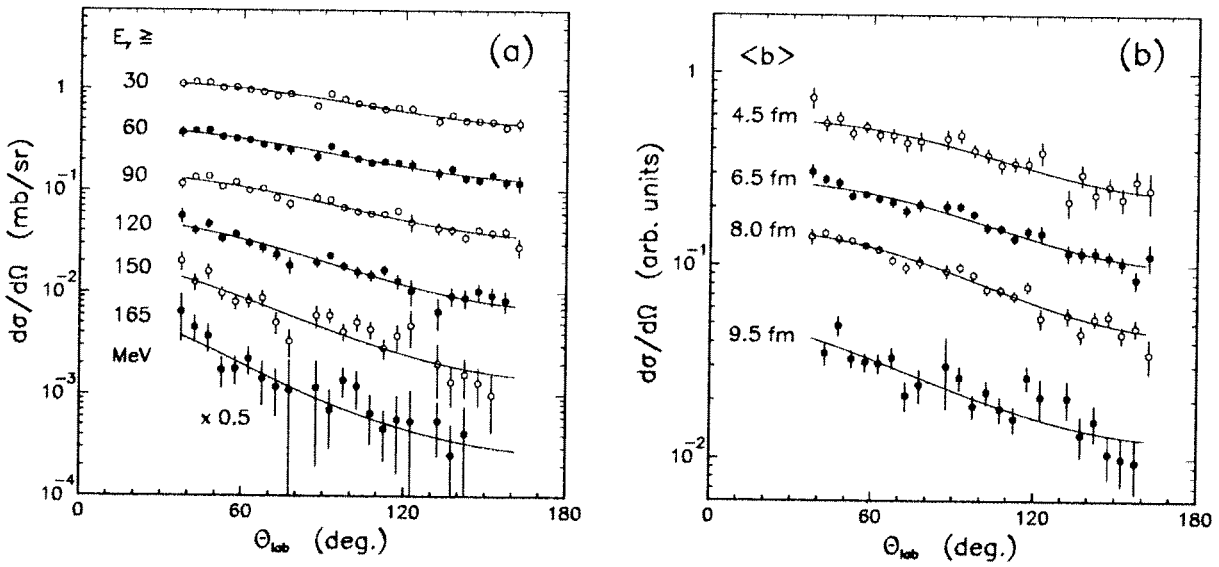


Fig. 1. (a) Bremsstrahlung laboratory angle-differential cross sections measured for $^{36}Ar+^{197}Au$ at 95 MeV/u, with different cuts on the photon energy. (b) Bremsstrahlung ($E_\gamma^{lab} \geq 30$ MeV) laboratory angular distributions measured for different mean impact parameters. The four distributions are arbitrarily normalized to each other.

We have furthermore studied the photon source velocities as a function of impact parameter $b$, by requiring photons with $E_\gamma \geq 30$ MeV in coincidence with light charged particles in the FW, selecting thus central to mid-peripheral collisions ($b = 3 - 9$ fm), or in coincidence with a projectile-like fragment in the magnetic spectrometer, covering mostly peripheral collisions ($b = 8 - 11$ fm). The FW multiplicity has been related to $b$ through a statistical fragmentation calculation done with the code FREESCO, and the correspondence between the PLF charge and $b$ has been obtained from an abrasion-ablation model. Figure 1(b) shows a representative sample of bremsstrahlung angular distributions measured in Ar+Au for different $b$. From the moving-source fits it appears that, as one goes from central ($b < 5$ fm) to the most peripheral collisions ($b > 9$ fm), $\beta_S$ increases from 0.14 to 0.21, i.e. approaches $\beta_{NN}$. Again, in the Ar+C system, no changes of the photon spectra with $b$ are observed. This is in line with the results of BUU[3] and TDHF[4] calculations which indeed predict for $\simeq$100 MeV/u heavy ions a large degree of stopping only in central collisions of reaction systems with $A_P + A_T > 200$.

## 4 Pion Polar and Azimuthal Distributions

With our experimental set-up it was possible to measure $\pi^0$ angular distributions over the (nearly) full angular range. Figure 2(a) shows response-corrected inclusive polar distributions of neutral pions produced in $^{36}$Ar+$^{12}$C and $^{36}$Ar+$^{197}$Au collisions, respectively, transformed into the $N-N$ cm frame (with $v/c = 0.22$); a pronounced forward-backward asymmetry is apparent in both cases. In the laboratory frame the pion polar distribution is determined by three effects : (i) the intrinsic angular distribution from the elementary production process; superimposed on this (ii) the source-frame motion and finally (iii) a distortion from pion absorption and scattering. The pion final-state interactions prohibit a straightforward moving-source analysis, as it can be done for photons, and make it impossible to extract a source velocity directly. This problem can however be circumvented by selecting very peripheral events, where the particular geometry of the collision (the two nuclei are side by side) lifts the forward-backward asymmetry due to shadowing and restores a symmetric polar distribution in the source frame. Selecting thus projectile-like

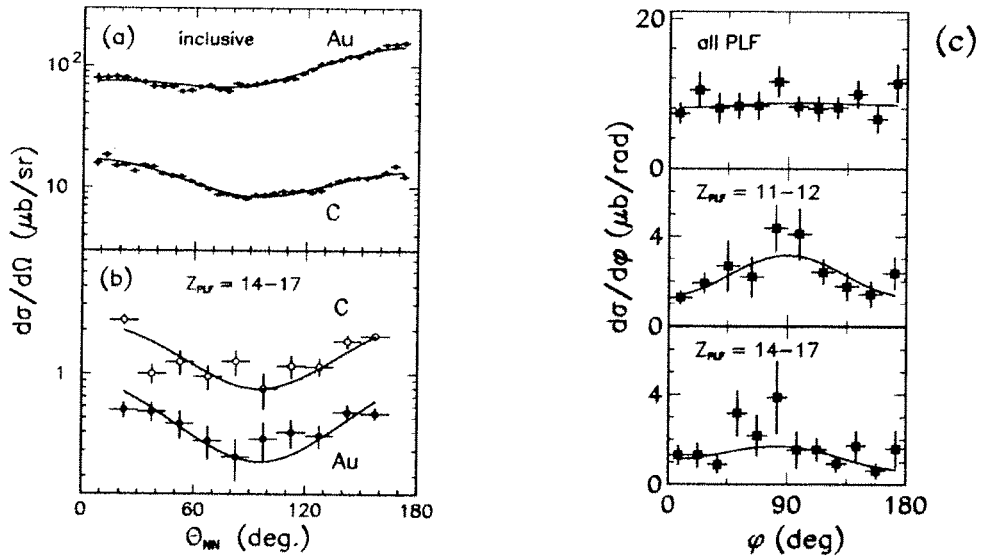


Fig. 2. (a) Inclusive $\pi^0$ polar distribution measured for $^{36}$Ar+$^{197}$Au and $^{36}$Ar+$^{12}$C, transformed into the $N-N$ cm frame. (b) same as (a), but for very peripheral collisions, selected by requiring $Z_{PLF}$ in the range 14–17. The solid curves are shadowing calculations normalized to the integral of the data (see Ref. 5 for details). (c) $\pi^0$ azimuthal distributions in $^{36}$Ar+$^{197}$Au (with $36^o < \theta_{CM} < 162^o$) for different cuts on $Z_{PLF}$. The solid lines represent a cosine expansion fitted to the data.

fragments with charge $Z$=14–17, impact parameters larger than 9 fm (4 fm) are sampled in Ar+Au (Ar+C) collisions. The polar distributions of pions coincident with these PLF's are shown for the two targets in Fig. 2(b): they are indeed symmetric in the $N-N$ cm frame, confirming a source velocity of $v/c = 0.22$ (in contrast to 0.07 for the Ar+Au cm frame, and 0.32 for the Ar+C frame). This result supports again the picture of pion generation in first-chance $N-N$ collisions.

For peripheral collisions, leading to finite scattering angles, an event plane $\varphi_o$ can be defined using the beam direction and the PLF momentum vector measured in SPEG. With respect to the event plane, the azimuthal distribution $d\sigma/d\varphi$ of neutral pions is almost flat, if all PLF's are allowed, but if PLF charges in the range 14–17 (11–12) are selected, corresponding to peripheral (semi-peripheral) collisions, a strong azimuthal anisotropy develops (Fig. 2). A cosine expansion $d\sigma/d\varphi = N(1 + S_1 \cos\varphi + S_2 \cos 2\varphi)$ fitted to the data shows that pion emission is enhanced by a factor $\simeq 2$ around $\varphi_\pi = 90^o$, that is perpendicular with respect to the reaction plane; in-plane the projectile and target spectator matter introduce shadowing due to strong pion reabsorption.

Within the shadowing picture one expects for an asymmetric collision system, besides the out-of-plane enhancement, a 0°/180° asymmetry in the pion azimuthal distributions; here $\varphi = 0^0$ is defined as the projectile side and $\varphi = 180^0$ as the target side. Sensitivity to such an asymmetry is demonstrated by the parameter $S_1$ of the cosine fits to the $\pi^0$ azimuthal distributions of Fig. 2(c). For the most peripheral event selection ($Z_{PLF} = 14-17$), $S_1$ is 0.17, corresponding to a larger yield at $\varphi = 0°$. For semi-peripheral events ($Z_{PLF} = 11-12$) however we find $S_1 \simeq 0$, i.e. consistent with symmetric yields. In the case of e.g. Ar+Au, the pion yield should indeed be larger on the projectile side (the smaller of the two nuclei), if there is positive, i.e. repulsive deflection (near-side collision), and smaller, if the deflection is to negative angles, i.e. if it is attractive (far-side collision). Our results point in fact at a change of the force balance with $b$: whereas repulsive Coulomb forces dominate at very large impact parameters ($S_1 > 0$), the less peripheral collisions already seem to be largely influenced by the attractive mean field ($S_1 \simeq 0$). Evidently compression is not yet strong enough to ensure repulsion also at smaller impact parameters.

## 5 Conclusions

In summary we have measured inclusive and exclusive hard-photon and $\pi^0$ emission in the reactions $^{36}$Ar+$^{197}$Au and $^{36}$Ar+$^{12}$C at 95 MeV/u. Whereas the observed characteristics of the photon source are fully consistent with the picture of production in leading $p-n$ collisions in the Ar+C system, a strong deviation of the source velocity from $\beta_{NN}$ has been observed in the heavier Ar+Au system. There $\beta_S$ is approaching $\beta_{NN}$ only for very peripheral collisions or for photon energies in excess of 150 MeV. We conclude therefore that, while very high-energy photons do indeed probe the very first phase of heavy-ion reactions, medium-energy photons also carry information on the later, stopping stage of the collision. The measured $\pi^0$ polar distributions can be described for both reaction systems in terms of a mid-rapidity pion source, in combination with strong final-state effects. Taking advantage of the strong pion reabsorption, we demonstrate a novel way to investigate the balance between attractive and repulsive deflection in intermediate-energy nucleus-nucleus collisions.

(1) H.K.W. Leegte et al., Nucl. Instr. Meth. **A313** (1992) 26.
(2) H. Nifenecker and J.A. Pinston, Prog. Part. Nucl. Phys. **23** (1989) 271.
(3) W. Bauer, Phys. Rev. Lett. **61**, 2534 (1988).
(4) J. Aichelin and H. Stöcker, Phys. Lett. **163B**, 59 (1985).
(5) R.S. Mayer et al., Phys. Rev. Lett. **70** (1993) 904.

# HIGH ENERGY PHOTON PRODUCTION IN THE $^{40}Ar + ^{51}V$ REACTION AT 44 MeV/u

P.Sapienza[1], R.Coniglione[1], C.Agodi[1], R.Alba[1], G.Bellia[1,2], A.Del Zoppo[1], P.Finocchiaro[1]
K.Loukachine[1],+E.Migneco[1,2], C.Maiolino[1], P.Piattelli[1], D.Santonocito[1], A.Peghaire[3]

(1) *Istituto Nazionale di Fisica Nucleare - Laboratorio Nazionale del Sud (ITALY)*
(2) *Dipartimento di Fisica dell'Università di Catania (ITALY)*
(3) *GANIL, Caen (FRANCE)*

## 1. Motivations

Hard photons, subthreshold pions and very energetic nucleons have been indicated by theoretical calculations as the best probes to investigate the first stages of the nucleus-nucleus collisions at intermediate energy. Due to their electromagnetic nature, hard photons can provide unperturbed information on the nuclear dynamics. Consequently their emission in heavy ion collisions at intermediate energy has been intensively studied in the last years[1,2]. In particular, the $\gamma$ emitting source velocity has been found to be close to the half-beam velocity independently of the projectile-target mass asymmetry[3]. Since this velocity coincides with the average nucleon-nucleon center of mass velocity, this result strongly supports the commonly accepted interpretation of these hard photons as bremsstrahlung radiation from first n-p collisions. Some *exclusive* experiments, aimed mainly at the study of the hard photon emission dependence on the centrality of the reaction, have also been performed[4-9]. However, it is very important to perform more *exclusive* experiments in order to clarify if and to what extent photons, pions and very energetic nucleons can be considered sensitive probes of the initial stages of the collision.

## 2. The experiment

In the following we will present some of the experimental results obtained with the MEDEA detector at GANIL with regards to the production of hard photons. We have measured, on an event-by-event basis, hard photons ($E_\gamma \geq 25$ MeV) in coincidence with light charged particles (Z=1,2) (LCP) in the reaction $^{40}Ar+^{51}V$ at 44 MeV/u. The LCP multiplicity can be assumed as an indicator of the impact parameter: the larger the multiplicities the more violent the collisions (small impact parameters). The experiment was performed with the MEDEA detector[10]. 150 $BaF_2$ detectors, covering the angular range $42^o \leq \theta \leq 180^o$, and 80 plastic phoswhich detectors covering the polar angles $10^o \leq \theta \leq 30^o$ were operating with a total geometrical efficiency of 80%. Hard photons were measured in the $BaF_2$ ball while the LCP were measured and identified

+ On leave from S.Peterburg Nuclear Physics Institute, Russia

both in the $BaF_2$ ball and in the phoswich wall.

## 3. Data analysis and results

In the analysis the high energy $\gamma$-rays were identified by combining the time of flight and pulse shape information. To get rid of the cosmic ray contamination in the $\gamma$ energy spectra the events triggered by cosmic rays were rejected off-line requiring a coincidence with at least one LCP detected in the phoswich wall. From a simultaneous fit of the unfolded inclusive $\gamma$ spectra at different angles in the laboratory we have extracted the $\gamma$ emitting source velocity, the anisotropy and the $\gamma$ cross section which are in good agreement with the existing systematics.

However, in order to get more information one has to study the hard photon emission dependence on the impact parameter which allows a more detailed comparison with the models.

For the conversion of the LCP multiplicity into impact parameter $b$ we have adopted the method of Cavata et al.[11] which is based on the assumption that the impact parameter and the multiplicity are connected by a monotone correlation.

The experimental hard photon multiplicity, defined as $M_\gamma(b) = \frac{d\sigma_\gamma(b)}{d\sigma_R(b)}$, is reported in fig.1 and increases steeply with increasing centrality from peripheral (large $b$) to mid-central collisions and then saturates for the most central collisions. The behaviour of $M_\gamma(b)$ agree with the trend of the BNV[12] calculations.

On the other hand, it is worth noticing that also the geometrical model based on the first n-p collision bremsstrahlung hypothesis[1] (solid line of fig.1) reproduces the data quite well, at least up to the mid-central collisions. In this model $M_\gamma$ is parametrized as $M_\gamma(b) = P_\gamma \cdot N_{np}(b)$ where $P_\gamma$ is the probability of emitting a nucleon in a n-p collision and $N_{np}(b)$ is the number of n-p collisions at a given $b$, evaluated on the basis of the surface dependence proposed by Bauer et al.[13] which follows the data better than standard volume prescription proposed by Nifenecker et al.[1]. The geometrical model indicates that $M_\gamma(b)$ is mainly affected by the size of the participant region formed during the collision, while the flattening observed for the most central collisions needs further investigations.

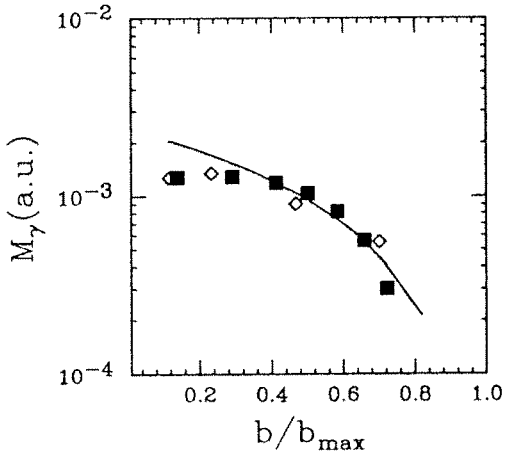


**Fig.1** - Experimental (squares) and BNV (diamonds) photon production multiplicity $M_\gamma$ ($E_\gamma \geq 40$ MeV) as a function of the impact parameter for the reaction $^{40}$Ar + $^{51}$V at 44 MeV/u. The solid line is the result of a geometrical model calculation (see text).

Another piece of information concerns the dependence of the inverse slope parameter $E_o$ on the centrality of the reaction. In fig.2 the value of $E_o$ in four bins of impact parameter is reported for the reaction $^{40}$Ar+$^{51}$V at 44 MeV/u. $E_o$ is almost constant

for the central reactions while decreases for the most peripheral ones. A similar trend has been also observed in other experiments[6,7,9] and it is usually interpreted, still in the frame of the n-p bremsstrahlung hypothesis, as due to the softening of the nucleon momenta at the nuclear surface and could give very interesting information on the nucleon momentum distributions during the collision.

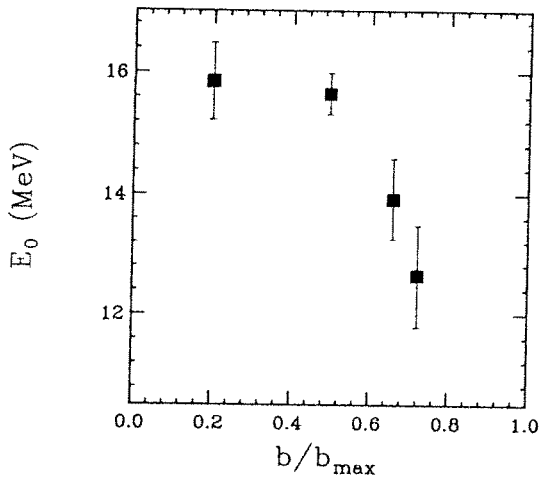


**Fig.2** - Experimental inverse slope parameter $E_o$ for four impact parameter bins for the reaction $^{40}$Ar + $^{51}$V at 44 MeV/u.

A clear signature of the hard photon production mechanism could be found by looking at the correlation between very energetic protons and hard $\gamma$. In fact several experimental data support the hypothesis that the hard photons and pre-equilibrium proton originate from the first collision between the most energetic projectile and target nucleons[14-16].

In the frame of the first chance n-p bremsstrahlung, the probability of observing a coincidence between a hard photon and a very energetic proton should decrease with increasing proton energy. In fact, if a very energetic $\gamma$ is emitted, the energy of the bremsstrahlung-generating proton is constrained by the limited energy available in the n-p collision. On the other hand, in the case of the emission from higher order n-p collisions or from a more thermalized system in a later stage of the reaction the $\gamma$ and proton emission are almost independent and therefore no correlation is expected.

In our analysis the correlation factor $R(E_p) = \frac{\sigma_{\gamma p}(E_p)}{\sigma_\gamma \cdot \sigma_p(E_p)}\sigma_R$ has been investigated as a function of the proton energy $E_p$ for the reaction $^{40}$Ar+$^{51}$V at 44 MeV/u in very central collisions. The preliminary results are shown in fig.3. For $E_\gamma \geq 25$ MeV $R(E_p)$ is close to one and it doesn't show any significant dependence on the proton energy as expected for indipendent $\gamma$-proton emission. This result is consistent with the data by Lampis et al[17] for $E_\gamma \geq 20$ MeV/u in the reaction $^{14}$N + Zn at 40 MeV/u. On the other hand, if we rise the $\gamma$ threshold up to 70 MeV, in spite of the very large error bars, a different trend is observed. In fact in this case the correlation factor is close to one for the lower proton energies but decreases with increasing energy indicating an anticorrelation between the most energetic $\gamma$ and protons.

## 4. Conclusions

To summarize we have studied hard photon production and its dependence on the impact parameter. The bremsstrahlung generated by the n-p collisions occurring at the first stage of the reaction gives a satisfactory description of the data. The preliminary

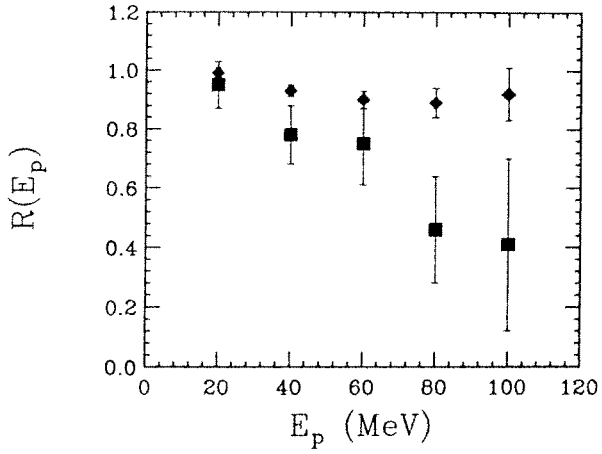


**Fig.3** - Experimental correlation factor $R(E_p)$ as a function of the proton energy for ($E_\gamma \geq 25$ MeV) (diamonds) and ($E_\gamma \geq 70$ MeV) (squares) (central collisions).

results on the $\gamma$-proton correlations strongly indicate that at least the most energetic photons and pre-equilibrium protons are produced by first chance n-p collisions.

## References


1. H. Nifenecker and J.A. Pinston, *Annual Rev. Nucl. Part. Science* **40**, (1990) 113.
2. W. Cassing et al., *Phys. Rep.* **188**, (1990) 365.
3. V. Metag, *Nucl. Phys.* **A488**, (1988) 483c.
4. R. Hingmann et al., *Phys. Rev. Lett.* **58**, (1987) 759.
5. H. Herrmann et al., *Phys. Rev. Lett.* **60**, (1988) 1630.
6. M. Kwato Njock et al., *Nucl. Phys.* **A489**, (1988) 368.
7. T. Reposeur et al., *Phys. Lett. B* **276** (1992) 418.
8. S. Riess et al., *Phys. Rev. Lett.* **69**, (1992) 1504.
9. E. Migneco et al., *Phys. Lett. B* **298** (1993) 46.
10. E. Migneco et al., *Nucl. Instr. and Meth.* **A314** (1992) 31.
11. C. Cavata et al., *Phys. Rev. C* **42** (1990) 1760.
12. A. Bonasera et al., *Phys. Lett. B* **246** (1990) 337 and *Il Nuovo Cimento A* **105** (1992) 301.
13. W. Bauer et al., *Phys. Rev. C* **34** (1986) 2127.
14. Luke et al., *Phys. Rev. C* .. (1993) ...
15. H. Fuchs and H. Homeyer, *International workshop on particle correlation and interferometry in nuclear collisions*, Nantes (1990) 305.
16. R. Alba et al., *XXXI International Winter meeting on nuclear physics* , Bormio(1993) and this compilation
17. A.R. Lampis et al., *Phys. Rev. C* **38** (1988) 1961.

# SEARCH FOR COHERENCE IN $\pi^0$ SUBTHRESHOLD EMISSION IN Kr + Ni AT 60 $A$·MeV*)

J. Québert[1], Y. Schutz[2], P. Lautridou[2], F. Lefèvre[2], T. Matulewicz[2], W. Mittig[2], R.W. Ostendorf[2], P. Roussel-Chomaz[2], F. Ballester[3], J. Díaz[3], A. Marín[3], M. Marqués[3], G. Martínez[3], M. Franke[4], R. Holzmann[5], A. Schubert[5], R.S. Simon[5], H.Löhner[6], J. Van Pol[6], R.H. Siemssen[6], H.W. Wilschut[6], S. Hlávač[7], V. Wagner[8], Z. Sujkowski[9]

[1] *Centre d'Etudes Nucléaires de Bordeaux-Gradignan, 33175 Gradignan, France*
[2] *Grand Accélérateur National d'Ions Lourds, BP 5027, 14021 Caen, France*
[3] *IFIC (CSIC - Univ. de Valencia) y Dpto. de Física Atómica, Molecular y Nuclear, 46100 Burjassot, Spain*
[4] *II Physikalisches Institut Universität Gießen, D-6300 Gießen, Germany*
[5] *Gesellschaft für Schwerionenforschung, D-6100 Darmstadt, Germany*
[6] *Kernfysisch Versneller Instituut, 747 AA Groningen, The Netherlands*
[7] *Institute of Physics of the Slovak Academy of Sciences, 842 28 Bratislava, Slovakia*
[8] *Nuclear Physics Institut of the Czech Academy of Sciences, 250 68 Řež, Czech Republic*
[9] *Soltan Institute for Nuclear Studies, 05-400 Swierk, Poland*
*) *Experiment performed with TAPS*

In 1992, the TAPS detector was set up at GANIL and $\gamma\gamma$ correlations were measured in the reaction $^{86}$Kr + $^{nat}$Ni at 60 $A$·MeV. In this experiment the purpose was chiefly to evidence the so-called HBT effect of bremsstrahlung photons[1].

We wish to present here another facet, concerning subthreshold $\pi^0$ emission, which can be developed in the framework of the correlation functions. Such $\pi_0$'s are identified by the peak occurring at an invariant mass of 135 MeV for the two detected photons (see bottom part of fig.1).

Whereas both sources of $\gamma\gamma$ emissions trigger apparent coincidences at the electronic level of detection, bremsstrahlung emission, due to n-p collisions, is in fact completely incoherent in the range of the collision time. The principle of intensity interferometry (second order correlation functions) is based on the presence of such an incoherence. The other process (the $\pi^0$ decay), on the contrary, is coherent in space and time (inside or outside the source) since it concerns the decay of an unstable resonance. An elementary detection, i.e., when two $\gamma$ detectors fire in the TAPS array for the specific invariant mass of 135 MeV, is analog to a detection by a single virtual counter with which the total momentum of the two $\gamma$'s is measured (i.e., the $\pi^0$ momentum).

In the framework of the correlation functions, this specific $\gamma\gamma$ decay cannot be studied by using second order correlation functions[3] because only one quantum is in fact detected with only one counter. For this emission, a first order correlation

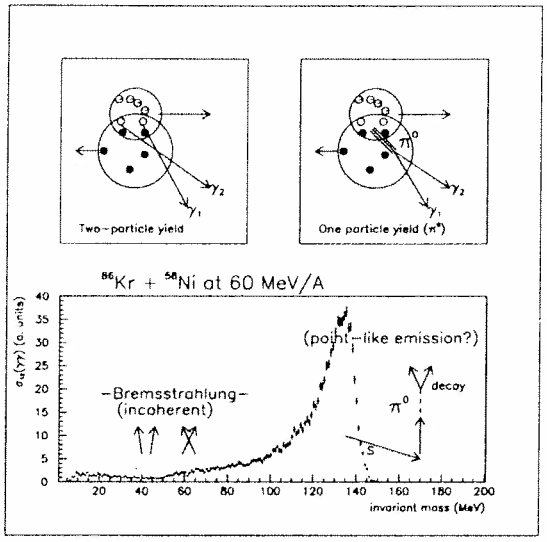


Figure 1: *Top: two different mechanisms of $\gamma\gamma$ emission from the point of view of space and time: Left: incoherent space-time bremsstrahlung emission; right: coherent space-time resonance decay ($\pi^0$). Below, the coincidence yield presents the two components.*

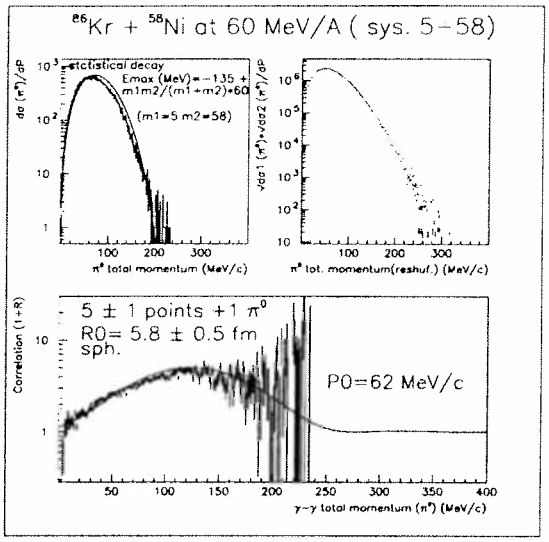


Figure 2: *Top: $\pi^0$ total spectra ($\gamma\gamma$ coincidences and reshuffled data). Below, the correlation function of first order is obtained by dividing the two spectra. A fit is performed with relation (1) in which it is necessary to include a source momentum $P_0$*

function can however be defined instead of a second order correlation function. This function is a tool to probe any cooperative effect in the emission[4] as first order functions probe coherence only.

The interest of using a first order correlation also lies, if there is coherence, in its sensitivity to the number of possible coherent participants in the source, (i.e., to the amplitude of possible cooperative effects), whereas the second order correlation function, considered in HBT measurements, does not present this specificity[2, 4]. The first order correlation function can be written (in analogy with the calculations for a N slit-interference pattern in optics):

$$1 + R = 1 + (N - 1)|\rho(|\vec{k}_1 + \vec{k}_2|)|^2 \qquad (1)$$

where the total momentum $\vec{P} = \vec{k}_1 + \vec{k}_2$ , $\rho$ is the Fourier transform and N the number of active source points (the granularity of the source). The maximum of this function should give the amplitude of the cooperative effects.

The experimental correlation function is obtained by dividing the total coincidence yield, versus P (upper left part of fig. 2), by the spectrum obtained with the product of the square-roots of the reshuffled distributions of $\pi_0$'s (upper right part of fig. 2). It appears that this complex procedure gives an analogy with the definition of first order correlation functions in optics ($\frac{I_{meas.}}{\sqrt{I_1}\sqrt{I_2}}$, with $I_{meas.} = I_1 + I_2$ and $I_{1,2}$

the two source-point intensities; $I_{meas.} \equiv \pi_0$ yield).
The study of the correlation function versus the sum of the two $\gamma$ momenta unfortunately introduces an effect due to the intrinsic momentum of the source of $\pi^0$'s. This latter quantity cannot be removed as this can be done in HBT measurements (where the difference of momenta is used). This effect can be noticed in the correlation displayed at the bottom part of fig. 2 (there is a displacement of the maximum of $< 2P_{source} > \simeq$ 125 MeV/c and the curve is roughly symmetric around this value).

A fit to the data with relation (1), where an average source momentum is introduced, leads to: N=5±1 (maximum of the curve) and $R_{source} \simeq$ 6 fm (shape of the curve).
The possible origin of this number of points is under study. It seems that such a number cannot be assigned to 5 coherent N-N collisions for the two following reasons:

a) the available energy due to 5 N-N collisions (without the kick of intrinsic Fermi motion) is not sufficient to create a $\pi_0$ with a kinetic energy corresponding to the spectrum shown in the upper left part of fig. 2 (Pmax$\simeq$ 220 MeV/c).

b) a careful study of the $\pi_0$ invariant distribution (not shown here) shows that the rapidity plot does not present a strong displacement towards the N-N rapidity. This plot is slightly shifted on the right of the target rapidity and thus, presumably characterizes a capture of a few nucleons by the target in the collision; thanks to the heavy partner, these nucleons bring enough energy in the phase-space of a few bodies to expect a statistical emission for instance (see the fit of the spectrum in the upper left part of fig. 2, using this hypothesis[6]).

In conclusion, there are a number of independent and complementary mesurements in this study which seem to reveal a cooperative effect of a few nucleons. A possible interpretation considers that they are captured by a heavy mass to produce a $\pi_0$. This interpretation, based on inclusive data, has to be compared to the results of exclusive data correlated to the spectrometer SPEG[7], which seem to evidence that a $\pi_0$ is created in a first chance peripheral N-N collision, then strongly reabsorbed to suffer final-state interactions with one of the participants.

# References


[1] M. Marqués *et al.*, in this issue.

[2] M. Gyulassy *et al.*, Phys. Rev. **C20** (1979) 2267

[3] D. Neuhauser, Phys. Lett. **B182** (1986) 289.

[4] J. Québert, in Proceedings of the II TAPS Workshop, Guardamar, Spain (1993), edited by J. Díaz and Y. Schutz, World Scientific, to be published.

[5] J. Québert, Ann. Phys. Fr. **17** (1992) 99

[6] G.E. Uhlenbeck and S. Goudsmit, P. Zeeman-Martinus Nijhoff's, Gravenhage(1935) - Netherland

[7] A. Schubert et al; submitted to Phys. Lett. B and this issue

# IMPACT PARAMETER DEPENDENCE OF $\pi^\circ$ PRODUCTION IN HEAVY ION COLLISIONS AT SUBTHRESHOLD ENERGIES

A.Badalá[1], R.Barbera[1,2], A.Palmeri[1], G.S.Pappalardo[1], F.Riggi[1,2]
A.C.Russo[1], G.Russo[2] and R.Turrisi[1,2]

C. Agodi[3], R. Alba[3], G. Bellia[2,3], R. Coniglione[3], A. Del Zoppo[3],
P. Finocchiaro[3], C. Maiolino[3], E.Migneco[2,3], P. Piattelli[3], and P. Sapienza[3]

A. Peghaire[4]

[1] *Istituto Nazionale di Fisica Nucleare, Sezione di Catania*
[2] *Dipartimento di Fisica, Università di Catania*
[3] *Istituto Nazionale di Fisica Nucleare, Laboratorio Nazionale del Sud*
[4] *GANIL, Caen*

## 1. - Motivations

Several indications on the central character of heavy ion collisions producing pions at subthreshold energies have been accumulated in recent years by semiexclusive experiments[1-5]. All these experiments were carried out detecting charged pions in a range telescope, whereas light charged particles (LCP), detected by large area multidetectors, were used as an indicator of the violence of the collision.

Unfortunately, quantitative estimates of the impact parameter scale for the pion production could not be extracted by these experiments due to the incomplete coverage of the total solid angle for LCP detectors and also to the small solid angle usually subtended by range telescopes. In case of neutral pions, which mainly decay into two gamma rays, some of the experimental difficulties which are inherent to the detection of charged pions could be overcome, due to the recent availability of 4 $\pi$ multidetectors which are able in principle to detect simultaneously energetic photons and charged particles [6-8].

The experiment presented here was carried out at GANIL with the multidetector MEDEA [7], coupled to a forward hodoscope, with the aim to get such a quantitative estimate for the impact parameter involved in the pion production mechanism. The charged particle multiplicity was used in the present analysis as a global variable to extract the impact parameter scale within the modified fireball model.

## 2. - Experiment and data analysis

The experiment was carried out at GANIL, with a beam of $^{36}Ar$ at 95 MeV/nucleon. The multidetector array MEDEA, coupled to a forward hodoscope of

plastic scintillators, was used to detect $\pi^\circ$ and charged particles. For this experiment MEDEA had 168 $BaF_2$ modules, arranged into 7 rings of 24 detectors each, covering the zenithal angular range between 30° and 138° and 120 phoswiches arranged into 5 rings of 24 detectors each, covering the angles from 10° to 30°. An additional hodoscope, made by 16 plastic scintillators in 2 rings, covered the angular range from 2.5° to 10° to detect light charged particles and fragments. The properties of MEDEA as a $\pi^\circ$ spectrometer have been already reported [8]. Part of the inclusive and exclusive data on $\pi^\circ$ production, measured with the same detector, have been published in previous papers [9-11]. Fig. 1 shows the invariant mass spectrum obtained in the present experiment, together with the result of a GEANT3 simulation. Results from GEANT3 simulations allowed to extract $\pi^\circ$ efficiency, and to correct data wherever required.

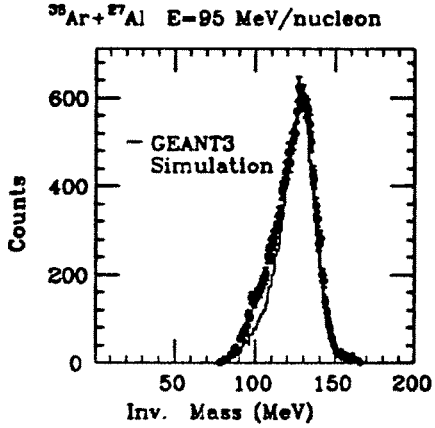


Fig.1: Invariant mass spectrum from the $^{36}Ar+^{27}Al$ reaction at 95 MeV/nucleon by the multidetector array MEDEA. Solid line is a GEANT3 simulation.

Simulations done in the framework of a modified fireball model [12] were used to search for global variables giving a good correlation to the impact parameter [13]. In the present analysis the charged particle multiplicity was chosen to classify the events into three classes, roughly corresponding to central, intermediate and peripheral collisions.

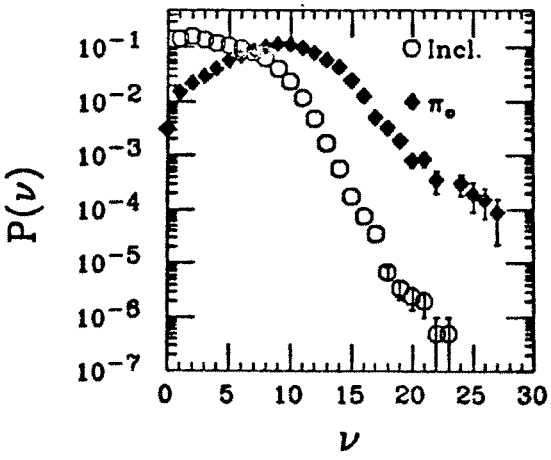


Fig.2: Multiplicity distribution of inclusive and $\pi^\circ$-triggered events for the reaction $^{36}Ar+^{27}Al$ at 95 MeV/nucleon.

## 3. - Results and discussion

Some of the inclusive results on $\pi^\circ$ production at 95 MeV/nucleon for the $^{36}Ar + ^{27}Al$ system have been already reported [11]. Among these, the kinetic energy spectra measured at several angles as well as their angular distribution and the integrated total cross section show evidence for the intervention of strong reabsorption effects, and claim for the necessity of a proper inclusion of the reabsorption in the dynamical calculations. The selection of impact parameters in pion events from heavy ion collisions could help, together with dynamical calculations, to investigate the role of reabsorption effects. A strong dependence of the pion production cross section on the impact parameter is observed in fig.2 which shows the inclusive and $\pi^\circ$-triggered charged particle multiplicity distributions. The three multiplicity bins, roughly corresponding to central (b=0-2 fm), intermediate (b=2-4 fm) and peripheral (b=4-6 fm) collisions, containg 57 %, 32% and 11% respectively of the pion events. This filter can be used to investigate how different features of the process depend on the character of the collision. As an example, angle-integrated kinetic energy spectra of the emitted pions were extracted for central, intermediate and peripheral collisions (fig.3). A calculation, taking into account reabsorption effects, was carried out introducing in a standard BNV code the effect of the distance traversed by the pion after its emission according to the nuclear matter in the surroundings and the dependence of the pion mean free path as a function of its kinetic energy as calculated in Ref.[14]. The results are promising in this respect since both the slopes and the absolute values are correctly reproduced (fig.4) at variance with the standard BNV version.

In conclusion, exclusive experiments on pion production give useful informations on the dynamics of the process, especially when collisions can be classified according to their impact parameter. It is expected that further information could come from a quantitative analysis of all particles associated to the pion production.

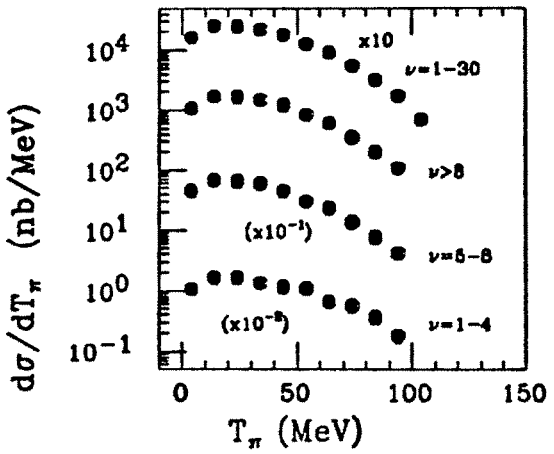


Fig.3: Angle-integrated pion energy spectra, for different bins of the charged particle multiplicity m.

Fig.4: Comparison of the pion energy spectra at different detection angles with the result of a BNV dynamical calculation taking into account the effect of the reabsorption in the nuclear matter and the energy dependence of the pion mean free path (solid histogram). The dashed histogram shows the result of the BNV calculation without reabsorption effects.

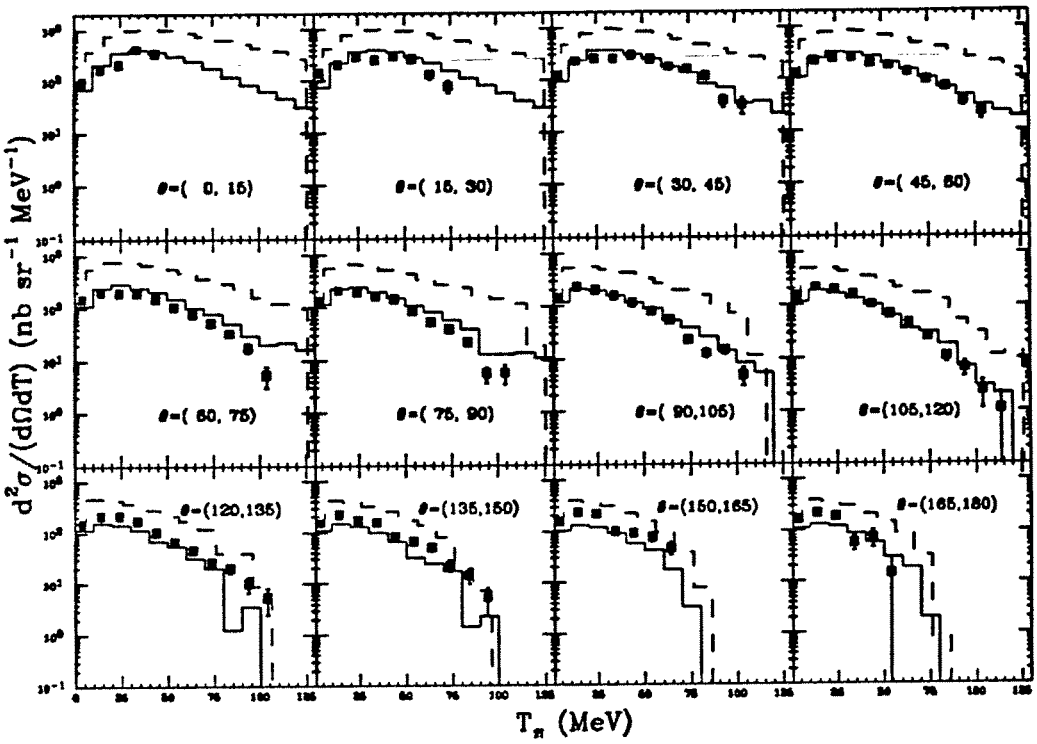


## References


[1] B.Erazmus et al., Nucl.Phys. A481(1988)821.
[2] S.Aiello et al., Europhys.Lett. 6(1988)25.
[3] R.Barbera et al., Nucl.Phys. A518(1990)767.
[4] R.Barbera et al., Nucl.Phys. A519(1990)231c.
[5] J.L.Laville et al., Report LPC Caen LPCC92-12(1992); Nucl.Phys. A, in press.
[6] W.Kuhn,H.Lohner (eds), Report GSI-91-21.
[7] E.Migneco et al., Nucl.Instrum. and Methods A314(1992)31.
[8] A.Badalà et al., Nucl.Instrum. and Methods A306(1991)283.
[9] A.Badalà et al., Phys. Rev.C47(1993)231.
[10] A.Badalà et al., Z.Phys. A346(1993)293.
[11] A.Badalà et al., Phys. Rev. C48(1993), in press.
[12] A.Bonasera, M.Di Toro and C.Gregoire, Nucl.Phys. A483(1988)738.
[13] A.Badalà et al., Z.Physik A344(1993)455.
[14] J.Hufner and M.Thies, Phys. Rev.C20(1979)273.

# A neural network to identify neutral mesons

Frédéric Lefèvre, Pascal Lautridou, Miguel Marqués, Tomasz Matulewicz, Reint Ostendorf, Yves Schutz,
for the TAPS collaboration : GANIL-Gießen-Groningen-GSI-Valencia

Neutral mesons like $\pi^0$ and $\eta$ are commonly used in heavy ion physics to probe the in-medium charactesistics of the NN interaction and the properties of hot and dense nuclear matter. These mesons are short lived and decay long before they can reach a detector. Both $\pi^0$ and $\eta$ decay predominantly by emission of two photons. They are identified by constructing the invariant mass of the photons.

$$m_{inv} = \sqrt{2 * E_1 * E_2 * (1 - \cos\theta)}$$

where $E_1$ and $E_2$ are energy of photons and $\theta$ their relative angle.

## The combinatorial problem

Beside the spatial and energy acceptance and resolution of detectors, another difficulty resides in the fact that we can misidentify mesons due to ambiguity in associating photons. It is always possible that two photons produced from two different sources have an invariant mass corresponding to a meson. With high photon multiplicities the number of pairs falling into one meson mass region by chance becomes higher than the number of mesons produced in the reaction.

One way to get rid of some of the combinatorial pair is to consider that one photon cannot be emitted from two different meson, so that it is not allowed for a photon to participate in more than one pair. The problem is then to select which pair is the most likely to be a physical one rather than a chance one. In a first step we calculate for each pair $C_l$ a confidence level that this pair was produced from an actual meson. The simplest funcion for $C_l$ is the mass ratio between the invariant mass and the rest mass of the closest meson, but others choices can be made. The simplest selection method is then to choose the case with the highest confidence level as the true pair, then removing all the remaining combinaisons containing these two photons, and select again the highest confidence level. It is well know that this strategy is not a very good one [1].

## A neural network to solve combinatoric problems.

The previous strategy has the fatal draw back to select what remains at the end of the process. A better strategy is to maximize the sum of confidence levels. The problem is complicated by the fact that we allow photons not to be paired (or to be paired with themselves), to represent direct photons and to take into account the geometrical acceptance of the detector [2]. The problem we are faced with is a typical optimization problem. No perfect solution within reasonable computing time is known for these class of problem, so we have to look for approximate solutions. Neural network are able to give quite good answers to optimisation problems[3]. For an introduction to neural network we refer the reader to references [4,5]

The shape of the neural network we designed to solve this problem is a triangle. One row and one column are assigned to every photon in an event. The diagonal represents photons paired to themselves, while all cells above the diagonal represent all possible pairs of photons. One cell (neuron) is assigned for every pair, including the diagonal. Each cell has a value called activity which changes during the evolution of the network in a domain [0,1]. A cell containing the photon is connected to all others cells containing the same photon. All links between cells are negative. So during the evolution of the

network, a cell with a high activity will decrease the activity of all others cells containing the same photon.

The neural network described above is an example of the Hopfield Neural net. There exists a convergence proof stating under which conditions the neural calculation converges [3]. However, this network doesn't solve our problem well enough. In fact with this configuration all the activities converge rapidly toward zero excepted the highest one and we implement the simplest selection method described above. To improve the solution we have to slow down the computation in order to let the network explores several states and to impose activities to converge toward one for all selected pairs (including photons paired with themselves).This is achieved by adding links connecting each cell to itself. Although this network is not any more of the Hopfield type, we have found a set of conditions for the weights sufficient to ensure convergence and to reach a state where each photon is used exactly once [2].

## Performance of the network [2]

We have applied this method to identify $\pi^0$ in simulated events. The simulations have been performed for the system $^{132}Xe + ^{197}Au$ at three different bombarding energies : 0.5 GeV/u ; 0,8 GeV/u and 1.0 GeV/u. The resulting average $\pi^0$ multiplicity is 0.64 ; 2 and 4 respectively. The simulated detector consisted of 216 identical units arranged on a sphere covering 2/3 of the total solid angle leaving two openings in the forward and backward hemisphere. The energy resolution of the individual unit is 13 %. Compared with the usual method which consists in integrating the $\pi^0$ peak in the invariant mass spectrum and subtracting a background, the network finds less $\pi^0$. However, the performance of the network must be judged on the signal to noise ratio. For the lowest energy the neural network raises the ratio true pions over detected pions from 81 % to 94 %, and for the highest energy from 42 % to 64 %. The network may be more advantageous when one need to identify pairs of $\pi^0$. The ratio of events with 2 true pions over events with two identified pions raises from 29 % to 88 % for the lowest energy and from 15 % to 41 % for the highest one. Moreover the number of events with 2 pions identified with the network is comparable to or even larger than the number given by the usual method. This can be explained by the ability of the network to eliminate combinatoric pairs in events having $\pi^0$ multiplicity larger than 2. Therefore the network will be the right tool for $\pi^0$ interferometry or to search for particle like $K_S^0$ meson decaying with the emission of 2 neutral pions.

To approach an experimental situation we have diminished the solid angle covered by the detector. For a small coverage of the solid angle, below 15 % the network and the usual method give comparable results. This can be explained by the fact that the background is not combinatoric but essentially due to photons that have lost their partner. For a larger coverage the nature of the background changes to become fully combinatoric at a coverage of 100%. The transition can be clearly seen when the ratio true/detected suddenly drops for both methods when 17 % of the solid angle is covered. The network performance is already better but with the usual method this ratio saturates at about 40 % when one third of the solid angle is covered, whereas with the network the ratio continues to increase up to 90 % for a full coverage. The price to pay is a serious reduction of the detection efficiency.

[1] D.W. Tank, J.J. Hopfield ; Scientific American 257 (1987) 62
[2] F. Lefèvre ; thèse de doctorat ; université de Caen 1993.
[3] J.J. Hopfield, D. W. Tank ; Biol. Cyber 52 (1985) 141
[4] R. Baele and T. Jackson ; Neural computing : an introduction ; Adam Hilger ed. Bristol 1990.
[5] C. Peterson, T Rögnvaldsson ; 1991 CERN School of computing.

# C - MISCELLANEOUS

# Search for Colour Van der Waals Force in $^{208}$Pb+$^{208}$Pb Mott Scattering

A.C.C. Villari[1,2], W. Mittig[1], A .Lépine-Szily[1,2], R. Lichtenthäler Filho[2], G. Auger[1], L. Bianchi[1], R. Beunard[1], M.E. Brandan[5], J.M. Casandjian[1,2], J.L. Ciffre[1], A. Cunsolo[3], A. Foti[3], L. Gaudard[1], C.L. Lima[2], A. Menchaca-Rocha[5], N. Orr[6], E. Plagnol[1], Y. Schutz[1], R.H. Siemssen[4], J.P. Wieleczko[1]

*(1) GANIL, B.P. 5027, 14021 Caen Cedex, France*
*(2) IFUSP, DFN, C.P. 20516, 01498, São Paulo, S.P., Brazil*
*(3) Dipartimento di Fisica and INFN - Sez. CT,95129 Catania,*
*(4) KVI, 9747 AA Groningen, The Netherlands*
*(5) Instituto de Fisica, UNAN, Mexico, Mexico*
*(6) L.P.C., 14050 Caen, France*

Precision measurements of subcoulomb barrier elastic scattering of heavy ions have been used successfully in the past [1,2] to study the influence of vacuum polarisation and relativistic effects and were found to be consistent with standard QED. The possibility of the existence of long range forces between hadrons has been suggested in the framework of QCD [3-8], though they also have been disputed on theoretical grounds [9]. The exchange of two gluons may give rise to a colour Van der Waals force (CVDWF) of the form $V = \hbar c(\lambda_N/r_0)(r_0/r)^N$ with a length scale $r_0$= 1fm and with $N \leq 7$. The limits on $\lambda_N$ were established from the measurement of the bound state energies of exotic atoms [4,6,7] and subcoulomb scattering of p, d, $^{16}$O on $^{208}$Pb [8]. It was recently proposed [10] to determine the strength of the CVDWF in a study of Mott scattering of two heavy nuclei.

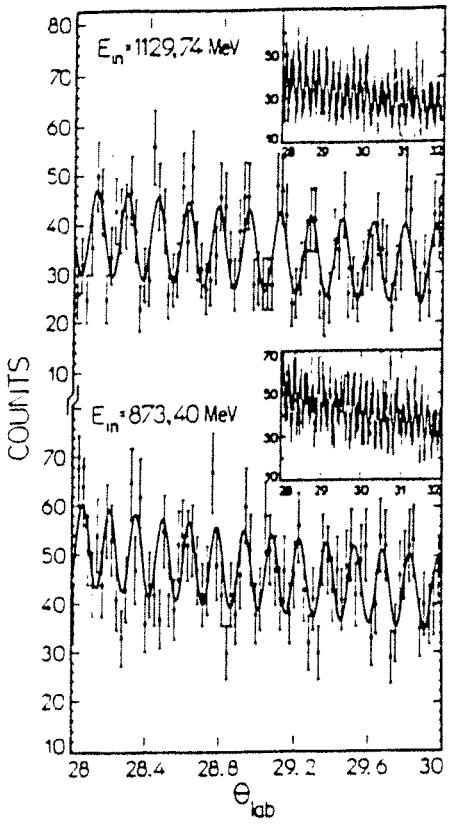


FIG 1. Mott scattering angular distributions at two bombarding energies. The inserts show the total angular domain covered. The solid lines are the best fits to the experimental measurements.

We report here on a high-precision measurement of the subcoulomb barrier scattering of $^{208}$Pb+$^{208}$Pb at two energies around 5 MeV/u in which we obtain a new upper limit on the existence of CVDWF. The relative precision needed for measuring these effects, which has been obtained in the present investigation, is of the order of $10^{-4}$ for the absolute angle and for the absolute beam energy. The absolute energy was determined by a velocity measurement of the beam. The time-of-flight (TOF) of the beam bunches was measured between two beam scanners, with the distance between them (~48m) determined to an accuracy of 1mm. The incident energies used in the experiment and their standard

deviations were $E_1^{beam}$=(873.48±0.06) MeV and $E_2^{beam}$=(1129.86±0.09) MeV, which corresponds to a relative error of $8.10^{-5}$. The absolute precision in the angle measurement was obtained by placing the target, the detectors, and the beam scanner behind the target on a common circle with a diameter of 7m. The scattered particles were detected in four x-y position sensitive drift chambers, that were mounted such as to allow kinematic coincidence measurements at $\theta_{lab}$= 30°- 60° and 45°- 45°. The determination of the absolute scattering angles to a precision of the order of 0.001° was achieved by the measurements of the distances to 0.1 mm between all components of the experimental set-up. The measured elastic scattering angular distributions at angles close to 30° show clearly the rapid oscillations (see FIG 1) of the differential cross section with periods that are about 0.14° and 0.18° at the two energies of 873.40 and 1129.74 MeV, respectively. The oscillations observed at both energies exhibit an angular shift with respect to pure Mott-scattering. Theoretical estimates including vacuum polarisation, relativistic effects, nuclear polarisability of target and projectile, and electronic screening underestimate the angular shifts slightly at 873.40 MeV and more significantly at 1129.74 MeV (see FIG 2).The comparison of the angular shift produced by a CVDWF folded into the nuclear matter distribution of the target and projectile allows the determination of a new upper limit for the strength of this force.

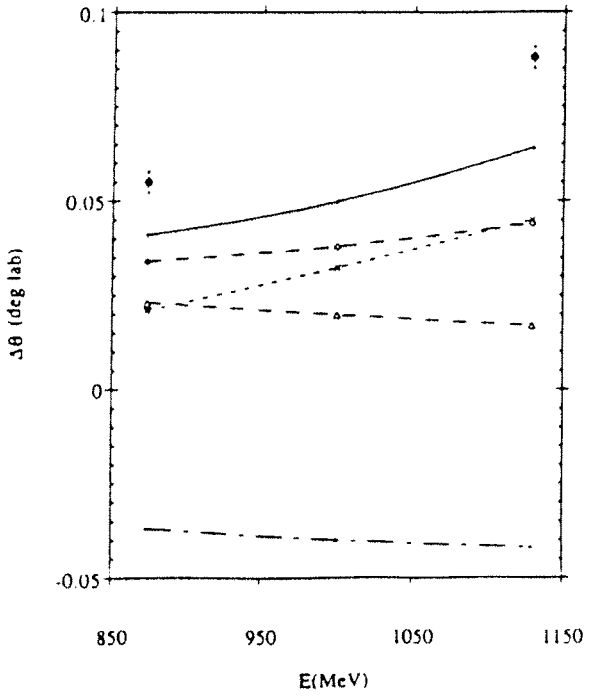


FIG 2. Comparison of the measured angular shift at the two energies with the theoretical predictions including vacuum polarization(dash-dotted line), nuclear polarizability (short-dashed line with crosses), relativistic effects (long-dashed line) and electronic screening with $^{+}$23 charge ( long-dashed line with triangles). The sum of these effects is shown by the solid line. The points with error bars are the result of the present experiment.

The introduction of an effective negative Q-value that takes into account the production of δ-electrons was necessary to explain the coincidence angle measurement data. The coupling to the δ-electron channel and to other atomic effects might well lead to an effective potential similar to that of the nuclear polarizability. Our high quality data for the first time show clearly the influence of atomic effects other than screening in this type of experiment and call for a careful theoretical analysis.

A new set of data were taken in July 1993 at energies of 787.42 MeV, 948.78 MeV, 1030.39 MeV, and 1306.93 MeV. We added to the experimental set-up described above two silicium detectors in the target chamber at $\theta_{lab}$ =27° and 73°, detecting the two lead nuclei in coincidence, in order to obtain the target position with a higher precision. In this

new measurement we used thicker and more homogeneous rotating $^{208}Pb$ targets and more intense incident beam, which resulted in much better statistics. These data are now being analysed.


1. W. Lynch et al., Phys. Rev. Lett. **48**, 979 (1982)
2. D. Vetterli et al., Phys. Rev. Lett. **62**, 1453 (1989)
   Nucl. Phys. **A533**, 505 (1991)
3. T. Appelquist and W. Fishler, Phys. Lett. **77B**, 405 (1978)
4. G. Feinberg and J. Sucher, Phys. Rev. **20D**, 1717 (1979)
5. T. Sawada, Phys. Lett. **100B**, 50 (1981)
6. G. Feinberg, Comm. on Nucl. Part. Phys. **19**, 51 (1989)
7. J.C. Batty, Phys. Lett. **115B**, 278 (1982)
8. C.V.K. Baba, Pramana -J. Phys. **29**, 143 (1987)
9. see for example: L. Villets in" Physics of strong fields",
   ed. W. Greiner, Plenum Press New York and London, 1987, p 735
11. M.S. Hussein, C.L. Lima, M.P. Pato and C.A. Bertulani,
    Phys. Rev. Lett. **65**, 839 (1990)
12. J. Raynal, ECIS code, unpublished

# THE FORMATION OF HOT AND DENSE NUCLEAR MATTER (E208)

R.W. Ostendorf, P.G. Kuijer, R.J.M. Snellings, T.M.V. Bootsma, A. van den Brink, A.P. de Haas, R. Kamermans, C.T.A.M. de Laat, G.J. van Nieuwenhuizen, C.J.W. Twenhöfel

*R.J. van de Graaffiaboratorium, Rijksuniversiteit Utrecht, P.O. Box 80000, 3508 TA Utrecht, The Netherlands*

A. Péghaire

*GANIL, BP 5027, 14021 Caen Cedex, France*

## 1 Introduction

The properties—formation and decay—of excited nuclear matter and its equation of state have since long been studied at Utrecht [1]. Employing a relatively small set-up, consisting of an ionization chamber and a few Si-CsI(Tl) telescopes, the formation of a compound system in heavy-ion reactions at energies between 10 and 35 $A$·MeV was investigated on a *statistical* basis, by looking at the evaporation-decay channel.

Recently, the Huygens detector system has been constructed. This detection system covers 80% of the total solid angle, allowing to study heavy-ion reactions on an *event by event* basis, without introducing a priori constraints on the analysis by only considering specific decay-channels.

## 2 The Huygens Detector System

The Huygens detector system is shown in figures 1 and 2.

The heart of the detector system is formed by a TPC-like drift chamber spanning polar angles ($\theta$) between 10° and 90°. It consists of a cylindrical gas-filled volume with a radius of 28 cm and a length of 54 cm. As counting gas argon-ethane and isobuthane have been used at a pressure of 60 mbar. The chamber is read out using three concentric rings of in total 128 microstrip detectors [2]. The microstrip signals are sampled by a flash ADC and *on-line* processed using a Digital Signal Processor (DSP). It should be noted that the sampling by the flash ADCs makes it possible to disentangle multiple hits. The TPC thus gives the direction of the particle as well as three independent measurements of a partial energy ($\Delta E$).

The TPC is backed by plastic (NE102A) scintillators. Around the gas volume at $\theta$ between 30° and 90°, 32 scintillators with a thickness of 10 cm, dimensioned to stop protons with energies up to 100 MeV, are used as stopping detectors. Forward angles, $\theta$ between 10° and 30°, are covered by 16 scintillators with a thickness of 1 cm. At these angles the identification of light charged particles is achieved in co-operation with the MUR [3], that also covers the very forward angular region from 3° to 10°.

Because of the thin foils around the gas volume the low-energy cut-offs are small, with a maximum of 0.5 MeV per nucleon for heavy fragments. The spatial resolution of the detector amounts to $\sim 5$ mm in the gas-volume in the direction of the electric field. The resolution in $\theta$ thus varies between 0.5° to 1.5°, depending on $\theta$. Due to the mounting of the microstrips, an azimuthal ($\phi$) resolution of $\sim 3°$ is achieved. The combination of the TCP-information with the various scintillating detectors enables a $Z$-identification up to $Z = 8$.

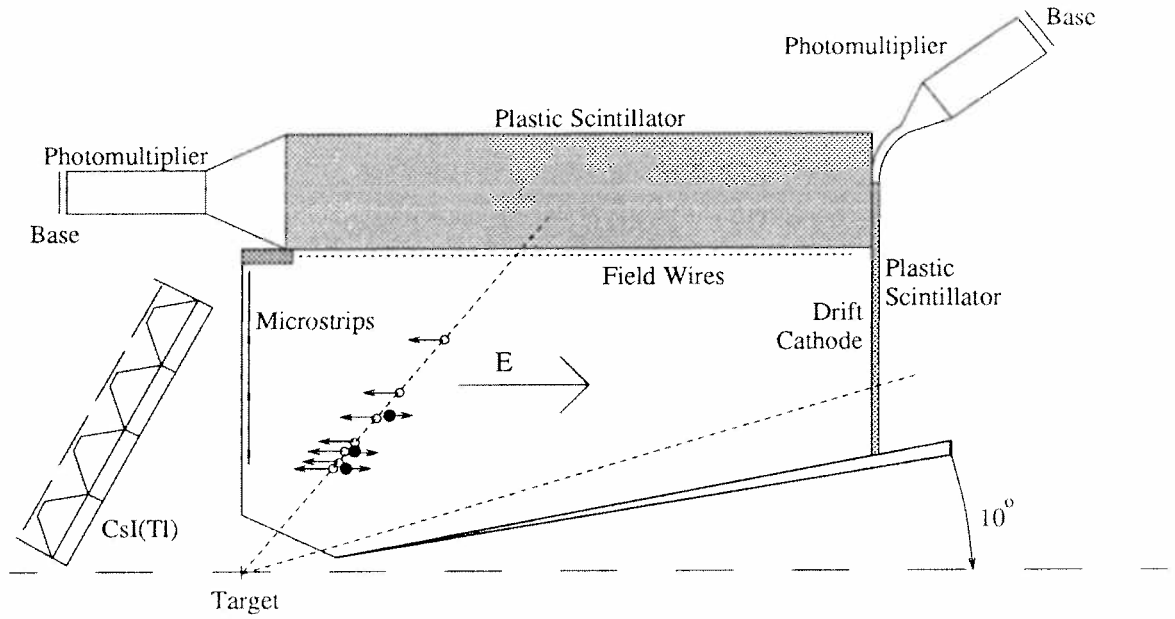


Figure 1: *A schematic view of the Huygens detector system.*

At backward angles one mainly expects light particles originating from an evaporation process, with $Z$-values up to 3. The backward detector consists of 4 walls of 16 CsI(Tl) crystals with a size of $5 \times 5 \times 1$ cm$^3$ [4], designed to stop protons with energies up to 50 MeV. The low energy threshold is of the order of 500 keV. Particle identification is achieved by means of the rise-time of the pre-amplifier pulse, sampled by a flash-ADC and analyzed *on-line* by a DSP.

The Huygens detection system has been developed to be a general purpose $4\pi$ scattering facility for heavy-ion collisions in the intermediate energy regime between 10 and 100 $A$·MeV. Compared to other existing $4\pi$ detectors, it shows a very good spatial resolution in the forward hemisphere for light charged particles and intermediate mass fragments with $Z < 8$.

## 3 The physics program

Measurement of flow is still a very active topic in studies of heavy-ion collisions at intermediate and relativistic (10 to 1000 $A$·MeV) energies. Flow is an enhanced transverse collective motion within the reaction plane due to a combination of mean field and nucleon-nucleon collision effects and is observed in the whole intermediate energy range. At lower energies (below 40 $A$·MeV) the observed colective motion of light particles can be described by a mean field approximation. At higher energies (above 100 $A$·MeV) the heavy-ion reaction is governed by nucleon-nucleon collisions. Since both mechanisms work in opposite directions, these effects cancel at the so-called balancing energy ($E_{\rm bal}$), around 75 $A$·MeV [5].

The basic idea is to compare experimental data on flow with theoretical calculations, like BUU and QMD type of simulations, in order to obtain information about the equation of state, the incompressibility constant of nuclear matter ($K_\infty$) and/or the in-medium nucleon-nucleon cross section ($\sigma_{\rm NN}$). Flow should be determined in exclusive measurements (impact parameter selection) utilizing reaction systems varying in incident energy

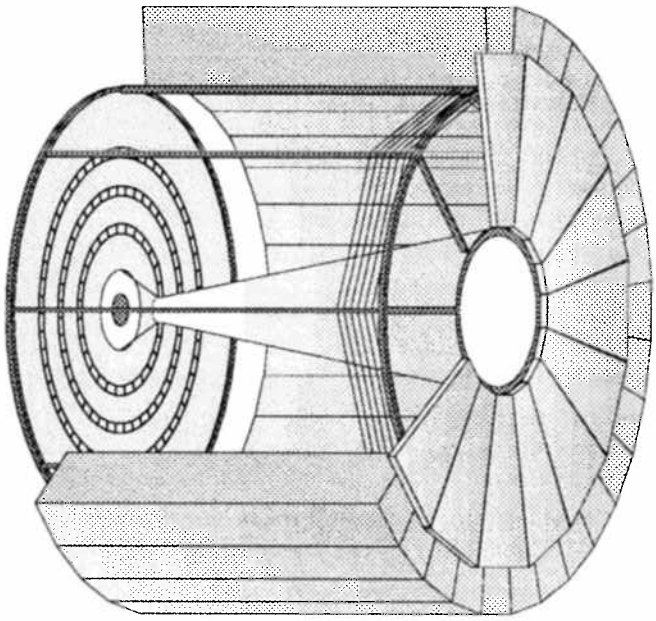

Figure 2: *A three-dimensional view of the Huygens detector system.*

and in size, to maximally constrain the theoretical models.

As a start, we have studied the system $^{36}Ar + ^{48}Ti$ at two incident energies: at 15 and 95 MeV/u. The analysis of the experimental data is under way.

## 4 Acknowledgements

We would like to acknowledge the availability and installation of the MUR by the laboratory LPC.

## References

[1] E.A. Bakkum *et al.*, Phys. Rev. **C39** (1989) 2094.
K.A. Griffioen *et al.*, Phys. Rev. **C40** (1989) 1647.
E.A. Bakkum *et al.*, Nucl. Phys. **A511** (1990) 117.
K.A. Griffioen *et al.*, Phys. Lett. **B237** (1990) 24.
R.J. Meijer *et al.*, Phys. Rev. **C44** (1991) 2625.
P. Decowski *et al.*, Phys. Rev. **C46** (1992) 667.

[2] A. Oed, Nucl. Instr. Meth. **A263** (1988) 351.
A. Oed *et al.*, Nucl. Instr. Meth. **A284** (1989) 223.

[3] G. Bizard *et al.*, Nucl. Instr. Meth. **A264** (1986) 483.

[4] P. Schotanus *et al.*, Nucl. Instr. Meth. **A310** (1991) 523.

[5] C.A. Ogilvie *et al.*, Phys. Rev. **C40** (1989) 2592.

[6] T.M.V. Bootsma *et al.*, Nucl. Instr. Meth. **A324** (1992) 399.

[7] T.M.V. Bootsma *et al.*, Nouvelles du GANIL **43** (1992) 19.

[8] T.M.V. Bootsma, PhD thesis Utrecht University (1993).

# Test and Calibration of Particle Detector ERNE

M. Lumme, E. Valtonen and T. Eronen
Space Research Laboratory, University of Turku, Finland

M. Lewitowicz and D. Bazin
GANIL Caen, France

## 1. Introduction

ERNE (Energetic and Relativistic Nuclei and Electrons experiment) will be launched into a halo type orbit around the L1 liberation point of the Earth-Sun system on-board the Soho spacecraft, which is a joint mission of ESA and NASA. ERNE will study the solar processes which produce energetic ions and electrons in the interplanetary space.

ERNE has two detector systems: the Low Energy Detector (LED) measures ions up to a few tens of MeV/n and the High Energy Detector (HED) extends the energy ranges of ions up to hundreds of MeV/n. Both sensors are capable of identifying ions from hydrogen up to the iron group of elements.

The purpose of the experiment at GANIL was to test the overall performance of the ERNE Flight Model as well as to calibrate the instrument. Further, acquisition of data needed for calculating the response of particles in the two HED scintillator detectors was foreseen as one important outcome of the test runs.

## 2. LED (Low Energy Detector)

LED consists of detector layers D1, D2, and AC. Layer D1 is composed of seven circular detectors D11-D17 in order to minimize the path length variation. Two of these are surface barrier detectors with a nominal thickness of 20 μm and the others are 80 μm thick ion implanted detectors. D2 is a 1000 μm ion implanted surface passivated detector. Each D1 detector operates in coincidence with D2 and in anticoincidence with AC.

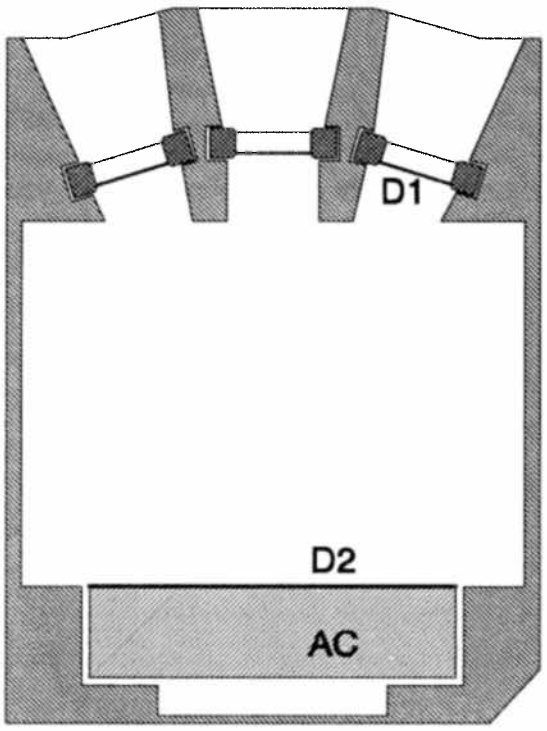


The energy range is 1.3 - 13 MeV/n for protons and $^4$He and higher for heavier nuclei. The geometrical factor of the detector is 0.9 cm$^2$ sr.

## 3. HED (High Energy Detector)

HED consists of two pairs of silicon strip detectors (S1, S2), a pair of thick conventional silicon detectors (D1), and of two scintillators (D2, D3). D2 is an 8 mm thick CsI(Tl) crystal and D3 a 15 mm thick BGO. The scintillators are surrounded by an active anti-coincidence shield (AC).

The energy range is 11-120 MeV/n for protons and $^{4}$He and 25-540 MeV/n for heaviest nuclei (Z < 30). The geometrical factor varies from 25 to 40 cm$^2$ sr depending on particle type and energy.

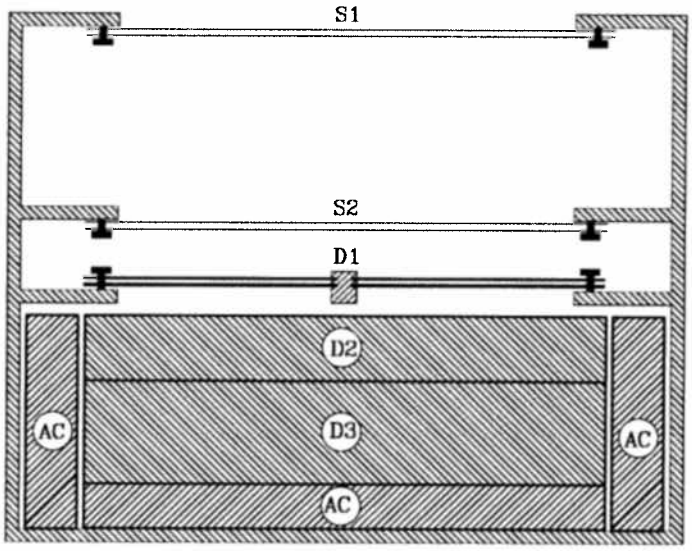


## 4. Experiment E217 (1993)

Total of nine test runs were carried out at GANIL in August 1993 by using a 60 MeV/n $^{84}$Kr primary beam together with various targets and LISE spectrometer setups. The rigidity of secondary particles ranged from 388 to 844 MV giving good coverage of energy ranges of the instrument. Excellent coverage of the elements which will be measured in space was achieved.

ERNE Sensor Unit (ESU) was mounted on a stand at the end of the beam line at ambient pressure. ESU contains the sensors and all the necessary electronics. This includes a data processing unit, which collects digitized signals and periodically transfers the observed events to the data collecting system.

## 5. Results/LED

In this test only particles incident in the D17 section were used. LED electronics is a relatively simple construction with two amplifier gain ranges in D1 and three in D2. Calibration of these five amplifiers included determination of offset and a linear coefficient. The result of the calibration has now been implemented into the on-board analysis software table and this table will further be updated by in-flight calibration.

Since a great majority of the particles which matched the low energy range covered by LED were those with A >> 2Z, which is not well covered by our analysis software, the isotopes were identified directly from scatter plots. An example of the analyzed particles is shown in the figure below where the gains were D17=HI and D2=MED. The Particle Identification Number (PIN) is defined by the relation:
PIN = Z + 0.12(A-2Z).

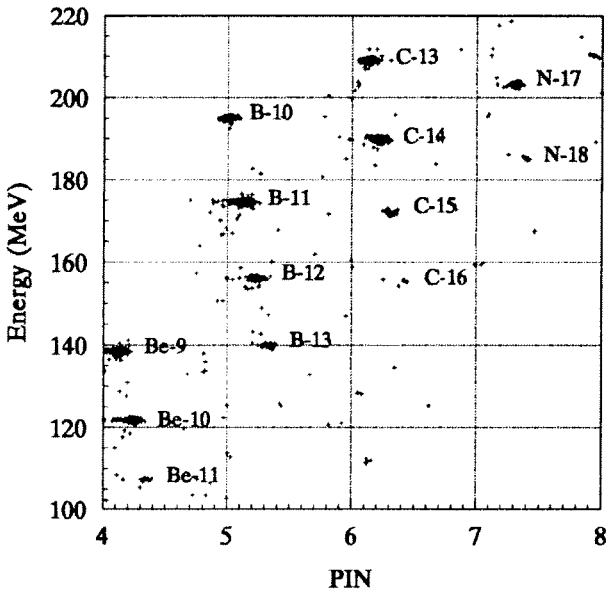


## 6. Results/HED

Analysis of HED data was started by a performance check where the digital electronics Gate Array STATUS-Word was inspected to see if any internal errors are present. The error rate was of order of 2 % which is very satisfactory and is usually caused by two or more particles hitting the detector simultaneously.

The calibration of the various HED amplifiers is an elaborate task since the total number of calibration parameters is 60. In this experiment only one quadrant was exposed and since the scintillators were not calibrated in this work the number of parameters was reduced down to 28.

The spatial resolution of the position sensitive 300 μm thick Si-strip detectors is determined by the charge propagation in the strip detector capacitive chain and by the noise of the electronics. By using the data from previous accelerator tests in modeling of each strip detector individually we have determined the ERNE Technical Model charge propagation functions in detector layers S1 and S2. This procedure was now repeated for the Flight Model by using the present data, and in that procedure both the charge propagation functions and the S-detector offsets and amplifier ratios were determined. However, since the beam was narrow and only a part of the detector layers were covered the uncertainty in this requires further calibration during the Soho flight.

The energy calibration was started with four high rigidity light particles (deuteron, triton, $^{4}$He and $^{7}$Li) which could be easily identified in the scatter plots by comparing the pulse heights in several detector layers. In this procedure we used data from one

test run only (number 6) and this gave the pulse height-to-energy coefficients in the HI-gain channels. We also obtained a confirmation for the previously determined offsets.

The next step was to calibrate the MED-gain channels. The particles needed in this were easily identified and the calibration was done with acceptable accuracy.

The last step was to calibrate the LO-gain channels. This was difficult due to the straggling of the heavy particles which stopped in the lower part of S2 or in D1. However, also this calibration was successful and as a result all the Si-detectors of the ERNE Flight Model have now been calibrated.

The final procedure in the analysis is to compare the events with typical behavior of particles with theory and remove the events which do not fit in due to straggling or errors in pulse height. This significantly improves isotopic resolution. Below are shown two figures, the first one giving a sample of data in measurement 3 and the second one where events with error higher than 7 % have been rejected. The total number of events was 2146 and the number of rejected events was 468.

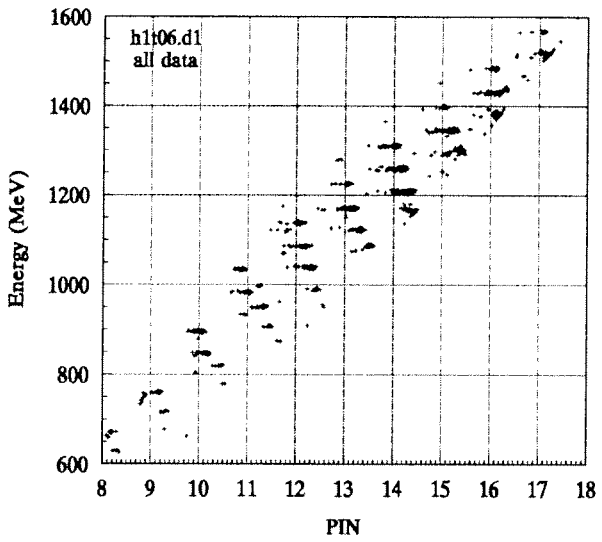


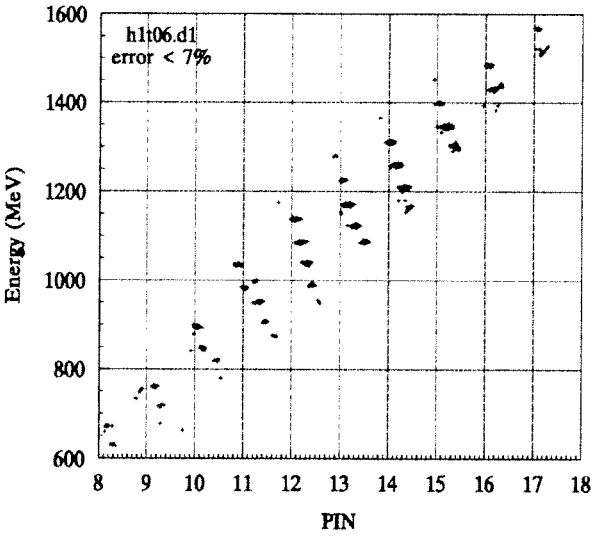



## Acknowledgements

We wish to thank the "Comité des Expériences de Physique Nucléaire du GANIL" for giving us the test opportunity and the GANIL staff for the work done during the tests.

# STOCHASTIC MEAN FIELD APPROACH AND INSTABILITIES

*Ph.Chomaz*[1], *M.Colonna*[1,2] *and A.Guarnera*[1,2]

[1])*GANIL, B.P. 5027, F-14021 Caen Cedex, France*

[2])*Laboratorio Nazionale del Sud, INFN*
*44, Via S.Sofia, 95125 Catania, Italy*
*and*
*Dipartimento di Fisica dell' Universitá di Catania*

ABSTRACT

Concerning nuclear matter, we discuss the spinodal instability. We first explain why any reduced description, such as a mean field approximation, is stochastic in nature. We show that the introduction of this stochastic dynamics leads to a predictive theory in a statistical sence whatever the individual trajectories are characterized by the occurence of bifurcations,instabilities or phase transitions. In such a critical situation, we explore the possibility to replace the stochastic part of the collision integral in the *Boltzmann − Langevin* model by the numerical noise associated with the finite number of test particles in ordinay *BUU* treatment.

The complete treatment of a many-body dynamics requires the consideration of the correlated evolution of a huge number of degrees of freedom which is in general impractical. A tractable approximation is to retain only a small part of the dynamical information (namely the most pertinent variables such as the one-body observables or collective modes) and to project the evolution onto the associated manyfold [1]. In particular, conserving only the one-body density leads to the well known mean field approximation. In general, the projected equation of evolution for the retained variables will be non-linear and therefore the dynamics may exhibit features such as instabilities, bifurcations and chaos.

The lack of full information about the state of the system, both initially and in the course of time, acts as a stochastic term in the effective equation of motion for the retained variables, because they characterize an entire ensemble of microscopically different states of the system. In effect, this ensemble acts as the heat bath in Brownian motion and the equation of motion will be of the *Langevin* type. In this case one is forced to consider not only one single trajectory, in the projected manyfold, but an ensemble of trajectories which differ because small fluctuations in the evolution may be propagated very differently by the deterministic but non-linear part of the effective equation of motion. In such a case, when chaos and bifurcations are encountered during the evolution, the mean average trajectory (mean field trajectory in the case of the projection on one-body observables) is no more defined. However, it must be noticed that the stochastic ensemble of trajectories is

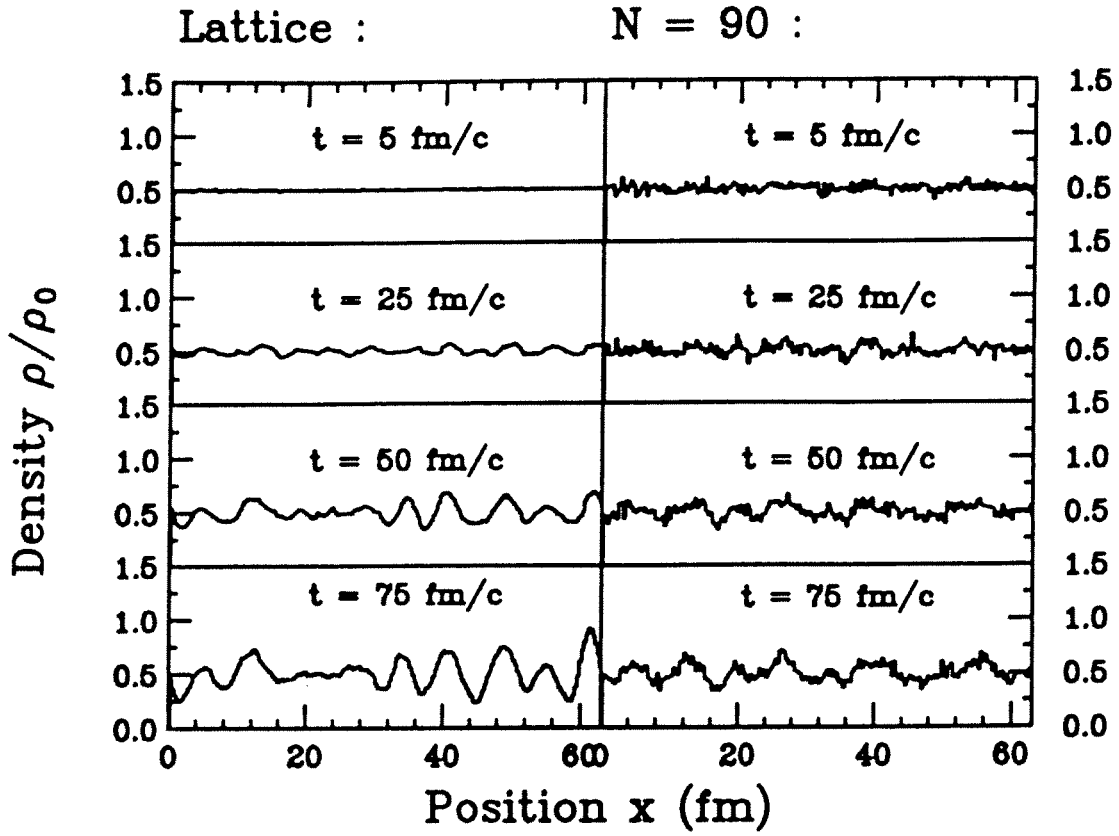


**Fig. 1.** The density profile $\rho(x,t)$ associated with one particular trajectory at four different times $t$, for the lattice calculation (part *a*) and for the test-particle simulation (part *b*).

perfectly defined.

This is in fact a general property of stochastic approaches: whatever the underlying (without stochasticity) dynamics is unpredictable (such as in deterministic chaos) the introduction of a stochastic term will suppress its deterministic character but will restaure its predictive power. Let us consider in the following, as a stochastic mean field approach, the *Boltzmann – Langevin* (*B. – L.*) theory [2,3]. This approach has been carefully tested in many physical scenarii [4]. In particular, it was shown that the ensemble of trajectories does converge to the right statistical equilibrium. In presence of instability the *Langevin* term provides a mechanism to break the possible symmetries and to test the mean field instabilities.

To illustrate these ideas we have considered an idealized case of a two-dimensional torus at half normal density and at a temperature T=3 $MeV$. For the considered force, (see ref. [5] for more details) this system lies in the spinodal instability region, i.e. the region where the system is unstable against variation of its density.

Fig. 1a presents a lattice simulation [6] of the *Boltzmann – Langevin* evolution in which the one-body distribution function $f$ experiences a stochastic evolution and therefore fluctuates, in response to the random effect of the *Langevin* force.

Since the mean field is unstable, these fluctuations are amplified and eventually lead to the formation of fragments. It is important to remark that at the initial time the density distribution is flat; as the time increases, fluctuations coming from the stochastic part of the collision integral are breaking this initial symmetry, leading to clusterization. Since calculations of the $B. - L.$ type are not feasible in 3D, because they need a huge computer time, we propose to replace the complicated *Langevin* term by a simple noise. In particular, we try to take advantage of the noise associated to the use of a finite number of test particles in ordinary $BUU$ simulations. In Fig. 1b, we show the same time evolution in the case of a $BUU$ calculation using 90 test particles. Now fluctuations are present since the beginning due to the finite sampling of the phase space distribution but starting from a given time ( $t \approx 50\ fm/c$) the evolution becomes comparable to that of the lattice calculation (part a), reaching finally a similar structure. One can see from the figure that if the used number of test particles is suitable, it is possible to reproduce the results of the lattice calculations. In our case it happens using 90 test particles per nucleon. Anyway, there is a range of test particle numbers which could be used obtaining not very much different results. This is due to the fact that since the instabilities are exponentially increasing the time to reach a given amplitude of the fluctuation is a logarithmic function of the number of test particles per nucleon.

In conclusion, we have justified the use of stochastic mean field approaches and clarified the possible role of chaos. We have discussed dynamical spinodal instabilities and proposed a simplified stochastic approach to deal with the study of the critical situations that may appear in nuclear collisions at intermediate energies. Many thanks are due to P. Fox for his important role in the elaboration of this Work.

## References

1. R. Balian, Y. Alhassid, and H. Reinhart, Phys. Rep. **131**(1986)1.
2. S. Ayik and C. Gregoire, Phys. Lett. B212 (1988) 269; Nucl. Phys. A513 (1990) 187
3. J. Randrup and B. Remaud, Nucl. Phys. A514 (1990) 339
4. G.F. Burgio, Ph. Chomaz, and J. Randrup, Nucl. Phys. A529 (1991) 157
5. M. Colonna, G.F. Burgio, Ph. Chomaz, M. Di Toro, and J. Randrup, Phys. Rev. C, in press.
6. G.F. Burgio, Ph. Chomaz, and J. Randrup, Phys. Rev. Lett. 69 (1992) 885

# PawGx an On-line, off-line data analysis for TAPS

Frédéric Lefèvre, Pascal Lautridou, Miguel Marqués, Tomasz Matulewicz, Reint Ostendorf, Yves Schutz,
for the TAPS collaboration : GANIL-Gießen-Groningen-GSI-Valencia

The TAPS detector was at GANIL during the fall 1993. The experimental setup consisted of TAPS with its 320 $BaF_2$ detectors each equipped with a plastic veto, the SPEG a magnetic spectrometer, and a forward wall for detecting light charged particles composed with 64 phoswitchs. We describe here the new on-line, off-line control and analysis environment specifically developed for this experimental sertup.

## Goals

The primary goal of the on-line control and analysis software is to provide the user a way to monitor individual detectors, like a drift chamber in the SPEG, and to correlate parameters from one or more detectors. Hence not only individual detector failure could be detected, but also physical data, like invariant mass spectrum, could be calculated on-line allowing us to optimize more global parameter like trigger's scaledown. As secondary requirement this on-line control software has to look like the off line analysis software.

## The acquisition software

In the fall of 1993,the taps acquisition software was based on GOOSY [1] running on a stand alone VaxStation 3200. This computer wrote data on exabyte and was able to distribute raw data by Decnet to other VaxStations on a separate Vax cluster. On this cluster the on-line analysis could be performed with GOOSY. Despite its on-line off-line analysis capabilities, GOOSY was not suitable for our use.

## The PawGx environment

As the usual analysis package at GANIL is the PAW [2] system, we chose to use it as a base for the on-line control software. As a starting point we used the libraries developed at GSI for the FOPI detector analysis [1]. We defined data structures for each detector, TAPS, SPEG, Forward Wall using the CERN dynamic memory manager for the fortran language, ZEBRA [3]. This allowed us to write independent algorithms to handle each detector separatly, and to collect all results in an easy way. Every part of the analysis can be turned on or off using flags that can be set or reset interactively during a run.The resulting software is named PawGx [5].

We wrote a new communication routine, between PawGx and GOOSY by using a Global section. A single GOOSY analysis process reads the raw data coming from the acquisition via Decnet, and copied these data on a VMS Global Section. Then this Global Section, which is one way to implement shared memory for VMS, is read by a PawGx analysis process. PAW is a single process program, so it is not possible for PAW, and therefore for PawGx to collect data while running an interactive session. To overcome this drawback, we used a scheme called writer-drawers.

## The PawGx writer process

A PawGx process called the writer, is linked to the GOOSY analysis and reads the global section. The writer is configured to do some physical analysis on an event by event basis. In this analysis there are low level features like energy and time calibration, particle

discrimination, as well as higher level features like shower reconstruction, cosmic ray identification, fragment identification in SPEG, two photon invariant mass reconstruction, and so on. The configuration of the analysis is controlled by flags which can be set interactively. Results of this analysis are stored into NTuples[4]. The NTuples contain physical parameters like energy, momentum, type of particle, multiplicities, from the three detectors individually and/or from the three detectors together allowing for correlation. NTuples are automaticaly stored on disk when full, and a new NTuple file is opened.

## The histogram builder

In a second layer, there are histogram builders. These programs automatically read NTuples and update histograms for all raw or calibrated parameters of each detector by projecting NTuples. The histograms are stored in PAW controlled global sections. Histograms builders are also in charge of clearing the NTuples files in order to avoid disk overflows.

## The PawGx drawer process

One or several PawGx or standart PAW processes called drawers can read NTuples and histograms and display their content in a fully interactive way. A library of KUIP macros (also called Kumacs) has been written to simplify the execution of repetitive tasks.

## Software testing

In addition to this software, a test bed was written in C to simulate an acquisition process. This simulation allowed us to debug all the PawGx environment before the setting of TAPS at GANIL, and thus saving time for setting up TAPS, and obtaining a reliable software environment. All this software ran during the 110 shifts of GANIL beam time without any failure.

## Off Line analysis

The software architecture described above evolved to give birth to the TAPS off-line analysis. This analysis is able to fully reconstruct TAPS events. The reconstruction is based on a complete pulse shape analysis, time of flight analysis, and shower reconstruction, and can therefore identify, and monitor rare events such $\gamma$–$\gamma$ and $\pi^0$ events.

Acknowledgement :
We wish to thank Robert Warner from Oak Ridge National Laboratory for his help during the building of the GOOSY-PAW link.

[1] GSI scientific report 1990 p 341
[2] PAW CERN Program library Q121
[3] ZEBRA CERN Program library Q100
[4] HBOOK CERN Program library Y250
[5] F.Lefèvre thèse de doctorat; Université de Caen ; 1993

# AUTHOR INDEX

# AUTHOR INDEX

# II - ACCELERATOR

# OPERATION AND MACHINE IMPROVEMENTS

## A.STATISTICS

This part summarises the beam statistics during the last three years.
Ganil was in operation for 36 weeks in 1991, 33 in 1992 and 37 in 1993. The operation is based continuously on several periods of 5 up to 9 weeks .

| Year | Weeks | runs | weeks per run | hours |
|---|---|---|---|---|
| 1991 | 36 | 7 | 4,6,5,7,4,6,4 | 5652 |
| 1992 | 33 | 5 | 7,6,7,6,7 | 5261 |
| 1993 | 37 | 5 | 8,7,9,7,6 | 5933 |

Table 1 : Organisation of the Operations

Next table show some aspects of the operation from the 1991 to 1993 periods.

| | **Planned Time (hours)** | **Effective Time (hours)** | **Eff./Plan. %** | **Effective %** |
|---|---|---|---|---|
| **Beam Tuning** | 3439 | 3347.5 | 97.34 | 20.57 |
| **Physics Experiments** | 10867 | 11006 | 101.28 | 67.61 |
| **Industrial Applications** | 530 | 504 | 95.09 | 3.10 |
| **Machine Studies** | 1272.5 | 1193 | 93.5 | 7.33 |
| **Miscellaneous** | 194 | 227 | 117.01 | 1.39 |
| **Total** | 16302.5 | 16277.5 | | 100 |

Table 2 : Time repartition

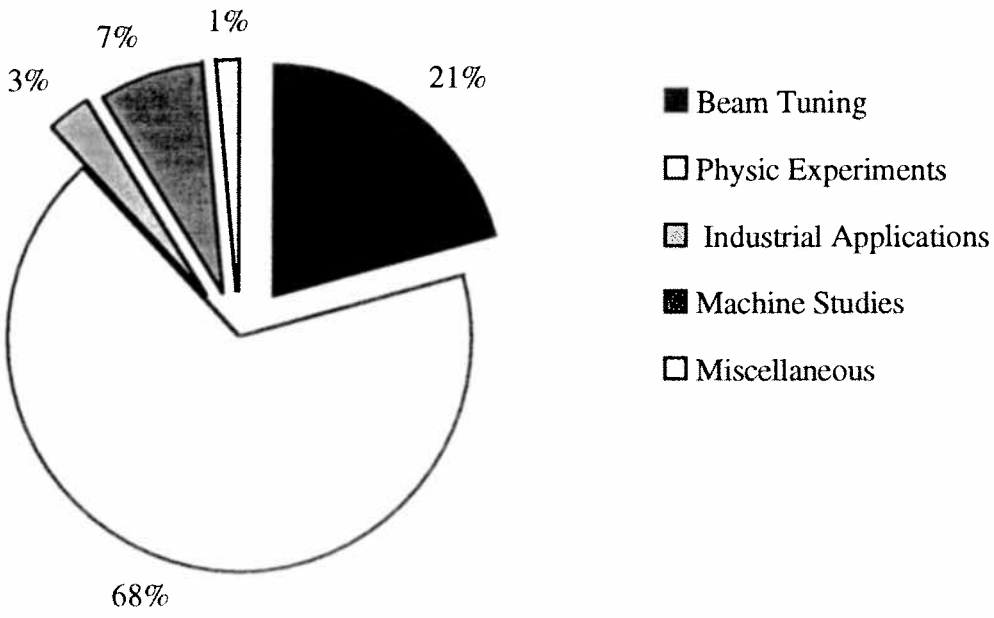

| | Hours | % |
|---|---|---|
| **Available beam** | 10233 | 88.90% |
| **Unavailability : tuning** | 493.75 | 4.29% |
| **Unavailability : failures** | 687.25 | 5.97% |
| **Maintenance** | 96.25 | 0.84% |
| **Total physics operation** | 11510.25 | 100 |

Table 3 : Availability beam to users (as shown in table 3, failure rates are low, less than 6%)

**Effective beam availibility** $\frac{\mathbf{10233}}{\mathbf{11510.25 - 96.25}}$ **x 100 = 89.65%**

| | Rate % | Hours |
|---|---|---|
| **Power supply** | 13.97 | 158 |
| **Equipment's** | 14.24 | 161 |
| **Electronics** | 3.76 | 42.5 |
| **Safety** | 5.70 | 64.5 |
| **Vacuum** | 8.20 | 92.75 |
| **RF System** | 26.69 | 301.75 |
| **Cooling** | 8.03 | 90.75 |
| **Electricity** | 4.80 | 54.25 |
| **Software** | 8.84 | 100 |
| **Miscellaneous** | 5.77 | 65.25 |

Table 4 : Distribution of failures

| Nature | IONS | Energy (MeV/u) | Hours | Rate % |
|---|---|---|---|---|
| Gas | 12 C 3/6+ | 60-75-95 | 930 | 6.26 |
| Gas | 14 N 3/7+ | 95 | 444 | 2.99 |
| Gas | 16 O 3/8+ | 44 | 128 | 0.86 |
| Gas | 16 O 4/8+ | 95 | 106 | 0.71 |
| Gas | 17 O 4/8+ | 84 | 141.25 | 0.95 |
| Gas | 18 O 4/8+ | 63 | 750 | 5.05 |
| Gas | 22 Ne 6+ | 14.35 | 122 | 0.82 |
| Gas | 20 Ne 3/10+ | 48 | 176 | 1.18 |
| Gas | 20 Ne 5/10+ | 95 | 288.5 | 1.94 |
| Gas | 20 Ne 6/10+ | 95 | 189.5 | 1.28 |
| Metal. | 24 Mg 5/12+ | 70 | 170 | 1.14 |
| Metal. | 24 Mg 7/12+ | 95 | 186 | 1.25 |
| Gas | 36 Ar 4/16+ | 27 | 251 | 1.69 |
| Gas | 36 Ar 5/16+ | 32 | 118.5 | 0.80 |
| Gas | 36 Ar 5/17+ | 37-44 | 544 | 3.66 |
| Gas | 36 Ar 9/18+ | 95 | 222 | 1.49 |
| Gas | 36 Ar 10/18+ | 95 | 1547 | 10.41 |
| Gas | 40 Ar 7/17+ | 45 | 144 | 0.97 |
| Gas | 40 Ar 9/18+ | 77.2 | 263 | 1.77 |
| Metal. | 52 Cr 10/23+ | 75 | 121 | 0.81 |
| Metal. | 58 Ni 7+ | 5 | 146.5 | 0.99 |
| Metal. | 58 Ni 10/26+ | 68.7 | 229 | 1.54 |
| Metal. | 64 Ni 10/26+ | 61 | 155 | 1.04 |
| Metal. | 64 Zn 13/29+ | 79 | 241.5 | 1.62 |
| Gas | 84 Kr 13+ | 9.1 | 61.5 | 0.41 |
| Gas | 84 Kr 11/31+ | 39.5 | 193 | 1.30 |

| Nature | IONS | Energy (MeV/u) | Hours | Rate % |
|---|---|---|---|---|
| Gas | 84 Kr 13/33+ | 60 | 325 | 2.19 |
| Gas | 86 Kr 13+ | 8 | 146.5 | 0.99 |
| Gas | 86 Kr 14+ | 9.1 | 135.5 | 0.91 |
| Gas | 86 Kr 12/31+ | 43.1 | 83 | 0.56 |
| Gas | 86 Kr 14/34+ | 60 | 713 | 4.80 |
| Metal. | 93 Nb 14/33+ | 31 | 93.5 | 0.63 |
| Metal. | 107 Ag 18/38+ | 36.4 | 64.5 | 0.43 |
| Metal. | 109 Ag 18/38+ | 35 | 79.5 | 0.53 |
| Metal. | 112 Sn 17/43+ | 58 | 248 | 1.67 |
| Gas | 125 Te 17/38+ | 27 | 243.5 | 1.64 |
| Gas | 129 Xe 18+ | 6.7 | 128 | 0.86 |
| Gas | 129 Xe 15/41+ | 30.6 | 189 | 1.27 |
| Gas | 129 Xe 18/44+ | 44 | 719.5 | 4.84 |
| Gas | 129 Xe 19/46+ | 50 | 225 | 1.51 |
| Gas | 132 Xe 18/45+ | 45.4 | 499.5 | 3.36 |
| Metal. | 155 Gd 19/47+ | 36.1 | 235 | 1.58 |
| Metal. | 157 Gd 19/47+ | 35.1 | 54.5 | 0.37 |
| Metal. | 181 Ta 23/57+ | 39.5 | 265 | 1.78 |
| Metal. | 181 Ta 24/55+ | 36 | 102 | 0.69 |
| Metal. | 181 Ta 24/57+ | 39.6 | 167.5 | 1.13 |
| Metal. | 208 Pb 24+ | 4.98 | 62 | 0.42 |
| Metal. | 208 Pb 25+ | 5,4 | 193.5 | 1.30 |
| Metal. | 208 Pb 23/56+ | 29 | 874 | 5.88 |
| Metal. | 238 U 24/58+ | 24 | 240 | 1.61 |
| Metal. | 238 U 24/59+ | 24 | 907 | 6.10 |

Table 5 : Beam performances during these three years and diagram of beams into specific domains at GANIL

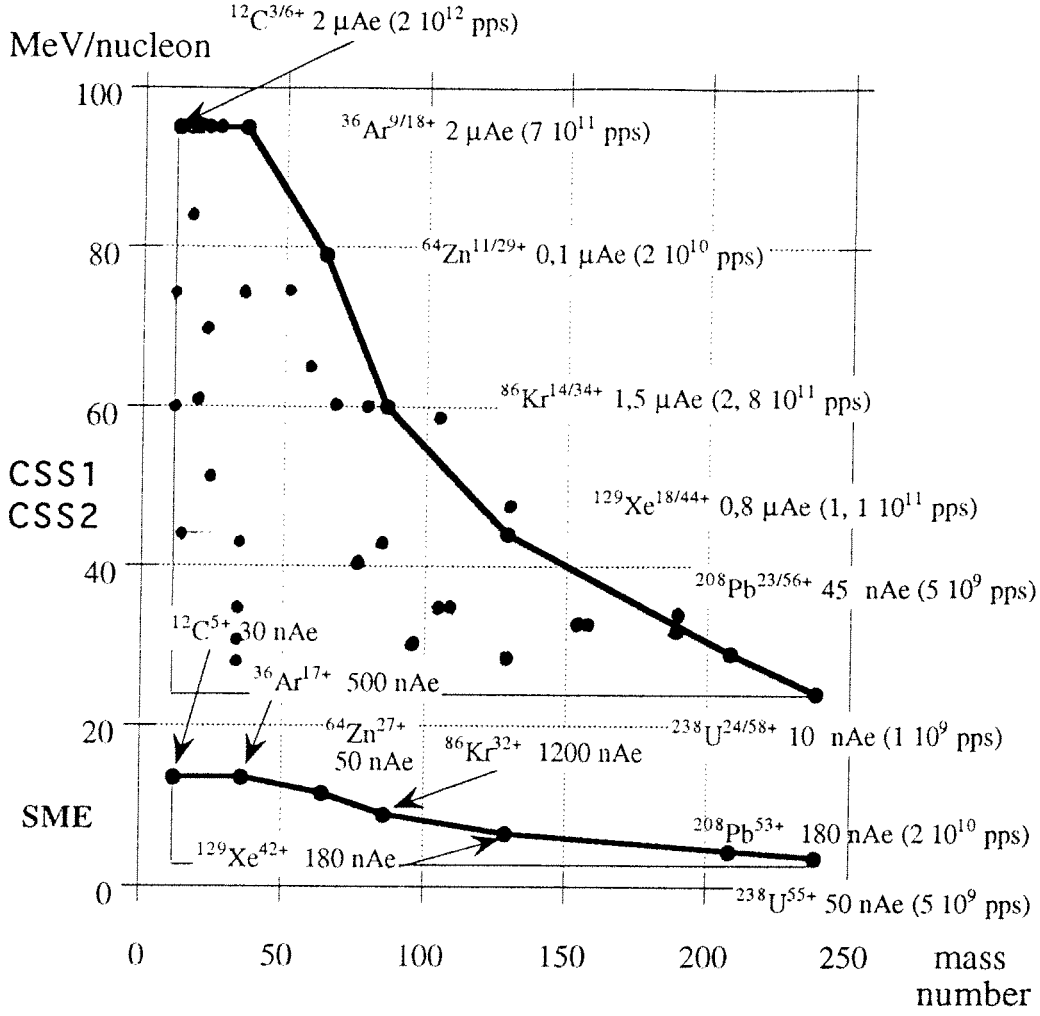


| EXPERIMENTAL AREAS | EXPERIMENTS NUMBER | HOURS | RATE % |
|---|---|---|---|
| D1 | 39 | 1259.25 | 11.23 |
| SIRA | 8 | 709 | 6.32 |
| LISE | 32 | 2825.75 | 25.19 |
| INDRA | 17 | 845.75 | 7.54 |
| NAUTILUS | 11 | 525 | 4.68 |
| ORION | 7 | 685.75 | 6.11 |
| DEMON | 3 | 353.75 | 3.15 |
| SPEG | 20 | 2359.75 | 21.04 |
| SAIF | 24 | 1336.25 | 11.91 |
| CSS | 6 | 316 | 2.82 |
| TOTAL | 167 | 11216.25 | 100 |

Table 6 : Time distribution into the different experimental areas

Table 7 List of the actual beam capabilities at GANIL

| ION/M | ETAT DE CHARGE | FREQUENCE HF (MHz) | ENERGIE FINALE (MEV/u) | INTENSITE REGLEE SUR CIBLE (6) | | CARACTERISTIQUES DES FAISCEAUX | | |
|---|---|---|---|---|---|---|---|---|
| | | | | pps x $10^{11}$ | nAe | ± ΔW/W mi-hauteur ($10^{-3}$) | Δt mi-hauteur ns | INTENSITE nAe |
| C 12 | 3/6 | 13,45 | 96,3 | 20,8 | 2000 | 0,30 | - | 173 |
| C 13 | 3/6 | 10,97 | 60 | 31,25 | 3000 | | | |
| C 13 | 3/6 | 12,13 | 75,03 | 25 | 2400 | | | |
| N 14 | 3/7 | 13,45 | 95 | 18,75 | 2100 | | | |
| O 16 | 3/8 | 9,52 | 44 | 15,6 | 2000 | | | |
| O 16 | 3/8 | 11,76 | 70 | 11,7 | 1500 | | | |
| O 16 | 4/8 | 13,37 | 95 | 11,7 | 1500 | | 0,5 | 130 |
| O 16 | 4/8 | 13,45 | 95 | 15,6 | 2000 | | | |
| O 16 | 5/8 | 13,45 | 95 | 16,40 | 2100 | | | |
| $^{(5)}$O 17 | 4/8 | 12,75 | 84 | 9,8 | 1250 | | 0,64 | 150 |
| $^{(1)}$O 18 | 3/8 | 10,1 | 50 | 11,7 | 1500 | | | |
| $^{(1)}$O 18 | 4/8 | 11,225 | 63 | 7,03 | 900 | | | |
| $^{(1)}$O 18 | 4/8 | 12,2 | 76 | 16,4 | 2100 | 0,64 | 0,2 | 6 |
| Ne 20 | 3/10 | 9,893 | 48 | 21,87 | 3500 | 0,32 | | |
| $^{(4)}$Ne 20 | 5/10 | 13,45 | 95 | 18,75 | 3000 | - | 0,45 | 1000 |
| $^{(4)}$Ne 20 | 6/10 | 13,45 | 95 | 12,5 | 2000 | | | |
| $^{(4)}$Mg 24 | 5/12 | 11,77 | 70 | 3,1 | 600 | | | |
| $^{(4)}$Mg 24 | 7/12 | 13,45 | 95 | 1,88 | 360 | | | |
| $^{(1)}$Ar 36 | 4/16 | 7,55 | 27,1 | 3,54 | 900 | | 0,84 | 150 |
| $^{(1)}$Ar 36 | 5/16 | 8,19 | 32 | 4,88 | 1250 | | | |
| $^{(1)}$Ar 36 | 5/17 | 8,77 | 37 | | | | | |
| $^{(1)}$Ar 36 | 5/17 | 9,31 | 42 | 3,67 | 1000 | 0,50 | | |
| $^{(1)}$Ar 36 | 5/17 | 9,478 | 44 | 2,94 | 800 | | 0,9 | |
| Ar 36 | 9/18 | 13,45 | 95 | 1,4 | 400 | | 0,26 | 10 |
| Ar 36 | I0/18 | 13,45 | 95 | 2,8 | 800 | | 0,3 | 10 |
| Ar 40 | 6/15 | 8,66 | 36 | 2,1 | 500 | | | |
| Ar 40 | 7/17 | 9,6 | 45 | 3,68 | 1000 | 0,35 | | 1000 |
| Ar 40 | 7/17 | 11,77 | 70 | 3,67 | 1000 | 0,79 | 0,5 | 340 |
| Ar 40 | 7/18 | 7,94 | 30 | | 300 | | | |
| Ar 40 | 9/18 | 12,27 | 77,18 | 2,8 | 800 | | 0,44 | |
| Ca 40 | 6/19 | 10,1347 | 50,4 | 1 | 300 | | | |
| Ca 40 | 9/20 | 13,455 | 95 | | | | | |
| $^{(2)}$Ca 48 | 8/19 | 11 | 60,3 | 2,78 | 800 | | 0,3 | 360 |
| Cr 52 | 10/23 | 12,15 | 75 | 0,68 | 250 | | | |
| Ni 58 | 10/26 | 11,651 | 68,5 | 1,92 | 800 | | < 1 | 180 |
| Ni 58 | 10/26 | 11,95 | 72,5 | | | | | |
| $^{(5)}$Ni 64 | 10/26 | 11,061 | 61 | 0,72 | 300 | | | |
| $^{(4)}$Zn 64 | 13/29 | 12,42 | 79 | 0,2 | 100 | | < 0,8 | 10 |
| $^{(3)}$Kr 84 | 14/33 | 11 | 60 | 2,8 | 1500 | 0,59 | 0,6 | 900 |
| $^{(3)}$Kr 84 | 11/31 | 9,055 | 39,55 | 1,61 | 800 | 0,45 | 1,2 | 200 |
| $^{(3)}$Kr 84 | 11/36 | 9,055 | 33,18 (C) ralenti | 0,2 | 120 (5π x 5π) | 5 | | |
| $^{(3)}$Kr 84 | 13/33 | 11 | 60 | 0,95 | 500 | | | |
| $^{(1)}$Kr 86 | 12/31 | 9,43 | 43,1 | 0,8 | 400 | | | |
| $^{(1)}$Kr 86 | 14/34 | 11 | 60 | 1,10 | 600 | 0,5 | 0,6 | 10 |
| $^{(4)}$Nb 93 | 14/33 | 8,075 | 31 | 0,53 | 280 | | 1,8 | 250 |
| $^{(4)}$Ag 107 | 18/38 | 8,71 | 36,4 | 0,2 | 120 | | | |
| $^{(4)}$Ag 109 | 18/38 | 8,55 | 35 | 0,2 | 120 | | 1,5 | 80 |
| $^{(3)}$Sn 112 | 17/43 | 10,8 | 57,9 | 0,29 | 200 | | | |
| $^{(5)}$Te 125 | 17/38 | 7,55 | 27 | 0,03 | 16 | | | |
| $^{(2)}$Xe 129 | 14/37 | 7,55 | 27 | 0,42 | 250 | | | |
| $^{(2)}$Xe 129 | 15/38 | 7,935 | 30 | | | | | |
| $^{(2)}$Xe 129 | 15/41 | 8,012 | 30,65 | 0,35 | 230 | 0,5 | 0,6 | 20 |
| $^{(2)}$Xe 129 | 20/44 | 9,4 | 42,8 | 0,99 | 700 | | | |
| $^{(2)}$Xe 129 | 18/44 | 9,52 | 44 | 1,15 | 800 | 0,90 | 0,2 | 18 |
| $^{(2)}$Xe 132 | 18/45 | 9,649 | 45,4 | 0,61 | 440 | 0,6 | | |
| $^{(4)}$Gd 155 | 19/47 | 8,672 | 36,1 | 0,05 | 40 | 0,5 | | |
| $^{(4)}$Gd 157 | 19/47 | 8,562 | 35,1 | 0,03 | 25 | 0,5 | | |
| $^{(4)}$Gd 158 | 19/47 | 8,5073 | 34,7 | 0,07 | 50 | | | |
| $^{(4)}$Ta 181 | 23/57 | 9,055 | 39,5 | 0,044 | 40 | 0,64 | 1,4 | 40 |
| $^{(4)}$Ta 181[a] | 24/55 | 8,66 | 36 | 0,34 | 300 | | 0,8 | |
| $^{(4)}$Ta 181[a] | 24/57 | 9,055 | 39,6 | 0,18 | 160 | | | |
| $^{(4)}$Pb 208 | 23/56 | 7,82 | 29 | 0,049 | 45 | 0,61 | < 1,9 | 30 |
| $^{(4)}$U 238 | 24/59 | 7,13 | 24 | 0,01 | 10 | 0,32 | 1 | 5 |

| ION/M | ETAT DE CHARGE | FREQUENCE HF (MHz) | ENERGIE FINALE (MEV/u) | INTENSITE REGLEE SUR CIBLE (6) | | CARACTERISTIQUES DES FAISCEAUX | | |
|---|---|---|---|---|---|---|---|---|
| | | | | pps x $10^{11}$ | nAe | ± ΔW/W mi-hauteur ($10^{-3}$) | Δt mi-hauteur ns | INTENSITE nAe |
| | | | CSS1 seul | | | | | |
| (1)Ne 22 | 6 | 13,75 | 14,43 | 10,5 | 1000 | | | |
| Ar 36 | 10 | 13,45 | 13,6 | 6,78 | 1085 | | | |
| Ar 40 | 9 | 13,35 | 13,5 | 13,9 | 2000 | | | |
| Ni 58 | 7 | 8,24 | 5 | 2,7 | 300 | | | |
| (3)Kr 84 | 13 | 11 | 9,1 | 10,6 | 2200 | | | |
| (1)Kr 86 | 13 | 10,214 | 7,9 | 9,6 | 2000 | | | |
| (1)Kr 86 | 13 | 10,313 | 8 | 14,4 | 3000 | | | |
| (1)Kr 86 | 14 | 11 | 9,1 | 8,9 | 2000 | | | |
| (4)Gd 157 | 19 | 8,56 | 5,43 | 0,21 | 65 | | | |
| (4)Pb 208 | 24 | 8,16 | 4,98 | 0,62 | 250 | | | |
| (4)Pb 208 | 25 | 8,50 | 5,4 | 1,0 | 400 | | | |

(1) enrichi 99% ; (2) enrichi 70% ; (3) enrichi 90% ; (4) naturel ; (5) enrichi 50% ; (6) pour les ions légers l'intensité est volontairement réduite afin de diminuer le taux de radiation produit avec ECR4 et C01.

- All the beams from CSS1 are available for the SME (with energy between 4 and 13 MeV/u).
- The power of the beam from CSS2 is limited to 400 Watts for the equipment safety.
- Other energies are available by beam slowing-down after CSS2.
- Exotic beams can be produced by fragmentation of primary beams, before the high-energy spectrometer ($^{14}O$ - 70 MeV/u and $^{12}N$ - 65 MeV/u have been produced).
- Light ion beams (p, d, α) can be produced at different energies for detector calibrations.
- Parallel beams and pencil beams can also be obtained on the target.
- $\frac{\varepsilon H}{\varepsilon V}$ ≤ 5 πmm.mrad
- $\frac{\Delta W}{W}$ ≅ some $10^{-4}$ (at half-height)
- $\Delta t$ ≅ 0.5 to 1 ns (at half-height)

for the standard beams from CSS2

**At GANIL, three different beams are performed at the same time. Two concern the high energy physics and the third, the mean energy experiments (SME). 156 experiments during 53.85 per cent of the available beam time for physics.**

**Total for SME : 5510 hours**

## B. MACHINE IMPROVEMENTS

To maintain the actual level of performance of the machine, to follow the increasing demand of users for new characteristics and better quality of beams, to study new equipments, and projects , require to assign a part of operation time for these topics. For the last two years 1991 and 1992, we may distinguish the following items in different applications :

**• UPGRADING PERFORMANCES**
- tuning of CSS2 cyclotron as a rebuncher
- capacitive beam position monitors and automatic beam centring

**• NEW FUNCTIONS**
- a cyclotron as a mass spectrometer

**• MATERIAL EVOLUTIONS**
- commissioning of the new high intensity axial injection
- implementing the new control system at GANIL
- energy deposited by neutrons and gamma rays in the cryogenic system of SISSI
- latest development of multicharged ECR sources
- an on-line isotopic separator test bunch at GANIL

• **OTHER IMPROVEMENTS**
- charge exchange of very heavy ions in carbon foils

Each items is shortly resumed (see below), name of authors, references of full articles, abstracts and short presentations of the results.

## 1. TUNING OF CSS2 CYCLOTRON AS A REBUNCHER

Author : M.H. Moscatello - internal report GANIL561.91/ml

The reduction of the length pulses at a given distance of a cyclotron may be obtained by tuning this cyclotron as a rebuncher. For that, a perturbation of the magnetic field is applied only by correction coils on the last turns of the acceleration process and minimises the increase of energy dispersion and radial length of the beam. This method was calculated for CSS2 cyclotron, so several tunings were made on the machine and up to the experimental areas ; as at least encouraging results were obtained.

*Results*
- reduction by a factor of two of the longitudinal beam length
- beam intensity less than 20% only
- greater beam stability to RF variations

*Difficulties*
- additional beam tuning of 3 to 4 hours
- difficulty to get the optimal value after an incident with the RF phase.

## 2. CAPACITIVE BEAM POSITION MONITORS AND AUTOMATIC BEAM CENTRING

Authors : P. Gudewicz, E. Petit - IEEE Particle Accelerator Conference - May 6-9 1991 San Francisco - p1142

A non-interceptive beam position monitor, made of four capacitives electrodes, has been, designed at GANIL in order to allow a permanent measurement of the ion beam position over a large intensity range (50 enA to 10 eμA). Signal processing is based on a 10 kHz heterodyne and an amplitude to phase conversion in order to measure the beam position. The accelerator is equipped with ten of these probes, six of them on the first beam line. An immediate application of these monitors is the automatic beam centring. For this, two algorithms have been developed using the information on the centre of gravity given by the beam position monitors which is then fed back to the steerers. The first is an iterative method based on an optimisation algorithm (Patter Search, Hooke and Jeeves). The second is a variational method which consists in determining for each steerer and each position monitor, the variation coefficient (mm/A) and solves a linear system. Both of these methods have been used on a section of beam line and have given similar and encouraging results. The next step is to centre the beam on the completely equipped line.

## 3. A CYCLOTRON AS A MASS SPECTROMETER

Authors : P. Bricault, G. Auger, M. Bajard, E. Baron, D. Bibet, A. Chabert, J. Fermé, L. Gaudart, A. Joubert, M. Lewitowicz, W. Mittig, E. Plagnol, Ch. Ricaud, Y. Schutz GANIL Caen,
G. Audi CSNSM Orsay
A. Gillibert CEN/Saclay Gif Sur Yvette
K. Fifield Australia National University Camberra
presented at the 13th International Conference on Cyclotron and their Applications - Vancouver 6-10 July 1992

Taking advantage of the system of coupled cyclotrons at GANIL, a method for mass measurements has been developed. The secondary nuclei are produced in a target located

between the two separated sector cyclotrons by the interaction of a beam coming from the first cyclotron. The prior tuning of this cyclotron for those very low intensities is accomplished using a beam having the same q/A ratio at the right velocity. For fine tuning, a probe inside one sector of the cyclotron has been developed.

*Results*

Despite the complexity of the spectra of the secondary ions, they are sufficiently similar from one species to the other, so that, using one of them as a calibration, it is possible to estimate the masses of the others. Assuming the mass of one nuclei as the reference we are able to derive the masses of the others. The attainable mass resolution is $\frac{\Delta m}{m} = 5\ 10^{-6}$.

## 4. COMMISSIONING OF THE NEW HIGH INTENSITY AXIAL INJECTION

Authors : Ch. Ricaud, E. Baron, J. Bony, M.P. Bourgarel, B. Bru GANIL Caen
R. Vienet LNS CEN/Saclay Gif sur Yvette
presented at the 13th International Conference on Cyclotron and their Applications - Vancouver 6-10 July 1992

The "O.A.I." project, now completed, was undertaken at GANIL in order to obtain a better transmission efficiency and to control the space charge effect with an ECR source installed on a high voltage platform. The first measurements made with various sorts of ions show that a 40% to 50% transmission is routinely achieved through the used for the heaviest ions (Pb, Ta, U) for which the stripper efficiency is weak.

The goal is now the production of exotic nuclei with light ion beams (C, O, Ne, Ar), but the full intensity will be only allowed when safe operation of the other parts of the machine is achieved.

The C01 injector was connected to the CSS's and two beams, Ta and Ne, have already been used for experiments. For 5 and 3 days respectively, 4 eμA of $Ne^{6+}$ were extracted from C01, 50 to 60% of these beams suitable for further acceleration through the CSS's. The stability and the availability of these beams on the target were excellent.

Two main conclusions can be drawn from the results :

- concerning the available intensities out of C01 we obtain for the heaviest ions at least a factor of 10 higher than with C02, which was one of our goals,
- Concerning the very high intensities needed for exotic ion production either by fragmentation or by the ISOL method, we are still faced with the large emittances of the beams extracted from C01. The large values of transverse emittances ($\cong$ 40 - 50 $\pi$ mm.mrad) and of the energy dispersion ($\cong$ 1.5%) do not fit the CSS's acceptance for an acceleration with manageable losses.

Therefore, we will have either to cut in the beam in front of CSS1 or, better, to understand and cure the causes of these large emittances.

## 5. IMPLEMENTING THE NEW CONTROL SYSTEM OF GANIL

Authors : T.Luong, T.André, D.Bibet, L.David, P.de Saint Jores, P.Duneau, C.Galard, J.Galvez, P.Gillette,P.Gudewicz,C.Leboucher, E .Lecorché, E.Lemaître, P.Lermine, J.M.Loyant, C.Maugeais, M.Moscatello, C.Maugeais, D.Outin, P.Pain, E.Petit, F.Regnault, J.Rozé, A.Souf, M.Ulrich, G.Vega
The Accelerator Operation Division GANIL Caen

The new computer control system is conducting the heavy ion accelerator GANIL since the outset of 1993, in a continuous and fully encouraging way. This paper highlights two leading issues :

-a/ The control system implementation featuring hardware architecture and software options ,

-b/ The accelerator controls emphasising man-machine interfaces and user applications. Finally, experience of the first semester is reported and future considerations are addressed.

## 5.1. INTRODUCTION

1.1 The Ganil control system has been rejuvenated in order to keep on matching its capabilities and performances with the escalating requirements of the accelerator operation. These requirements cover the vast spectrum of operator activities (beam setting and tuning, supervision, diagnostics, etc..) within a comfortable environment to achieve efficient and productive machine controls. Evolution potentiality is an additional important issue, considering the current Ganil project to accelerate very high intensity beams and its trend towards radioactive beams.

1.2. The control system renewal has to undergo two kinds of constraints :

-a/ Manpower by having to support, simultaneously and continuously, the old control system (based on a 16bit MITRA computer) which went on conducting the accelerator,

-b/ Operation by having to migrate to the new system in a smooth fashion, i.e. without perturbation of the experimental program.

1.3. The following considerations guided the design and the implementation of the new; system :

- Adopt the distributed architecture boosted by mature local area network technologies and communication protocol, which favours modular structures and easy extensions,
- Buy and don't build hardware and software components which comply with acknowledged open standards, to save development time and to minimise investment over the life of the system,
- Consider ergonomics and stick to windowing, colour graphic oriented operator interface, to achieve efficient man-machine interaction.

The new control system results from the joint effort of the Controls Group and the Electronics Group, the Operation Group, the Parameter Group of the Accelerator Operation Division. This paper reviews its main features.

## 5.2 THE NEW CONTROL SYSTEM

### 2.1. ARCHITECTURE

In contrast with the first control system, the new generation control system features highly distributed intelligence, deployed along three functional levels which intercommunicate by means of an Ethernet local area network (Fig.1) :

i. The HOST level, built around the VAX 6410/VMS and its peripherals, provides a cosy environment for miscellaneous off-line activities : software programming, debugging, data management, look-up displays, theoretical parameter calculations, simulation,... This level may access other facilities of the laboratory (e.g. Physics Acquisition VAX cluster) through the Ethernet LAN or remote laboratories via wide area networks (WAN).

ii. The OPERATOR CONTROL level is devoted to human accelerator controls. This level is ruled by a VAX 4400/VMS. Operator consoles are based on workstations VS4000 and Xterminals VXT2000 for multi-windowing colour graphic displays and shaft knob board for incremental controls (more details in §3.1). The VAX6410 and the VAX4400 are clustered for resource sharing.

iii.The FRONT END level provides local intelligence for field controls. At this level are used :

- Camac front end controllers (FECs) KSI3968 from KINETIC SYSTEMS. Camac FECs integrate the RTVAX300 chip and execute real-time applications under the VAXELN operating system,
- Programmable logic controllers (PLC) S5-135U from SIEMENS and PB400 from TELEMECANIQUE/APRIL. Camac FECs and SIEMENS PLC are directly hooked to the controls Ethernet LAN, while PB400 PLCs are connected to the VAX4400 via a master-slave JBUS link.

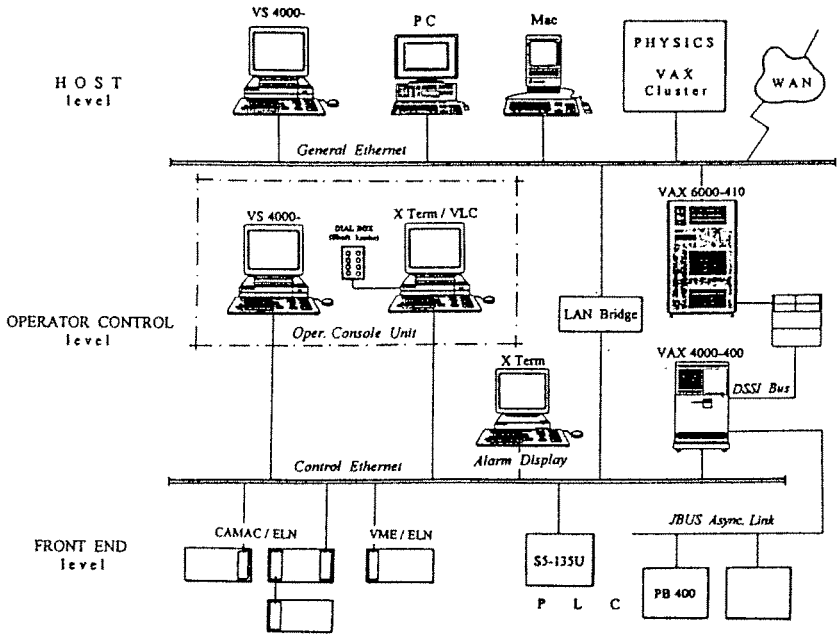


Fig.1 Architecture of the New Control System

## 2.2. SOFTWARE

### 2.2.1. Controls

A key software layer, named GANICIEL, was designed and written in ADA language to match the accelerator environment and to support its controls. GANICIEL rules over the whole control system and makes widely use of the client-server model to fully benefit from the distributed architecture adopted. In particular, it permits to drive the operator consoles and to interface the various components (about 2000) of the machine. At the front-end level, each Camac FEC controls its own set of components (e.g. stepper motors, power converters, ..) through dedicated drivers named "handlers". Basic actions are therefore performed by local intelligence and local live databases. Command messages arriving from the operator consoles are dispatched to the right processing Camac crates.

### 2.2.2. DATA Management

Data management is a strategic issue, owing to the large spectrum of information to handle (e.g. acceleration conditions, beam parameters, real-time controls, operation logs,..) and the overwhelming amount of data to master. Major realisations include Database for front-end equipment controls hosted in the VAX and fragmented into live databases to be downloaded into the Camac FECs, - Alarm system at management and real-time levels, Operation logs and statistics reporting, Database related to the beam parameters, following an object-oriented approach.

The currently used INGRES RDBMS (Relational Database Management System from the ASK Group) provides a considerable boost in functionality and flexibility. It complies with the SQL standard and supports the W4GL fourth generation language which allows to build graphic database user interface.

### 2.2.3. Supervision

Supervision of PLC at GANIL is based on the IMAGIN software package from SFERCA[1]. In use since fall 1989, it embodies our first step towards the new control system. Its scope spreads wider as time goes by.

[1] With satellite subsets such as a graphic editor, a real-time database, an acquisition module, etc ... Applications are written in ADA and in FORTRAN.

### 2.2.4. User applications

User applications are specifically developed for operators to conduct the accelerator and aim at achieving a high performance control level [2].

## 5.3 FIRST EXPERIENCE AND FUTURE

### 3.1. Commissioning

The new control system was installed in situ and commissioned during the accelerator shut-down, from December'92 to February'93. All hands on deck actively prepared the control environment ( clustering the VAX, upgrading the Camac controllers and restructuring the modules to fit the new network), and proceeded to exhaustively control all the components of the accelerator, in individual mode as well as in global mode.

### 3.2. First user impact

The new control system was rapidly adopted by the user community, thanks to the familiar twin mode of man-machine interaction, and the innovative colour graphic-oriented interface provided.

The operator application set needs to be improved . This weak point, which is normal considering the youth of the system, will be overcome progressively, in the near future.

The experience of this first semester is rather satisfactory. It definitely qualifies the new control system to conduct the accelerator.

## 5.4 CONCLUSIONS

**4.1.** A crucial step was accomplished to provide the accelerator with a high performance and flexible computer control environment.

**4.2.** This long haul effort reached its challenging goal on schedule, thanks to two deciding factors:

-a/ a proper strategy of "buy-don't-build" standard off the shelf products (hardware and software) to benefit from state-of-the-art industry techniques and to save manpower, -b/ a strong-willing staff who provided about 40 man-years of highly skilled and productive work spread over three years.

**4.3.** The control system renewal is conducted to completion and switched over in the smoothest possible fashion for the Ganil operation : no disruption of round-the-clock beam acceleration, no beam production program specifically tailored to back up the commissioning of the new system.

**4.4.** The accelerator is operating under the control of the new system since the beginning of this year. Getting started with this system is fast and pleasant, owing to the user-friendly interfaces provided. Though the basic user application environment was experienced as rather adequate, the impact of the users during this first semester was quite positive. No unscheduled shut-down of the machine is caused by a malfunction of the new control system.

**4.5.** To benefit from the large potential capabilities of the new control system, efforts are, from now on, channelled along two main axis regarding : -a/ controls techniques to fulfil dependable services and performances, -b/ accelerator operation to significantly improve the operation timing figures , to provide a high degree of beam availability and to achieve productivity, within comfortable operator controls conditions.

## 6. ENERGY DEPOSITED BY NEUTRONS AND GAMMA RAYS IN THE CRYOGENIC SYSTEM OF SISSI

Authors : E. Baron, L. Bianchi, C. Grunberg, A. Joubert GANIL Caen
J. Dural CIRIL Caen
presented at the 3rd European Particle Accelerator Conference Berlin 24-28 March 1992

SISSI is an ion-optical system consisting of two cryogenic solenoids separated by a target which produces secondary particles under the impact of intense heavy ion beams. Besides the

[2] A considerable effort was undertaken to implement the first wave of ADA applications.

problem of shielding the cryogenic parts against the heat and the charged particles coming from the target, care must be taken of the power deposited in the solenoid windings by neutrons and gamma rays ; although this power is supposedly very small, the cooling capacity of the closed cycle refrigerator (a few watts) must take it into account. Measurements were made by means of a calorimeter simulating the windings and traversed by the neutral particle fluxes produced by C, N, Ne and Ar hitting C and Ta targets ; the results are presented and compared to approximate theoretical predictions.

The experimental results show that the neutron power dissipated in the cold-temperature parts of SISSI can be reduced to a level comparable to the maximum tolerable value under the condition that these parts are shielded by a double layer : a thin cadmium foil wrapped around a more massive copper piece. However, this is only possible if the target thickness is such that it stops no more than 0.5 to 1 kW of incoming beam at 95 MeV/nucleon. On the other hand, the results given by the theoretical model are overestimated by a factor of several units.

## 7. LATEST DEVELOPMENT OF MULTICHARGED ECR SOURCES

Authors : P. Sortais, M. Bisch, M.P. Bourgarel, P. Bricault, P. Lehérissier, R. Leroy, J.Y. Pacquet, J.P. Rataud GANIL Caen
presented at the 3rd European Particle Accelerator Conference Berlin 24-28 March 1992

Since now ten years, the field of multicharged ECR ion source shows a continuous development in order to improve performances, technology and reliability of sources. The very last developments made at GANIL are :

- operation of a copy of the ECR4 source in the afterglow tuning mode (application to the CERN accelerator) and
- design of NANOGAN, an ECR type source using permanent magnets only.

The results associated with new applications of ECR ion sources show that it would be now possible to design new ECR devices especially adapted to pulse operation or highly charge radioactive ion production.

## 8. AN ON-LINE ISOTOPIC SEPARATOR TEST BENCH AT GANIL

Authors : P. Bricault, R. Leroy, M. Lewitowicz, J.Y. Pacquet, M.G. Saint-Laurent, P. Sortais GANIL Caen
A.C. Mueller, J. Obert, J.C. Putaux IPN Orsay
C.F. Liang, P. Paris CSNSM Orsay
J.C. Steclmeyer LPC-ISMRa Caen
presented at the 3rd European Particle Accelerator Conference Berlin 24-28 March 1992

It is planned to use the high energy heavy ion beams provided by the GANIL cyclotron facilities to produce "exotic" beams. At the moment the primary beam intensities are limited to 2 $10^{12}$ pps for light ions. With the new high intensity axial injection system the primary beam intensity will be multiplied by a factor of 10 for light ions from $^{12}C$ to $^{40}Ar$.

In order to determine if heavy ions can be competitive compare to high energy protons for the production of "exotic" nuclei an isotopic separator on-line test bench installed. This test bench is equipped with a very compact ECR ion source made entirely from permanent magnets, operating at 10 GHz.

The first run was with a $^{20}Ne$ beam at 95 MeV/nucleon on a MgO thick target.

Summary of the observed isotopes :

| Isotope | Half life (s) | Primary beam ($nA_p$) | Yield* (particle/s$\mu A_p$) |
|---|---|---|---|
| $^{19}Ne^{1+}$ | 17.2 | 35 | $4.8\ 10^7$ |
| $^{19}Ne^{2+}$ | 17.2 | 35 | $8.9\ 10^6$ |
| $^{19}Ne^{3+}$ | 17.2 | 32 | $1.6\ 10^6$ |
| $^{18}Ne^{2+}$ | 1.67 | 95 | $1.9\ 10^6$ |
| $^{18}Ne^{4+}$ | 1.67 | 90 | $1.9\ 10^5$ |
| $^{23}Ne^{1+}$ | 37.5 | 100 | $6.3\ 10^5$ |
| $^{24}Ne^{1+}$ | $2\ 10^2$ | 110 | $1.5\ 10^5$ |
| $^{13}N^{1+}$ | $6\ 10^2$ | 40 | $3.8\ 10^5$ |

* yield observed on the transport tape, efficiency of the transport system is not taken into account

Table 1

*Results*

Isotopes $^{18,19}Ne$, $^{23,24}Ne$ and $^{13}N$ were extracted and ionised (see Table 1).

The intensity on the target was limited to 1 μAe for handling and damages caused to the thin window at the entrance of the target.

A new site is under study to avoid problems coming from the slow neutrons and background in the experimental room. A new separator is also under consideration ; its resolving power should be much greater than a few thousands in order to have a clean separation for mass numbers less or equal to 100.

## 9. CHARGE EXCHANGE OF VERY HEAVY IONS IN CARBON FOILS

Authors : E. Baron, M. Bajard, Ch. Ricaud GANIL Caen

presented at the 6th Conference on Electrostatic Accelerators and Associated Boosters Montegrotto Terme (Padova) 1st-5th June 1992

The results of several years of operation with heavy to very heavy ions in the GANIL accelerators, along with specific measurements concerning stripping through carbon foils, led to a set of valuable recipes for predicting the characteristics required to obtain a desired charge state distribution. The ion species under study range from Ar to U and the energies from 3.8 to 10.6 MeV/nucleon. A series of measurements was also set up to evaluate the beam losses during acceleration in the three cyclotrons ; with the help of existing models for charge exchange cross-sections, it is shown that vacuum requirements can be fairly accurately determined.

Results :

A series of measurements were carried out with $Xe^{18+}$, $Pb^{23+}$ and $U^{24+}$ in the injector, $Pb^{23+}$ in CSS1 and $Pb^{56+}$ in CSS2. Concerning the injector, in all three cases, the results lie between the two predictions used. At energies higher than 1.4 MeV/nucleon, the fit of the Erb's results should not be extrapolated and only the prediction based on the Betz-Schmelzer approximation was used, providing as good agreements for CSS1 as for the injector. It is only above 5 MeV/nucleon that all estimates fail : the pressure estimated from the Franzke predictions for Pb ions in CSS2 based is 5 times higher that indicated by the measurements.

*Conclusion*

In the absence of detailed knowledge on charge exchange cross-sections for heavy ions traversing solids or gases, simple measurements over a wide range of projectile masses and velocities allow predictions which are significant for the design of injectors and boosters in coupled accelerator systems.

# III - PUBLICATION LIST

# 1992

**EXCITATION OF GIANT RESONANCES 208 PB, 120 SN, 90 ZR, AND 60 NI BY 84 MEV/NUCLEON 17 O IONS**

ALAMANOS N., LIGUORI-NETO R., ROUSSEL-CHOMAZ L., ROCHAIS L., AUGER F., FERNANDEZ B., GILLIBERT A., LACEY R., PIERROUTSAKOU D., BARRETTE J., MARK S.K., TURCOTTE R., BLUMENFELD Y., FRASCARIA N., GARON J.P., ROYNETTE J.C., SCARPACCI J.A., SUOMIJARVI T., VAN-DER-WOUDE A., VAN DER BERG A.M.

*CEN - SACLAY, MC GILL UNIV. - MONTREAL, IPN - ORSAY, KVI - GRONINGEN*

*TOURS SYMPOSIUM ON NUCLEAR PHYSICS*

*TOURS (FR)*

**MEASUREMENT OF GIANT RESONANCES AT ZERO DEGREE : WHY AND HOW ?**

GILLIBERT A., ALAMANOS N., AUGER F., LIGUORI NETO R., PIERROUTSAKOU D., SIDA J.L., BLUMENFELD Y., FRASCARIA N., LAMEHI M., LE FAOU J.H., ROYNETTE J.C., SUOMIJARVI T., CABOT C., MITTIG W., SILVEIRA GOMES P.R.

*DAPNIA/CEN SACLAY, IPN - ORSAY, GANIL - CAEN, UFF (BRASIL)*

*PROCEEDINGS OF THE XXX INTERNATIONAL WINTER MEETING ON NUCLEAR PHYSICS*

*BORMIO*

*INTERNATIONAL WINTER MEETING ON NUCLEAR PHYSICS.30*

RICERCA SCIENTIFICA ED EDUCAZIONE PERMANENTE.91

**ENERGY DAMPING AND INTERMEDIATE-VELOCITY FRAGMENT EMISSION IN PERIPHERAL Kr + Au COLLISIONS AT 43 MeV/u**

STUTTGE L., ADLOFF J.C., BILWES B., BILWES R., COSMO F., GLASER M., RUDOLF G., SCHEIBLING F., BOUGAULT R., COLIN J., DELAUNAY F., GENOUX-LUBAIN A., HORN D., LE BRUN C., LECOLLEY J.F., LOUVEL M., STECKMEYER J.C., FERRERO J.L.

*CRN - STRASBOURG, LPC/ISMRA - CAEN, IFIC/CSIC - BURJASOT*

NUCL. PHYS. A539 (1992) 511.

**DECAY MODES OF 31 Ar AND FIRST OBSERVATION OF BETA-DELAYED THREE-PROTON RADIOACTIVITY**

BAZIN D., DEL MORAL R., DUFOUR P., FLEURY A., HUBERT F., PRAVIKOFF M.S., ANNE R., BRICAULT P., DETRAZ C., LEWITOWICZ M., ZHENG Y., GUILLEMAUD-MUELLER D., JACMART J.C., MUELLER A.C., POUGHEON F., RICHARD A.

*CENB - GRADIGNAN, GANIL - CAEN, IPN - ORSAY*

PHYS. REV. C45, 1 (1992) 69.

**DETERMINATION OF THE 13 N(p,gamma) REACTION RATE THROUGH COULOMB BREAK-UP OF A RADIOACTIVE BEAM**

KIENER J., LEFEBVRE A., AGUER P., BACRI C.O., BIMBOT R., BOGAERT G., BORDERIE B., CLAPIER F., COC A., DISDIER D., FORTIER S., GRUNBERG C., KRAUS L., LINCK I., PASQUIER G., RIVET M.F., SAINT-LAURENT F., STEPHAN C., TASSAN-GOT L., THIBAUD J.P.

*CSNSM - ORSAY, IPN - ORSAY, CRN - STRASBOURG, GANIL - CAEN*

*SECOND INTERNATIONAL CONFERENCE ON RADIOACTIVE NUCLEAR BEAMS*

*LOUVAIN-LA-NEUVE*

*RADIOACTIVE NUCLEAR BEAMS*

**FRAGMENTATION OF NEUTRON DRIP-LINE NUCLEI AT 30 MeV/u**

RIISAGER K., ANNE R., ARNELL S.E., BIMBOT R., EMLING H., GUILLEMAUD-MUELLER D., HANSEN P.G., JOHANNSEN L., JONSON B., LATIMIER A., LEWITOWICZ M., MATTSSON S., MUELLER A.C., NEUGART R., NYMAN G., POUGHEON F., RICHARD A., RICHTER A., SAINT-LAURENT M.G., SCHRIEDER G., SORLIN O., WILHELMSEN K.

*AARHUS UNIV. - AARHUS, GANIL - CAEN, CHALMERS TEKNISKA HOGSKOLA - GOTEBORG, IPN - ORSAY, GSI - DARMSTADT, MAINZ UNIV., INST.FUR KERNPHYSIK - DARMSTADT*

*SECOND INTERNATIONAL CONFERENCE ON RADIOACTIVE NUCLEAR BEAMS*

*LOUVAIN-LA-NEUVE*

*RADIOACTIVE NUCLEAR BEAMS*

**STUDY OF LIGHT NEUTRON-DEFICIENT NUCLEI WITH THE LISE3 SPECTROMETER**
BORREL V., ANNE R., BAZIN D., BORCEA C., CHUBARIAN G.G., DEL MORAL R., DETRAZ C., DOGNY S., DUFOUR J.P., FAUX L., FLEURY A., FIFIELD L.K., GUILLEMAUD-MUELLER D., HUBERT F., KASHY E., LEWITOWICZ M., MARCHAND C., POUGHEON F., PRAVIKOFF M.S., SAINT-LAURENT M.G., SORLIN O.
*IPN - ORSAY, GANIL - CAEN, CENB - GRADIGNAN, LPC - CAEN, MSU - EAST LANSING, JINR - DUBNA*
*SECOND INTERNATIONAL CONFERENCE ON RADIOACTIVE NUCLEAR BEAMS*
*LOUVAIN-LA-NEUVE*
*RADIOACTIVE NUCLEAR BEAMS*

**STUDY OF NEUTRON-RICH NUCLEI WITH THE LISE SPECTROMETER**
LEWITOWICZ M., ANNE R., ARTUKH A.G., BAZIN D., BORCEA C., BORREL V., BRICAULT P., DETRAZ C., DOGNY S., GUILLEMAUD-MUELLER D., JACMART J.C., JONSTON C., KASHY E., KLAPDOR H.V., LUKYANOV S.M., MUELLER A.C., PENIONZHKEVICH YU.E., POUGHEON F., RICHARD A., SAINT-LAURENT M.G., STAUDT A., SCHMIDT-OTT W.D.
*GANIL - CAEN, JINR - DUBNA, CENB - GRADIGNAN, IPN - ORSAY, MSU - EAST LANSING, MPI - HEIDELBERG, GOTTINGEN UNIV., TORONTO UNIV.*
*SECOND INTERNATIONAL CONFERENCE ON RADIOACTIVE NUCLEAR BEAMS*
*LOUVAIN-LA-NEUVE*
*RADIOACTIVE NUCLEAR BEAMS*

**THE DECAY MODES OF PROTON DRIP-LINE NUCLEI WITH A BETWEEN 42 AND 47**
BORREL V., ANNE R., BAZIN D., BORCEA C., CHUBARIAN G.G., DEL MORAL R., DETRAZ C., DOGNY S., DUFOUR J.P., FAUX L., FLEURY A., FIFIELD L.K., GUILLEMAUD-MUELLER D., HUBERT F., KASHY E., LEWITOWICZ M., MARCHAND C., MUELLER A.C., POUGHEON F., PRAVIKOFF M.S., SAINT-LAURENT M.G., SORLIN O.
*INP - ORSAY, GANIL - CAEN, CENB - GRADIGNAN, LPC - CAEN, MSU - EAST LANSING, JINR - DUBNA*
Z. PHYS. A344 (1992) 135.

**TWO-NEUTRON REMOVAL REACTIONS FOR VERY NEUTRON-RICH NUCLEI**
RIISAGER K., ANNE R., ARNELL S.E., BIMBOT R., EMLING H., GUILLEMAUD-MUELLER D., HANSEN P.G., JOHANNSEN L., JONSON B., LATIMIER A., LEWITOWICZ M., MATTSSON S., MUELLER A.C., NEUGART R., NYMAN G., POUGHEON F., RICHARD A., RICHTER A., SAINT-LAURENT M.G., SCHRIEDER G., SORLIN O., WILHELMSEN K.
*AARHUS UNIV. - AARHUS, GANIL - CAEN, CHALMERS TEKNISKA HOGSKOLA - GOTEBORG, IPN - ORSAY, GSI - DARMSTADT, MAINZ UNIV. - MAINZ, INST. FUR KERNPHYSIK - DARMSTADT*
NUCL. PHYS. A540 (1992) 365.
*92 11 C*

**DYNAMICS AND THERMALIZATION IN ARGON INDUCED COLLISIONS AROUND 30 MeV/NUCLEON**
RIVET M.F., BORDERIE B., JOUAN D., CABOT C., FUCHS H., GAUVIN H., HANAPPE F., GARDES D., MONTOYA M.
*IPN - ORSAY, FNRS - BRUXELLES*
*FIRST EUROPEAN BIENNIAL WORKSHOP ON NUCLEAR PHYSICS*
*MEGEVE*

**ENERGY DISSIPATION IN HEAVY ION COLLISIONS AROUND THE FERMI ENERGY STUDIED BY NEUTRON MULTIPLICITY MEASUREMENTS**
JACQUET D., GATTY B., BRESSON S., CREMA E., GALIN J., GUERREAU D., MORJEAN M., PAULOT C., POUTHAS J., PIASECKI E., KORDYASZ A., JASTRZEBSKI J., PIENKOWSKI L., SKULSKI W., LOTT B., BOUGAULT R., COLIN J., GENOUX-LUBAIN A., HORN D., LEBRUN C., LECOLLEY J.F., LOUVEL M., QUEDNAU B., SCHROEDER W.U., TOKE J., JAHNKE U.
*IPN - ORSAY, GANIL - CAEN, WARSAW UNIV. - WARSAWA, CRN - STRASBOURG, LPC - CAEN, ROCHESTER UNIV. - ROCHESTER, HMI - BERLIN*
*TOURS SYMPOSIUM ON NUCLEAR PHYSICS*
*TOURS (FR)*

**EXCITATION ENERGY DISTRIBUTIONS IN FUSION REACTIONS INDUCED BY Ar PROJECTILES AT 50 AND 70 MeV/u**

VIENT E., BADALA A., BARBERA R., BIZARD G., BOUGAULT R., BROU R., CUSSOL D., COLIN J., DURAND D., DROUET A., HORN D., LAVILLE J.L., LE BRUN C., LECOLLEY J.F., LEFLECHER C., LOUVEL M., PATRY J.P., PETER J., REGIMBART R., STECKMEYER J.C., TAMAIN B., AUGER G., PEGHAIRE A., EUDES P., GUILBAULT F., LEBRUN C., ROSATO E., OUBAHADOU A., GONIN M.

*LPC - CAEN, GANIL - CAEN, LPN - NANTES, INFN - NAPOLI, LPN - RABAT, TEXAS A&M - COLLEGE STATION*

*PROCEEDINGS OF THE XXX INTERNATIONAL WINTER MEETING ON NUCLEAR PHYSICS*

*BORMIO*

*INTERNATIONAL WINTER MEETING ON NUCLEAR PHYSICS.30*

RICERCA SCIENTIFICA ED EDUCAZIONE PERMANENTE.91

**FISSION OF SPIN-ALIGNED PROJECTILE-LIKE NUCLEI IN THE INTERACTIONS OF 29 MeV/NUCLEON 208 Pb WITH 197 Au**

BRESSON S., MORJEAN M., PIENKOWSKI L., BOUGAULT R., COLIN J., CREMA E., GALIN J., GATTY B., GENOUX-LUBAIN A., GUERREAU D., HORN D., JACQUET D., JAHNKE U., JASTRZEBSKI J., KORDYASZ A., LE BRUN C., LECOLLEY J.F., LOTT B., LOUVEL M., PAULOT C., PIASECKI E., POUTHAS J., QUEDNAU B., SCHRODER W.U., SKULSKI W., TOKE J.

*GANIL - CAEN, WARSAW UNIV., WARSAW, LPC - CAEN, SAO PAULO UNIV., IPN - ORSAY, CHALK RIVER LAB., HMI - BERLIN, CRN - STRASBOURG, ROCHESTER UNIV.*

PHYS. LETT. B294 (1992) 33.

**HOT NUCLEI WITH HIGH SPIN STATES IN COLLISIONS BETWEEN HEAVY NUCLEI**

GALIN J.

*GANIL - CAEN*

*FIRST EUROPEAN BIENNIAL WORKSHOP ON NUCLEAR PHYSICS*

*MEGEVE*

**PB INDUCED FISSION AT 29 MEV/NUCLEON ON A SERIES OF TARGETS : C, AL, NI, AU**

PIENKOWSKI L., BRESSON S., BOUGAULT R., COLIN J., CREMA E., GALIN J., GATTY B., GENOUX-LUBAIN A., GUERREAU D., HORN D., JACQUET D., JAHNKE U., JASTRZEBSKI J., KORDYASZ A., LE BRUN C., LECOLLEY J.F., LOTT B., LOUVEL M., MORJEAN M., PAULOT C., PIASECKI E., POUTHAS J., QUEDNAU B., SCHROEDER W.U., SCHWINN E.S., SKULSKI W., TOKE J.

*GANIL - CAEN, HEAVY ION LAB. - WARSZAWA, LPC - CAEN, UNIVERSIDADE DE SAO PAULO, IPN - ORSAY, CHALK RIVER LAB. - CHALK RIVER, HMI - BERLIN, INST.OF EXP.PHYS. - WARSZAWA, CRN - STRASBOURG, ROCHESTER UNIV. - ROCHESTER*

*PROCEEDINGS OF THE XXX INTERNATIONAL WINTER MEETING ON NUCLEAR PHYSICS*

*BORMIO*

*INTERNATIONAL WINTER MEETING ON NUCLEAR PHYSICS.30*

RICERCA SCIENTIFICA ED EDUCAZIONE PERMANENTE.91

**PRODUCTION AND DECAY OF HOT NUCLEI**

JAHNKE U., BRESSON S., CHARVET J.L., GALIN J., GATTY B., GUERREAU D., JACQUET D., LOTT B., MORJEAN M., PIASECKI E., POUTHAS J., SCHWINN E., SOKOLOV A.

*HMI - BERLIN, GANIL - CAEN, CE - BRUYERES-LE-CHATEL, IPN - ORSAY, CRN - STRASBOURG, WARSAW UNIV. - WARSAW*

*FIRST EUROPEAN BIENNIAL WORKSHOP ON NUCLEAR PHYSICS*

*MEGEVE*

**PRODUCTION OF THREE NEARLY EQUAL MASS FRAGMENTS IN THE Xe + Cu REACTION AT 45 MeV/u**

BRUNO M., D'AGOSTINO M., FIANDRI M.L., FUSCHINI E., MILAZZO P.M., CUNSOLO A., FOTI A., GRAMEGNA F., GULMINELLI F., IORI I., MANDUCI L., MORONI A., SCARDAONI R., BUTTAZZO P., MARGAGLIOTTI G.V., VANNINI G., AUGER G., PLAGNOL E.

*INFN - BOLOGNA, INFN - CATANIA, INFN - LEGNARO, INFN - MILAN, INFN - TRIESTE, GANIL - CAEN*

PHYS. LETT. B292 (1992) 251.

**SEQUENTIAL LCP EMISSION ASSOCIATED WITH MULTIFRAGMENTATION OF THE Pb+Au SYSTEM AT 29 MeV/u**

CHBIHI A., BOUGAULT R., BRESSON S., COLIN J., CREMA E., GALIN J., GATTY B., GENOUX-LUBAIN A., GUERREAU D., HORN D., JACQUET D., JAHNKE U., JASTRZEBSKI J., KORDYASZ A., LE BRUN C., LECOLLEY J.F., LOTT B., LOUVEL M., MORJEAN M., PAULOT C., PIASECKI E., PIENKOWSKI L., POUTHAS J., QUEDNAU B., SCHRODER W.U., SCHWINN E., SKULSKI W., TOKE J.

*GANIL - CAEN, LPC - CAEN, UNIV. SAO PAULO, IPN - ORSAY, CHALK RIVER, HMI - BERLIN, HEAVY ION LAB. - WARSAW, UNIV. WARSAW, CRN - STRASBOURG, UNIV. ROCHESTER*

NUCL. PHYS. A545, 1,2 (1992) 229c.

*PROCEEDINGS OF THE INTERNATIONAL WORKSHOP ON DYNAMICAL FLUCTUATIONS AND CORRELATIONS IN NUCLEAR COLLISIONS*

*AUSSOIS*

**STUDY OF COLLECTIVE FLOW IN HEAVY ION COLLISIONS**

BIZARD G., PETER J., SHEN W.Q., SULLIVAN J.P., BROU R., CUSSOL D., LOUVEL M., PATRY J.P., REGIMBART R., STECKMEYER J.C., TAMAIN B., CREMA E., DOUBRE H., HAGEL K., JIN G.M., PEGHAIRE A., SAINT-LAURENT F., CASSAGNOU Y., LEGRAIN R., LEBRUN C., ROSATO E., MACGRATH R., JEONG S.C., LEE S.M., NAGASHIMA Y., NAKAGAWA T., OGIHARA M., KASAGI J., MOTOBAYASHI T.

*LPC-CAEN, GANIL-CAEN, CEN-SACLAY, LPN-NANTES, UNIV.DI NAPOLI, TEXAS A&M UNIV.-COLLEGE STATION, SUNY-STONY BROOK, INST.MOD.PHYS.-LANZHOU, TSUKUBA UNIV., TOKYO INST.TECHNOLOGIE, RIKKYO UNIV.-TOKYO*

*TOURS SYSMPOSIUM ON NUCLEAR PHYSICS*

*TOURS*

**THE EFFE PROJECT**

SIDA J.L., ALAMANOS N., AUGER F., GILLIBERT A., LIGUORI R., PIERROUTSAKOU D., POLLACO E.C., VOLANT C., BORCEA C., LEWITOWICZ M., MITTIG W., ROUSSEL-CHOMAZ P., CUNSOLO A., FOTI A., SILVEIRA GOMES P.

*DAPNIA/CEN SACLAY, GANIL - CAEN, INFN - CATANE, UFF (BRAZIL)*

*PROCEEDINGS OF THE XXX INTERNATIONAL WINTER MEETING ON NUCLEAR PHYSICS*

*BORMIO*

*INTERNATIONAL WINTER MEETING ON NUCLEAR PHYSICS.30*

RICERCA SCIENTIFICA ED EDUCAZIONE PERMANENTE.91

**THREE FRAGMENT SEQUENTIAL DECAY OF HEAVY NUCLEI AROUND 3 MeV/u EXCITATION ENERGY**

BIZARD G., DURAND D., GENOUX-LUBAIN A., LOUVEL M., BOUGAULT R., BROU R., DOUBRE H., EL-MASRI Y., FUGIWARA H., HAGEL K., HAJFANI A., HANAPPE F., JEONG S., JIN G.M., KATO S., LAVILLE J.L., LE BRUN C., LECOLLEY J.F., LEE S., MATSUSE T., MOTOBAYASHI T., PATRY J.P., PEGHAIRE A., PETER J., PROT N., REGIMBART R., SAINT-LAURENT F., STECKMEYER J.C., TAMAIN B.

*LPC/ISMRA - CAEN, GANIL - CAEN, FNRS/ULC - LOUVAIN LA NEUVE, TSUKUBA UNIV., TEXAS A&M UNIV. - COLLEGE STATION, ULB - BRUSSELS, INST.OF MODERN PHYS. - LANZHOU, SHINSHY UNIV. - MATSUMOTO, RIKKYO UNIV. - TOKYO*

PHYS. LETT. B276 (1992) 413.

**WIDE RANGE OF EMISSION TIMES IN MULTIFRAGMENT DECAY OF HOT NUCLEI BETWEEN 3 AND 5.5 MeV/u EXCITATION ENERGY**

LOUVEL M., BIZARD G., BOUGAULT R., BROU R., BUTA E., DURAND D., GENOUX-LUBAIN A., HAJFANI A., HAMDANI T., LAVILLE J.L., LE BRUN C., LECOLLEY J.F., PATRY J.P., PETER J., PROT N., REGIMBART R., STECKMEYER J.C., TAMAIN B., BADALA A., DOUBRE H., EL-MASRI Y., FUGIWARA H., HAGEL K., HANAPPE F., JEONG S., JIN G.M., KATO S., LEE S., MATSUSE T., MOTOBAYASHI T., PEGHAIRE A., SAINT-LAURENT F.

*LPC - CAEN, GANIL - CAEN, FNRS-ULC - LOUVAIN LA NEUVE, TSUKUBA UNIV., TEXAS A&M UNIV. - COLLEGE STATION, ULB - BRUXELLES, IMP - LANZHOU, SHINSHU UNIV., RIKKYO UNIV. - TOSHIMA-KU, INFN - CATANIA*

*PROCEEDINGS OF THE XXX INTERNATIONAL WINTER MEETING ON NUCLEAR PHYSICS BORMIO*

*INTERNATIONAL WINTER MEETING ON NUCLEAR PHYSICS.30*

RICERCA SCIENTIFICA ED EDUCAZIONE PERMANENTE.91

**EXCLUSIVE MEASUREMENTS OF THE HIGH ENERGY PHOTON PRODUCTION IN THE 129 Xe + 197 Au AT 44 MeV/u REACTION**

MIGNECO E., AGODI C., ALBA R., BELLIA G., CONIGLIONE R., DEL ZOPPO A., FINOCCHIARO P., MAIOLINO C., PIATELLI P., RUSSO G., SAPIENZA P., BADALA A., BARBERA R., PALMERI A., PAPPALARDO G.S., RIGGI F., RUSSO A.C., PEGHAIRE A., DE LEO R.

*INFN - CATANIA, CATANIA UNIV. - CATANIA, INFN - CATANIA, GANIL - CAEN, LECCE UNIV. - LECCE*

*PROCEEDINGS OF THE XXX INTERNATIONAL WINTER MEETING ON NUCLEAR PHYSICS BORMIO*

*INTERNATIONAL WINTER MEETING ON NUCLEAR PHYSICS.30*

RICERCA SCIENTIFICA ED EDUCAZIONE PERMANENTE.91

**MEASUREMENT OF THE IMPACT PARAMETER IN INTERMEDIATE ENERGY HEAVY ION COLLISIONS**

RIESS S., ENDERS G., HOFMANN A., KUHN W., METAG V., NOVOTNY R., MITTIG W., SCHUTZ Y., VILLARI A.C.C., EMLING H., GREIN H., GROSSE E., HENNING W., HOLZMANN R., KULESSA R., MATULEWICZ T., WOLLERSHEIM H.J.

*GIESSEN UNIV., GANIL - CAEN, GSI - DARMSTADT*

PHYS. REV. LETT. 69, No. 10 (1992) 1504.

**SUBTHRESHOLD KAON PRODUCTION IN HEAVY IONS COLLISIONS**

ALAMANOS N., BIANCHI L., CASSAGNOU Y., DABROWSKI H., ERAZMUS B., JULIEN J., LE BRUN C., LEBRUN D., LECOLLEY J.F., LEGRAIN R., MOUGEOT A., PERRIN G., DE SAINTIGNON P., SIDA J.L., WIELECZKO J.P.

*DAPNIA/CEN SACLAY, GANIL - CAEN, LPN - NANTES, LPC - CAEN, ISN - GRENOBLE*

*PROCEEDINGS OF THE XXX INTERNATIONAL WINTER MEETING ON NUCLEAR PHYSICS BORMIO*

*INTERNATIONAL WINTER MEETING ON NUCLEAR PHYSICS.30*

RICERCA SCIENTIFICA ED EDUCAZIONE PERMANENTE.91

**PHOTON AND SUBTHRESHOLD PION PRODUCTION CORRELATED WITH LIGHT FRAGMENTS : A STATISTICAL PROCESS**

LAVILLE J.L., BADALA A., BARBERA R., BIZARD G., DURAND D., PALMERI A., PAPPALARDO G.S., RIGGI F.

*LPC - CAEN, INFN - CATANIA*

*FIRST EUROPEAN BIENNIAL WORKSHOP ON NUCLEAR PHYSICS MEGEVE*

**PION PRODUCTION IN HEAVY ION REACTIONS INDUCED BY 16 O AND 84 Kr BEAMS AT 60 MeV PER NUCLEON**

PERRIN G., DABROWSKI H., DUHAMEL-CHRETIEN G., LEBRUN D., DE SAINTIGNON P., BOUGAULT R., DURAND D., GENOUX-LUBAIN A., LE BRUN C., LECOLLEY J.F., LOUVEL M.

*ISN - GRENOBLE, LPC - CAEN*

Z. PHYS. A342 (1992) 199.

**SUBTHRESHOLD PION PRODUCTION FROM NUCLEUS-NUCLEUS COLLISIONS AROUND 100 MeV/NUCLEON : IMPACT PARAMETER DEPENDENCE WITHIN THE MODIFIED FIREBALL MODEL**
BADALA A., BARBERA R., PALMERI A., PAPPALARDO G.S., RIGGI F., RUSSO A.C.
*INFN - CATANIA, CATANIA UNIV. - CATANIA*
Z. PHYS. A344 (1992) 455.

## H - ACCELERATEUR

**A CYCLOTRON AS A MASS SPECTROMETER**
BRICAULT P. ET AL.
*GANIL - CAEN, CSNSM - ORSAY, CEN SACLAY - GIF SUR YVETTE,*
*AUSTRALIA NATIONAL UNIV. - CAMBERRA*
*INTERNATIONAL CONFERENCE ON CYCLOTRONS AND THEIR APPLICATIONS.13*
*VANCOUVER (CN)*
*CYCLOTRONS AND THEIR APPLICATIONS*

**A HEAVY ION LINAC FOR THE CERN ACCELERATOR COMPLEX**
AMENDOLA G., ANGERT N., BOURGAREL M.P., BRU B., CERVELLERA F., FORTUNA G., HASEROTH H., HILL C., HUTTER G., KLABUNDE J., KLEIN H., KUGLER H., LISKA D., LOMBARDI A., LUSTIG H., MALWITZ E., MUSSO A., O'HANLON H., PARISI G., PISENT A., RAICH U., RATZINGER U., RICCATI L., RICCI R., SCHEMPP A., SHERWOOD T., SORTAIS P., TANKE E., TETU P., VAN DER SCHUEREN A., VRETENAR M., WARNER D., WEISS M.
*CERN - GENEVE, GSI - DARMSTADT, GANIL - CAEN, INFN - LEGNARO,*
*FRANKFURT UNIV. - FRANKFURT, LANL - LOS ALAMOS, INFN - TORINO*
*THIRD EUROPEAN PARTICLE ACCELERATOR CONFERENCE*
*BERLIN*
*EPAC 92*

**AN ON-LINE ISOTOPIC SEPARATOR TEST BENCH AT GANIL**
BRICAULT P. ET AL.
*GANIL - CAEN, IPN - ORSAY, CSNSM - ORSAY, LPC ISMRA - CAEN*
*CYCLOTRONS AND THEIR APPLICATIONS*
*VANCOUVER (CN)*
*INTERNATIONAL CONFERENCE ON CYCLOTRONS AND THEIR APPLICATIONS.13*

**COMMISSIONING OF THE NEW HIGH INTENSITY AXIAL INJECTION SYSTEM FOR GANIL**
RICAUD CH. ET AL.
*GANIL - CAEN, LNS CEN SACLAY - GIF SUR YVETTE*
*INTERNATIONAL CONFERENCE ON CYCLOTRONS AND THEIR APPLICATIONS.13*
*VANCOUVER (CN)*
*CYCLOTRONS AND THEIR APPLICATIONS*

**CYCLOTRON TUNNING AS A REBUNCHER**
BIBET D., MOSCATELLO M.H.
*GANIL - CAEN*
*INTERNATIONAL CONFERENCE ON CYCLOTRONS AND THEIR APPLICATIONS.13*
*VANCOUVER (CN)*
*CYCLOTRONS AND THEIR APPLICATIONS*

**GANIL STATUS REPORT**
BAJARD M.
*GANIL - CAEN*
*INTERNATIONAL CONFERENCE ON CYCLOTRONS AND THEIR APPLICATIONS.13*
*VANCOUVER (CN)*
*CYCLOTRONS AND THEIR APPLICATIONS*

**LATEST DEVELOPMENTS ON MULTICHARGED E.C.R. ION SOURCES AT GANIL**
SORTAIS P., BISCH M., BOURGAREL M.P., BRICAULT P., LEHERISSIER P., LEROY R., PACQUET J.Y., RATAUD J.P.
*GANIL - CAEN*
*THIRD EUROPEAN PARTICLE ACCELERATOR CONFERENCE*
*BERLIN*
*EPAC 92*

**NUMERICAL SIMULATION OF ECRIPAC PLASMA BEHAVIOUR WITH VLASOV EQUATIONS INCLUDING ELECTRON AND ION COLLECTIVE EFFECTS**
BERTRAND P.
*GANIL - CAEN*
*THIRD EUROPEAN PARTICLE ACCELERATOR CONFERENCE*
*BERLIN*
*EPAC 92*

**REVIEW OF LATEST DEVELOPMENTS OF ION SOURCES**
BEX L.
*GANIL - CAEN*
*PROCEEDINGS OF THE THIRD EUROPEAN PARTICLE ACCELERATOR CONFERENCE*
*BERLIN*
*EPAC 92*

**SECONDARY BEAMS AT GANIL**
DOUBRE H.
*GANIL - CAEN*
*INTERNATIONAL WORKSHOP ON THE PHYSICS AND TECHNIQUES OF SECONDARY NUCLEAR BEAMS*
*DOURDAN*
*PHYSICS AND TECHNIQUES OF SECONDARY NUCLEAR BEAMS*

**THE NEXT GENERATION CONTROL SYSTEM OF GANIL**
LUONG T.T. ET AL.
*GANIL - CAEN*
*INTERNATIONAL CONFERENCE ON ACCELERATORS AND LARGE EXPERIMENTAL PHYSICS CONTROL SYSTEMS*
*TSUKUBA (JP)*

**WHAT COULD BE A RADIOACTIVE ION BEAM FACILITY AT GANIL**
CHABERT A.
*GANIL - CAEN*
*THIRD EUROPEAN PARTICLE ACCELERATOR CONFERENCE*
*BERLIN*
*EPAC 92*

## I - INSTRUMENTATION

**HEAVY IONS DETECTION BY USING BaF2 CRYSTALS COUPLED TO THIN PLASTIC SCINTILLATOR**
LANZANO G., PAGANO A., DE FILIPPO E., POLLACCO E., BARTH R., BERTHIER B., BERTHOUMIEUX E., CASSAGNOU Y., CAVALLARO SL., CHARVET J.L., CUNSOLO A., DAYRAS R., FOTI A., HARAR S., LEGRAIN R., LIPS V., MAZUR C., NORBECK E., URSO S., VOLANT C.
*INFN - CATANIA, CEN SACLAY - GIF-SUR-YVETTE, LAB.NAZ. DEL SUD - CATANIA, INST.FUR KERNPHYSIK - DARMSTADT, GSI - DARMSTADT, GANIL - CAEN, IOWA UNIV. - IOWA*
NIM A323 (1992) 694.

**INDRA : A NEW 4pi DETECTOR FOR CHARGED PARTICLES AND NUCLEI AT THE GANIL FACILITY**
CHIBHI A.,AUGER G.,BENKIRANE A.,BIANCHI L.,BOURGAULT P.,HUGUET Y.,LE GUAY M., PLAGNOL E.,POUTHAS J.,SAINT-LAURENT F.,SPITAELS C.,TRIPON M.,WIELECZKO J.P., BERTHIER B.,CASSAGNOU Y.,CHARVET J.L.,DAYRAS R.,LEGRAIN R.,MAZUR C.,PASSERIEUX J., POLLACCO E.,VOLANT C.,BACRI C.O.,BARBEY S.,CHARLET D.,BORDERIE B.,RICHARD A., RIVET M.F.,TASSAN-GOT L.,CUSSOL D.,GAUTIER J.M.,LAVILLE J.L.,STECKMEYER J.C.,.....
*GANIL - CAEN, CEN - SACLAY, IPN - ORSAY, LPC - CAEN*
*FIRST EUROPEAN BIENNIAL WORKSHOP ON NUCLEAR PHYSICS*
*MEGEVE*

**THE GANIL RNB PROJECT**
CHABERT A., BRICAULT P., JOUBERT A., SORTAIS P.
*GANIL - CAEN*
*SECOND INTERNATIONAL CONFERENCE ON RADIOACTIVE NUCLEAR BEAMS*
*LOUVAIN-LA-NEUVE*
*RADIOACTIVE NUCLEAR BEAMS*

**THE INDRA 4pi DETECTOR : SOME FACETS OF THE PHYSICS PROGRAM**
BORDERIE B.
*IPN - ORSAY*
*INTERNATIONAL CONFERENCE ON NEW NUCLEAR PHYSICS WITH ADVANCED TECHNIQUES*
*LERAPETRA (GR)*
*NEW NUCLEAR PHYSICS WITH ADVANCED TECHNIQUES*

**WHAT KIND OF PHYSICS WITH NEW MULTIPARTICLE DETECTORS**
RIVET M.F.
*IPN - ORSAY*
*TOURS SYMPOSIUM ON NUCLEAR PHYSICS*
*TOURS (FR)*

## T - THEORIE

**A STOCHASTIC APPROACH TO FISSION**
BOILLEY D., SURAUD E., ABE Y., AYIK S.
*GANIL - CAEN, KYOTO UNIV. - KYOTO, TENNESSEE TECH.UNIV. - COOKEVILLE*
*PROCEEDINGS OF THE XXX INTERNATIONAL WINTER MEETING ON NUCLEAR PHYSICS*
*BORMIO*
*INTERNATIONAL WINTER MEETING ON NUCLEAR PHYSICS.30*
RICERCA SCIENTIFICA ED EDUCAZIONE PERMANENTE.91

**APPLICATIONS OF BOLTZMANN-LANGEVIN EQUATION TO NUCLEAR COLLISIONS**
SURAUD E., AYIK S., BELKACEM M., STRYJEWSKI J.
*GANIL - CAEN, TENNESSEE TECHN. UNIV. - COOKEVILLE*
NUCL. PHYS. A542 (1992) 141.

**COMMENTS ON THE WIDTH AND THE LIFETIME OF MULTIPHONON STATES**
CHOMAZ PH. ET AL.
*GANIL - CAEN, IPN - ORSAY*
PHYSICS LETTERS B282 (1992) 13.

**EXCITATION ENERGY EVOLUTION AND MULTI-PARTICLE CORRELATIONS IN HEAVY ION PERIPHERAL COLLISIONS AT INTERMEDIATE ENERGIES**
DORE D., BEAULIEU L., LAFOREST R., POULIOT J., ROY R., ST-PIERRE C., AUGER G., BRICAULT P., GROULT S., PLAGNOL E., HORN D.
*LAVAL UNIV. - STE-FOY, GANIL - CAEN, AECL - CHALK RIVER*
NUCL. PHYS. A545, 1,2 (1992) 363c.
*PROCEEDINGS OF THE INTERNATIONAL WORKSHOP ON DYNAMICAL FLUCTUATIONS AND CORRELATIONS IN NUCLEAR COLLISIONS*
*AUSSOIS*

**FINITE SIZE EFFECTS IN THE INTERMITTENCY ANALYSIS OF THE FRAGMENT-SIZE CORRELATIONS**
BOZEK P., PLOSZAJCZAK M., TUCHOLSKI A.
*GANIL - CAEN, INST.OF NUCL.PHYS. - KRAKOW, GSI - DARMSTADT, SOLTAN INST. FOR NUCL.STUDIES - SWIERK*
NUCL. PHYS. A539 (1992) 693.

**FLUCTUATIONS IN THE HADRONIZATION**
BOZEK P., PLOSZAJCZAK M.
*GANIL - CAEN, INST. OF NUC. PHYS. - KRAKOW*
NUCL. PHYS. A545, 1,2 (1992) 297c.
*PROCEEDINGS OF THE INTERNATIONAL WORKSHOP ON DYNAMICAL FLUCTUATIONS AND CORRELATIONS IN NUCLEAR COLLISIONS*
*AUSSOIS*

**FLUCTUATIONS IN THE MULTIFRAGMENTATION**
PLOSZAJCZAK M., BOZEK P., TUCHOLSKI A.
*GANIL - CAEN, INP - KRAKOW, SOLTAN INST.FOR NUCL. STUDIES - SWIERK*
*PROCEEDINGS OF THE XXX INTERNATIONAL WINTER MEETING ON NUCLEAR PHYSICS*
*BORMIO*
*INTERNATIONAL WINTER MEETING ON NUCLEAR PHYSICS.30*
RICERCA SCIENTIFICA ED EDUCAZIONE PERMANENTE.91

**FRAGMENTATION-INACTIVATION BINARY MODEL**
BOTET R., PLOSZAJCZAK M.
*PARIS-SUD UNIV. - ORSAY, GANIL - CAEN*
PHYS. REV. LETT. 69 (1992) 26.

**FROM EXPERIMENTAL MONOPOLE CROSS-SECTIONS TO NUCLEAR INCOMPRESSIBILITIES**
CHOMAZ PH. ET AL.
*GANIL - CAEN, IPN - ORSAY*
PHYSICS LETTERS B281 (1992) 6.

**INTERMITTENCY IN THE PARTICLE PRODUCTION AND IN THE NUCLEAR MULTIFRAGMENTATION**
BOZEK P., PLOSZAJCZAK M.
*GANIL - CAEN, INST.OF NUCL.PHYS. - KRAKOW*
*TOURS SYMPOSIUM ON NUCLEAR PHYSICS*
*TOURS (FR)*

**QUANTUM TUNNELING IN THE DRIVEN SU(2) MODEL**
KAMINSKI P., PLOSZAJCZAK M., ARVIEU R.
*GANIL - CAEN, INST.NUCL.PHYS. - KRAKOW, ISN - GRENOBLE*
*PROCEEDINGS OF THE XXX INTERNATIONAL WINTER MEETING ON NUCLEAR PHYSICS*
*BORMIO*
*INTERNATIONAL WINTER MEETING ON NUCLEAR PHYSICS.30*
RICERCA SCIENTIFICA ED EDUCAZIONE PERMANENTE.91

**SIGNATURES OF THE NUCLEAR EQUATION OF STATE IN THE COLLECTIVE FLOW OF HEAVY-ION REACTIONS**
DE LA MOTA V., SEBILLE F., FARINE M., REMAUD B., SCHUCK P., IDIER D., HADDAD F.
*LPN - NANTES, GANIL - CAEN, ISN - GRENOBLE*
*TOURS SYMPOSIUM ON NUCLEAR PHYSICS*
*TOURS (FR)*

**STOCHASTIC AND DETERMINISTIC SOLUTIONS OF THE 2-D BOLTZMANN EQUATION**
TOHYAMA M., SURAUD E.
*KYORIN UNIV. - TOKYO, GANIL - CAEN*
NUCL. PHYS. A549 (1992) 461.

**STOCHASTIC TDHF AND LARGE FLUCTUATIONS**
REINHARD P.G., SURAUD E.
*ERLANGEN UNIV., GANIL - CAEN*
NUCL. PHYS. A545, 1,2 (1992) 59c.
*PROCEEDINGS OF THE INTERNATIONAL WORKSHOP ON DYNAMICAL FLUCTUATIONS AND CORRELATIONS IN NUCLEAR COLLISIONS*
*AUSSOIS*

**STOCHASTIC TDHF FOR REACTIONS WITH LARGE FLUCTUATIONS**
REINHARD P.G., SURAUD E.
*INST.F.THEOR.PHYSIK - UNIV.ERLANGEN, GANIL - CAEN*
*PROCEEDINGS OF THE 7th ADRIATIC INTERNATIONAL CONFERENCE ON NUCLEAR PHYSICS*
*ISLANDS OF BRIONI*
*HEAVY-ION PHYSICS TODAY AND TOMORROW*

**THE BOLTZMANN-LANGEVIN EQUATION DERIVED FROM THE REAL-TIME PATH FORMALISM**
REINHARD P.G., SURAUD E., AYIK S.
*ERLANGEN UNIV. - ERLANGEN, GANIL - CAEN, TENNESSEE TECH. UNIV. - COOKEVILLE*
ANNALS OF PHYSICS 213, 1 (1992) 204.

**THE BOLTZMANN-LANGEVIN MODEL FOR NUCLEAR COLLISIONS**
AYIK S., SURAUD E., BELKACEM M., BOILLEY D.
*TENNESSEE TECHN.UNIV. - COOKEVILLE AND JOINT INST.FOR HEAVY-ION RES. - OAK RIDGE, GANIL - CAEN*
NUCL. PHYS. A545, 1,2 (1992) 35c.
*PROCEEDINGS OF THE INTERNATIONAL WORKSHOP ON DYNAMICAL FLUCTUATIONS AND CORRELATIONS IN NUCLEAR COLLISIONS*
*AUSSOIS*

# 1993

**ANOMALOUS HEAVY ION SCATTERING NEAR THE COULOMB BARRIER**
LEPINE-SZILY A., SCIANI W., WATARI Y.K., MITTIG W., LICHTENTHALER R., OBUTI M.M., OLIVEIRA Jr. J.M., VILLARI A.C.C.
*SAO PAULO UNIV. - SAO PAULO, GANIL - CAEN*
PHYSICS LETTERS B304 (1993) 45.

**ELECTRIC ISOVECTOR NUCLEAR RESPONSE FROM 13 C INDUCED CHARGE-EXCHANGE REACTIONS**
BERAT C., BUENERD M., HOSTACHY J.Y., MARTIN P., BARRETTE J., BERTHIER B., FERNANDEZ B., MICZAIKA A., VILLARI A., BOHLEN H.G., KUBONO S., STILIARIS E., VON OERTZEN W.
*ISN - GRENOBLE, DAPNIA/CE SACLAY - GIF SUR YVETTE, GANIL - CAEN, HMI - BERLIN*
NUCLEAR PHYSICS A555 (1993) 455.

**EXCITATION OF GIANT RESONANCES IN 208Pb, 120 Sn, 90 Zr AND 60 Ni BY 84 MeV/NUCLEON 17 O IONS**
LIGUORI NETO R. ET AL.
*DAPNIA CEN SACLAY - GIF SUR YVETTE, FOSTER RADIATION LAB. - MONTREAL, IPN - ORSAY, KVI - GRONINGEN*
NUCL. PHYS. A560 (1993) 733.

**MEASUREMENT OF DEVIATIONS FROM PURE MOTT-SCATTERING IN THE SYSTEM 208 Pb + 208 Pb BELOW THE COULOMB BARRIER**
AUGER G. ET AL.
*GANIL - CAEN, IFN - SAO PAULO, INFN - CATANIA*
*FRANCO-JAPANESE COLLOQUIUM ON NUCLEAR STRUCTURE AND INTERDISCIPLINARY TOPICS.6*
*SAINT-MALO (FR)*
*NUCLEAR STRUCTURE AND INTERDISCIPLINARY TOPICS*

**SEARCH FOR COLOR VAN DER WAALS FORCE IN 208 Pb + 208 Pb MOTT SCATTERING**
VILLARI A.C.C. ET AL.
*GANIL - CAEN, INSTITUTO DE FISICA - SAO PAULO, INFN - CATANIA, KVI - GRONINGEN*
PHYSICAL REVIEW LETTERS 71, 16 (1993) 2551.
*93*

**THE GIANT DIPOLE RESONANCE IN VERY HOT NUCLEI STUDIED WITH THE MEDEA DETECTOR**
LE FAOU J.H. ET AL.
*IPN - ORSAY, INFN - CATANIA, DAPNIA CEA SACLAY - GIF-SUR-YVETTE, GANIL - CAEN, NBI - COPENHAGEN*
RICERCA SCIENTIFICA ED EDUCAZIONE PERMANENTE.96, p. 417 (1993)
*INTERNATIONAL WINTER MEETING ON NUCLEAR PHYSICS.31*
*BORMIO (IT)*

**16 O BREAKUP ON Al, Ni AND Au TARGETS AT 94 MeV/NUCLEON**
BADALA A., BARBERA R., PALMERI A., PAPPALARDO G.S., RIGGI F., POLLAROLO G., DASSO C.H.
*INFN - CATANIA, CATANIA UNIV. - CATANIA, TORINO UNIV. AND INFN - TURIN, NBI - COPENHAGEN*
PHYS. LETT. B299 (1993) 11.

**BREAKUP OF THE PROJECTILE IN 16 O-INDUCED REACTIONS ON 27 Al, 58 Ni, AND 197 Au TARGETS AROUND 100 MeV/NUCLEON**
BADALA A. ET AL.
*INFN - CATANIA*
PHYS. REV. C48, 2 (1993) 633.

**MEASUREMENTS IN THE BEAM DIRECTION OF THE 40 Ar PROJECTILE FRAGMENTATION AT 44 MeV/A**

BACRI CH.O., ROUSSEL P., BORREL V., CLAPIER F., ANNE R., BERNAS M., BLUMENFELD Y., GAUVIN H., HERAULT J., JACMART J.C., POUGHEON F., SIDA J.L., STEPHAN C., SUOMIJARVI T., TASSAN-GOT L.

*IPN - ORSAY, GANIL - CAEN, DAPNIA/CE SACLAY - GIF SUR YVETTE*

NUCLEAR PHYSICS A555 (1993) 477

**MEASUREMENTS IN THE BEAM DIRECTION OF THE 40 Ar PROJECTILE FRAGMENTATION AT 44 MeV/A**

BACRI CH.O. ET AL.

*GANIL - CAEN, DAPNIA CEA SACLAY - GIF SUR YVETTE*

RICERCA SCIENTIFICA ED EDUCAZIONE PERMANENTE.96, p. 117 (1993)

*INTERNATIONAL WINTER MEETING ON NUCLEAR PHYSICS.31*

*BORMIO (IT)*

**PRODUCTION CROSS SECTIONS AND MOMENTUM DISTRIBUTIONS FROM 500 MeV/u 86 Kr FRAGMENTATION**

WEBER M., DONZAUD C., DUFOUR J.P., FAUERBACH M., GEISSEL H., GREWE A., GUILLEMAUD-MUELLER D., KELLER H., LEWOTOWICZ M., MAGEL A., MUELLER A.C., MUNZENBERG G., NICKEL F., PFUTZNER M., PIECHACZEK A., PRAVIKOFF M., ROECKL E., RYKACZEWSKI K.,
SAINT-LAURENT M.G., SCHALL I., STEPHAN C., SUMMERER K., TASSAN-GOT L., VIEIRA D.J., VOSS B.

*GSI - DARMSTADT, IPN - ORSAY, CEN BORDEAUX - GRADIGNAN,*
*INST. FUR KERNPHYSIK - DARMSTADT, GANIL - CAEN, LANL - LOS ALAMOS*

*INTERNATIONAL CONFERENCE ON NUCLEI FAR FROM STABILITY.6 / AND INTERNATIONAL CONFERENCE ON ATOMIC MASSES AND FUNDAMENTAL CONSTANTS.9*

*BERNKASTEL-KUES*

*NUCLEI FAR FROM STABILITY/ATOMIC MASSES AND FUNDAMENTAL CONSTANTS 1992*

**PROJECTILE BREAKUP STUDY IN 16 O INDUCED REACTIONS ON 27 Al, 58 Ni AND 197 Au TARGETS AROUND 100 MeV/NUCLEON**

BADALA A. ET AL.

*INFN - CATANIA, INFN - TORINO, NBI - COPENHAGEN*

RICERCA SCIENTIFICA ED EDUCAZIONE PERMANENTE.96, p. 316 (1993)

*INTERNATIONAL WINTER MEETING ON NUCLEAR PHYSICS.31*

*BORMIO (IT)*

*93 51 B*

**ASTROPHYSICAL RADIATIVE CAPTURE CROSS SECTIONS : MEASUREMENTS USING THE BREAKUP OF RADIOACTIVE BEAMS**

KIENER J., AGUER P., BOGAERT G., BORDERIE B., COC A., DISDIER D., FORTIER S., GRUNBERG C., KRAUS L., LEFEBVRE A., LINCK I., RIVET M.F., ROUSSEL-CHOMAZ P., SAINT-LAURENT F., STEPHAN C., TASSAN-GOT L., THIBAUD J.P.

*CSNSM - ORSAY, IPN - ORSAY, CRN - STRASBOURG, GANIL - CAEN*

*INTERNATIONAL SYMPOSIUM ON NUCLEAR ASTROPHYSICS HELD AT KARLSRUHE.2*

*KARLSRUHE*

*NUCLEI IN THE COSMOS*

**DECAY PROPERTIES OF EXOTIC N 28 S AND Cl NUCLEI AND THE 48 Ca/46 Ca ABUNDANCE RATIO**
SORLIN O. ET AL.
*IPN - ORSAY, MAINZ UNIV. - MAINZ, JINR - DUBNA, GANIL - CAEN, CENBG - GRADIGNAN, LPC - CAEN, HARVARD-SMITHSONIAN CENTER FOR ASTROPHYSICS - CAMBRIDGE, MPI - GARCHING*
PHYS. REV. C47, (1993) 2941.

**DETERMINATION OF THE 13 N(p,gamma) 14 O REACTION RATE THROUGH THE COULOMB BREAK-UP OF A 14 O RADIOACTIVE BEAM**
KIENER J., LEFEBVRE A., AGUER P., BACRI C.O., BIMBOT R., BOGAERT G., BORDERIE B., CLAPIER F., COC A., DISDIER D., FORTIER S., GRUNBERG C., KRAUS L., LINCK I., PASQUIER G., RIVET M.F., SAINT-LAURENT F., STEPHAN C., TASSAN-GOT L., THIBAUD J.P.
*CSNSM - ORSAY, IPN - ORSAY, CRN - STRASBOURG, GANIL - CAEN*
NUCL. PHYS. A552 (1993) 66.

**DISSOCIATION REACTIONS OF THE 11 Be ONE-NEUTRON HALO. THE INTERPLAY BETWEEN STRUCTURE AND REACTION MECHANISM**
ANNE R., ARNELL S.E., BIMBOT R., DOGNY S., EMLING H., ESBENSEN H., GUILLEMAUD-MUELLER D., HANSEN P.G., HORNSHOJ P., HUMBERT F., JONSON B., KEIM M., LEWITOWICZ M., MOLLER P., MUELLER A.C., NEUGART R., NILSSON T., NYMAN G., POUGHEON F., RIISAGER K., SAINT-LAURENT M.G., SCHRIEDER G., SORLIN O., TENGBLAD O., WILHELMSEN ROLANDER K., WOLSKI D.
*GANIL-CAEN, CHALMERS TEKN.HOGSKOLA-GOTEBORG, IPN-ORSAY, GSI-DARMSTADT, ANL-ARGONNE, AARHUS UNIV.-AARHUS, INST.FUR.KERNPHYSIK-DARMSTADT, INST.FUR.PHYSIK-MAINZ, CERN-GENEVE, SOLTAN INST.PROBLEMOW JADROWYCH-OTWOCK-SWIERK*
PHYSICS LETTERS B304 (1993) 55.

**ELASTIC SCATTERING OF 29 MeV/n 11 Li IONS ON A 28 Si TARGET**
LEWITOWICZ M. ET AL.
*GANIL - CAEN, JINR - DUBNA, IPN - ORSAY, CENT.INST.OF PHYS. - BUCHAREST, NUCL.PHYS.INST. - REZ, IFD UW - WARSAW, INST. FOR NUCL.RES. - KIEV*
*INTERNATIONAL CONFERENCE ON EXOTIC NUCLEI*
*FOROS (CRIMEA)*
*EXOTIC NUCLEI*

**ELASTIC SCATTERING OF A SECONDARY 11 Li BEAM ON 28 Si AT 29 MeV/NUCLEON**
LEWITOWICZ M. ET AL.
*GANIL - CAEN, IPN - ORSAY, LNR/JINR - DUBNA, NUCL. PHYS. INST. - REZ*
NUCLEAR PHYSICS A562 (1993) 301.

**ELASTIC SCATTERING OF A SECONDARY 11 Li BEAM ON 28 Si AT 29 MeV/u**
LEWITOWICZ M., ANNE R., ARTUKH A.G., BIMBOT R., BORCEA C., BORREL V., CARSTOIU F., DLOUHY S., GAREEV F.A., ERSHOV S.N., KAZACHA G.S., GUILLEMAUD-MUELLER D., KORDYASZ A., LUKYANOV S., MUELLER A.C., PENIONZHKEVICH YU., SKOBELEV N., SVANDA J., TRETYAKOVA S.
*GANIL - CAEN, INST.OF ATOMIC PHYS. - BUCAREST, JINR - DUBNA, IPN - ORSAY, NUCL.PHYS.INST. - REZ, IFD UW - WARSAW*
*INTERNATIONAL CONFERENCE ON NUCLEI FAR FROM STABILITY.6 / AND THE INTERNATIONAL CONFERENCE ON ATOMIC MASSES AND FUNDAMENTAL CONSTANTS.9*
*BERNKASTEL-KUES*
*NUCLEI FAR FROM STABILITY/ATOMIC MASSES AND FUNDAMENTAL CONSTANTS 1992*

**EMISSION OF NEUTRONS AND THE NEUTRON HALO OF 11 Li**
LEWITOWICZ M. ET AL.
*GANIL - CAEN, FYSISKA INSTITUTIONEN - GOTEBORG, IPN - ORSAY, GSI - DARMSTADT, AARHUS UNIV. - AARHUS, MAINZ UNIV. - MAINZ, INST.FUR KERNPHYSIK - DARMSTADT*
*INTERNATIONAL CONFERENCE ON EXOTIC NUCLEI*
*FOROS (CRIMEA)*
*EXOTIC NUCLEI*

**EXPERIMENTS TO DETERMINE THE STRUCTURE OF LIGHT NEUTRON-RICH NUCLEI**
MUELLER A.C.
*IPN - ORSAY*
*INTERNATIONAL CONFERENCE ON NUCLEI FAR FROM STABILITY.6 / AND THE INTERNATIONAL CONFERENCE ON ATOMIC MASSES AND FUNDAMENTAL CONSTANTS.9*
*BERNKASTEL-KUES*
*NUCLEI FAR FROM STABILITY/ATOMIC MASSES AND FUNDAMENTAL CONSTANTS 1992*

**EXPERIMENTS WITH SECONDARY BEAMS OF DRIP-LINE ISOTOPES**
MUELLER A.C.
*IPN - ORSAY*
*FRANCO-JAPANESE COLLOQUIUM ON NUCLEAR STRUCTURE AND INTERDISCIPLINARY TOPICS.6*
*SAINT-MALO (FR)*
*NUCLEAR STRUCTURE AND INTERDISCIPLINARY TOPICS*

**INVESTIGATIONS OF THE NEUTRON HALO BY RADIOACTIVE BEAM EXPERIMENTS**
MUELLER A.C.
*IPN - ORSAY*
RICERCA SCIENTIFICA ED EDUCAZIONE PERMANENTE.96, p. 477 (1993)
*INTERNATIONAL WINTER MEETING ON NUCLEAR PHYSICS.31*
*BORMIO (IT)*

**MASS MEASUREMENTS OF EXOTIC NUCLEI**
GILLIBERT A.
*CEN SACLAY - GIF SUR YVETTE*
*FRANCO-JAPANESE COLLOQUIUM ON NUCLEAR STRUCTURE AND INTERDISCIPLINARY TOPICS.6*
*SAINT-MALO (FR)*
*NUCLEAR STRUCTURE AND INTERDISCIPLINARY TOPICS*

**MASS-MEASUREMENTS OF EXOTIC NUCLEI**
MITTIG W.
*GANIL - CAEN*
NUCL. PHYS. A553 (1993) 473c
*INTERNATIONAL NUCLEAR PHYSICS CONFERENCE*
*WIESBADEN*

**NEUTRON DIFFERENTIAL CROSS SECTIONS FROM THE BREAK-UP OF 41 MeV/u 11 Be**
ANNE R., ARNELL S.E., BIMBOT R., DOGNY S., EMLING H., GUILLEMAUD-MUELLER D., HANSEN P.G., HORNSHOJ P., HUMBERT F., JONSON B., KEIM M., SAINT-LAURENT M.G., LEWITOWICZ M., MOLLER P., MUELLER A.C., NEUGART R., NILSSON T., NYMAN G., POUGHEON F., RIISAGER K., SCHRIEDER G., SORLIN O., TENGBLAD O., WILHELMSEN ROLANDER K., WOLSKI D.
*GANIL - CAEN, CHALMERS TEKNISKA HOGSKOLA - GOTEBORG, IPN - ORSAY, GSI - DARMSTADT, AARHUS UNIV. - AARHUS, INST. FUR KERNPHYSIK - DARMSTADT, MAINZ UNIV. - MAINZ, CERN - GENEVE, SOLTAN INSTYTUT PROBLEMOW JADROWYCH - OTWOCK-SWIERK*
*INTERNATIONAL CONFERENCE ON NUCLEI FAR FROM STABILITY.6 / AND INTERNATIONAL CONFERENCE ON ATOMIC MASSES AND FUNDAMENTAL CONSTANTS.9*
*BERNKASTEL-KUES*
*NUCLEI FAR FROM STABILITY/ATOMIC MASSES AND FUNDAMENTAL CONSTANTS 1992*

**PRESENT STATUS OF MASS MEASUREMENTS OF NUCLEI FAR FROM STABILITY USING A CYCLOTRON**
MITTIG W. ET AL.
*GANIL - CAEN, CEN SACLAY - GIF SUR YVETTE, IFUSP - SAO PAULO*
*INTERNATIONAL CONFERENCE ON EXOTIC NUCLEI*
*FOROS (CRIMEA)*
*EXOTIC NUCLEI*

**PRODUCTION AND STUDY OF NUCLEI OF ASTROPHYSICAL INTEREST WITH THE LISE SPECTROMETER**
SORLIN O., GUILLEMAUD-MUELLER D., MUELLER A.C., BORREL V., DOGNY S., POUGHEON F., KRATZ K.L., GABELMANN H., PFEIFFER B., SCHAFER F., SOHN H., WOHR A., PENIONZHKEVICH YU.E., LUKYANOV S.M., SALAMATIN V.S., ANNE R., BORCEA C., FIFIELD L.K., LEWITOWICZ M., SAINT-LAURENT M.G., BAZIN D., THIELEMANN F.K.
*IPN - ORSAY, INST. FUR KERNCHEMIE - MAINZ, JINR - DUBNA, GANIL - CAEN, CEN BORDEAUX - GRADIGNAN, ASTROPHYSICS HARVARD*
*INTERNATIONAL CONFERENCE ON NUCLEI FAR FROM STABILITY.6 / AND INTERNATIONAL CONFERENCE ON ATOMIC MASSES AND FUNDAMENTAL CONSTANTS.9*
*BERNKASTEL-KUES*
*NUCLEI FAR FROM STABILITY/ATOMIC MASSES AND FUNDAMENTAL CONSTANTS 1992*

**PROJECTILE BREAKUP STUDY IN 16 O INDUCED REACTIONS ON 27 Al, 58 Ni AND 197 Au TARGETS AROUND 100 MeV/NUCLEON**
BADALA A. ET AL.
*INFN - CATANIA, INFN - TORINO, NBI - COPENHAGEN*
RICERCA SCIENTIFICA ED EDUCAZIONE PERMANENTE.96, p. 316 (1993)
*INTERNATIONAL WINTER MEETING ON NUCLEAR PHYSICS.31*
*BORMIO (IT)*
*93 51 B*

**ASTROPHYSICAL RADIATIVE CAPTURE CROSS SECTIONS : MEASUREMENTS USING THE BREAKUP OF RADIOACTIVE BEAMS**
KIENER J., AGUER P., BOGAERT G., BORDERIE B., COC A., DISDIER D., FORTIER S., GRUNBERG C., KRAUS L., LEFEBVRE A., LINCK I., RIVET M.F., ROUSSEL-CHOMAZ P., SAINT-LAURENT F., STEPHAN C., TASSAN-GOT L., THIBAUD J.P.
*CSNSM - ORSAY, IPN - ORSAY, CRN - STRASBOURG, GANIL - CAEN*
*INTERNATIONAL SYMPOSIUM ON NUCLEAR ASTROPHYSICS HELD AT KARLSRUHE.2*
*KARLSRUHE*
*NUCLEI IN THE COSMOS*
*93 34 C*

**DECAY PROPERTIES OF EXOTIC N 28 S AND Cl NUCLEI AND THE 48 Ca/46 Ca ABUNDANCE RATIO**
SORLIN O. ET AL.
*IPN - ORSAY, MAINZ UNIV. - MAINZ, JINR - DUBNA, GANIL - CAEN, CENBG - GRADIGNAN, LPC - CAEN, HARVARD-SMITHSONIAN CENTER FOR ASTROPHYSICS - CAMBRIDGE, MPI - GARCHING*
PHYS. REV. C47, (1993) 2941.
*93 79 C*

**DETERMINATION OF THE 13 N(p,gamma) 14 O REACTION RATE THROUGH THE COULOMB BREAK-UP OF A 14 O RADIOACTIVE BEAM**
KIENER J., LEFEBVRE A., AGUER P., BACRI C.O., BIMBOT R., BOGAERT G., BORDERIE B., CLAPIER F., COC A., DISDIER D., FORTIER S., GRUNBERG C., KRAUS L., LINCK I., PASQUIER G., RIVET M.F., SAINT-LAURENT F., STEPHAN C., TASSAN-GOT L., THIBAUD J.P.
*CSNSM - ORSAY, IPN - ORSAY, CRN - STRASBOURG, GANIL - CAEN*
NUCL. PHYS. A552 (1993) 66.
*93 14 C*

**DISSOCIATION REACTIONS OF THE 11 Be ONE-NEUTRON HALO. THE INTERPLAY BETWEEN STRUCTURE AND REACTION MECHANISM**

ANNE R., ARNELL S.E., BIMBOT R., DOGNY S., EMLING H., ESBENSEN H., GUILLEMAUD-MUELLER D., HANSEN P.G., HORNSHOJ P., HUMBERT F., JONSON B., KEIM M., LEWITOWICZ M., MOLLER P., MUELLER A.C., NEUGART R., NILSSON T., NYMAN G., POUGHEON F., RIISAGER K., SAINT-LAURENT M.G., SCHRIEDER G., SORLIN O., TENGBLAD O., WILHELMSEN ROLANDER K., WOLSKI D.
*GANIL-CAEN, CHALMERS TEKN.HOGSKOLA-GOTEBORG, IPN-ORSAY, GSI-DARMSTADT, ANL-ARGONNE, AARHUS UNIV.-AARHUS, INST.FUR.KERNPHYSIK-DARMSTADT, INST.FUR.PHYSIK-MAINZ, CERN-GENEVE, SOLTAN INST.PROBLEMOW JADROWYCH-OTWOCK-SWIERK*
PHYSICS LETTERS B304 (1993) 55.
*93 21 C*

**STUDY OF THE BETA DECAY OF 20 Mg AND ITS IMPLICATION FOR THE ASTROPHYSICAL rp-PROCESS**

PIECHACZEK A., MOHAR M.F., ANNE R., BORREL V., CORRE J.M., GUILLEMAUD-MUELLER D., ISHIHARA M., KELLER H., KUBONO S., KUNZE V., LEWITOWICZ M., MAGNUS P., MUELLER A.C., NAKAMURA T., PFUTZNER M., ROECKL E., RYKACZENSKI K., SAINT-LAURENT M.G., SCHMIDT-OTT W.D., SORLIN O.
*GSI - DARMSTADT, GANIL - CAEN, IPN - ORSAY, RIKEN - WAKO, INS - TOKYO, GOTTINGEN UNIV. - GOTTINGEN, WASHINGTON UNIV. - SEATTLE, TOKYO UNIV. - TOKYO, INST. OF EXP. PHYS. - UNIV. OF WARSAW*
*INTERNATIONAL CONFERENCE ON NUCLEI FAR FROM STABILITY.6 / AND THE INTERNATIONAL CONFERENCE ON ATOMIC MASSES AND FUNDAMENTAL CONSTANTS.9*
*BERNKASTEL-KUES*
*NUCLEI FAR FROM STABILITY/ATOMIC MASSES AND FUNDAMENTAL CONSTANTS 1992*

**SYNTHESIS AND PROPERTIES OF EXOTIC NUCLEI AT GANIL WITH THE LISE SPECTROMETER**

GUILLEMAUD-MUELLER D.
*IPN - ORSAY*
*INTERNATIONAL CONFERENCE ON EXOTIC NUCLEI*
*FOROS (CRIMEA)*
*EXOTIC NUCLEI*

**THE DECAY MODES OF PROTON DRIP LINE NUCLEI WITH A BETWEEN 42 AND 47**

BORREL V., DOGNY S., GUILLEMAUD-MUELLER D., MUELLER A.C., POUGHEON F., SORLIN O., ANNE R., BORCEA C., FIFIELD L.K., LEWITOWICZ M., SAINT-LAURENT M.G., BAZIN D., DEL MORAL R., DUFOUR J.P., FAUX L., FLEURY A., HUBERT F., MARCHAND C., PRAVIKOFF M.S., DETRAZ C., KASHY E., CHUBARIAN G.G.
*IPN - ORSAY, GANIL - CAEN, CENBG - GRADIGNAN, LPC - CAEN, MSU - EAST LANSING, JINR - DUBNA*
*INTERNATIONAL CONFERENCE ON NUCLEI FAR FROM STABILITY.6 / AND THE INTERNATIONAL CONFERENCE ON ATOMIC MASSES AND FUNDAMENTAL CONSTANTS.9*
*BERNKASTEL-KUES*
*NUCLEI FAR FROM STABILITY/ATOMIC MASSES AND FUNDAMENTAL CONSTANTS 1992*

**THE SEARCH FOR NEW RADIOACTIVITIES AT THE PROTON DRIP LINE**
POUGHEON F., BORREL V., GUILLEMAUD-MUELLER D., MUELLER A.C., ANNE R., DETRAZ C., LEWITOWICZ M., BAZIN D., DUFOUR J.P., FLEURY A., HUBERT F., PRAVIKOFF M.S.
*IPN - ORSAY, GANIL - CAEN, CEN BORDEAUX - GRADIGNAN*
*INTERNATIONAL CONFERENCE ON NUCLEI FAR FROM STABILITY.6 / AND THE INTERNATIONAL CONFERENCE ON ATOMIC MASSES AND FUNDAMENTAL CONSTANTS.9*
*BERNKASTEL-KUES*
*NUCLEI FAR FROM STABILITY/ATOMIC MASSES AND FUNDAMENTAL CONSTANTS 1992*

**CHARGED PARTICLE CALORIMETRY OF 40 Ar + 27 Al AND 64 Zn + nat Ti REACTIONS AT INTERMEDIATE ENERGIES**
CUSSOL D. ET AL.
*LPC - CAEN, GANIL - CAEN, DAPNIA CEA SACLAY - GIF SUR YVETTE, FNRS IPN/UCL - LOUVAIN LA NEUVE, LPN - NANTES, TEXAS A&M UNIV. - COLLEGE STATION, INST.OF PHYS. - TSUKUBA*
RICERCA SCIENTIFICA ED EDUCAZIONE PERMANENTE.96, p. 250 (1993)
*INTERNATIONAL WINTER MEETING ON NUCLEAR PHYSICS.31*
*BORMIO (IT)*

**COMPONENTS OF COLLECTIVE FLOW AND AZIMUTHAL DISTRIBUTIONS IN 40 Ar + 27 Al AND 40 Ar + 58 Ni COLLISIONS BELOW 85 MeV/u**
SHEN W.Q., PETER J., BIZARD G., BROU R., CUSSOL D., LOUVEL M., PATRY J.P., REGIMBART R., STECKMEYER J.C., SULLIVAN J.P., TAMAIN B., CREMA E., DOUBRE H., HAGEL K., JIN G.M., PEGHAIRE A., SAINT-LAURENT F., CASSAGNOU Y., LEGRAIN R., LEBRUN C.,
ROSATO E., MAcGRATH R., JEONG S.C., LEE S.M., NAGASHIMA Y., NAKAGAWA T., OGIHARA M., KASAGI J., MOTOBAYASHI T.
*LPC - CAEN, GANIL - CAEN, SEPN/CEN SACLAY - GIF SUR YVETTE, LPN - NANTES, NAPOLI UNIV. - NAPLES, SUNY - STONY BROOK, IMP - LANZHOU, TSUKUBA UNIV. - TSUKUBA, TOKYO INST. OF TECH. - TOKYO, RIKKYO UNIV. - TOKYO*
NUCL. PHYS. A551 (1993) 333.

**DAMPED REACTION DYNAMICS IN 197 Au + 208 Pb COLLISIONS AT 29 MeV/NUCLEON**
QUEDNAU B.M. ET AL.
*NSRL - ROCHESTER, HMI - BERLIN, GANIL - CAEN, IPN - ORSAY*
PHYS. LETT. B309 (1993) 10.

**DYNAMICS OF VIOLENT COLLISIONS INDUCED BY AR ON AG BETWEEN 27 AND 60 MeV/NUCLEON : PERSISTENCE OF BINARY DISSIPATIVE COLLISIONS AND TEMPERATURE LIMITS**
RIVET M.F. ET AL.
*IPN - ORSAY, IPN - LOUVAIN-LA-NEUVE, FNRS - BRUXELLES, LPN - NANTES*
RICERCA SCIENTIFICA ED EDUCAZIONE PERMANENTE.96, p.92 (1993)
*INTERNATIONAL WINTER MEETING ON NUCLEAR PHYSICS.31*
*BORMIO (IT)*

**EMISSION OF COMPLEX FRAGMENTS IN THE REACTION Ar + Au AT 44 AND 77 A.MeV**
SOKOLOV A. ET AL.
*GANIL - CAEN, CEN - BRUYERES-LE-CHATEL, HMI - BERLIN, IPN - ORSAY, BEIJING UNIV. - BEIJING, CRN - STRASBOURG, INST. OF EXP. PHYS. - WARSAW*
NUCLEAR PHYSICS A562 (1993) 273.

**EVIDENCE FOR FAST AND SIMULTANEOUS MULTI-FRAGMENT EMISSION IN CENTRAL Kr + Au COLLISIONS AT 60 MeV/u**
LOPEZ O. ET AL.
*LPC - CAEN, INFN - CATANIA, CRN - STRASBOURG, AECL - CHALK RIVER, GANIL - CAEN*
PHYSICS LETTERS B315 (1993) 34.

**FISSION STUDY FOR THE SYSTEM 84 Kr + 232 Th AT 25, 35 AND 45 MeV/u**
POLLACCO E.C. ET AL.
*DAPNIA/CEN SACLAY - GIF-SUR-YVETTE*
ZEITSCHRIFT FUR PHYSIK A 346 (1993) 63.

**FROM BINARY FISSION TO MULTIFRAGMENTATION IN THE DECAY OF HEAVY EXCITED NUCLEI**
BIZARD G., BOUGAULT R., BROU R., COLIN J., DURAND D., GENOUX-LUBAIN A., LAVILLE J.L., LE BRUN C., LECOLLEY J.F., LOUVEL M., PETER J., STECKMEYER J.C., TAMAIN B., BADALA A., MOTOBAYASHI T., RUDOLF G., STUTTGE L.
*LPC/ISMRA - CAEN, INFN - CATANIA, RIKKYO UNIV. - RIKKYO, CRN - STRASBOURG*
PHYS. LETT. B302 (1993) 162.

**INCLUSIVE EXCITATION-ENERGY DISTRIBUTIONS OF HOT NUCLEI FROM 44 MeV/NUCLEON Ar- AND 32 MeV/NUCLEON Kr-INDUCED REACTIONS**
LOTT B. ET AL.
*CRN - STRASBOURG, CEN - BRUYERES-LE-CHATEL, GANIL - CAEN, IPN - ORSAY, HMI - BERLIN, BEIJING UNIV. - BEIJING, WARSAW UNIV. - WARSAW*
ZEITSCHRIFT FUR PHYSIK A 346 (1993) 201.

**INCLUSIVE FRAGMENT PRODUCTION IN 84 Kr + 197 Au AT E/A = 35 MeV**
MILKAU U. ET AL.
*GSI - DARMSTADT, FRANKFURT UNIV. - FRANKFURT, INFN - CATANIA, CEN SACLAY - GIF-SUR-YVETTE, TEXAS A&M UNIV. - COLLEGE STATION*
ZEITSCHRIFT FUR PHYSIK A 346 (1993) 227.

**LES NOYAUX CHAUDS**
GUERREAU D.
*GANIL - CAEN*
BULLETIN DE LA SOCIETE FRANCAISE DE PHYSIQUE 89 (1993) 5.

**MULTIFRAGMENT DECAY OF HIGHLY EXCITED NUCLEI**
LOUVEL M. ET AL.
*LPC ISMRA - CAEN, GANIL - CAEN, FNRS/UCL - LOUVAIN LA NEUVE, TSUKUBA UNIV. - IBARAKI-KEN, TEXAS A&M UNIV. - COLLEGE STATION, FNRS/ULB - BRUSSELS, IMP - LANZHOU, SHINSHU UNIVERSITY - RIKKYO UNIV. - TOKYO*
NUCLEAR PHYSICS A559 (1993) 137.

**REACTION-MECHANISM EVOLUTION FOR THE SYSTEM 20 Ne + 60 Ni AT INTERMEDIAIRE ENERGIES : FROM MASSIVE TRANSFER TO FRAGMENTATION**
ANDREOZZI F. ET AL.
*DIPART. DI SCIENZE FISICHE AND INFN - CATANIA, CE SACLAY - GIF SUR YVETTE, ORNL - OAK RIDGE*
NUCL. PHYS. A564 (1993) 441.

**RECENT RESULTS ON NUCLEAR FLOW MEASUREMENTS AT GANIL**
ANGELIQUE J.C. ET AL.
*LPC - CAEN, GANIL - CAEN, DAPNIA CEA SACLAY - GIF SUR YVETTE, IPN - LOUVAIN LA NEUVE, LPN - NANTES, TEXAS A&M UNIV. - COLLEGE STATION, DIPART.DI SCIENZE FISICHE - NAPOLI, IMP - LANZHOU*
RICERCA SCIENTIFICA ED EDUCAZIONE PERMANENTE.96, p. 213 (1993)
*INTERNATIONAL WINTER MEETING ON NUCLEAR PHYSICS.31*
*BORMIO (IT)*

**FRAGMENTATION PATTERN IN SEQUENTIAL EMISSION SPECTRA**
RUDOLF G. ET AL.
*CRN - STRASBOURG, LPC - CAEN, CEN SACLAY - GIF SUR YVETTE, IFIC UNIV. DE VALENCIA - BURJASOT, LPN - NANTES, GANIL - CAEN*
PHYSICS LETTERS B307 (1993) 287

**LIGHT CHARGED PARTICLE EMISSION IN PERIPHERAL COLLISIONS IN Kr + Au AT 60 MeV/u IN EXCLUSIVE MEASUREMENTS**
RUDOLF G. ET AL.
*CRN - STRASBOURG, LPC - CAEN, GANIL - CAEN*
RICERCA SCIENTIFICA ED EDUCAZIONE PERMANENTE.96, p. 276 (1993)
*INTERNATIONAL WINTER MEETING ON NUCLEAR PHYSICS.31*
*BORMIO (IT)*

**MULTIPLICITY DISTRIBUTIONS OF PREEQUILIBRIUM PROTONS IN INTERMEDIATE ENERGY HEAVY ION COLLISIONS**
ALBA R. ET AL.
*INFN - CATANIA, DIPART.DI FISICA DELL'UNIVERSITA - CATANIA, GANIL - CAEN, INFN - MILANO*
RICERCA SCIENTIFICA ED EDUCAZIONE PERMANENTE.96, p. 284 (1993)
*INTERNATIONAL WINTER MEETING ON NUCLEAR PHYSICS.31*
*BORMIO (IT)*

**ON THE BREAKUP OF EXCITED 16 O PROJECTILES INTO FOUR ALPHAS AT INTERMEDIATE ENERGIES**
POULIOT J., DORE D., LAFOREST R., ROY R., ST-PIERRE C., LOPEZ J.A.
*LPN LAVAL UNIV. - QUEBEC, TEXAS UNIV. - EL PASO*
PHYS. LETT. B299 (1993) 210.

**STRONG IMPACT PARAMETER DEPENDENCE OF HARD PHOTON PRODUCTION N INTERMEDIATE ENERGY HEAVY ION COLLISIONS**
MIGNECO E., AGODI C., ALBA R., BELLIA G., CONIGLIONE R., DEL ZOPPO A., FINOCCHIARO P., MAIOLINO C., PIATTELLI P., RUSSO G., SAPIENZA P., BADALA A., BARBERA R., PALMERI A., PAPPALARDO G.S., RIGGI F., RUSSO A.C., PEGHAIRE A., BONASERA A.
*INFN - CATANIA, CATANIA UNIV. - CATANIA, GANIL - CAEN*
PHYS. LETT. B298 (1993) 46.

**AZIMUTHAL ASYMMETRY OF NEUTRAL PION EMISSION IN Au + Au REACTIONS AT 1 GeV/NUCLEON**
VENEMA L.B. ET AL.
*KVI - GRONINGEN, PHYSIKALISCHES INST. - GIESSEN, GSI - DARMSTADT, PHYSIKALISCHES INST. - HEIDELBERG, FORSCHUNGSZENTRUM ROSSENDORF - DRESDEN, GANIL - CAEN, INST. FUR KERNPHYSIK - MUNSTER*
PHYSICAL REVIEW LETTERS 71, 6 (1993) 835.

**INVESTIGATION OF PION ABSORPTION IN HEAVY-ION INDUCED SUBTHRESHOLD pi o PRODUCTION**
MAYER R.S.,HENNING W.,HOLZMANN R.,SIMON R.S.,DELAGRANGE H.,LEFEVRE F.,MATULEWICZ T., MERROUCH R.,MITTIG W.,OSTENDORF R.W.,SCHUTZ Y.,BERG F.D.,KUHN W.,METAG V.,NOVOTNY R., PFEIFFER M.,BOONSTRA A.L.,LOHNER H.,VENEMA L.B.,WILSCHUT W.,ARDOUIN D., DABROWSKI H.,ERAZMUS B.,LEBRUN C.,SEZAC L.,BALLESTER F.,CASAL E.,DIAZ J., FERRERO J.L.,MARQUES M.,MARTINEZ G.,NIFENECKER H.,FORNAL B.,FREINDL L.,SUJKOWSKI Z.
*GSI-DARMSTADT, GANIL-CAEN, GIESSEN UNIV.-GIESSEN, KVI-GRONINGEN, LPN-NANTES, IFC-BURJASSOT, ISN-GRENOBLE, INP-CRACOW, SOLTAN INST.FOR NUCL. STUDIES - SWIERK*
PHYS. REV. LETT. 70, 7 (1993) 904.

**LIGHT CHARGED PARTICLES ASSOCIATED WITH SUBTHRESHOLD NEUTRAL PION EMISSION IN THE 16 O + 27 Al REACTION**
BADALA A. ET AL.
*INFN - CATANIA*
ZEITSCHRIFT FUR PHYSIK A 346 (1993) 293.

**NEUTRAL PION PRODUCTION IN THE 16 O + 27 Al REACTION AT 94 MeV/NUCLEON**
BADALA A., BARBERA R., PALMERI A., PAPPALARDO G.S., RIGGI F., RUSSO A.C., AGODI C., ALBA R., BELLIA G., CONIGLIONE R., DEL ZOPPO A., FINOCCHIARO P., MAIOLINO C., MIGNECO E., PIATTELLI P., RUSSO G., SAPIENZA P., PEGHAIRE A.
*INFN - CATANIA, CATANIA UNIV. - CATANIA, GANIL - CAEN*
PHYS. REV. C47, 1 (1993) 231.

**PERIPHERAL PION PRODUCTION IN PROJECTILE BREAKUP REACTIONS AT 94 MeV/NUCLEON**
BADALA A. ET AL.
*INFN - CATANIA, LPC - CAEN*
PHYSICS LETTERS B316 (1993) 240.

**PROTON AND SUBTHRESHOLD PION PRODUCTION CORRELATED WITH LIGHT FRAGMENTS : A STATISTICAL PROCESS ?**
LAVILLE J.L. ET AL.
*LPC ISMRA - CAEN, INFN - CATANIA*
NUCL. PHYS. A564 (1993) 564.

**BEYOND THE NUCLEUS**
DETRAZ C.
*CNRS - PARIS*
PHYSICS WORLD DEC. 1993, p. 28.

**ZEHN JAHRE GANIL**
VON OERTZEN W.
*HMI - BERLIN*
PHYS. BL. 50, Nr.1 (1994) 13.

**ABSOLUTE MEASUREMENT OF THE GANIL BEAM ENERGY**
MITTIG W. ET AL.
*GANIL - CAEN, IFUSP - SAO PAULO, INFN - CATANIA, KVI - GRONINGEN*
NIM A334 (1993) 301.

**CHARGE EXCHANGE OF VERY HEAVY IONS IN CARBON FOILS AND IN THE RESIDUAL GAS OF GANIL CYCLOTRONS**
BARON E., BAJARD M., RICAUD CH.
*GANIL - CAEN*
NIM A328 (1993) 177.
*INTERNATIONAL CONFERENCE ON ELECTROSTATIC ACCELERATORS AND ASSOCIATED BOOSTERS.6*
*PADOVA*
*ELECTROSTATIC ACCELERATORS AND ASSOCIATED BOOSTERS*

**PROPOSALS FOR A RADIOACTIVE ION BEAM FACILITY AT GANIL**
BOURGAREL M.P., BRICAULT P., CHABERT A., DUVAL M., JOUBERT A., RICAUD CH., SORTAIS P.
*GANIL - CAEN*
NIM A328 (1993) 321.
*INTERNATIONAL CONFERENCE ON ELECTROSTATIC ACCELERATORS AND ASSOCIATED BOOSTERS.6*
*PADOVA*
*ELECTROSTATIC ACCELERATORS AND ASSOCIATED BOOSTERS*

**SECONDARY BEAMS AT GANIL**
DOUBRE H.
*GANIL - CAEN*
*FRANCO-JAPANESE COLLOQUIUM ON NUCLEAR STRUCTURE AND INTERDISCIPLINARY TOPICS.6*
*SAINT-MALO (FR)*
*NUCLEAR STRUCTURE AND INTERDISCIPLINARY TOPICS*

**THE STANDARD GANIL DATA ACQUISITION SYSTEM**
RAINE B. ET AL.
*GANIL - CAEN*
*CONFERENCE RECORD OF THE EIGHTH CONFERENCE ON REAL-TIME COMPUTER APPLICATIONS IN NUCLEAR, PARTICLE AND PLASMA PHYSICS*
*VANCOUVER (CN)*

**A MULTI-ELEMENT DETECTOR ARRAY FOR HEAVY FRAGMENTS EMITTED IN INTERMEDIATE ENERGY NUCLEAR REACTIONS**
IORI I., MANDUCI L., MORONI A., SCARDAONI R., SUN CHONG WEN, ZHANG YUZHAO, ZHANG GUANGMING, GIGLIO F., MORA E., DI PIETRO G., DELLERA L., CORTESI A., BASSINI R., BOIANO C., BRAMBILLA S., MALATESTA M., BRUNO M., D'AGOSTINO M., FIANDRI M.L.,
FUSCHINI E., MILAZZO P.M., BUSACCHI G., CUNSOLO A., FOTI A., GIANINO C., SAVA G., GRAMEGNA F., BUTTAZZO P., MARGAGLIOTTI G.V., VANNINI G., AUGER G., PLAGNOL E.
*INFN - MILANO, INFN - BOLOGNA, INFN - CATANIA, INFN - LEGNARO, INFN - TRIESTE, GANIL - CAEN*
NIM A325 (1993) 458.

**A NONINTERCEPTIVE HEAVY ION BEAM PROFILE MONITOR BASED ON RESIDUAL GAS IONIZATION**
ANNE R., GEORGET Y., HUE R., TRIBOUILLARD CH., VIGNET J.L.
*GANIL - CAEN*
NIM A329 (1993) 21.

**LOSS OF LIGHT CHARGED PARTICLES BY NUCLEAR INTERACTIONS IN BaF 2 CRYSTALS**
LANZANO G. ET AL.
*INFN - CATANIA, DAPNIA CEN SACLAY - GIF SUR YVETTE, CRN - STRASBOURG*
NIM A332 (1993) 161.

**QUENCHING OF SCINTILLATION IN BaF 2 FOR LIGHT CHARGED PARTICLES**
MATULEWICZ T.
*GANIL - CAEN*
NIM A325 (1993) 365.

**REDUCTION OF THE ENERGY OF SECONDARY BEAMS DOWN TO THE COULOMB BARRIER**
YANG YONG FENG ET AL.
*GANIL - CAEN, DAPNIA CEA SACLAY - GIF SUR YVETTE, INFN - CATANIA, IPN - ORSAY*
NIM B82 (1993) 175.

**RESPONSE OF THE BaF 2 SCINTILLATOR TO LIGHT CHARGED PARTICLES**
DEL ZOPPO A., AGODI C., ALBA R., BELLIA G., CONIGLIONE R., FINOCCHIARO P., MAIOLINO C., MIGNECO E., PEGHAIRE A., PIATTELLI P., SAPIENZA P.
*INFN - CATANIA, CATANIA UNIV. - CATANIA, GANIL - CAEN*
NIM A327 (1993) 363.

**SELECTION OF VIOLENT COLLISIONS BY MEANS OF A NEUTRON CALORIMETER FOR INTERFEROMETRY MEASUREMENTS**
SEZAC L. ET AL.
*LPN - NANTES, CENBG - GRADIGNAN, GANIL - CAEN, INST.OF NUCL.PHYS. - CRACOW, JINR - DUBNA, WARSAW TECH.UNIV. - WARSAW, KVI - GRONINGEN*
RICERCA SCIENTIFICA ED EDUCAZIONE PERMANENTE.96, p. 293 (1993)
*INTERNATIONAL WINTER MEETING ON NUCLEAR PHYSICS.31*
*BORMIO (IT)*

**THE INDRA 4 PI DETECTOR AND ITS PHYSICS PROGRAM**
BORDERIE B. ET AL.
*IPN - ORSAY, DAPNIA CEA SACLAY - GIF SUR YVETTE, GANIL - CAEN, LPC - CAEN*
RICERCA SCIENTIFICA ED EDUCAZIONE PERMANENTE.96, p. 238 (1993)
*INTERNATIONAL WINTER MEETING ON NUCLEAR PHYSICS.31*
*BORMIO (IT)*

**THE RESPONSE OF BGO SCINTILLATOR DETECTORS TO LIGHT CHARGED NUCLEI**
DLOUHY Z. ET AL.
*NUCL. PHYS. INSTITUTE - REZ, GANIL - CAEN, IPN - ORSAY, JINR - DUBNA*
*INTERNATIONAL CONFERENCE ON EXOTIC NUCLEI*
*FOROS (CRIMEA)*
*EXOTIC NUCLEI*

**ENERGY DEPENDENCE OF INTERMITTENCY IN NUCLEAR REACTIONS AT INTERMEDIATE ENERGIES**
LI B.A., PLOSZAJCZAK M.
*HMI - BERLIN, GANIL - CAEN*
PHYS. LETT. B317 (1993) 300.

**EVEN-ODD ANOMALOUS TUNNELING EFFECT**
KAMIMSKI P., DROZDZ S., PLOSZAJCZAK M., CAURIER E.
*GANIL - CAEN, INP - KRAKOW, CRN - STRASBOURG*
PHYSICAL REVIEW C47, 4 (1993) 1548.

**EXCITATION OF GIANT MODES AND DECAY OF HOT NUCLEI**
CHOMAZ PH.
*GANIL - CAEN*
*FRANCO-JAPANESE COLLOQUIUM ON NUCLEAR STRUCTURE AND INTERDISCIPLINARY TOPICS.6*
*SAINT-MALO (FR)*
*NUCLEAR STRUCTURE AND INTERDISCIPLINARY TOPICS*

**FLUCTUATION IN NUCLEAR DYNAMICS AND MULTIFRAGMENTATION**
CHOMAZ PH. ET AL.
*GANIL - CAEN, LNS - CATANIA, LBL - BERKELEY, GSI - DARMSTADT*
RICERCA SCIENTIFICA ED EDUCAZIONE PERMANENTE.96, p. 107 (1993)
*INTERNATIONAL WINTER MEETING ON NUCLEAR PHYSICS.31*
*BORMIO (IT)*

**HEAVY RESIDUE PROPERTIES IN INTERMEDIATE ENERGY HEAVY ION INTERACTIONS WITH GOLD**
ALEKLETT K., YANEZ R., LOVELAND W., SRIVASTAVA A., LILJENZIN K.O.
*UPPSALA UNIV. - NYKOPING, OREGON STATE UNIV. - CORVALLIS,*
*CHALMERS UNIV. OF TECH. - GOTEBORG*
PROG. PART. NUCL. PHYS. 30 (1993) 297.

**K+ PRODUCTION FAR BELOW THE FREE NUCLEON-NUCLEON THRESHOLD IN HEAVY-ION COLLISIONS**
BELKACEM M., SURAUD E., AYIK S.
*GANIL - CAEN, TENNESSEE TECH. UNIV. - COOKEVILLE*
PHYS. REV. C47, 1 (1993) R16.

**MULTIFRAGMENTATION : A TOOL FOR THE STUDY OF NUCLEAR MATTER**
AUGER G. ET AL.
*GANIL - CAEN*
NUCLEAR PHYSICS NEWS 3, No.3 (1993) 21.

**MULTISCALING IN THE HADRONIZATION IN HIGH ENERGY COLLISIONS**
BOZEK P., PLOSZAJCZAK M.
*GANIL - CAEN - INP - KRAKOW*
ZEITCHRIFT FUR PHYSIK C 59 (1993) 585.

**NEW PIECES IN THE HOT GIANT DIPOLE RESONANCE PUZZLE**
CHOMAZ PH. ET AL.
*GANIL - CAEN, INFN - CATANIA, DIPART.DI FISICA - CATANIA, IMP - LANZHOU*
RICERCA SCIENTIFICA ED EDUCAZIONE PERMANENTE.96, p. 427 (1993)
*INTERNATIONAL WINTER MEETING ON NUCLEAR PHYSICS.31*
*BORMIO (IT)*

**SIMULATING THE LANGEVIN FORCE BY SIMPLE NOISE IN NUCLEAR ONE-BODY DYNAMICS**
COLONNA M., BURGIO G.F., CHOMAZ PH., DI TORO M., RANDRUP J.
*GANIL - CAEN, LNS - CATANIA, LBL - BERKELEY, GSI - DARMSTADT*
PHYSICAL REVIEW C47, 4 (1993) 1395

**SINGLE-PARTICLE AND COLLECTIVE STATES IN TRANSFER REACTIONS**
LHENRY I. ET AL.
*IPN - ORSAY, GANIL - CAEN*
NUCL. PHYS. A565 (1993) 524.

**THE ANALYSIS OF THE CHARGED-FRAGMENT CORRELATIONS USING A FRAGMENTATION-INACTIVATION BINARY MODEL**

BOTET R., PLOSZAJCZAK M.
*PARIS-SUD UNIV. - ORSAY, GANIL - CAEN*

PHYSICS LETTERS B313 (1993) 30.

Imprimerie CAEN-REPRO
Dépôt légal Avril 1994

GANIL

GRAND ACCELERATEUR D'IONS LOURDS
BP 5027 - 14021 CAEN CEDEX FRANCE - TEL. : 31 45 46 47
TELEX 170 533 F - FAX 31 45 46 65